INTERNATIONAL CONFERENCE on Wind Energy Harvesting

April 20-21, 2017
University of Coimbra
Coimbra, Portugal

THE INTERNATIONAL CONFERENCE ON
WIND ENERGY HARVESTING 2017
20-21 April 2017
Coimbra, Portugal

Editors:
Baniotopoulos C (Action Chair)
Rebelo C (Local Organiser)
Simões da Silva L (SC Chair)
Borri C (Action Vice Chair)
Blocken B (WG1 Chair)
Hemida H (WG1 Vice Chair)
Veljkovic M (WG2 Chair)
Morbiato T (WG2 Vice Chair)
Borg R P (WG3 Chair)
Huber S (WG3 Vice Chair)
Efthymiou E (Dissemination)

Paper book: ISBN 978-989-99226-4-8
Electronic book: ISBN 978-989-99226-5-5

April 20-21, 2017
Coimbra, Portugal

Gold Sponsor

sidenor

Silver Sponsors

SALZGITTER MANNESMANN RENEWABLES

Supported by

cmm ASSOCIAÇÃO PORTUGUESA DE CONSTRUÇÃO METÁLICA E MISTA · U · C · isise

cost EUROPEAN COOPERATION IN SCIENCE AND TECHNOLOGY

Aeolus future

Scientific Committee

Simões da Silva L. (Portugal, Chair)

Ahmet G. (Turkey)
Allegrini J. (Switzerland)
Alterman R. (Israel)
Aran J. (Spain)
Baker C. (UK)
Bakon T. (Poland)
Bard D. (Sweden)
Bartoli G. (Italy)
Blok R. (Netherlands)
Chaudhari A. (Finland)
Conde B. (Spain)
Coker D. (Turkey)
Correia J. (Portugal)
Cundeva S. (FYR of Macedonia)
Efstathiades C. (Cyprus)
Efthymiou E. (Greece)
Genc M. (Turkey)
Gervasio H. (Portugal)
Godinho L. (Portugal)
Hadjimitsis D. (Cyprus)
Höffer R. (Germany)
Hubova O. (Slovakia)
Huvaj N. (Turkey)
Jaisli I. (Switzerland)
Joffre S. (Finland)
Kalkman I. (Netherlands)
Kayran A. (Turkey)
Keysan O. (Turkey)
Konecna L. (Slovakia)
Kubilay A. (Switzerland)
Marciukaitis M. (Lithouania)
Marino E. (Italy)
Markovic Z. (Serbia)
Montazeri H. (Netherlands)
Murphy P. (Ireland)
Netusil M. (Czech Rebublic)
Norton C. (Ireland)
Pinto P. (Portugal)
Pires Neves L. (Portugal)
Polak A. (Croatia)
Ramponi R. (UK)
Rebelo C. (Portugal)
Sari R. (Turkey)
Schaumann P. (Germany)
Shiff G. (Israel)
Simões R. (Portugal)
Sokolov A. (Lithouania)
Spiteri Staines C. (Malta)
Srsen M. (Croatia)
Starosta K. (Poland)
Stathopoulos T. (Canada)
Stavroulakis G. (Greece)
Sterling M. (UK)
Tamura Y. (Japan)
Tanyer A. M. (Turkey)
Thomassen P. (Norway)
Todorovic J. (Bosnia and Herzegovina)
Tominaga Y. (Japan)
Tuncer I. (Turkey)
Uzol N. (Turkey)
Van Beeck J. (Belgium)
Van Hooff T. (Belgium

Steering Committee

Baniotopoulos C. (UK, Chair)
Blocken B. (Netherlands)
Borg R. (Malta)
Borri C. (Italy)
Efthymiou E. (Greece)
Hemida H. (UK)
Huber S. (Switzerland)
Morbiato T. (Italy)
Rebelo, C. (Portugal)
Veljkovic M. (Sweden)

Organizing Committee

Carlos Rebelo (Portugal, co-Chair)
Charalampos Baniotopoulos (UK, co-Chair)
Constança Rigueiro (Portugal)
Helena Gervásio (Portugal)
José Antonio Correia (Portugal)
Luis Simões da Silva (Portugal)
Rui Simões (Portugal)
Rui Matos (Portugal)

Table of Contents

FOREWORD

Dear Colleagues,

welcome to the International Conference on Wind Energy Harvesting – WINERCOST'17!

The Conference is organized in the scope of the TUD COST Action TU1304 *Wind energy technology reconsideration to enhance the concept of smart cities (WINERCOST)* and intends to provide a forum for the presentation and discussion of different aspects of wind energy and wind energy technologies. Following the aims of the COST action, the Conference addresses the research in the context not only of large onshore and offshore wind farms but also of urban and suburban built environment applications, which can have a decisive contribution to enhance the concept of Smart Future Cities.

The participation of young researchers in this Conference has been encouraged and pursued by giving the opportunity to the early stage researchers of the Marie-Curie Innovative Training Network AEOLUS4FUTURE to present their projects and the already available results in two special sessions during the conference. This project provides the funding for hiring the fifteen early stage researchers working in the ten different European universities, research institutes and companies, which are the project partners.

WINERCOST'17 addresses a wide variety of topics included in five themes: (i) Wind Characteristics and Loads; (ii) Structures, Materials and Dynamics; (iii) Grid Integration, Operations and Control; (iv) Markets, Strategies, Policies and (v) Socio-economics Smart Cities and Environmental Aspects.

The scientific committee has chosen a total number of about seventy extended abstracts for oral presentation during the two days that last the conference. These papers address topics included in the above-mentioned themes with special incidence in the first two of them.

The Conference has been organized in seven plenary sessions and ten parallel sessions. Internationally recognized experts will give four keynote lectures addressing the general themes of the Conference.

The organizers wish all the participants a fruitful work and a pleasant stay in the University of Coimbra, one of the oldest European universities.

Associate Professor Carlos Rebelo (University of Coimbra, Portugal)
Professor Charalampos Baniotopoulos (University of Birmingham, UK)
Chairs of Organizing Committee.

Keynote Lectures

THE INTERNATIONAL CONFERENCE ON
WIND ENERGY HARVESTING 2017
20-21 April 2017
Coimbra, Portugal

Paper keynote

NON-STATIONARY WINDS AND SOME IMPLICATIONS FOR THE BUILT ENNVIRONMENT

Mike Jesson[1]
University of Birmingham
Birmingham, UK

Chris Baker[2]
University of Birmingham
Birmingham, UK

Mark Sterling[3]
University of Birmingham
Birmingham, UK

ABSTRACT

In the vast majority of cases, winds are considered to be stationary and as such are treated in the same way for design purposes. However, not all wind is the same, and non-stationary winds such as thunderstorm downbursts and tornadoes need to be considered using a different framework. This paper outlines two possible analytical models for such winds and introduces a possible framework which may be of use to the urban designer.

NOMENCLATURE

D	=	Initial diameter of the downburst (m)
r	=	Radial distance from the centre of the tornado-like vortex (m)
r_m	=	Radial distance corresponding to U_m (m)
$\bar{r}$	=	Normalized radial distance (r/r_m)
U	=	Radial velocity (m/s)
U_m	=	Reference radial velocity (m/s)
$\bar{U}$	=	Normalized radial velocity ($\bar{U} = U/U_m$)
x	=	Horizontal distance (m)
z	=	Vertical distance above the ground (m)
z_m	=	Vertical distance above the ground corresponding to U_m (m)

INTRODUCTION

Wind is inherently non-stationary, but for most practical (design) purposes is usually considered to be statistically stationary over a given period of time, typically of the order of 30 minutes to 1 hour. Arguably the roots of this assumption can be traced back to the existence of the spectral gap, which was first postulated by [1]. However, van der Hoven noted that this may be a result of the way in which the data was analyzed and, subsequently, [2] and [3] have queried whether the spectral gap exists, and, if it does, whether it is as pronounced as first thought. Whilst this debate is interesting, the lack of frequent wind-related design failures suggests that there is merit in assuming that the most wind is stationary (over given periods) for most of the time. However, it is important to note that not all wind is the same and, as such, it is possible that for some winds the assumption of stationarity is fundamentally incorrect. For example, during thunderstorms, it is possible for downbursts and tornadoes to occur. Fig. 1 illustrates the recorded wind speed against time, during a series of downburst-type events [4]. Not only is the non-stationarity of the downburst events evident in Fig. 1 but also the significant

1 Research Fellow, School of Engineering, School of Engineering, University of Birmingham, Birmingham, UK. Department, University, M.A.Jesson@bham.ac.uk
2 Professor of Environmental Fluid Mechanics, School of Engineering, University of Birmingham, Birmingham, UK. Department, University, C.J.Baker@bham.ac.uk
3 Head of School and Beale Professor of Civil Engineering, School of Engineering, University of Birmingham, Birmingham, UK. Department, University, M.Sterling@bham.ac.uk

variations that can occur between such events. Similar variations between tornado events can also be observed, as well as the rapid changes in wind speed and direction.

Noting the above, the authors contend that it is important to consider these events separately when analyzing their effects on the built environment. As a result, two separate analytical models have been developed, one for thunderstorms and one for tornadoes, and are outlined in what follows. These models are then incorporated into a general risk framework which could be adopted for assessing the impacts of non-stationary winds in the built environment.

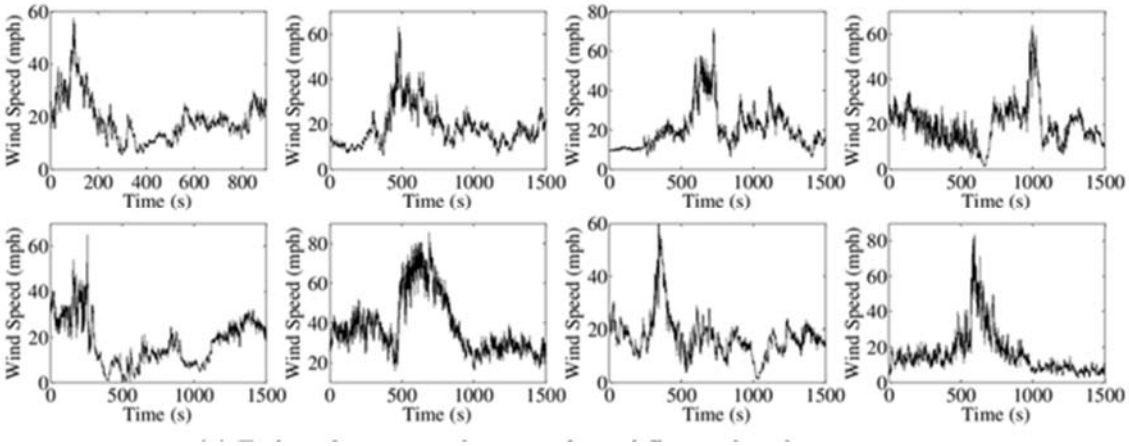

Figure 1. A family of measured downburst-type events[4]

DOWNBURST MODEL

Inspired by the findings of [5], the downburst model assumes that main flow field of a downburst arises as a result of the interaction of a primary vortex and secondary vortex (Fig. 2), and a constant outflow velocity. In order to model the "no-flow" condition across the ground plane, each vortex is mirrored in the ground plane. This method is taken from Potential Flow modelling, as is the superposition of the velocity fields to give the net velocity. Unlike the inviscid vortex of Potential Flow model, with its inherent singularity at the centre, the vortices are modelled as viscous, Rankine vortices. For a given size downburst, the initial location, size and shape of these vorticities are initially defined. As the simulation progresses the vortices are allowed to deform and translate, at rates based on the results of [6], [7], [8], and [9]. At this point, we note that we are using a one-dimensional model, developed for low Reynolds number flows, to describe what is ultimately a high Reynolds number, three-dimensional flow. As such, we acknowledge the weakness of this approach but note (a) the turbulence intensities in downbursts tend to be lower than those in stationary winds ([5]) and (b) the generated flow field appears to be capture the main components of the flow (Fig. 3). Fig. 3 illustrates the radial velocity (i.e., the streamwise velocity from at normalized height (z/D) above the ground of 0.02) against time, recorded at a normalized distance from the point of the impingement (x/D) of 1.50, where z is the distance above the ground, x is the distance from the centre of impingement and D is the diameter of the initial downburst)

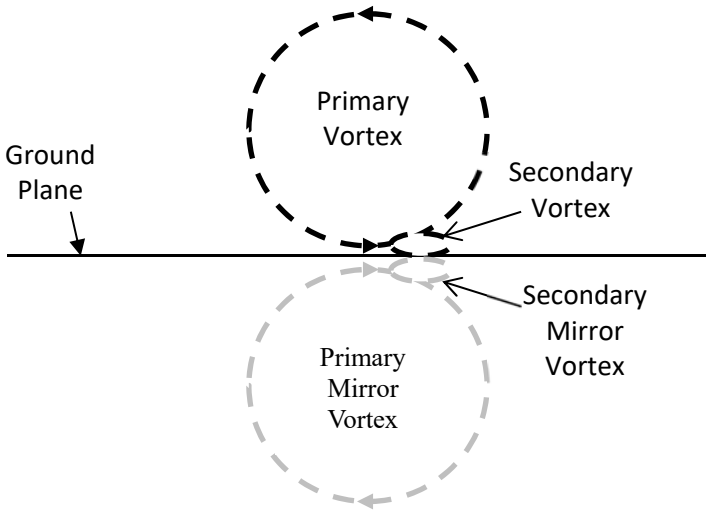

Fig. 2. Schematic illustrating the primary and secondary vortex used in the downburst model

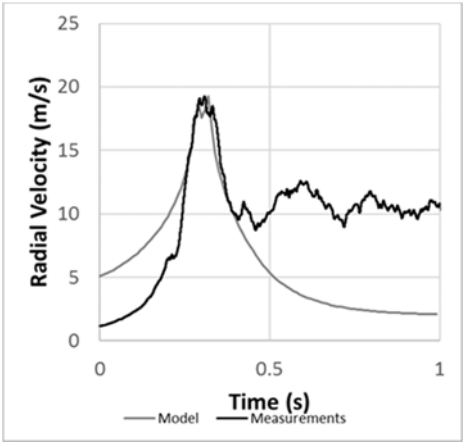

Fig. 3. Velocity time series for the model against actual data.

TORNADO MODEL

The development of the tornado model is based on a solution of the high Reynolds number Navier-Stokes and assumes that the radial velocity takes the form similar to:

$$\bar{U} = \frac{-4\bar{r}\bar{z}}{(1+\bar{r}^2)(1+\bar{z}^2)} \quad (1)$$

where, $\bar{U} = U/U_m$, where U is the radial velocity; $\bar{r} = r/r_m$ and $\bar{z} = z/z_m$ and r and z are the radial and vertical distances from the centre of the vortex. We thus assume that the velocity is normalised with a reference radial velocity U_m, and that the lengths are normalised with the radial (r_m) and vertical lengths (z_m) for which this reference velocity occurs, as outlined above. This represents an inflow into the tornado centre, with a maximum value of the inflow at $\bar{r} = \bar{z} = 1$, with the reference velocity in this case representing the maximum radial velocity. It shows a peak in radial velocity both in the radial and vertical directions, and the velocity goes to zero at the core and at infinity in a physically plausible way. A full derivation of the model is given [10] and results of the model are illustrated in Fig. 4.

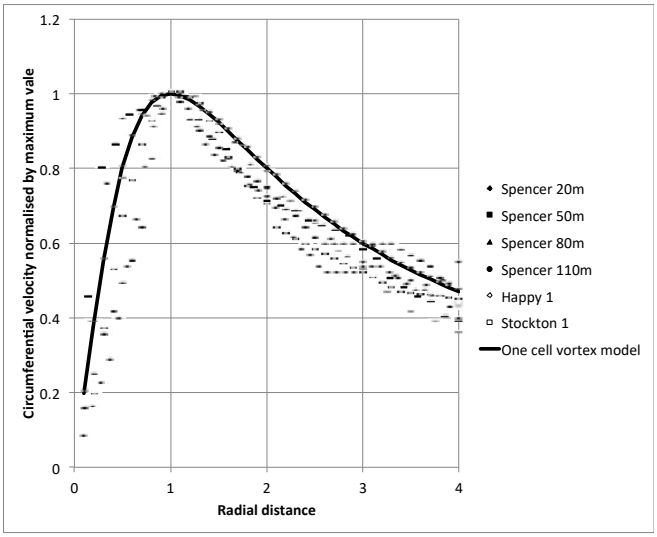

Fig. 4 A comparison of the radial velocity predicted by equation (1) (one cell vortex model) with full-scale data.

UNIFIED FRAMEWORK

Given the relative frequency with which thunderstorm downbursts and tornadoes occur in certain countries and the non-stationary flow fields generated, it is important to reflect on how the above analytical models could be incorporated into a framework for a variety of wind related issues in the urban environment (e.g., structural design, etc.). Fig. 5 illustrates such a possible framework which has both (or either) of the above models at its heart and enables probabilities of the wind resource to be established. There are a number of elements to this framework which would need to be informed either by modelling (physical/numerical) or full-scale data. However, much of the required data is already available or is in the process of being acquired.

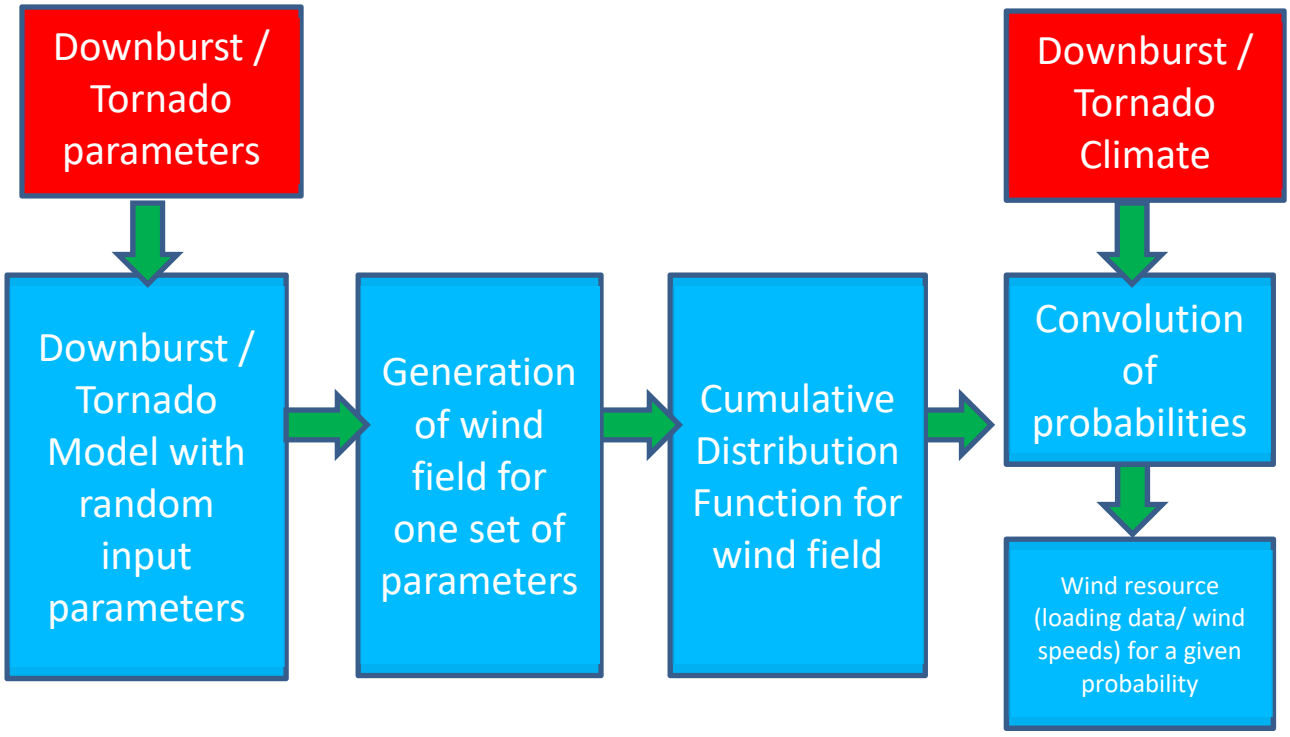

Fig. 5 A generic framework for non-stationary winds in the urban environment.

CONCLUSIONS

In this extended abstract, we have outlined two possible analytical models which appear to be capable of capturing the important features of two non-stationary types of winds, i.e., thunderstorm downbursts and tornadoes. The outline of a framework has been put forth in order to illustrate how these models could be incorporated into a resource, which may be of use to the urban designer.

ACKNOWLEDGEMENTS

The downburst elements of this work arise from research supported through the ESPRC (grant number EP/J008281/1) and as such, the authors would like to express their gratitude for the funding. In addition, the authors would also like to thank Mr Mike Vanderstam for the tireless technical support he has provided during his 40-year career at the University of Birmingham.

REFERENCES

[1] van der Hoven, I., (1957). "Power spectrum of horizontal wind speed in the frequency range from 0.0007 to 900 cycles/h". Journal of Meteorology. 14, 160–164

[2] Baker, C. J (2010) Discussion of The macro-meteorological spectrum – A preliminary study" by R I Harris. Journal of Wind Engineering and Industrial Aerodynamics, 90, 945–947. http://dx.doi.org/10.1016/j.jweia.2009.08.004

[3] Richards, P.J, Hoxey, R.P. and Short, J.L. (2000) Spectral models for the neutral atmospheric surface layer. Journal of Wind Engineering and Industrial Aerodynamics, 87, 167–185 http://dx.doi.org/10.1016/j.jweia.2009.08.004

[4] Lombardo, F T, Smith, D. A., Schroeder, J. L., and Mehta, K. C (2013) "Thunderstorm characteristics of importance to wind engineering". Journal of Wind Engineering and Industrial Aerodynamics. 125, 121-132

[5] Jesson, M., Sterling, M., Letchford, C and Baker, C. J. (2015). Aerodynamic forces on the roofs of low-, mid- and high-rise buildings subject to transient winds. *Journal of Wind Engineering and Industrial Aerodynamics.* Vol 143, August 2015, 42-49. doi: 10.1016/j.jweia.2015.04.020

[6] Haines, M.R., 2015. *The simulation of non-synoptic effects and their implications for engineering structures*. University of Birmingham, UK, Birmingham.

[7] McConville, A.C., Sterling, M., Baker, C.J., 2009. The physical simulation of thunderstorm downbursts using an impinging jet. Wind and Structures. 12, 133–149

[8] Mason, M.S., James, D.L., Letchford, C.W., (2009). Wind pressure measurements on a cube subjected to pulsed impinging jet flow. Wind and Structures 12, 77–88.

[9] Kim, J., Hangan, H., 2007. Numerical simulations of impinging jets with application to downbursts. Journal of Wind Engineering and Industrial Aerodynamics. 95, 279–298. doi:10.1016/j.jweia.2006.07.002

[10] Baker, C.J and Sterling, M (2017). Modelling wind fields and debris flight in tornadoes**.** Submitted to the Journal of Wind Engineering and Industrial Aerodynamics

THE INTERNATIONAL CONFERENCE ON
WIND ENERGY HARVESTING 2017
20-21 April 2017
Coimbra, Portugal

Paper: Keynote

RECENT DEVELOPMENTS OF ANALYSIS AND DESIGN OF FLOATING WIND TURBINES

Torgeir Moan[1]
Norwegian University of Science and Technology (NTNU)
Trondheim, Norway

ABSTRACT

Offshore wind provides an important source of renewable energy. Offshore wind turbines with a monopile support structure fixed to the sea bed in shallow water, have already been industrialized, while fixed turbines in deeper water are emerging and floating wind turbines are still at an early stage of development. Various floating concepts have been proposed for offshore wind application. Wind turbine concepts should be developed in a life cycle perspective – i.e. the design, fabrication/installation and operation. In this paper recent developments of concepts and methods is briefly described followed by a review of design and analysis features relating to the design phase with a focus on design criteria and integrated dynamic analysis under environmental loads. Typical features of their behaviour are also illustrated through some numerical studies.

INTRODUCTION

Increased focus on renewable energy is needed in view of the climate challenges [1-2]. Globally, there is a significant potential for offshore wind energy. Wind power is produced offshore by wind turbines that consist of a rotor, a drivetrain and an electric generator, supported on a tower and a bottom fixed or floating structure. The core unit is the rotor with a drivetrain to the electric generator. Most turbines are horizontal axis with 3 blades, however, 2 bladed rotors are also of interest. Geared drive train is applied to increase the rotational speed from about 10 rpm to 1800 rpm relevant for traditional generators. Alternatively a direct drive, i.e. without gear is applied. The balance between advantages/ disadvantages, in terms of cost is not yet clarified. A significantly different alternative would be to use a vertical axis turbine – with different types of rotors envisaged, using curved or straight blades, see e.g. [3-4]. Various types of vertical axis turbines have been proposed (Fig. 1) but are only commercial in small scale.

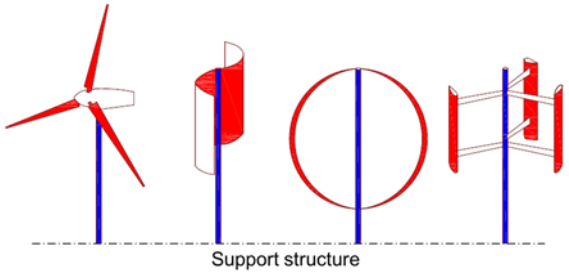

HAWT Savonius- Darrieius- H-type- VAWT

Figure 1. Types of wind turbines. (Courtesy Zhengshun Cheng)

For traditional HAWT with gear transmissions (Fig. 2), the gearbox is among the most expensive components. However, gearbox failure rates are high. Therefore, it is necessary to develop methods to better understand the effects of the dynamic load conditions in the drivetrain components. Since the load effect in the drivetrain is a result of the global performance of the wind turbine system, integrated analysis becomes crucial.

[1] Professor, Department of Marine Technology, NTNU, NO-7491 Trondheim, Norway. Email:tormo@ntnu.no

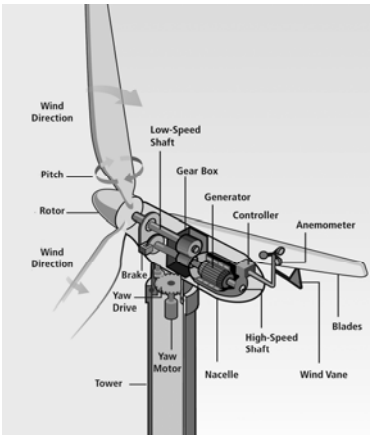

Figure 2. Wind turbine drivetrain for a HAWT (Courtesy NREL).

Up to now, fixed foundations, such as monopile, gravity-base and tripod, are used in offshore wind farms in relatively shallow water, i.e. 10-30 m. Jacket wind turbines have been installed in water depths up to 45 m and will play an important role in the near-future development. In deeper water, say, beyond 80 m, it may be more cost-effective to exploit this energy potential by using floating wind turbines – see Fig. 3. This is because the foundation cost of a fixed wind turbine will increase significantly when the water depth increases, while the cost of a floater is less sensitive to the water depth.

In the last few years, research work about floating wind turbines has been intensified. Proposed concepts mainly have been a spar [5-8], or a semi-submersible [9-14], with catenary, taut or tension leg mooring system. Comparative studies of several types of floating concepts have been presented in [15-19].

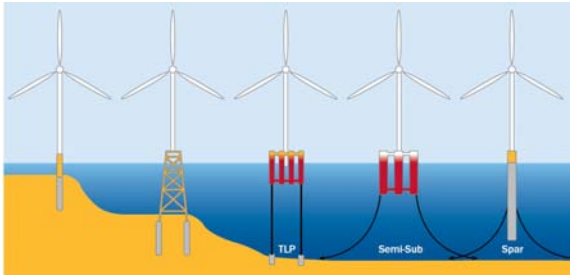

Figure 3. Selected concepts for supporting a horizontal axis wind turbine. (Courtesy: EWEA, 2013)

After being installed, turbines experience operational, shutdown, and parked conditions during their 20-year service life. Moreover, they are exposed to a variety of load conditions that can failure in different modes. Structures supported on the seafloor can experience failure of the structure, foundation or soil, while buoyant structures can experience capsizing or sinking, hull or mooring system failure. In addition the rotor and drivetrain experience various failure modes. While the experienced failure rates for electrical and mechanical components can be of the order of 0.5, large mechanical components/gears/bearings have a failure rate of the order 0.05-0.25 [20]; implying that these components don't reach a 20 years life expectancy. The failure rate of the rotor and tower was estimated by [21] to be of the order of 10^{-1} - $3{\cdot}10^{-3}$ and $7{\cdot}10^{-4}$ - $1{\cdot}10^{-4}$, respectively. Support structures are usually designed to have an even smaller likelihood. Although the failure rate of gearboxes is much lower than that of other subassemblies, gearbox failures contribute to a significant amount of downtime because of the complexity to repair or replace the gearbox [22].

A rational approach for safety assessment should be based on [23]:

- Goal-setting; not prescriptive
- Probabilistic; not deterministic
- First principles; not purely experimental
- Integrated total; not separately
- Balance of safety elements; not hardware

Failure of wind turbines on site normally implies only economic consequences, and not fatalities nor environmental damage. Safety criteria should therefore be decided on a cost benefit basis in economic terms. To make renewable energy from offshore wind more competitive, cost reduction is a crucial issue.

The development of floating wind turbines is still at an early stage and further studies are required to demonstrate which of the concepts is the best one for certain site conditions, i.e. water depth and metocean conditions. This does not only refer to the support structure but also the rotor and drivetrain because the wind turbine facility is a tightly coupled system where the different subsystems interact.

The purpose of this paper is to highlight recent developments of wind turbine concepts, design criteria and methods for integrated dynamic analysis, primarily with respect to the operational phase of floating wind turbines, with an highlight on the effect of fault conditions on blades, tower and hull structure, as well as the performance of the drivetrain in normal operational conditions needed for documenting the design for serviceability and safety. Besides design inspection, monitoring, maintenance and repair during operation is briefly addressed.

METHODOLOGY

General

The International Electrotechnical Commission (IEC) [24] design standard specifies the design requirement for land-based wind turbines and the IEC [25] design standard supplements the design standard [24] with design requirements for bottom-fixed offshore wind turbines. The guidelines and standards from Germanischer Lloyd (GL) and Det Norske Veritas (DNV) are also extensively used [26-27]. For the design of floating wind turbine structures, DNV-JS-103 is one of a very few references to date [28]. Design specifications for wind turbine gearboxes are given in [29]. Current design approaches, especially for the drivetrain, are semi-empirical and based on allowable stress approaches, even with respect to fatigue.

For proper design of the wind turbine rotor, tower, floater and mooring system, dynamic response analysis of the wind turbine to simultaneous action of wind and wave loads needs to be addressed. Different concepts have different dynamic performance, which may influence wind power generation, system design and eventually the cost of power.

Design criteria

Wind turbine systems are in general designed for serviceability and safety. The main serviceability criterion relates to a stable power production. Even if a proper control system can compensate e.g. motions it is relevant to introduce criteria for steady tilt and motions, say of the order of 5-8º. The drift-off and motions may also have to be limited due to the response in the power cable. The tilt and motions responses also have implications on the performance of the drivetrain.

In detailed design for safety, compliance with limit state criteria for ultimate, fatigue and possibly accidental collapse (ALS) criteria should be demonstrated. For floating wind turbines criteria for overall stability as well as ultimate and fatigue strength apply.

Floating structures are normally designed for intact and damage stability corresponding to ULS and ALS criteria. However, since the consequences of failure is only economical, there is a discussion about to which extent ALS and especially damage stability criteria should be satisfied, unless it is decided based on cost-benefit considerations. According to the IEC codes (e.g. IEC61400 series) explicit ULS design checks should be carried out for fault conditions e.g. internal faults due to control system and grid. This is because they occur relatively frequently. Whether ALS checks relating to stability of floating turbines and strength of the structure and mooring system in “low probability” damaged condition (ALS criterion, [23], is still under debate. A cost benefit assessment should anyway be the basis for such a criterion.

While rotor blades, tower and hull structure are designed based on explicit ultimate and fatigue strength criteria and predicted response for the different load cases, simplified empirical safety criteria are applied to the drive train. Sometimes, it is assumed that the simplified design check of the drivetrain is acceptable if the (horizontal) acceleration of the nacelle is limited to 0.3 - 0.6 g (g being the acceleration of gravity). However, the inertia forces (on the rotor) only represent part of the loads acting on the drive train shaft and hence govern the loads in the gear and bearings. The thrust and all the three moments acting on the shaft, as obtained in an integrated global dynamic analysis, should be considered in a limit state design check of the drivetrain mechanical components.

There is clearly a need for further development of rational design criteria for different failure modes, especially for drivetrain components, e.g. based on assessment of load effects by first principles.

Luan et al. [30] describes the design of a 5 MW semi-submersible wind turbine, addressing stability, dynamic behaviour and a simplified ultimate strength check.

Inspection, Monitoring, Maintenance and Repair during Fabrication and In-Service

Inspection and condition monitoring (IM), and, if necessary, maintenance and repair (MR) are important measures for maintaining an adequate safety level, especially with respect to fatigue, wear, corrosion and other

degradation phenomena. The main challenge is concerned with deterioration phenomena, especially crack growth, because the significant dynamic loading. An inspection and repair approach can contribute to the safety only when there is a certain structural damage tolerance. This implies that there is an interrelation between design criteria (fatigue life, damage tolerance) and the inspection and repair criteria [31]. While the initial IMMR plan is made at the design stage, it is updated depending upon findings during inspections.

While inspection and repair strategy serves as basis for ensuring the safety of the hull structure, condition monitoring is important for the drive train, especially based on vibration-based monitoring of the drivetrain [32] (Coronado and Fischer, 2015). Gear-box-oil based CMM is also gaining importance as a complementary system.

Importance of dynamic behaviour

Offshore wind turbines are subjected to dynamic wind and wave loads, possibly ice and seismic loads, as well as rotor loads with a wide range of frequencies.

A wind turbine experiences loads at the rotation frequency of the rotor, denoted 1P (typically 0.12 – 0.2 Hz) and the blade passing frequency of N (number of blades) times the frequency P.

From the aerodynamics point of view, all of the 6-DOF (degrees of freedom) resonant rigid-body motions might be excited, due to a wide range of wind force excitation frequencies. Moreover, the wind turbine loads might excite flexible modes of the tower and blades with natural frequencies of 0.3-1.0 Hz. This is important to consider for structural design of the tower and blades, but does not affect the motions of floating wind turbines. On the other hand, the motions might affect the magnitude of the aerodynamic loads.

First order wave excitation corresponds to frequencies in the range of 0.04 - 0.3 Hz. Moreover, second-order difference-frequency wave forces can excite the resonance of horizontal rigid-body motions (surge, sway and yaw) with typical natural frequencies of 0.005 - 0.02 Hz. Second-order sum-frequency wave forces may excite flexural modes of bottom fixed wind turbines as well as heave, roll and pitch modes with typical natural frequency above 0.2 Hz of tension-leg turbines. For a spar with a single tension-leg excitations occur due to a nonlinear coupling between heave, pitch/roll, surge/sway motions, which leads to excitation at several frequencies.

It is noted that for a spar WT, the natural frequencies of heave and pitch (or roll) motions could be close and the so-called Mathieu instability (e.g. [33-34] might occur. Hence, the design should aim at differentiating the natural frequencies in heave and pitch (or roll). The unsymmetrical aerodynamic forces on the rotor may lead to a large yaw moment.

With a conventional mooring system with radial lines through the center of the spar, the yaw stiffness will be small. However, a delta-configuration adjacent to the spar hull ensures an adequate yaw stiffness and yaw natural frequency.

The pitch/roll natural frequency of a tension-leg WT with a rigid tower may be of the order 0.3 – 0.5 Hz which is usually close to the lowest natural frequency of a flexible tower fixed at the transition to the floater [19, 35-36]. This fact would imply a coupled pitch and flexible tower mode. In such a case it is important to model the tower as a flexible structure.

The natural frequencies of the mechanical drivetrain between the rotor and generator are much higher than the rigid and flexible structure and blade modes which allow the drivetrain responses to be determined in an uncoupled manner.

It is important to consider wind and wave misalignment. For instance resonant yaw motions may occur due to the yaw moment induced by the thrust force when the floater rolls under the wave loads. The dynamic yaw motions of the spar in such conditions are significant. Modelling of aerodynamic damping becomes important in this connection.

Due to the facts described above, it is important to analyze the dynamic responses, especially of floating wind turbines by taking into account the wind and wave loads simultaneously. In other words, a coupled analysis tool is needed, considering aerodynamic and hydrodynamic loads, as well as models of the structure, mooring and drive drain in an integrated analysis. Moreover, automatic control is needed to ensure maximum power at low (below rated) wind speeds; stable power and limited structural responses in the operational conditions.

Integrated dynamic analysis

The response analysis needs to be carried out for different design load cases, (Ch.5 of [4], [25]) which include a variety of design situations such as power production, power production plus occurrence of fault, normal shutdown and parked condition. Some of load cases come from ‘abnormal’ events of the wind turbine such as shutdown, loss of electrical network connection, faults in control system, faults in protection system and so forth [25, 28]. Metocean conditions such as gusts, turbulence and shift in wind direction are also important. Some of these loads imply transient events. The load conditions specified for bottom-fixed wind turbines are taken to be relevant for floating turbines also, but the time-domain analysis for floating wind turbines is much more demanding

because of the low frequency excitations and responses require much longer samples to limit the statistical uncertainty in the simulation.

The response needs to be determined in terms of extreme values for ultimate strength check and response histories for fatigue and wear assessment.

It follows that in order to determine the load effects in the support structure and towers, a model of the whole system, including e.g. the rotor/drivetrain, is needed in order to account for all relevant loads and system features. The integrated dynamic analysis provides load effects in all subsystems, such as the rotor, drivetrain, tower, support structure, mooring or foundation and can serve as a basis for the design of them. Normally, the global analysis can be done with a simplified model of e.g. the drivetrain, while the responses for the design checks of the gears and bearings will be based on a high fidelity model, as illustrated later.

The equations of motion for floating wind turbines are formulated in the time- (TD) or frequency domain (FD), considering wind and wave loads and possibly ice loads.. The advantage of FD methods the computational efficiency and ease of dealing with frequency dependent features, while the disadvantage is the need for linearization of possible nonlinear features, handling transient response effects, and control. Frequency domain analysis of land-based and bottom-fixed offshore turbines have been made e.g in [37]. The applicability of frequency domain methods for floating turbines has been investigated in [36,38] based on separate analysis of wind and wave-induced response but carefully accounting for the aerodynamic damping from the rotor and hydrodynamic damping was included in calculations of the wave motions.

Hydrodynamic loads for slender structures can normally be modelled by using the Morison formula, e.g. [33].

$$F = \frac{1}{2}\rho D C_d v|v| + \frac{1}{4}\rho D^2 C_m a \tag{1}$$

Which expresses the lateral force on a slender member with a diameter D. C_d and C_m are drag and inertia coefficients, respectively and ρ is the water density.

The loads on large volume structures should be estimated by potential theory, considering the incoming and diffracted wave pattern. The hydrodynamic loads on floating structures need to be estimated by simultaneously calculating the motions of the structures. In general potential theory is applied. Both the first- and second-order wave loads due to the difference- and sum-frequency effects need to be considered. In the linear analysis, both the diffraction and radiation effects are addressed, which results in the wave excitation forces and the added mass and potential damping forces, respectively. Second-order difference-frequency wave loads might be calculated using a full quadratic transfer function or based on the Newman's approximation, while a fully quadratic transfer function is normally used for sum-frequency loads. The wave forces on floating structures are in general frequency-dependent. and in the time-domain simulation, they are generated based on a given wave time series.

Viscous effects are normally modelled as drag forces and added to the potential forces. .

In addition particular phenomena, such as wave slamming and ringing loads e.g. on large diameter wind turbines need to be considered. For tension leg structures second order high and low frequency loads as well as (third order) ringing loads should be considered, e.g. [36, 39].

Aerodynamic analysis is especially carried out to determine the wind loads acting on the rotor blades, which is strongly related to both the inflow wind velocity and the induced velocity due to the presence of the rotor. Numerical methods have been developed with different levels of detail, such as Blade Element Momentum (BEM), Geralized Dynamic Wake (GDW) method, vortex method, panel method and Navier-Stokes solver, e.g. [3-4, 40-43]. The BEM method is widely used and often combined with structural analysis tools, e.g. the Finite Element Method (FEM), to obtain the dynamic responses of wind turbine tower and blades, by accounting for aero-elasticity.

Refined methods are particularly relevant to establish or validate simplified methods and partly develop fast simplified methods for design analyses. Examples of the former type of analyses are a) a study of the effect of icing on rotor blades by combining using a CFD and BEM method (e.g. Etemaddar et al. 2014a).

It is also of interest to establish simplified methods especially for use in conceptual studies. An example of a simplified aerodynamic model for the rotor [5, 19, 44] is based on the thrust curve only. This model has been validated by comparing with a comprehensive aero-hydro-servo-elastic approach for two different spar FWTs [44]. It is noted that the computer time for a 1 hour real time simulation is 24 hours and 15 min for the full and the simplified models, respectively.

For VAWTs a variety of aerodynamic models have been developed, including the single streamtube model, multi-streamtube model, Double Multi-Streamtube (DMS) model, Actuator Cylinder (AC) flow model, panel method, vortex method and CFD method [45]. A numerical comparison of these models were conducted in [46, 47].

To model the dynamic behavior of flexible floating bodies, generalized modes for the system may be applied [48-49]. Hydrodynamic loads corresponding to the radiation are evaluated for unit modal response and are

then integrated into the equations of motion where the wave exciting forces are included. Alternatively, the so-called direct method [50] where the hydrodynamic boundary value problem (pressure distribution) and the elastic response are solved simultaneously. Therefore, although the direct method avoids the incorporation of any modes into the solution of response, the method is computationally expensive and requires interfacing between the hydrodynamic and structural numerical techniques such as the boundary element method (BEM) and the FEM.

Typically the time domain approach is based on the linear frequency-domain model which is transformed into the time domain and add nonlinear features. Such a model is referred to as a hybrid frequency- and time-domain model in this context and was initially introduced by Cummins [51]. To date, it has been used successfully in different motion analysis applications, see, e.g. [49, 52-54]. The resulting equation for a stationary rigid structure may be written as:

$$\left[\mathbf{M}+\mathbf{A}^{\infty}\right]\ddot{\mathbf{r}}(t)+\int_0^{t_{mem}}\mathbf{k}(t-\tau)\dot{\mathbf{r}}(\tau)\,d\tau+\mathbf{K}\mathbf{r}(t)=\mathbf{R}(t) \tag{2}$$

$$\mathbf{k}(t)=\frac{2}{\pi}\int_0^{\infty}\left[\mathbf{B}(\omega)-\mathbf{B}^{\infty}\right]\cos(\omega t)\,d\omega \tag{3}$$

where $\mathbf{A}^{\infty},\mathbf{B}^{\infty}$ denote the high-frequency limit of added mass and potential damping, respectively. It is noted that Equation (2) can be reformulated by a set of first order differential equation – and hence reduce the effort in evaluating the convolution integral in the step by step solution of the dynamic equations of motion, e.g. [55]. Since the retardation kernel $\mathbf{k}(t)$ in the integral in Equation (3) vanishes for times passing a certain value, t_{mem}, the integration may be taken to t_{mem} instead of infinity.

One can now add nonlinearities such as viscous drag forces, 'exact body' hydrostatic or Froude-Krylov force, etc., to the rhs of Equation (2).

Wind turbines are obviously also subjected to aerodynamic loads which normally are treated in the time domain, and depend on the relative velocity of the components subjected to aerodynamic loads. Since the velocities of structural parts depend on both the wave and wind loads – there is an interaction between the corresponding load effects.

For rigid floating structures, the buoyancy and mooring lines provide stiffness (restoring), while the water provides added mass, and the water, air and mooring contribute to damping.

The hull of floating wind turbines moored with (soft) catenary mooring lines can normally be considered as a rigid body. However, an elastic finite element model may be useful in order to easily determine the internal forces in the hull for structural design. In particular it is noted that the tower on various floaters (semi-submersible, tension-leg) wind turbines is flexible enough to imply structural dynamic effects, as documented in [35, 38]. Moreover, structural damping needs to be based on empirical data.

The mooring system primarily prevent drift off due to steady wind, wave and current loads and also affect the low frequency excitation due to wind and wave loads. The mooring system does not influence the magnitude of the first order wave induced motions (which however cause mooring tension). Mooring lines could be modelled as nonlinear springs when global responses are determined. More proper FE models of mooring lines including the line dynamics (drag due to lateral forces) should be used when the line tension is estimated.

The drivetrain is obviously a crucial component in a wind turbine system.

When the aerodynamic and hydrodynamic loads are given, the dynamic responses are obtained in the time domain. Coupled mooring analysis might be applied, where the floater motions and the mooring line tension are solved simultaneously.

In response analysis of wind turbines subjected to simultaneous wind and wave loads, conditions with misaligned wind and wave, should be especially considered, partly because such excitations might involve conditions with limited damping.

Automatic Control

The purpose of control systems at the wind farm, turbine, and component levels is to manage the safe, automatic operation of the turbine (Ch. 8 of [3]). In order to respond to environmental changes or changes in the operational condition, the turbine-level controller provides some input to dynamic controllers, such as generator torque or blade pitch controllers. Large horizontal axis wind turbines are normally of pitch-regulated variable speed control (Ch.8.3 of [3], Ch.8.2 of [4]). type to regulate the power output and structural loads. For such systems both the rotor speed and the blade pitch can be varied.

For wind speeds between cut-in and rated speed (typically 3 to 12m/s), the blade pitch is kept constant and the generator torque varies such that the WT operates as close as possible to the optimal tip speed ratio. In this

region, the thrust and torque increase quadratically with wind speed. At the rated wind speed, the wind turbine reaches the rated torque, rotational speed, and thrust. In the above-rated wind speed region, the blade pitch is varied in order to minimize the structural loads and the generator torque is chosen to give the rated power output. Fig. 4a indicates a typical power-wind speed relationship for a turbine with a rated power of 5 MW. Namik and Stol [56]studied individual blade pitch control (IBPC) as an alternative to collective pitch control for FWTs.

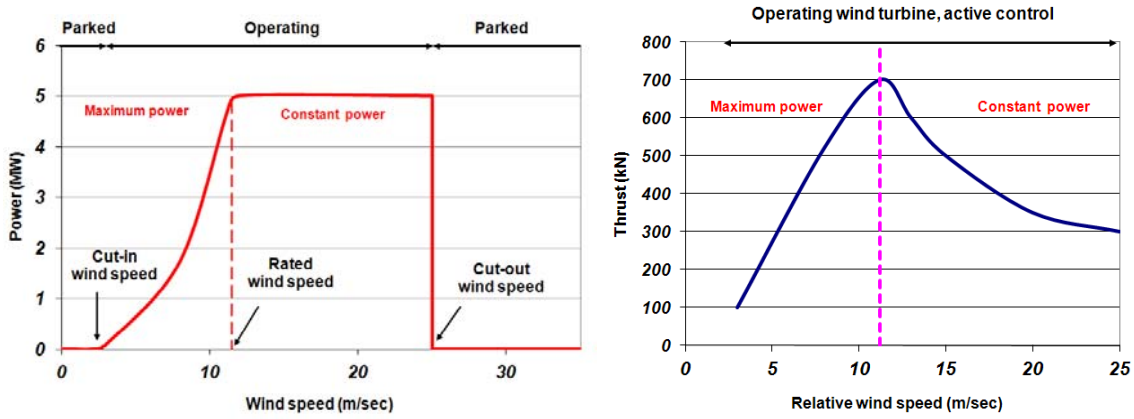

Figure 4. Power (Fig. 4a) and thrust curve (Fig. 4b) of the NREL 5 MW HAWT.

The "large" nacelle motions of FWTs present an additional challenge for the control system. For systems with low-frequency surge or pitch motions, there may be a negative feedback mechanism between the nacelle velocity and the blade pitch controller [57-58], as implied by the negative "damping" at over-rated wind speeds. This feature can be seen as a negative slope of the thrust force with respect to the relative wind speed, as indicated in Fig. 4b.

The initial studies especially focused on spar turbines. Karimirad & Moan [59] addressed this issue for a tension-leg spar system.

For a TLPWT, the platform pitch natural frequency is generally higher than the controller frequency, thus eliminating the need for control system modications in most operating conditions. On the other hand, the surge natural frequency is lower than the control frequency and could theoretically lead to instability [60]. In the studies [35-36, 61-62] the land-based controller was applied to all TLPWTs except in certain studies, particularly related to ringing.

Coupled analysis of floating wind turbines is time consuming. A simplified method, proposed by Statoil (2012), is convenient to apply to model the integrated rotor loads (i.e. the thrust) as a point force on the tower top, especially for spar turbines [19]. It has been shown that this simplified model gives global responses within 10% accuracy compared with the model using the BEM method [44]. However, simplifications and hence the limitations of the method should be observed in [19].

The control strategy for large megawatt VAWTs is somewhat different from that of HAWTs, since large scale VAWTs usually operates with variable rotational speed at a fixed blade pitch angle, and the aerodynamic loads acting on the rotor vary periodically when it rotates [64-65].

So far the control issues relating to normal operational conditions, have been briefly addressed. However, the design standard [24] requires the consideration of control system fault or loss of electrical network. The exact nature of the faults to be analyzed is, however, not specified and needs to be identified by a Failure Mode and Effect Analysis (FMEA).

For pitch-regulated wind turbines, the blade pitch control system contributes significantly to the failure rate [20]. The control system must then recognize the fault and react in some way, typically by shutting down the turbine (by quickly pitching the remaining functional blades to full feather) [66]. While sensor faults were investigated in [67,68], fault cases involving pitch actuator that becomes stuck and grid faults in terms of a short circuit resulting in a complete loss of torque, were considered in [61, 66, 69]. The latter is considered a worst case scenario for grid faults. In this connection it is assumed that the blade pitch control mechanism is still able to function, such that all three blades are pitched to feather shortly after the generator torque is lost. Detection and isolation of faults in drivetrain and rotor blades were investigated in [70] and [71], respectively.

Computational strategy

In the design of wind turbines many load conditions need to be considered to account for the variation in the combined wave and wind conditions, operational versus parked (survival) condition. It is noted that operational conditions include start up and shut down, fault occurrence and emergency shutdown. Hence, the reference is a

so-called long-term analysis, in which results from a set of short term analyses in which the metocean conditions are assumed to be stationary, are combined based on the probability of occurrence of the various short term metocean conditions, e.g. [72]. The long-term variability is accounted for by considering relevant short-term conditions and their probability. While there are methods, like the contour (line) surface to select a sufficient number of short-term conditions to determine extreme load effects, fatigue analysis would generally have to include a large number of short-term conditions. Use of the contour method to determine extreme load effects for wind turbines is illustrated in [73]. Cyclic load histories for fatigue (and possibly wear) design checks normally need to be based on long term analysis.

Analyses also need to be carried out for conceptual or detailed design requiring different degree of refinement. A variety of methods – refined and simplified – is hence desirable for dealing with the aerodynamics, hydrodynamics, structural and possible soil mechanics. In general highly efficient methods are required to accomplish analysis in the early design stages when alternative designs need to be assessed. Hence, simplified mechanics models need to be pursued.

An important issue in connection with the time domain analysis is the discretization of the metocean parameter space (wave height, -period and mean wind speed) which determines the number of simulations that need to be carried out – to determine extremes or fatigue load effects.

The basic integrated dynamic analysis is a short term analysis considering the stochastic nature of waves and turbulence of wind. Since some natural frequencies may be as small as 0.02 Hz a long sample may be needed in a time domain analysis to capture the load effects (motions) due to wind and low frequency hydrodynamic loads. On the other hand the time step needs to be small to capture all phenomena – including high frequency features associated with e.g. a mechanical or hydraulic drivetrain. Jiang et al. [74] found that a stable analysis of a hydraulic drivetrain for a 5 MW wind turbine required time steps of the order of 10-4 s to yield stable numerical solution. In such a case it is clear that uncoupled analysis is necessary.

In the simulation of the load effects in short-term conditions it is important that the sampling time is sufficiently long to limit the statistical uncertainty, especially when determining extreme values. Stress ranges for fatigue analysis essentially depend on the standard deviation of the load effects (at least for a narrow band process) and are less sensitive to the sampling time [75]. Moreover, when estimating extreme values efforts to use realistic methods to fit the sample and then extrapolate to extreme values. Alternative methods, such as Weibull tail, global maxima and a recently proposed extrapolation method (ACER) based on the mean upcrossing rates, can be used for obtaining the extreme values, see e.g. [76].

A full long-term analysis (FLTA) is the most accurate approach to determine the effects due to environmental loads, both in terms of extreme load effects for ULS design check and load effect histories (i.e. stress ranges) for FLS design check [55]. Since the full long-term analysis is time consuming simplified methods such as the environmental contour method (ECM) [77-78] and simplified full long-term analysis (SLTA) [79, 73] have been proposed.

Since wind turbines might experience the maximum load effects when they operate or when they are parked the methodology needs to be modified [80, 81, 73].

SLTA is the same as FLTA except that it only include the important environmental conditions and ignore the others that do not contribute much to the long-term results. It has been studied for offshore structures and wind turbines. For a bottom fixed wind turbine, it is found that less than 10% of all the environmental conditions are required to simulate to achieve practically the same result as the FLTA [73].

Since there is an interaction between the response due to waves and wind, an integrated analysis of wind and wave load effects is in principle desirable, considering simultaneously the two loads in the time domain, with due account of the wind turbine controller.

However, various types of uncoupled analysis are useful in view of the computational efforts involved in a full long term coupled analysis. In particular, uncoupled analysis by first carrying out a global analysis of the system followed by substructure analysis based on input from the global analysis.

Determination of internal forces in the hull structures is possible in some computer codes for special cases; i.e. when the hydrodynamic loads are determined by Morison formula and the structure is modelled as a frame consisting of beams. In general, determination of internal forces in large volume floating wind turbines requires a finite element model of the hull and a potential theory of hydrodynamic loads that account for radiation and diffraction effects. A general time-domain method for determining internal forces in floating wind turbine support structures is presented and applied for a semi-submersible wind turbine in [82].

RESULTS

Various case studies which illustrate the issues highlighted in this paper, have been accomplished at the Centre for Ships and Ocean Structures and recently in the Centre for Autonomous Marine Operations and Systems

at NTNU in Trondheim. Most studies have been made using the NREL GRC 750 kW and the NREL 5 MW HAWT [83]; the DTUWind 10 MW HAWT as well as the Darrieus VAWT [84]. In particular the development of a 3 stage drivetrain with two main bearings for the 5 MW turbine is noted [85]. See also Fig. 5.

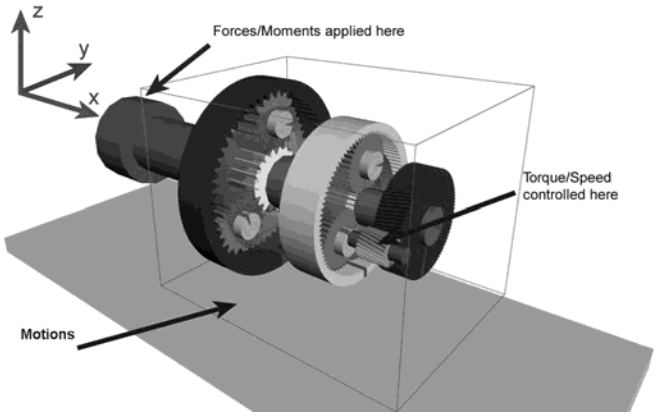

Figure 5. Drivetrain design for a 5 MW turbine [85]

Various support structures, including different versions of monopiles, jackets and spar, semi-submersible and tension-leg floaters as well as land-based towers for reference, have been used in the case studies, partly in comparative studies.

In addition to numerical analysis, full or model scale physical investigations can be used to gain insight into the behaviour of OWTs. Full-scale laboratory tests of components such as generators or blades are more commonly carried out than large scale support structure tests, although support structure data may be collected from demonstration projects at large scale in natural environments; and are crucial due to the limitations of model scale tests; especially of a full wind turbine system involving scaling of hydrodynamic, aerodynamics and elasticity as well as combined with control. However, model tests are useful e.g. for various reasons [86], and especially confirming feasibility of the system, separate validation of hydrodynamics and aerodynamics models under controlled conditions. An example of validation by using model tank testing will be presented in this section.

In this section only examples relating to HAWT are considered. Regarding the performance of VAWT reference is made to [47].

In the following a brief overview of studies related to the behaviour of turbines in fault conditions and the performance of the drive train in various conditions.

Analysis of wind turbine response experiencing fault conditions

Wind turbines are subjected to faults and failures in their lifetime. A vast number of sensors are installed on a modern wind turbine to detect and isolate faults. Faults such as bearing wear or gear tooth wear are hard to detect at early stages, but they may result in a total breakdown of drivetrain [87]. The EU Reliawind project provided wind turbine reliability profiles by analyzing the long-term operational data and fault records of 350 onshore wind turbines [20]. The pitch system has the highest failure rate among the components. Because of this, the contribution of the pitch system fault to downtime is also large. There exist a suite of techniques for fault detection and isolation. Upon the detection of faults, the supervisory controller selects a remedial action based on existing protection strategies. If the fault is controllable, it will be accommodated by techniques such as signal correction and fault tolerant control. If the situation is severe and the turbine is not in a safe state, the supervisory controller brings the turbine to stop. In the worst case, if the main control system fails to stop the turbine safely, the safety system takes over. It normally consists of a hard-wired fail-safe circuit linking a number of normally open relay contacts [4]. If any of the contacts is lost, the safety system trips, causing the appropriate fail-safe actions, to operate. In the present context it is assumed that severe faults are detected and actions to get the turbine is taken. Turbine shutdowns can either be normal or emergency. For emergency shutdown, the common practice is to pitch all blades to feather simultaneously at the maximum pitch rate.

For wind turbines, the change of the aerodynamic loads is the key driver to the dynamic responses of turbines in fault and shutdown conditions.

Design of wind turbines according to IEC 61400 [25] should include considerations of the transient responses caused by faults, e.g. grid loss and blade blockage due to loss of pitch control.

Fig. 6 shows the bottom moment response in the tower of a land based turbine when a blade blockage occurs at the time: 400s. After a time delay of s, an emergency shutdown takes place. The tower bottom bending moment has a change in the mean values during this event. The large negative bending moment is caused by the

aerodynamic forces acting at the tower top during the three-blade shutdown. The first tower fore-aft natural bending frequency can be observed in the shutdown process. Significant main shaft bending moment is caused by the imbalanced load acting on the rotor plane. If one blade is seized and hindered from the normal pitch-to-feather activity, the transient response for both fault cases is seen to be large. Obviously the response would also depend on in which instant it occurs in relative to the steady response.

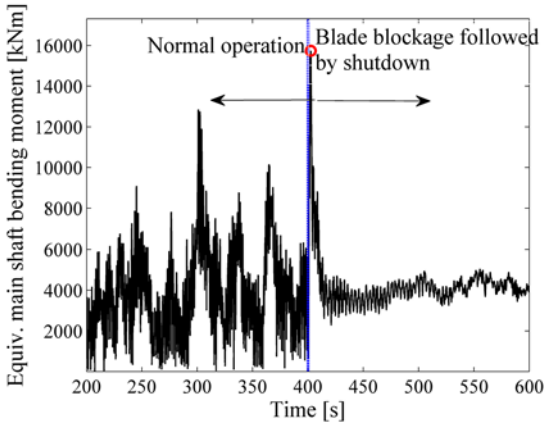

Figure 6. Time series of the structural responses, Uw=17 m/s, TI=0.2 s, Tf=400 s, Td=0.1 s, Pr=8°/s, land-based wind turbine, HAWC2 simulation [88, 89].

In Fig. 7 extreme response in the upper part of the tower, which corresponds to the shaft bending moment, for land-based and floating wind turbines are compared, considering extreme environmental and fault conditions. The metocean conditions are specified in Table 1 and the fault cases A-D are defined as follows:

A) Fault-free: normal power generation in ECs F1-F5 and F7, idling in EC F6 (see Table 1).
B) Blade seize: the pitch actuator of one blade is blocked at time and the turbine continues to operate, with the controller trying to maintain the desired rotational speed by pitching the other two blades.
C) Blade seize followed by shutdown: the pitch actuator of one blade is blocked at time , and the controller reacts by shutting down after detection time .
D) Grid loss followed by shutdown: the grid is disconnected at time , and the controller reacts by shutting down after detection time.

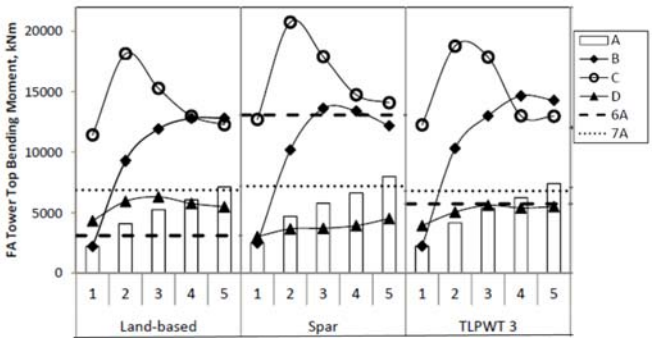

Figure 7. Expected maximum tower top side-side bending moment for all platforms and conditions. F1-5 are shown with bars (A), diamonds (B), open circles (C), and triangles (D). The expected maxima for F6 and F7 for each concept are shown as horizontal lines for comparison [61].

When shutdown occurs, the grid is disconnected and all lades with working actuators are pitched to feather (90º) at the pitch rate PR. In the current work, the pitch rate during shutdown is chosen to be PR = 8 deg/s, the maximum pitch rate suggested in [90]. The pitch rate can have a significant impact on the loads and motions, as studied in [66, 88, 89].

For fault types B, C, and D, the fault occurred after 400 seconds of normal operation. An additional 600 seconds after fault were simulated in order to capture several subsequent cycles of low-frequency events. For fault types C and D with second, which is approximately 10 times the sampling frequency of the controller [61].

Table 1: Metocean/Fault conditions. The wind and wave direction is in the positive x-direction, and the wind speed is reported for the hub height. The NTM and ETM models are applied for Class C.

Condition	F1	F2	F3	F4	F5	F6	F7
H_s (m)	2.5	3.1	3.6	4.2	4.8	14.1	3.1
T_p (sec)	9.8	10.1	10.3	10.5	10.8	13.3	10.1
U (m/sec)	8.0	11.2	14.0	17.0	20.0	49.0	11.2
I	0.17	0.15	0.14	0.13	0.12	0.10	0.24
Faults	A-D	A-D	A-D	A-D	A-D	A	A
Num. Seeds	30	30	30	30	30	6	6
Sim Length (sec)	1000	1000	1000	1000	1000	10800	10800

Drivetrain responses

Global response analyses of wind turbines are generally carried out with a simple model of the drivetrain. In order to shed light on the effect of global responses on the drivetrain a comparative study of the response of a 750 kW drivetrain [91,92] on an onshore and a floating spar turbine (in Fig. 8) has been assessed by [93]. The drivetrain studied is a high speed generator, one stage planetary, two stage parallel and three-point support type. The response analysis is carried out in two steps. First, global aero-hydro-elastic-servo time domain analyses are performed using HAWC2. The main shaft loads are obtained in this integrated wind-wave response analysis. These loads are then used as inputs for the multibody drivetrain time domain analyses in SIMPACK [94], see e.g. [92].

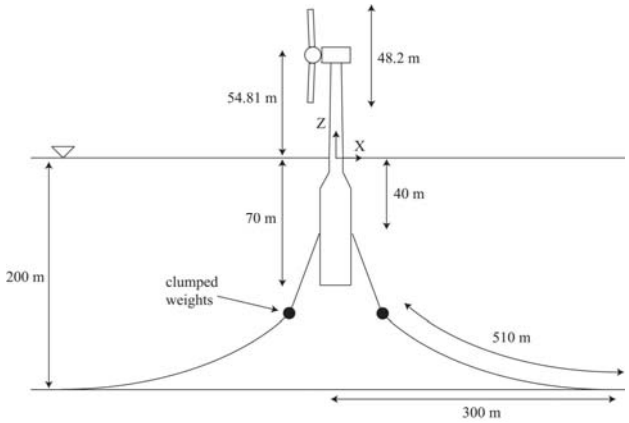

Figure 8. The floating spar support for the 750 kW turbine [93].

Fig. 9 shows the percentage difference in the standard deviations of the shaft loads that have the largest influence on the internal drivetrain responses, for the floating and land-based wind turbines. These differences are largest for the low speed planetary stage, but do also propagate to the intermediate and high speed stage in some load cases. Comparisons of the frequency spectra show that wave-induced responses appear both in the main shaft loads and internal drivetrain response variables. Main shaft non-torque loads are very important in the prediction of accurate internal drivetrain responses, in particular for the bearing loads and gear displacements.

This drivetrain is further studied using an uncoupled model for the drivetrain on a land-based turbine focusing on the contact forces on gear teeth surface and the corresponding fatigue damage [95, 96]. This analysis has been extended to deal with the load effects in the bearings of the drivetrain [97] and the structural reliability of the gear [96].

Moreover, studies have been performed to assess the bearings of the drivetrain [97] and manufacturing imperfections in gears [98].

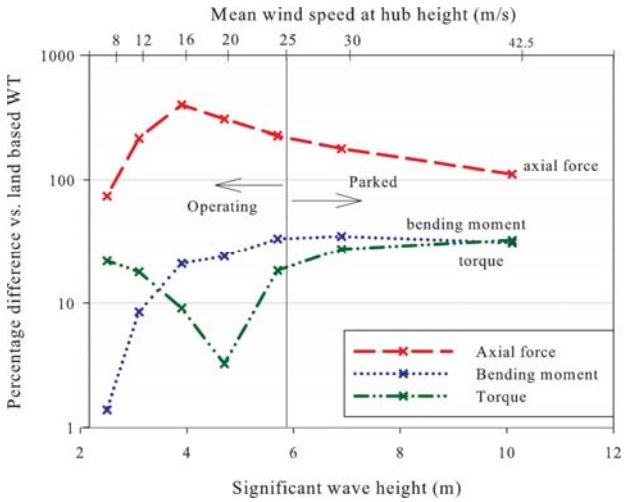

Figure 9. Comparison of the standard deviation of the response of the main shaft in the floating and land based wind turbines [93].

The direct load effect analysis approach relating to drivetrains has been further employed in wind turbine drivetrain maintenance planning and condition monitoring. [99] established a ranking for inspection/monitoring of gear and bearing components based on fatigue damage estimates. A prognostic method for fault detection in wind turbine gearboxes was developed [100], addressing the performance of a 5 MW three stage reference gearbox (Fig. 6) supported by a land-based tower, spar, TLP and two semi-submersible, respectively. The fatigue damage of mechanical components inside the gearbox and main bearings was compared for different environmental conditions.

In the previous section the performance of HAWT under fault conditions was illustrated. The use of the global-local analysis approach may also be used to determine the drive train response in fault conditions [101]. The 5 MW reference gearbox (Fig. 5) was used in this study. This turbine is a pitch-regulated, variable-speed, three-bladed upwind wind turbine. The cut-in, rated, and cut-out wind speed is 3 m/s, 11.4 m/s, and 25 m/s. The drivetrain is a 4-point support drivetrain with two stage planetary and one stage parallel gear system (Fig. 10). Two load cases were analysed: one for normal operation and one in which an actuator fault occurred after 400 s, resulting in a seize of blade 2 (fixing its pitch angle). After 0.1 s an emergency shut-down is initiated by pitching to feather the other two blades at the maximum pitch rate of 8 deg/s. The generator remains disconnected during this period. The results for the wind speed of 14 m/s and the normal turbulence model (NTM) of class A for a land based turbine are presented in this paper.

Novel wind turbine concept combined with wave energy converter

With a rapid development of offshore wind industry and increased research activities on wave energy conversion in recent years, there is an interest in investigating the technological and economical feasibility of combining offshore wind turbines (WTs) with wave energy converters (WECs). In the EU FP7 MARINA Platform project, three floating combined concepts, namely the spar torus combination (STC), the semi-submersible flap combination (SFC) and the oscillating water column (OWC) array with a wind turbine, were selected and studied in detail by numerical and experimental methods. The STC and SFC concepts are shown in Fig. 10a.

The 5-MW-CSC (SFC) concept is a braceless steel semi-submersible platform designed for supporting the 5-MW NREL reference wind turbine at offshore sites with harsh environmental conditions, e.g. the northern North Sea. Numerical analyses show that the 5-MW-CSC has very good intact stability and motion performance. Compared to spar and TLP wind turbines, the semi-submersible design has greater flexibility with respect to water depth and ease of installation. Conventional semi-submersibles consist pontoons and columns that are connected by braces to form an integrated structure. Even though the column-pontoon joints in the novel concept are challenging, it might be a cheaper solution that the multiple tubular joints in a conventional semisubmersible. Moreover, an important aspect of this concept was that it could facilitate a combination of wave energy converters.

The design of the steel 5-MW-CSC, initially inspired the concrete semi-submersible wind turbine concept by Dr.techn.Olav Olsen, is documented in [102, 30]

A 1:50 model test of the combined wind and wave energy converter concept was carried out at ECN, Nantes, see Fig. 10b [103,104]. A 1:30 model test of the wind turbine was carried out in the ocean basin of SINTEF Ocean, using a real-time hybrid model testing approach (ReaTHM^®) was applied. The experimental and numerical

results are compared and used to validate a numerical time-domain approach for determining forces and moments in the structural components of floating wind turbines [105].

The 5-MW-CSC is used as a reference design by researchers and industry to validate numerical and experimental methods to analyse the performance.

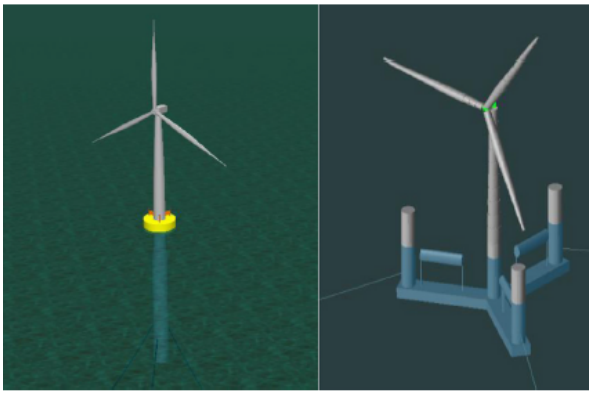

a) Layout: of the STC and SFC concepts

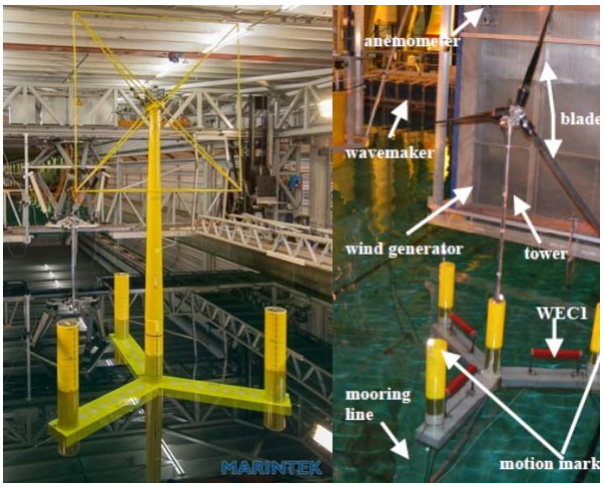

b) 1:30 scalemodel of the wind turbine for the hybrid model testing of the 5-MW-CSC at SINEF Ocean; and the 1:50 model test of the the SFC with three flap-type wave energy converters at ECN, Nantes.

Figure 10 Combined wind turbine and wave energy converters.

The experimental results are compared with numerical analyses in [105]. The paper [106] focuses on validating a time-domain numerical approach for determining internal forces and moments in structural components of floaters. A finite element model is developed to represent global stiffness of the structural components. The external and inertia loads on the structural components are modeled as distributed loads. Hydrodynamic loads on each structural component are obtained by the potential theory. A 1:30 scaled braceless semi-submersible model (the left Fig. 10b) was carried out in the ocean basin of SINTEF Ocean. Measurements of the global forces and moments at the base of a side column of the model and rigid-body motions of the model are compared to the corresponding simulations.

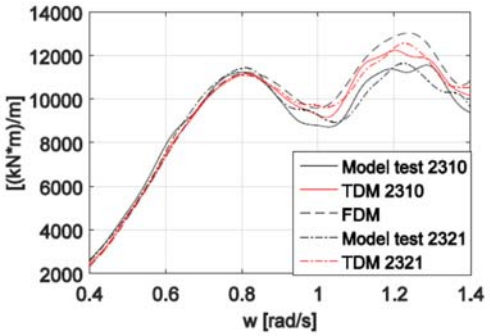

Figure 11 Transfer function for the fore-aft bending moment at the tower base, derived from 1-hour realizations, pink noise, H_s = 2 m (model test 2310) and H_s = 4 m (model test 2321)[106]

Transfer functions for the wave-induced bending moment in the column base are obtained from 1-hour measurements of the pink noise model tests, i.e. model tests 2310 and 2321, and the corresponding simulations. Reasonable good agreement between the RAOs of the experimental and numerical models is observed, as shown in Fig. 11. The frequency domain method (FDM) gives the transfer functions in a straight forward manner and is used as a reference model. In the comparisons we focus on frequency range from 0.4 rad/s to 1.4 rad/s where the major wave energy of the pink noise model tests is distributed. Comparisons for more severe conditions will be made in a future paper.

CONCLUSIONS

Floating wind turbines are expected to play an increasing role in harvesting the abundant wind energy resources offshore, when the wind industry moves into water depths, say, beyond 80 m. This paper deals with recent developments of analysis and design of floating wind turbines.

The need for carrying out an integrated dynamic analysis as a basis for design, is highlighted, based on a proper hydro-, aero-, servo-elastic model. At the same time simplified models need to be developed to provide efficiency in design analyses. For instance, a simplified aerodynamic model is shown to be two orders of magnitude faster than the full aerodynamic analysis and hence suitable for conceptual studies of global behaviour of the support structure/tower. However, its limitations regarding assessment of the response of the rotor and drivetrain, should be observed.

It is important to have a controller to avoid the 'negative damping' effect from the thrust force for wind speeds larger than the rated one and thus limit the pitch motion for the spar wind turbine. The effect of such a controller on the pitch motions of the semi-submersible or the tension-leg wind turbine, is small.

The need to do a fully coupled global analysis especially for large turbines is recognized. The results from such an analysis can serve as input to a detailed analysis of the crucial subsystem of the wind turbine, namely the drive train, to keep computational efforts at a reasonable level. Such an uncoupled analysis is feasible if the natural frequencies in the global and local systems are sufficiently far apart.

The effect of pitch control and grid faults has been investigated and it is shown that such conditions could be governing in the ultimate limit state design checks.

It is shown that a drivetrain supported by a floating support structure mightl have larger response than the land-based one, and especially a larger standard deviation, and should be further pursued in the context of more rational design of drivetrains based on direct load effect analysis.

Due to the possible significant response in the drive train caused by faults, more work needs to be carried out in the future to establish relevant fault conditions for floating wind turbines and estimate their effect on the response and hence, the turbine design. More efforts should also be devoted to fatigue analysis and design of floating wind turbines.

ACKNOWLEDGEMENTS

The author wishes to acknowledge the support from the Research Council of Norway through Centre for Ships and Ocean Structures (CeSOS) and the Centre for Autonomous Marine Operations and Systems (AMOS), Norwegian University of Science and Technology.

REFERENCES

[1] IEA 2012. "Energy Technology Perspectives 2012-Pathways to a Clean Energy System", ISBN 978-92-64-17488-7, IEA Publications, 2012.

[2] IPCC 2011. "IPCC Special Report on Renewable Energy Sources and Climate Change Mitigation. Prepared by Working Group III of IPCC". Cambridge University Press, Cambridge, United Kingdom and New York, NY, USA, 2011.

[3] Manwell, J., McGowan, J. G., &Rogers, A. L., "Wind Energy Explained". John Wiley & Sons, Ltd., 2009.

[4] Burton, T., Jenkins, N., Sharpe, D., & Bossanyi, E., "Wind Energy Handbook". Chishester:John Wiley & Sons Ltd., 2011.

[5] Nielsen, F.G., Hansen, T.D. & Skaare, B., "Integrated Dynamic Analysis of Floating Offshore Wind Turbines", Proc. EWEC Conf., 2006, Athens, Greece.

[6] Karimirad, M. & Moan, T., "Extreme dynamic structural response analysis of catenary moored spar wind turbine in harsh environmental conditions", J. OMAE, Vol. 133, No. 4, 2011, pp. 0411031.

[7] Muliawan, M.J., Karimirad, M., Moan, T. & Gao, Z., "STC (Spar-Torus Combination): A Combined Spar-Type Floating Wind Turbine and Large Point Absorber Floating Wave Energy Converter – Promising and Challenging", Proc. 31st OMAE Conf., 2012, Rio de Janeiro, Brazil.

[8] Muliawan, M.J., Karimirad, M. & Moan, T., "Dynamic Response and Power Performance of a Combined Spar-Type Floating Wind Turbine with Large Point Absorber Floating Wave Energy Converter", Renewable Energy, Vol. 50, 2013, pp. 47-57.

[9] Henderson, A.R. & Patel, M.H., "Floating Offshore Wind Energy", Proc. OMAE Conf., 1998.

[10] Withee, J.E. & Sclavounos, P.D., "Fully Coupled Dynamic Analysis of a Floating Wind Turbine System", Proc. 8th World Renewable Energy Congress, 2004, Denver, USA.
[11] Suzuki, H., Yamaguchi, H., Akase, M., Nakada, S. & Imakita, A., "Development of TLP Type Floating Structure for Offshore Wind Farms", Technology Report of Mitsui Engineering and Shipbuilding Co. Ltd., 2009 (in Japanese).
[12] Roddier, D., Cermelli, C. & Weinstein, A., "Windfloat: A floating foundation for offshore wind turbines; Part I: Design basis and qualication process", Proc. 28th OMAE Conf., 2009, Honolulu, Hawaii, USA.
[13] Roddier, D., Peiffer, A., Aubault, A. & Weinstein, J., "A Generic 5 MW WindFloat for Numerical Tool Validation & Comparison against a Generic Spar", Proc. 30th OMAE Conf., 2011, Rotterdam, Netherlands.
[14] Myhr, A., Maus, K. J. & Nygaard, T. A., "Experimental and computational comparisons of the OC3-HYWIND and tensionleg-buoy (TLB) floating wind turbine conceptual designs", Proc. 21st ISOPE Conf., 2011, Maui, Hawaii, USA.
[15] Butterfield, S., Musial, W., Jonkman, J. & Sclavounos, P., "Engineering challenges for floating offshore wind turbines", Technical report NREL/CP-500-38776, 2007, National Renewable Energy Laboratory, CO, USA.
[16] Matsukuma, H. & Utsunomiya, T., "Motion Analysis of a Floating Offshore Wind Turbine Considering Rotor-Rotation", The IES Journal Part A: Civil and Structural Engineering, Vol. 1, No. 4, 2008, pp. 268-279.
[17] Jonkman, J.M. & Matha, D., "Dynamics of offshore floating wind turbines–analysis of three concepts", Wind Energy, Vol. 14, No. 4, 2011, pp. 557–569.
[18] Robertson, A.N. & Jonkman, J.M., "Loads analysis of several offshore floating wind turbine concepts", In Proc. 21st ISOPE Conf., 2011, Maui, Hawaii, USA.
[19] Gao, Z., Luan, C., Moan, T., Skaare, B., Solberg, T., Lygren, J.E., "Comparative Study of Wind- and Wave-Induced Dynamic Responses of Three Floating Wind Turbines Supported by Spar, Semi-Submersible and Tension-Leg Floaters", Proc. ICOWEOE Conference, 2011, Beijing.
[20] Wilkinson, M., Harmann, K., Spinato, F., Hendriks, B. & van Delft, T., "Measuring wind turbine reliability - results of the reliawind project". In European Wind Energy Conference (EWEA 2011), 2011, Brussels, Belgium.
[21] Robinson, C.M.E., Paramasivam, E.S.,Taylor, E.A., Morrison, A.J.T. & Sanderson, E.D., "Study and development of a methodology for the estimation of the risk and harm to persons from wind turbines", Health and Safety Executive, RR968 Research Report, 2013, UK.
[22] Spinato, F., Tavner, P.J., van Bussel, G.J.W. & Koutoulakos, E. "Reliability of wind turbine subassemblies", Renewable Power Generation, IET, Vol. 3, No. 4, 2009, pp. 387–401.
[23] Moan, T., "Safety of Offshore Structures", Keynote lecture, Offshore Structural Reliability Conference, 2014, Houston, USA.
[24] IEC 61400-1, "61400-1 wind turbine. part 1: Design requirements", 3rd ed. 2007, Geneva, Switzerland.
[25] IEC 61400-3. "61400-3 wind turbines. part 3: Design requirements for offshore wind turbines". 3rd ed. 2009, Geneva, Switzerland.
[26] GL, "Guideline for the certification of Wind Turbines", 2010, Germanischer Lloyd, Hamburg, Germany.
[27] DNV, "Design of Offshore Wind Turbine Structures", DNV-OS-J101, 2014.
[28] DNV, "Design of Floating Wind Turbine Structures", DNV-OS-J103, 2013.
[29] IEC 61400-4. "61400-4 wind turbines. part 4: Design requirements for wind turbine gearboxes", 1st ed. 2012, Geneva, Switzerland.
[30] Luan, C., Gao, Z. & Moan, T., "Design and Analysis of a Braceless Steel 5 MW semi-submersible wind turbine", Proc. OMAE Conference, 2016, Pusan, Korea.
[31] Moan, T., "Reliability-based management of inspection, maintenance and repair of offshore structures", Structure and Infrastructure Engineering, Vol. 1, No. 1, 2005, pp. 33 – 62.
[32] Coronado, D. and Fischer, K., "Condition Monitoring of Wind Turbines: State of the Art, User Experience and Recommendations", 2015, Fraunhofer, IWES, Bremerhafen.
[33] Faltinsen, O.M., "Sea Loads on Ships and Offshore Structures", Cambridge University Press, 1990, UK.
[34] Koo, B.J., Kim, M.H. & Randall, M., "Instability of a Spar Platform with Mooring and Risers". Ocean Engineering, Vol. 31, No. 17-18, 2004, pp. 2175-2208.
[35] Bachynski, E.E. & Moan, T., "Design considerations for tension leg platform wind turbines", Marine Structures Vol. 29, No. 1, 2012, pp. 89–114.
[36] Bachynski, E.E. & Moan, T., "Linear and Nonlinear Analysis of Tension Leg Platform Wind Turbines", Proc. ISOPE Conf., 2012, Rhodes, Greece.

[37] Van der Tempel, J., "Design of support structures for offshore wind turbines". PhD thesis, 2006, University of Technology, Delft.
[38] Kvittem, M.I. & Moan, T., "Frequency versus time domain fatigue analysis of a semi-submersible wind turbine tower". J. of OMAE, Vol. 137, No. 1, 2015, pp. 011901.
[39] Bachynski, E.E. & Moan, T., "Ringing loads on tension leg platform wind turbines", Ocean Engineering, Vol. 84, 2014, pp. 237–248.
[40] Hansen, M.O.L., "Aerodynamics of Wind Turbines", 2nd Ed. 2008, London, Earthscan, UK.
[41] Hansen, M.O.L., Sorensen, J.N., Voutsinas,S., Sorensen, N. & Madsen, H.A., "State of the Art in Wind Turbine Aerodynamics and Aeroelasticity", Progress in Aerospace Sciences, Vol. 42, No. 4, 2006, pp. 285-330.
[42] FLUENT. "Theory Guide", ANSYS R.13, 2010.
[43] Hansen, M.O.L. & Madsen, H.A., "Review paper on wind turbine aerodynamics", Journal of Fluids Engineering, Vol. 133, No. 11, 2011, pp.114001.
[44] Karimirad, M. & Moan, T., "A Simplified Method for Coupled Analysis of Floating Offshore Wind Turbines". Marine Structures, Vol. 27, No. 1, 2012, pp. 45-63.
[45] Borg, M., Shires, A., Collu, M., "Offshore floating vertical axis wind turbines, dynamics modelling state of the art. part I: Aerodynamics", Renewable & Sustainable Energy Reviews, Vol. 39, 2014, pp. 1214-1225.
[46] Ferreira, C.S., Madsen, H.A., Barone, M., Roscher, B., Deglaire, P., Arduin, I., "Comparison of aerodynamic models for vertical axis wind turbines", Journal of Physics: Conference Series Vol. 524, No. 1, 2014, pp. 012125.
[47] Cheng, Z., Moan,T. and Gao, Z., "Dynamic Response Analysis of Floating Wind Turbines with Emphasis on Vertical Axis Rotors", MARE-WINT. Springer International Publishing, 2016.
[48] Newman, J.N., "Wave effects on deformable bodies", Applied Ocean Research, Vol. 16, No. 1, 1994, pp. 47–59.
[49] Kashiwagi, M., "Transient response of a VLFS during landing and take-off of an airplane", Journal of Marine Science and Technology", Vol. 9, 2004, pp.14–23.
[50] Yasuzawa,Y., Kagawa,K., Kawano, D. & Kitabayashi, K., "Dynamic response of a large flexible floating structure in regular waves". Proc. 16th OMAE Conf., 1997, New Orleans, USA.
[51] Cummins,W.E., "The impulse response function and ship motions", Schifftechnik Vol. 47, No. 9, 1962, pp. 101–109.
[52] Wu, M.K. & Moan, T., "Linear and Nonlinear Hydroelastic Analysis of High Speed Vessels", J. Ship Research, Vol. 40, No. 2, 1996, pp.149–163.
[53] Taghipour, R., Perez, T. & Moan, T., "Hybrid frequency-time domain models for dynamic response analysis of marine structures". Ocean Engineering, Vol. 35, 2008, pp. 685-705.
[54] Taghipour, R., Perez,T. & Moan,T., "Time-Domain Hydroelastic Analysis of a Flexible Marine Structure Using State-Space Models", J. OMAE , Vol. 131, No. 1, 2009, pp. 011603.
[55] Naess, A. & Moan, T., "Stochastic Dynamics of Marine Structures". Cambridge University Press, 2013.
[56] Namik, H. & Stol, K., "Performance analysis of individual blade pitch control of offshore wind turbines on two floating platforms", Mechatronics, Vol. 21, No. 4, 2011, pp. 691-703.
[57] Larsen, T. J., & Hanson, T. D., "A method to avoid negative damped low frequent tower vibrations for a floating, pitch controlled wind turbine", Journal of Physics Conf. Series, Vol. 75, No. 1, 2007.
[58] Skaare, B., Hanson, T. D., Nielsen, F. G., Yttervik, R., Hansen, A. M., "Thomsen, K. & Larsen, T. J., "Integrated dynamic analysis of floating offshore wind turbines", European Wind Energy Conference and Exhibition, 2007.
[59] Karimirad M. & Moan T., "Ameliorating the Negative Damping in the Dynamic Responses of a Tension Leg Spar-Type Support Structure with a Downwind Turbine", Sci. proc. the European Wind Energy Conference (EWEC2011), 2011, Brussels, Belgium.
[60] Matha, D., "Model development and loads analysis of an offshore wind turbine on a tension leg platform, with a comparison to other floating turbine concepts". MSc thesis, 2009, University of Colorado-Boulder.
[61] Bachynski, E.E., Etemaddar, M., Kvittem, M.I., Luan, C. & Moan, T., "Dynamic analysis of floating wind turbines during pitch actuator fault, grid loss, and shutdown", Energy Procedia, Vol. 35, 2013. pp. 210–222.
[62] Bachynski, E.E., Kvittem, M.I., Luan, C. & Moan, T., "Wind-wave misalignment effects on floating wind turbines: Motions and tower load effects", J. OMAE, Vol. 136, No. 4, 2014, pp.041902.
[63] Statoil, "Priv. communication with the Wind Turbine Group", 2012, Bergen, Norway.
[64] Merz, K.O., Svendsen, H.G., "A control algorithm for the deepwind floating vertical-axis wind turbine", Journal of Renewable and Sustainable Energy, Vol. 5, No. 6, 2013, pp. 063136.

[65] Cheng, Z., Madsen, H.A., Gao, Z., Moan, T., "A fully coupled method for numerical modeling and dynamic analysis of floating vertical axis wind turbines", Renewable Energy, Vol. 107, 2017, pp. 604-619.
[66] Jiang, Z., Karimirad, M. & Moan. T., "Dynamic response analysis of wind turbines under blade pitch system fault, grid loss, and shutdown events", Wind Energy, Vol. 17, 2014, pp. 1385–1409.
[67] Etemaddar, M., Gao, Z., & Moan, T., "Structural load analysis of a wind turbine under pitch actuator and controller faults", Journal of Physics: Conference Series, Vol. 555, 2014, pp. 012034.
[68] Etemaddar, M., Blanke, M., Gao, Z. & Moan, T., "Response analysis and comparison of a spar type and a land-based wind turbine under blade pitch controller faults", Wind Energy, Vol. 19, 2016, pp. 35-50.
[69] Jiang, Z., Xing, Y., Dong, W., Moan, T. & Gao, Z., "Long-term probability distribution of wind turbine planet roller bearing loads". In WINDPOWER 2013 Conference & Exhibition, 2013, Chicago, USA.
[70] Ghane, M., Rasekhi Nejad, A., Blanke, M., Gao, Z. and Moan, T., "Condition monitoring of spar-type floating wind turbine drivetrain using statistical fault diagnosis", submitted to J. Wind Energy, 2017.
[71] Cho, S., Gao, Z. and Moan, T. "Model-based fault detection of blade pitch system in floating wind turbines", Journal of Physics, Conference Series, Vol. 753, 2016.
[72] Li, L., Gao, Z. & T. Moan,T., "Joint Environmental Data at Five European Offshore Sites for Design of Combined Wind and Wave Energy Devices", Proc. OMAE Conf., 2013Nantes, France.
[73] Li, Q.; Gao, Z.; Moan, T., "Modified Environmental Contour Method for Predicting Long-term Extreme Responses of Bottom-fixed Offshore Wind Turbines", Marine Structures, Vol. 48, 2016, pp. 15-32
[74] Jiang, Z., Yang, L., Gao, Z. & Moan, T., "Numerical simulation of a wind turbine with a hydraulic transmission system", Energy Procedia, Vol 53, 2014, pp. 44-55.
[75] Kvittem, M.I. & Moan, T., "Time domain analysis procedures for fatigue assessment of a semi-submersible wind turbine", Marine Structures, Vol. 40, 2015, pp. 38-59.
[76] Saha, N., Gao, Z., Moan, T. & Naess, A. "Short-Term Extreme Response Analysis of a Jacket Supporting an Offshore Wind Turbine", Wind Energy, Vol. 17, No. 1, 2014, pp. 87-104.
[77] Haver, S., and Winterstein, S., "Environmental contour lines: A method for estimating long term extremes by a short term analysis", Transactions, Society of Naval Architects and Marine Engineers, Vol. 116, 2009, pp. 116–127.
[78] Winterstein, S., Ude, T., Cornell, C., Bjerager, P., and Haver, S., "Environmental parameters for extreme response: Inverse form with omission factors", In Proceedings of 6th International Conference on Structural Safety and Reliability, 1993.
[79] Videiro, P. M., and Moan, T., "Efficient evaluation of long-term distributions". In Proceedings of the 18th International Conference on Offshore Mechanics and Arctic Engineering, 1999.
[80] Saranyasoontorn, K., and Manuel, L., "On assessing the accuracy of offshore wind turbine reliability-based design loads from the environmental contour method", In International Society of Offshore and Polar Engineers, Vol. 1, 2004, pp. 128–135.
[81] Agarwal, P., and Manuel, L., "Simulation of offshore wind turbine response for long-term extreme load prediction". Engineering Structures, Vol. 31, No.10, 2009, pp. 2236 – 2246.
[82] Luan, C., Gao, Z. and Moan, T., "Development and verification of a time-domain approach for determining forces and moments in structural components of floaters with an application to floating wind turbines". Marine Structures. Vol. 5, 2017, pp. 87-109.
[83] Jonkman, J.M., Butterfield, S., Musial, W. & Scott, G., "Definition of a 5-MW reference wind turbine for offshore system development", Technical report NREL-TP-500-38060, 2009, NREL,CO, USA.
[84] Paraschivoiu, I., "Wind turbine design: with emphasis on Darrieus concept", Montreal Polytechnic International Press, 2002.
[85] Nejad A.R., Guo Y., Gao Z. & Moan T., "Definition of a 5 MW reference gearbox for offshore wind turbine development", Wind Energy, Vol. 19, No. 6, 2015, pp. 1089-1106.
[86] Nielsen, F.G., "Experts' Meeting on Computer Code Validation for Offshore Wind System Modeling", 2012, Boulder, CO, USA.
[87] Odgaard, P.F., Stoustrup, J. & Kinnaert, M., "Fault tolerant control of wind turbines - a benchmark model", In the 7th IFAC Symposium on Fault Detection, Supervision and Safety of Technical Processes, 2009, Barcelona, Spain, pp. 155-160.
[88] Jiang, Z., Moan, T., Gao, Z. & Karimirad, M., "Effect of shut-down procedures on dynamic responses of a spar-type floating wind turbine", Proc. of the 32nd OMAE, 2013, Nantes, France.
[89] Jiang, Z., Moan, T. & Gao, Z., "A comparative study of shutdown procedures on the dynamic responses of wind turbines", J. Offshore Mech. Arct. Eng, Vol. 137, No.1, 2015, pp. 011904.

[90] Jonkman, J.M. & Musial, W., "Final Report – Subtask 2 - The Offshore Code Comparison Collaboration (OC3)", IEA Wind Task 23 - Offshore Wind Technology and Deployment, 2010.
[91] Oyaque, F., "Gearbox reliability collaborative (GRC) description and loading", Technical report NREL/TP-5000-47773, 2009, National Renewable Energy Laboratory, CO, USA.
[92] Xing, Y. & Moan, T., "Multi-body modelling and analysis of a planet carrier in a wind turbine gearbox", Wind Energy, Vol. 16, No. 7, 2013, pp. 1067–1089.
[93] Xing, Y., Karimirad, M. & Moan, T., "Modelling and analysis of floating spar-type wind turbine drivetrain", Wind Energy, Vol. 17, No. 4, 2014, pp. 565–587.
[94] Rulka, W., "SIMPACK-a computer program for simulation of large-motion multibody systems", Multibody System Handbook. Springer-Verlag Inc., 1990, New York, USA.
[95] Dong, W., Xing, Y., Moan, T. & Gao, Z., "Time domain-based gear contact fatigue analysis of a wind turbine drivetrain under dynamic conditions", I.J. of Fatigue, Vol. 48, 2012, pp. 133–146.
[96] Nejad A.R., Gao Z. & Moan T., "On long-term fatigue damage and reliability analysis of gears under wind loads in offshore wind turbine drivetrains", I.J. of Fatigue, Vol. 61, 2014, pp. 116–128.
[97] Jiang, Z., Xing, Y., Guo, Y., Moan, T. & Gao, Z., "Long-term contact fatigue analysis of a planetary bearing in a land-based wind turbine drivetrain", Wind Energy, Vol. 18, No. 4, 2014, pp. 591-611.
[98] Nejad A. R., Xing Y., Guo Y., Keller J., Gao, Z. & Moan T., "Effects of floating sun gear in a wind turbine's planetary gearbox with geometrical imperfections", Wind Energy, Vol. 18, No. 12, 2015, pp. 2105-2120.
[99] Nejad A.R., Gao Z. & Moan T., "Fatigue reliability-based inspection and maintenance planning of gearbox components in wind turbine drivetrains", Energy Procedia, Vol. 53, 2014, pp. 248–257.
[100] Nejad, A. R., Odgaard, P. F., Gao, Z. & Moan, T., "A prognostic method for fault detection in wind turbine drivetrains", Engineering Failure Analysis, Vol. 42, 2014, 324-336.
[101] Nejad, A.R., Jiang,Z., Gao,Z. and Moan, T., "Drivetrain load effect in a 5 MW wind turbine under blade-pitch fault condition and emergency shutdown", J. Phys.: Conf. Ser., Vol. 753, 2016, pp. 112011.
[102] Luan, C., Michailides, C., Gao, Z., and Moan, T., "Modeling and analysis of a 5 MW semi-submersible wind turbine combined with three flap-type wave energy converters", In 33th International Conference on Ocean, Offshore and Arctic Engineering, 2014, San Francisco, USA.
[103] Michailidis, C., Gao, Z., and Moan, T., "Experimental and numerical study of the response of the offshore combined wind/wave energy concept SFC in extreme environmental conditions". Marine Structures. Vol. 50, 2016, pp. 35-54.
[104] Michailidis, C., Gao, Z., Moan, T., "Experimental study of the functionality of a semisubmersible wind turbine combined with flap-type Wave Energy Converters". Renewable Energy, Vol. 93, 2016, pp. 675-690.
[105] Berthelsen, P. A., Bachynski, E. E., Karimirad, M., and Thys, M., "Real-time hybrid model testing of a braceless semi-submersible wind turbine. Part III: Calibration of a numerical model", In 35th International Conference on Ocean, Offshore and Arctic Engineering, 2016.
[106] Luan, C., Chabaud, V., Bachynski, E., Gao, Z., and Moan, T., "Experimental validation of a time-domain approach for determining forces and moments in a floating wind turbine subjected to pink noise waves". Submitted to Energy Procedia, 2017.

THE INTERNATIONAL CONFERENCE ON
WIND ENERGY HARVESTING 2017
20-21 April 2017
Coimbra, Portugal

Paper keynote

URBAN WIND ENERGY: POTENTIAL AND CHALLENGES

Ted Stathopoulos
Concordia University
Montreal, Canada

ABSTRACT

Urban wind energy consists of the utilization of wind energy technology in applications to the urban and suburban built environment. The paper highlights some of the progress made recently in the areas of quantification of wind resources available in the urban habitat; the utilization of suitable wind turbines for the enhancement of exploiting these resources; and the significant role of the application of building and urban aerodynamics concepts towards an optimal arrangement of interfacing augmented wind with its extraction mechanisms.

ACKNOWLEDGMENT

There are several graduate students and researchers contributed to the research work and concepts presented in this paper, who should be acknowledged properly. Here is a list in alphabetical order: Hatem Alrawashdeh, Ayman Al-Quraan, Bert Blocken, Aierken Dilimulati, Marius Paraschivoiu and Pragasen Pilay. Financial support from the Natural Sciences and Engineering Research Council of Canada (NSERC) is also greatly appreciated.

1. INTRODUCTION

Wind has been used by human beings as an energy source since a very long time ago. The power of wind was used to sail ships, to mill grain and to pump water, or both. Wind power is currently considered as a friendly alternative to fossil fuels, this is because it is renewable, widely distributed, clean with no greenhouse gas emissions produced during operation. In most cases, the energy of the wind is harnessed through constructing large wind-power plants to supply economical clean power. However, in urban and suburban areas, the land is limited and this is considered a major restriction for the installation of large plants. An alternative option is to construct building-integrated energy systems. Figure 1 shows the Bahrain World Trade Center Towers, where three wind turbines facing the predominant wind direction are suspended on bridges between the two towers of the center.

Figure 1: Urban Wind Turbines: Bahrain World Trade Center Towers.
(https://commons.wikimedia.org/wiki/File:Bahrain_World_Trade_Center.jpg?uselang&equal;nl)

Urban wind energy generation such as that produced by small-scale wind turbines installed on or around buildings can be defined as micro-generation. There is a growing interest in the use of wind power in buildings for distributed generation. Since the generated power is a function of the cube of the wind speed, a small increase in the wind speed leads to a large difference in wind power generation. Therefore, it is to our interest to assess properly the wind resource in an area and attempt to enhance it by using various aerodynamics techniques. This is contrary to the traditional wind engineering approach where the focus is in reducing wind speeds and pressures to minimize wind-induced building loads and contribute to the economy of a safe building design.

2. ESTIMATON OF WIND SPEEDS ON AN URBAN LOCATION

The prediction of the wind speed in the built environment is difficult, due to the varying roughness and the frictional effects which reduce the wind speed close to the ground. In addition, several adjacent buildings influence the wind regime around a specific building in the urban environment. The most dependable method for the wind assessment in the urban environment is to directly measure the wind speed, ideally at the position and the height of the proposed wind turbine. However, measuring the wind speed at a site is both time consuming and expensive, i.e. normally not appropriate for the early stages of wind power development. Fortunately, several methods are available for the initial assessment of wind resource in urban areas, with varying degrees of resolution and accuracy. These are, in order of increasing accuracy, wind atlases, wind tunnel modeling and direct wind resource measurement (European Commission, 2007).

Recent research by Al-Quraan et al (2016) has provided evidence that appropriate utilization of atmospheric boundary layer wind tunnel technology can provide an excellent methodology to assess realistic estimates of urban wind energy potential within reasonable accuracy. Two actual building cases in Montreal with different upstream roughness homogeneity were considered. Figure 2 shows these two cases along with a part of the corresponding wind tunnel model.

In the first case, field wind speed measurements are used to evaluate the wind energy potential for the EV building of Concordia University, a building with upstream rather homogeneous urban/suburban type of terrain – see Figure 2 (a). In the second case, the Equiterre building upstream terrain is very rough and highly inhomogeneous – see Figure 2 (b).

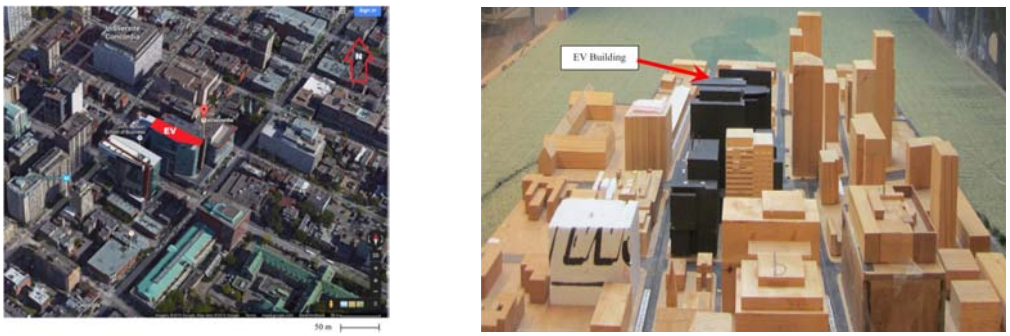

(a)

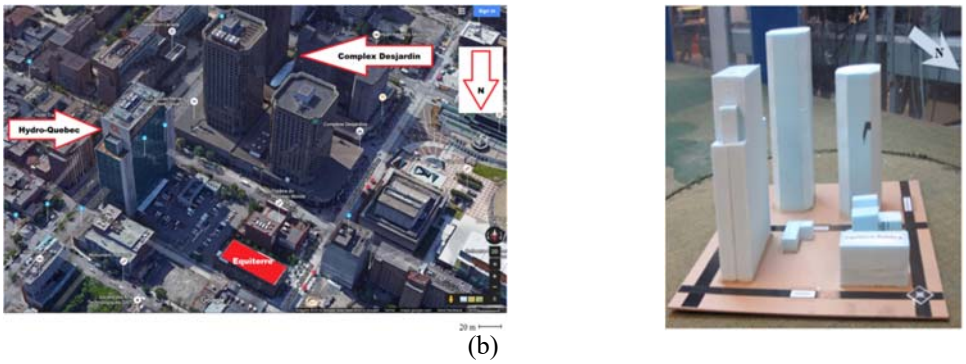

(b)

Figure 2: Perspective View of the Considered Building Cases (https://www.google.ca/maps) and their Models in the Wind Tunnel: (a) EV Building case (homogenous). (b) Equiterre Building case (nonhomogeneous) (Al-Quraan et al 2016).

In order to compare the calculated wind energy using the field measurements over the EV building roof and the estimated value using the proposed methodology, a three-cup anemometer was installed in one roof corner at a height of 2m above the roof. The anemometer was programed to take one measurement every 5s. The field measurement data were collected from the beginning of August 2013 to the end of October 2013. Also, another three-cup anemometer was installed in one corner above the roof of the Equiterre building, identical to the one on the roof of the EV building and with the same settings. The field measurement data - magnitude of the wind speed only - were collected for a 3-month period: November 1, 2012 to January 31, 2013.

The obtained data were used to calculate the total wind energy for the corresponding period. Figures 3 (a) and (b) show comparisons between the field measurements of wind energy and their estimation for the two building cases considered. It can be shown that the error in the wind energy, evaluated by [(field–estimated)/field] *100%, is less than 5% in case of homogenous terrain – see Figure 3 (a), whereas the obtained results show that the error between the wind energy field measurement and the estimation using the wind tunnel is less than 20% for nonhomogeneous terrain – see Figure 3 (b).

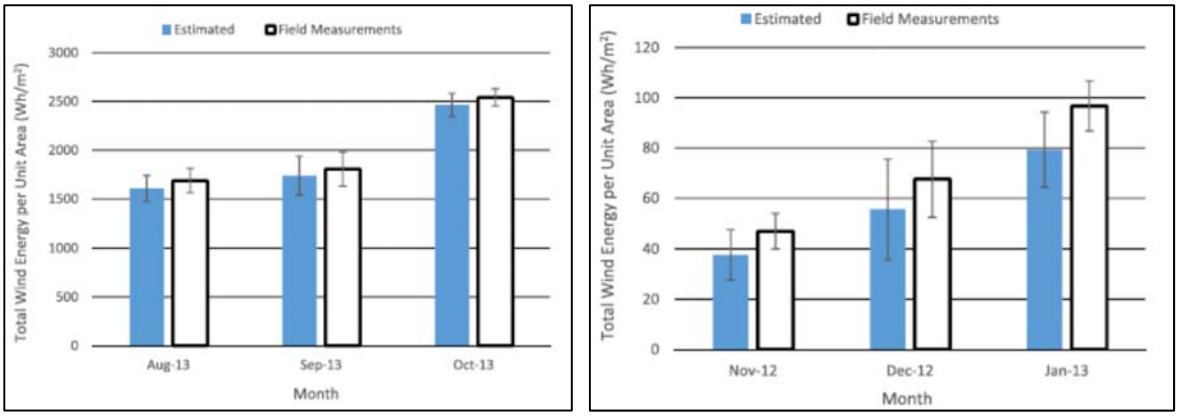

(a) (b)

Figure 3: Field Measurement Data and Estimated Total Wind Energy Potential per Unit Area with the Corresponding Error Bars above the Roof of (a) EV Building (homogeneous terrain) (b) Equiterre Building (nonhomogeneous terrain) (Al-Quraan et al 2016).

Comparison of the wind tunnel results with corresponding field measurement wind data in order to examine the validity of wind tunnel in providing realistic estimates of urban wind energy potential has shown that the suggested methodology is sufficiently accurate to be used, at least in the case of homogeneous terrain. Thus, high correlation between the estimation of the wind energy using the wind tunnel approach and the calculation based on field measurements above the roof of a building in homogeneous terrain has been noticed. On the other hand, in case of highly nonhomogeneous terrain, the discrepancy is higher but may still be acceptable for purposes of initial evaluation. In all cases the estimated values were lower than the measured values, so the assessment is on the conservative side.

3. WIND TURBINE DESIGNS

A large variety of wind turbine types and designs is available at present. Typically, efficient designs with high performance are influenced by several requirements related mainly to the application to serve and the location where the turbine is to be installed. As well, other constraints may play role in the efficiency of the designs, e.g. size constraints, noise limitations, visual disturbances and low start-up wind speeds. Among these requirements and constrains, the performance of one particular wind turbine may be more optimized compared to the others.

Savonius rotor is a vertical axis low speed wind turbine characterized as more inexpensive and simpler in construction. Savonius rotors are considered to be some of the oldest designs for wind turbines and they have proven to be well-suited to micro scaled urban operations due to their simple design and relatively low cut-in wind

velocity (Saha et al, 2008). The Darrieus vertical axis wind turbine (VAWT) is one of the most suitable for rooftop integration, as it is visually unobtrusive and produces low-level acoustic emissions (Balduzzi et al, 2012). In addition, recent designs of Darrieus wind turbines show good self-startup abilities (Batista et al, 2015).

Horizontal axis wind turbines (HAWTs) are the most widespread types of wind turbines. Their use spreads a lot for urban applications despite the nature of wind, which is highly turbulent and blowing from multiple directions. The HAWTs are very sensitive to the direction of the wind and do not cope well with turbulent flow and buffeting. Wind tunnel tests at the Delft University of Technology examining the effect of wind approaching from an angle from below revealed that the Vertical helical rotor wind turbines have power coefficient of about 0.4. Due to the 3-dimensional nature of the wind flow, VAWTs are very robust with different directions of wind and are better suited for exploiting turbulent flow (Ragheb, 2012). Based on the Wineur Project report (Cace et al, 2007), Table 1 summarizes the advantages and disadvantages of the common types of urban wind turbines.

Table 1. Summary of advantages and disadvantages of urban wind turbines based on Wineur Project report (Cace et al, 2007)

	Urban HAWTs	**Lift VAWTs**	**Drag VAWTs**
Advantages	• Efficient, • Proven technology • Widely used in wind • Economical • Wind range of commercial product options	• Almost as efficient as HAWT at given wind speed • Performs well in different wind directions and turbulence • Less vibration and buffeting (low noise)	• Proven product • Less acoustic emission • Reliable and robust • Performs well in different wind directions and turbulence • Less vibration, can benefit from turbulence
Disadvantages	• Does not cope well with buffeting • Performs poorly in changing wind direction	• Not yet proven • More sensitive to turbulence than drag based VAWTS	• Not efficient • Comparatively uneconomic

Pagnini et al (2015) presented an in situ experimental analysis for power performance of two small size wind turbines of identical rated power, but realized with vertical and horizontal axis. The turbines were placed in the same place exposing to two distinct regimes, low turbulence (wind blowing from the sea) and high turbulence (wind blowing from the land). Figure 4 shows the values of power coefficients (C_p) that were evaluated from the power output gathered from January to August 2012. The HAWT and VAWT have a swept area of 78.5 m^2 and 46.5 m^2 respectively. The C_p is evaluated based on the power output and the measured mean velocity. The density of air is assumed to be 1.225 kg/m^3. It should be mentioned that there is inconsistency in wind speeds obtained by the anemometer and what is the wind turbine experienced, also interval used to measure the power production. As shown in Figure 4, the calculated C_p violates Betz's coefficient (0.59), which is considered as the ideal maximum theoretical kinetic energy that can be captured by the wind turbine. However, the results can be used for comparison purposes for the performance of VAWT and HAWT. It was observed that the HAWT was extremely sensitive to the direction of wind while the VAWT was able to capture energy carried by strong gust of wind much more efficiently (Pagnini et al, 2015).

Although urban wind power has attracted much attention, several questions arise regarding the power output performance of wind turbines, particularly in urban areas. Thus, seeking for new wind turbine designs with higher power efficiency needs further investigation. As such, brimmed diffuser structure to envelope a rooftop VAWT in recent years has attracted the attention of research. For instance, Ohya and Karasudani (2010) have tested a wind turbine system consisting of a diffuser shroud with a broad-ring flange at the exit periphery and a wind turbine inside it. It was found that the power output of the Diffuser Augmented Wind Turbine (DAWT) is increased by 4-5 times compared to conventional wind turbines due to concentration of the wind energy. Figure 5 compares the power curves of a conventional Savonius wind turbine (C_p = 0.09) with a Building Integrated Wind Turbine (BIWT) for C_p = 0.381 based on data from Saha et al (2008). The BIWT results, which are more than 4 times higher, fit well to the field data measured.

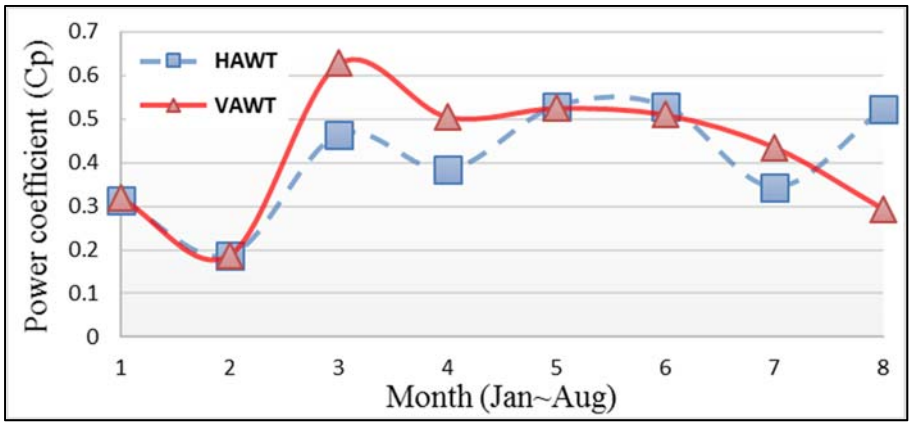

Figure 4: Monthly-averaged power coefficients of two wind turbines based on the data from Pagnini et al (2015)

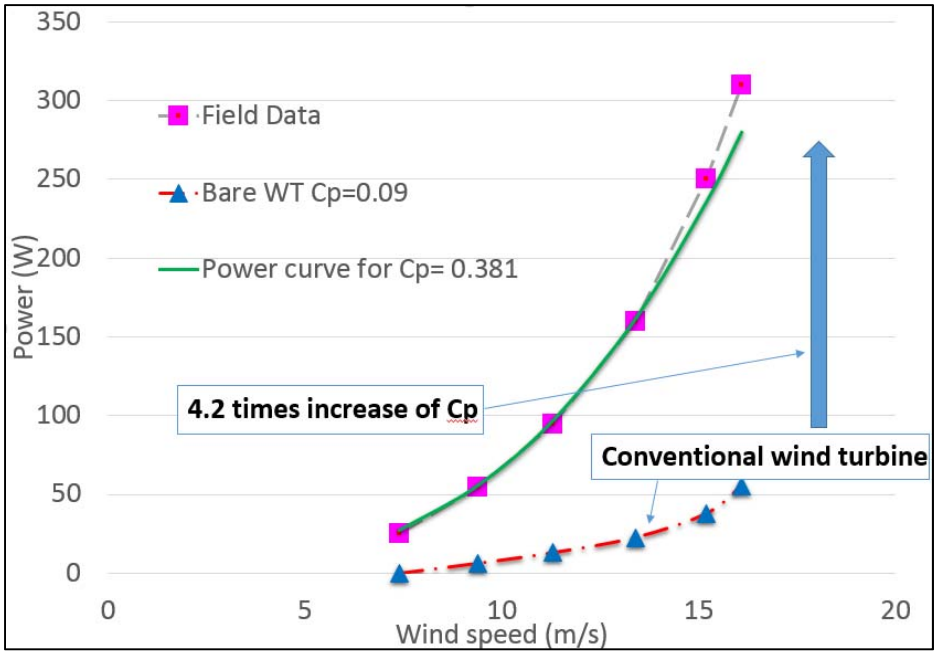

Figure 5: Performance comparison of BIWT based on data from Saha et al (2008) and Park et al (2015)

Urban wind turbines are still at the primary stage of technological development. Lacking experimental data of wind turbines installed in urban settings stands as a strong drawback on the evaluation of turbine efficiencies and, consequentially, their viability. Although conventional wind turbines directly located in urban built-environment do not perform well, other wind turbines, especially VAWTs, still show good results but need further optimization for urban applications. Diffusers and shrouded brims around conventional wind turbines may lead to significant power output increases.

4. URBAN AERODYNAMICS

The wind flow in urban areas blows with high turbulence due to high roughness of the ground surface and comes from multiple directions. Flow turbulence negatively influences the power output performance of the turbine, induced wind loads and noise propagation. On the other hand, the velocity and the density of the air flow

may increase in urban areas due to flow channeling and corner stream effects. This positively influences the power output performance of the turbine. Barlow et al (2015) reviewed the various boundary layer scales and the influence of urban morphology on the potential enhancement of wind speeds in the vicinity of buildings and above building roofs, as well.

The Bahrain World Trade Centre (WTC), which is located at the edge of the Arabian Gulf, was completed in 2008 costing about $150 million. It is considered the world's first skyscraper with integrated wind turbines. The twin towers have a height of 240 m (787 ft) and support three 29 m diameter large scale horizontal axis wind turbines. The towers have an aerodynamic shape like a funnel creating a wind flow path to improve the power-generation efficiency. Measurements carried out by the meteorological stations documented that the average annual wind speed in Bahrain at 10 m height is 4.8 m/s with predominant north-to-north-west direction. This level of wind speed was considered moderate and not economically viable for wind energy potential (Bachellerie, 2012).

The Bahrain WTC design would have yielded higher wind energy output if the buildings were positioned in diverging rather than the existing converging configuration – see Figure 6. Thus, from the wind energy point of view and based on wind-tunnel testing and Computational Fluid Dynamics simulations carried out by Blocken (2016) on the modeled Bahrain WTC, it was found that the towers would produce 14 percent more energy output per year if they were turned 180º around. Moreover, integrating the wind turbines further back would have increased the efficiency up to 31% – see Figure 7.

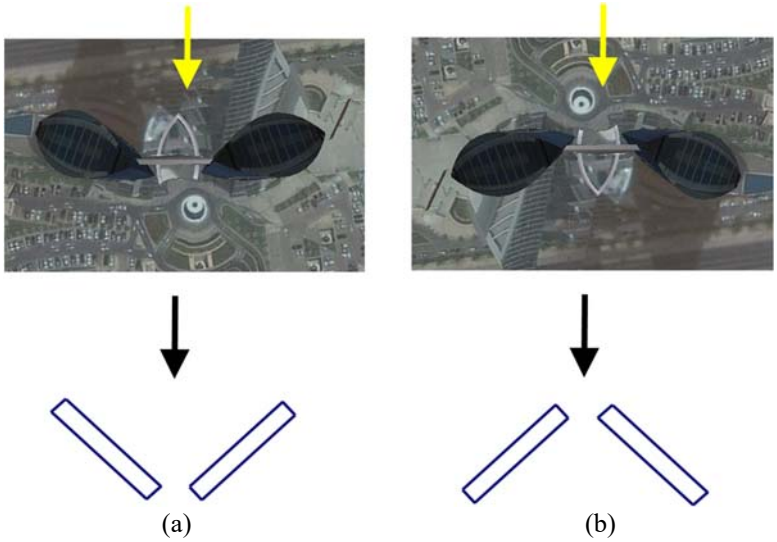

Figure 6: Bahrain World Trade Center Configurations: (a) Converging (chosen). (b) Diverging (Highest Wind Speed) (Blocken, 2016).

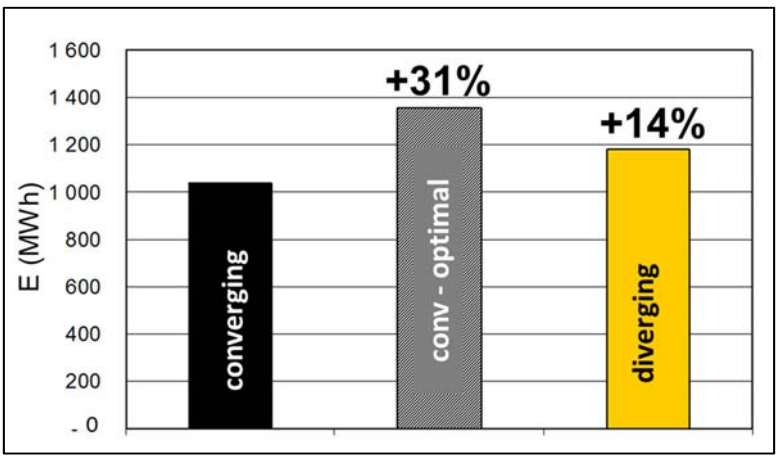

Figure 7: Estimated Yearly Wind Energy Output using CFD (Blocken, 2016).

Clearly, the study of building and urban aerodynamics becomes extremely relevant to the location and configuration of urban wind turbines for optimal performance.

5. SUMMARY AND CONCLUSIONS

The paper refers to the potential and challenges encountered in an attempt to capitalize on urban wind energy. Wind resource assessment, selection of appropriate wind turbines and application of knowledge of building and urban aerodynamics have been discussed and the progress made in this area has been identified. There is a need for additional comprehensive research in these areas in order to optimize the generation and utilization of urban wind energy.

REFERENCES

Al-Quraan A., Stathopoulos T., Pillay P. 2016. Comparison of wind tunnel and on site measurements for urban wind energy estimation of potential yield. Journal of Wind Engineering and Industrial Aerodynamics 158, 1-10.

Bachellerie, I.J. 2012. Renewable energy in GCC countries: Resources, potential, and prospects. Jeddah, Gulf Research Centre.

Balduzzi, F., Bianchini, A., Carnevale, E.A., Ferrari, L., Magnani, S. 2012. Feasibility analysis of a Darrieus vertical-axis wind turbine installation in the rooftop of a building. Applied Energy 97, 921-9.

Batista, N.C., Melício, R., Mendes, V.M.F., Calderón, M., Ramiro, A. 2015. On a self-start Darrieus wind turbine: Blade design and field tests. Renewable and Sustainable Energy Reviews 52, 508-522.

Cace, J., Horst, E., Syngellakis, K., Niel, M., Clement, P., Heppener, R., Peirano, E. 2007. Urban Wind Turbines, Guidelines for small wind turbines in the built environment 2016, 41. Available: http://www.urbanwind.net/pdf/SMALL_WIND_TURBINES_GUIDE_final.pdf. Last Accessed: February 26, 2016

Drew, D.R., Barlow, J.F., Cockerill, T.T. 2015. Estimating the potential yield of small wind turbines in urban areas: A case study for Greater London, UK. Journal of Wind Engineering and Industrial Aerodynamics 115, 104-111.

European Commission, 2007. Urban wind resource assessment in the UK. Report about the wind resource assessment in the urban environment.

https://commons.wikimedia.org/wiki/File:Bahrain_World_Trade_Center.jpg?uselang&equal;nl

Ohya, Y., Karasudani, T. 2010. A shrouded wind turbine generating high output power with wind-lens technology. Energies 3, 634-649.

Pagnini, L.C., Burlando, M., Repetto, M.P. 2015. Experimental power curve of small-size wind turbines in turbulent urban environment. Applied Energy 154, 112-21.

Park, J., Jung, H., Lee, S., Park, J. 2015. A new building-integrated wind turbine system utilizing the building. Energies 8, 11846-11870.

Ragheb, M. 2012. Wind turbines in the urban environment. Available: http://mragheb.com/NPRE%20475%20Wind%20Power%20Systems/Wind%20Turbines%20in%20the%20Urban%20Environment.pdf. Last accessed: February 26, 2016

Saha, U.K., Thotla, S., Maity, D. 2008. Optimum design configuration of Savonius rotor through wind tunnel experiments. Journal of Wind Engineering and Industrial Aerodynamics 96, 1359-1375.

PORTUGUESE EXPERIENCE IN SUCCESSFULLY INTEGRATING 5000MW WIND POWER

José Medeiros Pinto[1]
APREN
Lisbon, Portugal

ABSTRACT

Portugal is a world reference in terms of renewables integration in the electricity grid, namely the wind. Actually, the wind energy represents more than 24% of the Portuguese electricity consumption, the second highest penetration in the world until 2015, only overpassed by Denmark at that time. In 2016, this figure was also overcame by Ireland. However, the intrinsic Portuguese characteristics as a peripherical European country only connected with Spain make this achievement more challenging and notable.

In this speech, it will be focused and referred the strategy followed by the Portuguese authorities, Entities and Promoters to reach that number which results from more than 5000MW installed, running smoothly and with no significant technical problems or network restrictions.

I will be mentioned the main obstacles that have been considered to overcome the risks of the wind variability, the initial wind turbine technological low performances compared with conventional generation and the approaches to face them.

It will be emphasized the results of the wind, and in general the renewables, development in Portugal and the trade-off between the benefits and the costs compared with a "business as usual" approach.

The speech will finish with a description of the APREN's (Portuguese Renewable Association) point of view about the futures developments and the challenges that the Renewable Sector is facing.

[1] Director of the Portuguese Association for Renewable Energies (APREN), http://www.apren.pt/en/

Wind Characteristics and Loads

THE INTERNATIONAL CONFERENCE ON
WIND ENERGY HARVESTING 2017
20-21 April 2017
Coimbra, Portugal

Paper 201

A NUMERICAL WAKE ALIGNMENT METHOD FOR HORIZONTAL AXIS WIND TURBINES WITH THE LIFTING LINE THEORY

D. B. Melo[1]
Instituto Superior Técnico
Lisboa, Portugal

J. Baltazar[2]
Instituto Superior Técnico
Lisboa, Portugal

J. A. C. Falcão de Campos[3]
Instituto Superior Técnico
Lisboa, Portugal

ABSTRACT

A method to analyze the flow around horizontal axis wind turbines based on the lifting line theory is herewith presented. The strong relation between the reliability of the results and the proper alignment of the vortex wake is well known and documented. Hence, a non-linear vortex wake alignment scheme is proposed. The numerical results are presented and compared to the NREL turbine experimental data.

NOMENCLATURE

$C_{D,L}$	=	Drag coefficient, lift coefficient	$\vec{S}$	=	Vector radius from the integration point to the field point, $\|\vec{S}\| = S$ (m)
$C_{n,t}$	=	Force coefficient (normal, tangential to the section chord)	$\vec{U}$	=	Inflow velocity, $\|\vec{U}\| = U$ (m/s)
C_P	=	Power coefficient	$\vec{U}_\infty$	=	Incoming velocity field in the rotating reference frame (m/s)
D	=	Turbine rotor diameter (m)	$\vec{V}$	=	Total velocity (m/s)
L_k	=	k[th] lifting line	v_t	=	Tangential induced velocity (m/s)
$\vec{L}$	=	Lift force per unit span (N/m)	$\vec{v}$	=	Induced velocity (m/s)
M	=	Number of lifting lines elements	x_a	=	Axial coordinate of the alignment sections, $a = 1, \ldots, n$ (m)
N	=	Number of segments in which we discretize a trailing vortex	$x_{fw,ew}$	=	Axial coordinate of the far wake section and end wake section (m)
N_θ	=	Number of increments in which we discretize a blade rotation	Z	=	Number of blades
P	=	Power (W)	α	=	Angle of attack (rad)
p	=	Wake pitch (m)	$\vec{\Gamma}$	=	Circulation in the lifting line (m^2/s)
R	=	Turbine rotor radius (m)	$\vec{\gamma}$	=	Vortex sheet strength (m/s)
r_h	=	Rotor hub radius (m)	λ	=	Tip speed ratio, TSR
r_v	=	Radius of the image vortices (m)	ν	=	Kinematic viscosity (m^2/s)
r'	=	Element corner point radius (m)	ρ	=	Density of the fluid (kg/m^3)
$\bar{r}$	=	Control point radius (m)	$\vec{\omega}$	=	Angular velocity, $\|\vec{\omega}\| = \omega$ (rad/s)
S_k	=	k[th] vortex sheet			

1 MSc Student, Department of Mechanical Engineering (DEM), Instituto Superior Técnico, Universidade de Lisboa, Av. Rovisco Pais 1, 1049 Lisboa, Portugal/daniela.brito.melo@tecnico.ulisboa.pt/+351 963010946
2 Marine Environment and Tecnology Center (MARETEC), Instituto Superior Técnico, Universidade de Lisboa, Av. Rovisco Pais 1, 1049 Lisboa, Portugal/joao.baltazar@tecnico.ulisboa.pt
3 Marine Environment and Tecnology Center (MARETEC), Instituto Superior Técnico, Universidade de Lisboa, Av. Rovisco Pais 1, 1049 Lisboa, Portugal/falcao.campos@tecnico.ulisboa.pt

INTRODUCTION

The complexity of the flow around wind turbines makes it difficult to fully understand all the phenomena involved. Its modelling is therefore challenging and simplifications are naturally made. The models are both analytically and numerically complex, even if one reduces the viscosity to zero and assumes a steady state condition. Being originally introduced by Lanchester-Prandlt, the lifting line theory has been used to model marine propellers [1] and, more recently, axial turbines [2]. A number of researchers have contributed to the development of the theory. The correct modelling of the rotor wake is of the utmost importance for the quality of the numerical results [3]. Rigid or semi-empiric wake models are typically used. Ideally, the vorticity should be aligned with the local velocity field. However, it is not feasible to do it on its full extent. A vortex wake alignment scheme is proposed. The wake geometry is forced to be parallel to the flow in multiple sections downstream of the rotor. Finally, the numerical results are compared to the NREL turbine experimental data [4].

FORMULATION OF THE LIFTING LINE THEORY

Consider the rotor of a horizontal axis turbine with radius R, diameter D and with Z blades symmetrically placed around a cylindrical hub of radius r_h. The rotor is rotating with constant angular velocity $\vec{\omega}$ in a uniform inflow moving with velocity $\vec{U}$. The fluid is assumed to be inviscid and incompressible. We introduce a cartesian coordinate system (x, y, z) and a cylindrical coordinate system (x, r, θ) in a reference frame rotating with the turbine rotor. The flow is steady in the rotating reference frame and the relative velocity field is given by $\vec{U}_\infty = \vec{U} - \vec{\omega} \times \vec{r}$, as illustrated in Fig. 1.

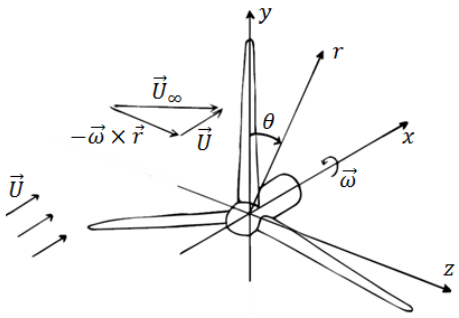

Fig. 1 Adopted coordinate system and incoming velocity field

In the lifting line model each turbine blade is represented by a radial bound vortex, extending from the root to the blade tip. The circulation along the lifting lines, $\vec{\Gamma}$, continuously varies and a vortex sheet of strength $\vec{\gamma}$ is shed from each lifting line. The velocity induced by the Z lifting lines and corresponding vortex sheets, $\vec{v}$, at a field point is given by the Biot-Savart law:

$$\vec{v}(x,y,z) = \frac{1}{4\pi} \sum_{k=1}^{Z} \left(\int_{L_k} \frac{\vec{\Gamma} \times \vec{S}}{S^3} dl + \int_{S_k} \frac{\vec{\gamma} \times \vec{S}}{S^3} dA \right), \quad (1)$$

where L_k denotes the k[th] lifting line, S_k the corresponding vortex sheet, $\vec{S}$ is the vector radius from the integration point to the field point and S is its module.

The total velocity field, $\vec{V} = \vec{U}_\infty + \vec{v}$, is related to the lift force per unit span, $\vec{L}$, by the Kutta-Joukowski theorem: $\vec{L} = \rho \vec{V} \times \vec{\Gamma}$, where ρ is the density of the fluid. The blade section lift coefficient, C_L, and drag coefficient, C_D, are obtained from 2D experimental data [5].

NUMERICAL METHOD

In the vortex lattice model the lifting lines and the shed vortex sheets are discretized by a lattice of concentrated vortices [3]. The lifting lines are discretized in M elements along the radius. On each element, the circulation is assumed to be constant. At the elements corner points the circulation is discontinuous and a concentrated vortex of constant intensity is shed. The trailing vortices are discretized in N straight-line segments.

The radial coordinate of the control points, $\bar{r}$, and of the elements corner points, r', are defined by a cosine distribution which allows a successful numerical convergence [2].

The turbine wake model considers a free vortex wake aligned in multiple sections, similarly to the work of Baltazar [6]. The coordinates of the wake straight-line edges are defined by the following expressions, with all variables in their dimensionless form (using R and U for coordinates and velocities, respectively):

$$x_2 = x_1 + p|_1 \left(1 + \frac{v_t}{\lambda r'}\right)\Big|_1 \frac{2}{N_\theta}, \tag{2}$$

$$\theta_2 = \theta_1 + \left(1 + \frac{v_t}{\lambda r'}\right)\Big|_1 \frac{2\pi}{N_\theta}, \tag{3}$$

where N_θ is the number of increments in which we discretize a full rotation of the blades, p is the wake pitch, v_t is the tangential induced velocity and λ is the tip speed ratio (TSR), $\lambda = \omega \mathrm{R}/U$. The indexes 1 and 2 refer, respectively, to the upstream and downstream edges of each straight-line segment.

The wake expansion is neglected. Hence, the radial coordinate of the trailing vortices remain unchanged. The wake is extended downstream and truncated at a station with axial coordinate x_{ew}. The vortex wake is divided into two parts: a transition wake region from the lifting line to a far wake station with axial coordinate x_{fw}, where variations of pitch and tangential velocities take place and an ultimate region from x_{fw} to x_{ew}, where the wake parameters remain constant and assume the values of the far wake station. In the transition wake, n sections of alignment, characterized by an axial coordinate $x_a, a = 1, \dots, n$, are defined.

The induced velocities at M control points are calculated at each alignment section. The radial coordinates of the alignment control points are given by $\bar{r}$. The axial and tangential coordinates are radially interpolated from the coordinates of the straight-line edges immediately below the axial position x_a (Fig. 2).

The new wake geometry is generated from equations (2) and (3), considering p and v_t interpolated/extrapolated from the values obtained in the alignment sections. In the ultimate region, p and v_t are assumed constant and identical to those obtained at the far wake station.

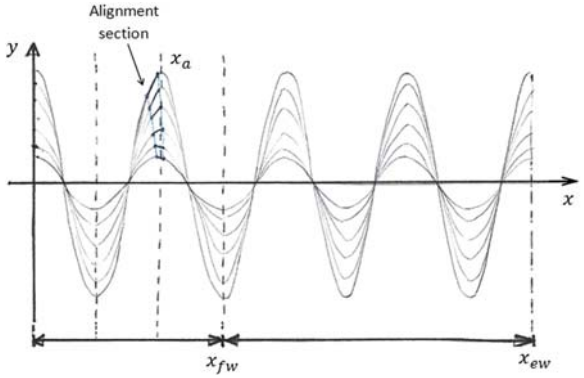

Fig. 2 Wake model: representation of the alignment sections

The turbine hub is modeled by an infinite cylinder. For this purpose an image vortex system is established as suggested in [7]. It is constituted by straight-line vortices with the same axial and tangential coordinates of the trailing vortex and radial coordinates, r_v, given by $r_v = r_h^2/r'$.

It is possible to establish a system of equations and compute the circulation on each lifting line element. The wake geometry must be prescribed in order to start the iterative process. Having the circulation on the M elements one can compute the induced velocities and a new wake geometry is established.

RESULTS

The incoming flow conditions are summarized in Tab.1. The analysis conditions were set by an upwind NREL/NASA Ames wind tunnel test [4]. The blades geometry can be found in [8].

TSR	U (m/s)	ω (rpm)	ρ (kg/m^3)	$\nu \times 10^{-5}$ (m^2/s)
5.41	7	71.9	1.246	1.4197

Tab.1 Incoming flow conditions

The lifting lines are discritized in M = 30 elements. The wake trailing vortices are truncated at x_{ew}/R=10 and discretized in $N_\theta = 200$ straight-line segments per turn. The wake alignment model was tested for three and two sections of alignment. The results are presented for the last ($n = 2$), where the vortices were lined up at $x/\mathrm{R} = 0$ (lifting line) and $x/\mathrm{R} = 1$. The radial distributions of the dimensionless pitch and tangential induced velocity on the alignment sections are presented in Fig.3.

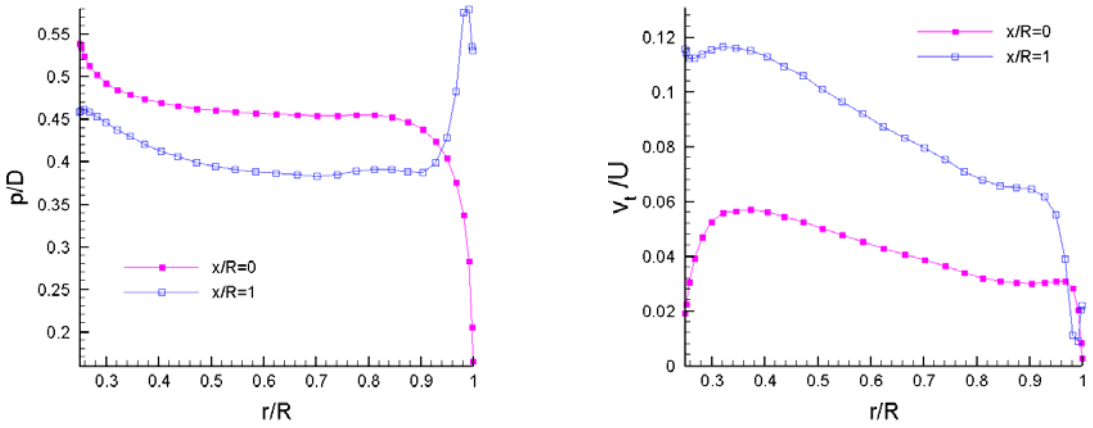

a) b)

Fig. 3 Radial distribution of (a) pitch and (b) tangential induced velocity at the alignment sections ($n = 2$)

The effect of the alignment on the power coefficient, $C_P = P/\left(\frac{1}{2}\rho U^3 \pi \mathrm{R}^2\right)$, where P is power, is shown in Tab.2. The mean experimental value is also presented for comparison purposes [4]. The wake alignment in the downstream section, $x/\mathrm{R} = 1$, increases the power coefficient by 19%.

The $n = 3$ wake, aligned at $x/\mathrm{R} = 0$, $x/\mathrm{R} = 1$ and $x/\mathrm{R} = 2$, and the $n = 2$ wake produced similar results. The radial distribution of pitch and tangential induced velocity on $x/\mathrm{R} = 2$ were, in fact, very close to the distributions registered on section $x/\mathrm{R} = 1$. The power coefficient decreased 0.007% with the extra alignment section.

Wake	C_P
Constant pitch ($\boldsymbol{n = 1}$, aligned on $\boldsymbol{x/\mathrm{R} = 0}$)	0.2790
Aligned on $\boldsymbol{x/\mathrm{R} = 0}$ and $\boldsymbol{x/\mathrm{R} = 1}$ ($\boldsymbol{n = 2}$)	0.3332
Mean experimental value	0.3548

Tab.2 Power coefficient, C_P, for a wake of constant pitch ($n = 1$) and a wake aligned in two sections ($n = 2$). Mean experimental value obtained in NASA/Ames wind tunnel test [4]

The force coefficients, C_n and C_t (normal and tangential to the section chord, respectively) are defined as a function of the lift and drag coefficients:

$$C_n = C_L \cos\alpha - C_D \sin\alpha, \tag{4}$$

$$C_t = C_L \sin\alpha + C_D \cos\alpha, \tag{5}$$

where α is the angle of attack.

The numerical predictions of the radial distributions of C_n and C_t are plotted in Fig.4 and compared with the experimental measurements presented in [4].

The alignment in $x/\mathrm{R} = 1$ leads to an increase of C_n and C_t in the whole blade extent. An agreement between the experimental data and the $n = 2$ resultant power coefficient and force coefficients' radial distribution can be observed. The discrepancies near the hub are directly related to its modelling. As previously stated it is simulated by an infinite cylinder. However, its radius is far bigger than the real turbine hub.

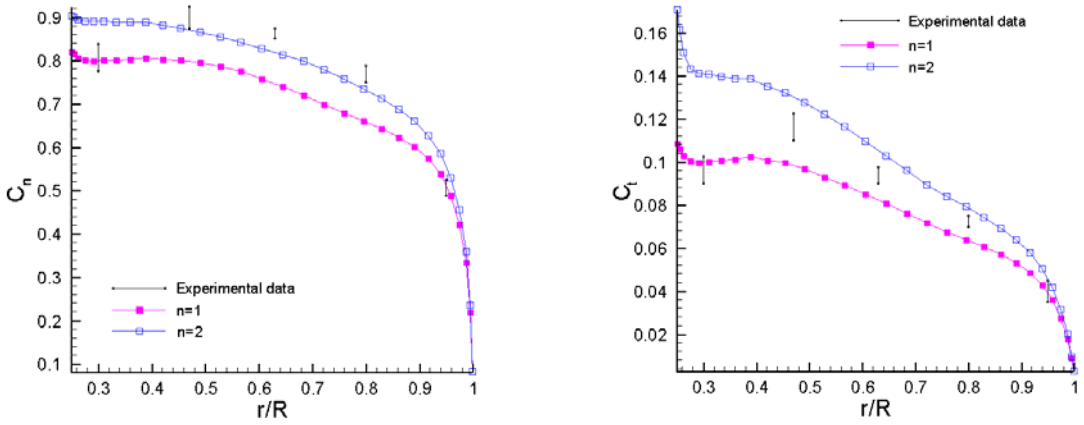

a) b)

Fig.4 Radial distribution of (a) C_n and (b) C_t for two wakes: constant pitch ($n = 1$) and aligned in two sections ($n = 2$); comparison with experimental data [4]

CONCLUSIONS

A method to analyze the flow around horizontal axis wind turbines with the lifting line theory is presented. A non-linear vortex wake alignment scheme is proposed. Results are presented for a wake aligned in the lifting line and in one section downstream. An increase in the power coefficient is obtained. An additional alignment section downstream did not significantly change the results. The numerical predictions are compared to the NREL turbine experimental data. The non-linear vortex wake alignment scheme considerably improves the predicted force coefficients' radial distributions with respect to the classical alignment at the lifting line.

REFERENCES

[1] Morgan, W., Wrench, J., "Some Computational Aspects of Propeller Design", Methods in Computacional physics: Aplications in Hydrodynamics, ISSN 0076-6860, Vol.4, 1965, pp. 301-330

[2] Falcão de Campos, J., "Hydrodynamic Power Optimization of a Horizontal Axis Marine Current Turbine with Lifting Line Theory", In INTERNATIONAL OFFSHORE AND POLAR ENGINEERING CONFERENCE, 3, Lisboa, 2007 – Seventeenth International Offshore and Polar Engineering Conference. California: ISOPE, 2007, pp. 307-313

[3] Kerwin, J., Lee, C. "Prediction of a Steady and Unsteady Marine Propeller Performance by Numerical Lifting-Surface Theory", SNAME Transactions, ISSN 0081-161, Vol.86, 1978, pp. 218-253

[4] Sorensen, N., Michelsen, J., Schreck, S. "Navier-Stokes Predictions of the NREL Phase VI Rotor in the NASA Ames 80 ft x 120 ft Wind Tunnel", Wind Energy, ISSN 1099-1824, Vol.5, 2002, pp. 151-169

[5] Hand, M., Simms, D., Fingersh, L. J., Jager, D., Cotrell, J., Schreck, S., Larwood, S., "Unsteady Aerodynamics Experiment Phase VI: Wind Tunnel Test Configurations and Available Data Campaigns", Colorado: NREL, 2001, NREL/TP-500-29955

[6] Baltazar, J., "On the Modelling of the Potential Flow About Wings and Marine Propellers Using a Boundary Element Method", Lisboa: Universidade de Lisboa, Instituto Superior Técnico, PhD Thesis, 2008

[7] Kerwin, J., "Lecture Notes on Hydrofoils and Propellers", Cambridge MA: MIT, 2001

[8] Simms, D., Schreck, S., Hand, M., Fingersh, L. J., "NREL Unsteady Aerodynamics Experiment in the NASA-Ames Wind Tunnel: A Comparison of Predictions to Measurements", Colorado: NREL, 2001, NREL/TP-500-29494

THE INTERNATIONAL CONFERENCE ON
WIND ENERGY HARVESTING 2017
20-21 April 2017
Coimbra, Portugal

Paper 202

ASSESSMENT OF EDDY VISCOSITY MODELS FOR THE MULTISCALE MODELLING OF THE NEUTRAL ATMOSPHERIC BOUNDARY LAYER

Orkun Temel[1]
von Karman Institute
Brussels, Belgium
Universite de Mons
Mons, Belgium

Laurent Bricteux[2]
Universite de Mons
Mons, Belgium

Jeroen van Beeck[3]
von Karman Institute
Brussels, Belgium

ABSTRACT

This study is devoted to the investigation of the performances of 6 different $k-\epsilon$ closures for coupled computational fluid dynamics (CFD) and numerical weather prediction (NWP) simulations. The methodology being applied is based on the reformulation of Reynolds-Averaged Navier-Stokes models based on the features of mesoscale turbulence closures. Simulations have been performed for the Askervein Hill case. The inflow conditions have been acquired by performing mesoscale simulations using the Weather Research and Forecasting (WRF) model and the microscale/CFD computations have been conducted with the open source CFD toolbox OpenFOAM v.2.3.1. The numerical results have been compared with the wind speed and turbulent kinetic energy measured during the campaign.

INTRODUCTION

The numerical and laboratory-scale modelling of the flows over complex terrains is one of the most challenging topics in the field of atmospheric boundary layer [1] due to many different engineering applications like heavy gas dispersion [2] and wind energy assessment studies [3]. Diurnal variation of near-surface winds over complex terrains is directly related with a larger meteorological scale, so called mesoscale. For instance, the convection of clouds with different water vapor concentrations changes the absorption coefficient of atmosphere which also directly affects the surface radiative heat flux. When the surface radiative heat flux changes, the surface temperature gradient changes too and this affects the budget of the turbulence kinetic energy and finally the near-surface winds changes during the day.

This complicated physical process arises questions on the applicability of classical logarithmic law profile based on the Monin-Obukhov theory [4]. For extreme stability conditions like low-level-jets or extremely unstable conditions, the applicability of the Monin-Obukhov theory is open to question. Moreover, the Monin-Obukhov theory is only applicable for the surface layer. Nowadays, due to the improvements in the wind engineering, the hub-height of wind turbines are increasing so that the region physically governed by the Monin-Obukhov theory falls below to the region that is aimed to achieve technologically. Even though, there are some attempts to extend the Monin-Obukhov theory above the surface layer, their universality is still open to question [5].

Mesoscale or generally speaking NWP models stand as a potential tool to obtain realistic inflow conditions thanks to their multiphysical nature which covers many different atmospheric phenomenas including atmospheric radiation, phase change of water, heat and mass transfer within soil and turbulence within the atmospheric boundary layer. The main idea is to perform mesoscale simulations and use the wind speed, wind direction, potential temperature values in the upstream of the microscale domain as inflow conditions.

Many researchers had reported that the standard RANS closures are not developed for the atmospheric boundary layer flows and their closure coefficients must be determined according to the physics of the atmospheric boundary layer [6]. Many different approaches had been proposed by various researchers from analytical

[1] PhD Candidate, Environmental and Applied Fluid Dynamics, von Karman Institute for Fluid Dynamics, Brussels, Belgium, orkun.temel@vki.ac.be
[2] Professor, Department Mecanique, Universite de Mons, Mons, Belgium, Laurent.BRICTEUX@umons.ac.be
[3] Professor, Environmental and Applied Fluid Dynamics, von Karman Institute for Fluid Dynamics, Brussels, Belgium,

derivations [7] to making use of look-up tables [8]. However, it must be noted that all these models devoted to the microscale simulations not for the coupled CFD/NWP simulations. The problem with the current model was the fact that when the turbulent scalars which are computed by the mesoscale model are imposed directly as boundary conditions to the turbulence model, the computed turbulent viscosities of mesoscale and microscale model must match. In other words, the turbulence closure coefficients must be convenient between two models. In order to solve this problem, 8 different mesoscale turbulence models have been adapted as variants of $k-\epsilon$ models for coupled RANS simulations of CFD/NWP [9].

In this present study, different to our previous work [9], further modifications and improvements have been tested for the developed base model. In addition to $k-\epsilon$ closures, based on our another previous work [10], a variant of Re-normalization Group (RNG) $k-\epsilon$ model which is developed for atmospheric boundary layer flows has been updated to be able to work for coupled simulations.

The time period of interest is the TU-03B turbulence run of Askervein Hill full scale experiments [11], which corresponds to the 03/10/1983 - 14:00-17:00. Mesoscale results of the previous work [9] has been used. Mesoscale simulations had been performed for 4-nested domain covering a region of 4000 km x 4000 km and having the finest resolution as 1.5 km for the smallest domain which covers a region of 135 km x 135 km . Simulations have been performed with an algebraic turbulence parameterization scheme so called Yonsei University Scheme (YSU). Kain-Fritsch cumulus parameterization [12] is used only for domains D1 and D2. For longwave and shortwave radiative fluxes the Rapid Radiative Transfer Model (RRTM) [13] is used within all domains. For the microphysics parameterizations, Thompson scheme [14] is applied and classical 5 layer land-surface scheme which is being widely used for NWP codes is used [15].

TURBULENCE CLOSURES

Derivation of inflow conditions

Planetary boundary layer schemes being used within this study are first-order turbulence parameterization schemes which defines turbulent momentum diffusivity within the atmospheric boundary layer based on the bulk parameters of atmospheric boundary with the following formulation [10]:

$$\nu_t = w_* \kappa z \left(1-\frac{z}{z_i}\right)^2 \tag{1}$$

Therefore, the turbulent scalars must be derived by using some empirical formulations related to the atmospheric boundary layer. The detailed derivation can be found in [9]. Turbulence kinetic energy and the dissipation rate of the turbulence kinetic energy are as follows:

$$\epsilon = \frac{(u_* \kappa z)^3 \left(1-\frac{z}{z_i}\right)^6}{\mathrm{B}_1 \left(\frac{\kappa z l_\infty}{\kappa z + l_\infty}\right)^4} \tag{2}$$

$$k = \frac{(u_* \kappa z)^2 \left(1-\frac{z}{z_i}\right)^4}{\left(\frac{\kappa z l_\infty}{\kappa z + l_\infty}\right)^2} \tag{3}$$

In Eq.2 and Eq.3, u_* is the friction velocity, κ is the von Karman constant, z_i is the boundary layer thickness and B_1 is a model coefficient which is taken as 24.0 [14] and l_∞ is the asymptotic length scale which is also taken as 200 m [10].

Turbulence closures

Transport equations for the turbulent scalars are as follows for the standard $-\epsilon$:

$$u_i \frac{\partial k}{\partial x_i} = \frac{\partial}{\partial x_i}\left[\frac{\nu_t}{\sigma_k}\frac{\partial k}{\partial x_i}\right] + P - \epsilon \tag{4}$$

$$u_i \frac{\partial k}{\partial x_i} = \frac{\partial}{\partial x_i}\left[\frac{\nu_t}{\sigma_k}\frac{\partial k}{\partial x_i}\right] + \frac{\epsilon}{k} C_1 P - \frac{\epsilon^2}{k} C_2 \quad (5)$$

Based on the relationship between production of turbulence and dissipation and making use of Monin-Obukhov relationships, turbulence closure coefficients had been determined for non-neutral conditions [10], the simplified relationship between C_1 and C_2 for neutral conditions is:

$$C_{\epsilon 1} = C_{\epsilon 2} - \frac{\kappa^2}{C_\mu^{0.5}\sigma_\epsilon} \quad (6)$$

To extend this approach above the boundary layer, the approach proposed by Detering and Etling [16] has been used and the Eq.6 becomes:

$$C_1 = C_1^0 + \frac{C_f}{Ro^{-1}} \quad (7)$$

$$C_{\epsilon 2} = C_1^0 + \frac{C_f}{Ro} + \frac{\kappa^2}{C_\mu^{0.5}\sigma_\epsilon} \quad (8)$$

C_1^0 is the classical model coefficient which is taken as 1.44, Ro is the Rossby number based on the friction velocity and turbulent macroscale ($= u_*/|f|L$). Finally based on our theoretical derivation in [9], C_μ can be taken as 0.0417.

For the RNG $k-\epsilon$ model, transport equations for turbulence kinetic energy and the dissipation rate of turbulence:

$$u_i \frac{\partial k}{\partial x_i} = \frac{\partial}{\partial x_i}\left[\frac{\nu_t}{\sigma_k}\frac{\partial k}{\partial x_i}\right] + P - \epsilon \quad (9)$$

$$u_i \frac{\partial k}{\partial x_i} = \frac{\partial}{\partial x_i}\left[\frac{\nu_t}{\sigma_k}\frac{\partial k}{\partial x_i}\right] + \frac{\epsilon}{k}(C_1^0 - R) P - \frac{\epsilon^2}{k} C_2 \quad (10)$$

$$C_1 = C_1^0 + \frac{C_f}{Ro} \quad (11)$$

$$C_{\epsilon 2} = C_1^0 + \frac{C_f}{Ro} + \frac{\kappa^2}{C_\mu^{0.5}\sigma_\epsilon} \quad (12)$$

Another approach being used to adapt RANS closures for atmospheric boundary layer is the length-scale limitation [17].

$$C_1 = C_1^0 + (C_2 - C_1)\frac{L}{L_\epsilon} \quad (13)$$

where L_ϵ can be computed Blackadar formulation which is also based on the asymptotic length scale.

$$\frac{1}{l_\epsilon} = \frac{1}{\kappa z} + \frac{1}{l_\infty} \quad (14)$$

Blending approach

It must be noted that these closure coefficients are based on the homogeneous state of atmospheric boundary layer which will not be valid for the regions where the flow is deviating from the homogeneous state. In order to provide a better modeling for the wake regions, the blending approach developed by Parente [18] has been adapted to our current model. The blending approach is based on the gradual transition of closure coefficients from the ones proposed for homogeneous state to the ones would perform better within the wake region by using a blending

function. For instance, $\bar{\gamma}$ being a generic variable which can be $C_{\epsilon 1}$, $C_{\epsilon 2}$, σ_k or σ_ϵ, it is blended with the values being used in standard $k-\epsilon$ by using the following formulation:

$$\bar{\gamma} = \gamma_{std} + (1-\delta^{\alpha})(\gamma_{ABL} - \gamma_{std}) \tag{15}$$

where δ is the blending function based on a dependent variable (velocity, turbulence kinetic energy etc.) and α is the shape function of transition which is taken as 2. In this present study, we apply the velocity gradient as the marker of blending function. For homogeneous atmospheric boundary layer only the vertical gradient of stream-wise velocity will be equal to a non-zero value and it can be approximated as $\sim u_*/\kappa z$. We use the %10 of this estimated velocity gradient as the threshold value and use the horizontal gradient of stream-wise velocity as the marker as follows:

$$\delta = \min\left[\left(\frac{\left|\frac{\partial u}{\partial x} - 0.1\frac{u_*}{\kappa z}\right|}{0.1\frac{u_*}{\kappa z}}\right), 1\right] \tag{16}$$

Finally, 6 different turbulence models are as shown in Table.1.

Table 1. Description of cases

	Description	$C_1 - C_2$	C_μ
Case I	Standard $k-\epsilon$ model without blending	$C_{\epsilon 2} = C_1^0 + \frac{C_f}{Ro} + \frac{\kappa^2}{C_\mu^{0.5}\sigma_\epsilon}$	0.0417
Case II	Standard $k-\epsilon$ model with blending		
Case III	RNG $k-\epsilon$ model without blending		
Case IV	RNG $k-\epsilon$ model with blending		
Case V	Standard $k-\epsilon$ model without blending (2)	$C_1 = C_1^0 + (C_2 - C_1)\frac{L}{L_\epsilon}$	
Case VI	Standard $k-\epsilon$ model with blending (2)		

MICROSCALE CFD SIMULATIONS

Developed turbulence closure has been applied to Askervein Hill case based on a previous study performed with conventional microscale CFD approach by Balogh [19] where the inflow conditions are defined based on the measurements acquired during the Askervein Hill campaign. In order to compare the effectiveness of the developed methodology, the same computational domain has been used (see Fig.1).

The selected time period, TU03-B campaign, is reported to have near-neutral stratification [20]; therefore, the simulations have been performed by neglecting the heat transfer within the boundary layer. Gradient Richardson number was determined to be −0.0074 which corresponds to the 'very slightly unstable' condition; therefore, the atmospheric stability is considered to be neutral.

SIMPLE solution algorithm has been used with the second order upwind discretization schemes for convective fluxes and the inlet boundary conditions have been determined by using the results of mesoscale simulations.

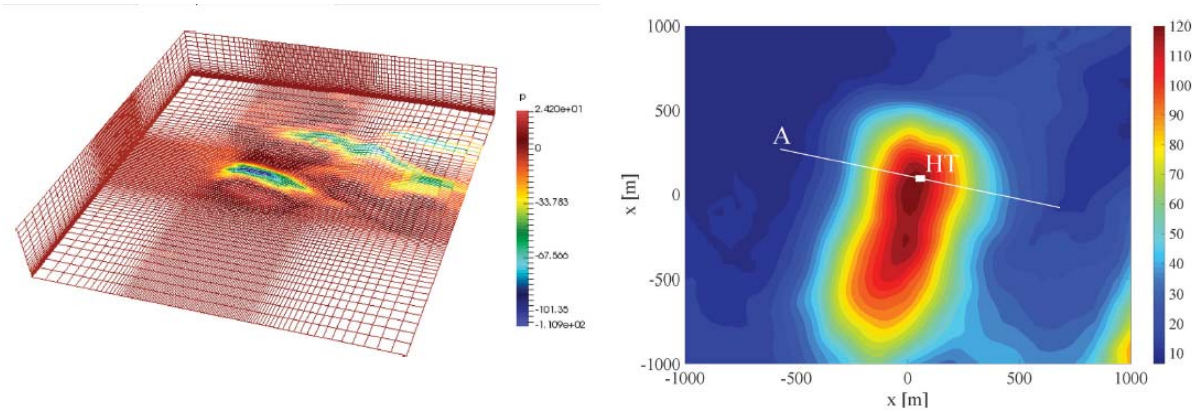

Figure 1. Computational domain

The preliminary results have been compared with the velocity and turbulence kinetic energy profiles at the hill top (HT) and presented in Fig.2.

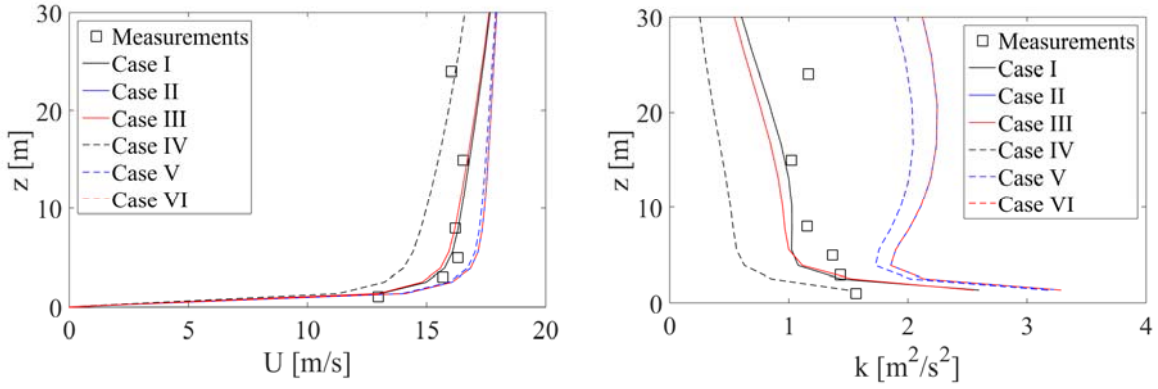

Figure 2. Comparison of wind speed and turbulence kinetic energy profiles at the top of Askervein Hill

CONCLUSIONS

Preliminary results have shown that the blending approach does not improve the quality of estimations. This can be related with the fact that the blending approach is actually developed for flows around building where the flow totally deviates from its upstream state which can be represented by the theories devoted to the atmospheric boundary layer, which is not the case for the Askervein Hill case. The approach proposed by Detering and Etling [16] performs much better than the approach based on the length-scale limitation. Additionally, at the hill top, it is likely to claim that RNG and standard $k-\epsilon$ closures behaved quite similarly. However the final conclusion will be drawn after a full quantitative comparison with the measurements.

ACKNOWLEDGEMENTS

This study has been supported and funded by the Fonds de la Recherche Scientifique de Belgique (FRS-FNRS).

REFERENCES

[1] Wood, N. (2000). Wind flow over complex terrain: a historical perspective and the prospect for large-eddy modelling. Boundary-Layer Meteorology, 96(1-2), 11-32.
[2] Scargiali, F., Di Rienzo, E., Ciofalo, M., Grisafi, F., & Brucato, A. (2005). Heavy gas dispersion modelling over a topographically complex mesoscale: a CFD based approach. Process safety and environmental protection, 83(3), 242-256.
[3] Cabezón, D., Iniesta, A., Ferrer, E., & Martí, I. (2006). Comparing linear and non linear wind flow models. In Proceedings of the European Wind Energy Conference EWEC (Vol. 2006).

[4] Foken, T. (2006). 50 years of the Monin–Obukhov similarity theory. Boundary-Layer Meteorology, 119(3), 431-447.
[5] Gryning, S. E., Batchvarova, E., Brümmer, B., Jørgensen, H., & Larsen, S. (2007). On the extension of the wind profile over homogeneous terrain beyond the surface boundary layer. Boundary-Layer Meteorology, 124(2), 251-268.
[6] Parente, A., Gorlé, C., Van Beeck, J., & Benocci, C. (2011). Improved k–ε model and wall function formulation for the RANS simulation of ABL flows. Journal of wind engineering and industrial aerodynamics, 99(4), 267-278.
[7] Pontiggia, M., Derudi, M., Busini, V., & Rota, R. (2009). Hazardous gas dispersion: a CFD model accounting for atmospheric stability classes. Journal of hazardous materials, 171(1), 739-747.
[8] Alinot, C., & Masson, C. (2002, January). Aerodynamic simulations of wind turbines operating in atmospheric boundary layer with various thermal stratifications. In ASME 2002 Wind Energy Symposium (pp. 206-215). American Society of Mechanical Engineers.
[9] Temel, O., & van Beeck, J. (2016). Adaptation of mesoscale turbulence parameterisation schemes as RANS closures for ABL simulations. Journal of Turbulence, 17(10), 966-997.
[10] Temel, O., & van Beeck, J. (2016). Two-equation eddy viscosity models based on the Monin–Obukhov similarity theory. Applied Mathematical Modelling.
[11] Taylor, P. A., & Teunissen, H. W. (1987). The Askervein Hill project: overview and background data. Boundary-Layer Meteorology, 39(1-2), 15-39.
[12] Kain, John S., 2004: The Kain–Fritsch convective parameterization: An update. J. Appl. Meteor., 43, 170–181.
[13] Mlawer, Eli. J., Steven. J. Taubman, Patrick. D. Brown, M. J. Iacono, and S. A. Clough (1997), Radiative transfer for inhomogeneous atmospheres: RRTM, a validated correlated–k model for the longwave. J. Geophys. Res., 102, 16663–16682.
[14] Thompson, Gregory, Paul R. Field, Roy M. Rasmussen, William D. Hall, 2008: Explicit Forecasts of Winter Precipitation Using an Improved Bulk Microphysics Scheme. Part II: Implementation of a New Snow Parameterization. Mon. Wea. Rev., 136, 5095–5115.
[15] Dudhia, Jimy, 1996: A multi-layer soil temperature model for MM5. the Sixth PSU/NCAR Mesoscale Model Users' Workshop.
[16] Detering, H. W., & Etling, D. (1985). Application of the E-ε turbulence model to the atmospheric boundary layer. Boundary-Layer Meteorology, 33(2), 113-133.
[17] Apsley, D. D., & Castro, I. P. (1997). A limited-length-scale k-ε model for the neutral and stably-stratified atmospheric boundary layer. Boundary-Layer Meteorology, 83(1), 75-98.
[18] Parente, A., Gorlé, C., van Beeck, J., & Benocci, C. (2011). A comprehensive modelling approach for the neutral atmospheric boundary layer: consistent inflow conditions, wall function and turbulence model. Boundary-layer meteorology, 140(3), 411-428.
[19] Balogh, M., RANS simulation of the neutral atmospheric boundary layer using OpenFOAM, Research Master Report, 2010, von Karman Institute for Fluid Dynamics
[20] Chow FK, Street RL. Evaluation of turbulence closure models for large-eddy simulation over complex terrain: flow over Askervein Hill. J. Appl. Meteorol. Climatol. 2009; 48:1050–1065.

THE INTERNATIONAL CONFERENCE ON
WIND ENERGY HARVESTING 2017
20-21 April 2017
Coimbra, Portugal

Paper 203

COMPARISON OF WIND LIDAR MEASUREMENTS WITH PREDICTIONS FROM AIRPORT DATA

Francesco Ricciardelli[1]
Università degli stuudi della Campania "Luigi Vanvitelli"
Aversa, Italy

Stefano Pirozzi[2]
Università degli stuudi della Campania "Luigi Vanvitelli"
Aversa, Italy

Alberto Mandara[3]
Università degli stuudi della Campania "Luigi Vanvitelli"
Aversa, Italy

ABSTRACT

The prediction of the mean and extreme wind climate at a site from airport historical data contains intrinsic errors coming from the not necessarily good quality of the original data, from the approximations adopted when defining orography and roughness at the sites of measurement and at the site of interest, from the possible presence of sheltering effects at the site of measurement and from the approximations embedded in the mathematical models used for transferring the measured data to the site of interest.
In this paper the wind velocities predicted at e site from airport measurement are compared with wind LIDAR measurements, with the purpose of quantifying inaccuracies and possibly detecting their causes.

INTRODUCTION

Both for the prediction of the mean wind climate in wind energy assessments, and for the prediction of wind loads for structural design, the use of airport historical wind data is often the first step. This, however, contains intrinsic inaccuracies due to several reasons, some of which are:

a) historical data are often unreliable due to incompleteness, measurement errors, poor maintenance and change of the instruments, modifications in the characteristics of the surroundings, length of the records;

b) the definition of the characteristics of orography and of terrain roughness in the surroundings of the measurement sites and of the site of interest depend on the availability of maps, on the accuracy and resolution of these, and on the ability of translating these into boundary conditions for the mathematical model adopted;

c) mathematical models for Atmospheric Boundary Layer wind flow must properly account for thermal conditions and stratification, especially when used for analyzing the mean wind climate.

As a result, the predicted statistics of the mean and extreme wind speed can also be inaccurate, and the inaccuracy is amplified when the square of the this is used for assessing wind loads and its third power is used for assessing wind resource.

On the other hand, more recently wind LIDARS have appeared, and are becoming more and more common for the assessment of wind power and for the monitoring of wind characteristics in wind farms. Wind LIDARS provide a direct measurement of the wind velocity at the site and at the height of interest, which is therefore much more accurate than any prediction from airport data. On the other hand, wind LIDAR measurements are limited in time, and the data available often insufficient for a reasonably accurate statistical description of the wind climate.

In addition, wind LIDARS, and in particular wind scanners also offer the possibility of analyzing the spatial distribution of mean and fluctuating wind speed. In doing this, one has to be aware of the inaccuracies associated with averaging, and validation and refinement of the techniques is still in progress.

Finally, the availability of even short duration wind LIDAR measurements at the site of interest, together with much longer historical records from neighboring airports allows calibration of the procedures for assessing wind climate at the site. In fact, by comparing wind LIDAR measurements and predicted wind velocities at the site one can calibrate the prediction technique, and when this is applied to the entire historical record one has to expect that the accuracy of the prediction of the wind climate at the site of interest is improved.

1 Associate Professor, SUN, DICDEA, Via Roma, 9, 81031, Aversa (CE), Italy, friccia@unina2.it
2 Graduate Student, SUN, DICDEA,Via Roma, 9, 81031, Aversa (CE), Italy, stefanopirozzi@gmail.com
3 Professor, SUN, DICDEA,Via Roma, 9, 81031, Aversa (CE), Italy, alberto.mandara@unina2.it

This paper deals with the aspect above. In a first stage data from three anemometric stations have been used to assess the generalized mean and extreme wind climate of a region north of Napoli, in southern Italy. The projected wind velocities at a reference site have been calculated and are discussed. Meanwhile, in October 2015 a wind LIDAR has been installed at the reference site, and measurements have started to be taken. Three months of measurement will be used to calibrate the prediction of the wind climate at the site of interest, by comparison with the projected wind velocities. At the end of the calibration process the historical records will be used again to calculate the statistics of the mean and extreme, and these will be compared with those obtained before calibration, so to quantify the differences in terms of wind resource and of wind loads.

PROCEDURE

The three measurement sites are the Napoli Capodichino International Airport, the Carlo Romagnoli Grazzanise Airport and the Capri Damecuta Heliport. The site of interest is in the city if Aversa, where buildings of the Faculty of Engineering of the Seconda Università di Napoli are located.

The Napoli Capodichino International Airport (40°53'02"N, 14°17'10"E, WMO: 16289, IATA: **NAP**, ICAO: **LIRN**) is located within the metropolitan area of Napoli, at an elevation of 80 m above sea level and a distance from the sea of 4.5 Km. The surroundings are densely build. SYNOP historical three-hourly records from 1952 to 2011 are available for this site, together with METAR historical hourly records from 1974 to 1999 and semi-hourly from 2000 to 2011. The mean wind climate is dominated by north-north easterly and south-south westerly winds. Orography effects may affect the measurements. (Figure 1).

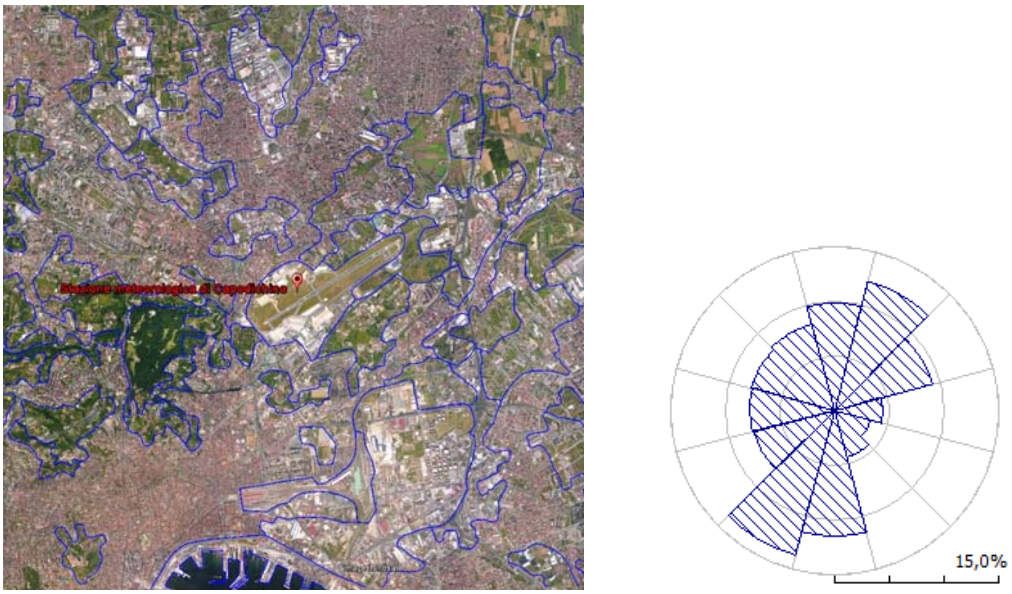

Figure 1. Napoli Capodichino International Airport site and wind frequency rose.

The Carlo Romagnoli Grazzanise Airport (41°03'39,"N, 14°04'55"E, IATA: **QTC**, ICAO: **LIRM**) is located 27 km north of Napoli, at an elevation of few metres above sea level and a distance from the sea of 12 km. The surroundings are flat agricultural areas. SYNOP historical three-hourly records from 1976 to 2011 are available for this site. The mean wind climate is dominated by north-easterly and west-south westerly winds. (Figure 2).

The Capri Damecuta Heliport (40°33'30"N, 14°12'05"E, ICAO: **LIQC**) is located on the western coast of the island, at the top of a 150 m cliff and at a distance from the sea of 300 m. Orography effects are expected to be very strong. SYNOP historical three-hourly records from 1955 to 2011 are available for this site, with many missing measurements. The mean wind climate is rather omnidirectional, only slightly dominated by west-south westerly winds. (Figure 3).

Finally, the Aversa site (40°58'00"N, 14°12'00"E) is located 15 km north of Napoli, at an elevation of 50 m above sea level and a distance from the sea of 15 Km. The surroundings are flat and densely build. (Figure 4).

Figure 2. Carlo Romagnoli Grazzanise Airport site and wind frequency rose.

Figure 3. Capri Damecuta Heliport site and wind frequency rose.

Figure 4. Aversa site.

The generalized mean and extreme wind climate at the three sites was analyzed using WAsP and WAsP Engineering software. The roughness height was calculated for 12, 30° degree sectors, using the CORINE Land Cover data 2000 (CLC 2000). Orography maps were obtained from SRTM (Shuttle Radar Topography Mission) 1" resolution (30 m) data.

Measurements are presently being taken at the Aversa site using a pulsed wave WindCube V2 wind LIDAR, installed at 10 m of elevation (Figure 5). Measurements started in mid October.

Figure 5. WindCube V2 installation.

PRELIMINARY RESULTS

In Table 1 the Weibull parameters *A* and *k* and mean wind speed for the Aversa site evaluated from different historical data are shown. In Tables 2 and 3 the Fifty-year wind speed evaluated from different historical data through Extreme Value Analysis and Peak Over Threshold method are shown.

Table 1. Weibull parameters *A* and *k* and mean wind speed for the Aversa site evaluated from different historical data.

Site	z = 10 m a.g.l.				z = 50 m a.g.l.				z = 100 m a.g.l.			
	A [m/s]	k	U [m/s]	P [W/m^2]	A [m/s]	k	U [m/s]	P [W/m^2]	A [m/s]	k	U [m/s]	P [W/m^2]
Capodichino METAR	1.6	1.10	1.6	12	3.3	1.3	3.0	61	4.1	1.4	3.8	100
Capodichino SYNOP	1.7	1.11	1.6	13	3.4	1.3	3.1	68	4.3	1.4	3.9	111
Grazzanise	1.6	1.15	1.5	9	3.1	1.3	2.8	48	4.0	1.4	3.6	84
Capri	1.7	0.95	1.7	22	3.4	1.0	3.3	120	4.4	1.1	4.1	195

Table 2. Fifty-year wind speed for the Aversa site evaluated from different historical data through Extreme Value Analysis.

Site	z = 10 m a.g.l.		z = 50 m a.g.l.		z = 100 m a.g.l.		z = 150 m a.g.l.		z = 200 m a.g.l.	
	U_{50} [m/s]	*dev.*	U_{50} [m/s]	*dev.*	U_{50} [m/s]	*dev.*	U_{50} [m/s]	*dev.*	U_{50} [m/s]	*dev.*
Capodichino METAR	21.6	1.89	34.1	2.97	39.4	3.42	42.5	3.69	44.7	3.91
Capodichino SYNOP	22.2	1.85	35.5	2.98	41.2	3.46	44.4	3.73	46.6	3.92
Grazzanise	17.8	1.54	28.5	2.47	32.7	2.82	34.9	2.99	36.6	3.13
Capri	21.1	2.96	33.8	4.72	39.4	5.51	42.5	5.93	44.5	6.22

Table 3. Fifty-year wind speed for the Aversa site evaluated from different historical data through Peak Over Threshold Method.

Site	z = 10 m a.g.l.		z = 50 m a.g.l.		z = 100 m a.g.l.		z = 150 m a.g.l.		z = 200 m a.g.l.	
	U_{50} [m/s]	*dev.*	U_{50} [m/s]	*dev.*	U_{50} [m/s]	*dev.*	U_{50} [m/s]	*dev.*	U_{50} [m/s]	*dev.*
Capodichino METAR	24.1	3.04	38.4	4.92	43.8	5.39	46.8	5.63	49.0	5.84
Capodichino SYNOP	23.2	2.25	38.2	3.96	43.1	4.21	45.7	4.28	47.7	4.41
Grazzanise	17.2	0.86	27.5	1.17	31.8	1.71	34.2	1.98	35.8	2.07
Capri	24.8	3.75	41.0	6.54	47.1	7.35	50.2	7.71	52.4	8.02

It is clear how the results depend very much on historical data and on the method of evaluation adopted.

Finally, as an example in figure 6 a comparison is presented of the measured data at 10 m (Capodichino) and of the projected data at 50 m (Aversa) for the dominant sector (195°-225°) and omnidirectional. All the directional data are found to correlate very well, while omnidirectional data show a larger scatter. This suggests that when projections are made at a site of interest using directional data, these can be quite accurate, given that the model is properly calibrated.

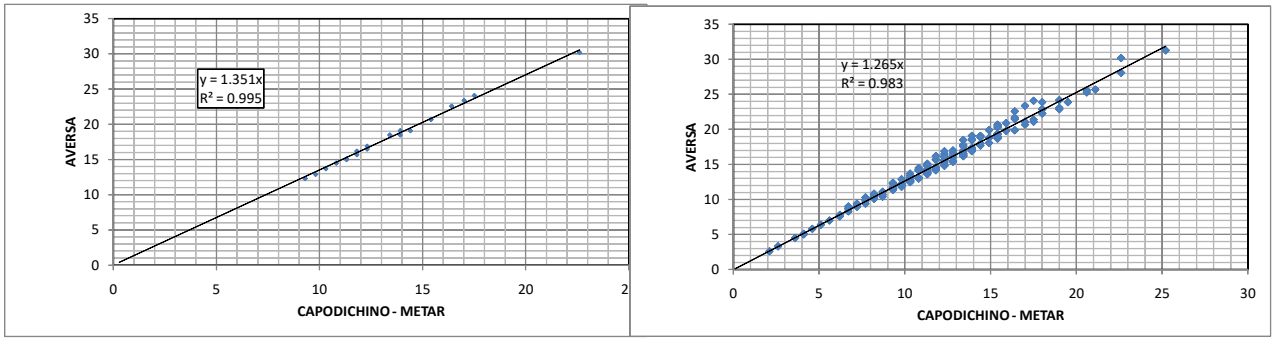

Figure 6. Comparison of measured data at 10 m (Capodichino) and predicted data at 50 m (Aversa): 195°-225° sector (left) and omnidirectional (right).

ACKNOWLEDGEMENTS

The results presented in this paper have been produced in the framework of the research project GELMINACAL, founded by the Italian Ministry for University (MIUR).

REFERENCES

[1] Stull R.B. “An Introduction to Boundary Layer Meteorology”. Kluwer, Dordrecht, 1988.
[2] Manwell J.F., McGowan J.G., Rogers A.L. “Wind energy explained: theory, design and application” 2002.

THE INTERNATIONAL CONFERENCE ON
WIND ENERGY HARVESTING 2017
20-21 April 2017
Coimbra, Portugal

Paper 204

EFFECTS OF STABLE ATMOSPHERIC CONDITOIN AND VARIOUS FOREST DENSITIES ON WIND RESOURCE

Ashvinkumar Chaudhari[1]
Lappeenranta University of Technology
Lappeenranta, Finland

Boris Conan[2]
Ecole Centrale de Nantes
Nantes, France

Antti Hellsten[3]
Finnish Meteorological Institute
Helsinki, Finland

ABSTRACT

The wind profile over a forested terrain is characterized by strong shear and high turbulence level. In addition, diurnal and seasonal variations in weather conditions highly affect the Atmospheric Boundary Layer (ABL) characteristics. Therefore, studies on the combined impact of forest and thermal stratifications are of utmost importance for wind resource assessment. In this work, Large-Eddy Simulations are carried out under neutral and stable conditions to study the effects of thermal stratifications on the ABL profile developed over a forest. Three different types of forests are tested, using different Leaf Area Densities, to evaluate how the wind resource is affected in both, neutral and stable, conditions. Comparisons are performed in order to elucidate the combined effect of a forest cover and stable conditions.

NOMENCLATURE

H	=	Height of forest (m)
U	=	Mean horizontal velocity (m/s)
U_{hub}	=	Mean horizontal velocity at hub height (m/s)
U_g	=	Geostrophic wind (m/s)
$\sigma_x, \sigma_y, \sigma_z$	=	Root-Mean-Square of the velocity fluctuations (m/s)
α	=	Wind shear (-)
k	=	Turbulent kinetic energy, TKE (m^2/s^2)
$\overline{(u'w')}$	=	Reynolds shear stress (m^2/s^2)
Q_H	=	Heat-flux on the canopy-top ($K \cdot m/s$)
γ	=	Wind direction (°)
u_*	=	Frictional velocity (m/s)
x, y, z	=	Cartesian coordinates, z is the vertical coordinate (m)
z_0	=	Roughness length (m)

INTRODUCTION

Forest areas are of increasing interest for the wind energy industry, as such locations have a huge benefit in terms of the social acceptance of wind energy. However, the wind profile over a forested terrain is characterized by strong vertical shear and high turbulence levels. As a result, wind turbines installed within forest areas are expected to have high aerodynamic loads, which would eventually affect their life-time and maintenance costs. In addition, diurnal and seasonal variations in weather conditions induce drastic changes to the atmospheric boundary

1 Post-doctoral researcher, School of Engineering Science, Lappeenranta University of Technology (LUT), P.O. Box 20, FI-53851 Lappeenranta, Finland, Email: Ashvinkumar.Chaudhari@lut.fi
2 Assistant professor, Equipe Dynamique de l'Atmosphère Urbaine et Côtière, Ecole Centrale de Nantes, F-44321 NANTES Cedex 3, France, Email: boris.conan@ec-nantes.fr
3 Senior Research Scientist, Atmospheric Dispersion Modelling, Finnish Meteorological Institute, P.O. Box 503, SF-00101, Helsinki, Finland, Email: Antti.Hellsten@fmi.fi

layer (ABL). Among the other ABL conditions, Stable boundary-layers (SBLs) are relatively shallow and are characterized by lower and sometimes intermittent turbulence levels, strong vertical variations in wind speed (shear) and direction (veer), and a relatively high wind near the top of SBL. At this height, the local wind can become super-geostrophic and form a Low Level Jet (LLJ) [1]. As a result, for the same geostrophic wind, SBLs may provide larger energy potential compared to neutral and convective ABLs. However, the SBL may induce high deformation strain on the blade as well as greater structural fatigue loads due to strong shear and veer [1]. Seasonal variations also influence forest properties as trees drop their leaves in autumn but sprout new leaves in spring and they start growing again. Thus forest properties are being changed during a year, and this leads to changes in the lower part of the ABL. These observations emphasize the need for a more detailed understanding of the wind resource over forest areas under the influence of stably stratified atmospheric conditions. This is utmost important for new wind-energy harvesting in the Northern countries, where the cold climate condition is typical as well as the share of forest in the total land-area is much higher, for example up to 75% in Finland. From a numerical point of view, little literature [2, 3] is available on coupling forest and stable conditions. Therefore, more research is needed to improve our understanding of the wind characteristics and the turbulence organization in the lower part of the ABL, as this regime is highly relevant to wind energy.

This work aims at studying the effect of stable stratification over a forest cover compared to that of neutral stratification. Further, the effects of a number of forest densities, representing seasonal variations in tree, on wind resources are studied for the both thermal conditions in order to see how forest properties influence the local wind and that how it affects the wind resource. The study is based on numerical simulations which are carried out using the Large-Eddy Simulations (LES) approach. To distinguish thermal effects (SBL) and dynamic effects (presence of the forest), all simulations are also carried out without forest (i.e. over flat-terrain situations). In the present abstract, numerical results of the wind characteristics over a dense forest under the influence of neutral and stable conditions are presented and discussed. The result comparison is shown into perspective for wind energy applications.

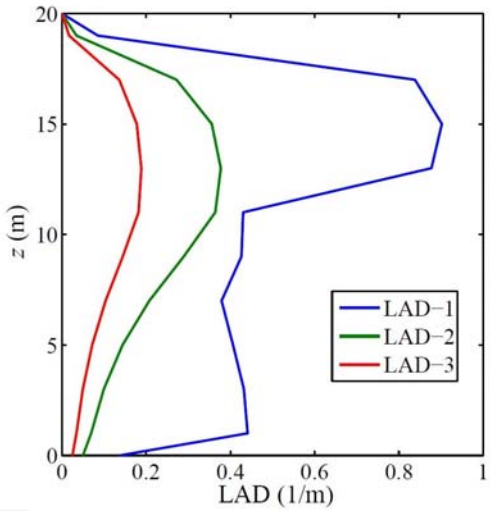

Fig. 1: Vertical distributions of the three LAD profiles used in the study

METHODOLOGY

For both atmospheric conditions, different forest properties are considered to see the influence of a forest cover on the ABL. Three different Leaf Area Densities (LAD) are set up (Figure 1), representing tree's biomass-area per unit volume (1/m). The three forest types are considered horizontally homogenous but vertically heterogeneous. Among the LAD profiles utilized in this work, the first one (LAD-1) is adopted from the wind-tunnel experiment [4], which represents a sort of artificial forest made of metallic meshes. The second LAD profile (LAD-2) represents pine forest located at the Ryningsnäs site in Sweden [5]. Pine forests are typical in the northern countries. Originally, Nebenfuhr and Davidson (2015) estimated this profile and used in their recent numerical study [2]. The third LAD profile (LAD-3) uses the same shape of the LAD-2, but with less amplified density. In this way, the LAD-3 profile represents the same type of trees as in the case with LAD-2, but with less biomass area. In all cases, the forest height is fixed to 20 m.

In the numerical simulations, the drag-force approach [6] is used to model the presence of the forest canopies on the ground. To consider the flow over an infinitely long forest, periodic boundary conditions are used

in both horizontal directions. The incompressible filtered Navier-Stokes equations, along with a potential-temperature equation, are solved including the Coriolis and buoyancy forces. The simulations are performed using a computational domain of $80H \times 40H \times 20H$ in longitudinal (x), transversal (y) and vertical (z) directions, respectively. Here, $H = 20$ m is the height of the forest in all cases. The domain is discretized into $320 \times 160 \times 126$ grid-cells in x, y and z directions respectively. In this way, the grid resolution in both horizontal (longitudinal and transversal) directions is fixed to 5 m. In the vertical direction, the grid resolution is set to 2 m in the forest ($z < 20$ m), and is then gradually decreased to reach 5 m at the top boundary. The flow is driven by fixing the pressure gradient force which adjusts the geostrophic wind to $U_g = (6.13,0,0)$ m/s at the height of 400 m. The Monin-Obukhov scaling laws are used at the lower boundary. In the stable case, the potential temperature θ is initialized to rise from 297 K at the ground to 300 K at the top boundary. Below 100 m, random fluctuations with amplitudes of 0.1 K and 0.5 m/s are added to the initial potential-temperature and horizontal-velocity fields, respectively. Following [2], the stable case is based on the observations of the Ryningsnäs field measurement [5], with a heat flux of $Q_H = 0.005\ \mathrm{K \cdot m/s}$ at the top of the canopy. The latitude is set to 57° that corresponds to the Ryningsnäs field-measurement site.

RESULTS

In this section, only the results obtained using LAD-1 profile are presented. However, in the full paper, the present results will be compared with other results which will be obtained using the rest of the two forest properties (LAD-2 and LAD-3). Figure 2 compares the LES results from the two thermal conditions normalized by the friction velocity. The LES results are time-averaged for 50-hour after the flow development. According to Figure 2, the normalized mean wind-speed in the stable condition is higher by 34% at $z = 5H$ (at hub height) and 40% at $z = 20H$ as compared to the neutral case. The maximum difference is found to be 71% at $z = 13.4H$ due to the LLJ. Such velocity speed-ups observed under the stable conditions may lead to high power potential. Further, the Root-Mean-Square (RMS) of the longitudinal velocity fluctuation (σ_x) is smaller in the stable case compared to that in the neutral case at every height above the forest. The transversal (σ_y) and vertical (σ_z) fluctuations are found to be of similar amplitudes for $1 \leq z/H < 5$ (Fig. 2b). The resolved turbulent kinetic energy (Fig. 2d) is smaller by about 71% in the stable case at $z = 5H$ with respect to that in the neutral case. The boundary-layer height in the stable case is found to be at $z/H = 15$, which is about 75% of the boundary-layer depth in the neutral case. The boundary-layer depth in the neutral case is the same as the height of the computational domain ($20H$). The lower boundary-layer height is generally responsible for the decreased level of turbulence in the stable case.

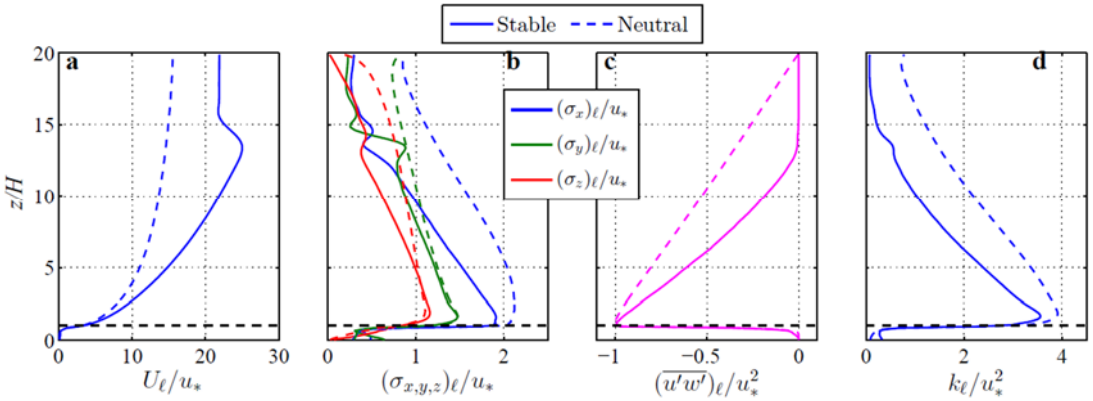

Fig. 2: Vertical profiles of the normalized horizontal mean wind-speed (a), the RMS of the fluctuations (b), the resolved Reynolds shear stress (c), and the resolved turbulent kinetic energy (d). The solid and dashed lines represent the stable and neutral cases respectively

To discuss the results from a wind energy perspective, a typical middle size wind turbine (≈ 2.5MW) with a diameter of 90 m and hub height of 100 m is selected. Figure 3 compares the normalized LES results from the two stability conditions as well as with the VDI norms [7]. In Figure 3, the altitude is normalized with the hub height, and the light-grey background depicts the rotor diameter. The comparison of the velocity profiles between the VDI norms [7] (neutral & no forest) and the neutral simulation with forest in Figure 3(a) clearly shows an increased wind shear (due to the forest) affecting the entire rotor area. The shear exponent α (Figure 3d) is very high due to the forest and the stable conditions amplify it. Further, Figure 3(b) indicates that the stably stratified condition dramatically affects the change in the wind direction. A rotation of 10° is observed through the rotor in stable conditions, whereas only 3° is observed in neutral conditions. Such changes in wind direction (due to the

prevailing of the Coriolis forces compared to the inertial forces and turbulent mixing) are expected to affect power production and to increase the yawing moment with possibly harmful consequences for turbine lifetime.

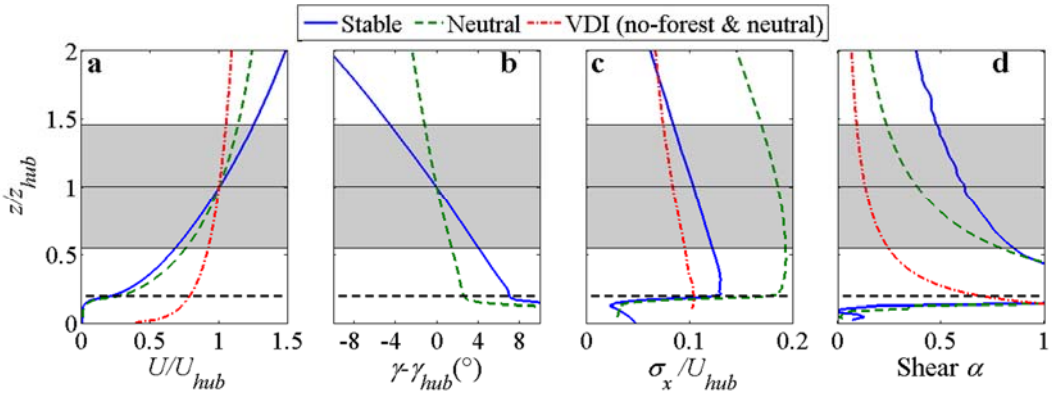

Fig. 3 Comparison of the wind characteristics in neutral (dashed lines) and stable (solid lines) conditions over the forest compared to the VDI norms [7] (dash-dotted lines) over a flat terrain. (a) The normalized horizontal mean wind speed, (b) the mean wind angle with respect to the wind direction at hub height, (c) the turbulence intensity in the longitudinal direction, and (d) the wind shear factor

The global Turbulence Intensity ($TI = \sigma_x/U_{hub}$) is shown in Figure 3(c). Under neutral condition, the forest introduces a turbulence level of about 18% at hub height, and maintains it throughout the boundary layer. This is a very high increase compared to the VDI norms [7] in neutral conditions without forest (9%). The shear exponent (Table 1) is also drastically increased compared to the VDI norms. In stable conditions, the negative thermal flux reduces the turbulence level down to about 11% at hub height and again decreases to 9% at the rotor-top position. Less or sometime internment turbulence level is one of the characteristics of stably stratified conditions in general. However, the shear exponent in the stable case is drastically increased compared to the VDI [7] and to the neutral case.

Table 1 compares the LES statistics with the IEC standards [8]. The IEC standards are used for the selection of the turbine by providing the shear exponent, the reference speed, and the reference turbulence intensity specific of each turbine category. The TI under neutral conditions reaches to the maximum limit of the IEC standards, but stable conditions reduce it back to within the IEC limits. For both condition, the shear is outside the IEC recommendations. Thus forest violates, especially under neutral conditions, the IEC standards of safe turbine operation.

Table 1. Calculated shear exponent and TI at hub height from the simulations compared to the norms [7, 8]

	Shear α	TI
Stable (forest)	0.62	11%
Neutral (forest)	0.41	18%
VDI (Neutral-flat)	0.14	9%
Max IEC	0.2	18%

CONCLUSIONS

For alone-standing turbine in forest, stably stratified conditions are may be favorable as they damp some of the extra turbulence coming from forest as well as they increase wind speed. With respect to a flat terrain, the shear and turbulence levels at hub height are increased by the presence of the forest in both conditions. In the neutral case, a high (18%) turbulent level is observed at hub height, which in practice might be harmful to wind-turbine operation, as it is on the verge of the IEC limits [8]. The stable stratification is found to amplify the shear factor (by 56% at hub height compared that of the neutral case) and to increase the angle deviation. These two parameters are prejudicial to wind turbines, as high shear may trigger fatigue.

In both conditions, due to the forest, the shear factor is out of the IEC recommendations. However, the stable conditions damp the intensity of the turbulence cause by the forest in an important manner. The TI is decreased from 18% (in neutral) to 11% (in stable) at the hub height. Therefore, neutral stratification is found to be the worst case for turbulence intensity, but stable stratification the worst case for shear factor. It must be

mentioned that the IEC evaluation accounts only for hub height values, whereas numerical results show significant variations vertically even within rotor diameter.

Currently, LES calculations focusing on the LAD-2 and LAD-3 profiles are being carried out. In the full paper, the effects of neutral and stable stratifications on the ABL developed over the three different forests will be discussed in detail. Also, simulations without any forest (i.e. flat terrain) will be carried in order to see the global influence of forest on wind resources under neutral and stable stratifications.

ACKNOWLEDGEMENTS

The computational resources for the numerical simulations were provided by CSC-Finnish IT Center for Science, Espoo (Finland). The author, A. Chaudhari, acknowledges with thanks the support of the TU1304 action "WINERCOST".

REFERENCES

[1] Porté-Agel F., Lu H., and Wu Y. T., “Interaction between large wind farms and the atmospheric boundary layer”, Procedia IUTAM, Vol. 10, 2014, pp 307-318.

[2] Nebenfuhr B. and Davidson L., “Large-Eddy Simulation Study of Thermally Stratified Canopy Flow”, Boundary-Layer Meteorol., Vol. 156, 2015, pp 253–276.

[3] Chaudhari A., Conan B., Aubrun S., Hellsten A., “Numerical study of how stable stratification affects turbulence instabilities above a forest cover: application to wind energy”, Journal of Physics: Conference Series, Vol. 753 (3), Article ID: 032037, 2016, pp. 1-12.

[4] Conan B., Aubrun S., Coudour B., Chetehouna K. and Garo J.-P., “Contribution of coherent structures to momentum and concentration fluxes over a flat vegetation canopy modelled in a wind tunnel”, Atmos. Environ., Vol. 107, 2015, pp 329–341.

[5] Arnqvist J., Segalini A., Dellwik E. and Bergström H., “Wind statistics from a forested landscape”, Boundary-Layer Meteorol., Vol. 156, 2015, pp 53–71.

[6] Shaw R.-H. and Schumann U., “Large-eddy simulation of turbulent flow above and within a forest”, Boundary-Layer Meteorol., Vol. 61, 1992, 47–64.

[7] VDI-Guideline, “Environmental meteorology, physical modelling of flow and dispersion processes in the atmospheric boundary layer–applications of wind tunnels”, Report no. 3783/12, 2000.

[8] International Electrotechnical Commission (IEC), “Wind turbines-part 1: Design requirements”, Tech. rep. IEC-61400-1, 2007.

THE INTERNATIONAL CONFERENCE ON
WIND ENERGY HARVESTING 2017
20-21 April 2017
Coimbra, Portugal

Paper 205

ENERGY HARVESTING FROM DIFFERENT AEROELASTIC INSTABILITIES OF A SQUARE CYLINDER

Thomas ANDRIANNE[1]
University of Liège
Liège, BELGIUM

Renar P. ARYOPUTRO[2]
University of Liège
Liège, BELGIUM

Philippe LAURENT[3]
University of Liège
Liège, BELGIUM

Gérald Colson[4]
University of Liège
Liège, BELGIUM

ABSTRACT

This paper presents an experimental and numerical investigation of the power extraction from the oscillations of a square beam due to aeroelastic instabilities. The energy harvesting is performed using a coil-magnet arrangement connected to a variable resistance load with the target objective to auto-power a remote sensor. Two aeroelastic phenomena are investigated: Vortex Induced Vibration (VIV) and cross-flow galloping. The first instability (VIV) is analyzed on a free-standing vertical structure. A second experimental set-up is developed on a horizontal square cylinder supported by springs, free to oscillate vertically as a rigid body. In this case, both galloping and VIV are interacting, leading to interesting characteristics in order to harvest energy from the wind. For both harvesting systems, the characteristics of the aeroelastic phenomena are first studied numerically using a wake oscillator model (for VIV) and a quasi-steady model (for galloping). Then the behavior of each electro-mechanical aeroelastic system is investigated for different reduced wind speeds and load resistances in a wind tunnel. It is shown that the efficiency of the current harvesting device is low, but large enough to power a remote sensor with an adapted measuring strategy.

INTRODUCTION

The amount of smart remote sensors has constantly increased over the last years. The objective of such sensors is to obtain information about the environment (temperature, luminosity, noise, humidity,...) or to take part to communication networks. A main drawback of such systems is the need to supply power to the sensors: conventional power supplies, such as battery or supply cables, consist in the main obstacle to reach a higher integration of microsystems in engineering applications. The *energy harvesting* concept can relax this constrain by using free and renewable energy to power ultra-low power devices.

The objective of this work is to harvest energy from the vibration induced by the wind: in an aeroelastic system a fraction of the energy of the flow is transferred to the structure beyond a critical wind speed. The difficulty concerns the coupling of the harvesting system to the aeroelastic system, which might change the behavior of the global electro-aeroelastic model. Many research works have been dedicated to this topic. Some of them are purely experimental [1-3], numerical [4] or in-between, without modeling the harvester [5].

In the scope of this work, we focus on an experimental and numerical investigation on two types of aeroelastic phenomena: (i) VIV of a vertical structure and (ii) VIV-Galloping of a horizontal structure. The modeling part is devoted to the quantification of the energy harvesting potential of the aeroelastic phenomena. The second part aims to validate the model output and measures the power output of the energy harvester.

[1]Head of Wind Tunnel Laboratory, Aerospace & Mechanical Engineering, University of Liège, Belgium, corresponding author: t.andrianne@ulg.ac.be
[2]Master student in Aerospace Engineering, University of Liège, Belgium
[3]Research Engineer, Microsys Laboratory, Electrical Eng. and Computer Science, University of Liège, Belgium
[4]Research Engineer, Microsys Laboratory, Electrical Eng. and Computer Science, University of Liège, Belgium

METHODOLOGY

For each structure, a wind tunnel test campaign is carried out to measure the amplitude of motion and the electrical power (P_{EH}) as a function of the reduced velocity, for different values of the load resistance. In parallel, the aeroelastic behavior is investigated by adequate numerical models:

- For VIV, the model proposed by Tamura [6] is selected. This model is a wake oscillator type (two degrees of freedom), having the advantage to involve parameters that can be related to static aerodynamic quantities.
- For galloping, the traditional Parkinson model using a fifth order polynomial form of the vertical force coefficient is selected [7]. The empirical constants of this model are available from the literature, as a function of the Reynolds number of interest.

These non-linear models are able to capture the complex aeroelastic behavior of the systems (lockin for VIV and subcritical bifurcation for galloping). In the case of the horizontal beam, where VIV and galloping are expected to interact, the two models are coupled to reproduce this interaction effect, which changes the form of the traditional bifurcation diagram of a square cylinder [8].

In addition, an experimental identification of the dynamic properties of the harvesting system (coil-magnet assembly) is performed. The resulting representation of the harvesting part is coupled to the aeroelastic models presented above in order to obtain a global electro-aeroelastic model.

The models are used to quantify the potential energy transfer between the flow and the structure. Barrero et al. proposed a similar approach using a fluid force model based on experimental data from forced vibration tests [5]. The Root Mean Square (RMS) value of the mechanical power of the aeroelastic motion, denoted P', is calculated by

$$\boldsymbol{P' = \sqrt{1/T \int_0^T \left[F_y(t)\dot{y}(t)\right]^2 dt}} \quad (1)$$

where $\boldsymbol{F_y(t)}$ and $\boldsymbol{\dot{y}(t)}$ correspond to the force along the cross-wind direction and the motion velocity respectively.

The theoretical/model estimations of the efficiency of the systems will be compared to the experimental measurements carried out in the wind tunnel.

EXPERIMENTAL SET-UP

The tests are performed in the multi-disciplinary wind tunnel of University of Liège, in uniform low turbulence flow conditions (TI<0.2%). For each set-up, the model is installed in the test section and the coil-magnet assembly is installed at the tip of the vertical model (figure 1) and on one site of the horizontal one (figure 2). The beam is made of aluminum, has a square section with a side of 50mm, a thickness of 2mm and a length of 1650mm and 1340mm for the vertical and horizontal apparatus respectively.

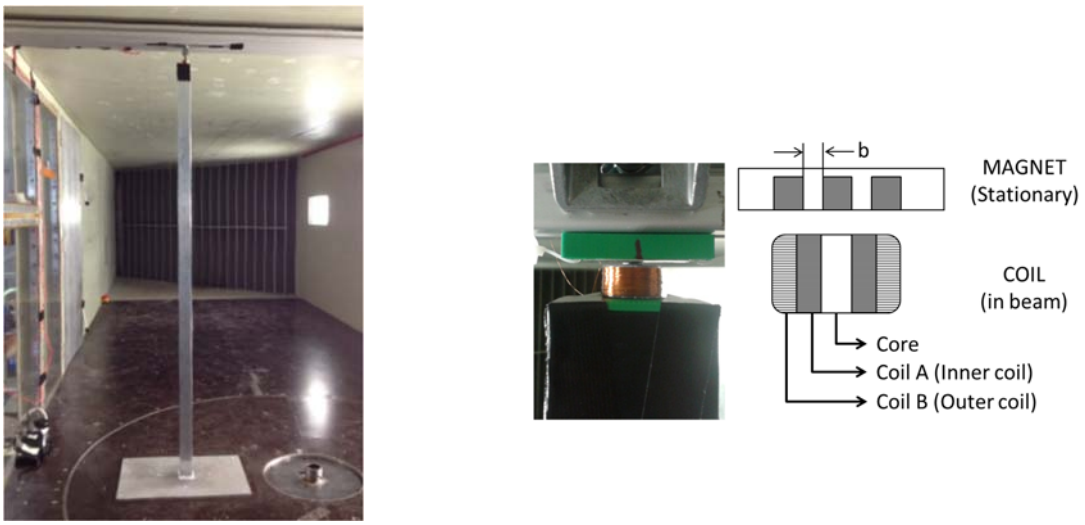

Figure 1. Vertical experimental set-up installed in the test section (left) - Coil/magnet assembly (right)

Figure 2. Horizontal set-up installed in the test section (left) - Coil/magnet assembly (right)

The instrumentation of the model consists in a laser to measure its displacement. The modal properties of the structure with and without the harvester are identified through free responses (hammer impacts) imposed to the beam. A voltmeter measures the voltage through the load resistance (V_L) and the electrical power produced by the harvesting system is calculated by $P_{EH}=V_L^2/ R_L$.

EXPERIMENTAL RESULTS

The electrical power extracted by the coil-magnet assembly in the case of the vertical structure (VIV only) is presented in figure 3. It is observed that the VIV oscillation starts around U^*~7.2~1/0.13, where St=0.13 is a good estimate of the Strouhal number of the square cylinder. The lockin range is equal to $\Delta U^* = 2.5$, which is not very large because of the large value of the Scruton number of the system ($\boldsymbol{Sc} = \frac{2\pi m\xi}{\rho D^2} = 6$).

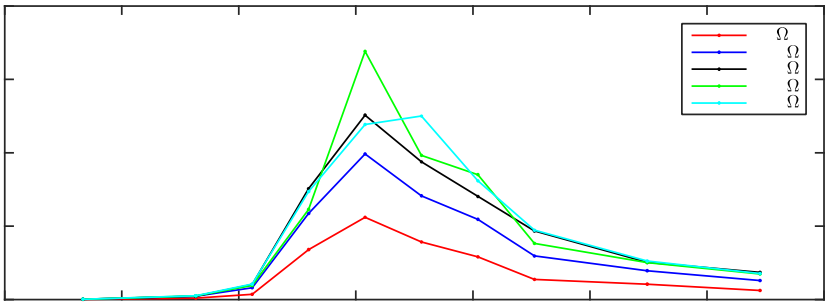

Figure 3. Vertical set-up (VIV): Electrical Power output vs. U^*, for different values of the load resistance

The maximum electrical power is reached around $U^* \sim 8$ and for a load resistance around 400Ω. The optimum value of the load resistance matches the resistance of the coil (406Ω) in accordance with the Maximum Power Transfer Theorem.

Figure 4 presents the VIV-galloping power output as a function of the reduced velocity for the horizontal set-up. In this case, there is a clear interaction between VIV (the critical VIV velocity is shown as a black square) and galloping. The galloping phenomenon is triggered by the VIV instability and the resulting bifurcation branch follows a linearly the reduced velocity U^*. It is observed that the load resistance has a strong effect on the resulting

oscillation amplitude and R_L=255Ω corresponds to the optimal value, matching the internal resistance of the coil (R_C=257Ω), similarly to the case of the vertical set-up presented above.

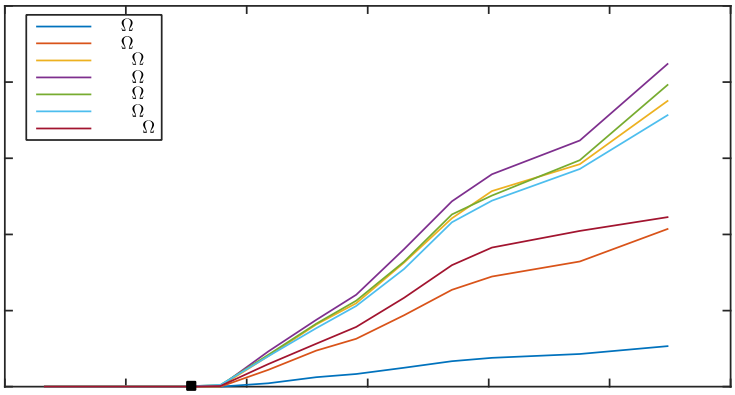

Figure 4. Horizontal set-up (VIV-Galloping): Electrical Power output vs. U^*, for different values of the load resistance

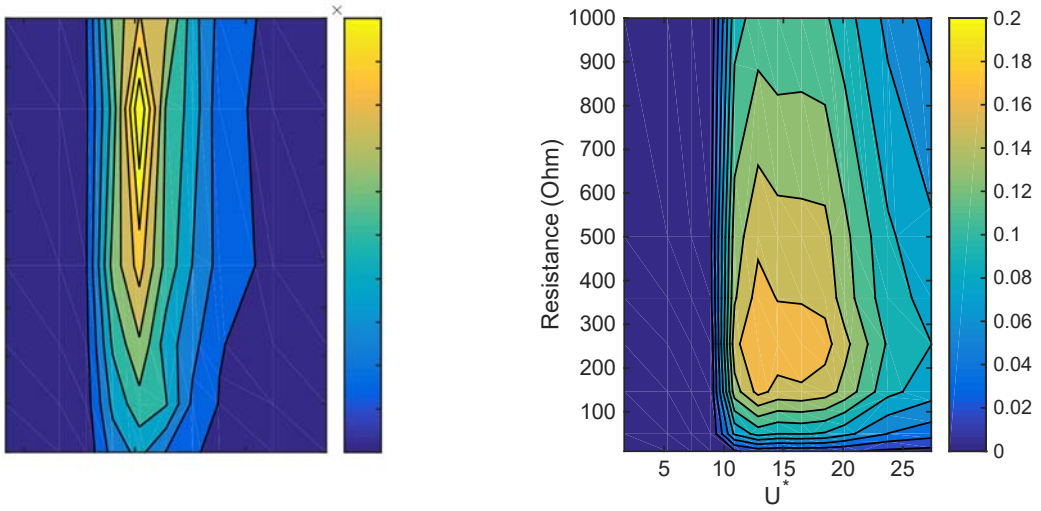

Figure 5. Efficiency (in %) of the harvesting systems: Vertical set-up (left) and horizontal set-up (right)

Figure 5 presents the efficiency (P_{EH}/P_{WIND}) in the plane (U^*,R). In the left plot, the VIV optimal efficiency is clearly localized on a peak, centered on (8,400). Beyond this peak (U^*>10), no more energy can be extracted by the system since the lockin phenomenon ended. In the right plot, the situation is different: beyond the critical velocity (U^*=10), the system is unstable and energy can be harvested up to U^*=30 (which is the limit of the test). Nevertheless, the optimum harvesting region ranges between U^*=10 and U^*=20 and R=150Ω and R=350Ω. This is a clear difference between the two harvesting apparatus.

On the energy harvesting point of view, the electrical power output the ratio P_{EH} / P_{WIND} is lower than 10^{-5} for the VIV set-up (2 10^{-3} for the VIV-galloping). This result brings out the poor efficiency of the current design choice for the coil/magnet assemblies to harvest the mechanical energy of motion.

On the auto-powering point of view, it is worth mentioning that the value of P_{EH}, around 0.15mW, can be sufficient to carry out measurements with ultra-low power devices. Such devices can be operational and provide measurements from 0.01mW (at low acquisition frequency). In addition, small size electrical storing devices (batteries, capacitors or super-capacitors) can be used in order to establish a measuring strategy for which the measuring time is adapted to the available power (including sleeping times of the sensor). If needed, an electrical storing device (e.g. battery) can be used to power the wireless sensor node set with a proper duty cycle in order to

achieve a balanced energy equation. Rather than wasting this mechanical energy, the energy induced by the VIV phenomenon can be used to self-monitor the harvesting apparatus itself, for predictive maintenance purpose [9].

CONCLUSIONS

The present work investigates the potential energy harvesting from the VIV and galloping phenomena of a square cylinder in an airflow. In this abstract, primary experimental results are presented and the electrical power output is shown for the two tested configurations (vertical and horizontal). As expected, the global efficiencies values (P_{EH}/P_{WIND}) are very low (~0.15mW for VIV and ~15mW for VIV-galloping) but sufficient to power sensors with an adapted strategy. In the conference paper, numerical models are used to compute the amount of mechanical power of the beam undergoing oscillations.

REFERENCES

[1] Sousa V. C., Anicezio M de M, De Marqui Jr, C., Erturket A., "Enhanced Aeroelastic Energy Harvesting by Exploiting Combined Nonlinearities: Theory and Experiment", Smart Materials and Structures 20 (2011) doi:10.1088/0964-1726/20/9/094007

[2] P. Hémon X. Amandolèse and T. Andrianne, Galloping oscillations of prisms and energy harvesting in wind tunnel, First International Symposium on Flutter and its Application, Tokyo, 15-17 May 2016, Japan

[3] Bernitsas M. M., Raghavan K., Ben-Simon Y., Garcia E.M., "VIVACE (Vortex Induced Vibration Aquatic Clean Energy): A New Concept in Generation of Clean and Renewable Energy From Fluid Flow", Journal of Offshore Mechanics and Arctic Engineering. ASME Trans. 130 (2008) 041101.

[4] Tang L., Païdoussis M.P., Jian J., "Cantilevered flexible plates in axial flow: Energy transfer and the concept of flutter-mill", Journal of Sound and Vibration 326 (2009) 263-276

[5] Barrero-Gil A., Pindado S., Avila S., "Extracting energy from Vortex-Induced Vibrations: A parametric study", Applied Mathematical Modelling, Volume 36, Issue 7, 2012, 3153-3160

[6] Tamura Y. and Matsui G., "Wake-oscillator model of vortex-induced oscillation of a circular cylinder", Proceedings of the 5th International Conference on Wind Engineering, Vol.2, Fort Collins, Colorado, USA, July 1979, pp. 1085-1092

[7] Parkinson, G. V., Smith, J. D., 1964. The Square Prim as an Aeroelastic Non-linear Oscillator. Quarterly Journal of Mechanics and Applied Mathematics, XVII, 225-239.

[8] Mannini C., Marra A. M., Bartoli G., "VIV–galloping instability of rectangular cylinders: Review and new experiments", Journal of Wind Engineering and Industrial Aerodynamics 132 (2014), 109-124

[9] Ph. Laurent, F. Dupont, S. Stoukatch, F. Axisa. "Ultra-low power microsystems integrated", Proc. Smart Systems Integration Conf. (SSI2015), Copenhague, Danemark, 11-12 Mars 2015

THE INTERNATIONAL CONFERENCE ON
WIND ENERGY HARVESTING 2017
20-21 April 2017
Coimbra, Portugal

Paper 206

HIGH-ORDER DETACHED-EDDY SIMULATION OF UNSTEADY FLOW AROUND NREL S826 AIRFOIL

Özgür Yalçın[1]
METU
Ankara, Turkey

Kenan Cengiz[2]
METU
Ankara, Turkey

Yusuf Özyörük[3]
METU
Ankara, Turkey

ABSTRACT

Delayed-detached eddy simulation (DDES) is a promising approach for unsteady turbulent problems. The several weaknesses of the model limit its use to detached flows. However, recent studies have enhanced it considerably through several modifications, such that DDES has been applicable to attached flows as well. In this study, flow around the NREL S826 airfoil designed for use in HAWTs is aimed to simulate using a DDES model with a shear-layer-adaptive length scale, which is a recent enhancement over DES models. The solver, which has been developed for aeroacoustic purposes, used features fourth-order spatial accuracy with dispersion-relation-preserving (DRP) scheme. Simulations will be done at a Reynolds number of 145000 and near stall angles of attack to analyze the stall characteristics of the airfoil. Then, the aerodynamic coefficients will be compared with the METUWIND experimental data and the DDES results from another study in METU. This study aims to improve the results with eliminating the mentioned limitations of DDES in low-Reynolds number flows as well as with reducing the grid cells thanks to the low-dissipation and low-dispersion scheme of the solver.

INTRODUCTION

In modern wind turbines, the blade noise is the primary noise source which are mostly related to turbulent flow structures around the blades and these structures generate the noisiest waves of wind turbines [1,2]. Accurate turbulent flow solutions for aeroacoustic purposes need proper numerical schemes and turbulence modeling. Since acoustic waves can propagate without dissipation and dispersion losses over long distances, numerical schemes employed must be non-dissipative and non-dispersive. For this purpose, a Navier-Stokes solver based on the fourth-order (in spatial accuracy) finite volume approach of [3] with low-dissipation and low dispersion benefits has been developed. While low dissipation is provided with a fourth-order scheme, low dispersion is provided with 'dispersion-relation-preserving' (DRP) feature proposed by Tam and Webb [4]. The development process of this solver and validation test results have demonstrated and discussed in the study of Cengiz and Özyörük [5]. Despite the fact that the solver is designed for aeroacoustic purposes, the inherent features of the numerical scheme, such as fourth-order DRP discretization, would benefit proper resolution of the turbulent structures in the flow.

Instead of directly resolution of eddies in turbulent flow situations, there are several turbulence modelings in use to reduce the computational cost down to feasible levels. For instance, unsteady Reynolds-averaging Navier-Stokes (URANS) models all eddies by a universal model; on the other hand, large eddy simulation (LES) models small eddies and resolves the large ones. However, they both have some drawbacks. While RANS could not give accurate results for large separation cases, LES needs extremely fine mesh domains in boundary layers. Although

1 Research Assistant, Aerospace Engineering Department, METU, Turkey / oyalcin@ae.metu.edu.tr
2 Research Assistant, Aerospace Engineering Department, METU, Turkey / kcengiz@ae.metu.edu.tr
3 Professor, Aerospace Engineering Department, METU, Turkey / yusuf.ozyoruk@ae.metu.edu.tr

detached eddy simulation (DES), aimed to overcome these drawbacks, models eddy viscosities in boundary layers via unsteady RANS and activates LES at the outer boundary layer regions, it may develop less eddy viscosity in boundary layers by activating LES earlier due to severe grid cases (modelled-stress depletion (MSD) problem). Consequently, delayed detached eddy simulation (DDES), which solves the MSD problem by limiting the length scales with eddy viscosities, is introduced in [6]. On the other hand, DES models are mainly designed for detached flow cases, as the name infers. When properly adjusted, nevertheless, it may even resemble wall-modeled LES (WMLES) except that it uses RANS equations for eddy viscosity in its LES mode as well, instead of Smagorinsky-type subgrid viscosity definitions typically used in LES approaches. Properly adjusting the model here is meant to be the modifications designed to overcome certain weaknesses proposed and cured in [7,8]. A more recent modification is designed by [9] additionally accelerates the transition to LES mode in shear layers. This version of DES, which is called "shear-layer-adaptive DES (SLADDES)", is implemented and tested in this study, in an aim to obtain good results even in attached flow cases. In this study, SLADDES simulations are performed around the NREL S826 blade section profile which was designed for HAWTs of 10-15 meters by the National Renewable Energy Laboratory (NREL). The simulation will be conducted for flow with Reynolds number of 145000 and 8°, 10° and 12° angles of attack which are around the stall threshold of the airfoil. The blade section is located inside a wind tunnel so that the aerodynamic results will be compared with the available experimental test results of METUWIND wind tunnel [10]. Moreover, the results will be compared with the study of Çakmakçıoğlu et al. [11] which performed the same problem with CFD++ commercial software.

METHODOLOGY

The numerical scheme and the turbulence modeling being used will be explained in detail in the final manuscript.

Simulation Setup

H-mesh topology is created in cross section view and extruded along spanwise direction for two chord lengths. Since the wind tunnel has fixed inlet flow direction parallel to its wall surfaces, various attack angles is induced by rotating the airfoil itself. The METUWIND wind tunnel test section dimensions are (1 X 1 X 2) m. The chord length is 0.2 m. However, in this study span/chord length ratio is preferred as 2 rather than the original one which is 5 due to computational cost concerns. 2 chord length in spanwise direction is enough to develop turbulent structures along the blade section. The mesh has 353 X 65 X 65 grid cells. The first grid distance on the wall boundary is set to satisfy $y^+ \sim 1$. Note that the benchmark study has simulated the same problem having approximately 11 million grid cells with $y^+ << 1$. Geometry and block structure together with a view of mesh around the airfoil can be seen in Figure 1.

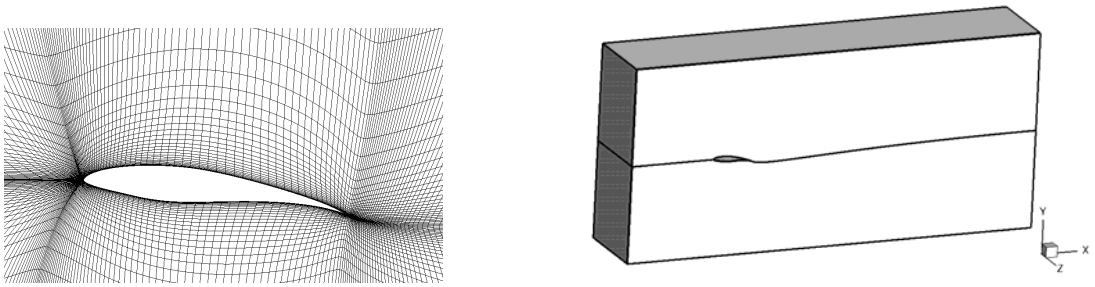

Figure 1. Two block approach and the mesh around the airfoil for 8° angle of attack (2D view on left, 3D view on right). Only odd numbered grid points are shown in 2D view.

Boundary Conditions

Since the influence of boundary layers at top and bottom tunnel walls can be neglected, slip wall boundary condition is applied. The same condition is applied to the lateral walls. On the inlet, free stream velocity and pressure is supplied with use of Riemann invariants, whereas on the outlet the downstream boundary of the tunnel, free stream pressure outlet condition is enforced.

CONCLUSIONS

In the final manuscript of this paper, the SLADDES results will be demonstrated around NREL S826 blade profile at a Re number of 145000. The lift and drag coefficients at angles of attack, 8°, 10°, and 12° near stall will be compared with METUWIND experimental results and another DDES study. In the benchmark study, near stall angles DDES has not shown any improvements over RANS at the Re number of interest while at higher Re numbers, such as 970000, it has obtained more accurate results. DES approaches do not include Kelvin-Helmholtz instability phenomena as required before transition so that they delay the transition. This is why they might have

a trouble at low Re numbers where massively separated flows do not occur. SLADDES has been developed to overcome this weakness. Therefore, this paper aims to test SLADDES implementation into the solver for an attached flow case and improve the DDES results.

ACKNOWLEDGEMENTS

The authors are thankful to METU Center for Wind Energy (METUWIND) for providing parallel computing resources.

REFERENCES

[1] S. Oerlemans. Detection of aeroacoustic sound sources on aircraft and wind turbines. University of Twente, 2009

[2] A.L. Rogers and J.F. Manwell. Wind turbine noise issues. Renewable Energy Research Laboratory, University of Massachusetts, 2004

[3] J.C. Kok. A high-order low-dispersion symmetry-preserving finite-volume method for compressible flow on curvilinear grids. Journal of Computational Physics , 228(18):6811–6832, 2009

[4] C.K.W. Tam and J.C. Webb. Dispersion-relation-preserving finite difference schemes for computational acoustics. Journal of Computational Physics, 107(2):262–281, 1993

[5] K. Cengiz Y. Özyörük. Detached eddy simulation using a high-order low-dissipation low-dispersion computational method for aeroacoustic purposes. In Ankara International Aerospace Conference, 2015

[6] P.R. Spalart, S. Deck, M.L. Shur, K.D. Squires, M.K. Strelets, and A. Travin. A new version of detached-eddy simulation, resistant to ambiguous grid densities. Theoretical and Computational Fluid Dynamics, 20(3):181-195, 2006

[7] S. Deck. Recent improvements in the zonal detached eddy simulation (ZDES) formulation. Theoretical and Computational Fluid Dynamics, 26(6):523-550, 2012

[8] M. L. Shur, P. R. Spalart, M. K. Strelets, and A. K. Travin. A hybrid RANS-LES approach with delayed-DES and wall-modelled LES capabilities. International Journal of Heat and Fluid Flow, 29(6):1638-1649, 2008

[9] M. L. Shur, P. R. Spalart, M. K. Strelets, and A. K. Travin. An enhanced version of DES with rapid transition from RANS to LES in separated flows. Flow, Turbulence and Combustion, 95(4):709-737, 2015

[10] Y. Ostavan, H. Amiri, and O. Uzol. Aerodynamic Characterization of NREL S826 Airfoil at Low Reynolds Numbers. RUZGEM 2013 Conference on Wind Energy Science and Technology, METU Ankara Campus, 2013

[11] S.C. Çakmakçıoğlu, I.O. Sert, O. Tuğluk and N. Sezer-Uzol. 2-D and 3-D CFD Investigation of NREL S826 Airfoil at Low Reynolds Numbers. In Journal of Physics: Conference Series (Vol. 524, No. 1, p. 012028), 2014

THE INTERNATIONAL CONFERENCE ON
WIND ENERGY HARVESTING 2017
20-21 April 2017
Coimbra, Portugal

Paper 207

IMPACT OF THE OFFSHORE WIND FARM ALPHA VENTUS ON THE LOCAL WIND CLIMATE IN THE NORTH SEA – ANALYSIS OF DATA FROM FINO1

Cornelia Kalender[1]
Ruhr-Universität Bochum,
Wind Engineering and Flow Mechanics
Bochum, Germany

Simon Tewolde[2]
Ruhr-Universität Bochum,
Wind Engineering and Flow Mechanics
Bochum, Germany

Simon Wiedemann[3]
Ruhr-Universität Bochum,
Wind Engineering and Flow Mechanics
Bochum, Germany

Rüdiger Höffer[4]
Ruhr-Universität Bochum,
Wind Engineering and Flow Mechanics
Bochum, Germany

ABSTRACT

Seven years before the first German wind farm alpha ventus was built in the North Sea the research platform FINO1 was put in operation in 2003. Equipped with many different measurement techniques for meteorological and oceanographic parameters the aim of FINO1 is to document the local environment before and after the wind farm was build. Along the mast with 100m in height the measured wind velocities and directions are analysed in this work. The influence of the wind farm on the local measured wind climate can be clearly shown. The mean velocities in sectors where turbines are located decreases while the turbulence intensity increases.

NOMENCLATURE

A	=	Scaling factor of Weilbull distribution (m/s)
k	=	Shape factor of Weilbull distribution
u	=	Wind velocity (m/s)
$\bar{u}$	=	10 minutes mean wind velocity (m/s)
I_u	=	Turbulence intensity (%)
σ_u	=	Standard deviation of wind velocity

INTRODUCTION

Due to the planned exit from nuclear and fossil fuel energy in the next future, the importance of renewable energy is still growing. Especially the energy generation with offshore wind farms is promising to carry a higher output than onshore wind-farms. On one hand this is caused by the stronger wind velocities close to the water level compared to wind over terrain and on the other hand by the more uniform sea-weather. Contrary to these advantages, the construction and operating costs of offshore farms are higher. In order to keep this as low as possible, particularly the repair and service costs, a detailed knowledge about the dynamic loads from wind and

1 Postdoctoral researcher., Wind Engineering and Flow Mechanics, Faculty of Civil and Environmental Engineering, Ruhr-Universität Bochum, Universitätsstraße 150, 44801 Bochum, Germany / cornelia.kalende@rub.de
2 Doctoral researcher, Wind Engineering and Flow Mechanics, Faculty of Civil and Environmental Engineering, Ruhr-Universität Bochum, Universitätsstraße 150, 44801 Bochum, Germany / simon.tewolde@rub.de
3 Graduate student, Wind Engineering and Flow Mechanics, Faculty of Civil and Environmental Engineering, Ruhr-Universität Bochum, Universitätsstraße 150, 44801 Bochum, Germany / simon.wiedemann@rub.de
4 Professor, Wind Engineering and Flow Mechanics, Faculty of Civil and Environmental Engineering, Ruhr-Universität Bochum, Universitätsstraße 150, 44801 Bochum, Germany / ruediger.hoeffer@rub.de

waves is necessary. Therefore, the research platform FINO 1, shown in Figure 1, was put in operation in 2003 in the North Sea of Germany, 45 Kilometers northwards of the city Borkum. Their task is to monitor the local wind climate and the sea condition in order to provide an extensive continue database for harvesting and design of offshore wind energy converters and farms. Besides the data for operational concepts, the environmental conditions and the impact of the wind farms on the environment shall be investigated [1]. This is possible since 2010 the first German offshore wind farm alpha ventus was built in the neighborhood close to this research platform (see Figure 1).

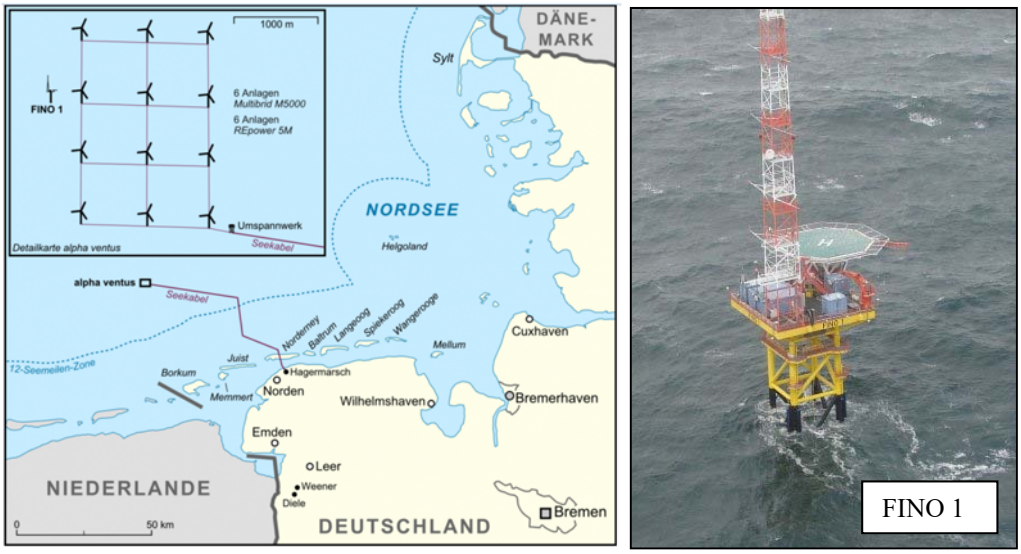

Figure 1 Location of the research platform FINO 1 and of the wind farm alpha ventus in the North Sea [2]

METHODOLOGY

The Platform is equipped with several techniques for meteorological and oceanographic measurements. This includes amongst other things wind velocities and directions with ultrasonic and cup anemometers as well as temperature, atmospheric pressure and humidity in different heights along the measurement mast of 80m in height. The measured data are sent to the coast site with 32 Mbits/s directional radio link and processed to the project institutes. Most of the results are stored as ASCII files in the BSH-FINO-database and available for the public [3]. This data are used in this study to analyse the local wind climate, the swell and the influence of the wind farm on these.

The used measurement data were edit in order to build up an own database consisting of 10 minutes mean values for the period from 01.01.2004 until the 31.12.2014. Velocities from cup anemometers are available in eight different heights along the mast; ultrasonic anemometers were placed only in three heights. The measurement height is given in meter above the mean value of sea level. Besides the ultrasonic anemometers the wind direction is measured in four heights with wind vanes. Using the standard deviation σ_u and the 10 minutes mean values $\bar{u}$ of the wind velocities the turbulence intensity is calculated after Equ.(1). The distribution of the wind velocities during the period between 2004 and 2014 is shown as Weilbull-distribution in Equ.(2).

$$I_u = \sigma_u / \bar{u} \tag{1}$$

$$f(u) = \frac{k}{A}\left(\frac{u}{A}\right)^{k-1} e^{-\left(\frac{u}{A}\right)^k} \tag{2}$$

RESULTS

The local wind climate in 100m or rather 90m height above the mean sea level is shown in Figure 2. The left hand side gives the Weilbull-distribution of 10min mean values of the wind velocity in 100m height. On the right hand side, the wind rose in 90m height is drawn. The wind comes mainly from west to south-west. In the north-west sector of the wind rose the influence of the mast is visible due to the very low wind velocities.

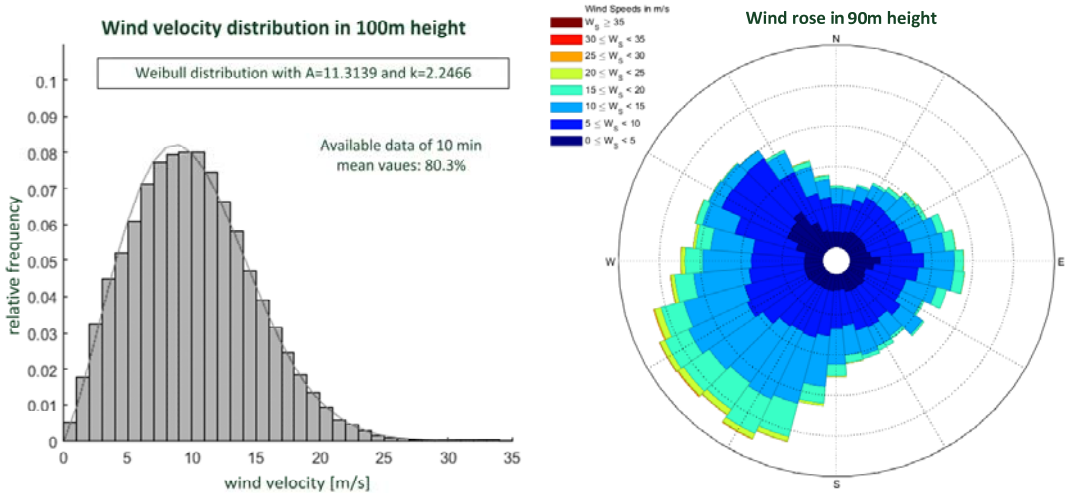

Figure 2 Visualisation of the local wind climate. Left: Distribution of the 10min mean values of the wind velocity in 100m height. Right: Wind rose in 90m height

Along the wind measuring mast the variation of the Weilbull parameters A and k in different measurement heights indicates the developed boundary layer flow. This atmospheric flow is classified in general by low wind and high turbulence close to the surface and higher wind speed and lower turbulence in the upper part away from the surface. Starting from 30m in Figure 3 the scaling factor A increases up to 100m height, which means higher turbulence and lower mean wind velocities close to the sea level and high wind speeds in 100m height. The shape factor k decreases along the mast height and shows values around k = 2,3 which is typical for this region [4].

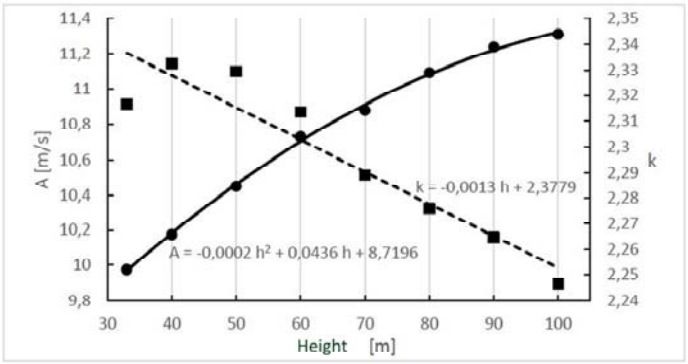

Figure 3 Development of the Weilbull scaling factor A (circles) and the shape factor k (squares) along the height of the measurement mast of FINO1

The offshore wind park alpha ventus was build seven years after FINO1 was put in operation. The wind park consists of twelve wind turbines from two different types and with a height of hub around 90m. To analyse the influence of the operating wind farm on the local wind climate the turbulence intensity in different wind directions is calculated for different measurement periods. Figure 4 shows in the upper scatter plot the turbulence intensities measured in 90m height before the wind farm was build. Beneath the second scatter plot of the turbulence intensity in Figure 4 clearly illustrate its change due to the peaks in the point cloud. This increased turbulence intensities results from the operating wind turbines in the first and second row near to Fino1, whose location agree well with the wind sectors of the peak areas. Additionally one can show, that especially the distribution of the turbulence intensities for the wind velocity classes between 4-10 m/s - were the turbines normally operates - changed after the wind park was build. Due to the wind farm the mean wind velocity between 20° to 180° decrease while the turbulence intensity increase in this sectors. Also in the 320° sector the wind shadow of the mast itself is visible.

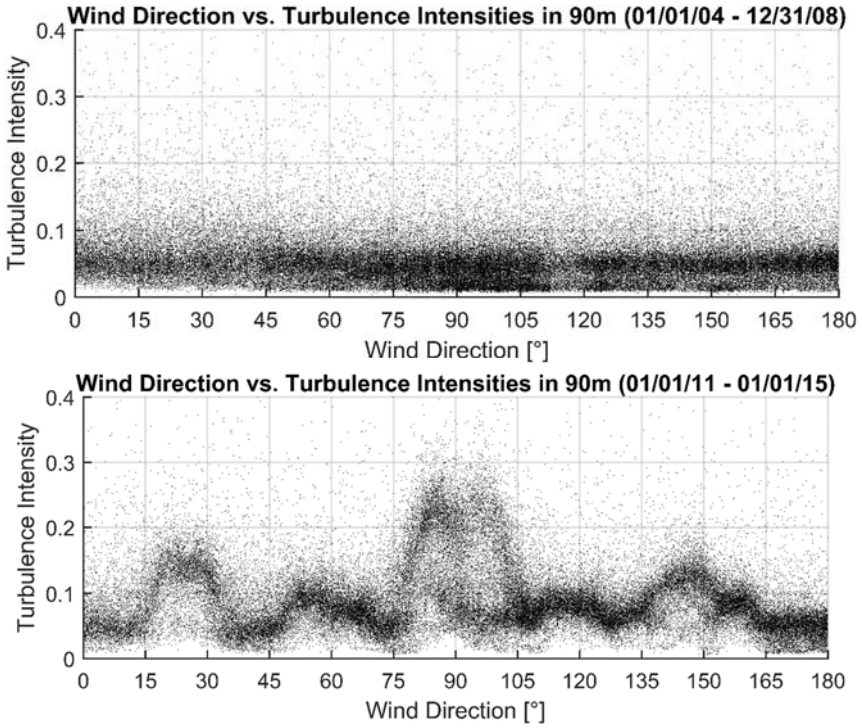

Figure 4 Turbulence intensities measured in 90m height. Upper part show the results before alpha ventus was build (2004-2008), lower part shows the measurement results from the period with alpha ventus (2011-2015).

FUTURE WORK WITH FINO 1 DATA

The cost of offshore wind energy significantly depends on minimizing the idle time during the installation and operation of the wind turbines. All activities during the construction of an offshore wind farm, starting from the pile driving to the assembling of rotors and finally installation of a condition monitoring system, are done within periods of favorable sea conditions and minimum impact to the environment. Therefore optimizing the safe time windows for installing wind turbines or accessing them becomes important.

An offshore wind turbine consists of many mechanical and electrical components, which fail more frequently compared to the structural components. These failures result in scheduled and unscheduled inspection and maintenance visits to the wind turbine. But organizing these visits is not an easy task considering the sometimes very dangerous sea conditions, especially in the North Sea. Therefore, in order to avoid idle periods, which can result in increased construction and operation cost of offshore wind energy, there arises a need to optimize favorable time windows for safe offshore operation.

The availability of many years' data for the environmental and sea state condition of FINO1 platform in North Sea creates a good opportunity to study these topics. Therefore, an optimum solution can be obtained by making use of the time history environmental and sea state data from FINO1 platform and develop models for long term and short term sea state prediction for safe offshore operation. The allowable limits of the environmental and sea state conditions for different types of offshore activities; ranging from installation of an offshore wind turbine structure to accessing the wind turbine for inspection and maintenance will be used as an input.

CONCLUSIONS

Since 2003 the research platform FINO1 is measuring the weather and sea condition amongst other thing in the North Sea close to the German coast. The aim is to monitor the local climate, the sea level and the environmental development. Especially since 2010 the wind farm alpha ventus starts to operate in the neighbourhood of FINO1 which allows now after some years a detailed view to its influence on the local environment, in particular on the wind climate. It can be shown, that the mean wind speed and the turbulence intensity changes due to the operating wind energy converters. The huge amount of recorded data allows a detailed and precise view and enable further analysis about the impact of offshore wind farms on the environment and helps to reduce the construction and operating costs.

REFERENCES

[1] Neumann, T.; Westerhellweg, A.; Cañadillas, B.; Herklotz, K.; Outzen, O. (2010), "New tasks or FINO1 – the research platform after installation of the first German offshore wind farm "alpha - ventus" and the start of "RAVE"". In: DEWEK. 10th German Wind Energy Conference. Bremen, germany, 17-18 November

[2] Homepage FINO 1 Research Platform. Online http://www.fino1.de/en/, 23.11.15

[3] FINO1 database. Online: http://www.bsh.de/en/Marine_data/Observations/MARNET_monitoring_network/FINO_1/index.jsp, 23.11.15

[4] Christoffer, Jürgen; Ulbricht-Eissing, Monika (1989), "Die bodennahen Windverhältnisse in der Bundesrepublik Deutschland. 2. Aufl. Offenbach am Main [Germany]: Selbstverlag des Deutschen Wetterdienstes (Berichte des Deutschen Wetterdienstes, 147)

THE INTERNATIONAL CONFERENCE ON
WIND ENERGY HARVESTING 2017
20-21 April 2017
Coimbra, Portugal

Paper 208

ON THE UNDERSTANDING OF THE ABOVE ROOF FLOW OF HIGH-RISE BUILDINGS FOR WIND ENERGY HARVESTING

Hassan Hemida[1]
School of Civil Engineering
University of Birmingham, Birmingham, UK

Anina Šarkić[2]
Institute of Numerical Analyses and the Theory of Structures, University of Belgrade, Serbia

Rüdiger Höffer[3]
Windingenieurwesen und Strömungsmechanik, Faculty for Civil and Environmental Engineering,
Ruhr-University Bochum, Germany

ABSTRACT

In order to increase wind energy harvesting from urban environment, the wind behavior around high-rise buildings need to be fully understood. In this paper, wind tunnel experiments of the flow around a high-rise building with a height to width ratio of 3:1 were performed to investigate the wind distribution in the above roof flow and the building surface pressure. The building was mounted in an environmental boundary layer wind tunnel resembling that of a built environment. Two shapes of the roof of the building were investigated; flat and tilted roofs. Four different wind angles, with respect to the side of the high-rise building, were investigated experimentally; 0, 15, 30, and 45 degrees. These results give a database for the validation of computational fluid dynamic simulations for further investigations and visualizations of the flow around the high-rise buildings in built environments.

INTRODUCTION

Wind energy is harvesting since the existence of human being. Wind mills have been used to extract water from deep wells and for agriculture purposes. Since the discovery of electricity, wind turbines have been used to convert the wind energy into electricity and with the continuous rise of fuel prices, increase in carbon emissions and reduction of fusel fuel, wind energy has received considerable attentions as alternative and cheap energy source. Although the production of wind energy is predominantly from on-shore and off-shore wind farms, there are many difficulties associated with these technologies. The large cost of transmitting the energy to the costumers, foundation of wind energy system, structural fatigue due to the interactions between waves, winds and structure of the wind energy system, difficulties in maintenance, corrosion of the structure due to the salinity of the water are some of the diffcatities associated with off-shore wind farms. For on-shore wind farms, the issues are related to use of land, visual effect, effect on wild life, expensive maintenance and public resistance that made some countries to ban construction of new on-shore wind farms. To overcome some of these issues and to promote the use of green energy from renewable resources, there is a strong trend in the European Union (EU) of promoting harvesting wind energy from built environment. This is evidenced by the recently awarded EU projects; COST action "TU1304" [1] and the H2020 ITN project "AEOLUS4FUTURE" [2]. The main aim of the first project is to investigate the possibility of harvesting wind energy from urban environment and for the second one is to transfer the established expertise from the on-shore and off-shore wind farms to the built environments. This is also supported by the Feed-in Tariff (FIT), a payment to people generating their own electricity from renewable

1 Associate Professor, School of Civil Engineering, University of Birmingham, E-mail: h.hemida@bham.ac.uk
2 Assistant Professor Institute of Numerical Analyses and the Theory of Structures, University of Belgrade, Bulevar kralja Aleksandra 73, sarkicanina@gmail.com
3 Professor, Faculty of Civil and Environmental Engineering, Ruhr-University Bochum, Universitätsstraße 150, 44801 Bochum, IC 5/127, Ruediger.Hoeffer@rub.de

sources, implemented by a number of EU governments, such as that implemented by the UK government in 2012. However, there are a number of issues associated with installing wind turbines in an urban environment, such as reduction in efficiency, noise, vibration, visual impact and many others that make social acceptance to these types of technologies difficult. The efficiency of wind energy system in urban environment is related to the reduced wind velocity and thus the amount of energy that can be harvesting. Also, the high turbulence intensity of the atmospheric boundary layer in urban environments decreases the turbine efficiency, increases noise and vibration and reduces life time of the wind energy device. Thus, more research is needed to investigate the best location to mount a wind turbine on the roof of a high-rise building, at which the wind velocity and turbulence are appropriate for wind energy harvesting.

The work of this paper has been undertaken as a part of a Short Term Scientific Mission of the EU COST Action "TU1304" to measure the flow around high-rise buildings for the purpose of wind energy harvesting. The main aim is to measure wind velocity at different locations in the above roof flow of a high-rise building and the surface pressure with a main focus on the roof. The building's height to width ratio is 3:1. Four different wind directions (angles), with respect to the side of the building, have been considered; 0°, 15°, 30° and 45°. These measurement data are considered as a base for validations of any further computational fluid dynamic (CFD) simulations.

METHODOLOGY

Two 1:300 scale models of the high-rise building have been used; one with a flat roof and the other with a tilted roof as shown in Figures 1(a) and 1(b), respectively. As shown in Figure 1(a), the height of the building is denoted by H (400 mm) and the width by B (133.3 mm). The height to width ratio of the building is H:B=3:1.

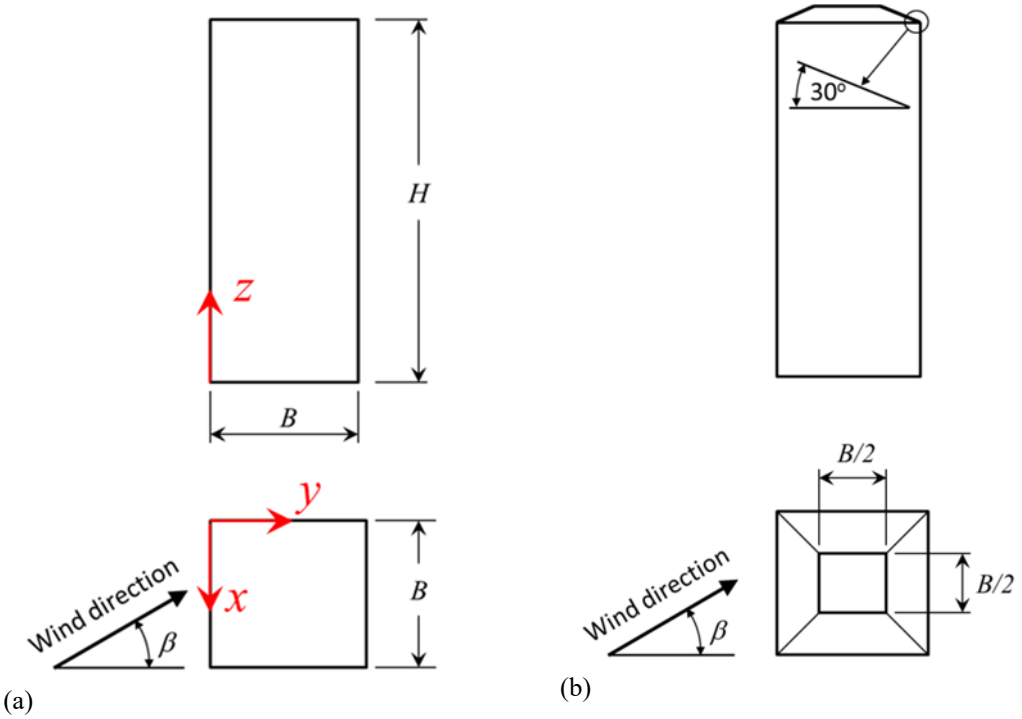

(a) (b)

Figure 1 High-rise building model used in the investigation, (a) with flat roof, (b) with a tilted roof.

The angle of the tilted roof in Figure 1(b) is 30°. The dimensions of the tilted roof are the same as those of the flat roof building with the added cap to the flat roof. The hypotheses here is that the tilted roof will help reducing both the separation and turbulence intensity in the above roof flow and hence enhance the quality and mean speed of the wind above the roof for the purpose of wind energy harvesting.

The experiments have been conducted in the atmospheric boundary-layer wind-tunnel of the Ruhr-University Bochum, Germany. The wind tunnel has a cross section of 1.6 m x 1.8 m and a test section length of 9.4 m. Figure 2 shows the wooden models mounted on a rotating table in the wind tunnel. A two velocity components hot wire anemometer has been used to measure the velocity components in the stream-wise and vertical directions. No attempt has been made to measure the span-wise velocity component. The sampling frequency of the hot wire was 2000 Hz. The anemometer has been calibrated in a calibration tunnel using laminar

flow. The atmospheric boundary layer has been simulated using a castellated barrier, turbulent generators and the roughness elements (cascaded small cubes of edge length 3.6 cm and 1.6 cm, respectively) as shown in Figure 2. In addition to the velocity measurements, the surface pressure has been obtained at different locations to give extra data for the CFD validation. The pressure sensors are connected to the bores in the wooden model by optimized pressure tubes with a length of about 0.9 m. Reference velocity was measured using Prandtl tube placed 1m in front of the model at the height corresponding to the height of the model.

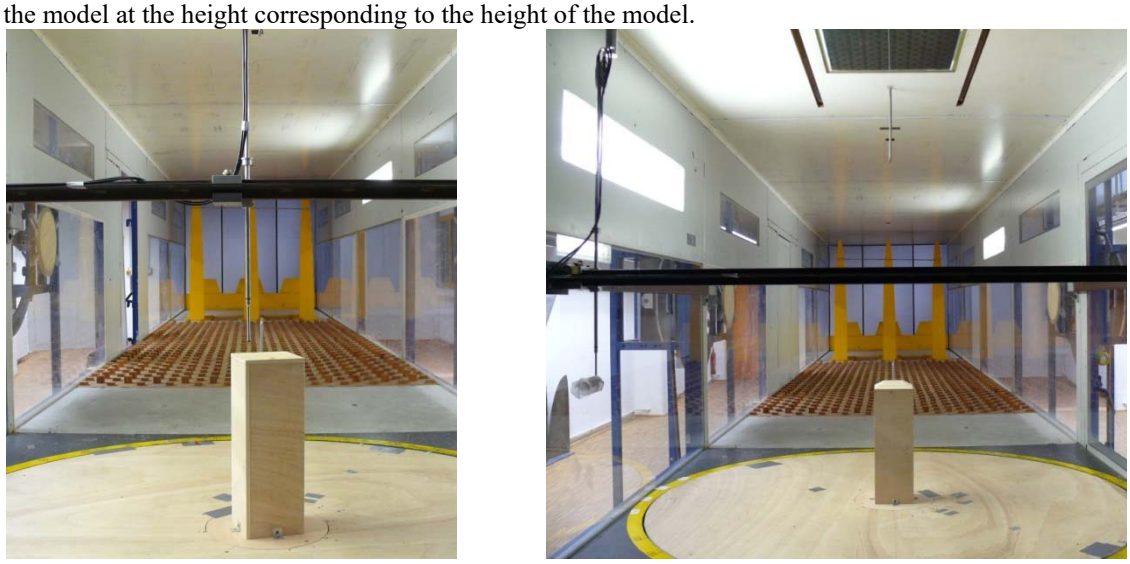

(a) (b)

Figure 2 The two building models mounted in the wind tunnel, (a) flat roof and (b) tilted roof.

The surface pressure was measured through ninety pressure taps distributed on the roof (64 taps) and sides (26 taps) as shown in Figures 3 and 4. The spacing between the different taps is also shown in Figure 3.

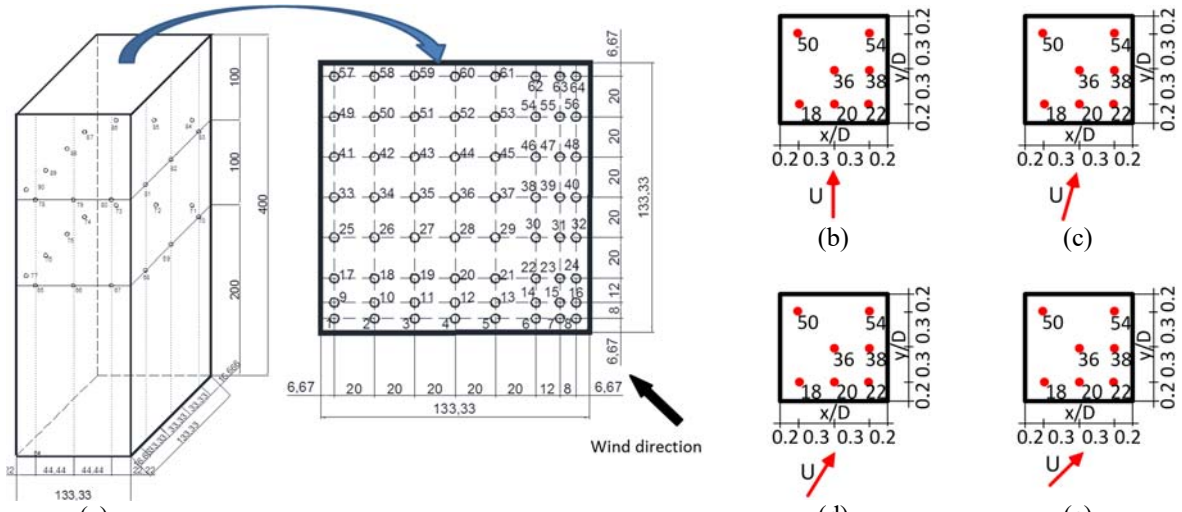

(a) (b) (c) (d) (e)

Figure 3 Distribution of pressure taps on the surface of the building (a) and positions of velocity measurements (a), (c), (d) and (e) for 0o, 15o, 30o and 45o, respectively.

Two types of pressure transducers have been used for this study:

- Honeywell 170 PC sensors
- AMSYS 5812-0001-D-B sensors.

The calibration establishes the pressure-voltage relations for each pressure sensor. For that purpose, a Betz manometer is used, allowing loading the sensors with a known pressure. This way the link between the measured voltage and known pressure is established. For these measurements these relationships are acquired: for Honeywell

sensors 5mbar corresponds to 5V and for AMSYS sensors 5mbar corresponds to 1V. The pressures are scanned with the sampling rate of 1000Hz in a sample-and-hold modus, which produces simultaneous sampling of pressures.

RESULTS

Figure 4 shows a sample of the velocity measurements ahead and in the above roof flow. It can be seen that the flow separates at the windward edge and reattaches to the roof after about the mid length of the roof. Further velocity measurements can be found in [3].

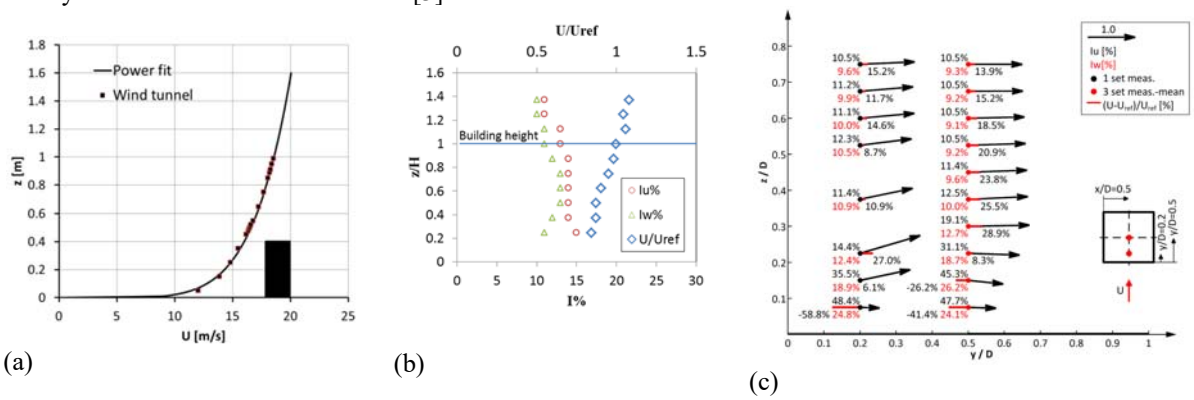

(a) (b) (c)

Figure 4 Velocity measurements; (a) ahead of the model, (b) turbulence intensity ahead of the model and (c) velocity above the model.

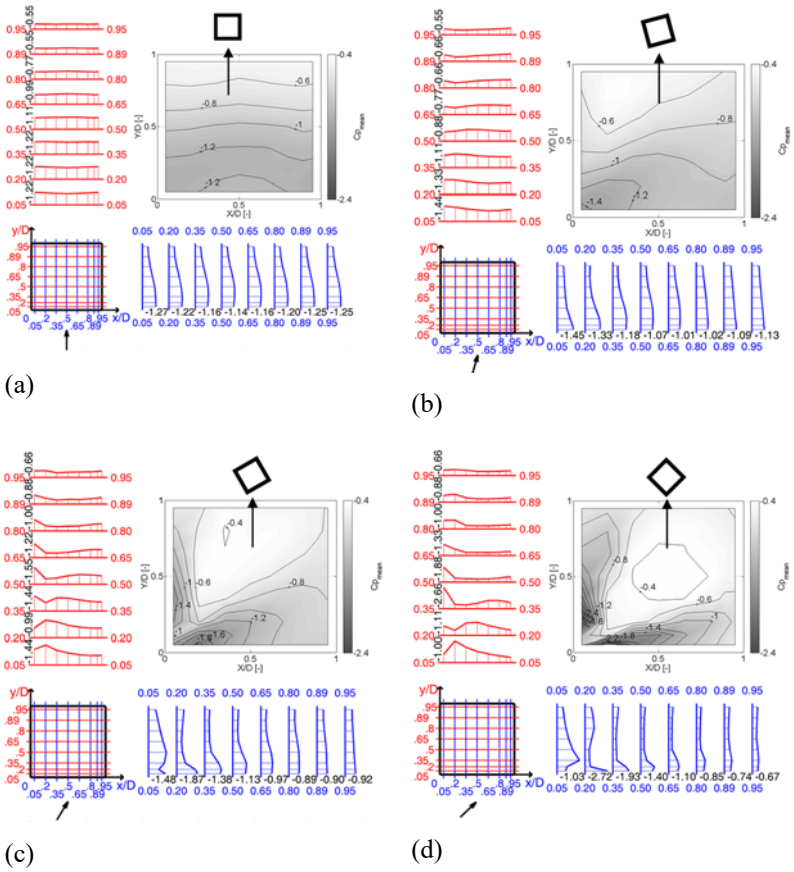

(a) (b) (c) (d)

Figure 5 Pressure coefficient on the roof of the flat-roof building at different wind angles; (a) 0º, (b) 15º, (c) 30º and (d) 45º.

Figure 5 shows the surface pressure on the roof of the flat-roof building. For 0º angle, the flow separates at the windward edge resulting in an area of low pressure on the roof of the building. The low pressure area is followed by a build up in the surface pressure and this is related to the flow reattachment. With the increase in the wind angles, the flow started to separates at the windward corner to make two separation cones. At 45º wind angle the surface pressure is symmetrical indicating that the two cones are similar in size.

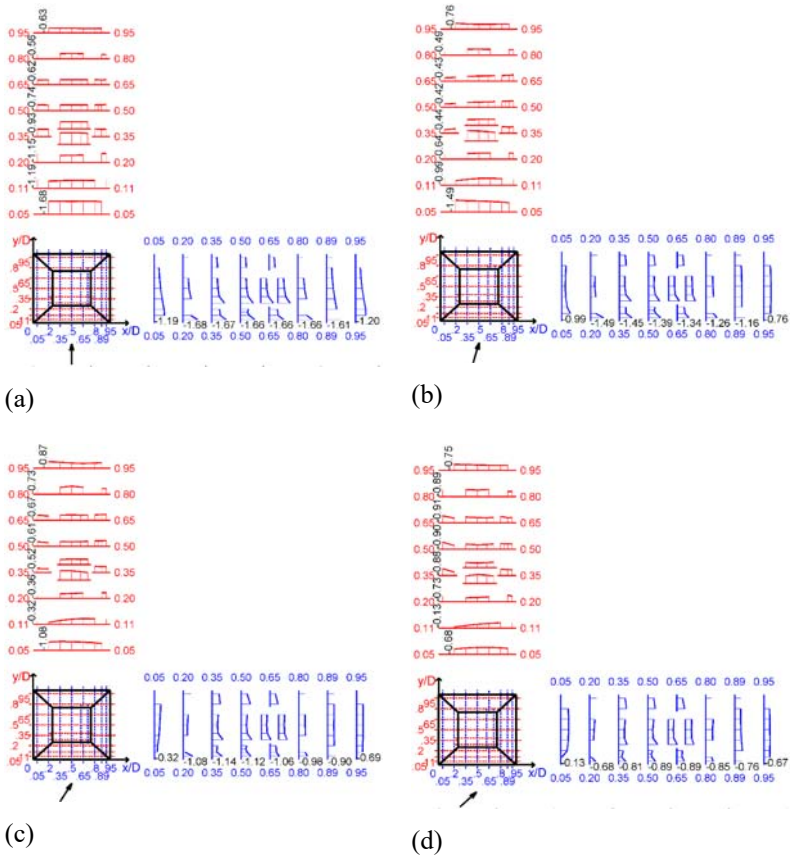

Figure 6 Pressure coefficient on the roof of the tilted-roof building at different wind angles; (a) 0º, (b) 15º, (c) 30º and (d) 45º.

Figure 6 shows the pressure distribution on the roof of the lilted-roof building at different wind angles. Dissimilar to the flat roof building, the separation region is not predominant and it is limited to a small area close to the windward edge. The work includes also measurements of the surface pressure on the different sides of the building, the instantaneous pressure at each taping position and the power spectral of each measurement. However, these are not included in this paper due to the length restriction.

CONCLUSIONS

This work represents the measurements of the surface pressure on two types of building roofs subjected to atmospheric winds. It has been found the flow separates from the surface of the flat roof to form a relatively large separation region while this region is relatively small in case of tilted roof shape. The work provides a database for validation of future numerical investigation of the flow around high-rise buildings.

ACKNOWLEDGEMENTS

The authors would like to acknowledge the support provided by the Chair of the COST-Action TU1304 Prof Charalampos Bianiatoplous and his encouragement to undertake such work. The time and support received at the Ruhr-University Bochum by the Lab technicians are also acknowledged.

REFERENCES

[1] WINERCOST, Online http://www.cost.eu/COST_Actions/tud/Actions/TU1304
[2] AEOLUS4FUTURE http://www.uc.pt/fctuc/dec/investigacao/areascientificas1/projeto/mecestru
[3] Hemida, H., Šarkic, A., Höffer, R., *The above roof flow of a high-rise building for wind energy extraction; wind tunnel and numerical investigations,* 14th International conference on wind engineering, Porto Alegre, Brazil, June 2015;

THE INTERNATIONAL CONFERENCE ON
WIND ENERGY HARVESTING 2017
20-21 April 2017
Coimbra, Portugal

Paper 209

TALL HYBRID WIND TURBINE TOWERS. LOAD ANALYSIS AND STRUCTURAL RESPONSE.

Michaela Gkantou[1]
Research Fellow/PhD Candidate
University of Birmingham
Birmingham, United Kingdom

Charalampos Baniotopoulos[2]
Professor
University of Birmingham
Birmingham, United Kingdom

Pedro Martinez-Vazquez [3]
Lecturer
University of Birmingham
Birmingham, United Kingdom

ABSTRACT

Wind energy, a clean and renewable energy source, has vastly found applications both in onshore and offshore locations. In order to further increase the power output, demand for taller applications, able to exploit intense velocities in higher altitudes, has appeared. To achieve this, hybrid wind steel towers, combining lattice and tubular parts for the support structure, could be a promising solution. Within the present study, the structural response of such a tall hybrid wind turbine tower is studied and the obtained results are discussed. Two Design Load Cases (DLC) from those established in IEC64100-1 standard [1], are considered. A series of 600 seconds simulations, with the wind speed ranging from 3 to 25 m/s, with an incremental step of 1 m/s, are executed. Time histories of the elemental forces and the nodal displacements are extracted in critical positions of both the lattice and the tubular part. The mean values of the output data are evaluated and plotted against the wind speed. Conclusions regarding the influence of the wind speed on the induced tower behaviour are drawn.

NOMENCLATURE

CHS	=	Circular Hollow Section
DLC	=	Design Load Case
NTM	=	Normal Turbulence Model
ETM	=	Extreme Turbulence Model

INTRODUCTION

The increased amount of greenhouse emission gases has enhanced the demand for clean and renewable energy. Wind farms consisting of fully lattice or all tubular wind turbine towers have substantially contributed to an increase in the renewable energy production. Recent demands for higher wind turbines with larger capacities, aimed to be installed at high altitudes or at places with high wind velocities, have emerged. In order to fulfil the required safety and durability verifications, whilst keeping the solution economically and environmentally sustainable, hybrid structures, efficiently combining tubular and lattice parts, could be used. Towards this direction, the present study performs numerical analysis on a tall hybrid structure.

METHODOLOGY

The current paper focuses on a 120 m wind turbine tower. As a first step, various parameters, including the height of its part, the number of legs, the arrangements and the angle of bracings, need to be defined. An initial study should be performed in order to find the most efficient structure, ensuring compromise between the lowest structural weight and the fabrication and assembly costs which usually come as a function of the number of connections. For the present study, a hybrid tower consisting of 60 m tube at the upper part and 60 m lattice

1 Research Fellow/PhD Candidate, School of Engineering, University of Birmingham, m.gkantou@bham.ac.uk
2 Professor, School of Engineering, University of Birmingham, c.baniotopoulos@bham.ac.uk
3 Lecturer, School of Engineering, University of Birmingham, p.vazquez@bham.ac.uk

structure at the lower part, as shown in Figure 1, has been selected. In order to increase the load distribution, six columns (legs) have been chosen for the lattice structure. The employed cross-sections were based on a preliminary study [2]. For both the tubular and the lattice part, cold-formed built-up polygonal cross-sections in steel grade S355 were used. The tubular part was tapered ranging from 5500 mm in the base to 4000 mm in the top, with constant plate thickness equal to 40 mm. The transition part was conservatively designed with bracings of large cross-sections. It should be noted that the transition piece is a critical component, aiming to transfer all the dynamic and self-weight loads to the lattice, and needs separate in-depth investigation, out of the scope of the present paper. Various cross-sections, as can be seen in Figure 1, were chosen for the lattice structure, in which the bending moment and the self-weight is expected to be supported by the axial forces in the columns, whilst the shear forces by the axial forces of the bracings. For the present study, it was deemed adequate to simulate the polygonal cross-sections with circular hollow sections (CHS).

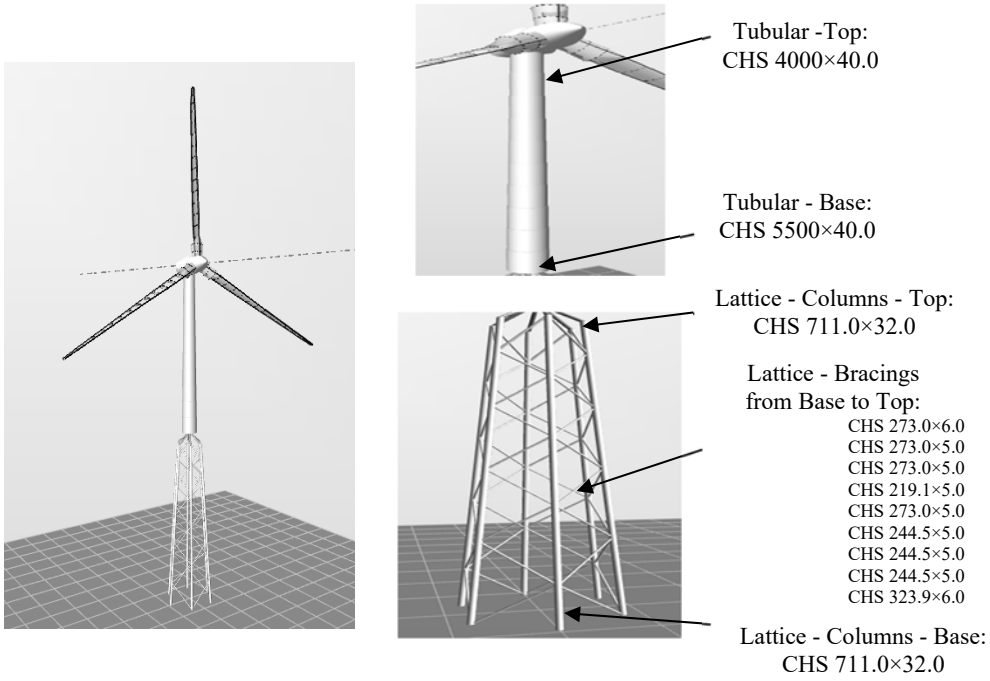

Figure 1. Wind turbine tower (60 m lattice & 60 m tubular)

In order to account for the interaction between elastic and inertia forces of the structure and the external aerodynamic force, ashes [3], an integrated analysis software, has been used for the numerical analysis. Ashes uses blade element momentum (BEM) algorithm for aerodynamics and combines it with finite element (FE) solver for the evaluation of the induced structural behaviour. Wind turbulence can be simulated with Turbsim tool [4], a stochastic, full-field, turbulence simulator, and imported into ashes. For the considered hybrid structure, a 5 MW class AII turbine [5] is assumed. After developing the wind turbine tower model, the turbulence models are generated. This depends on the considered design load cases. IEC6400-1[1] outlines the minimum requirements for wind turbines to ensure the engineering integrity of onshore wind structures by providing 15 and 7 design load cases (DLC) for the ultimate and the fatigue limit state respectively. Herein focus is set on DLC 1.1 and DLC 1.3 which corresponds to power production conditions and embody the requirements for loads resulting from atmospheric turbulence during normal (NTM) and extreme operating conditions (ETM) respectively. After creating the NTM and ETM models, 600 seconds simulations are performed. For both DLC 1.1 and DLC 1.3, parametric studies with the wind speed ranging from 3 to 25 m/s, with an incremental step of 1 m/s, are executed. The wind flow is assumed to be parallel to the hub axis. The extreme turbulence model together the extracted responses are shown in Figure 2. Note that in order to eliminate initial impact effects, the first 30s of each simulation which are expected to present instabilities, are disregarded.

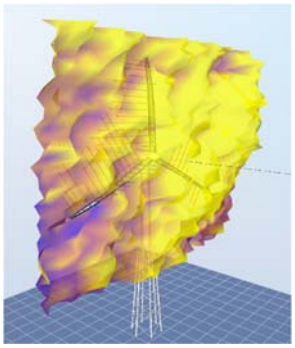

a) Extreme Turbulence Model

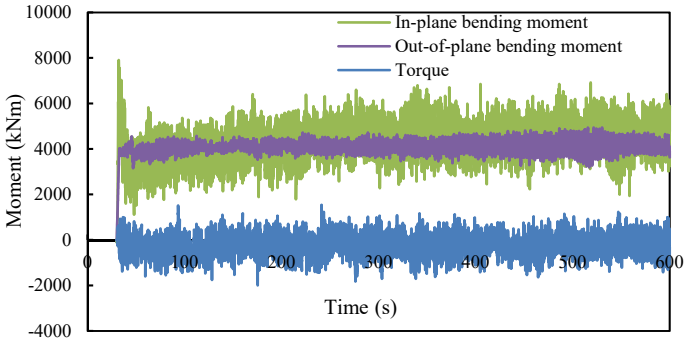

b) Moment time histories - tubular top -wind speed 12 m/s - DLC 1.3.

Figure 2. Aeroelastic analysis in ashes [3].

RESULTS

In order to evaluate the results, the mean values of elemental forces and nodal displacements are calculated and plotted against the wind speed. The observed response for DLC 1.1 is shown in Figures 3-5. In particular, Figure 3 presents the mean values of induced moments on the tubular structure for increasing wind speed. In order to verify the results, the data from measurements on a tubular structure [6] are included for comparison purposes. Even though the measurements refer to a different, still comparable, support structure, the similarity on the observed response is evident. For in-plane bending moments, peak values are achieved for wind speed 11 m/s. This is related with the pitch controller that decreases the angle of attack in order to mitigate the excitation load on the blade structure and keep RPM (rotations per minute) and the output constant. The influence of the aforementioned effect is less significant on the out-of-plane and torsional moments, which remain relatively stable for wind speeds higher than 11 m/s. The axial forces of the columns and the bracings of the lattice structure for increasing wind speed are depicted in Figure 4. An ascending curve for wind speed 3-11 m/s and a descending curve for wind speed 11-25 m/s are again noticeable. The axial forces are similar in the lower and the upper part of the lattice columns, justifying the selection of the same cross-section. In addition to the mean values, load matrices with maxima and minima have been formed. These can be subsequently used for the extreme load assessment for a certain cross-section at different heights. Besides the elemental forces, the mean values of in-plane and out-of-plane deflections, as illustrated in Figure 5, can be utilized for the serviceability limit state verifications. The overall structural response of DLC 1.3 was similar to that of DLC 1.1, with DLC 1.3 presenting slightly higher mean values (i.e .0.57% higher mean values for the axial forces of the lattice part, 2.45% higher mean values for the in-plane bending moments of the tubular part) compared to those of DLC 1.1.

a) Tubular - Base
In-plane bending moment vs wind speed

b) Tubular - Base
Out-of-plane bending moment vs wind speed

c) Tubular - Top
Torque vs wind speed

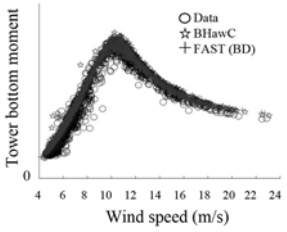

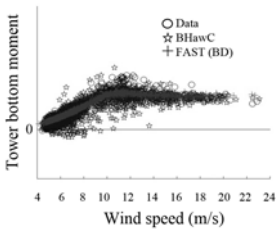

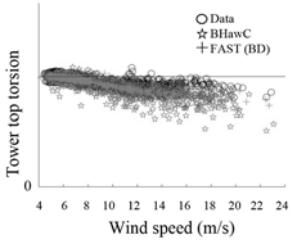

Measurements on wind turbine structure [6]

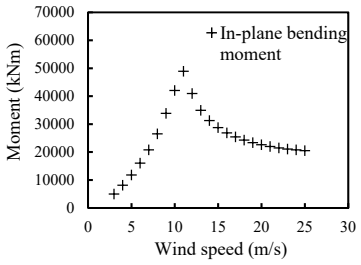

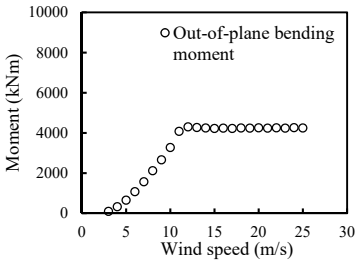

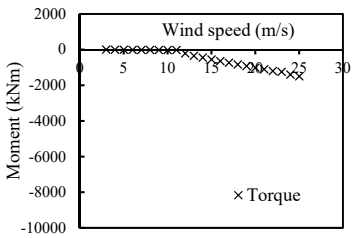

Numerical anlysis on a hybrid structure

Figure 3. 10-min mean values of moments - tubular structure.

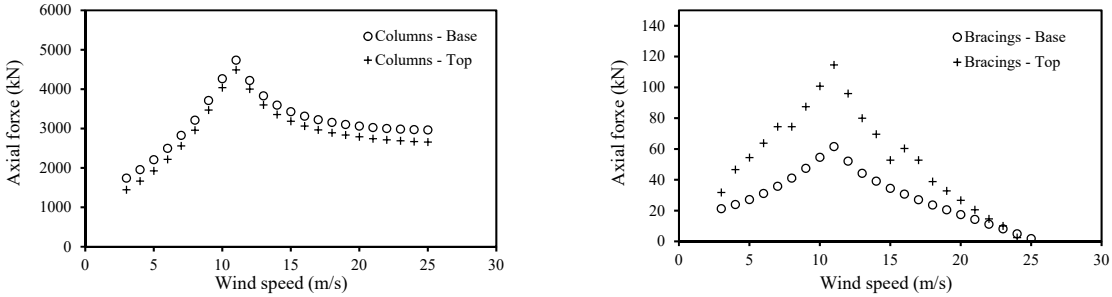

a) Lattice - Columns b) Lattice - Bracings

Figure 4. 10-min mean values of axial forces - lattice structure.

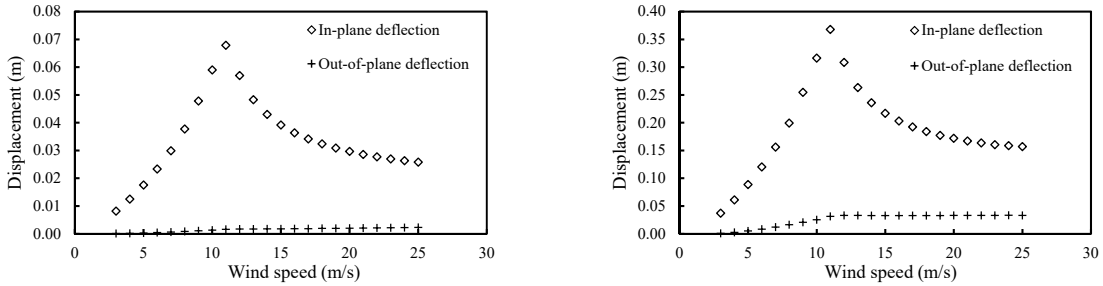

c) Lattice - Top d) Tubular - Top

Figure 5. 10-min mean values of displacements.

CONCLUSIONS

A numerical study on a hybrid wind turbine tower has been performed. The extracted structural response was compared with the measurements on a tubular wind turbine tower [6], finding similar trend with respect to the wind speed. As anticipated, for the in-plane bending moments of the tubular part, the axial forces of the lattice part and the in-plane deflections of the whole structure, mean peak values were achieved for wind speed 11 m/s. The obtained results can be used for further assessment of the wind structure's behaviour and for the execution of component checks and limit state verifications. Future research could be performed to investigate optimal configurations of hybrid structures, compare them with conventional wind turbine towers and assess the possibility of using higher steel grades in highly stressed regions.

ACKNOWLEDGEMENTS

The research leading to these results has received funding from the Research Fund for Coal and Steel (RFCS) under grant agreement RFSR-CT-2015-00021. The support of Mr. Mohammad Reza Shah Mohammadi to the software learning is gratefully acknowledged by the first author.

REFERENCES

[1] IEC 61400-1 (2005) Wind Turbines_Part 1: Design Requirements. International Electrotechnical Commission, Geneva, 3rd edition.
[2] Rebelo, C. and Mohammadi, M. (2016) "Steel Hybrid Onshore Wind Towers Installed with Minimal Effort", Technical Report. Deliverable D1.1.
[3] Ashes, Available from: http://www.simis.io/ [Accessed 7 January 2017].
[4] TurbSim, NWTC Information Portal, Available from: https://nwtc.nrel.gov/TurbSim [Accessed 7 January 2017].
[5] Jonkman, J., Butterfield, S., Musial, W., and Scott, G. (2009). "Definition of a 5-MW Reference Wind Turbine for Offshore System Development." Technical Report NREL / TP-500-38060, National Renewable Energy Laboratory, Golden, CO.
[6] Guntur, S., Jonkman, J., Schreck, S., Jonkman, B., Wang, Q., Sprague, M., Hind, M. and Sievers, R. (2016) January. "FAST v8 Verification and Validation for a MW-scale Wind Turbine with Aeroelastically Tailored Blades." In 34th Wind Energy Symposium (p. 1008).

THE INTERNATIONAL CONFERENCE ON
WIND ENERGY HARVESTING 2017
20-21 April 2017
Coimbra, Portugal

Paper 210

THE DESIGN OF AERODYNAMICALLY SHAPED HIGH-RISE BUILDINGS WITH INTEGRATED WIND TURBINES

Roland Antal[1]
STU in Bratislava, Faculty of Civil Engineering
Bratislava, Slovak Republic

Norbert Jendzelovsky[2]
STU in Bratislava, Faculty of Civil Engineering
Bratislava, Slovak Republic

Olga Hubova[3]
STU in Bratislava, Faculty of Civil Engineering
Bratislava, Slovak Republic

ABSTRACT

The current trend in the modern architecture is to combine an environmental and practical solutions together. One of the most popular green solutions is the use of wind turbines. The article focuses on innovative design of high-rise buildings with integrated wind turbines. The idea is to create two aerodynamically shaped high-rise buildings with two horizontal wind turbines placed between them. Correct shape and orientation of buildings due to the placement of horizontal wind turbines will be matter of interest here.

INTRODUCTION

Preliminary design of high-rise buildings and their mutual orientation is based on the assumption, that the air which flows around buildings is supposed to accelerate in zones, where wind turbines will be placed. In other zones, acceleration of wind is unwanted, due to unnecessary overloading of the structure. The design of the building is inspired by the shapes of rain drop and air wing "NACA 0024" [1], (Fig. 1). Both shapes were chosen because of their ingenious profile with very low drag coefficient and aesthetical appearance.

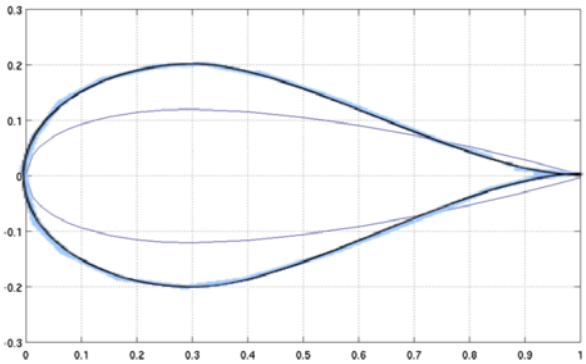

Figure 1. Inspiration of the shape of the building – air wing "NACA 0024" [1] (grey) and rain drop (blue).

[1] PhD. student, Department of Structural Mechanics, STU in Bratislava, Faculty of Civil Engineering, Radlinskeho 11, 810 05, Bratislava, Slovak Republic, roland.antal@stuba.sk
[2] Professor, Department of Structural Mechanics, STU in Bratislava, Faculty of Civil Engineering, Radlinskeho 11, 810 05, Bratislava, Slovak Republic, norbert.jendzelovsky@stuba.sk
[3] Associate professor, Department of Structural Mechanics, STU in Bratislava, Faculty of Civil Engineering, Radlinskeho 11, 810 05, Bratislava, Slovak Republic, olga.hubova@stuba.sk

METHODOLOGY

Before the final proposal was created, 6 CFD (Computational Fluid Dynamics) simulations were done. CFD analyses were aimed on finding the best orientation and the placement of buildings based on objectives that were previously set. For software analyzes wind characteristics of Bratislava-Slovakia were selected as a location of buildings. In the selected location, North-Western wind flow is predominate (21 % of the year). According to [2], average wind speed measured 10 m above ground is 5 m/s. The area can be characterized as an urban terrain between categories III and IV according to [3].

The CFD simulations are based on calculations by finite volume method, where discrete volume is divided to smaller control volumes, where variables are investigated.

Solution is iterative and in this case SST (Shear Stress Transport) mathematical model was used. This model belongs to the group of RANS models (Reynolds Averaged Navier-Stokes equation models). SST mathematical model was created by connection of two very popular mathematical models k-ε and k-ω. Best of both worlds were used, because k-ε reaches satisfying results in free stream and k-ω model is suitable for near wall turbulence analysis. Thus, SST model works by converting of the k-ε equations to k-ω formulation and automatically switches between them, depending on the location where turbulence of wind flow is investigated. More information about this mathematical model and can be found in [4, 5].

Boundary conditions for CFD simulations were set based on previous measurements verified by wind tunnel tests. Depending on the rotation of buildings, finite volume network was created (Fig. 2). In the boundary layer close to objects (buildings), turbulence and wind speed were investigated, therefore it was necessary to create very smooth layers of mesh. Hexahedral elements were used. The Smallest elements with the size of 1 mm were created directly on the contact of the fluid and objects. Larger elements with the size of 400 mm were created in zones where wind turbulence is no longer investigated.

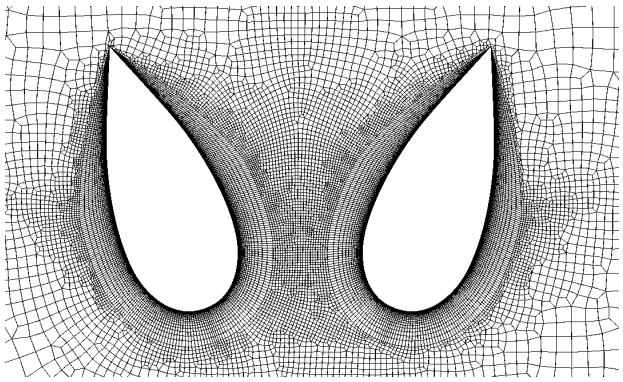

Figure 2. Mesh of control volumes created close to objects for the one of the analyzed wind flow.

Other boundary conditions were set as follows, (Fig. 3): wind speed at the inlet of the discrete volume: 5 m/s (constant for 2D simulations and logarithmic according to [3] in the 3D analysis), pressure at the outlet: 0 Pa, objects of interest (buildings) were created as a “no slip walls”, which means that the velocity of the wind speed on the contact of fluid and objects is equal to 0 m/s. Boarders of the discrete volume were created as a “free slip walls”, where the velocity on the contact of the wind flow and wall is the same as the velocity at the free stream.

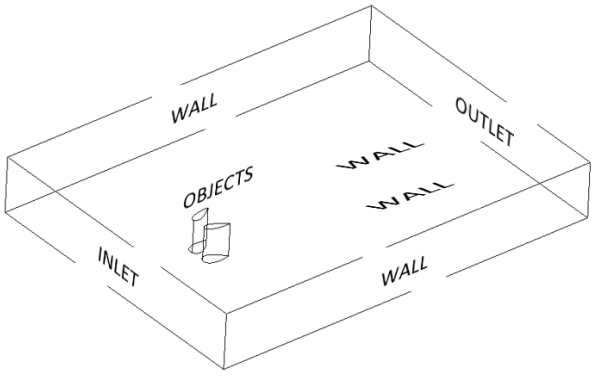

Figure 3. A schematic illustration of terminology used for definition of boundary conditions.

RESULTS

Before the final proposal, 6 CFD analyzes were calculated. Results of wind speed from 3 most interesting and fundamental placements of buildings are shown in the (Fig. 4). Wind flow direction is bottom up.

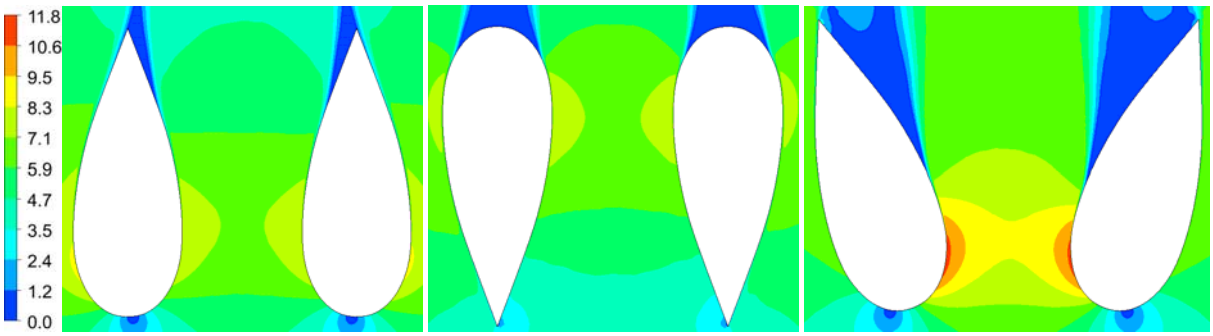

Figure 4. Wind speed [m/s], configuration number "1" (left), "2" (middle), "3" (right)

The comparison of results shows differences between wind speeds dependent on the mutual orientation of buildings. Configuration number "3" (Fig. 4 - right) meets the preferred conditions at the best, therefore it is used for the 3D analysis and the proposal of final design. Velocity in the assumed location of wind turbines reaches values of 8.4 m/s to 10.6 m/s. The placement and mutual configuration of buildings is also advantageous in terms of seizures of smaller ground area compared to other examples with similar wind speed.

By application of preferred conditions and by combining two shapes (air wing and rain drop) final shape was created (Fig. 5).

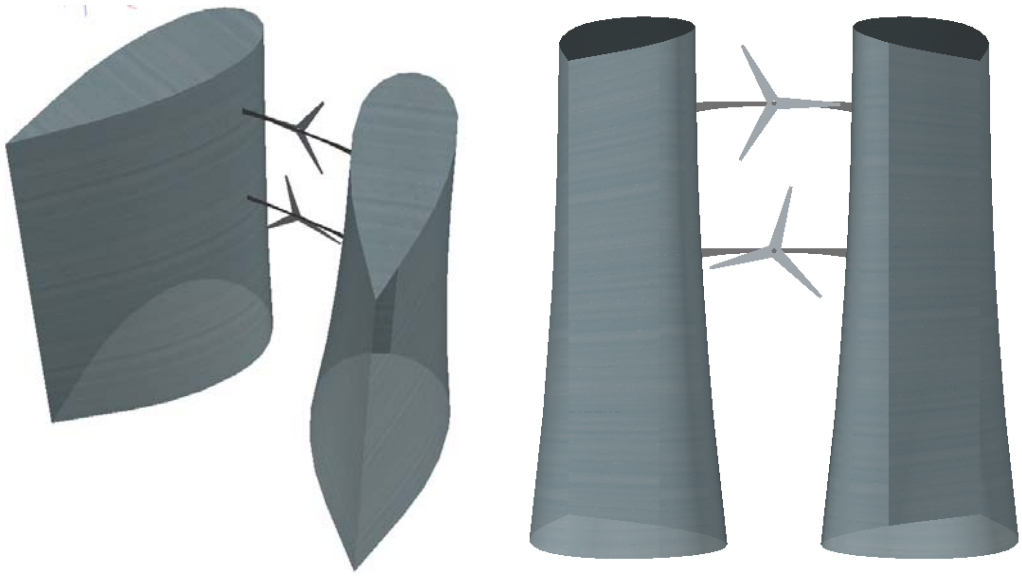

Figure 5. Final design of high-rise buildings complex with integrated wind turbines.

Dimensions and characteristics of the proposed buildings are as follows: building has 35 floors above ground, height of buildings is 105 m, width of the upper part is 24 m, length of the upper part is 75 m, width of the bottom part is 38 m, length of the bottom part is 75 m, the clearance between buildings in the level of the lower wind turbine is 30 m and the clearance in the level of the upper wind turbine is 32 m.

Two double ZECWP 75 kW [6] horizontal wind turbines with counter rotating rotors which diameters are 22 m respectively 10 m were used. First of the horizontal wind turbines was placed 60 m above ground. Second wind turbine was placed 90 m above ground. The manufacturer declares that wind turbines can produce 342 000 kWh per year per one wind turbine at the average wind speed 7.5 m/s. Considering the information from [2] and [6], it was calculated that, both wind turbines will be working at the full capacity approximately 70 % of the year. It means that they would produce approximately 12 % of total energy consumed by these buildings (479 000 kWh per year), which would be enough to cover the costs for electricity of 31 four members

households. It is declared that ZECWP wind turbines produce less than 60 dB of noise, what is considered as insignificant noise.

In the following figures we can see results of the final CFD simulation of wind flow.

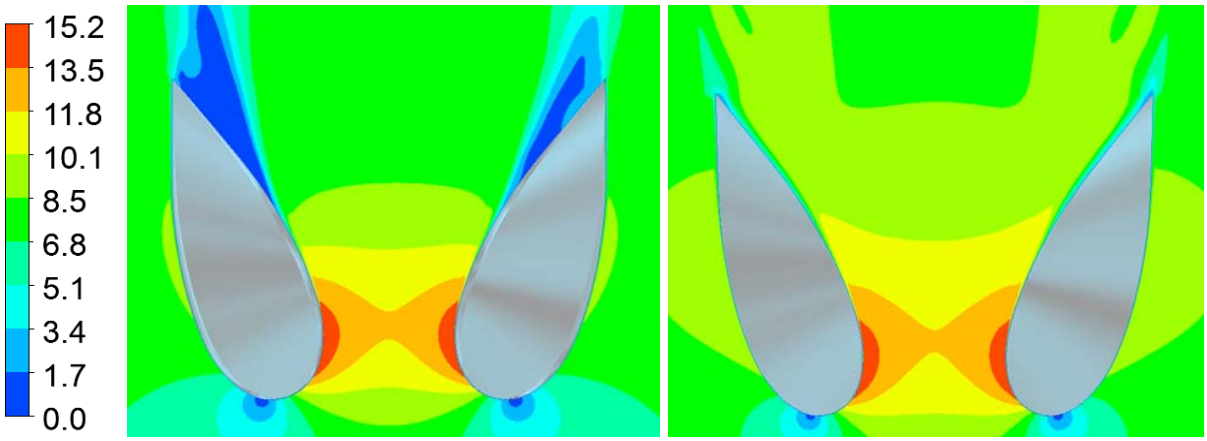

Figure 6. Velocity in the height of wind turbines in [m/s], lower wind turbine (left), upper turbine (right).

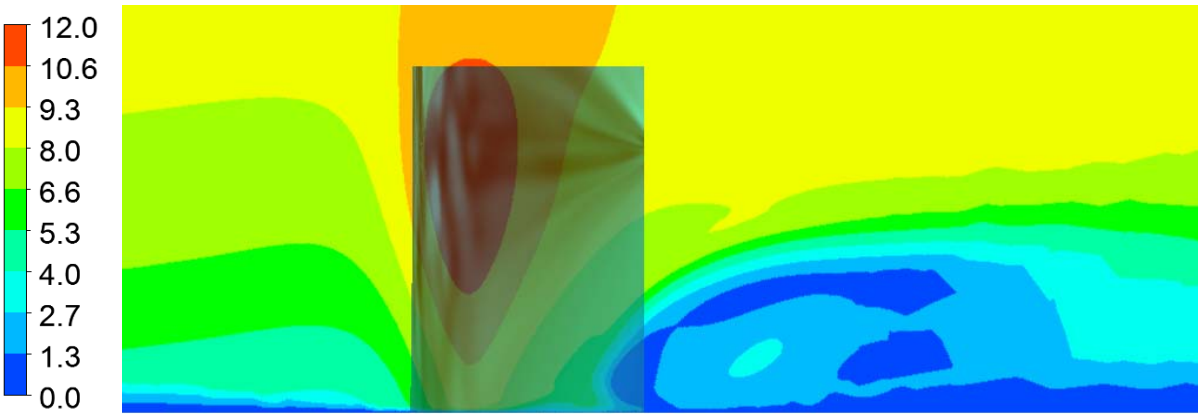

Figure 7. Velocity in the middle section between buildings in [m/s].

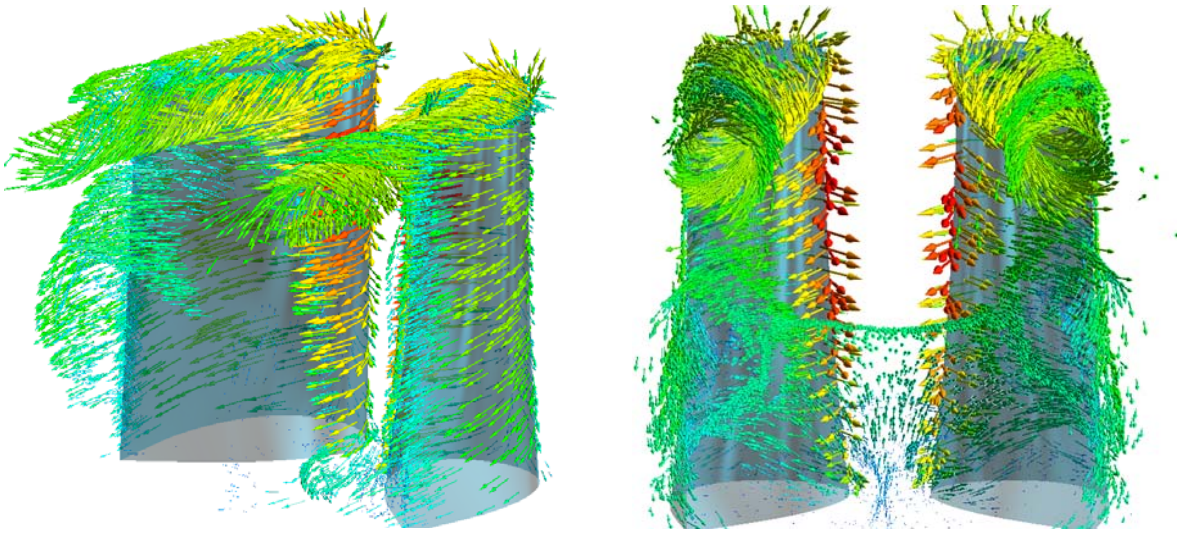

Figure 8. Illustration of vortexes.

CONCLUSIONS

The task of the final CFD simulation was to demonstrate verity of considerations defined at the beginning. As it is shown in the (Fig. 6), velocity in the placement of both wind turbines reaches values large enough to power drive turbines and produce provided value (12 %) of total energy consumed by these buildings. In the (Fig. 7), we can see that wind flows faster only in the upper part of buildings, thus pedestrians would not be exposed to significant wind effects related to extreme wind discomfort. In the (Fig. 8) creation of vortexes is shown. At the end, it can be said, that targets that were defined at the beginning were fulfilled and the aerodynamic design of ecology and "functional" buildings was created.

ACKNOWLEDGEMENTS

This paper was supported by Grant Agency VEGA, project No. 1/0544/15

REFERENCES

[1] UIUC Applied Aerodynamics Group - UIUS Airfoil Coordinated Database [online]. Available at: http://m-selig.ae.illinois.edu/ads/coord_database.html

[2] POLCAK, N. and P. STASTNY. Topography Influence on Wind Condition of Bratislava. Skalni Mlyn: Microclimate and mesoclimate of landscape structures and anthropogenic environment. 978-80-86690-87-2, 2422011.

[3] Eurocode 1: Actions on structures. Part 1-4 General actions - Wind actions, 2007.

[4] CHUNG, T. J. Computational Fluid Dynamics. 2nd. Cambridge University Press, 2014. ISBN 978-1-107-42525-5.

[5] KOZUBKOVA, M. Modeling of fluid flow, FLUENT, CFX. Ostrava: VSB - Technical University of Ostrava, 2008.

[6] ZEC Wind Power [online]. Available at: http://www.zecwindpower.com/

THE INTERNATIONAL CONFERENCE ON
WIND ENERGY HARVESTING 2017
20-21 April 2017
Coimbra, Portugal

Paper 211

THE WIND DISTRIBUTION IN WARSAW
A SOURCE FOR URBAN WIND ENERGY HARVESTING

Katarzyna Starosta[1]
Institute of Meteorology and Water Management
National Research Institute
Warsaw, Poland

Andrzej Wyszogrodzki[2]
Institute of Meteorology and Water Management
National Research Institute
Warsaw, Poland

ABSTRACT

The promotion of energy from renewable sources minimize the environmental impacts and even serve as an opportunity for mitigation of greenhouse gas emissions and reduction of the global warming. In recent years, there is observed significant development of new wind turbine and photovoltaic installations (up to 20% of total power production by 2020 according to European Union Directive), especially in the urban environment. With increased number of people living in large urban areas, there emerged an idea of smart cities with the cost effective renewable energy networks built in the urban subspace. Detailed knowledge of the meteorological conditions in the urban environment is an important factor for the growing renewable energy industry. The aim of our work is to study the wind distribution in Warsaw based on the observational and numerical model data sets acquired from the two-year period in 2014-2015. For the practical interpretation and further post-processing, results of the numerical model COSMO at 2.8km resolution were verified against data from five urban meteorological stations located within Warsaw metropolitan area. The verification is performed by comparison of the wind rose plots from model simulations and observations at individual station locations.

KEY WORDS

meteorology, climatology, wind power, smart city , wind speed and direction, numerical weather forecasts, weather forecast verification, post-processing

INTRODUCTION

With the sustained progress in the construction of new power micro-installations, public awareness of the significance of renewable energy sources (RES) in the urban space becomes an important subject and opens potential new directions of research. Illuminated road signs and information boards, lightings in parks, also small local silent turbines with a vertical axis of rotation on the building roof tops and walls in conjunction with solar photovoltaic installations reduce the load on the existing transmission network and also decrease the energy loss due to reduced transmission length. Municipal office in Warsaw provides support for the development of new power micro-installations in urban neighborhoods until 2020 [2]. Since the wind energy is natural weather element highly variable in time and space, it requires detailed studies using different approaches. For example, the climatology of wind speed is the first criterion for assessing the placement of wind turbines. The aim of our work is to develop methods for estimate wind energy potential, based on the available data from the urban meteorological stations in Warsaw in comparison with the data from the numerical model forecasts. For the practical analysis we use the WRPLOT [3] software.

[1] leader, IMGW-PIB, PL-01-673 Warsaw, 61 Podleśna str, katarzyna.starosta@imgw.pl
[2] researcher, IMGW-PIB, PL-01-673 Warsaw, 61 Podleśna str, andrzej.wyszogrodzki@imgw.pl

METHODOLOGY

Observational network and numerical model data.

Our studies are based on the wind speed and wind direction data in the years 2014 and 2015 attained from the small network of observational stations in Warsaw:

Meteorological stations in Warsaw

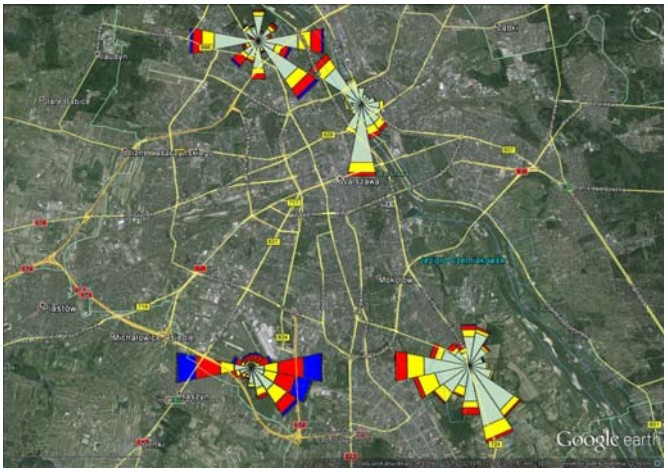

Synoptic station **Okęcie** (24h)

Climatologic station **Bielany** (6,12,18 h)

Three automatic meteorological stations project CLIMATE (24h)

- **ZOO** (zoological garden)
- **Wilanow** Palace
- **Kaweczyn** heat and power plant

Fig.1 Warsaw area with wind roses in 2014 year

COSMO (Consortium for Small-scale modelling) numerical weather prediction model

Model COSMO version 5.01 is run at IMGW-NRI operationally using two nested domains at horizontal resolutions of 7 km and 2.8 km. The model runs four times per day starting at 00, 06, 12, 18 UTC and produces 78 hour and 36 hour forecasts respectively at 7 and 2.8km resolutions. COSMO model runs in a deterministic mode using initial (IC) and boundary (BC) conditions from ICON global model.

Horizontal Grid Spacing [km]	7	2.8
Domain Size [grid points]	415 x 445	380 x 405
Forecast Range [h]	78	12
Initial Time of Model Runs [UTC]	00 06 12 18	1h frequency
Model Version Run	5.01	
Model providing LBC data	ICON	COSMO PL 7
LBC update interval [h]	3h	1h
Data Assimilation Scheme	Nudging	

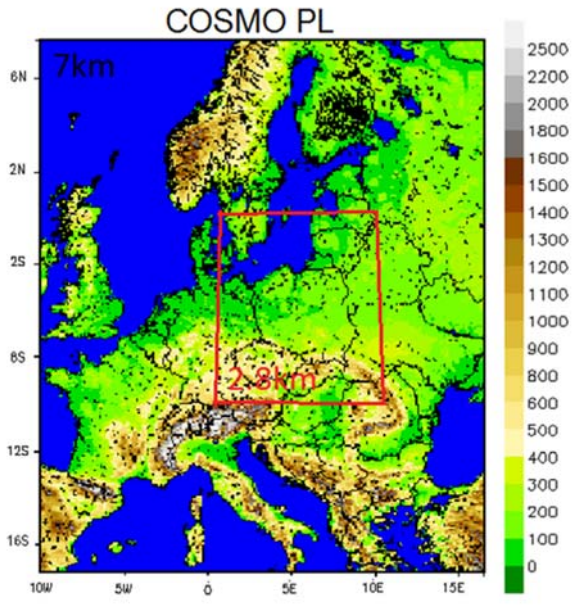

Fig2. Configuration model COSMO.PL

Implemented in COSMO model observational data assimilation (DA) system is based on the nudging technique and allows for ingesting weather data measurements - as these carried out on SYNOP stations acquired from the WMO/GTS network - to improve forecast's quality.

RESULTS

Seasonal variability of the wind speed.

The large seasonal variability of wind from year to year causes that these data should be analyzed with use at best the longer multiannual data sets. In our analysis we are currently employing urban observations and model forecasts from two-year period in 2014 and 2015 and also compare them with the averaged data available for full decade between 2005-2014. The current analysis extends results presented in [4] computed for the first half of 2014.

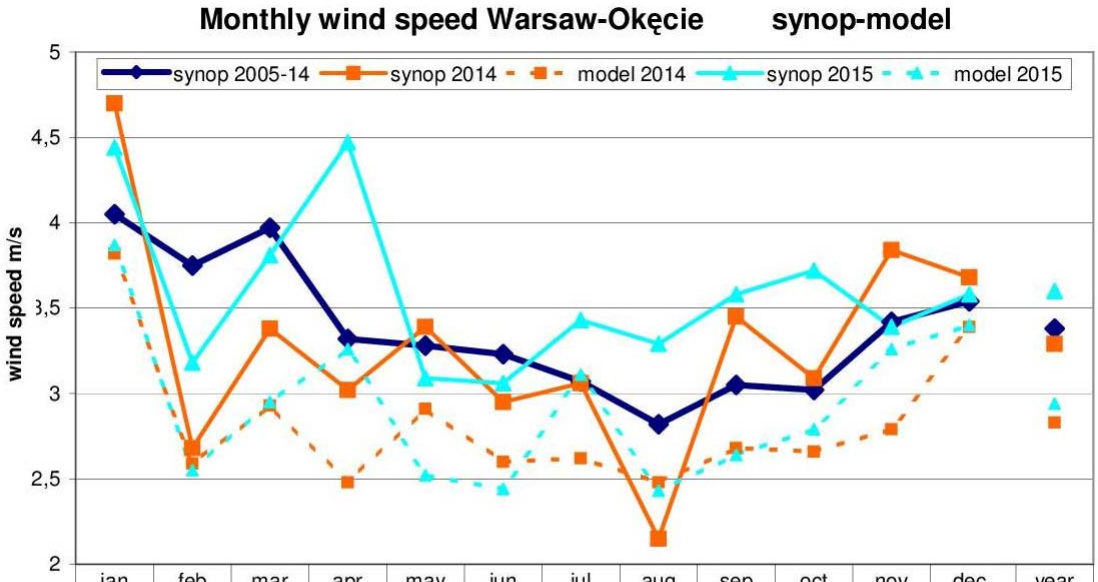

	jan	feb	mar	apr	may	jun	jul	aug	sep	oct	nov	dec	year
synop 2005-14	4,05	3,75	3,97	3,32	3,28	3,23	3,07	2,82	3,05	3,02	3,42	3,54	3,38
synop 2014	4,7	2,68	3,38	3,02	3,39	2,95	3,06	2,15	3,45	3,09	3,84	3,68	3,29
model 2014	3,82	2,59	2,93	2,48	2,91	2,6	2,62	2,48	2,68	2,66	2,79	3,39	2,83
synop 2015	4,44	3,18	3,81	4,47	3,09	3,06	3,43	3,29	3,58	3,72	3,39	3,58	3,6
model 2015	3,87	2,55	2,95	3,26	2,52	2,44	3,11	2,43	2,64	2,79	3,26	3,4	2,94

Fig 3. Monthly wind speeds at the Warsaw Okęcie station.

In analysis of monthly periods of wind velocity we observe the maximum speed in January and a minimum in August. Comparing the wind speed from the years 2014 and 2015, we observe in general the larger wind speeds in 2015. The COSMO model results (dashed lines at Fig 3) have larger systematic error (comparing to the average over full decade) than the observational data.

Wind roses.

A wind rose is a concise and illustrative product showing wind speed and wind direction at a certain location. It provides information about the frequency of winds blowing at certain speed ranges from the particular direction, as well as its time percentage. For the selected locations , we compare wind roses generated from NWP model with data from observational stations. Results are used both for the current meteorological analysis and studies of a longer period of time. For current analysis WRPLOT View program was used [3].

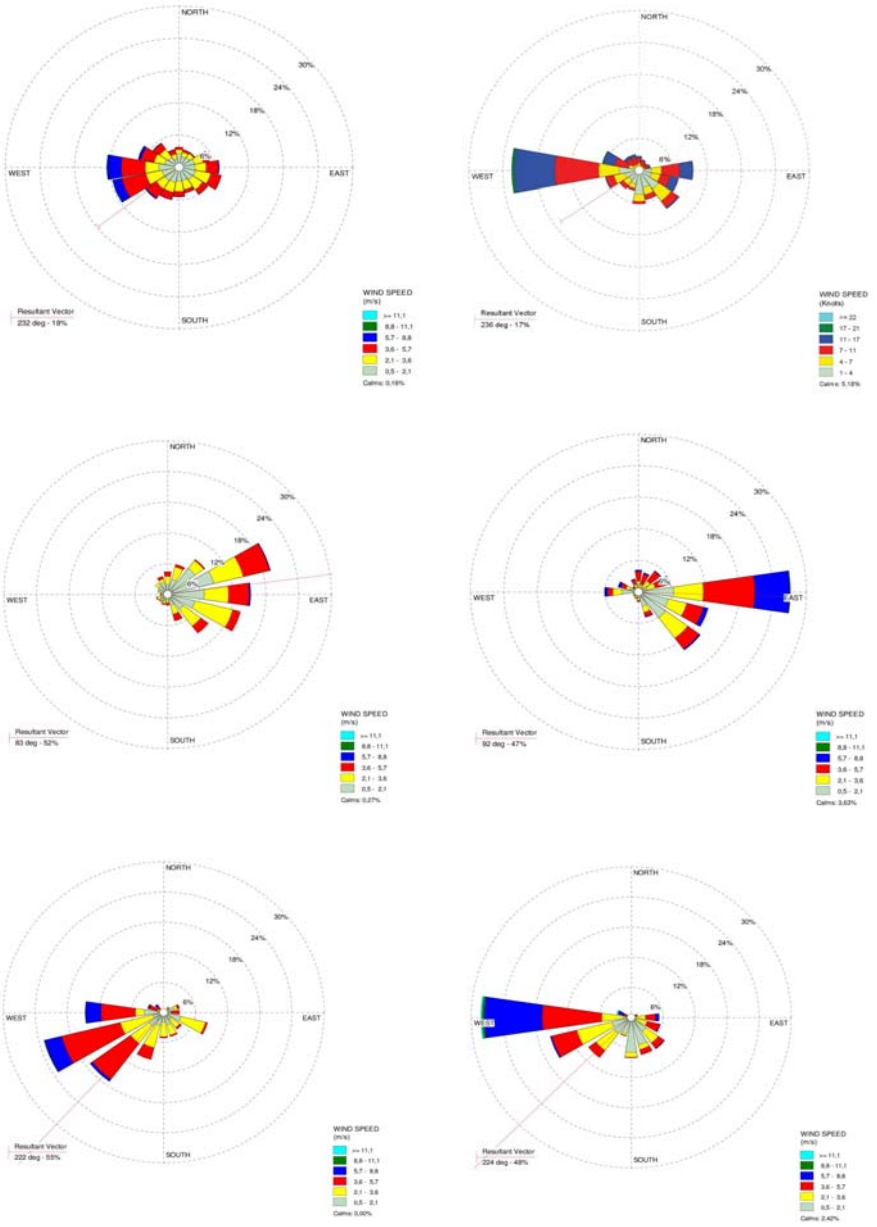

Fig.4 Wind roses at Warszawa Okęcie during 2015
(left model/right synop, top all year, middle August, bottom December).

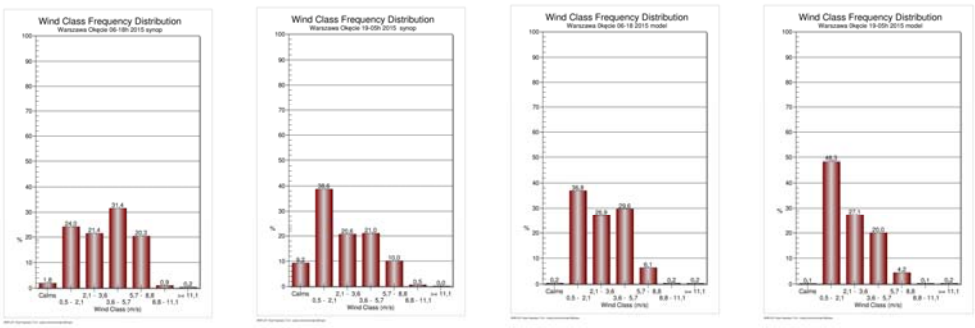

Fig.5 Wind class frequency distribution at Warszawa Okęcie during
day-night periods of 2015 (left synop 6-18h, 19-05h, right model 6-18h, 19-05h).

By comparing observational data at Okęcie with the prognostic model results (Fig 4) we can see that the model wind speeds are smaller and wind directions more scattered. Wind speeds are clearly marked by daily course (Fig

5). We are seeing greater speed daytime with a maximum between 12 (noon) and 16, and a minimum at the night time hours.

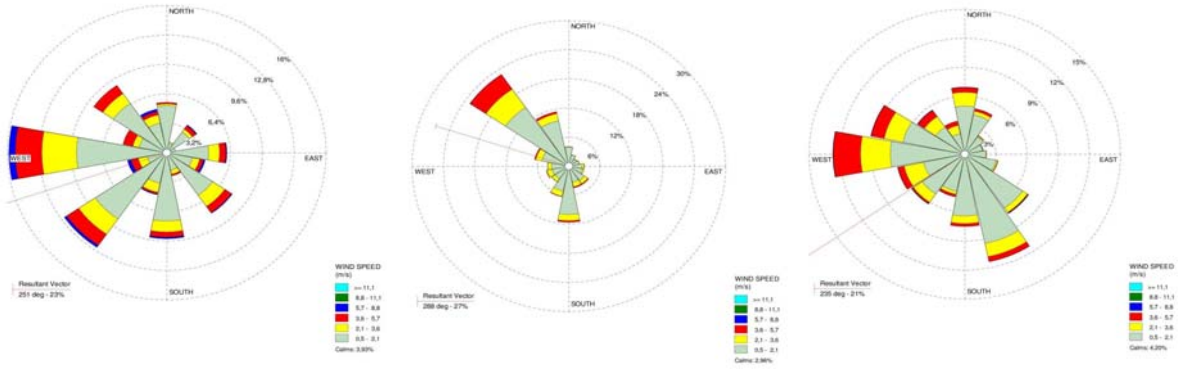

Fig. 6 From left: Bielany, ZOO, Wilanów observation data in 2015.

Fig. 6 presents observed wind distribution averaged over the 2015 year at three remaining Warsaw stations. In comparison to the wind rose at Okęcie station (Fig 4, top right corner) we can see much wider spread in wind direction at each location with predominant north-western component but significantly lower amplitude of the wind speed.

CONCLUSIONS

Warsaw is located in the zone of potential wind power 700-800 kWh/m2/year. Calculated by us indicative wind power value was approximately 500 kWh/m2/year in 2014 for the station Warsaw Okęcie. Micro wind installation, and small installations 1- 10 kW are planned in neighborhoods on the outskirts of the city. Poland has a transitional climate between the maritime climate (Atlantic) from the west and continental from the east of the country. Accordingly, the weather conditions in individual years are highly variable. Therefore, for the installation of wind turbines, it is necessary on a regular basis the study of a current weather conditions, so in addition to the observations we need data from numerical weather prediction models. At present COSMO model is introducing direct implementation of urban effects with the TERRA-URB (H.Wouters) parameterization. Further use of this model version will enable us to obtain more accurate forecasts in any grid points within the city. The verification and post-processing of the model data give us the opportunity to improve our research on meteorological conditions for renewable energy in the urban environment.

ACKNOWLEDGEMENTS

The authors would like to thank for making available data from the project IMGW-PIB “KLIMAT”.

REFERENCES

[1] Oke. T.R. Initial guidance to obtain representative meteorological observation at urban sites. WMO/TD-No.1250 2006
[2] Action Plan for renewable energy sources for Warsaw .Warsaw City Office - August 13, 2014 r. (in polish)
[3] Lakes environmental software WRPLOT View http://www.weblakes.com/products/wrplot/
[4] Starosta K., and Wyszogrodzki A.: Assessment of model generated wind energy potential in Poland. COSMO News Letter No. 16

THE INTERNATIONAL CONFERENCE ON
WIND ENERGY HARVESTING 2017
20-21 April 2017
Coimbra, Portugal

Paper 212

WIND ENERGY HARVESTING IN THE URBAN ENVIRONMENT - QUALITY ASSESSMENT OF LARGE EDDY SIMULATIONS OF FLOW SEPARATIONS

Ulf Winkelmann[1]
Ruhr-University
Bochum, NRW, Germany

Anina Šarkić Glumac[2]
University of Belgrade
Belgrade, Serbia

Rüdiger Höffer[3]
Ruhr-University
Bochum, NRW, Germany

ABSTRACT

This work assesses the quality of large eddy simulations (LES) for an atmospheric boundary layer flow around a wall-mounted cube by using verification and validation methods. Additionally, the flow separation characteristics over the bluff body are inspected. This method is performed especially with regard to the analysis of the velocity field and the turbulent kinetic energy in the vicinity of the roof for an effective positioning of small scale wind turbines in the urban environment. Various simulations settings are carried out and analyzed to optimize the computational time of the simulation while maintaining high quality results.

INTRODUCTION

The analysis of the characteristics of the flow field around bluff bodies is a significant task for the wind engineer for efficient wind harvesting in the urban environment using small scale wind turbines. The positioning of the small scale wind turbines on the roofs of buildings is of crucial importance as the flow characteristics of interest such as the flow velocity and the turbulent kinetic energy vary immensely between the inner and outer part of the separation region of the flow. In the CFD community it is widely accepted, that the transient LES are superior to the steady state Reynolds averaged Navier-Stokes simulations (RANS) for the calculation of average flow values for wind engineering purposes. Large eddy simulations have been gaining importance in recent years due to the increased available computational power and the promising quality of the results. LES seems to be a very good compromise between the accuracy of the results and the computational power needed to perform the simulations.

Quite recently, considerable attention has been paid to the use of methods to ensure the quality of LES for CWE problems. This approach is called validation and verification (V&V). The knowledge about the accuracy and errors of numerical simulations is crucial for creating reliable results. In this work the effects of different simulation settings are assessed using a V&V analysis for an atmospheric boundary layer flow over a wall mounted cube using the OpenFOAM software, with the aim of choosing an optimal setting to reduce the computational time while still preserving a high quality simulation. The results can be used as a guideline for economical LES with high quality results for the future research of bluff body aerodynamics. In general, this work follows a V&V approach similar to the work published by Gousseau et al. for a simplified high-rise building using the ANSYS Fluent software [8].

In the upcoming chapter the general methodology and the mathematical model of the governing equations and turbulence modeling is described first. Then geometry and domain, and boundary conditions are stated. Subsequently, a brief summary of the setup of the wind tunnel experiment is given and the validation methods performed are explained. After that the verification methods are explained in more detail. The final chapter of this work presents a conclusion of the work performed.

METHODOLOGY

[1] Teaching and Research Assistant, Faculty of Civil and Environmental Engineering, Ruhr-University Bochum, Universitätsstraße 150, 44801 Bochum, IC 5/123, Ulf.Winkelmann@rub.de

[2] Assistant Professor, Institute of Numerical Analyses and the Theory of Structures, University of Belgrade, Bulevar kralja Aleksandra 73, sarkicanina@gmail.com

[3] Professor, Faculty of Civil and Environmental Engineering, Ruhr-University Bochum, Universitätsstraße 150, 44801 Bochum, IC 5/127, Ruediger.Hoeffer@rub.de

The main aim of this work is to detect optimal simulation settings for the analysis of the separation flow characteristics for an atmospheric flow over a bluff body while assessing the quality of the simulations.
The influence on the quality of the results of different simulations settings is analyzed using the V&V techniques described below. The accuracy of the results is assessed, inter alia, by using the so called hit rate to validate the numerical results against results obtained in wind tunnel experiments [13]. The convergence of the simulations is checked by using a sampling window approach [1]. The applicability of different resolutions of numerical grids for the flow around the wall mounted cube is examined by adopting the LES index of quality method (LES_{IQ}) [3][4]. The numerical and the modeling error are gauged for each simulation by applying a systematic model and grid variation [4][7]. The main factor for the required computational time and the quality of a LES is the spatial discretization of the geometry and the numerical domain. In general, the higher the amount of numerical cells used for the spatial discretization, the better the results and the higher the computational time. Thus, the effects of different **mesh sizes** on the velocity field and the turbulent kinetic energy for the flow around a wall mounted cube are analyzed in this work. Further, different **time step lengths** for the transient simulation are examined to conceivably reduce the computational time. Overall, a higher time can step lead to a worse prediction or a non-converging simulation with the possible advantage of reducing the computational time. One of the most important methods for the quality of the simulation is the interpolation scheme used by the finite volume method for the convective term of the momentum equation of the Navier-Stokes equation (Eq.: (2)). The influence of several **interpolation schemes** is tested in this work. Additionally, the so called random spot method [10] is used to model a **turbulent inlet** flow, which influence on the flow around the cube is assessed by comparing the method to a **steady state inlet** condition without turbulence. Furthermore, different **turbulence modeling approaches**, namely the standard and dynamic Smagorinsky turbulence model are employed [11][12].
The governing equations for the numerical simulations are the instantaneous filtered Navier-Stokes equations for an isothermal, incompressible Newtonian fluid consisting of the filtered conservation of mass (Eq. (1)) and the filtered conservation of momentum (Eq. (2)):

$$\frac{\partial u_i}{\partial x_i} = 0, \tag{1}$$

$$\frac{\partial \rho u_i}{\partial t} + \frac{\partial \rho u_j u_i}{\partial x_j} = -\frac{\partial p}{\partial x_i} + \mu\left(\frac{\partial^2 u_i}{\partial x_j^2}\right) - \frac{\partial \tau_{ij}^s}{\partial x_j} \tag{2}$$

with the properties of the fluid, kinematic viscosity and density μ and ρ, respectively. u_j is the vector of the instantaneous velocity, x_i and x_j represent the spatial position with i=1,2,3 and j=1,2,3 and p is the pressure. The overbar denotes filtered values. τ^s_{ij} is the so called small scale stress:

$$\tau_{ij}^s = \rho\left(u_i u_j - \bar{u}_i \bar{u}_j\right). \tag{3}$$

The small scale stress τ^s_{ij} needs further turbulence modeling: In this work the Smagorinsky model and the dynamic Smagorinsky model are adopted, both using the Boussinesq hypothesis for obtaining the small scale stress tensor: $\tau_{ij}^s = 2\mu_t \bar{S}_{ij}$. The small scale stress tensor is modeled with the concept of the eddy viscosity $\mu_t = C_S^2 \rho L_{SGS}^2 |\bar{S}|$ and the filtered rate of strain $\bar{S}_{ij} = \left(\partial u_i / \partial x_j + \partial u_j / \partial x_i\right)/2$. C_S is treated as a constant in case of the standard Smagorinsky model, and as a dynamic parameter that varies in time when applying the dynamic Smagorinsky model. L_{SGS} is the length of the filter size which corresponds to the size of the numerical grid for the implicit filtering method employed in this work. The characteristic filtered rate of strain is defined as $|\bar{S}| = \left(\bar{S}_{ij}\bar{S}_{ij}\right)^{1/2}$.[12][10]

GEOMETRY, DOMAIN AND NUMERICAL GRID

The domain and the numerical grid are created according to the Guidelines by Franke et al. [5]. Overall, three different grid resolutions are created using the ICEM CFX software. An increasing ratio of the cells of 1.05 is applied from the cube to the boundaries of the domain. The distances between the windward surface of the cube to the inlet of the domain, the lateral surfaces of the cube and the lateral boundaries of the domain, the top surface of the cube and the top boundary of the domain are equal to 5 H. The distance between the leeside surface of the cube and the downstream boundary of the domain is 15 H, resulting in a blockage ratio of 1.51% for a 0° angle of attack of the flow. The geometry, the domain and a surface mesh for the 0° angle of attack of the flow is displayed in Fig. 1.

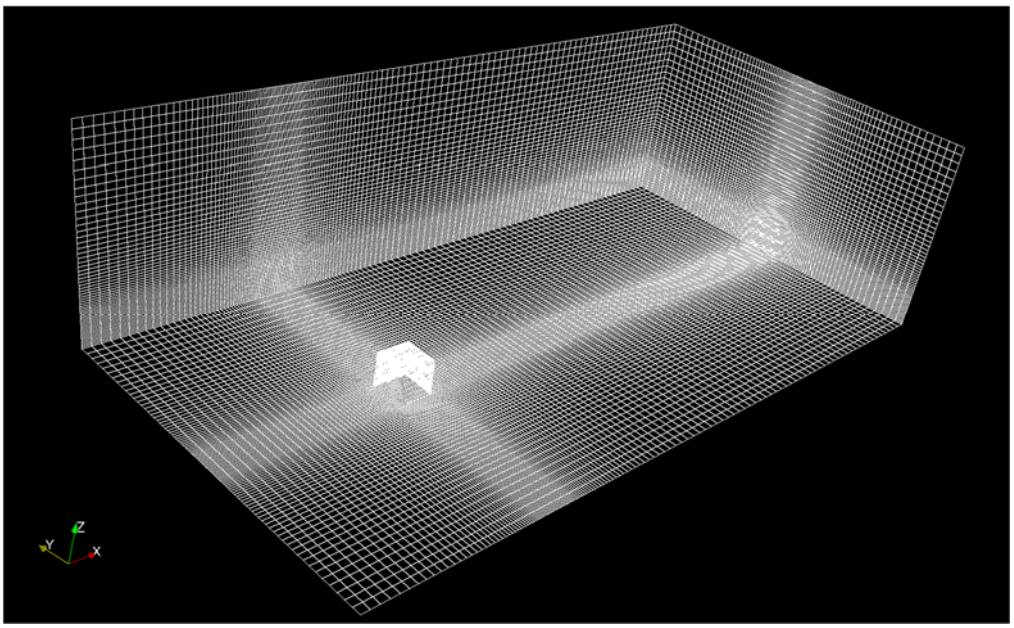

Fig. 1 Geometry, domain and surface mesh of the coarse mesh for 0° angle of attack

The lateral boundary conditions and the top boundary condition are modeled as symmetry planes. Therefore influence of the walls in the wind tunnel experiment is neglected.
The upstream surface is defined as an inlet using different approaches: a steady state inlet approach without turbulence, and an approach that models turbulent structures. The downstream boundary condition is modeled using a constant pressure. The cube and bottom surface of the domain are both modeled as smooth walls.

VALIDATION

The influence of the different simulation settings is validated, inter alia, by analyzing the non-dimensional averaged velocity components of the flow $\langle u_i^* \rangle = \langle u_i \rangle / \langle u_H \rangle$ and the non-dimensional averaged turbulent kinetic energy $\langle k^* \rangle = \langle k \rangle / \langle u_H^2 \rangle$ using the hit ratio q (Eq. (4)) [13]. Here, the chevrons $\langle\rangle$ denote averaged values, the asterisk * denotes a non-dimensional value, u_H is the upstream velocity of the atmospheric boundary layer at building height H and k is the turbulent kinetic energy:

$$q = \frac{}{N} \cdot \sum_{n=1} 1_n \quad \text{with} \quad 1_n \begin{cases} \\ 0 \text{ else} \end{cases} \tag{4}$$

with N representing the number of measurement points, S_n are the computed flow values, M_n are the flow values obtained from the wind tunnel experiment, Δr is the relative deviation threshold and Δa the absolute deviation threshold. For comparison to wind tunnel measurements and Δa equals the uncertainty of the measured values in the wind tunnel experiment.

The wind tunnel experiments, published via the website of the CEDVAL project, were performed by Bischof and Schatzmann [2]. The experiment was carried out in the BLASIUS wind tunnel at the Meteorological Institute of Hamburg University using modified Standen-Spires and a uniform LEGO-roughness to model the atmospheric boundary layer. Here, a wooden cube was used to model a building of 25 m size using a scaling factor of 1/200 in the middle of the floor in a test cross section of 1.5 m x 1 m size. The measurement of the velocities was performed using a 2D- laser Doppler anemometry and a Prandtl tube to obtain a reference velocity. Overall, 1314 individual measurements in the area of 2.5 H luv side, 5.5 H lee side, 3 H in vertical direction starting from the bottom of the wind tunnel and 2.5H in lateral direction have been performed.

VERIFICATION

Convergence check for the non-dimensional values of the velocity and the turbulent kinetic energy is performed by an estimating sampling window using the method proposed by [1]. Here, the moving average and the moving standard deviation of a flow value φ are observed over a window that is iteratively increasing by 50 non-dimensional time units of $T = \Delta t \cdot u_H / H$, with Δt representing the time step of the transient simulation. The residual of any tested variables φ is evaluated at the n-th sampling window in percentage to check convergence

$$\varphi_{res} = \left| (\varphi_n - \varphi_{n-1}) / \varphi_n \right| \cdot 100 \tag{5}$$

The magnitude of φ_{res} should decrease with increasing simulation time for a converging simulation. The simulation is assumed to be sufficiently converged when φ_{res} is below 5% for all considered flow values for averaged flow values and the standard deviations, respectively [1].
The systematic model and grid variation method aims to obtain the modeling and numerical error separately [4][9]. The governing idea is that the modeling error can be assessed by changing a modeling parameter. For the standard Smagorinsky this approach fits very well, because here the user can change the C_S modeling factor by himself before running the simulation. The numerical error can be estimated by obtaining the results of a defined decrease of the mesh size. This a posteriori method proposed by Klein uses three different simulations to estimate the model error $c_m h^m$ and the numerical error $c_n h^n$ [9]:

$$c_m h^m = (u_D - u_{G2}) / (1 - \alpha) \tag{6}$$

$$c_n h^n = \frac{(u_{G1} - u_{G2}) - (u_D - u_{G2}) \alpha^m}{1 - \beta^n}. \tag{7}$$

Here, u_{G2} represents the solution of the LES using a fine grid, u_D represents the solution using a different turbulence model parameter, u_{G1} represents the solution using a coarse mesh, α is the coarsening factor of the numerical grids, n is the order of the numerical error, m the exponent of the modeling error term and β represents the influence of the different coefficients of the Smagorinsky turbulence model. For this work m is set to 2/3 and the order of the numerical scheme n is set to 2 as proposed by Freitag and Klein [7].
Due to the implicit filtering applied in LES, that uses the grid size as a filter size, the obtained solution is dependent on the grid size. Therefore, a grid independent study usually performed for RANS simulations cannot be performed or LES. Thus, the quality of the numerical grid is examined using the LES_{IQ} proposed by Celik et al. [3][4] and recommended by Franke [6] for CWE problems. The governing idea of the LES_{IQ} is to assess the ratio of the actual, total turbulent kinetic energy k_{tot} of the case at hand to the resolved turbulent by the computed, large scales of the turbulent flow k_{res} (Eq. (8)). The closer this ratio gets to 1, the higher the resolved kinetic energy. For a DNS this ratio would become 1 and it is expected to decrease for LES with decreased mesh resolution. Now, the actual total kinetic energy of the case at hand is unknown and needs to be obtained. Two procedures are possible for attaining the total turbulent kinetic energy for the use of the LES_{IQ} method: On the one hand it is possible to measure the

total kinetic energy by using wind tunnel experiments k_{exp} and compare these to the resolved turbulent kinetic energy of the simulation k_{res}. On the other hand, the total turbulent kinetic energy can be approximated with the aid of two numerical simulations with different grids to retrieve the LES_{IQ}. In this work the calculation of the LES_{IQ} is twofold: It is assessed using results from the CEDVAL wind tunnel experiments and additionally gauged by a systematic grid refinement.

$$LES_{IQ} = 1 - \frac{|k - \bar{k}|}{k^{total}} \tag{8}$$

CONCLUSIONS

In this work LES of an atmospheric boundary layer flow over a wall mounted cube were performed for several cases with varying parameters using the open source software package OpenFOAM. This work successfully analyzes the effects of the different aforementioned simulations settings by using verification and validation methods. It shows the effects on the quality of the results and the errors of the numerical simulations. Additionally, the influence of the different simulation settings on the separated flow above the bluff body, the main flow region of interest for small scale wind turbines, is assessed. The insight given in this work allows future researches of flows around bluff bodies to produce economical LES simulations while maintaining a high quality.

REFERENCES

[1] Bruno, L.; Fransos, D.; Coste, N.; Bosco, A. (2010): 3D flow around a rectangular cylinder: A computational study. In: *Journal of Wind Engineering and Industrial Aerodynamics* 98 (6-7), p. 263–276.
[2] CEDVAL Database (2014): http://www.mi.uni-hamburg.de/CEDVAL_Validation_Data.427.0.html
[3] Celik, I. B.; Cehreli, Z. N.; Yavuz, I. (2005): Index of Resolution Quality for Large Eddy Simulations. In: *Journal of Fluids Engineering.* 127 (5), p. 949-958.
[4] Celik, I.; Klein, M.; Janicka, J. (2009): Assessment Measures for Engineering LES Applications. In: *Journal of Fluids Engineering.* 131 (3), S. 031102-1-031102-10.
[5] Franke, J.; Hellsten, A.; Schlünzen, H.; Carissimo B. (Eds.) (2007): Cost 732 best practice guideline for the CFD simulation of flows in the urban environment.
[6] Franke J. (2010): A review of verification and validation in relation to CWE. In: *The fifth International Symposium on Computational Wind Engineering CWE 2010,* Chapel Hill, North Carolina, USA.
[7] Freitag, M.; Klein, M. (2006): An improved method to assess the quality of large eddy simulations in the context of implicit filtering. In: *Journal of Turbulence* 7, No.40, p. 1-11.
[8] Gousseau, P., Blocken, B., van Heijst, G.J.., (2013): Quality assessment of Large-Eddy Simulation of wind flow around a high-rise building: Validation and solution verification. Computers & Fluids 79, pp. 120–133.
[9] Klein, M. (2005): An Attempt to Assess the Quality of Large Eddy Simulations in the Context of Implicit Filtering. In: *Flow Turbulence Combust* 75 (1-4), p. 131–147.
[10] Kornev, N., Hassel, E., (2006): Method of random spots for generation of synthetic inhomogeneous turbulent fields with prescribed autocorrelation functions. In: *Communications in Numerical Methods in Engineering 23*, p. 35–43.
[11] Lilly, D.K., (1992): A proposed modification of the Germano subgrid-scale closure method. In: *Physics of Fluids* A 4, 633-635.
[12] Smagorinsky, J., (1963): General circulation experiments with the primitive equations. In: *Monthly Weather Review 91*, p. 99-164.
[13] VDI 3793 Part 9 (2005): Environmental meteorology. Prognostic microscale wind field models. Evaluation for flow around buildings and obstacles.

THE INTERNATIONAL CONFERENCE ON
WIND ENERGY HARVESTING 2017
20-21 April 2017
Coimbra, Portugal

Paper 213

WIND ENERGY POTENTIAL OF THE HIGH-RISE BUILDING INFLUENCED BY NEIGHBOURING BUILDINGS – AN EXPERIMENTAL INVESTIGATION

Anina Šarkić Glumac[1]
University of Belgrade
Belgrade, Serbia

Hassan Hemida[2]
University of Birmingham
Birmingham, UK

Rüdiger Höffer[3]
Ruhr-University
Bochum, NRW, Germany

ABSTRACT

In order to increase wind energy harvesting from urban environment, the wind behaviour and the effect of the surrounding buildings needs to be fully understood. In this paper, wind tunnel experiments of the flow around a high-rise building with a height to width ratio of 3:1 surrounded by four high-rise buildings of the same geometry were performed to investigate the interference effect on the above roof flow. Velocity measurements as well as surface pressure measurements are presented. Two scale models of the high-rise building have been used; one with a flat roof and the other with a tilted roof and four different wind angles, with respect to the side of the high-rise building, were investigated; 0°, 15°, 30°, and 45°.

INTRODUCTION

Renewable energy can bring economic, environmental and social benefits. One potential strategy related to energy is to maximize city's own energy generation of renewable energy and in the same way to minimize its impact on health and environment [1]. Therefore, well suited renewable technology to urban environments could be wind power generation. Nevertheless, due to large roughness length, the built environment has relatively lower average wind speeds and higher turbulence levels. However, the disturbed flows around buildings can locally increase wind speeds. In particular, positions with the highest wind speed and lowest turbulence intensity are suitable for energy extraction and there are usually occurring at the roofs of the buildings.

Related to the studies of wind flow in urban environment, some authors have focused their attention on local wind loads on roofs and facades ([2], [3]), whereas some others have focused on the overall structural loads on buildings, including the changes on the wind-induced dynamic response of tall buildings due to other upstream buildings [4]. Still only limited studies are dealing with wind energy harvesting potential related to urban area ([1]).

In this paper, the interference effect related to the flow above high-rise building surrounded by four buildings under the influence of different flow angles is presented. This work reports on the wind tunnel experiments that have been carried out in the ABL wind tunnel in the Ruhr-University Bochum as part of a Short Term Scientific Mission (STSM) sponsored by the COST-Action TU1304.

WIND TUNNEL EXPERIMENTS

The interference effect of the surrounding buildings was investigated in case of the high-rise building in the Atmospheric Boundary Layer Wind Tunnel of the Ruhr-University Bochum, Germany. The wind tunnel has a cross section of 1.6 m x 1.8 m and a test section length of 9.4 m.

Two 1:300 scale models of the high-rise building have been used; one with a flat roof and the other with a tilted roof as shown in Fig. 1a). The height of the building is denoted by H (400 mm) and the width by B (133.3 mm). The height to width ratio of the building is H:B=3:1. Interfering buildings are represented as a copy of the main building with the flat roof with exactly same dimensions. The used geometrical arrangement for the interference configuration is presented in Fig. 1b). Four different wind directions (angles), with respect to the

[1] Assistant Professor, Institute of Numerical Analyses and the Theory of Structures, University of Belgrade, Bulevar kralja Aleksandra 73, sarkicanina@gmail.com
[2] Professor, School of Civil Engineering, University of Birmingham, B152TT, UK , h.hemida@bham.ac.uk
[3] Professor, Faculty of Civil and Environmental Engineering, Ruhr-University Bochum, Universitätsstraße 150, 44801 Bochum, IC 5/127, Ruediger.Hoeffer@rub.de

side of the building, have been considered: 0°, 15°, 30° and 45°. Fig. 1c) presents the measured configuration placed in the wind tunnel. Velocity as well as surface pressure measurements are performed.

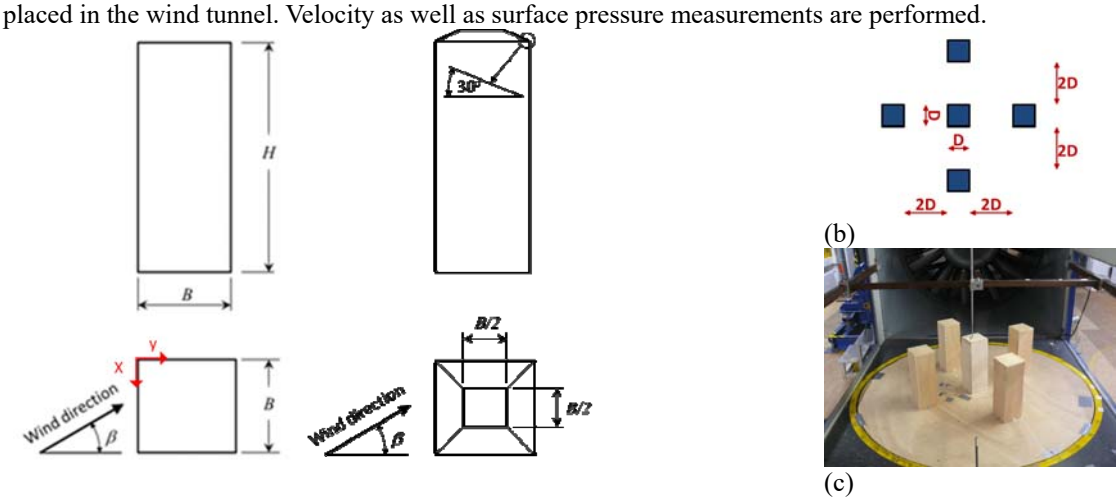

(a) (b) (c)

Figure 1. (a) Model of the single high-rise building with flat and tilted roof placed in wind tunnel, (b) arrangement of the buildings in interference configuration and (c) high-rise building in interference configuration placed in the wind tunnel

Hot wire anemometry and measurements of mean dynamic pressure were used to measure velocity. A Prandtl tube mounted one meter upstream of the model at the height of the roof of the principle model was used to set the reference wind tunnel velocity for each test. The velocities above the roof of the principal building in interfering configuration are measured at different locations at different heights.

The surface pressure was measured through ninety pressure taps distributed on the roof (64 taps) and sides (26 taps) as shown in Fig. 2. The spacing between the different taps is also shown in Fig. 2. For these pressure measurements the necessary equipment consists of pressure transducers (sensors), a tubing system, amplifiers and analog/digital (A/D) converters.

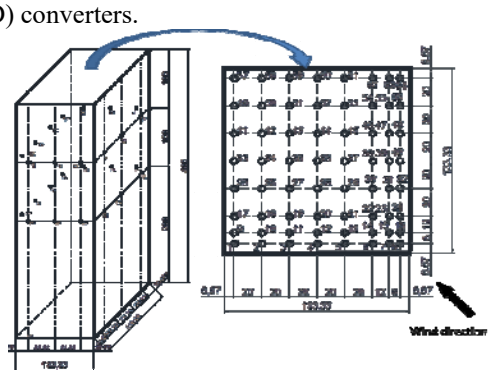

Figure 2. Distribution of pressure taps on the surface of the building with the flat roof

RESULTS

Fig. 3a) shows velocity distribution measured above two positions at the central line of the flat roof (point P20 and P36 from Fig. 2) for the 0° angel of flow attack. The velocity components in the y and z directions from Fig. 1a), u and w, respectively were measured. The lower upstream measurement position is slightly pointing downwards, suggesting a possible small separation at the upstream corner. However, all other positions are showing nearly parallel flow to the roof top, experiencing no significant increase in the streamwise wind velocity up to the height of z/D=0.675, where the magnitude of streamwise velocity suddenly increases to 14.5%. In addition, from this position upwards, observed turbulence intensities are becoming more comparable to the turbulence intensity that is measured in the upstream flow generated by the roughness elements and turbulence generators at the inlet of the wind tunnel. More detailed analysis of the velocity measurements related to interference configuration of the high-rise building with the flat roof can be found in [5].

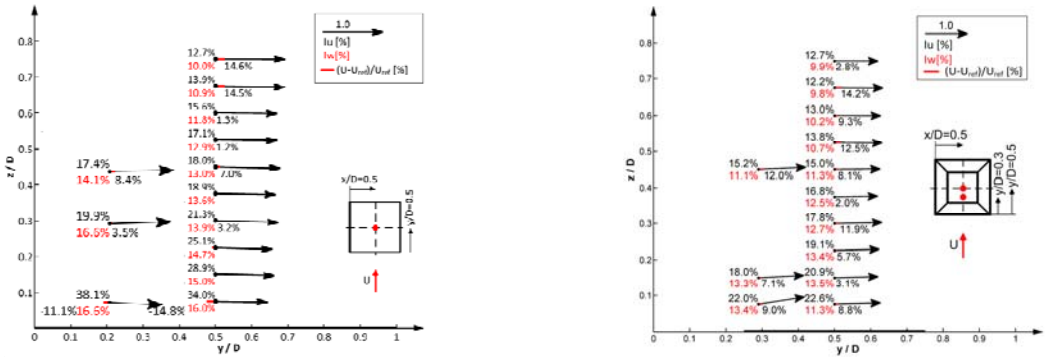

(a) (b)

Figure 3. Profiles of velocity vectors, turbulence intensity I_u (black number - marked next to the measurement points), turbulence intensity I_w (red number - marked next to the measurement points) and percentage increase in the wind speed (black number - marked aside of a vertical line defined by measurement points) over a single high-rise building under the influence of 4 surrounding high-rise buildings measured at P20 and P36 at 0° angle at (a) flat roof and (b) tilted roof.

Fig. 3b) shows corresponding flow field above similar positions over the tilted roof. The velocity vector above the upstream point suggests that the flow creates small separation at the windward edge. When compared with the flat roof case, the tilted roof generates velocity amplification of a similar magnitude (12.5%) only positioned slightly lower at z/D=0.525. In addition, the turbulence intensity is much lower close to the building than that of the flat roof.

Fig. 4 shows surface pressure coefficient at four measured wind angles. In case of 0˚ angle a significant reduction in the surface pressure close to the upstream edge can be observed that is directly followed by an increase in the surface pressure further downstream. This suggests a possible small separation at the upstream edge. More pronounced reduction of the pressure close to the upstream corner is occurring in the case of 15º yaw angle, suggesting larger separation bubble. In case of high yaw angles of 30º and 45º the flow separates at the upstream corner to form two separation cones along the upstream edges where the highest reduction in surface pressure exists.

In order to provide an improved understanding of the effect of wind direction on the surface pressure, the mean pressure coefficient and its standard deviation have been plotted along two vertical lines shown in the Fig. 5 and Fig. 6 at measured wind angles. For yaw angles 15º, 30º and 45º pressure coefficient distributions in Fig. 5. show similar pattern that is characterized with the upstream hump shape followed by pressure increase. This is typical for a flow with a separated region followed by a reattachment [6]. In the case of the mean pressure distribution, the hump shape is related to large negative pressure values in the separated region, where the largest suction was found to follow directly beneath the average moving vortex core [7]. The length of the mean recirculation region is related to the peak location of the standard deviation value since the peak occurs just upstream of the mean reattachment position [6]. Therefore, more pronounced separation is observed in case of 30º yaw angle. Comparing Fig. 5 and Fig. 6 for large wind angles can be observed that the cone-like separation grows in size along the side of the building.

Power spectra density plots for the roof surface pressures of all measurement points at the middle line of the flat roof for an approaching flow angle of 45° are shown in Fig. 7. The significant peak near $nD/U_{ref} \approx 0.33$ is prominent for all measurement points. Since it is observed in all signals it can be related to the shedding frequency of the structures of the flow generated from the upstream building. A second distinct peak is related to the frequency $nD/U_{ref} \approx 0.11$ and it is observed at upstream points P4 and P12. Further downstream, this peak seems to shift to slightly lower frequency $nD/U_{ref} \approx 0.07$. This frequency can be related to the low-frequency unsteadiness of the shear layer. This transition of the low-frequency peak location is accompanied by increase in the broad band energy levels that is occurring around the point P20. Here the broad band energy levels reach a maximum from which they decrease further downstream. This behavior usually occurs near reattachment point, as it is stated in [6], and it is correlated to the approximation of the reattachment point based on the standard deviation of the pressure coefficient. Similar pattern is observed in case of approaching angles of 15° and 30°.

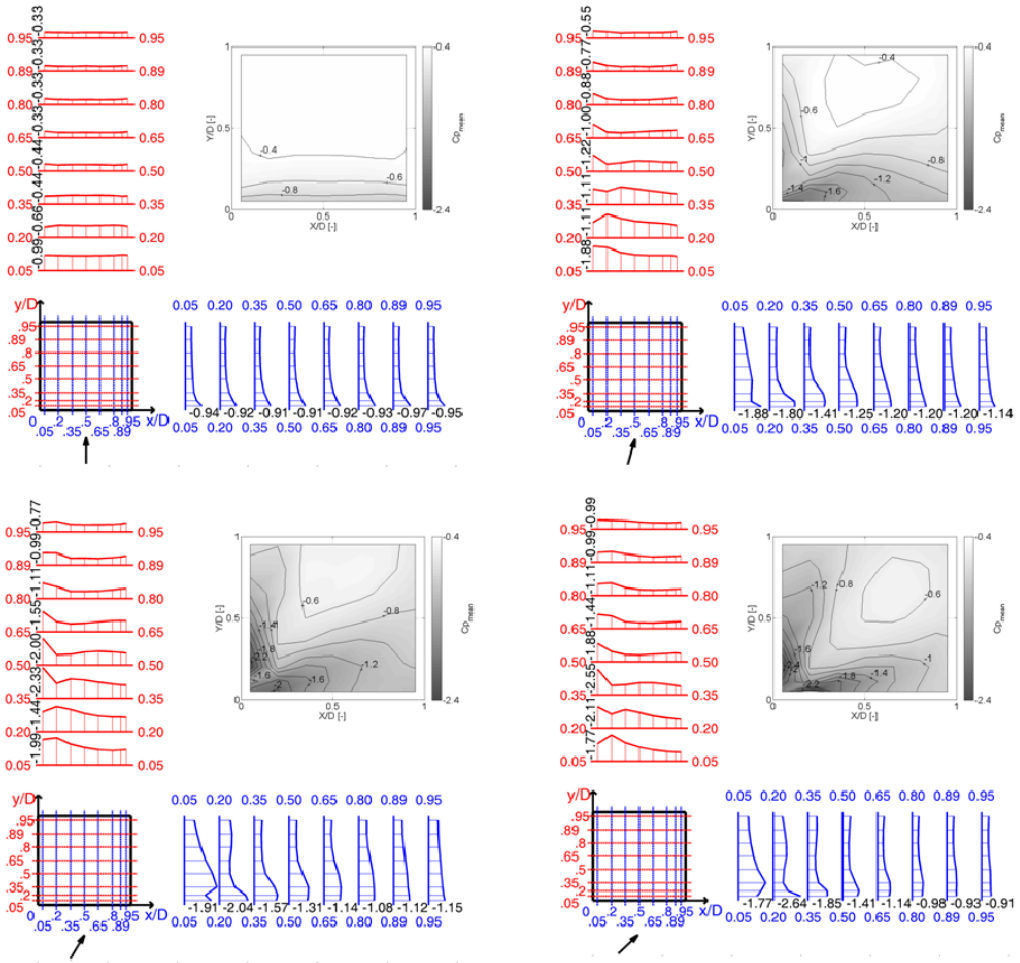

Figure 4. Surface pressure distributions on the flat roof for (a) 0˚, (b) 15˚, (c) 30˚ and (d) 45˚ yaw angle

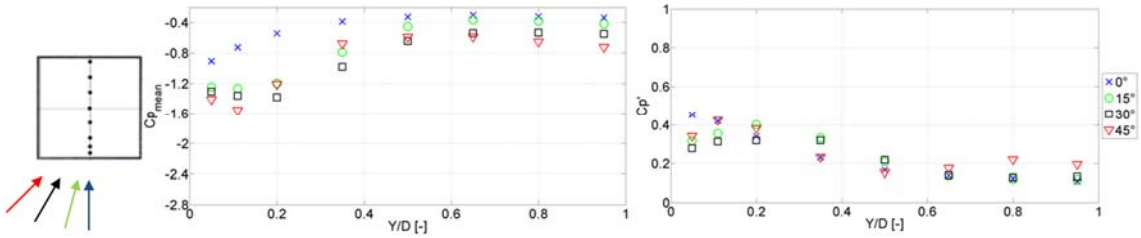

Figure 5. Mean and standard deviation distribution of pressure coefficient along vertical middle line at different wind angles

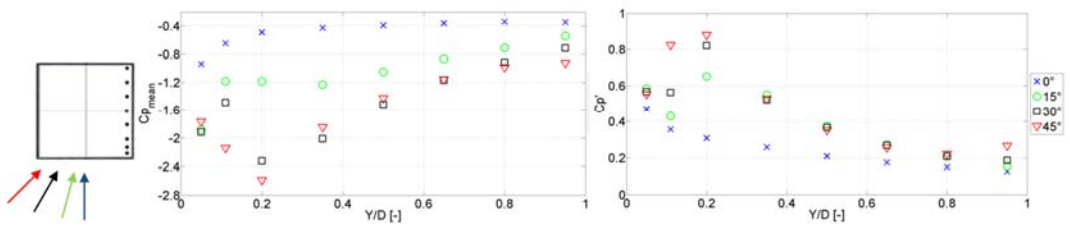

Figure 6. Mean and standard deviation distribution of pressure coefficient along vertical corner line at different wind angles

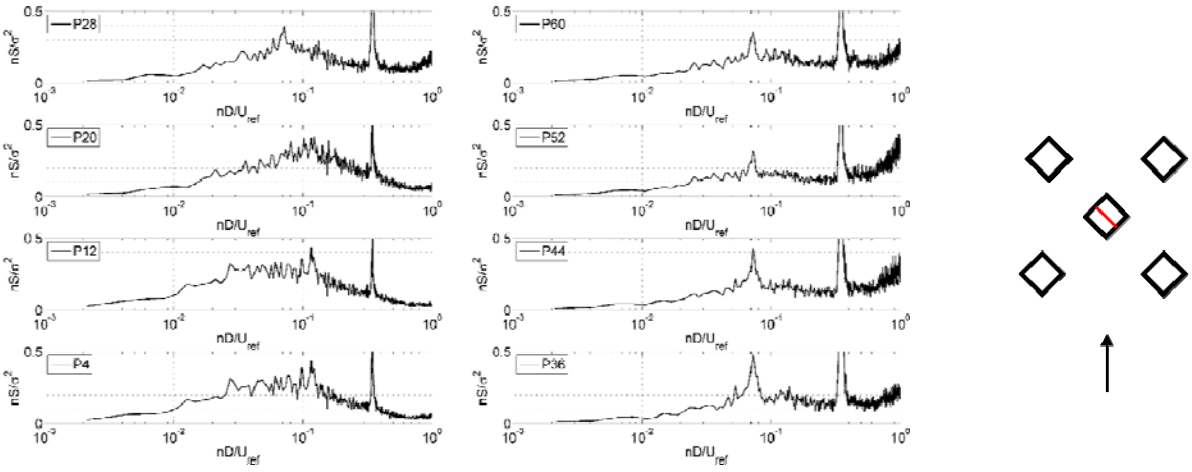

Figure 7. Energy spectra of the pressures for line x/D=0.5 on the flat roof top of the high-rise building under the influence of 4 surrounding high-rise buildings for approaching flow of 45°

CONCLUSIONS

This paper reports on wind tunnel tests related to the configuration of high-rise building surrounded by four identical buildings. The main idea is to obtain as possible detailed representation of the flow above the high-rise building influenced by neighbouring buildings by joining results of velocity and pressure measurements. The following conclusions can be made from the current study:

- At 0° of approaching flow, increase of streamwise velocity component, as well as decrease of the turbulence intensity to the level similar to the free stream occurs at about two thirds of the building width above the roof.
- The flow above the tilted roof building is less turbulent than that above a flat roof.
- For higher yaw angles, in particular 30° and 45° separation cones are generated at the upstream sides of the building.

ACKNOWLEDGEMENTS

The authors would like to acknowledge the support provided by the Chair of the COST-Action TU1304 Prof Charalampos Baniotopoulos and his encouragement to undertake such work. The time and support received at the Ruhr-University Bochum by the Lab technicians are also acknowledged.

REFERENCES

[1] L. Lu and K.Y. Ip, "Investigation on the feasibility and enhancement methods of wind power utilization in high-rise buildings of Hong Kong", Renewable and Sustainable Energy Reviews, 13, 2009, pp 450–461
[2] S. Ahmad and K. Kumar, "Effect of geometry on wind pressures on low-rise hip roof buildings", Journal of Wind Engineering and Industrial Aerodynamics, 90, 2002, pp. 755–779
[3] K.M. Lam, M.Y.H. Leung, J.G. Zhao, "Interference effects on wind loading of a row of closely spaced tall buildings", Journal of Wind Engineering and Industrial Aerodynamics 96, 2008, pp. 562–583.
[4] A.C. Khanduri, T. Stathopoulos, C. Bedard, "Wind-induced interference effects on buildings – a review of the state-of-the-art", Engineering Structures, 20, 1998, pp. 617–630.
[5] A. Šarkić, H. Hemida, K. Kostadinović, R. Höffer, "Experimental investigation of interference effect of high-rise buildings for wind energy extraction", WINERCOST Workshop 'Trends and Challenges for Wind Energy Harvesting', Coimbra, 2015.
[6] F.Haan, "The effects of turbulence on the aerodynamics of long-span bridges", PhD thesis, University of Notre Dame, Indiana, 2000.
[7] D. Banks et al. D. Banks, R.N. Meroney, P.P. Sarkar, Z. Zhao, F.Wu, "Flow visualization of conical vortices on flat roofs with simultaneous surface pressure measurement", Journal of Wind Engineering and Industrial Aerodynamics, 84, 2000, pp. 65-85.

THE INTERNATIONAL CONFERENCE ON
WIND ENERGY HARVESTING 2017
20-21 April 2017
Coimbra, Portugal

Paper 214

WIND FLOW AROUND A BUILDING OF AN ATYPICAL FORM

Olga Hubova[1]
Faculty of Civil Engineering STU Bratislava
Bratislava, Slovakia

Lenka Konecna[2]
Faculty of Civil Engineering STU Bratislava
Bratislava, Slovakia

ABSTRACT

This article deals with investigation of air flowing around an atypical building. Result is an important parameter of pressure coefficient on the structure, what is necessary for design of buildings and structures (or parts of structures) in terms of wind load calculations. Wind tunnel measurements of wind flow and wind pressures distributions around an atypical building whose cross section was quarter circle, were performed in BLWT STU in Bratislava for 24 wind directions and different speeds in steady and turbulent wind flow.

NOMENCLATURE

w_e	=	External wind pressure (Pa)
c_{pe}	=	External wind pressure coefficient (-)
I_v	=	Intensity of turbulence (%)
α	=	Local angle of wind attack (rad)
z_0	=	Roughness length (m)
q_p	=	Peak velocity pressure (Pa)
ρ	=	Air density (kg/m^3)
v_{ref}	=	Reference wind speed (m/s)

INTRODUCTION

Wind actions on structures or structural elements are determined by wind pressure on surfaces. The basic parameter for determination of the wind load on the structure is peak velocity pressure q_p, which contains mean wind velocity and fluctuating part of wind velocity- turbulence. This is influenced by the atmospheric conditions in the given locality, height above terrain and local influences - roughness and orography, season and wind direction. The peak velocity pressure is calculated as the pressure in conditions of the mean wind speed and short-term velocity fluctuations. Wind pressure acting on the external surfaces depends on the external wind pressure coefficient c_{pe}[8].It is possible for typical shapes of constructions to find the values c_{pe} in Section 7 EN 1991-1-4 [2].

In the standard it is not possible to find wind pressure coefficients for atypical shapes of buildings. The wind pressure distribution on these structures can be obtained by experimental measurements in the wind tunnel or by CFD simulation for a suitable model of turbulence. Recently a growing amount of high-rise structures in the shape of quarter circle (see Fig.1) has been built.

[1] Assoc. Prof., Department of Structural Mechanics, Slovak University of Technology, Radlinskeho 11, SK-810 05 Bratislava, Slovakia / email: olga.hubova@stuba.sk

[2] Researcher with Ph.D. title, Department of Structural Mechanics, Slovak University of Technology, Radlinskeho 11, SK-810 05 Bratislava, Slovakia / email: lenka.konecna@stuba.sk


a)

b)

Figure 1. Quarter circle shaped high-rise buildings

METHODOLOGY

Experimental measurements were performed at Boundary Layer Wind Tunnel of Slovak University of Technology in Bratislava. Wind tunnel was designed with open circuit scheme (see Fig.2) with overall length 26.3 m and two operation sectors of cross-section 2.6 ×1.6 m and with adjustable ceiling. Front operation sector provides steady wind flow up to the velocity 32 m/s (115 km/h). The sector is used for testing of sectional models. Rear operating sector (ROS) is suitable for detection of effects caused by turbulent wind flow with velocity from 0.3 to 18 m/s. Measurements of local pressures on the small-scale models in front and rear operating sectors gave us information about airflow in steady and turbulent wind flow under various wind directions.

Simulated boundary layer for urban terrain requires the similarity criteria in four basic parameters:

1. Profile of mean wind velocity,
2. Profile of turbulence intensity,
3. Integral length scale,
4. Power spectral density function.

Mean wind velocity and intensity of turbulence profiles were investigated for different roughness and we obtained information on type and quality of boundary layer. The special devices like grids or foil and 2D barriers were inserted along wind tunnel (see [3], [6]). Length of roughness field is 14.4 m. Finally, turbulent wind flow is created in rear operating space. In our case, the roughness of floor was created by plastic film FASTRADE 20 and 150 mm barrier (Fig. 4). From the evaluation of the vertical mean velocity profiles, it seems that this modification of floor of tunnel is in the match with terrain category III.– IV. (closely to IV.), according to [2] with roughness length z_0 = 0,69 m (see [7]).

We tested the model of building in two spaces in steady and turbulent wind flow (see Fig. 2) by changing of wind direction and wind velocity. Measurements were conducted using pressure scanner DSA 3217 from Scanivalve.

Measured profile - quarter circle with a radius of 0.16 m and length of 1.1 m was placed centrally in front of the measuring space, 0.8 m above the floor, where the steady flow was measured (see [3], [6]). Initial position of segment (rotation angle 0°), dimensions and 16 measured pressure taps are shown in Fig. 3. Wind velocity has been set by using software LabVIEW. The model was rotated every 15º, thereby was simulated the changing of wind direction acting on the object. The evaluation of the measured data enables to determine the most unfavorable position with maximum values of suction and wind pressure for different wind speeds.

a)

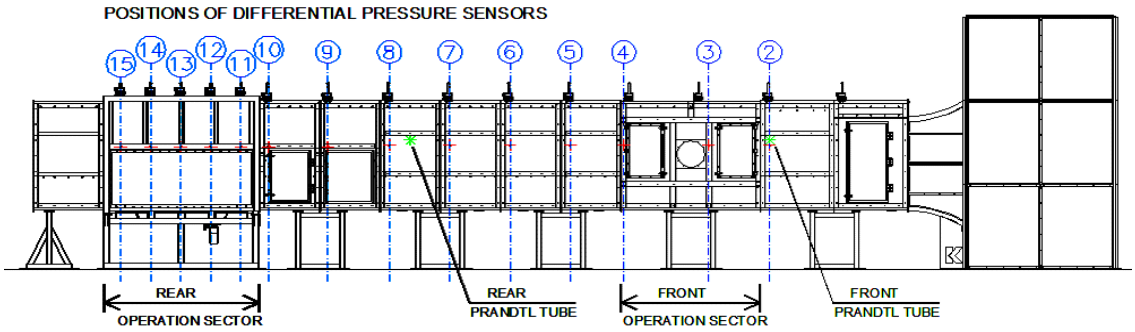

b)

Figure 2.BLWT STU wind tunnel in Bratislava with two measurements sectors

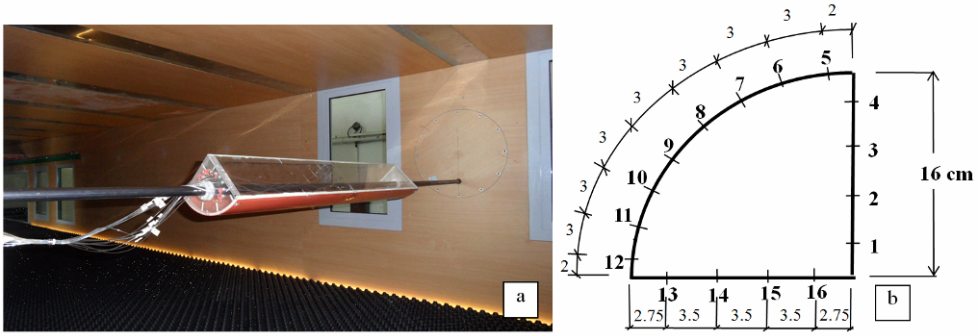

Figure 3. Model of quarter circle shape in steady wind flow (a) and initial position (b)

Second model with height h = 0.273 m and radius r = 0.11m (scale 1:380) was placed in the middle of turn table in turbulent wind flow and initial position of segment (rotation angle 0°) can bee seen in Fig. 4. Measurements were made at heights z_A = 0.258 m, z_B = 0.136 m and z_C = 0.015 m above the floor. Resultant value was determined as average of 1 000 samples (in each tap). The measurements were carried out for 2 frequencies (f_1 = 20 Hz, f_2 = 28 Hz). The reference wind velocities at the top of building were $v_{ref,1}$ = 8.94 m/s and $v_{ref,2}$ = 12.88 m/s. These values were measured by using the anemometer – Almemo.

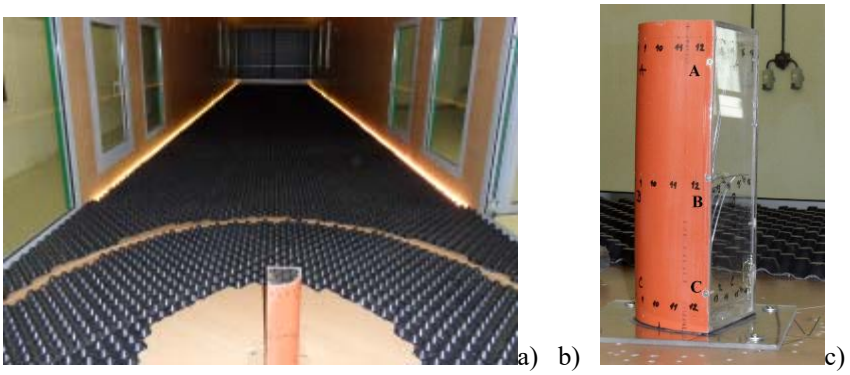

a) b) c)

Figure 4. Model of building in scale 1:380 placed in the turbulent wind flow

RESULTS

Obtained results - the wind pressure distribution and external wind pressure coefficients of examined structure are depicted in following graphs – Fig. 5.

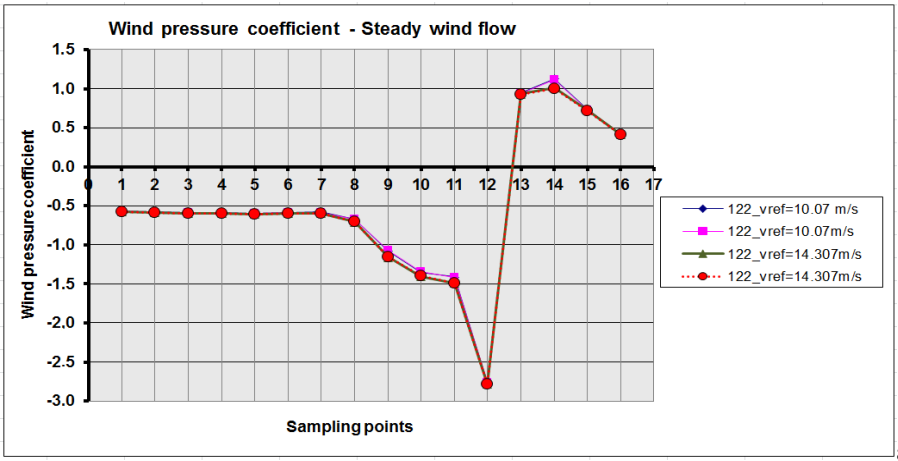

a)

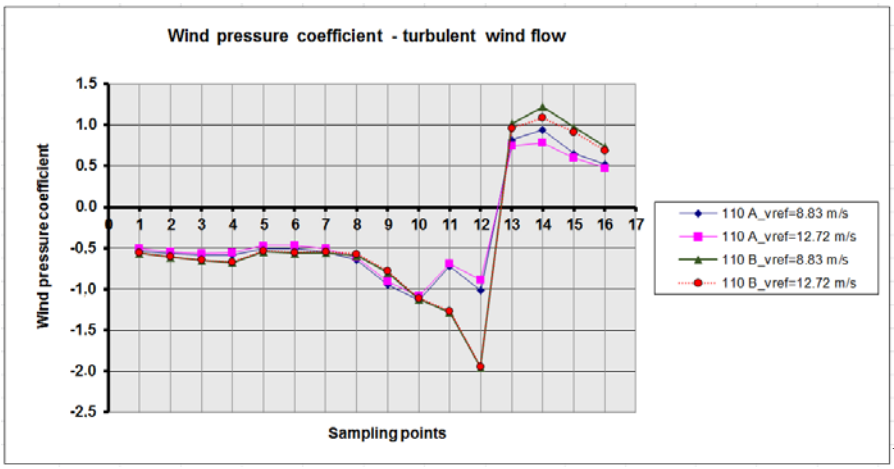

b)

Figure 5. Wind pressure coefficient in steady (a) and turbulent (b) wind flow

The results of experimental measurements were to determine the wind pressure distribution and external wind pressure coefficients for different wind direction and wind flow. Extreme values of the external wind pressure coefficient reached values of suction in steady wind flow c_{pe} = -2,78 and in turbulent wind flow at z_B = 0,136 m c_{pe} = -2,06 see Fig. 5.

In upper part of the structure (level A), the pressures are affected by specific wind flow around the free end of the structure, see Fig. 5b. The end-effect factor depends on the slenderness of the structure and on the wind direction.

CONCLUSIONS

The external wind pressure distribution and external wind pressure coefficients obtained from repeated experimental measurements made on model in steady and turbulent wind flow indicates the local extremes of suction in certain directions. Increased wind speed and suction of the corners of the building on the particular location of the object relative to the prevailing wind direction shows the danger areas on the façade of the structures.

ACKNOWLEDGEMENTS

The presented results were achieved under sponsorship of the Grand Agency VEGA of the SlovakRepublic (grants. reg. No. 01/0544/15). This paper was created with the support of the TU1304 COST action “WINERCOST”.

REFERENCES

[1] Counihan, J., “An Improved Method of Simulating an Atmospheric Boundary Layer in a Wind Tunnel”, Atmospheric Environment, Vol.3, 1969 pp. 197 – 214.

[2] EN 1991-1-4 Eurocode 1: Actions on structures-Part 1-4: General actions-Wind actions, 2005.

[3] Hubova, O. - Lobotka, P., “The multipurpose wind tunnel STU”, Civil and Environmental. Engineering, Scientific-Technical Journal, Vol. 10, Iss.1, 2014, pp. 2 - 9. ISSN 1336-5835, EV 3293/09

[4] ACSE Manuals and Reports on Engineering Practice, no.67, “Wind Tunnel studies of buildings and structures”, Aerospace Division of the American Society of Civil Engineers, 1999.ISBN 0-7844-0319-8.

[5] Hubova, O.,“Actual problems of the wind actions on structures and application of Eurocodes”, AD ALTA Journal of interdisciplinary research,Vol. 01, 2011. ISSN 1804-7890, ETTN 072 – 11 00001-01-4.

[6] Hubova, O. -Lobotka, P., “The Natural Wind Simulations in the BLWT STU Wind Tunnel“,ATF3rd Conference on Building Physics and Applied Technology in Architecture and Building Structures, May 6-7, 2014, TGM - Federal Institute of Technology, Vienna, Austria, pp.78-84.E-Book of reviewed papers.ISBN 978-3-200-03644-4.

[7] Wieringa, J., “Representative Roughness Parameters for Homogeneous Terrain”, In: Boundary Layer Meteorology, Vol. 63, Iss. 4, 1993, pp. 323-363.

[8] Holmes, J.D., “Wind loading of structures”, Spon Press, London, 2001.

[9] Stathopoulos, T. - Baniotopoulos, C.C., “Wind Effects on Buildings and Design of Wind Sensitive Structures”, CISM Courses and Lectures No. 493, International Centre for Mechanical Sciences, Springer, Vienna, 2007.

THE INTERNATIONAL CONFERENCE ON
WIND ENERGY HARVESTING 2017
20-21 April 2017
Coimbra, Portugal

Paper 215

WIND RESOURCE ASSESSMENT FOR THE POTENTIAL WIND FARM LOCATION AT FIELD OF WARSAW UNIVERSITY OF LIFE SCIENCES

Tomasz Bakoń[1]
Warsaw University of Life Sciences
Warsaw, Poland

Rafał Korupczyński[2]
Warsaw University of Life Sciences
Warsaw, Poland

ABSTRACT

In this study an evaluation of wind energy resources at a given area was presented. The location was a farmland of the Agriculture Experimental Institute of Warsaw University of Life Sciences – SGGW in Poland. On the basis of meteorological measurements for a few heights an average wind speeds, a Weibull shape and scale parameters as well as wind power density was investigated. Moreover, a preferred wind directions were determined. The results show a certain usefulness of given location at future as a place of a small wind farm for a teaching and research purposes.

NOMENCLATURE

AEI	=	Agriculture Experimental Institute (of Warsaw University of Life Sciences)
AGL	=	Above ground level
ASL	=	Above sea level
c	=	Weibull scale parameter (ms^{-1})
f	=	Probability of wind speed
F	=	Cumulative probability of wind speed
h	=	Height (m)
k	=	Weibull shape parameter
v	=	Wind speed (ms^{-1})
v_{av}	=	Average wind speed (ms^{-1})
WPD	=	Wind power density (Wm^{-2})
z_0	=	Roughness length (m)
α	=	Wind power law exponent
ρ	=	Density of air (kgm^{-3})

1 Assistant Professor, Faculty of Production Engineering, Energy Management Division, Warsaw University of Life Sciences – SGGW, Nowoursynowska 164, 02-787 Warsaw / Poland, tomasz_bakon@sggw.pl

2 Assistant Professor, Faculty of Production Engineering, Energy Management Division, Warsaw University of Life Sciences – SGGW, Nowoursynowska 164, 02-787 Warsaw / Poland, rafal_korupczynski@sggw.pl

INTRODUCTION

In the past few years an interest in wind power engineering in Poland went up. Some new and large wind farms arose. In the EU countries, there is requirement of 20% energy should be produced by renewable resources [1]. In the 2007 at the fields of Agriculture Experimental Institute of Warsaw University of Life Sciences at Żelazna (near the center of Poland) launched a meteorological station [2]. This place is potentially good for using of wind energy, because of quite strong winds. The measurement results were adopted in teaching and research. Moreover, brewed up the idea to build a wind farm for commercial and teaching reasons – partly as a business and partly as a laboratory. Hence, there is still a need to evaluate wind energy resource.

METEOROLOGICAL STATION

The station (fig. 1) was built above 174 m above the sea level on the farmland. Around the mast, at the radius about 500 to 700 m there are almost no buildings or trees. The aluminum mast is 12 m height. The first anemometer is on 6 m AGL, the second one on 12 m high. On 6 m AGL is also a barometer, thermometer and wind direction sensor. A data logger sends its measurement by the radio transmitter to the computer, which is localized in the main building of the AEI, about of 1 km from the mast. The data logger and sensors are supplied from one 12 V VRLA battery, which is changed one time for about two weeks. Moreover, there is a photovoltaic cell for the loading the battery, if the sun radiation is present. Measured parameters are: wind speeds (6 and 12 m AGL), atmospheric pressure, air temperature. The data are averaged every minute. In this study the results from the two years: 2008 and 2009 were presented.

Figure 1. Measuring mast on the field of AEI at Żelazna

RESULTS

The raw data: wind speeds (6 and 12 m AGL) and wind directions (6 m AGL) are presented in figures 2 and 3. Wind speed still is going up for 2 years. Preferred wind directions are west, south and south-west. If there are more than one wind turbine, they should not shade one another for wind from these directions. Wind speed at greater heights was calculated by the wind profile power law [3]:

$$v_{h2} = v_{h1}\left(\frac{h_2}{h_1}\right)^{\alpha}$$

where: v_{h2}, v_{h1} – wind speed at height h_2 and h_1 AGL respectively, α – exponent of the wind profile, which is dependent on characteristics of terrain.

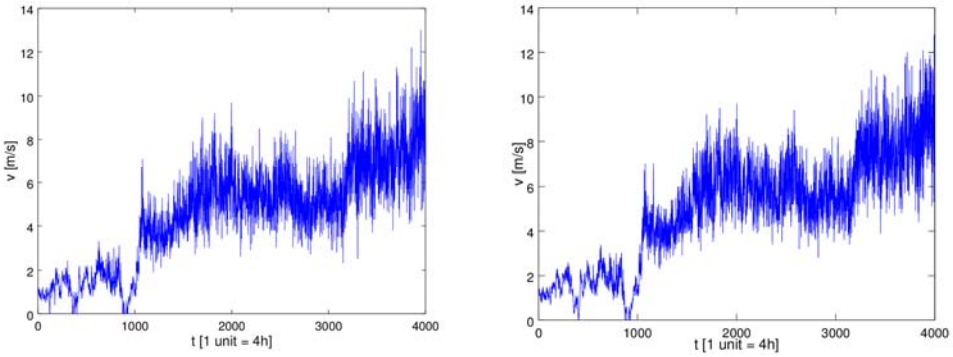

Figure 2. Wind speed at 6 m AGL (left) and 12 m AGL (right) vs. time

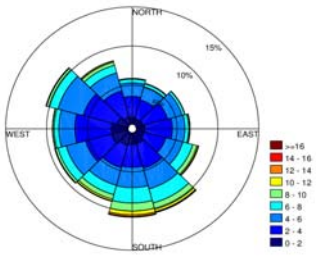

Figure 3. Wind rose at 6 m AGL

The exponent calculated from the average speeds at height 6m and 12 m is equal $\alpha = 0.175$. If we want to know the terrain class there is a need to know the roughness length z_0. It can be calculated from simple formula [4] after some conversion:

$$z_0 = \frac{h}{e^{\frac{1}{\alpha}}}$$

where: h is measurement height AGL (m). Because of α was calculated from two heights: (6 and 12 m), h has to be an average from the two heights, that is 9 m. Then z_0 is 0.030 m.

From [5] the roughness has to be calculated as:

$$z_0 = \frac{\sqrt{h_1 h_2}}{e^{\frac{1}{\alpha}}}$$

Calculated value of z_0 is equal 0.028 m. Both ways of roughness calculations provide very close results. On the figures 4 relations between wind speeds and time for the given heights are illustrated.

In [6] J. Wieringa updated Davenport Roughness Classification. For $z_0 = 0.03$ m there is class 3 "Open" terrain with only low plant and few high objects. Such terrain (farmland of AEI) is under discussion.

From [7] the average wind speed 6 ms^{-1} at 30 m is sufficient for small or medium wind projects. This context the business wind farm on the field of AEI is not valid from economic reasons. However, from

research and didactical point of view, there are some evidences to build small wind farm at aforementioned localization.

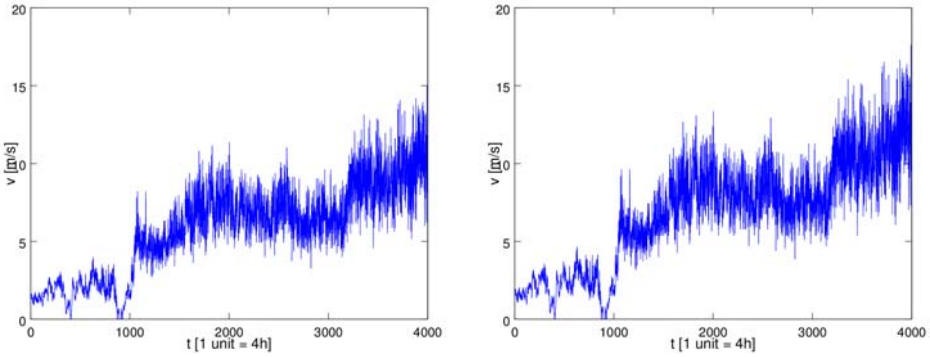

Figure 4. Wind speed at 30 m AGL (left) and 75 m AGL (right) vs. time

Because of randomized wind nature, there is a reason to use some statistical methods. One of them is the Weibull distribution which is widely used [8]:

$$f(v) = \frac{k}{c}\left(\frac{v}{c}\right)^{k-1} \exp\left(-\left(\frac{v}{c}\right)^{k}\right)$$

where: $f(v)$ – probability of speed v, k – dimensionless shape parameter, c – scale parameter (ms $^{-1}$).

Both parameters can be calculated by linear regression [9] which has to be applied to cumulative Weibull distribution. At figure 5 distributions and histograms are presented.

For a more practically heights (above 30 m), from wind power engineering point of view, the most probably wind speed is about 4 ms^{-1}. If the height is going up, the distribution shapes will be more flattened (compare a vertical scale of fig. 5). The approximations of the Weibull curves (red) is quite well compared to discrete data (blue bars).

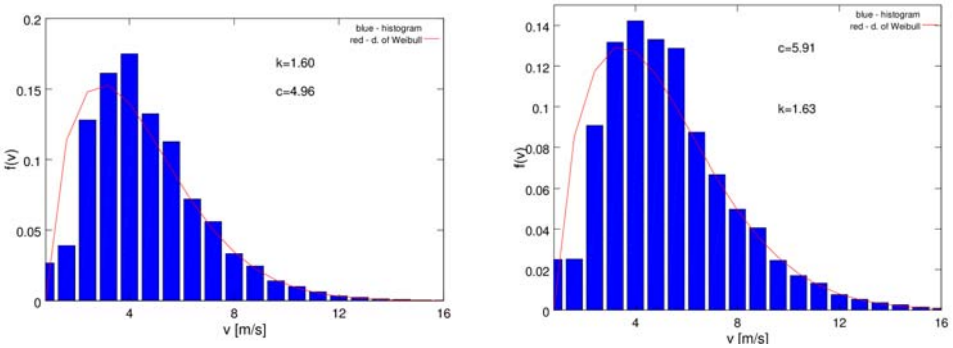

Figure 5. Wind speed distribution 30 m AGL (left) and 75 m AGL (right)

One of a wind energy resource parameters is wind power density WPD (W/m^2) [10]:

$$WPD = \frac{1}{2} \cdot \rho \cdot v_{av}^{\ 3}$$

where ρ is air density assumed to 1.22 kgm^{-3} for the standard atmosphere and v_{av} is average wind speed. In table 2 values of WPD, as well as average wind speeds, and Weibull parameters are presented. These last parameters are calculated for the every heights separately, based on measured (6 and 12 m) or calculated (30 and 75 m) wind speed time series. The values of WPD are quite low. At the 75 m AGL there is only above 100 Wm^{-2}.

Table 2. Wind power density and average speeds at given heights

h [m]	WPD [Wm^{-2}]	v_{av} [ms^{-1}]	k[-]	c[ms^{-1}]	Remarks
6	32.5	3.76	1.44	3.42	measuring height
12	41.9	4.09	1.54	4.04	measuring height
30	67.3	4.79	1.60	4.96	predicted height
75	109	5.63	1.63	5.91	predicted height

CONCLUSIONS

In this study, evaluation of wind energy resources at farmland of AEI was surveyed. Average wind speeds at few heights, wind roses, Weibull scale and shape parameters were determined. Moreover, wind power density was calculated at given heights. From point of view of the average wind speed, the localization which is being discussed, is not as good as possible for a commercial wind energy harvesting. Although, giving that is educational and scientific application of potential wind farm, the whole task has a chance of success.

ACKNOWLEDGEMENTS

Meteorological station was built by support of Rector of Warsaw University of Life Sciences [grant 50411250017 in 2007].

REFERENCES

[1] Directive 2009/28/EC of the European Parliament and of the Council of 23 April 2009 on the promotion of the use of energy from renewable sources and amending and subsequently repealing Directives 2001/77/EC and 2003/30/EC
[2] Czekalski D., Korupczyński R., Obstawski P., "Badanie zasobów energii wiatrowej w rejonie RZD SGGW w Żelaznej", Zeszyty Naukowe Politechniki Rzeszowskiej. Budownictwo i Inżynieria Środowiska , Vol.47, No.252, 2008, pp. 63-70
[3] Gualtieri G., Secci S. "Methods to extrapolate wind resource to the turbine hub height based on power law: A 1-h wind speed vs. Weibull distribution extrapolation comparison", Renewable Energy, Vol.43, 2012, pp. 183-200
[4] Hau E , "Wind Turbines Fundamentals, Technologies, Application, Economics, 2nd Edition", Springer, Germany, 2006, pp. 464
[5] Quaschning V., "Understanding Renewable Energy Systems". Earthscan London, UK, 2005, pp. 188
[6] Wieringa J., "Updating the Davenport Roughness Classification", Journal of Wind Engineering and Industrial Aerodynamics, Vol. 41, 1992, pp. 357-368
[7] Virtual Met Mast™ Plus, Met Office, Issue 5, 2013, www.metoffice.gov.uk/media/pdf/2/2/MO_VMM_datasheet_Issue_5_Nov13_FINAL.pdf
[8] Ulgen K., Hepbasli A., "Determination of Weibull parameters for wind energy analysis of Izmir, Turkey", International Journal of Energy Research, Vol. 26, 2002, pp.495-506
[9] Bhattacharya P., Bhattacharjee R., "A study on Weibull distribution for estimating the parameters", Journal of Applied Quantative Methods, Vol. 5, No. 2, 2010, pp. 234-241

THE INTERNATIONAL CONFERENCE ON
WIND ENERGY HARVESTING 2017
20-21 April 2017
Coimbra, Portugal

Paper 216

WIND RESOURCE ASSESSMENT AND IDENTIFICATION OF THE AVAILABLE WIND POTENTIAL IN URBAN AREAS - METHODOLOGY

Teresa Simões[1]
LNEG
Lisbon, Portugal

Ana Estanqueiro[2]
LNEG
Lisbon, Portugal

ABSTRACT

In the latest years the wind energy sector has experienced a huge growth all over the world. The deployment of onshore and offshore wind energy projects was recently followed by the interest in developing urban wind projects in order to respond to the integration of renewable energy systems in smart cities. This was followed by the need to find suitable and less costly methodologies for the urban wind resource assessment as well as the development of suitable planning methodologies in order to find the most interesting sites for urban wind energy deployment and to overcome the costly methods already existing for this purpose. This paper presents a methodology for the urban wind resource assessment and for the planning of the renewable integration in urban environments using geographical information systems. To illustrate the developed methodologies, a case study in an urban area is presented.

NOMENCLATURE

Fc_i	=	Correction factor
v_{ref_i}	=	Mean wind speed obtained with CFD-Urban (m/s)
v_{model_i}	=	Mean wind speed obtained with the CFD-Complex with the digital surface model for grid point i (m/s).
F_{ci_m}	=	Mean correction factor applied obtained from the average of the differences found between the results from CFD models
P_i	=	Grid point i
PD	=	Power density (W/m^2)
v_i	=	Mean wind speed in grid point i (m/s)
PD_i	=	Power density in grid point i (W/ m^2)
$v_{i,rec}$	=	v_i reclassified
$PD_{i,rec}$	=	PD_i reclassified
Pot_{sust}	=	Sustainable wind potential of the area under study (kW)
A_{tot}	=	Total area occupied by the grid points that obey the selection conditions
A_{min}	=	Minimum area needed for the installation of a small wind turbine
Pot_{WT}	=	Nominal power of a reference wind turbine
D	=	Wind turbine's diameter

[1] Junior Researcher, Energy analysis and networks research unit (UAER), LNEG – National Laboratory for Energy and Geology, Estrada do Paço do Lumiar, 22, 1649-038 Lisbon, Portugal, teresa.simoes@lneg.pt
[2] Senior researcher – Head of Research Unit, Energy analysis and networks research unit (UAER), LNEG – National Laboratory for Energy and Geology, Estrada do Paço do Lumiar, 22, 1649-038 Lisbon, Portugal, ana.estanqueiro@lneg.pt

INTRODUCTION

Urban wind energy has a large potential to be explored in the context of smart cities, whether through the installation of small wind turbines in the domestic sector (building rooftops and surrounding areas), or integrated in the building envelope providing that they are designed with wind energy exploitation in mind [1]. The wind potential in urban areas is difficult to characterize due to the high impact of obstacles and structures on the atmospheric flow. Buildings often cause flow separation, wind speed reduction and high turbulence on the top and around buildings. Also, in economic terms, the high costs of wind measurements campaigns are an important barrier to the development of this sub-sector of wind energy. Other data sources may be used for the characterization of the wind flow in urban environment, such as databases and national and regional wind potential atlas. These solutions are usually based on the application of data from mesoscale models (MM5 – Fifth Generation Mesoscale Model, WRF – Weather Research and Forecasting) to standard microscale models (e.g. WASP - Wind Atlas Analysis and Application Program [2]) that despite their validity, are not adapted to these environments. In both methods, the wind potential is often overestimated [3].

The use of CFD (*computational fluid dynamic*) models to characterize the wind behavior around buildings is nowadays state of the art. Nevertheless, the application of these models is highly time consuming, in particular when one needs to model large areas to adequately assess the impact of structures on the wind flow. In this context, a methodology was developed to characterize the urban wind potential, based on the construction of a surface involving the buildings' area, so that it can be treated as a very complex orography. In this particular case, the WindSim model [4] (referred subsequently as CFD-Complex) is used to model the surface of the buildings and the surrounding terrain (urban digital terrain model: U-DTM) and the Meteodyn model [5] (referred subsequently as CFD-Urban) is used to model the natural geometry of the buildings in a small area in order to introduce in the final resource map the influence of the obstacles (buildings) that are not considered with the detail in the generation of the surface. In both cases, the wind data from the Wind Potential Atlas for Mainland Portugal [6] are used.

After the resource maps elaboration, a methodology is developed to identify the suitable areas inside an urban area that can be further explored for the installation of small wind turbines. In this case a Geographical information system is used and interactive tool are developed having in mind the ability to update input and output data according to the objectives of each project the user wishes to study. The results obtained for the wind resource assessment and planning methodologies are illustrated in a case study and presented in this document.

METHODOLOGY

Wind Resource Assessment in Urban Areas

The proposed methodology is based on the generation of a digital terrain model which includes the terrain and the existing buildings as a whole, thus representing an *urban digital terrain model*: U-DTM. The urban DTM can be treated as a very complex terrain and used as input for a standard wind resource assessment model (e.g. Wasp, WindSim). This methodology strongly reduces the computational costs associated with standard CFD models to simulate groups of buildings; it simplifies the geometry of the urban mesh and enables to extend the area of simulation to a city scale. The U-DTM is inserted into the CFD-Complex and, by using synthetic wind data series obtained by mesoscale modeling, which enables the urban wind potential to be estimated in the absence of experimental wind data. Since the U-DTM will, in some regions, smooths the city geometry, and since wind data from numerical mesoscale modeling usually overestimates the wind potential in urban environments, it is also necessary to correct the obtained spatial wind resource maps in order to more accurately describe the urban wind flow. Therefore, in the proposed methodology some areas of a city are selected and modeled in CFD-Urban in order to establish correction factors to be applied to the results from the CFD-Complex. The results from both models are compared and the deviations analyzed to define the correction factors to be applied to the wind resource maps obtained with the U-DTM (equation 1).

$$Fc_i = 1 - \left(\frac{v_{ref_i}}{v_{model_i}}\right) \quad (1)$$

where Fc_i is the correction factor, v_{ref_i} is the mean wind speed obtained with CFD-Urban and v_{model_i} is the mean wind speed obtained with the CFD-Complex with the digital surface model for grid point i. Depending on the extension of the urban area under analysis, correction factors are defined for the area surrounding the buildings (area A) and for the building's rooftops (Area B), and the average of the differences is found and applied to the wind resource map using the expression in (1).

$$v_i = F_{c_{i_m}} \times v_{model_i}; \quad (3)$$

where $F_{c_{i_m}}$ is the mean correction factor obtained from the average of the differences found between the results from both models. The same formulation is performed for power density calculation (W/m2). The resource maps obtained after the correction factors application are inserted into a Geographical information system, and a set of tools are developed for the identification of the most suitable areas for wind energy systems installation. This methodology is described in detail and published in [7].

Identification of suitable areas for wind energy systems identification and quantification of the available wind potential.

The methodology for the identification of the avaliable wind potential is based on the establishment of a set of criteria which meets the minimum requirements for the instalation of wind energy systems that guarantee an efficient performance of each system. In a first stage, the definition of input conditions related to the wind resource is performed. For this purpose, a minimum capacity factor (Fc) that enables the efficient operation of the wind energy systems is established. As stated in [8] the limits between 10% and 20% are suitable for the Fc parameter. Also, in this work, a threshold of 5 m/s for mean wind speed and 130 W/m^2 are established. These input data are then reclassified in order to obtain a final map with the interest areas for the instalation of wind energy systems (eq. 2 and 3).

$$If\ v_i \geq 5.0\frac{m}{s}; \xrightarrow{reclassification} v_{i,rec} = 1; else\ v_{i,rec} = 0 \tag{2}$$

$$If\ PD_i \geq 130\frac{W}{m^2}; \xrightarrow{reclassification} PD_{i,rec} = 1; else\ PD_{i,rec} = 0 \tag{3}$$

Where v_i is the mean wind speed and PD_i is the power density, both in the corresponding in the grid-point i of the resource map. $v_{i,rec}$ and $PD_{i,rec}$ are the same values after reclassification.
The reclassified resource maps are them multiplied in order to obtain the resultant grid-points that obey all the conditions imposed to each parameter (eq. 4).

$$Pot_{0,1} = v_{i,rec} \times PD_{i,rec}\ ; \tag{4}$$

where $Pot_{0,1}$ corresponds to the resultant grid, populated with “0” and “1” (where “0” is not suitable and “1” is suitable). This grid can then be multiplied by one of the original resource grids in order to represent one of the variables, depending on the purpose of the study. After the selected areas are found, is the necessary to establish the mean suitable area to install a wind turbine. This area is determined according to the wind turbine model characteristics, namely the rotor diameter and the distance between wind turbines. In this case, the minimum distance to consider between is 3 diameters in the crosswind direction and 8 diameters in the along wind direction which corresponds to a final area of 24 D^2. The sustainable wind potential is then obtained by the equation 8.

$$Pot_{sust} = \frac{A_{tot} \times Pot_{WT}}{A_{min}} \tag{8}$$

Where Pot_{sust} is the sustainable wind potential of the área under study (in kW), A_{tot} is the total area occupied by the grid points that obey the selection conditions, Pot_{WT} is the nominal power of the wind turbine model selected for the study and A_{min} is the minimum area needed for the installation of a small wind turbine.

RESULTS

To test the methodologies described above, an urban area was selected and the results are presented in figures 1 and 2. Figure 1 presents the results obtained with the wind resource assessment methodology and figure 2 and table 1 present the results obtained with the methodology for the identification and quantification of the wind potential in the selected urban area.

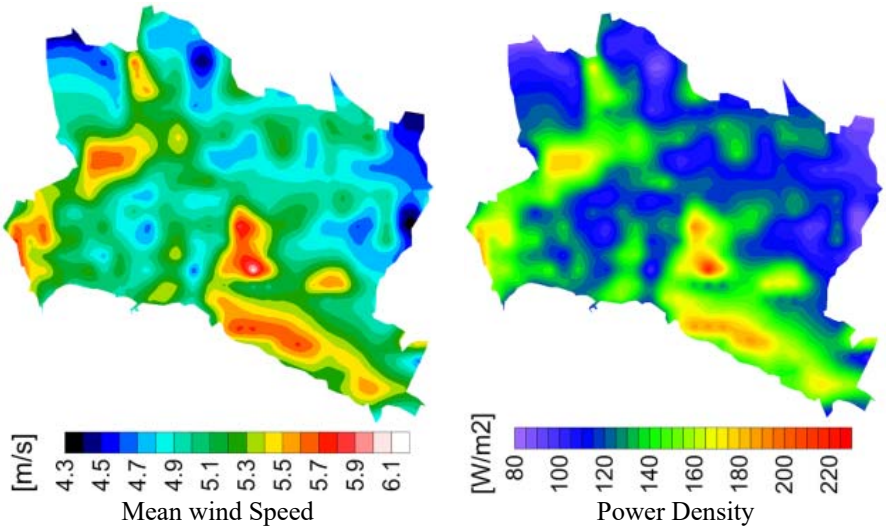

Figure 1. Resultant wind resource maps for an urban area representing, respectively Mean wind speed and Power Density for h=10m.

Table 1. Available potential in the urban area under study.

Total area (m^2)	Available area (m^2)	Available wind potential (MW)
8891376	1607856	11.152

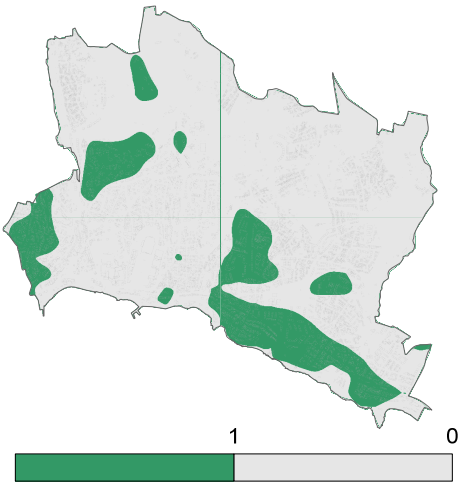

Figure 2. Available areas for wind energy systems installation

CONCLUSIONS

In this paper a methodology for urban wind resource assessment based on the generation of a surface involving the urban mesh and surrounding terrain was presented. It is based on simple and low-cost procedures which enable its replication to other urban areas. The results obtained are presented in detail and validated in [7]. Also a methodology for the identification of suitable areas for wind energy systems installation, as well as the quantification of the available wind potential is presented. It is based on the use of Geographical Information

systems and a set of interactive tools were developed for this purpose. The results here obtained are a valuable contribution for the determination of the sustainable wind resource in urban areas, for planning purposes, especially in the context of smart cities.

ACKNOWLEDGEMENTS

The authors wish to thank Prof. António Lopes from IGOT - Institute of Geography and Spatial Planning of the University of Lisbon and the municipality of Cascais for providing some of the data used in this work. The work developed for this paper was funded by the Portuguese Foundation for Science and Technology (FCT) under the grant: SFRH / BD / 41756 / 2007 and by the National Laboratory for Energy and Geology, I.P. (LNEG I.P.).

REFERENCES

[1] Stankovich, S., Campbell, N., & Harries, A. (2009). Urban Wind Energy. Earthscan - BDSP Partnership Ltd.

[2] Mortensen, N. G., Landberg, L., Troen, I., & Petersen, E. L. (1983). Wind atlas Analysis and Application Program (WASP), Vol. 1: Getting started. Roskilde: Risoe National Laboratory.

[3] Simões, T., Costa, P., & Estanqueiro, A. (2009). A first methodology for wind energy resource assessment in urbanised areas in Portugal. 2009 European Wind Energy Conference proceedings. Marseille.

[4] WindSim. (2009). WindSim, version 4.9.1.24234, copyright © 1997-2009 WindSim AS.

[5] Meteodyn. (2008). UrbaWind, version 1.5.0.0, copyright © Meteodyn 2008.

[6] Costa, P., Miranda, P., & Estanqueiro, A. (2006). Development and Validation of the Portuguese Wind Atlas. 2006 European Wind Energy Conference procedings. Athens.

[7] Simões, T., Estanqueiro, A., (2016). A new methodology for urban wind resource assessment. Renewable Energy, Elsevier, pages 598-605. Volume 89, April 2016.

[8] Trust, C. (2008). *Carbon Trust. Small-scale wind energy. Policy insights and practical guidance.* WindPower.

THE INTERNATIONAL CONFERENCE ON
WIND ENERGY HARVESTING 2017
20-21 April 2017
Coimbra, Portugal

Paper 217

URBAN WIND ENERGY ESTIMATES WITHIN A LISBON NEIGHBOURHOOD

Fernando Marques da Silva[1]
National Laboratory for Civil Engineering (LNEC)
Lisbon, Portugal

Gerardo Ibelli[2]
Lisbon University, Sciences Faculty
Lisbon, Portugal

ABSTRACT

Urban roughness increases wind natural variability both in time and space. This increased variability may change from a neighbourhood to the next one due to the change in layout, shape and buildings dimensions. The work presented here deals with the wind and SWT production assessments within a Lisbon neighbourhood where can be found different types of buildings under an irregular layout. Both wind tunnel tests and CFD simulations were used achieving a good match for the results showing the influence of building height and position. The estimated energy production, using a single SWT, is within the band of 1900 kWh <AEP< 2700 kWh 20 m above rooftops.

NOMENCLATURE

SWT	-	Small Wind Turbine
AEP	=	Annual energy production (kWh)
U	=	Wind velocity (m/s)
k	=	Weibull shape factor (-)
A	=	Weibull scale factor (m/s)

I. INTRODUCTION

Microgeneration in urban areas as a way to reduce energy demand is a concept getting increased support. If solar energy assessment and use is simple the same cannot be said about wind energy, moreover on urban environment. Wind energy use needs relatively strong and reliable (with a significant occurrence probability) winds, and as clean as possible (low turbulence levels). This statement almost means that one should forget urban wind power because the requirements are very difficult to obtain starting with the first one – frequent strong winds does not match with human settlements. It should be kept in mind that SWT has high design wind velocities. These difficulties may be increased by the urban aerodynamic roughness as the result of large built areas where layouts and buildings dimensions may change within short distances.

If in general wind assessment needs time in urban areas needs also to be evaluated at each point where a SWT is intended to be sited. Clearly this becomes easily too expensive to make such a project economically feasible. In order to reduce such initial costs it is important to have a clear idea on the site feasibility or what will be the best spots to install a SWT within a neighbourhood. To achieve such a purpose complementary techniques of wind tunnel tests and CFD models may be used allowing identifying those spots reducing the number of measuring stations and the monitoring time.

This work presents such a complementary study applied to a Lisbon neighbourhood with a particular layout and different types of buildings. A scaled model was used for the wind tunnel tests performed at LNEC's facility together with a CFD simulation using ENVI-met software.

II. CASE STUDY

1 Research Officer, Structures Department, LNEC, Av. Brasil, 101, 1700-066 Lisboa, Portugal/fms@lnec.pt
2 MSc Student, Geography, Geophysics and Energy Department, Lisbon Univ., Campo Grande, Lisboa, Portugal

The 3.5 km^2 studied area is a residential neighbourhood sited on flat ground in the end of low rise low dense construction area wind path. It is an area of apartment buildings of different heights and ensembles from isolated towers to lower rise bands and including a school ground, Figure 1.

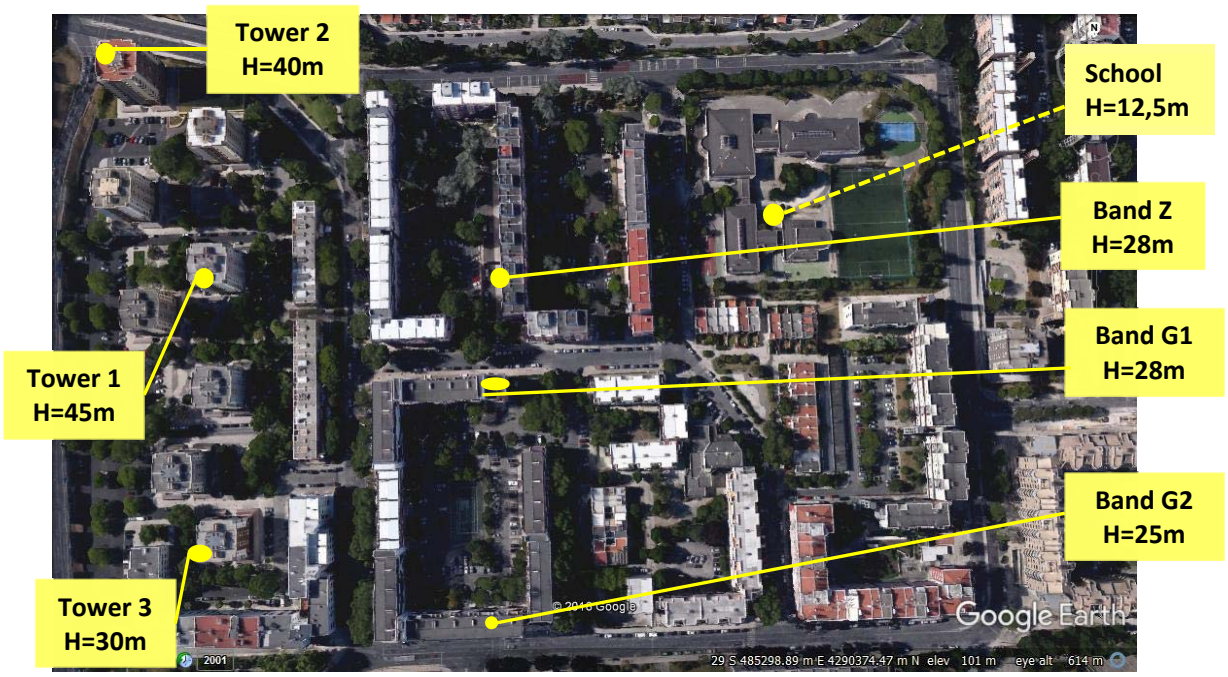

Figure 1. - Area under study

The "tower sector" on the left has eight taller buildings with heights from 30 to 45 m high and three bands with 15 to 25 m. The neighbour "band sector" show different arrangements of buildings all rising to 25 m high. On the top East corner there's an open school area with low rise buildings the taller having 12.5 m high. The zones on the bottom of the area under study are quite irregular showing buildings going from 3 to 30 m.

This area is around 3 km west of the Lisbon airport were the wind climate data was obtained, Fig. 3. The average for the velocity in Lisbon is U=3.7 m/s, 10 m above ground. The highest sectorial values, U=4.3 m/s, corresponding to North and Southwest incidences, but the largest occurrences are, by far, from North.

The Weibull parameters are k=1.82 and A=4.22 m/s and extrapolation for the height of 45 m brings U=5.3 m/s and the Weibull parameters to k=2.16 and A=5.96 m/s. both distributions are also presented in Figure 2.

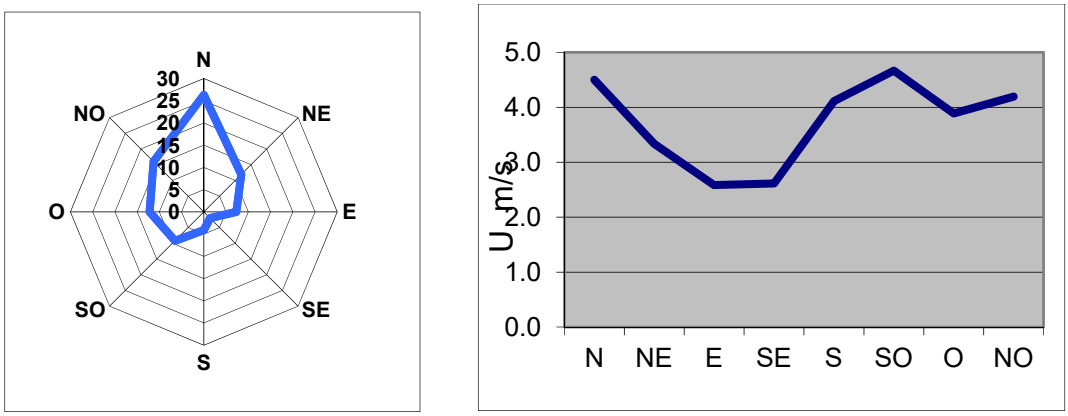

Figure 2. - Lisbon wind climate (1982-2005)

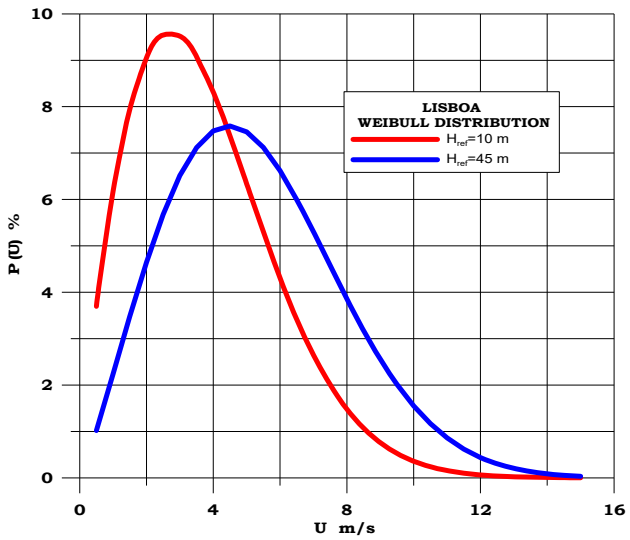

Figure 2 (cont.) - Lisbon wind climate (1982-2005)

III. METHODOLOGY

In order to evaluate the differences of wind potential production for small wind turbines (SWT) sited on building tops within the study area two approaches were used. i) wind tunnel tests over a physical model of the area, and ii) a CFD model.

3.1 - TESTING MODELS

The physical model reproducing and area of 650 x 320 m^2 was assembled at a 1/500 scale (Lopes, 2003), Figure 3, to be used in an open circuit wind tunnel with 3x2 m^2 of cross section and 9m long, the velocity going up to 18 m/s. The incoming flow simulates a boundary layer with a power law exponent of α=0.23 following Irwin's method (Irwin, 1981; Castanho, 2012). Three 1,22 m spires, 0.61 m apart each other, and a staggered array of 98 cubic roughness elements (10 cm edge) provided the incoming boundary layer profile, Figure 4.

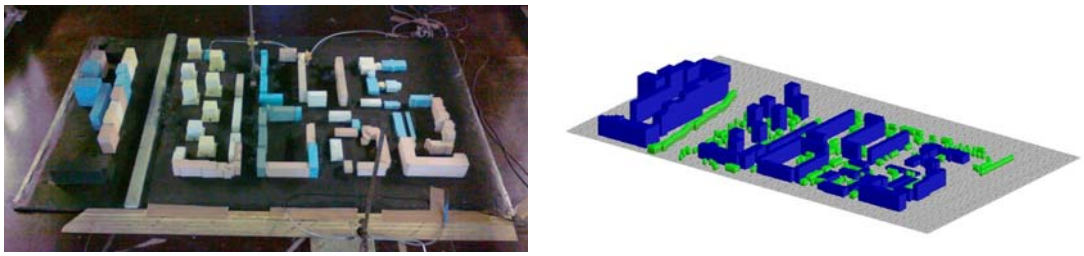

Figure 3. - Testing models: wind tunnel and CFD

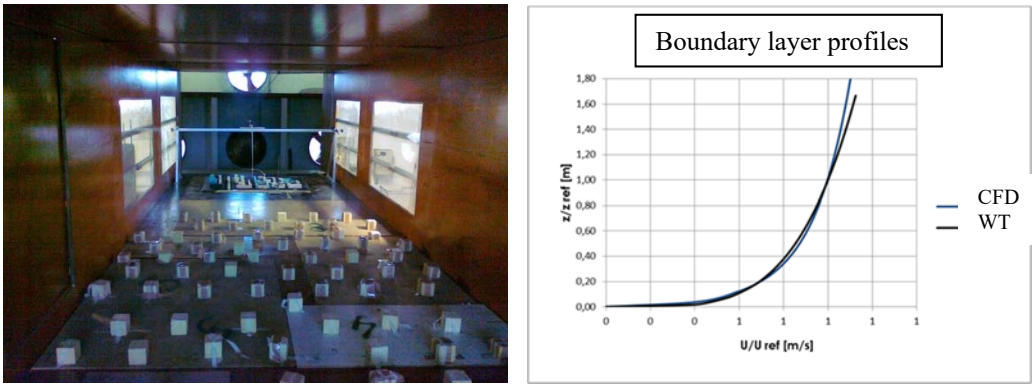

Figure 4. - Wind tunnel roughness elements and both BL flows.

3.2 - CFD MODEL

Figure 5 shows the correspondent CFD model used on free ENVI-met software (envi-met.com). The mesh has 159x89x30 cubic cells of 5 m^3 each except close to the ground where the height was reduced to the half. This 3D model goes up to 150 m high covering the same 3.5 km^2 area of the real one. The mesh has a telescopic vertical variation increasing its dimension in 10%, each step, above the height of 600 m. A boundary layer flow identical to the one inside the wind tunnel was imposed.

IV. RESULTS

When overcoming the obstacles presented by the buildings the flow separates immediately above rooftops generating areas of low and reversed velocity. Above such separated flow bubbles the velocity is increased from the reference undisturbed velocity at rooftop level – $U_{ref}(45)$=5,3 m/s. Figure 5 shows the velocity profiles above rooftop of Tower 1 for different wind directions expressed by the ratio to the reference velocity and the velocity distribution over the area at 35m a.g.l., for NW wind. Similar vertical profiles were obtained for the other referred buildings and so discarding the possibility of using the school for SWT because the estimated local wind speed showed no increasing factor.

Those profiles allowed estimating the different AEP for marked buildings (Figure 1) at three heights above rooftop – 5m, 10m and 20m. For that purpose a 2.5 kW at 13 m/s, 2.3 m rotor diameter T.URBAN wind turbine was used. Figure 6 show the SWT and its power curve. Results are resumed in Figure 7.

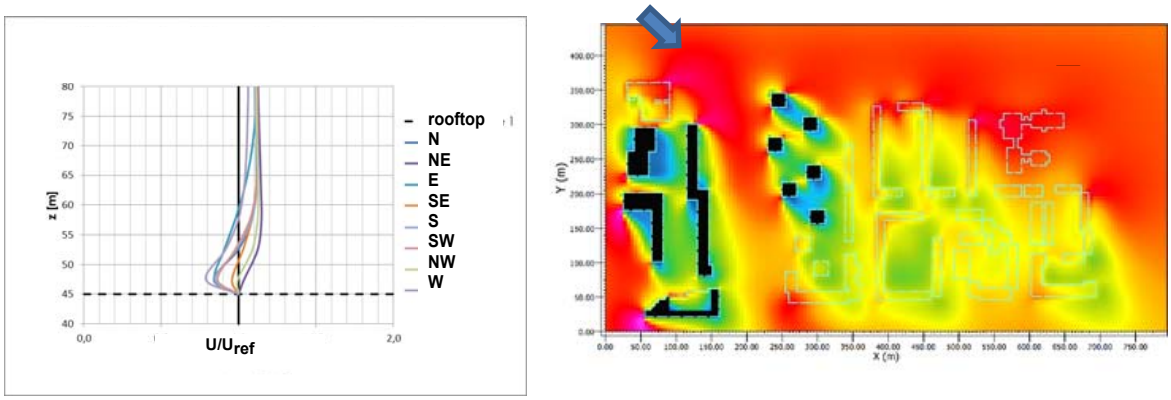

Figure 5. - Velocity profiles above Tower 1 and NW velocity distribution at z=35 m.

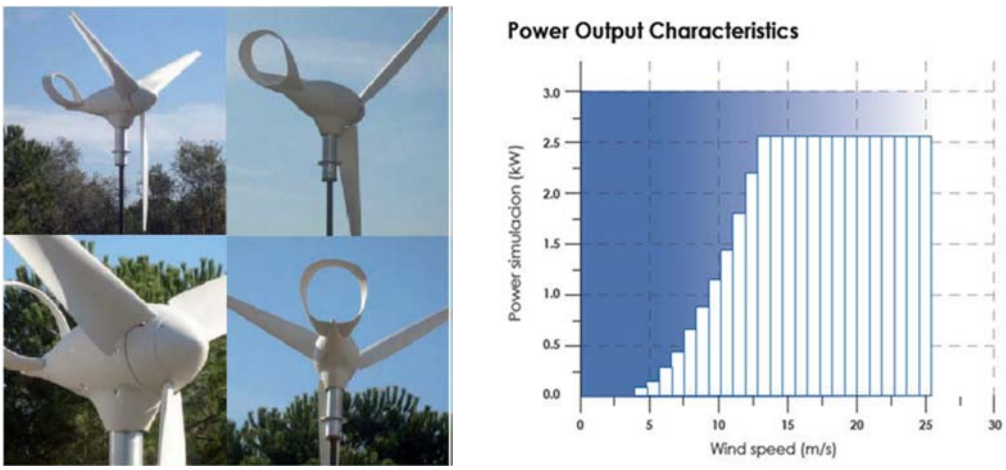

Figure 6. - T.URBAN wind turbine and its power curve

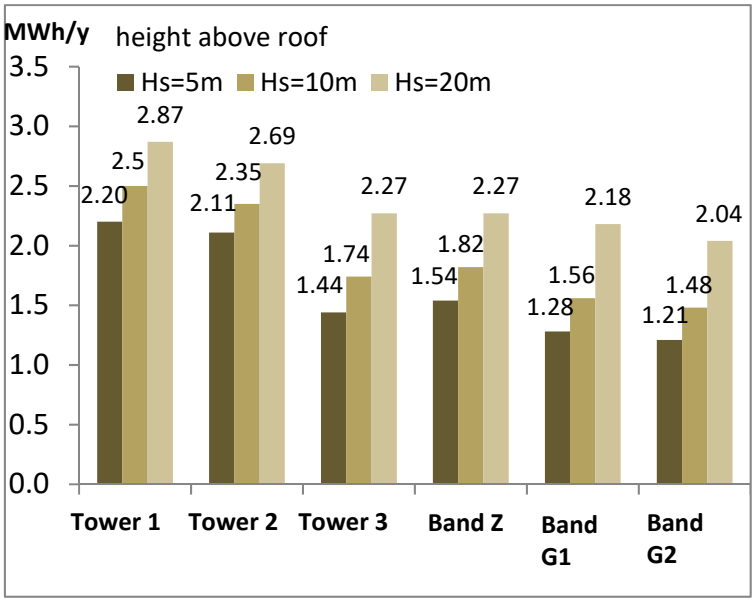

Figure 7 - Estimated AEP for the different buildings

V. CONCLUSIONS

A wind energy production assessment was performed for an urban neighbourhood inside Lisbon using complementary techniques of wind tunnel tests and CFD simulation. This allowed establishing vertical velocity profiles above selected buildings as a function of wind incidence.

Using reference wind velocities at rooftops heights, out from Lisbon wind data, and occurrence probabilities from a Weibull distribution it was possible to estimate the available wind power. Then using a small horizontal axis wind turbine with 2.3 m of rotor diameter and a rated power of 2.5 kW, at 13 m/s of wind velocity – T.URBAN -, estimates of power production were carried out for three heights above rooftop (h a. r. of 5, 10 and 20 m) for each of the selected buildings. The exception was the school because, due to its low rise buildings, of the insufficient available wind.

Lower rise buildings (T3 and bands) show higher power increase with height above roofs – 50% to 70% from 5m to 20m) than the taller ones (T1 and T2) where power increase is around 30%. Anyway even a 10 m tall SWT on rooftop may be excessive.

It may be concluded that the expected need of local evaluation of wind characteristics should be performed for each building or band of buildings in order to correctly estimate power production.

REFERENCES

[1] Irwin, H. “The Design of Spires for Wind Simulation” Journal of Wind Engineering and Industrial Aerodynamics, 7, 1981, 361-366.

[2] Castanho, A. S. “Experimental assessment of pedestrian comfort on urban environment”,: MSc Thesis, IST, Lisbon University, 2012. (in Portuguese)

[3] Henriques, J., Silva, F. M., Estanqueiro, A., & Gato, L. “Design of a new urban wind turbine airfoil using a pressure-load”. Renewable Energy, 34, 2009, pp. 2728-2734

[4] Simiu, E., & Scanlan, R. “Wind Effect on Structures”, 1996, Maryland: John Wiley & Sons, Inc.

[5] Ibelli G. “Urban wind power assessment. Telheiras case study” MSc Sciences Faculty, Lisbon University, 2013. (in Portuguese)

[6] Lopes, A. “Lisbon climate changes as a consequence of urban growth”, PhD Thesis Physical geography Sciences Faculty, Lisbon University, 2003. (in Portuguese)

[7] LNEG. “T.Urban Technical Details” on 16/11/2013, from T.Urban: http://turban.ineti.pt/entrada.htm

http://www.envi-met.com/#section/intro

THE INTERNATIONAL CONFERENCE ON
WIND ENERGY HARVESTING 2017
20-21 April 2017
Coimbra, Portugal

Paper 218

THEORETICAL-NUMERICAL ANALYSIS OF DYNAMIC BEHAVIOR OF CABLES SUBJECTED TO WIND LOADS

Hermes Carvalho[1]
UFMG
Belo Horizonte, Brazil

Gilson Queiroz[2]
UFMG
Belo Horizonte, Brazil

Ricardo H. Fakury[3]
UFMG
Belo Horizonte, Brazil

Paula M.L. Vilela[4]
UFMG
Belo Horizonte, Brazil

Patrícia Raposo[5]
INEGI & Faculty of Engineering, University of Porto, Porto, Portugal

Jose A.F.O. Correia[6]
INEGI & Faculty of Engineering, University of Porto, Porto, Portugal

A.M.P. de Jesus[7]
Faculty of Engineering, University of Porto, Porto, Portugal

Carlos Rebelo[8]
University of Coimbra
Coimbra, Portugal

ABSTRACT

Traditionally the analysis of cables subjected to wind is performed using an equivalent static analysis. However the occurrence of numerous accidents on structural systems composed of cables without the design speed being reached, indicates that collapse can be caused by dynamic action or errors on the estimates of wind forces. The objective of this paper is to present a methodology for dynamic analysis of cables subjected to wind, considering the geometric nonlinearity and the aerodynamic damping. The validation of the proposed procedure is performed by comparison with results obtained by other researchers and experimental results obtained in a wind tunnel. A comparison of the responses obtained for the dynamic analysis and the equivalent static analysis is presented.

INTRODUCTION

In transmission lines, the main load to be considered in the structural analyses is produced by wind, which acts dynamically on the system (towers, cables and insulator strings). Considering that several accidents involving towers of this type have occurred, although the wind speed used in the project was not reached, the collapse might be caused by dynamic actions or by some mistake in the wind effect estimate.

For the dynamic behavior, a space model of an isolated cable is evaluated, considering the geometric non-linear effects and the aerodynamic damping, with a huge influence in cases in which the structure assumes speeds next to the wind speed. The wind loading is modeled as a random process from statistical properties.

A numerical procedure which takes in account the aerodynamic damping is proposed and validated by confrontation with the formulae proposed by Davenport and Vickery and wind-tunnel tests presented by Loredo-

1 Associate Professor, Dept. Structural Engineering, University Federal of Minas Gerais, Av. Antônio Carlos, 6627, Belo Horizonte / MG, Brazil, hermes@dees.ufmg.br
2 Associate Professor, Dept. Structural Engineering, University Federal of Minas Gerais, Av. Antônio Carlos, 6627, Belo Horizonte / MG, Brazil, gilson@dees.ufmg.br
3 Full Professor, Dept. Structural Engineering, University Federal of Minas Gerais, Av. Antônio Carlos, 6627, Belo Horizonte / MG, Brazil, fakury@dees.ufmg.br
4 Master Degree, Dept. Structural Engineering, University Federal of Minas Gerais, Av. Antônio Carlos, 6627, Belo Horizonte / MG, Brazil, pmlv@ufmg.br
5 Research Assistant, INEGI/Faculty of Engineering, University of Porto, Rua Dr. Roberto Frias, 4200-465 Porto, Portugal, praposo@inegi.up.pt
6 Researcher, INEGI/Faculty of Engineering, University of Porto, Rua Dr. Roberto Frias, 4200-465 Porto, Portugal, jacorreia@inegi.up.pt
7 Professor, INEGI/Faculty of Engineering, University of Porto, Rua Dr. Roberto Frias, 4200-465 Porto, Portugal, ajesus@fe.up.pt
8 Associate Professor, Department of Civil Engineering, University of Coimbra, Coimbra, Portugal, crebelo@dec.uc.pt

Souza. The maximal values of the dynamic response obtained were compared with results produced by a static analysis in agreement with the prescriptions of the NBR 6123, with the application of the wind-gust coefficient.

NUMERICAL APROACH FOR DYNAMIC ANALYSIS OF CABLES

Succinct procedure description

A suspended cable, such as those employed in electric power overhead transmission lines, presents a catenary form. In the specific case of equal-height supports, this catenary will be symmetric about the central axis. Cable deflection depends on cable self-weight, span length, temperature and initial cable tension. For the simulation performed in this work, cables where modeled as non-linear truss elements (link 10) from ANSYS® commercial software. Keyoption 3 was set to 0 to allow elements to work only when submitted to tension. For the displacement calculations, both large displacement formulation and truss elements initial strains were considered. Fixed supports were considered at both cable ends. Dynamical analysis is performed in three main steps:

1st Step: Gravitational forces are applied gradually. Final cable configuration is obtained after a non-linear static analysis (dynamical effects are disabled);

2nd Step: Nodal forces corresponding to aerodynamic forces due to mean wind speed are applied on the cables. Loads should be introduced gradually with low increments, in a way that only low speeds are induced in the cables. The analysis is dynamic, therefore these speeds have to be small enough not to interfere on the next step results.

3th Step: Finally, the wind nodal forces (mean and fluctuant values) are set as arbitrary time functions. A transient dynamic analysis is then performed. For the numerical evaluations, a model composed by a simple conductor and leveled supports was built. The model had the dimensions of a real transmission line (span length equal to 400m).

For comparison with literature experimental results presented by Loredo-Souza [3], a similar but smaller model was built (span length equal to 150m). The other geometrical parameters were chosen according to Loredo- Souza [3].

Aerodynamic Damping

The aerodynamic damping is defined as a retardation effect produced by the relative displacement between air and structure. In the specific case of prismatic structures such as cables, moving in the wind direction and subjected to a uniform flow, a formulation was proposed by Davenport [1] e Vickery [2] to quantify the aerodynamic damping:

$$\zeta_{aj} = \left(\frac{C_D}{4\pi}\right)\left(\frac{\rho_a d^2}{m}\right)\left(\frac{V}{f_j d}\right) \quad (1)$$

where:

ζ_{aj} is the aerodynamic damping, for the j-th mode;
C_D is the drag coefficient;
ρ_a is the air density;
d is the cable diameter;
m is the mass per unit length of cable;
V is the wind speed;
f_j is the natural frequency of the cable, for the j-th mode in Hz.

The procedure proposed by this work takes directly into account the aerodynamic damping by considering the relative speeds between wind and cable, for the calculation of wind pressures. The basic formulation to obtain the wind pressure and the relative speed are presented in Equations (2) to (5):

$$V_R = (V(t) - V_{cable}) \quad (2)$$

$$V(t) = \bar{V}_z + v(t) \quad (3)$$

$$\bar{V}_z = \bar{V}_{10}(z/10)^p \quad (4)$$

$$q_{wind} = 0{,}613\,.V_R^2 \quad (5)$$

where:

q_{wind} is a dynamic pressure of wind;

V_R is the relative velocity between the wind and the cable;
$V(t)$ is the wind speed;
V_{cable} is the cable speed;
$v(t)$ is the fluctuating component of the longitudinal speed;
$\overline{V}_z$ is the average longitudinal velocity component of the project, in 10 minutes;
$\overline{V}_{10}$ is the average speed of project to 10 meters high, with a mean of 10 minutes;
z is the height from the ground point in the study, in meters;
p is the exponent coefficient on the roughness of the terrain.

With the formulation presented above, the procedure can be generalized and applied for any kind of structure which develops high relative speeds when excited by the wind.

Non-deterministic modeling of wind

To perform a non-deterministic dynamic analysis in the time domain, it is necessary to generate time functions to represent the fluctuant part of the wind longitudinal speed. In the present work, a random signal with zero mean value is generated from a PSD (Power Spectral Density). Equation (6) shows the time-history of the process variable $v(t)$ generated according to Pfeil [5]:

$$v(t) = \sqrt{2}\sum_{i=1}^{N}\sqrt{S^V(f_i)\Delta f}\cos(2\pi f_i t + \theta_i) \tag{6}$$

where:
$S^v(f)$ is the spectral density function;
N is the number of frequency ranges Δf considered in the spectrum;
f_i is the frequency, in Hz;
t is the time, in seconds;
Δf is the increased frequency, in Hz;
θ_i is the random phase angle between 0 and 2π.

The spectral density function employed, defined according to the studies of Kaimal (Blessmann [6]), is presented in Equation (7):

$$\frac{fS^V(z,f)}{u_*^2} = \frac{200\,x}{(1+50x)^{5/3}}\;;x(z,f) = \frac{z\,f}{\overline{V}_z} \tag{7}$$

where:
f is the frequency, in Hz;
u_* is the friction or tangential speed, in m/s;
z is the height from the ground point in the study, in meters;

For structures considered as big sized, several time series have to be generated. These series have to be spatially correlated. Spatial correlation is performed based on statistical formulations. The cross spectral density function and the cross correlation function employed are presented in equations (8) and (9), respectively:

$$S^{v_1,v_2}(f) = \int_{-\infty}^{+\infty} C^{v_1,v_2}(\tau)e^{-i2\pi f\tau}d\tau \tag{8}$$

$$C^{v_1,v_2}(\tau) = \int_{-\infty}^{+\infty} S^v(f)e^{-\hat{f}}e^{i2\pi f\tau}df \tag{9}$$

RESULTS

Figure 1 presents both the temporal evolution of the cable central node displacements and temporal evolution of the end support reaction in the wind direction (transversal to the cable). All the results are presented using the method proposed at this work, the Davenport's methodology and a simulation without the aerodynamic damping (with a wind gust of 32 m/s). The x-axis is longitudinal to the cable, the y-axis is horizontal and transversal to the cable (direction of the wind) and the z-axis is the vertical axis.

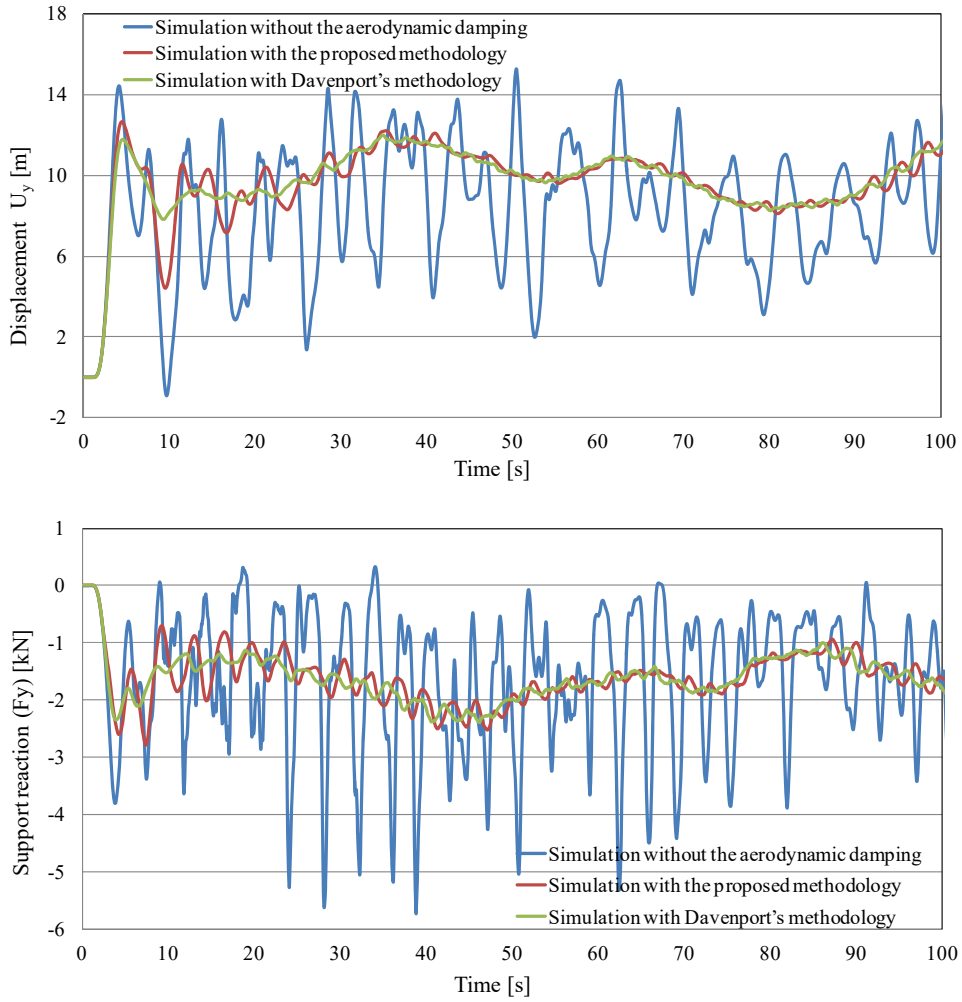

Figure 1. Temporal evolution of the cable's central node displacements and temporal evolution of the central support reaction in the wind direction for different methods

Table 1 presents the values of the cable's maximal reaction for a wind gust speed of 50 m/s for both dynamic and static analysis. The dynamic analysis is performed with the proposed procedure whereas the static analysis is performed using the wind gust factor, described at NBR 6123:1988.

Table 1: Proposed dynamic analysis versus static analysis.

Reactions	Proposed procedure	Static analysis
Fx [kN]	55,51	48,52
Fy [kN]	7,82	7,34
Fz [kN]	1,26	1,35

Figure 2 presents the temporal evolution of the support reaction, in the wind direction, obtained by the application of the proposed procedure model built according to Loredo-Souza (1996). Table 2 presents the comparison between the results of the simulation and those obtained from wind tunnel tests.

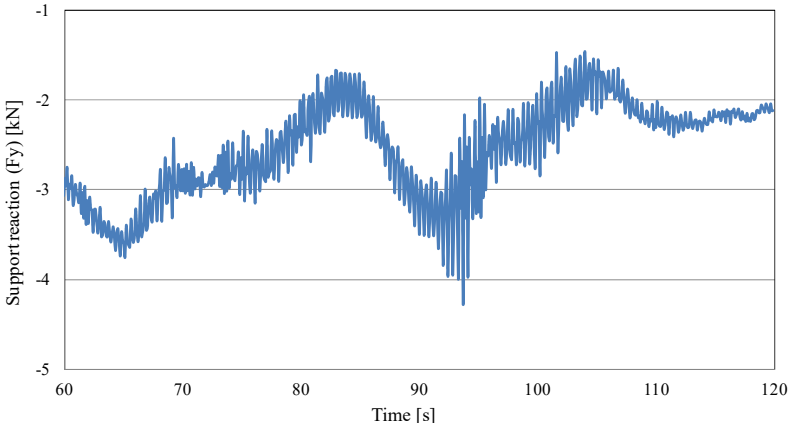

Figure 2. Temporal evolution of the support reaction obtained with proposed procedure.

Table 2: Proposed dynamic analysis versus experimental analysis.

Fy	Experimental analysis – reduced scale model Loredo-Souza [3]	Experimental analysis – real scale model Loredo-Souza [3]	Dynamic analysis	Error [%]
Minimum [kN]	1,36 x 10-5	1,7	1,5	11,5
Average [kN]	2,40 x 10-5	3,0	2,6	13,0
Maximum [kN]	3,60 x 10-5	4,5	4,3	4,5

CONCLUSIONS

A method to take in to account the aerodynamic damping in cables subjected to wind dynamic effects was proposed in this work. The proposed method consists in aerodynamic pressure calculations considering the relative speed between cable and wind. The proposed method results were compared with those based on the formulation proposed by Davenport (1988) and Vickery (1992). The results were also confronted with laboratory wind-tunnel results issued by Loredo-Souza (1996). Both comparisons showed good agreement.

It was showed by the results that cable response is reduced considerably when aerodynamic damping is considered. Even though cable response was reduced, maximal support reaction was above that obtained by the application of the wind gust factor in a static analysis (Loredo-Souza, 1996). Therefore, the usual engineering practice of using static analysis should be reconsidered and eventually substituted by a dynamic analysis of the structural assembly of tower, isolators and cables.

REFERENCES

[1] Davenport, A.G. “The response of tensions structures to turbulent Wind: the role of aerodynamic damping”. In: 1st International Oleg Kerensky Memorial Conference on Tension Structures, London, june, 1988.

[2] Vickery, B.J. “Advanced structural dynamics I. (Engineering Science 610) Course notes.” The University of Western Ontario, Canadá, 1992.

[3] Loredo-Souza, A.M. “The Behaviour of Transmission Lines Under High Winds.” 1996. Thesis (Doctorade) - Faculty of Engineering Science Department of Civil Engineering, The University of Western Ontario, Ontário.

[4] ASSOCIAÇÃO BRASILEIRA DE NORMAS TÉCNICAS – ABNT. NBR 6123: Forças devidas ao Vento em Edificações. Rio de Janeiro, 1988.

[5] Pfeil, M. S. “Comportamento aeroelástico de pontes estaiadas.” 1993. Thesis (Doctorade) - Departamento de Engenharia Civil, Universidade Federal do Rio de Janeiro, Rio de Janeiro.

[6] Blessmann, Joaquim. “Introdução as estudo das ações dinâmicas do vento”, 2. ed. Porto Alegre: Ed. Universidade/ UFRGS, 2005.

[7] Carvalho, H. “Efeitos do vento em linhas de transmissão”. 2015. Thesis (Doctorade) - Departamento de Engenharia de Estruturas, Universidade Federal de Minas Gerais, Belo Horizonte.

[8] ANSYS-11.0. Release 1.0 Documentation for Ansys. Canonsburg, United States.

Structures, Materials and Dynamics

THE INTERNATIONAL CONFERENCE ON
WIND ENERGY HARVESTING 2017
20-21 April 2017
Coimbra, Portugal

Paper 301

FATIGUE ANALYSIS OF WIND TURBINE BLADES

Ricardo E. Teixeira[1]
INEGI, University of Porto
Porto, Portugal

Pedro Moreira[2]
INEGI, University of Porto
Porto, Portugal

Paulo J. Tavares[3]
INEGI, University of Porto
Porto, Portugal

José A.F.O. Correia[4]
INEGI, University of Porto
Porto, Portugal

Miguel Calvente[5]
University of Oviedo
Gijón, Spain

Abílio De Jesus[6]
INEGI, University of Porto
Porto, Portugal

Alfonso Fernández-Canteli[7]
University of Oviedo
Gijón, Spain

ABSTRACT

This paper intends to show the methodology used to perform a fatigue analysis in wind turbine blades. Experimental results, obtained according to the standard IEC 61400-13, were used to develop a Matlab software solution. The software uses rainflow algorithm to count the cycles for each strain range, and calculate damage using Miner's law.

NOMENCLATURE

DLR = German Aerospace Center

INTRODUCTION

Renewable energy market is growing, leading to a need of sound evaluation of the structural integrity of the wind turbines blades. With this purpose good measurement campaigns should be performed in accordance with standard IEC 61400-13 "Wind turbines - Part 13: Measurement of mechanical loads", that describes the measurement of structural loads on wind turbines. [1]
Regarding wind turbines fatigue assessment, there are two main type of loads to consider:

- Flapwise direction due to aerodynamic loads (shear, drag, lift);
- Lead-lag directional due to inertial loads (gravity, blade dynamics).

These loads usually occur in orthogonal bending directions. Flapwise is the direction where highest loads occur. These loads vary strongly in amplitude and mean value. Regarding lead-lag loads, they are mainly originated by the own weight of the blade. Also the load direction changes twice during a single evolution and lead-lag loads are more regular than fapwise loads. [2] These two type of loads are cyclic so they are the leading cause to fatigue in wind turbine blades.
A Matlab code for the fatigue life analysis of wind turbine blades was developed. This software was developed taking into account real data from sensitized blades and guidelines given by the standard IEC 61400-13. The software is based on a rainflow algorithm to analyze the several loading cycles, and performs damage using Miner's law.

METHODOLOGY

1 Development Engineer, INEGI, University of Porto, Portugal, reteixeira@inegi.up.pt
2 Senior Researcher, INEGI, University of Porto, Portugal, pmoreira@inegi.up.pt
3 Senior Researcher, INEGI, University of Porto, Portugal, ptavares@inegi.up.pt
4 Assistant Researcher, INEGI, University of Porto, Portugal, jacorreia@inegi.up.pt
5 Researcher, Gijón Faculty of Engineering, University of Oviedo, Spain, munizmiguel.uo@uniovi.es
6 Assistant Professor, INEGI/Faculty of Engineering, University of Porto, Portugal, ajesus@fe.up.pt
7 Emeritus Professor, Gijón Faculty of Engineering, University of Oviedo, Spain, afc@uniovi.es

Fatigue is a local damage process caused by the application of cyclic loading even if the load is lower that the yield stress. Usually, fatigue loads can be divided in two different groups: constant and variable amplitude. In real load cases it is uncommon to have constant cyclic loads. The case of variable amplitude loads is named load spectrum or load history.

During its service life, a turbine blade is subjected to cyclic loads that can have constant or variable amplitude. For cases of constant amplitude loading the determination of the amplitude and the number of cycles is easy to be performed. Although, if the amplitude of the load changes with time, further processing is needed. Fatigue cycles can be counted using time histories of the loading parameter such as force, torque, stress, strain, etc. Cycle counting methods are used to summarize irregular and long load histories giving the number of cycles for different amplitudes. There are some counting methods of one parameter such as level-crossing, range-mean and range-crossing, however these methods are not able to deal with local stress-strain hysteresis behavior, and this has a lot of influence in fatigue failure. Two-parameter cycle counting methods like rainflow are widely used nowadays.

After the cycle counting there is the need to obtain the damage induced by the cycles. For this purpose Miner linear damage and accumulation rule can be used. [4]According to this law, a component stressed at σ_1 has a life of N_1 cycles and the damage after n_1 is given by n_1/N_1. This fraction of cycles n_1 creates a damage D_1 of the total damage D_1. Fatigue failures occurs when the total damage introduced by multi-level fatigue loading reaches the critical damage,

$$D_{total} = \sum D_i = \sum \frac{n_i}{N_i} \leq D_{cr}$$

Mathematically, the Miners rule is given by,

$$\sum \frac{n_i}{N_i} = 1$$

With the purpose of perform this analysis a matlab application was done. The main interface of the application is shown in Figure *1*.

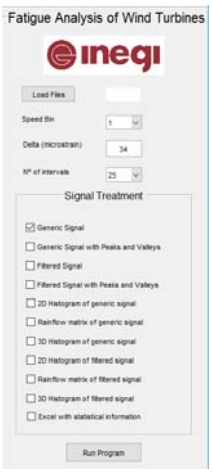

Figure 1 - Main interface of the application.

This application counts the number of cycles in each variable range (strain, stress or torque). To run the application the "load files" button should be pressed and a typical explorer window will open to allow the selection of the files to analyze (At this stage of the application only .mat extension is supported). As soon as files are loaded a message box appears confirming that the files were loaded successfully (Figure *2*).

There is a parameter called delta that is the minimum range of cycles that matters for the analysis. Cycles with lower range will be neglected. The units for this parameter in this stage of the application are micro-strain because the analyzed data was in micro-strain. It is also possible to select the number of range intervals that we pretend being that the standard suggests at least one hundred in order to have a good resolution. The speed bin is only important if the option "Excel with statistical information" is selected because the name of the excel file will be "Statistical_information (Speed Bin)".

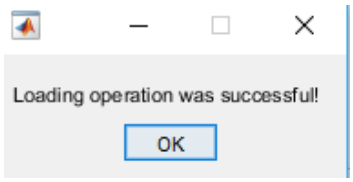

Figure 2 - Loading successful message box.

The software allows the analysis of more than one 10 minutes files and the outputs are:

- plot of generic and filtered signals (Figure *3* and Figure 4) respectively;
- plot of generic and filtered signal with peaks and valleys (Figure 5 and Figure 6 respectively);
- 2D and 3D histogram for generic and filtered signal (Figure 7, Figure 9, Figure 8 and Figure 10 respectively);
- Excel file with statistical information.

Each output can be selected checking the respective check box.
2D histograms are represented in terms of strain range and 3D histograms are represented in terms of strain range and mean value. The rainflow matrices shows the number of cycles for each strain range, as well as the average value of the amplitude and mean of each strain range. The excel file that is generated shows the statistical data for each bin, this is the maximum and minimum strain value for each file, as well as the minimum of the minimums and the maximum of the maximums. It also prints the average amplitude and mean value for each file as well as the average for all files. It also calculates the damage equivalent load and standard deviation.

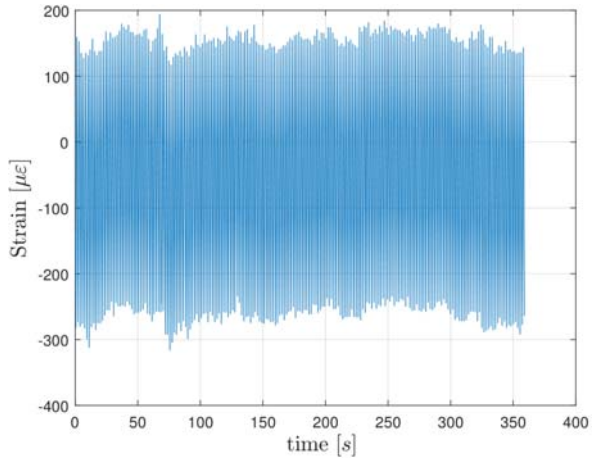

Figure 3 - Generic Signal.

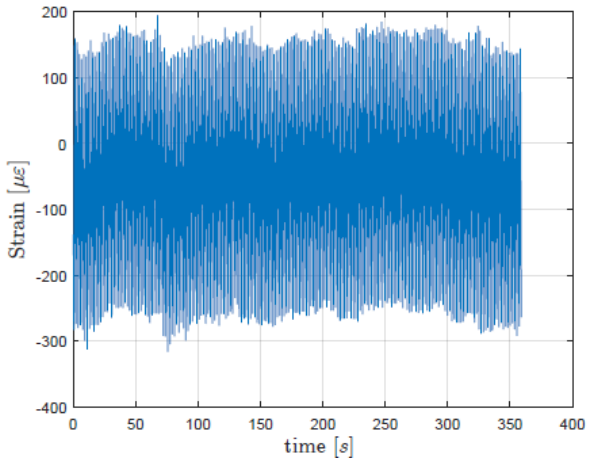

Figure 4 - Filtered signal.

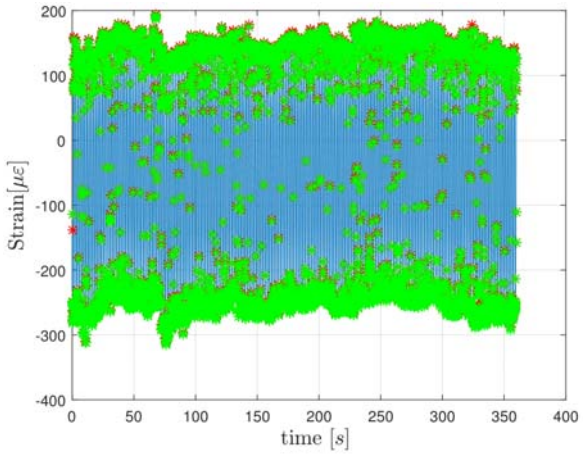

Figure 5 - Generic signal with peaks and valleys.

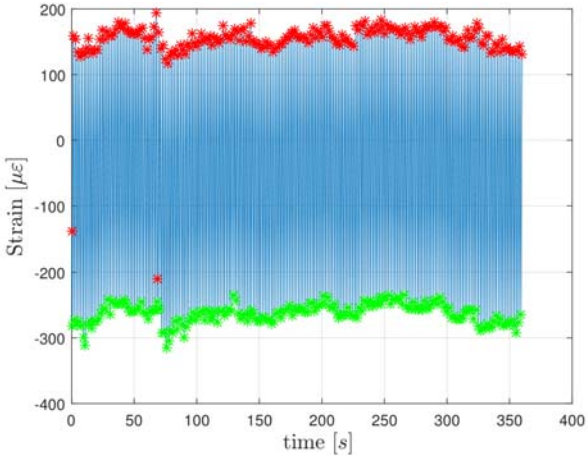

Figure 6 - Filtered signal with peaks and valleys

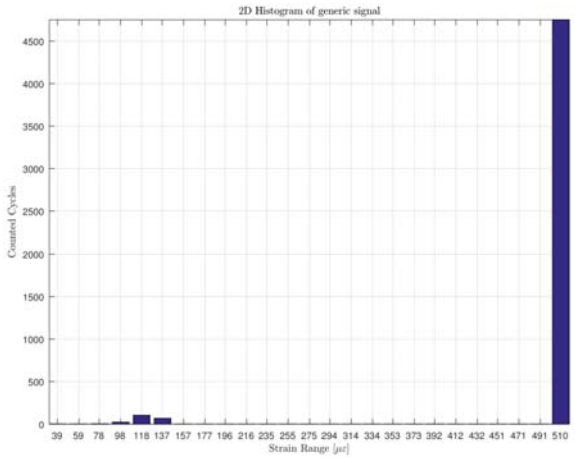

Figure 7 - 2D histogram of generic signal.

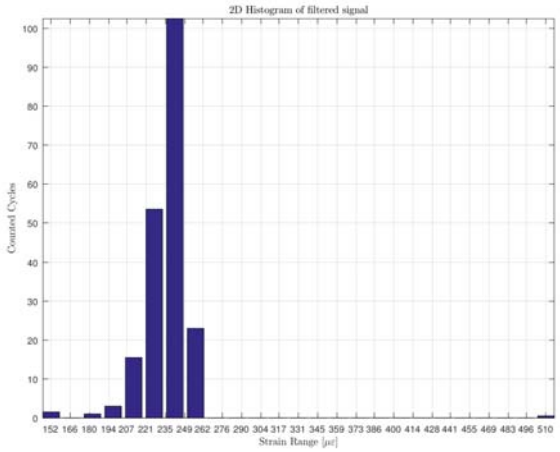

Figure 8 - 2D histogram of filtered signal.

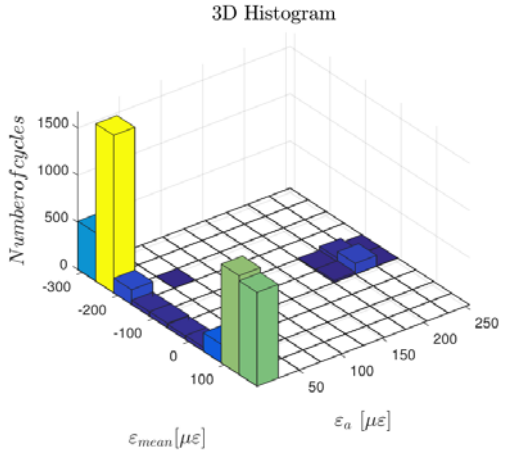

Figure 9- 3D histogram of generic signal.

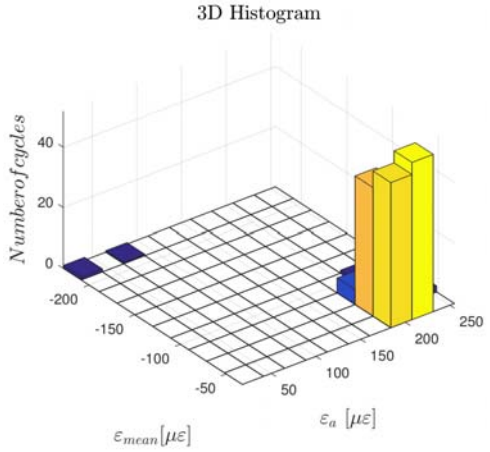

Figure 10 - 3D histogram of filtered signal.

RESULTS

The example shown in previous figures represents the analysis performed to one file corresponding to lead-lag direction.

Concerning the plots, it is possible to see that a great amount of cycles in the original signal correspond to noise, and for this reason the signal filtering is underlying as well as the definition of delta value.

In this particular case study the definition of the delta value was based in the $\varepsilon - N$ curve. The curve used was the same given by German Aerospace Center (DLR).[5] In this document only curves for $R = 0.1$ and $R = -1$ are given. For the case shown in Figure 3, $R = -1$ is the best approximation. The curve used is shown in figure

6. To obtain the value of delta a large number of cycles was considered, in this case $1E30$, so it was considered that the strain values corresponding to this number of cycles did not contribute to fatigue. This approach leaded to a delta value of $34\ \mu\varepsilon$.

Comparing Figure 7 with Figure 8 (or Figure 9 with Figure 10) it is possible to notice that a big amount of cycles with small strain range (approximately 4950 cycles) were neglected form generic signal to filtered signal. This improves the results and allows a bigger resolution in the results.

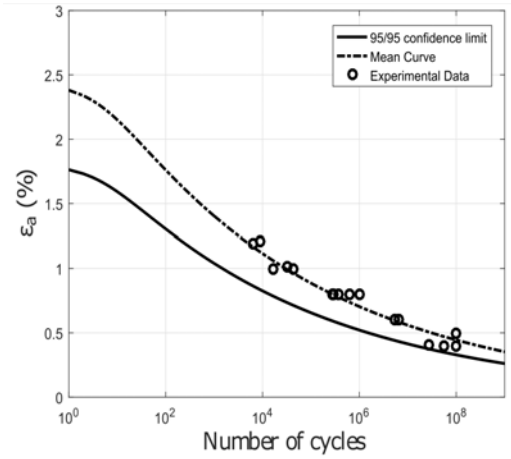

Figura 11- $\varepsilon - N$ curve.

CONCLUSIONS

As future works some tasks are defined,

- Perform fatigue tests to material specimens at different *R* values. This will allow to perform more accurate analysis as well as a better definition of delta value;
- Apply a probabilistic approach to obtain the fatigue curves of the material;
- Apply Miner's law to obtain the damage induced in the blades.

ACKNOWLEDGEMENTS

The authors of this work would like to express their gratitude to the SciTech-Science and Technology for Competitive and Sustainable Industries, R&D project NORTE-01-0145-FEDER-000022 co-financed by Programme Operational Regional do Norte ("NORTE2020") through Fundo Europeu de Desenvolvimento Regional (FEDER) and the Portuguese Science Foundation (FCT) through the post-doctoral grant SFRH/BPD/107825/2015 the for their collaboration, financial and technical support during this research works.

REFERENCES

[1] I. E. Commission, "WIND TURBINES – Part 13: Measurement of mechanical loads," ed, 2014.
[2] R. P. L. Nijssen, "Fatigue life prediction and strength degradation of wind turbine rotor blade composites," Knowledge Centre WMC and DPCS group of Aerospace Engineering, 2011.
[3] REN21, "Renewables 2016 Global Status Report," 2016.
[4] P. P. Milella, *Fatigue and corrosion in metals*: Springer Science & Business Media, 2012.
[5] G. A. R. Establishment, "Fatigue of materials and components for wind turbine rotor blades," 1996.

THE INTERNATIONAL CONFERENCE ON
WIND ENERGY HARVESTING 2017
20-21 April 2017
Coimbra, Portugal

Paper 302

AN INTEGRATED APPROACH FOR SMART MONITORING, INSPECTION AND LIFE-CYCLE ASSESSMENT OF WIND TURBINES

Imad Abdallah[1]
ETH Zürich
Zürich, Switzerland

Eleni Chatzi[2]
ETH Zürich
Zurich, Switzerland

Braulio Barahona[3]
ETH Zürich
Zürich, Switzerland

ABSTRACT

In this paper we present a new integrated approach for assessing the structural health and life-cycle of wind turbines. A major challenge in efficient condition assessment and residual life prediction for such systems lies in their continual exposure to highly stochastic loadings due to non-stationary environmental conditions, gravity, and inertial effects. Furthermore, wind turbines suffer from significant degree of interaction amongst their components comprising a variety of materials, which bears a large influence on the measured condition/health monitoring data. The challenge is compounded by the presence of advanced control systems trying to extract maximum power from the wind while maintaining the operating loads within the design limits. The objective is thus to develop methods and tools, which are able to account for the lack of precise loading information as well as operational, environmental and modelling uncertainties, toward the structural health monitoring, damage detection and life-cycle assessment for wind turbine components across two temporal scales, namely the short-term (gusts, extreme turbulence, faults) and long-term (fatigue). To this end we propose a novel framework that combines a easily deployed and relatively cheap sensor network, with state-of-the-art data processing methodologies and "near-real time" Aero-elastic simulations, with the standard stream of condition monitoring data (SCADA). We present the main thesis of this framework and illustrate one aspect of it, namely the data driven modelling part.

NOMENCLATURE

SHM	=	Structural Health Monitoring
CMS	=	Condition Monitoring Systems
WT	=	Wind Turbine
PCE	=	Polynomial Chaos Expansion
O&M	=	Operation and Maintenance

INTRODUCTION

There is a major challenge in efficient condition assessment and residual life prediction when wind turbine components are subjected to strongly varying loads, both on the short-term scale (seconds) due to varying rotor speed, gravitational, aerodynamic and inertial forces, and long-term scale (days, weeks) due to temperature, gusts, turbulence and seasonal variations. Furthermore, due to the narrow gap amongst their natural frequencies, wind turbines suffer from significant degree of interaction amongst their components, comprising a variety of materials, which bears a large influence on the measured condition/health monitoring data. This challenge is to some level compounded by the presence of advanced control systems aiming to extract maximum power from the wind, while maintaining the operating loads within the design limits. The current practice of monitoring and diagnostics of the health of wind turbine structures involves (1) Visual inspection which is subjective, labor-intensive, time-consuming, and periodic, (2) Non-Destructive Evaluation which is costly, labor-intensive, time-consuming,

1 Postdoc, Structural Mechanics, ETH Zürich, Stefano-Franscini-Platz 5, 8093 Zürich, Swizterland / abdallah@ibk.baug.ethz.ch
2 Professor Doctor, Structural Mechanics, ETH Zürich, Stefano-Franscini-Platz 5, 8093 Zürich, Swizterland / chatzi@ibk.baug.ethz.ch
3 Postdoc, Structural Mechanics, ETH Zürich, Stefano-Franscini-Platz 5, 8093 Zürich, Swizterland / barahona@ibk.baug.ethz.ch

periodic and requires trained personnel, and finally (3) Supervisory Control And Data Acquisition (SCADA) and/or component specific Condition Monitoring Systems. The motivation of this work stems from the obvious lack of decision making framework for O&M and lack of integration of SHM for both short-term damage detection and long-term Life-Cycle Management. Furthermore, uncertainties in measurements, wind turbine operation and environmental conditions are rarely considered in SHM, and finally "Near-real time" Aero-elastic simulations are rarely integrated into an SHM framework. The ERC funded WINDMIL project aims to develop appropriate performance assessment methodologies, which are able to account for the lack of precise input (loading) information as well as environmental and modeling uncertainties, toward the assessment of structural performance, damage detection and life-cycle assessment across two temporal scales, namely the short- and long-term one. The former refers to the handling of sudden anomalies typically linked to extreme events (strong winds, waves, earthquake), while the latter refers to deterioration processes that evolve across a lengthier time span and which form an adverse factor for extending the life-cycle of these structural components, as fatigue damage. To this end, we propose a novel framework that fuses multiple sources of information including: (1) a easily deployed and relatively cheap sensor network to capture the structure response, (2) with state-of-the-art data processing methodologies and "near-real time" Aero-elastic simulations, with (3) the standard existing stream of condition monitoring data and SCADA. We present the main thesis of this framework and illustrate one aspect of it, namely the data driven modelling part.

METHODOLOGY

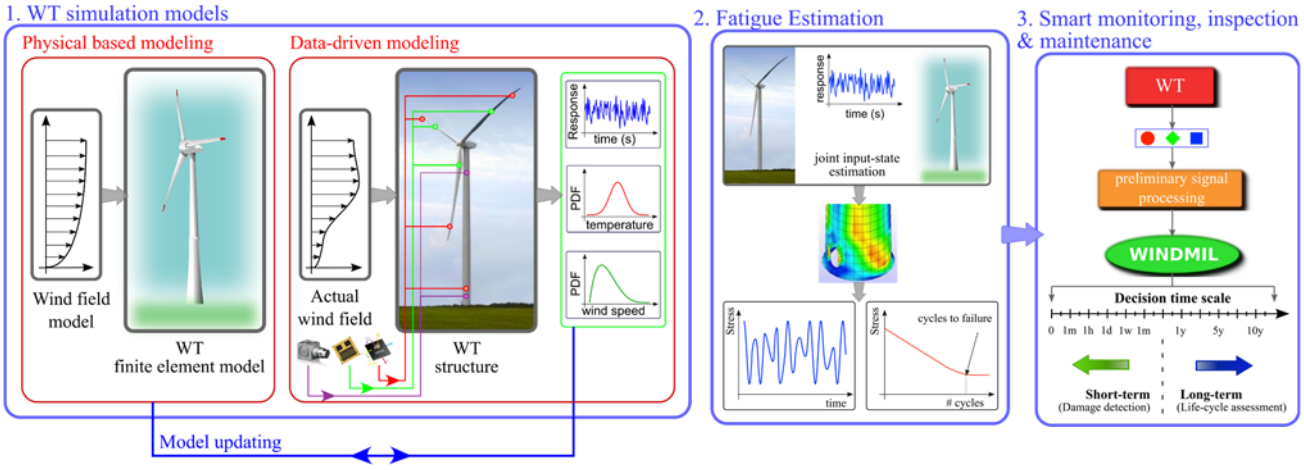

Figure 1. Integrated framework for Monitoring, inspection and life-cycle Assessment of wind turbines.

Figure 1 illustrates the integrated framework for Monitoring, inspection and life-cycle Assessment of wind turbines, which is defined on the basis of two separate time scales, one short-term and one long-term. The short-term assessment aims to provide early warning of the onset of damage or to register an extreme event (i.e. abnormal operation). The long-term framework is linked to the prediction of fatigue accumulation and the evidence of deterioration in the derived performance indicators.

The first level of the integrated approach is to establish the wind turbine simulation models, both physical (simulations) and data driven. In the physical based modeling a refined representation of the wind turbine components and their geometry and material properties is established. The refined model serves as a link between the system's characteristics (geometry, materials) and properties (stiffness, strength) and the resulting aero-servo-hydro-elastic response, which is the quantity measured in the field via sensors. Data-driven modeling relies on dynamic response measurements for extracting mathematical representations of the system. These representations can be delivered in a modal, regression or wavelet based form. Since the model is inferred from measurements of the response without necessarily a-priori knowledge of the system itself, this step comprises a task of inverse engineering. When the WT is parked, the structure is excited by ambient wind loads. During power production, the dynamics of the WT becomes non-stationary due to the rotation of the rotor, which induces a "periodic variability". This may be attributed to the effects of aerodynamic, gravitational and inertial forces [1], [2]. Time Varying Auto Regressive (TVAR) models constitute a suitable tool for tracking the time evolution of the dynamics using a compact parametric formulation:

$$y[t] + a_1[t]y[t-1] + a_2[t]y[t-2] + \cdots + a_n[t]y[t-n] = e[t], \quad e[t] \sim NID(0, \sigma_e^2[t])$$

where t designates discrete time, $y[t]$ the observed non-stationary signal, $e[t]$ the residual sequence, that is the un-modeled part of the signal, which is assumed to be normally identically distributed with zero mean and time-varying variance $\sigma_e^2[t]$, and $a_i[t]$ the time-varying AR parameters.
The second level builds onto the physics and data driven models for the prediction of fatigue accumulation. Toward this end, the physical and the data-driven models developed in Level 1 will be used in a synergistic way. The data-driven models will be used for the loading estimation through very recently developed system identification methods, which allow to infer the states of the system, i.e., its displacement and velocity time histories, under an unknown dynamic excitation (unknown input) via a limited number of sensors. This is known as a joint input-state estimation problem [3], [4], [5], [6] for fatigue prediction in civil structures. The extension of this theory to WTs, although not straightforward due to once again the particular dynamics involved, is a crucial task for treating the most commonly identified bottleneck for these systems, namely failure due to fatigue. In a next stage, the predicted response quantities will be linked to physical properties of the system, via use of the physics based models, leading to the estimation of strain time histories in hot-spot locations of the WT structures. The use of a physics based model in this case is vital for transiting from vibrational response data into strain information in unmeasured locations of the structure. The integration of appropriately adapted deterministic and stochastic fatigue theories will generate fatigue damage accumulation maps based on actual operational conditions. This in turn enables prediction of the residual fatigue lifetime and reliability of the structure minimizing down time, lowering the frequency of sudden breakdowns and associated maintenance and logistic costs. A subcomponent of this step necessarily entails the definition of suitable sensor configurations, able to monitor those quantities that are critical for allowing fatigue estimation in absence of load information [7]. In this sense, a successful sensor setup should ensure the realization of inference, numerical verification, and experimental validation of the developed simulation models, as well as, damage detection and prediction of fatigue accumulation. The measurement system delivered from this study should come as a complimentary low cost solution to the information standard SCADA systems routinely provided for WTs.
The third level, Smart Monitoring, Inspection and Maintenance, relies on the treatment of the data collected from the suggested monitoring system, which will inevitably deliver diverse information contaminated with a significant amount of uncertainties. Indeed, due to reasons relating to material properties, ageing processes, loading conditions, boundary conditions, and others, every structural system is characterized by uncertainty. As a result, we may only have a limited degree of confidence in a WT physical model, when the latter has to be employed for the assessment of the WT's reliability and safety through its life-cycle. A fundamental question that therefore arises is how does one deal with a system that is probabilistic in nature and continually changing? In this case we refer to "macro-temporal variability" which pertains to the loading and environmental conditions which are continually changing within the range of hours, or even minutes [8]: (i) non-periodic, stochastic loads caused by wind gusts and turbulence (within the order of minutes), (ii) changes in the input wind flow profile (within the order of minutes) and (iii) environmental conditions variation (temperature, humidity, solar radiation, wave loading and others; within the order of hours). For modeling the evolution of the system as a function of changing conditions, the parameters of the non-stationary representations obtained in Level 1 will be projected onto the stochastic spaces of the recorded operational and environmental conditions of the WT [9], [10]. In this way, a statistical model may be built, incorporating the effects of environmental and operational conditions and alleviating the danger of misinterpreting these as damage. A Polynomial Chaos Expansion (PCE) method, coupled with the TVAR models enables the transition from micro (structure on its own) to macro (structure in interaction with its environment) delivering performance indicators that ensure enforcement of this scheme in a uniform and repeatable manner. The formulation of performance indicators (indices) essentially requires a training period after which these are able to predict performance within regular. Deviations of these indices from normal bounds, indicate irregularity in the operation of the WT and serve as a warning/alarm. This "macro-temporal" stochastic framework provides a means of quantifying the uncertainty pertaining to the evolution of the dynamic behaviour of a WT during its complete operational spectrum. Once variability due to environmental conditions is quantified, damage detection may be accomplished by identifying within the robust performance indices distinct patterns that evidence different types of damage, from component failures to fatigue accumulation or material deterioration. A feature extraction approach will be pursued to this end [11].

RESULTS

In the context of this framework we will present the data-driven result of the framework. The WT under study is a V90 2MW Vestas generator of a wind farm in Lübbenau in northern Germany owned by Repower Deutschland GmbH. The vibration response of the WT were measured by triaxial accelerometers at five distinct locations of the WT tower. A 10-minute-long dataset was recorded every half hour for 29 days. The signals recorded at 200 Hz were low pass filtered and down sampled to 12.5 Hz (cutoff frequency at 5 Hz). An example

of the SCADA signals is shown in Figure 2. Figure 3 shows the non-stationary SP-TARMA model of the tower accelerations tracks with good accuracy the evolution of the dynamics when compared to the spectrogram shown in the background. Figure 5 shows how the PCE method, coupled with the SP-TARMA model, enables the transition from short-term (structure on its own) to long-term (structure in interaction with its environment) stochasticity delivering performance indicators of the structure [12].

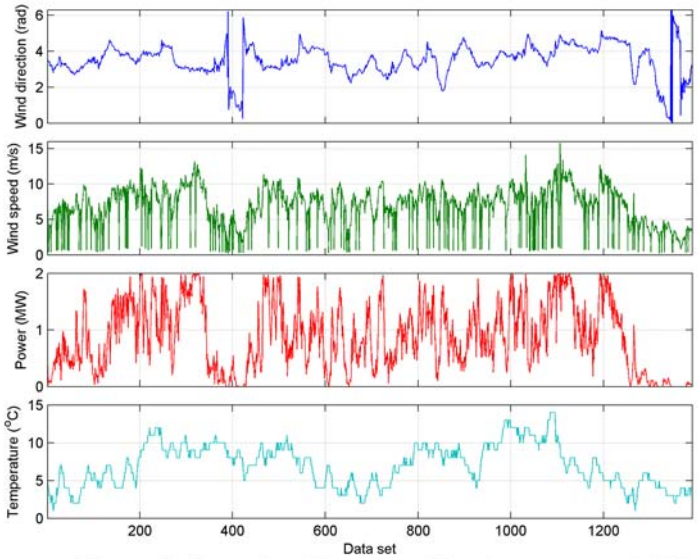

Variables	
1	Wind direction [deg]
2	Min wind speed [m/s]
3	Average wind speed [m/s]
4	Max wind speed [m/s]
5	Min power [kW]
6	Average power [kW]
7	Max power [kW]
8	Nacelle direction [deg]
9	Nacelle temperature [°C]
10	Ambient temperature [°C]

Figure 2. Example of long term 10-minute averaged SCADA data, and the list of available operational and environmental conditions through the SCADA system and the plot of the four selected input variables.

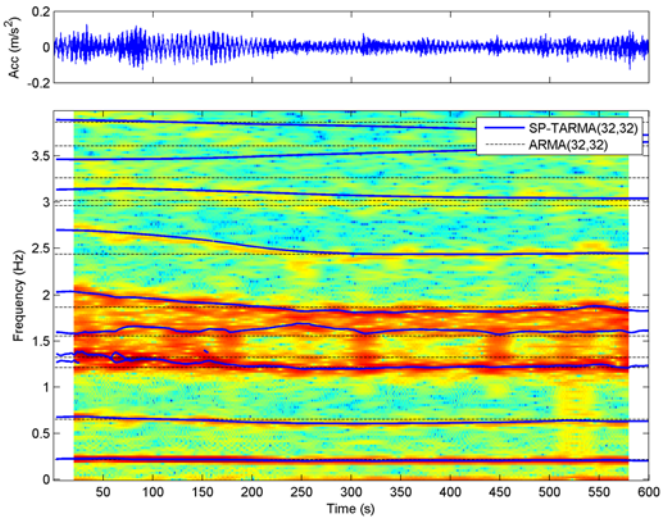

Figure 3. Dynamics of the WT under normal operation represented by a spectrogram of the accelerations time series. The non-stationary SP-TARMA model tracks with good accuracy the evolution of the dynamics when compared to the spectrogram shown in the background.

CONCLUSIONS

We presented an Integrated Approach for Smart Monitoring, Inspection and Life-Cycle Assessment of Wind Turbines. The proposed approach fulfils a lack of integration of SHM for both short-term damage detection and long-term Life-Cycle Management, addresses the uncertainties in measurements, wind turbine operation and environmental conditions and finally integrates, seamlessly, “Near-real time” Aero-elastic and physics based simulations into an SHM framework.

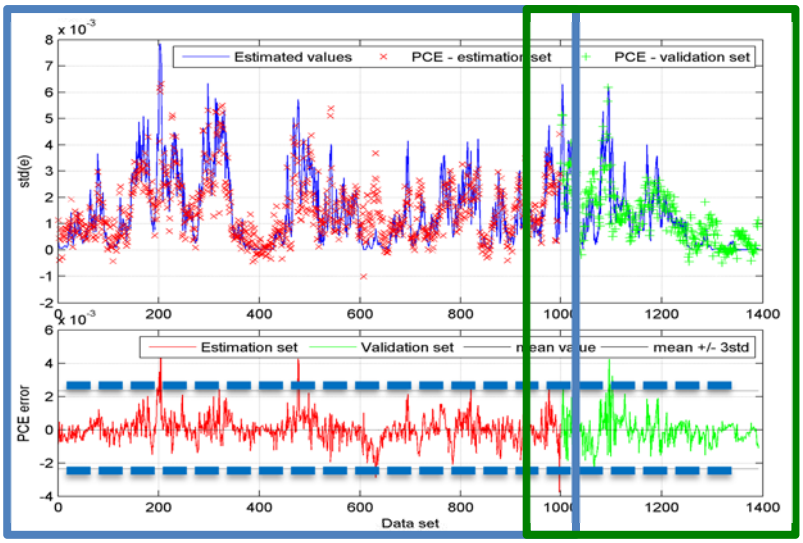

Figure 4. Long-term monitoring. SP-TARMA model residual *std* as obtained from the modelling of each vibration response dataset along with the PCE model expansion values. The PCE errors along with 95% confidence intervals (calculated from the estimation set) are also shown.

ACKNOWLEDGEMENTS

ERC Starting Grant 2015.

REFERENCES

[1] Hau E., Wind Turbines: Fundamentals, technologies, application, economics, 3rd edition, Springer 2013.
[2] Hameed Z., Hong Y.S., Cho Y.M., Ahn S.H., and Song C.K., Condition monitoring and fault detection of wind turbines and related algorithms: A review, Renewable and Sustainable Energy Reviews, 13(1): 1–39, 2009.
[3] Lourens, E., Papadimitriou, C., Gillijns, S., Reynders, E., De Roeck, G., and Lombaert, G., Joint input-response estimation for structural systems based on reduced-order models and vibration data from a limited number of sensors, Mechanical Systems and Signal Processing, 29: 310-327, 2012.
[4] Eftekhar-Azam, S., Chatzi, E., and Papadimitriou, C., A dual Kalman filter approach for state estimation via output-only acceleration measurements, Mechanical System and Signal Processing, in press.
[5] Eftekhar-Azam, S., Chatzi, E., Papadimitriou, C., and Smyth, A.W., Experimental Validation of the Dual Kalman Filter for Online and Real-time State and Input Estimation, Proceedings of IMAC-XXXIII, Orlando, United States, 2015.
[6] Lourens, E.M., Papadimitriou, C., and Chatzi, E., Global response monitoring of offshore wind turbine support structures based on a limited number of acceleration measurements, ECCOMAS Thematic Conference - UNCECOMP 2015, Crete Greece, 2015.
[7]Iliopoulos, A., Devriendt, C., Guillaume, P., and Van Hemelrijck, D., Continuous Fatigue Assessment of an Offshore Wind Turbine Using a Limited Number of Vibration Sensors, 7th European Workshop on Structural Health Monitoring, Nantes, France, 2014.
[8] Hyvärinen A. and Oja E., Independent component analysis: algorithms and applications, Neural Networks, 13(4–5): 411–430, 2000.
[9] Spiridonakos, M., and Chatzi, E., Metamodeling of structural systems with parametric uncertainty subject to stochastic excitation, Earthquakes and Structures - An International Journal for Earthquake Engineering & Earthquake Effects on Structures, 8(4), 2015, in press.
[10] Bogoevska, S., Spyridonakos, M., Chatzi, E., Dumova-Jovanoska, E., Höffer, R. "A novel bi-component Structural Health Monitoring strategy for deriving global models of operational Wind Turbines", 8th European Workshop On Structural Health Monitoring (EWSHM 2016), 5-8 July 2016, Spain, Bilbao
[11] Avendaño-Valencia, L.D., and Fassois, S.D., Stationary and non-stationary random vibration modeling and analysis for an operating wind turbine, Mechanical Systems and Signal Processing , 47(1-2): 263-285, 2014.
[12] Spiridonakos, M., Ou, Y., Chatzi, E., and Romberg, M., Wind turbines structural identification framework for the representation of both short- and long-term variability, proceedings of 7th International conference on Structural Health Monitoring of Intellightn Infrastructure (SHM-II), Torino, Italy, 1-3 July 2015.

THE INTERNATIONAL CONFERENCE ON
WIND ENERGY HARVESTING 2017
20-21 April 2017
Coimbra, Portugal

Paper 303

MULTIAXIAL FATIGUE BEHAVIOUR OF STRUCTURAL STEELS FOR FATIGUE DESIGN OF WIND TOWERS

Grzegorz Lesiuk[1]
Wrocław University of Science and Technology
Wrocław, Poland

Wojciech Wiśniewski[2]
Wrocław University of Science and Technology
Wrocław, Poland

Slobodanka Jovašević[3]
University of Coimbra
Coimbra, Portugal

José A.F.O. Correia[4]
University of Coimbra
Coimbra, Portugal

Abílio M.P. De Jesus[5]
University of Porto
Coimbra, Portugal

Carlos Rebelo[6]
University of Coimbra
Coimbra, Portugal

Luis Simões da Silva[7]
University of Coimbra
Coimbra, Portugal

ABSTRACT

Wind energy has been used for more than 3000 years. Today, when global warming has become one of the most serious environmental issues, the need for renewable energies is increasing. The high demand for wind energy is leading the development of more powerful wind energy converters that demand higher towers to reach zones of higher speed and less turbulent wind [1,2]. With the increase of the tower height also transportation, assembly, erection and maintenance of the tower becomes more difficult and costly. On the other hand, increase in height rises the generated energy. At the moment, the most commonly used type of tower for wind energy conversion (WEC) is steel tubular tower. However, for the heights above 100 m, this type of tower requires diameters at the tower base of more than 5 m which makes the usual assembling process unfeasible due to public road transportation limitations [3,4,5]. Some producers have proposed lattice solution. Comparing to tubular tower, lattice towers have many bolted connections that require frequent maintenance, do not provide protected area for workers and are aesthetically less appealing, but they are not affected by transportation limitations [6,7].

Another type of tower construction that allows greater heights is the hybrid solution. This type of tower is composed of three parts: the lower lattice part, tubular tower consisting of several parts bolted or welded together as in typical tubular tower solution, and transition piece which ensures the connection and transmission of forces between two main parts. The use of tubular tower for the upper portion beneficiates of all advantages of optimized technology for tubular steel towers with the diameters within public road transportation limitations, while the lattice portion enables the required extension of height [2,8]. Another advantage is that the lattice portion can be used to facilitate installation of the upper tubular portion and the turbine, therefore avoiding the need for very high cranes [3,8].

Lattice structures composed of hollow sections are widely used. They are used in buildings and halls, bridges, barriers, offshore structures, towers and masts. One main problem is the connections that can be used for tubular hollow sections. This has led to development of different types of welded and bolted connections between the sections. Within European project SHOWTIME [9] new type of tubular elements and connections are under development. These types of elements and connections (see Fig. 1) will allow improvements in the way of construction as well as in the fatigue resistance and in the maintenance needs during service life. The materials to be used are S355 and S690 steels [10].

1 Assistant Professor, Wrocław University of Science and Technology, Faculty of Mechanical Engineering, Department of Materials Science and Engineering, Wrocław, Poland/grzegorz.lesiuk@pwr.edu.pl
2 MSc Eng., Wrocław University of Science and Technology, Faculty of Mechanical Engineering, Department of Materials Science and Engineering, Wrocław, Poland
3 Research Assistant, Ph.D. student, ISISE/Department of Civil Engineering, University of Coimbra, Coimbra, Portugal/sjovasevic@uc.pt
4 Invited Assistant Professor and Assistant Researcher, Department of Civil Engineering, University of Coimbra, Coimbra, Portugal/jacorreia@inegi.up.pt
5 Assistant Professor, Department of Mechanical Engineering, University of Porto, Porto, Portugal/ajesus@fe.up.pt
6 Associate Professor, Department of Civil Engineering, University of Coimbra, Coimbra, Portugal/crebelo@dec.uc.pt
7 Full Professor, Department of Civil Engineering, University of Coimbra, Coimbra, Portugal/luisss@dec.uc.pt

Fatigue life evaluation of structural details may be carried out using different approaches. The global *S-N* approach was the first prediction technique developed [11]. This technique is generally used to predict the total life of a component. It is supported by experimental results and directly relates a global definition of stress range, $\Delta\sigma$, with total number of cycles to failure, N_f. Local approaches are associated with local failure models and could be described by strain-life and stress-life relations [12,13]. Strains and stresses are evaluated at a local hot spot. This approach considers only crack initiation life phase.

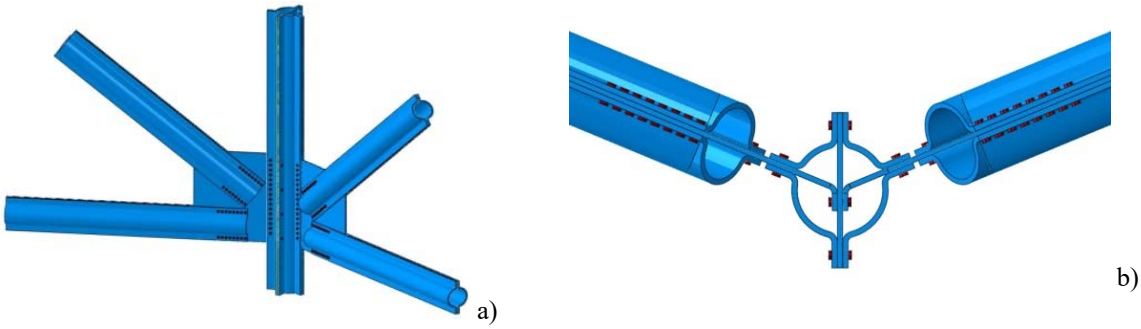

a) b)

Figure 1. Steel half-pipes bolted connection: a) 3D view; b) Cross-section view.

A procedure for multiaxial fatigue assessment of a steel half-pipe bolted connection is to be proposed in the SHOWTIME project and some ideas were explored in references [14,15]. The multiaxial fatigue life evaluations can be made using several approaches, such as based on strains [16,17,18,19], stresses [20] and energy [21,22,23]. There are a number of multiaxial damage parameters being proposed in the literature covering low-cycle fatigue, high-cycle fatigue, proportional and non-proportional loading conditions.

Findley and Tracy [16,17] proposed a fatigue life equation in low-cycle fatigue regime about the influence of normal stresses to the maximum shear stress plane, with the following form:

$$\left(k \cdot \sigma_n + \frac{\Delta\tau}{2}\right)_{max} = \tau_f^* (N_f)^b \tag{1}$$

where k is a material constant, $\Delta\tau/2$ ($=\tau_a$) is the alternating shear stress, $\sigma_{n,max}$ is the maximum normal stress, and variable τ^*_f is determined using the torsional fatigue strength coefficient, τ_f', in the equation:

$$\tau_f^* = \sqrt{1+k^2} \cdot \tau_f' \tag{2}$$

Brown and Miller [18] defined the damage critical plane and proposed the following equation:

$$\left(S \cdot \Delta\varepsilon_n + \frac{\Delta\tau}{2}\right)_{max} = A\frac{\sigma_f'}{E}(2N_f)^b + B\varepsilon_f'(2N_f)^c \tag{3}$$

where S is a Brown and Miller constant.

Fatemi and Socie [19] proposed a modified equation which was originated from Brown and Miller's relationship as follows:

$$\gamma_{max}\left(1 + n\frac{\sigma_n^{max}}{\sigma_y}\right) = (1+\nu_e)\frac{\sigma_f'}{E}(2N_f)^b + \frac{n}{2}(1+\nu_e)\frac{(\sigma_f')^2}{E\sigma_y}(2N_f)^{2b} + (1+\nu_p)\varepsilon_f'(2N_f)^c + \frac{n}{2}(1+\nu_p)\frac{\sigma_f'\varepsilon_f'}{\sigma_y}(2N_f)^{b+c} \tag{4}$$

where n is an empirical constant, ν_e and ν_p are Poisson's ratio in the elastic and plastic region, respectively.

Smith et al. [21] proposed a damage parameter, known as *SWT* parameter, to account for mean stress effects updating existing strain-based fatigue models. In multiaxial fatigue conditions the SWT parameter is determined for the critical plane which corresponds to the maximum principal stress and strain as follows:

$$SWT = \max\left(\sigma_n \cdot \frac{\Delta\varepsilon_1}{2}\right) \tag{5}$$

$$\sigma_n \cdot \frac{\Delta\varepsilon_1}{2} = \frac{(\sigma_f')^2}{E}(2N_f)^{2b} + \sigma_f'\varepsilon_f'(2N_f)^{b+c} \tag{6}$$

where σ_n is the maximum principal stress during the cycle and $\Delta\varepsilon_1/2$ is the principal strain amplitude. Socie [22] modified the *SWT* parameter taking into account the parameters that control the damage, such as:

$$SWT = \Delta\varepsilon_1^{max} \cdot \Delta\sigma_1 + \Delta\gamma_1^{max} \cdot \Delta\tau_1, for\ tensile\ mode \tag{7}$$

$$SWT = \Delta\gamma_{max} \cdot \Delta\tau \quad + \Delta\varepsilon_n \cdot \Delta\sigma_n, for\ shear\ mode \tag{8}$$

Ellyin [23] proposed a model based on the energy density associated to each cycle, ΔW^t, which is composed by two parts: plastic strain energy, ΔW^P, and the positive elastic strain energy, ΔW^{E+}. In the case of proportional or biaxial non-proportional loading, the total energy density associated to a cycle may be computed as:

$$\Delta W^t = \Delta W^P + \Delta W^{E+} = \int_t^{t+T} \sigma_{ij} d\varepsilon_{ij}^P + \int_t^{t+T} H(\sigma_i) H(d\varepsilon_i^e) \sigma_i d\varepsilon_i^e \tag{9}$$

where σ_{ij} and $\varepsilon^P{}_{ij}$ are the stress and plastic strain tensors, σ_i and ε_i^e are the principal stresses and the principal elastic strains, T is the period of one cycle and $H(x)$ is the Heaviside function. The fatigue failure criterion is defined according to the following expression:

$$\psi = \Delta W^t = \frac{\Delta W^P}{\bar{\rho}} + \Delta W^{E+} = \kappa \left(2N_f\right)^{\alpha} + C \tag{10}$$

where κ, α and C are material parameters to be determined from appropriate tests and $2N_f$ is the number of reversals to failure. The multiaxial constraint ratio, $\bar{\rho}$, can be determined using the following expression:

$$\bar{\rho} = (1 + \bar{\nu}) \frac{\hat{\varepsilon}_{max}}{\hat{\gamma}_{max}} \tag{11}$$

with

$$\hat{\varepsilon}_{max} = max[\varepsilon_a, \varepsilon_t] \tag{12}$$

$$\hat{\gamma}_{max} = max[|\varepsilon_a - \varepsilon_r|, |\varepsilon_t - \varepsilon_r|] \tag{13}$$

where ε_a and ε_t are principal in-plane strain (axial and transversal) parallel to the free surface, ε_r is the radial strain (perpendicular to the free surface), and $\bar{\nu}$ is an effective Poisson's ratio.

The steel half-pipes bolted connections presented in Figure 1 are subjected to complex loads. In this sense, the choice of a multiaxial damage criterion is required [14]. In order to apply a multiaxial/biaxial damage criterion it is necessary to carry out experimental tests of small-scale specimens to characterize the cyclic elastoplastic behavior under multiaxial/biaxial loading conditions of materials under study.

In this paper an experimental programme is designed (see Table 1) of multiaxial (axial+torsional) fatigue tests in low-cycle fatigue (LCF) regime using smooth specimens (see Fig. 2 and 3) for the S355 and S690 steels. These fatigue results are used to estimate the constants of local multiaxial criteria.

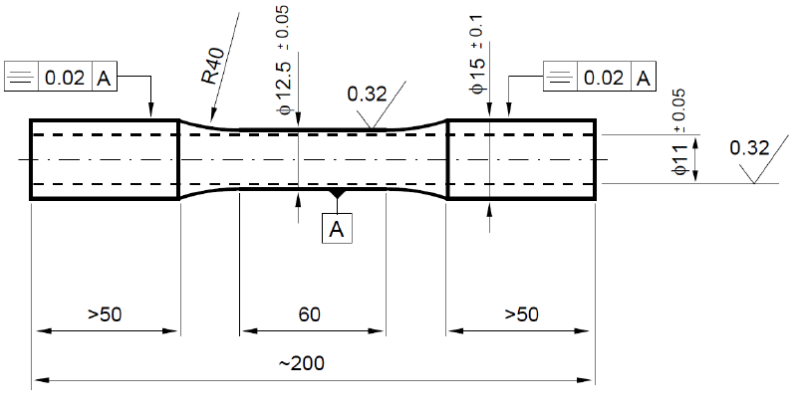

Figure 2. Geometry of the specimen to be used in the multiaxial (axial+torsional) fatigue tests (in mm).

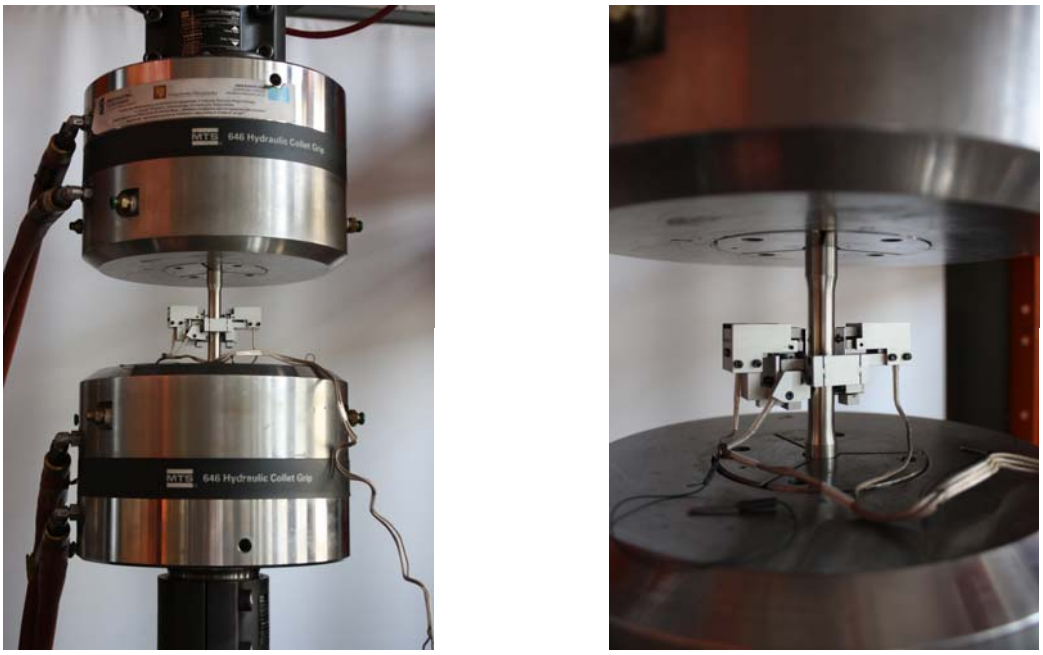

a) b)

Figure 3. Multiaxial (axial+torsional) fatigue test: a) Overview of the test; b) Specimen with biaxial axial-torsional extensometer. (colocar antes da tabela 1)

Table 1. Experimental programme to be used in multiaxial (axial+torsional) fatigue tests.

Δε (%)	Δγ (%)	Number of Specimens	Test Conditions
1.50	-	2	Pure Axial, R=-1
0.75		2	
0.50		2	
0.30		2	
1.50	-	2	Pure Axial, R=0 or 0.05
0.75		2	
0.50		2	
0.30		2	
-	1.50	2	Pure Torsional, R=-1
	1.00	2	
	0.75	2	
	0.50	2	
-	1.50	2	Pure Torsional, R=0 or 0.05
	1.00	2	
	0.75	2	
	0.50	2	
0.25	0.43	2	Proportional, R=0 or 0.05
0.50	0.87	2	
0.90	1.56	2	
0.25	0.43	2	Proportional, R=-1
0.50	0.87	2	
0.90	1.56	2	
0.40	0.70	2	Non-proportional, R=0
0.80	1.00	2	
0.40	0.60	2	Non-proportional, R=-1
0.80	1.00	2	

The connection presented in Fig. 1 that is to be used in the lattice part of a hybrid wind turbine tower, is not covered by design codes. A typified connection for this type of structural detail has been established in the SHOWTIME project, but an appropriate fatigue S-N curve is needed. A procedure for multiaxial fatigue assessment based on local approaches was proposed by Jovašević et al. [15]. This proposed procedure needs the the cyclic elastoplastic behavior under multiaxial/biaxial loading experimental tests to be performed. A local model based on multiaxial fatigue criteria can be used to obtain the S-N curve prediction.

ACKNOWLEDGEMENTS

The authors acknowledge with thanks the support of the European Commission's Framework Program "Horizon 2020", through the Marie Skłodowska-Curie Innovative Training Networks (ITN) "AEOLUS4FUTURE – Efficient harvesting of the wind energy" (H2020-MSCA-ITN-2014: Grant agreement no. 643167) to the present research project. José A.F.O. Correia acknowledges to the Portuguese Science Foundation (FCT) for the financial support through the post-doctoral grant SFRH/BPD/107825/2015. The authors also acknowledge the support of the Wroclaw University of Science and Technology – Department of Mechanics, Materials Science and Engineering.

REFERENCES

[1] C. Heistermann, "Behaviour of pretensioned bolts in friction connections", Lulea, Sweden, 2011.

[2] E Hau, "Wind turbines – Fundamentals, Technologies, Application, Economics" (3rd ed.), Springer, Germany, 2013.

[3] M Veljkovic, M. Feldmann, J. Naumes, D Pal, L. Simões da Silva, C. Rebelo, "Wind turbine tower design, erection and maintenance", in Wind energy systems: Optimising design and construction for safe and reliable operation Edited by J D Sørensen, Aalborg University and J N Sørensen, Technical University of Denmark, Denmark, Woodhead Publishing Limited, Cambridge, UK, (2011) ISBN: 978 1 84569 580 4.

[4] M. Veljkovic, M. Feldmann, J. Naumes, D. Pak, C. Rebelo, L. Simões da Silva, "Friction connection in tubular towers for a wind turbine", Stahlbau, 79: 660–668 (2010), doi: 10.1002/stab.201001365.

[5] M. Pavlovic, C. Heistermann, M. Veljkovic, D. Pak, M. Feldmann, C. Rebelo, L. Simões da Silva, "Friction connection vs. ring flange connection in steel towers for wind converters", Engineering Structures, 98, 151-162 (2015). http://dx.doi.org/10.1016/j.engstruct.2015.04.026

[6] J.F. Manwell, J.G. McGowan, A. L. Rogers, "Wind energy explained – Theory, Design and Application", Wiley, USA, 2002.

[7] K. Hüsemann, "Ruukki Wind towers – High truss towers for wind turbine generators", Ruukki, Finland, 2010.

[8] G. Figueiredo, C. Rebelo, "Structural behaviour of hybrid lattice – tubular steel wind tower", Univesity of Coimbra, Portugal, 2013.

[9] Rebelo et al. "Steel Hybrid Onshore Wind Towers Installed with Minimal Effort (SHOWTIME)", Project Proposal; Grant Agreement No. RFSR-CT-2015-00021, 2015.

[10] Rebelo et al., "Steel Hybrid Onshore Wind Towers Installed with Minimal Effort (SHOWTIME)", Grant Agreement No. RFSR-CT-2015-00021, Annual report, Technical Report No. 1, Issued on March 2016.

[11] W. Weibull, "Fatigue Testing and Analysis of Results", London: Pergamon Press LTD, 1961.

[12] F. Ellyin, "Fatigue Damage, Crack Growth and Life Prediction", London: Chapman & Hall, 1997.

[13] H. Chen, G.I. Grondin, R.G. Driver, "Fatigue Resistance Oh High Performance Steel", Structural Engineering Report No. 258, University of Alberta, Canada, 2005.

[14] F. Ozturk, J.A.F.O. Correia, C. Rebelo, A.M.P. de Jesus, L. Simoes da Silva, "Fatigue assessment of steel half-pipes bolted connections using local approaches", Procedia Structural Integrity 1 (2016) 118–125.

[15] S. Jovašević, J.A.F.O. Correia, M. Pavlović, C. Rebelo, A.M.P. De Jesus, M. Veljković, L. Simões da Silva, "Global fatigue life modelling of steel half-pipes bolted connections", Procedia Engineering, Volume 160, 2016, Pages 278–284.

[16] W.N. Findley, "Theories relating to fatigue of materials under combinations of stress", Colloquium on Fatigue, Stockholm (1955), Springer-Verlag, Berlin, 35.

[17] W.N. Findley, J.F. Tracy, "The Effect of the Intermediate Principal Stress on Triaxial Fatigue of 7075-T6 Aluminum Alloy", Journal of Testing and Evaluation, 1973, Volume 1, Issue 5.

[18] M.W. Brown, K.J. Miller, "A theory for fatigue failure under multiaxial stress–strain conditions", Proc Inst Mech Engrs 1973;187:745–55.

[19] A. Fatemi, D.F. Socie, D.F., "A critical plane to multiaxial fatigue damage including out-of-phase loading", Fatigue Fract Eng Mater Struct 1988;11(3):149–65.

[20] O.H. Basquin, "The exponential law of endurance tests", Proc Am Soc Test Mater 1910;10:625–30.

[21] K.N. Smith, P. Watson, T.H. Topper, "A Stress-Strain Function for the Fatigue of Metals", Journal of Materials 1970; 5(4): 767-78.

[22] D.F. Socie, "Multiaxial fatigue damage models", J Eng Mater Tech 1987;109:293–8.

[23] F. Ellyin, "Fatigue damage, crack growth and life prediction", Chapman & Hall, 1997.

THE INTERNATIONAL CONFERENCE ON
WIND ENERGY HARVESTING 2017
20-21 April 2017
Coimbra, Portugal

Paper 304

EVALUATION OF THE NONDETERMINISTIC DYNAMIC STRUCTURAL RESPONSE OF WIND TURBINE TOWERS

José Guilherme Santos da Silva[1]
Civil Engineering Postgraduate Programme (PGECIV)
Structural Engineering Department (ESTR)
State University of Rio de Janeiro (UERJ)
Rio de Janeiro/RJ, Brazil

Breno de Almeida Santos Oliveira[2]
Civil Engineering Postgraduate Programme (PGECIV)
State University of Rio de Janeiro (UERJ)
Rio de Janeiro/RJ, Brazil

ABSTRACT

This investigation develops an analysis methodology aiming the evaluation of the dynamic structural response of a typical wind turbine supporting steel tower, based on a numerical modelling, performed with the aid of the finite element program ANSYS. The study is initially centred on the evaluation of the natural frequencies and vibration modes of the analysed structural model. The numerical model calibration was made by comparisons to experimental data related to an experimental modal analysis acquired in a full scale tower structure and proved to be able to fully represent its structural dynamic performance. This way, with the objective of evaluating the results obtained according to the proposed analysis methodology, the wind tower dynamic structural response was investigated considering the rotor forces and the nondeterministic wind dynamic excitation loads applied to the structure.

INTRODUCTION

Based on the increasing demand on renewable and clean energy, wind turbine design has advanced significantly in terms of its size and type [1]. In Brazil, considering this advance, the conventional conical steel tower is a predominant type of supporting structure [2]. However, it should be noted that wind farms, widely used in Europe, still do not represent a significant parcel of the renewable energy sources utilized in Brazil and one of these reasons for this trend can be attributed to the wind farm high implementation costs [3]. This way, an optimization of the wind turbine supporting tower structure, see Figure 1, can contribute for the implementation of new and cost-effective wind farms plants in Brazil. On the other hand, these aims can only be achieved with the understanding of the static and dynamic behaviour of typical wind turbine supporting steel towers [2,3].

Having these thoughts in mind, on December 2014, around 1,800 megawatts (MW) were contracted with energy from 71 wind power plants scheduled to be delivered beginning in July 2012. While focusing domestically on wind-energy generation, Brazil is part of a larger international movement toward wind power as a primary source of energy. In fact, wind power has seen the highest expansion rate of all available renewable energy sources, with an average growth of 27% per year since 1990, according to the Global Wind Energy Council (GWEC) [4]. On the other hand, as a result of the efforts of PROINFA (Incentive Program for Alternative Energy Sources), Brazil possesses an installed capacity of more than 6,5 GW, contributing to 4,7% of the national energy production in Brazil, according to ABEEólica, the Brazilian Association of Wind Power. In fact, wind was the third main source of energy production in Brazil, trailing only to biomass with 9,1% and hydropower with 84,9%. The estimates for the end of 2017 are that wind energy production in Brazil will be about of 8,7 GW. According to CETESB, the State Environmental Company of the State of São Paulo, the production of wind energy reduces the emissions of CO2 in Brazil per year by more than 11.600.000 tons, which is good for the annual emission of 7 million vehicles [5].

Considering the relevance of this theme, this investigation aims to develop an analysis methodology to evaluate the nondeterministic dynamic structural response of a typical wind turbine supporting steel tower (MM92 wind tower), located in Algarve, Portugal, based on a numerical modelling, performed with the aid of the finite element computational program ANSYS [6]. The study is initially centred on the evaluation of the natural frequencies and vibration modes of the analysed structural model. This way, the model calibration was made by

1 Associate Professor, DSc, State University of Rio de Janeiro, Rio de Janeiro/RJ, Brazil, jgss@uerj.br
2 DSc Student, State University of Rio de Janeiro, Rio de Janeiro/RJ, Brazil, engbrenoalmeida@yahoo.com.br

comparisons to experimental data related to an experimental modal analysis acquired in a full scale wind tower structure [7], and proved to be able to fully represent its structural dynamic performance. In sequence, with the objective of evaluating both quantitative and qualitatively the results obtained according to the proposed methodology, the wind tower nondeterministic dynamic structural response was investigated considering the rotor forces and the nondeterministic wind loads applied to the tower [2].

a) Osório, Rio Grande do Sul, Brazil b) Sevilha, Spain c) Algarve, Portugal (MM92)

Figure 1. Typical wind tower structures in many countries around the world [3]

NONDETERMINISTIC WIND DYNAMIC LOADS

One of the dynamic loads of great importance to be considered in the structural analysis of typical wind turbine supporting steel tower is related to the wind forces. The towers wind-induced structural response consists of along-wind response, across-wind response and torsion response. Initially, in this investigation the along-wind response analysis was considered. In design practice, the flow of wind around typical wind turbine supporting steel tower is a complex and random process, so the wind action is considered as a nondeterministic process and presents unstable properties and also random characteristics, which indicate that the deterministic consideration should be avoided [2].

This way, aiming to simulate the nondeterministic wind actions, this investigation presents a numerical formulation based on the Monte Carlo's method. The Monte Carlo numerical procedure is then used to compute the power spectral density associated to the wind actions and to derive the statistics of the dynamic response, considering the uncertainty of the wind loadings [2]. The fluctuating parcel of the wind is decomposed into a finite number of harmonic functions proportional to the structure resonant frequencies with phase angles randomly determined. Thus, the present study assumed a frequency range of 0.01 to 5.791 Hz, which corresponds to the first five vibration modes of the investigated wind turbine supporting steel tower and 81 harmonics were used in the numerical analysis, with an increment frequency equal to 0.0728 Hz ($\Delta\omega$ = 0.0728 Hz). The fifth harmonic coincides with the fundamental frequency of the structure (resonant harmonic), while the remaining harmonics are multiples and submultiples of the resonant harmonic. The amplitude of each harmonic is obtained using an existing wind power spectrum density function, based on the Kaimal spectrum. The Kaimal spectrum was adopted due to the consideration of the tower height z in its formulation. The power spectrum is given by Eqs. (1) and (2) and the friction velocity is determined by Eq. (3).

$$\frac{fS_v(f,z)}{u_*^2} = \frac{200x}{(1+50x)^{5/3}} \tag{1}$$

$$x(f,z) = \frac{fz}{V_z} \tag{2}$$

$$u_* = \frac{\kappa v_Z}{\ln(z / z_0)} \tag{3}$$

Considering the Eqs. (1) to (3), f represents the frequency, $S^V(f)$ is related to the wind power spectral density in the frequency f, x is the dimensionless frequency, Vz is the velocity at height z and k is the Karman constant. Firstly, based on a single harmonic function, the fluctuating parcel of the wind can be represented by Eq. (4), with v_0 representing the basic wind speed. In sequence, assuming that the fluctuating parcel of the wind is associated to a second order ergodic stationary random process with mean equal to zero and also considering a superposition of the harmonic waves, the fluctuations can be expressed as in Eq. (5), where N is the total number of frequency increments in the power spectrum density, f_i is the frequency related to the harmonic i, Δf is the frequency increment and θi is the random phase angle normally distributed in the interval [0-2π]. The amplitude of the functions in time domain is given by Eq. (6). Finally, based on the use of the developed mathematical formulation, see Eqs. (1) to (6), the nondeterministic wind-induced response in along-wind direction can be calculated through the sum of a static parcel (along-wind translation) and a dynamic part (along-wind random vibration) [2]. It must be emphasized that the along-wind translation is mainly caused by the wind steady flow. The along-wind vibration is caused by the turbulent flow. The along-wind random vibration includes a quasi-steady background turbulence response to low frequency component and a narrow-band resonant response.

$$v(t) = v_0 \cos(2\pi f t) \tag{4}$$

$$v(t) = \sum_{i=1} \sqrt{2S^V(f_i)\Delta f}\, \cos(2\pi f_i t + \theta_i) \tag{5}$$

$$a_i = \sqrt{2S^V(f_i)\Delta f} \tag{6}$$

WIND TURBINE SUPPORTING STEEL TOWER MODELLING

Based on previous investigations [2,3], an actual MM92 wind turbine tower of 2 MW capacity (Repower model), with 78.1 m height (Hub height: H_{hub} = 78.1 m), characterised by a free standing steel tube varying its diameter and thickness throughout the height was modelled in the present work. The tower was divided in three parts to enable transportation and assembly at the construction site. These parts are depicted in Figure 2(a), where two doors, provided to enable ventilation and access for maintenance, can be observed near to the tower base plate, Figure 2(e). The connection between these parts was made by bolted connections, see Figure 2(b). Flange plates were considered in the numerical model to simulate this effect. The tube thickness varied along the wind tower height. The adopted thicknesses in the tower first, second and third segments varied from 30 to 21 mm, 20 to 16 mm and 15 to 12 mm, respectively [3].

A finite element model for the studied supporting steel tower wind tower was developed using four-nodes thick shell elements (SHELL181 [6]), that considers bending, shear and membrane deformations. The mesh was refined along the tower using well-proportioned finite elements to avoid numerical problems, as illustrated in Figure 2(c) to 2(e). The model was composed by 16625 shell finite elements with 16667 nodes. The tower main structure was made with a S355 steel grade with a bilinear constitutive law considering a 5% strain hardening young modulus [2,3]. The response of the nacelle and the turbine was considered as linear elastic. The adopted Young's Modulus and density was equal to 210000 N/mm^2 and 7850 kg/m^3. This strategy enabled an easy evaluation of the tower self-weight load. The adopted boundary conditions simulated a cantilever model with a fixed support at the tower base plate [2,3].

DYNAMIC STRUCTURAL ANALYSIS

Initially, the wind tower natural frequencies and vibration modes were determined with the aid of numerical simulations as presented in Figure 3 and Table 1. It can be clearly noticed from Table 1 results [2,3], that there is a good agreement between the structural model natural frequencies calculated using finite element simulations and the experimental results measured by Rebelo and Silva [7]. Such fact validates the numerical model here presented, as well as the results and conclusions obtained throughout this work. In sequence, the wind tower dynamic structural response under the action of the rotor forces and the nondeterministic wind loadings was calculated. The Newmark algorithm [2] was used to evaluate the structural system dynamic response and a time step equal to 2x10^{-3}s ($\Delta t = 2x10^{-3}$ s) was considered in the numerical analysis. It is also considered that the modal damping coefficient adopted in this investigation was equal to 1.5% (ξ= 1.5%) [2,3].

Based on work developed by Umut *et al*. [1], the rotor forces acting on the structure are produced due to rotating machinery and should be given by the manufacturer of the wind turbine according to each specific wind turbine tower design. A literature review also has indicated only one paper [1,8], which includes the rotor forces values for a wind turbine tower with a 450 kW capacity and 38 m height. This way, in this paper the rotor forces for a wind turbine of 450 kW capacity and 38 m height are used for the analysed wind turbine tower [1,2,8]. Thus, the rotor forces are increased linearly with increasing wind turbine power and these forces (F_x, F_y, F_z, M_x, M_y and M_z) are applied to the tower for the operational design situation [1,2]. The wind loads are applied longitudinally and the wind steel tower MM92 is analysed under gravity + rotor forces + wind dynamic loadings.

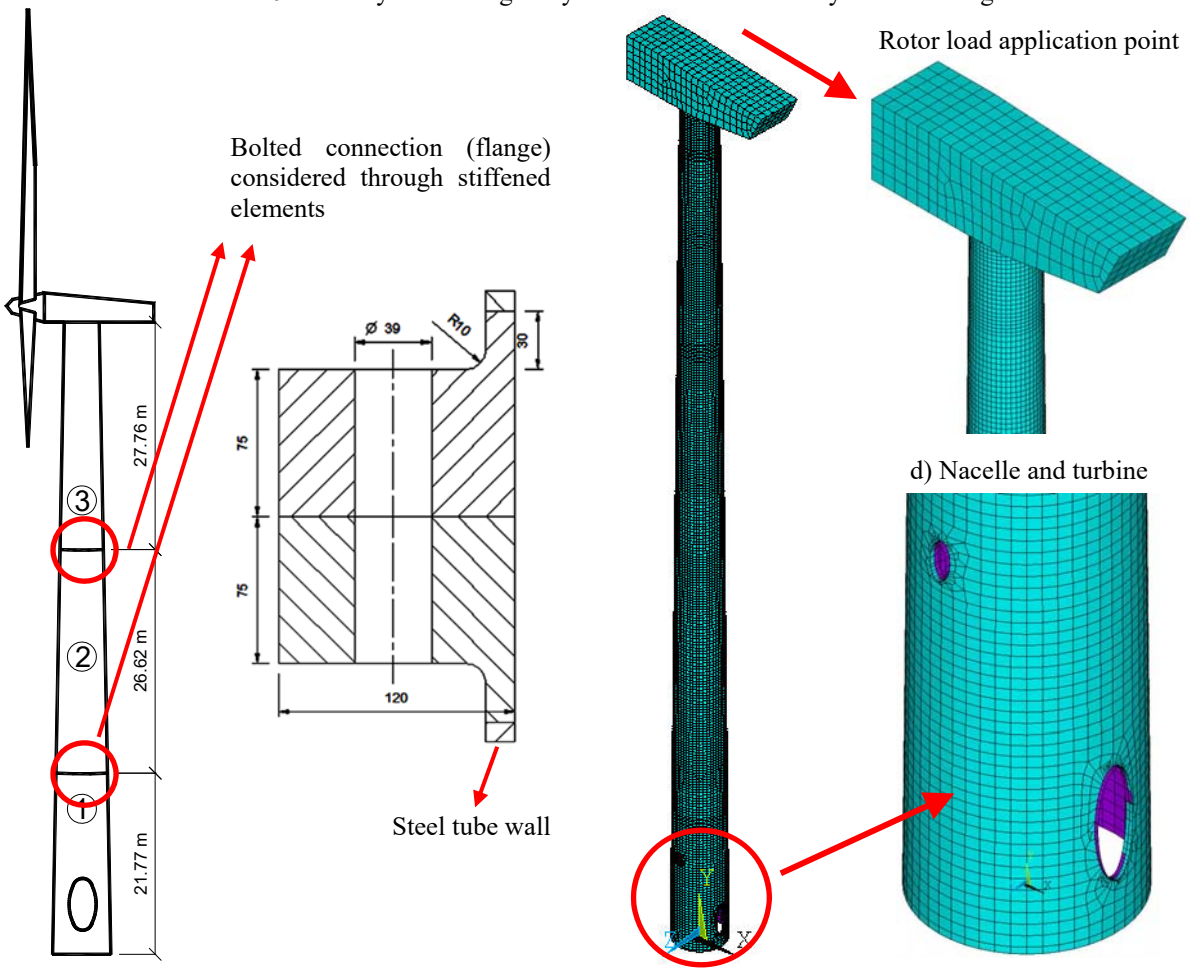

Figure 2. Structural model and finite element model of the investigated wind steel tower MM92 [3]

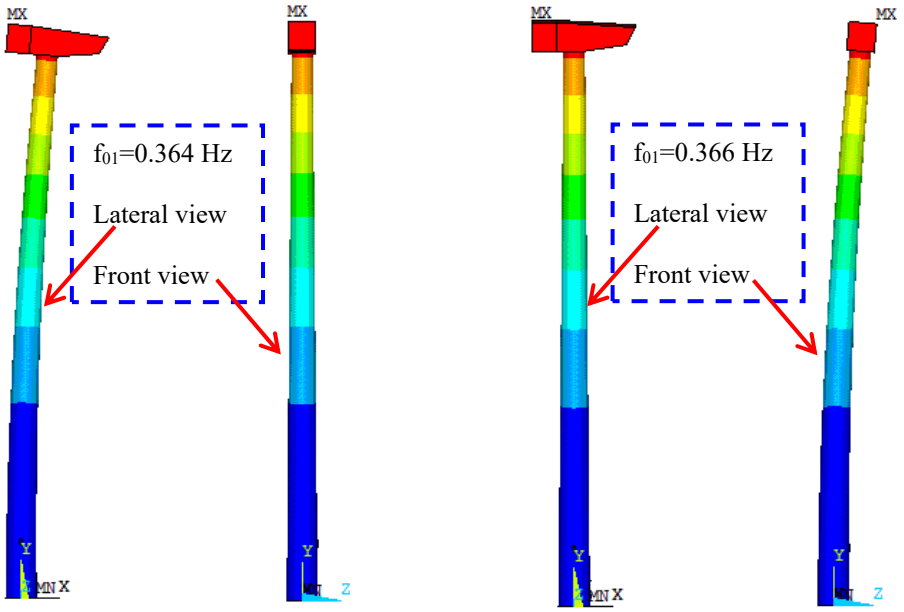

Figure 3. First and second vibration modes of the investigated wind turbine tower

Table 1. Experimental and numerical natural frequencies for the MM92 wind tower

Mode	Experimental [7]	Numerical [2,3]	Vibration Modes
Mode 1	f_{01} = 0.340 Hz	f_{01} = 0.364 Hz	1st Bending: Nacell direction (X-X)
Mode 2	f_{02} = 0.343 Hz	f_{02} = 0.366 Hz	1st Bending: Transversal to Nacell direction (Y-Y)

Figure 4 presents the horizontal translational displacements in time and frequency domain at the top of the investigated structural model (H_{Hub} = 78.1m). The horizontal displacements indicated that the wind tower dynamic response was gradually attenuated along the time due to the influence of the structural system damping. As expected, the maximum displacement [u_{max} = 68 mm: *steady state response*] is less than approximately one-hundredth of the total height and appears at the top of the tower. The wind turbine first vibration mode [f_{01} = 0.364 Hz: bending effects] represents the main peak of energy transfer in the dynamic response, see Figure 4.

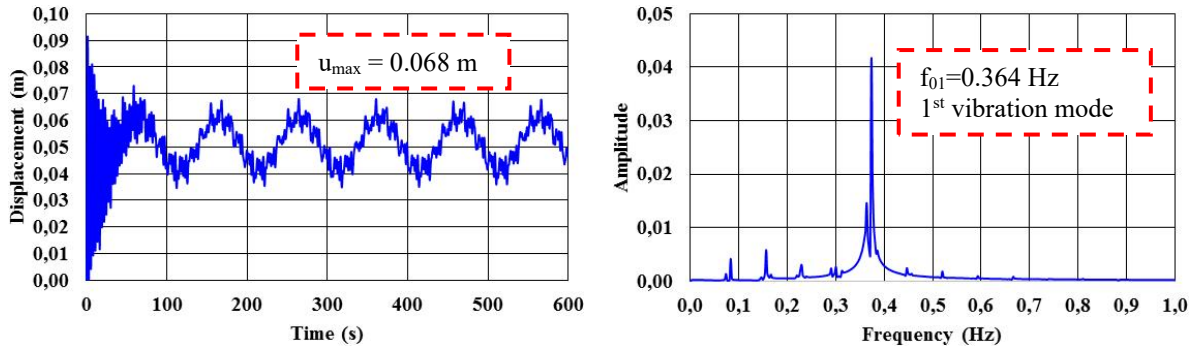

Figure 4. Dynamic structural response of the wind turbine steel tower MM92 (υ = 40 m/s)

CONCLUSIONS

In this work, a wind turbine steel tower is analysed under gravity + rotor forces + nondeterministic wind dynamic loads. The developed nondeterministic mathematical model proved to be an efficient solution method for the evaluation of the dynamic structural response of wind turbine towers. The present analysis has shown that the maximum displacement is less than approximately one-hundredth of the total height of the tower and there is no plastic hinge formation in the tower sections. The author's intention is to proceed the study, based on the development of fatigue and buckling analyses and also the vortex dynamic loads needs to be investigated.

ACKNOWLEDGEMENTS

The authors gratefully acknowledge the support for this work provided by the Brazilian Science Foundations CAPES, CNPq and FAPERJ.

REFERENCES

[1] O. Umut, B. Akbas, J. Shen, "Design Issues of Wind Turbine Towers", The 8th International Conference on Structural Dynamics, EURODYN 2011, Leuven, Belgium, 2011, pp. 1592-1598.

[2] B. de A.S. de Oliveira, "Numerical Modelling of the Dynamic Behaviour of Wind Turbine Steel Tower Structures", DSc Thesis (In Portuguese. In development), Civil Engineering Post-Graduate Programme, PGECIV, State University of Rio de Janeiro, UERJ, Rio de Janeiro, Brazil, 2017.

[3] A. da S. Sirqueira, "Structural Behaviour of Wind Turbine Steel Tower Structures", MSc Dissertation (In Portuguese), Civil Engineering Post-Graduate Programme, PGECIV, State University of Rio de Janeiro, UERJ, Rio de Janeiro, Brazil, 2008, pp. 1-108.

[4] Wikipedia, "Renewable energy in Brazil". See: http://thebrazilbusiness.com/article/wind-energy-in-brazil. Full text accessed in 20/12/2016.

[5] E.F. Nes, "Wind Energy in Brazil". See: https://en.wikipedia.org/wiki/Renewable_energy_in_Brazil. Full text accessed in 20/12/2016.

[6] ANSYS 12.1. ANSYS-Inc. Theory Reference. Swanson Analysis Systems, Inc., 2010.

[7] C. Rebelo, L.A.P.S da Silva, "Measurement Plan of a Wind Steel Tower in Espinhaço de Cão, Lagos, Algarve, Portugal". HISTWIN: High-Strength Steel Tower for Wind Turbines. Civil Engineering Department, Faculty of Sciences and Technology, University of Coimbra, 2007, pp. 1-11.

[8] N. Bazeos, G.D. Hatzigeorgiou, H., D.L. Karabalis, "Static, Seismic and Stability Analyses of a Prototype Wind Turbine Steel Tower", Engineering Structures, Vol. 24, 2002, pp.1015-1025.

THE INTERNATIONAL CONFERENCE ON
WIND ENERGY HARVESTING 2017
20-21 April 2017
Coimbra, Portugal

Paper 305

EXPERIMENTAL AND NUMERICAL INVESTIGATIONS OF THE S355 AND 42CrMo4 STEEL CRACKED COMPONENTS IN TERMS OF THE DYNAMIC RESPONSE AND ENERGY APPROACH

Grzegorz Lesiuk[1]
Wrocław University of Science and Technology, Wrocław, Poland

Jose A.F.O. Correia[2]
INEGI & Faculty of Engineering, University of Porto, Porto, Portugal

Bocian Mirosław[3]
Wrocław University of Science and Technology, Wrocław, Poland

A.M.P. de Jesus[4]
INEGI & Faculty of Engineering, University of Porto, Porto, Portugal

Maciej Panek[5]
Wrocław University of Science and Technology, Wrocław, Poland

Kucharski Paweł[6]
Wrocław University of Science and Technology, Wrocław, Poland

ABSTRACT

S355 and 42CrMo4 structural steels are commonly used in "green power energy" sector. S355 steel is commonly used for wind towers structures. The 42CrMo4 steel is widely used as a material for rotors and highly stressed component subjected to fatigue loading. The knowledge about the mechanical response and behavior of the cracked components is a crucial point in "safe life" strategy procedures. The initial aim of the experiments (and numerical analysis) was the examination of the effect of the length and orientation of fatigue cracks on the character and the natural frequencies of the object. 3PBs (three-point bending) beams were used with an initial crack length a = 8.7mm. These samples were subjected to cyclic loading, thereby causing the incremental (controlled) crack growth, respectively - 10.1 mm, and 12.2 mm. For three lengths of the obtained crack (smaller increments according to a first mode of rupture), experimental modal analysis was conducted. In addition to research on the real object also numerical analysis using the environment Abaqus 6.14 was performed. Based on Lanczos algorithm natural frequencies was evaluated, then set system response in the frequency domain (for harmonics function of loading). Analyzes were carried out in a linear manner. Exemplary results are shown in Fig. 1 which compares numerical and experimental results. The next step of the experimental works was to investigate a new energy model (introduced in. [1], [2]) usefulness in description of the FCGR (fatigue crack growth rate) diagram for 42CrMo4 steel – Figure 2. On the dynamic response (as frequency vibrations), the system can affect local,

1 PhD Eng., Wrocław University of Science and Technology, Faculty of Mechanical Engineering, Department of Materials Science and Engineering, Smoluchowskiego 25 St, PL-50370 Wrocław, Poland, grzegorz.lesiuk@pwr.edu.pl
2 PhD Eng., INEGI/Faculty of Engineering, University of Porto, Rua Dr. Roberto Frias, 4200-465 Porto, Portugal, jacorreia@inegi.up.pt
3 PhD Eng., Wrocław University of Science and Technology, Faculty of Mechanical Engineering, Department of Materials Science and Engineering, Smoluchowskiego 25 St, PL-50370 Wrocław, Poland, miroslaw.bocian@pwr.edu.pl
4 Professor, INEGI/Faculty of Engineering, University of Porto, Rua Dr. Roberto Frias, 4200-465 Porto, Portugal, ajesus@fe.up.pt
5 PhD Eng., Wrocław University of Science and Technology, Faculty of Mechanical Engineering, Department of Materials Science and Engineering, Smoluchowskiego 25 St, PL-50370 Wrocław, Poland, maciej.panek@pwr.edu.pl
6 MSc. Eng., Wrocław University of Science and Technology, Faculty of Mechanical Engineering, Department of Materials Science and Engineering, Smoluchowskiego 25 St, PL-50370 Wrocław, Poland, pawel.kucharski@pwr.edu.pl

plastic zones and the possible effect of the fatigue crack closure. During the experiments, the plastic zones were monitored using DIC (Digital Image Correlation) method - Figure 3. All calculations were performed with GOM DIC environment. As a conclusion should be underlined, that both, numerical analysis and experimental modal analysis, may be in the future used to assess the length and orientation of the imperfections in the material. The results encourage further analysis due to the large potential application of the presented method.

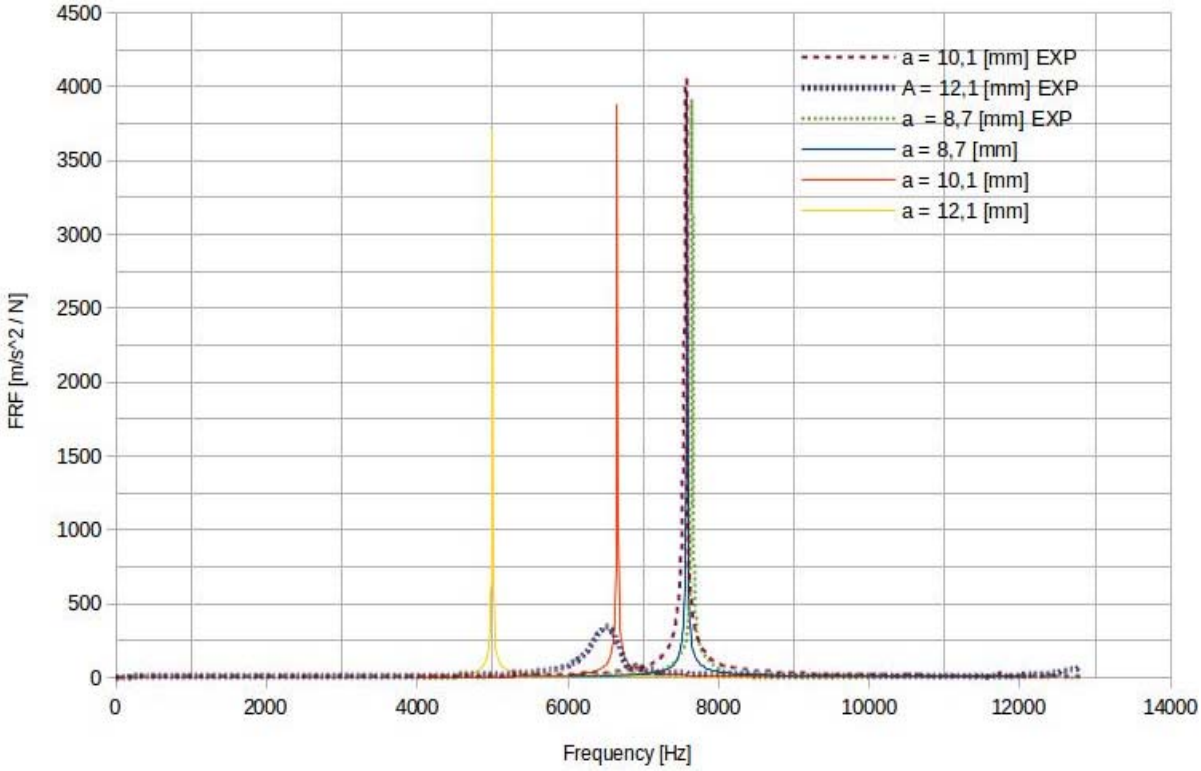

Figure 1. Experimental and numerical resonant frequencies obtained for fatigue cracked beam (W=20mm B=10mm), S355 steel.

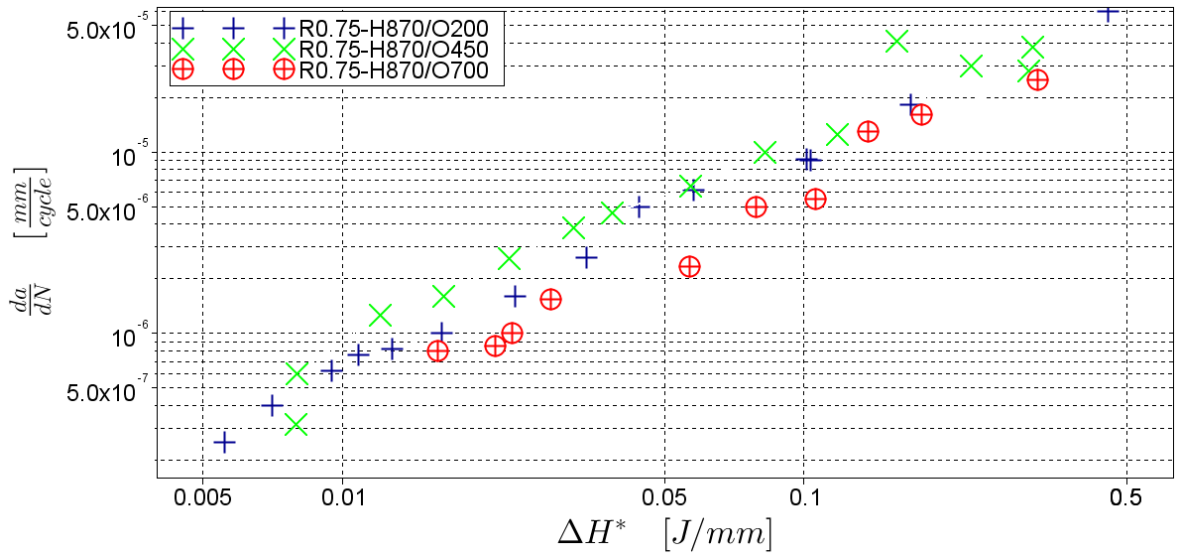

Figure 2. Fatigue fracture diagram based on energy parameter for the closure free (R=0.75) condition, 42CrMo4 steel with different heat treatment parameters.

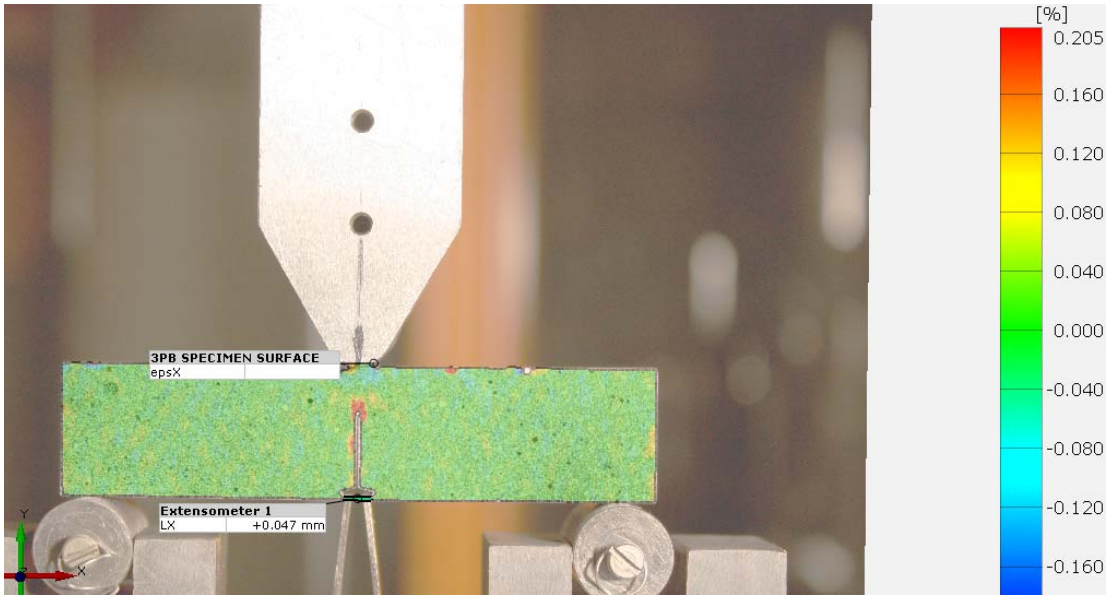

Figure 3. 3PB specimen (42CrMo4 steel) during test $-\varepsilon_{xx}$ strain distribution and plastic zone size evaluation during fatigue fracture and fracture toughness tests.

ACKNOWLEDGEMENTS

This work was financial supported by the Wroclaw University of Science and Technology – Department of Mechanics, Materials Science and Engineering internal, fundamental research program.

REFERENCES

[1] Szata M., Lesiuk G., "Algorithms for the estimation of fatigue crack growth using energy method", Archives of Civil and Mechanical Engineering, vol. 9., no 1, pp.119-134, Elsevier 2009.

[2] Kucharski P., Lesiuk G., Szata M., "Description of fatigue crack growth in steel structural components using energy approach-Influence of the microstructure on the FCGR", FATIGUE FAILURE AND FRACTURE MECHANICS XXVI: Proceedings of the XXVI Polish National Conference on Fatigue Failure and Fracture Mechanics, vol. 1780, AIP Publishing, 2016.

THE INTERNATIONAL CONFERENCE ON
WIND ENERGY HARVESTING 2017
20-21 April 2017
Coimbra, Portugal

Paper 306

EXTREME STEELS: A HIGH PERFORMANCE SOLUTION FOR WIND FASTENERS EXPOSED TO ADVERSE WEATHER CONDITIONS

Diego Herrero[1]
Sidenor I+D S.A.
Basauri, Basque Country, Spain

Jacinto Albarran[2]
Sidenor I+D S.A.
Basauri, Basque Country, Spain

ABSTRACT

The EXTREME technology was developed by Sidenor in order to allow the use of low-alloyed steels in the manufacturing of large wind fasteners and, at the same time, improve the performance of these components minimizing thus the risk of failure.

The extensive characterization study carried out on a 32CrB4 grade, manufactured through the EXTREME technology, shows that not only larger fasteners can be manufactured fulfilling the mechanical requirements (Ø > 50 mm vs Ø 36 mm for the conventional 32CrB4), but also an improvement of the mechanical properties is achieved with regards to the standard 32CrB4.

The fatigue performance of conventional steels is also improved with the EXTREME technology (the fatigue limit increases more than 10%). This improvement minimizes the risk of fatigue failures during the in-service life of the wind fasteners.

The application of the EXTREME technology in wind fasteners exposed to adverse climatological conditions will lead to a safer functioning of wind towers and to a reduction of the maintenance needs.

NOMENCLATURE

Ø	=	Diameter (mm)
Q&T	=	Quench and tempering
HV	=	Hardness in Vickers
UTS	=	Ultimate Tensile Stress (MPa)
$YS_{0,2\%}$	=	Yield Stress at 0,2 % (MPa)
El	=	Elongation (%)
RoA	=	Reduction of Area (%)
KV	=	Toughness of V-notched specimens (J)
σ_f	=	Fatigue limit (MPa)

INTRODUCTION

In order to optimize the wind turbine performance, wind farms are built in the most windy regions of the World, which usually coincide with extreme weather areas (where besides the hard winds, very low temperatures and/or corrosive environments, as in the case of off-shore wind farms, are common) [1].

That exposure to extreme weather conditions and the difficult accessibility to the places where wind towers are located increase the maintenance costs. The main way to reduce these costs is minimizing

[1] Researcher, Product Department, Sidenor I+D S.A., Bº Ugarte S/N, 48970, Basauri (Spain). diego.herrero@sidenor.com. T: +34 944871891; F: +34 944871844
[2] Department Manager, Product Department, Sidenor I+D S.A., Bº Ugarte S/N, 48970, Basauri (Spain). jacinto.albarran@sidenor.com

the number of interventions. In the case of wind fasteners, the three main causes of maintenance needs are: the low temperatures, the fatigue failures and the exposure to corrosive environments:

- *Low temperatures*: Low temperatures make the steel more brittle increasing the risk of failure caused by an impact [1]. In order to assure the correct functioning of the steel at low temperature, the standard ISO 898-1 [2] established all the requirements that the steels used in wind tower fasteners and foundations must fulfill. The most common steel class used in these applications is class 10.9 whose main requirements are shown in Table 1.

  Table 1. Requirements for the steel class 10.9 established by ISO 898-1 [2].

	Class 10.9
Min. UTS (MPa)	1040
Min. $YS_{0,2\%}$ (MPa)	940
Min. El (%)	9
Min. RoA (%)	48
Min. KV at -40 ºC (J)	27
Hardness range (HV)	320 - 380

- *Fatigue failures*: Fatigue damage is defined as a progressive damage that appears when the material is subjected to cyclic loads. The stress values that cause such damage are much lower than the material UTS or YS.

  The fatigue performance is not mentioned in the standard ISO 898-1. So, given that wind fasteners are subjected to cyclic loads, a fatigue failure could take place even having reached all the requirements established in the standard. The fatigue failure of the wind fasteners could lead to the collapse of the whole wind tower [3]. An improvement of the steel fatigue performance would directly lead to a safer tower operation.

- *Exposure to corrosive environments*: The exposure of the fasteners to corrosive environments drastically decreases their in-service life [4][5]. The way to face this question, contrary to the two previous cases, is focused on the use of protective coatings and not on the improvement of the steel properties. This is the reason why this problem will not be considered in this paper.

Figure 1. Accident in the Taikoyama wind power plant caused by a fatigue failure [3].

The previously described aspects lead to unexpected failures of the components increasing the maintenance needs. This paper is focused on the steel properties optimization (paying special attention to its fatigue performance) in order to improve the wind tower fasteners and foundations in-service performance, minimizing thus the maintenance interventions and the risk of accidents similar to the one occurred in the Taikoyama wind power plant [3].

The actual trend of building wind turbines of bigger and bigger power (> 5 MW) [6] leads to a considerable increase of the tower dimensions. Subsequently, to ensure the correct fastening of the different parts of the tower, the fasteners diameter must be also increased. This dimensional increase makes even more difficult the obtaining of the required mechanical properties.

Nowadays, to reach the previously mentioned mechanical properties with small fasteners (Ø < 36 mm) low alloyed steels (i.e. 32CrB4 or 33MnCrB6) are used. However, if bigger fasteners (Ø > 36 mm) want to be manufactured, the use of high alloyed steel grades (i.e. 30CrNiMo8) is needed in order to assure the required mechanical properties, mainly the combination of high strength and very high toughness at low temperatures. The main drawback of these alloyed grades is the high price of alloying elements (i.e. Ni, Mo…).

Sidenor developed the EXTREME technology which, thanks to the optimization of the steel manufacturing process, allows:

1. A maximization of the steel mechanical properties and fatigue performance.
2. To fulfill all the requirements established in the standard using low-alloyed steels in large diameter bars.

So, the application of the EXTREME technology will lead to a safer in-service performance of screws and studs exposed to very adverse climatological conditions. This technology will allow the use of low-alloyed steels in the manufacturing of fasteners in a wide range of diameters.

This paper is focused on the application of the EXTREME technology in the 32CrB4 steel grade, the most commonly used grade in small size fasteners, in order to establish the improvements provided by this technology with regards to the standard material.

METHODOLOGY

The basis of the EXTREME technology is the optimization of the chemical composition and the steel manufacturing process:

- *Chemical composition:* EXTREME steels are Cr-B grades with a possible Ni addition which allows the achievement of the desired mechanical properties in large diameters. The S and P content is controlled in order to maximize the toughness at low temperature.
- *Steel manufacturing process:* The improvement of the manufacturing process is focused on the optimization of the main parameters of the secondary metallurgy, the continuous casting and the heat treatment.

  In the secondary metallurgy, different stirring types and vacuum levels were considered to obtain the desired chemical composition.

  In the continuous casting of 185x185 mm billets, different electromagnetic stirring (EMS) levels and continuous casting speeds were tested to find those leading to the most homogeneous material.

  Finally, after the bars hot rolling, the corresponding heat treatment was carried out (Q&T in gas furnace for bolts, and induction hardening for studs). The main parameters of each heat treatment (austenization temperature and time and tempering temperature and time) were optimized[3].

The specimens needed to carry out the mechanical and fatigue tests were machined at 12,5 mm from the bar surface. The specimens extraction and preparation were carried out following the standard ISO 377 [7].

The tensile tests, performed on Ø 9 mm specimens, followed the standard ISO 6892-1 [8]. The Charpy impact tests were carried out at different temperatures (following the standard ISO 148-1 [9]) on V-notched specimens. Three repetitions of each mechanical test were carried out. Finally, tension-compression axial fatigue tests (R = -1) were performed on Ø 8 mm specimens, these tests were conducted following the ISO 12106 [10] using a testing frequency of 25 Hz and a run-out criteria of 10.000.000 cycles.

[3] Although both heat treatments were optimized, in the case of bolts the steel is supplied in as-rolled condition. Sidenor could share the most adequate values for the Q&T parameters with the bolts manufacturer in order to obtain the desired mechanical properties.

RESULTS

Among the different bar diameters tested for the 32CrB4 EXTREME steel, the results obtained with the diameters 56 mm (for Q&T) and 64 mm (for induction hardening) are shown below:

– *Chemical composition and microstructural assessment:* The chemical composition of the studied steel is shown in Table 2.

Table 2. Chemical composition of the 32CrB4 EXTREME steel (% in weight).

C	Cr	P	S	B
0,31	1,03	0,011	0,003	0,0021

The obtained microstructure for both cases is tempered martensite with some traces of tempered bainite at mid radius and at the center of the bars (as shown in Figure 2 and Figure 3). These microstructures perfectly fit the requirements established in the standard ISO 898-1.

Figure 2. Microstructures (100X) from the surface to the center of the bar, 32CrB4 EXTREME Q&T Ø 56 mm.

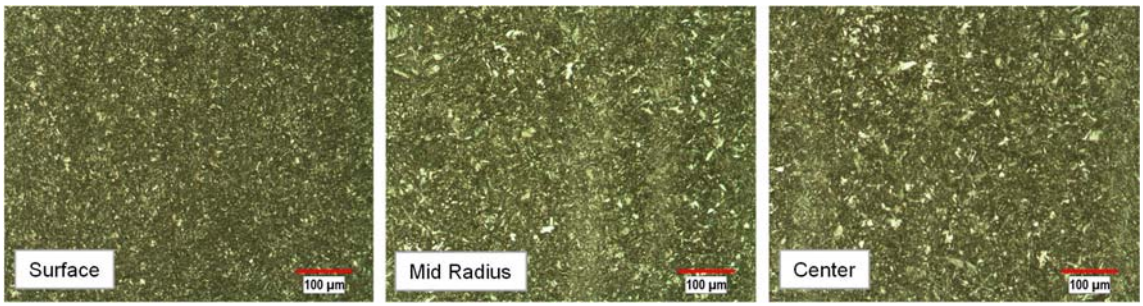

Figure 3. Microstructures (100X) from the surface to the center of the bar, 32CrB4 EXTREME Induction Hardened Ø 64 mm.

– *Mechanical properties:* The average hardness profiles (shown in Table 3) were obtained after three repetitions performed each 5 mm from the bar surface to the core. The material is quite homogeneous from the hardness point of view. The requirements stated by the standard ISO 898-1 are reached.

Table 3. Hardness profile (HV_{30kg}) for the 32CrB4 EXTREME Q&T and induction hardened.

Distance from bar surface (mm)	32CrB4 EXTREME Q&T Ø 56 mm	32CrB4 EXTREME Ind. Hard. Ø 65 mm
5	335	347
10	332	349
15	330	355
20	325	353
25	321	331
30	-	329

Figure 4 compares the results obtained in the tensile and impact tests for the 32CrB4 EXTREME steels (Q&T and induction hardened) with the minimum values demanded by

the ISO 898-1. Although in all the cases those minimum values are clearly reached, all the properties of the induction hardened steel are notably better than the Q&T one, especially considering its higher diameter (64 mm vs 56 mm).

The very high toughness at -40 ºC of the induction hardened 32CrB4 EXTREME steel assures an excellent response in case of impact during the in-service life of the fastener.

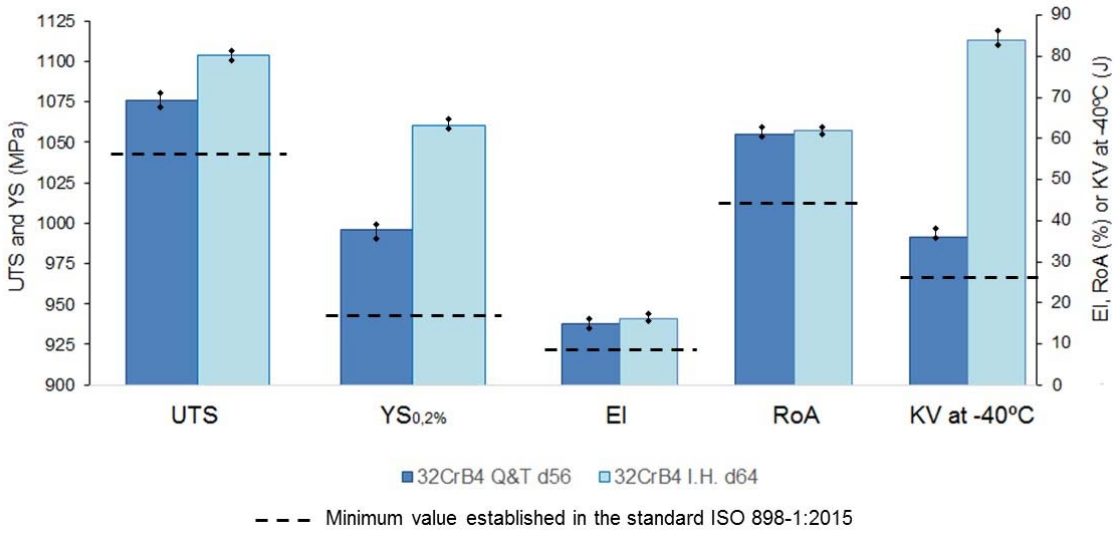

Figure 4. Mechanical properties of the 32CrB4 Q&T (Ø 56 mm) and induction hardened (Ø 64 mm).

– *Fatigue performance:* To evaluate the fatigue performance, tension-compression tests were carried out with 32CrB4 EXTREME Q&T and induction hardened steels. The obtained results were compared with the fatigue performance of the conventional 32CrB4.

In Figure 5 the S-N curves for the Q&T 32CrB4 EXTREME and conventional variants are represented. In the case of the conventional steel the fatigue specimens were machined from Ø 30 mm bars, while for the EXTREME steel Ø 56 mm bars were used. It is clearly seen that, even with a considerably higher bar diameter, the fatigue limit of the 32CrB4 EXTREME is about 15% higher than the one of the conventional 32CrB4. So, if similar diameters were compared, the fatigue improvement obtained with the EXTREME steel would be even higher.

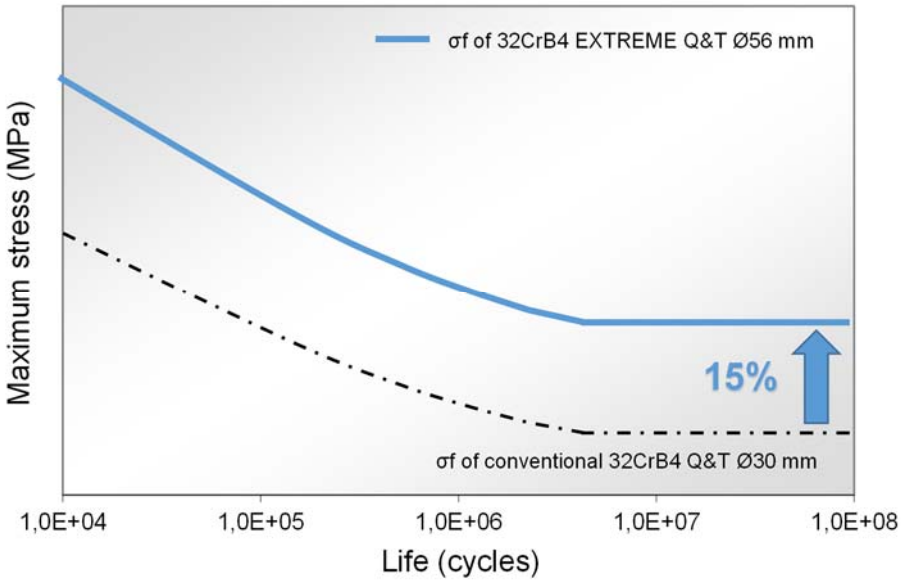

Figure 5. S-N curves for the 32CrB4 EXTREME and conventional Q&T grades.

Figure 6 also shows S-N curves, but in this case they correspond to the induction hardened EXTREME and conventional variants. The bar diameters used to make this comparison of the fatigue performance are 64 mm for the EXTREME steel and 30 mm for the conventional one. The fatigue performance of the conventional steel is improved in a 10% when the 32CrB4 EXTREME is used, even when the difference of the bar diameters is so high as the considered ones. As in the case of the Q&T steels, if similar diameters were considered, the improvement of the fatigue performance achieved with the EXTREME steel would be considerably higher.

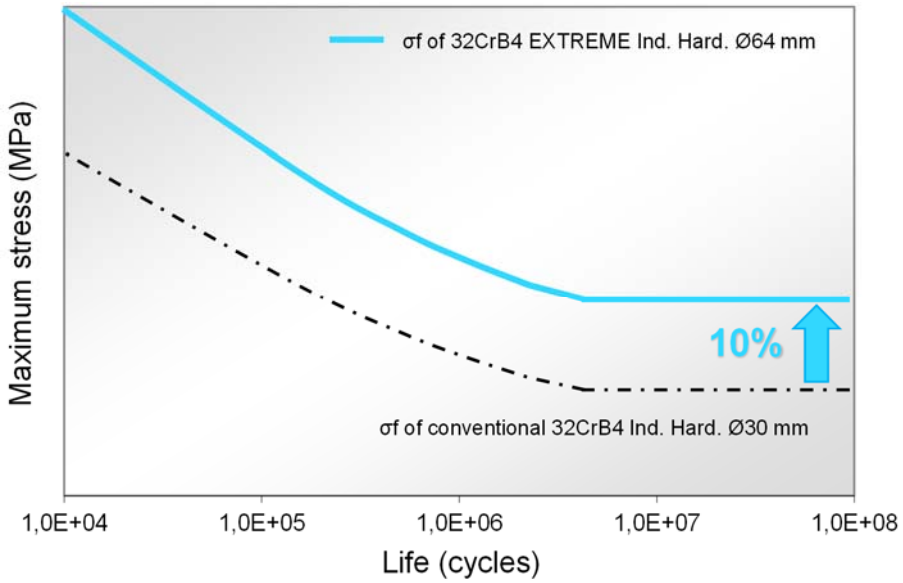

Figure 6. S-N curves for the 32CrB4 EXTREME and conventional induction hardened grades.

In summary, the EXTREME technology notably improves the steel fatigue performance and, consequently, the fasteners one. This will lead to a minimization of the risk of fatigue failures of these fasteners and will contribute to a safer operation of the wind tower.

– *Future work:* This extensive study of the EXTREME steels will be completed thanks to the participation of Sidenor in the SHOWTIME project, a European project developed in the frame of the RFCS (Research Fund for Coal and Steel) in which real connections, consisting in two pre-tensioned bolts (manufactured with EXTREME steels) connecting three steel plates, will be fatigue tested. In order to reproduce the in-service performance of these connections, besides non-corroded connections, two different corrosion levels will be considered.

  These fatigue tests, to be performed in the SHOWTIME project, will provide very valuable information regarding the in-service performance of the EXTREME steels.

CONCLUSIONS

The use of EXTREME steels leads to a safer in-service performance of the fasteners and reduces the maintenance needs:

– The very high toughness at -40 ºC reached with the induction hardened 32CrB4 EXTREME steel assures an excellent response in case of impact.

– The large improvement of the fatigue performance achieved with the EXTREME steels minimizes the risk of fatigue failure of the fasteners.

The EXTREME technology developed by Sidenor allows the use of low-alloyed steels in large fasteners in which, up to now, the required mechanical properties only could be reached using high-alloyed steels:

- For bolts (Q&T) the 32CrB4 EXTREME can be used up to Ø 56 mm when the conventional 32CrB4 can be only used up to Ø 36 mm.
- For studs (induction hardened) the 32CrB4 EXTREME can be used up to Ø 64 mm when the conventional 32CrB4 can be only used up to Ø 36 mm.

REFERENCES

[1] A. Lacroix and J. F. Manwell, "Wind Energy: Cold Weather Issues", PhD Thesis, Renewable Energy Research Laboratory, University of Massachussets at Amherst, 2000.
[2] ISO 898-1:2015, "Mechanical properties of fasteners made of carbon steel and alloy steel – Part 1: Bolts, screws and studs with specified property classes – Coarse thread and fine pitch thread", 2015.
[3] Y. Liu and T. Ishihara, "Fatigue failure accident of wind turbine tower in Taikoyama wind power plant". EWEA Conference. Paris (France), 2015.
[4] A. Rosborg Black, L. Rischel Hilbert and T. Mathiesen, "Corrosion protection of offshore wind foundations". NACE International Conference & Expo. Dallas (USA), 2015.
[5] H. van der Mijle Meijer, "Corrosion in offshore wind energy 'a major issue'", The offshore wind power conference "ESSENTIALS INNOVATIONS". Den Helder (The Netherlands), 2009.
[6] IPCC, "Report on mitigating climate change", 2012.
[7] ISO 377:2013, "Steel and steel products – Location and preparation of samples and test pieces for mechanical testing", 2013.
[8] ISO 6892-1:2016, "Metallic materials – Tensile testing – Part 1: Method of test at room temperature", 2016.
[9] ISO 148-1:2016, "Metallic materials – Charpy pendulum impact test – Part 1: Test method", 2016.
[10] ISO 12106:2013, "Metallic materials – Fatigue testing – Axial-strain-controlled method", 2013.

THE INTERNATIONAL CONFERENCE ON
WIND ENERGY HARVESTING 2017
20-21 April 2017
Coimbra, Portugal

Paper 307

FATIGUE LIFE ASSESSMENT OF A VERTICAL AXIS WIND TURBINE

Maria Pia Repettp[1]
Univ. of Genova
Genova, Italy

Luisa Pagnini[2]
Univ. of Genova
Genova, Italy

ABSTRACT

Starting from the experience gained in an experimental campaign over a vertical axis wind turbine, and availing of a numerical model of the structural details, this paper investigates possible critical conditions of wind induced fatigue, considering the operational conditions and the actual wind speed.
The wind turbine is located in the experimental facility of the Savona Harbor. Wind field is described using an advanced measuring network. Power production is recorded by the control system of the turbine. Structural response is acquired by servo-accelerometers and strain gages positioned on the supporting pole. After having identified the dynamic parameters of the system, the detailed numerical model of a limited portion of the structure allows to determine the suitable SN curve to be used in the fatigue life assessment.

INTRODUCTION

The study of wind actions and effects on wind turbines is usually carried out according to two different approaches. The former approach uses advanced computational models that integrate finite element analyses and Computational Fluid Dynamics. In this case, the analysis needs very advanced computer procedures. The latter approach recalls simplified models that can be found also in specific codes on wind turbines [1] and that apply only for horizontal axis technologies and in a limited number of simple situations. Wind tunnel assessments using scale models are very promising, but, at the current state of research, appears not fully mature from a technical viewpoint.

Small size wind turbines play a marginal role on the energy production and the economic return often does not pay back the use of very expensive and complicated calculations. Due to the small dimensions of the rotor and supporting structure, they are often designed using simplified procedures that do not reproduce the actual dynamic phenomena involved nor the turbulent action of the wind. As a matter of fact, their behavior is as much complex as the behavior of the large size turbines, and major shortcomings may affect both the power production and the structural safety. The structural response is very sensitive to turbulent and gusty wind; the variable wind speed mechanism may cause resonant conditions with the structural frequencies that cause frequent damage and may give rise to fatigue collapse both to the blades and to the supporting structure (Figure 1). Therefore, there is the need, from the one hand, to provide reliable characterizations of the power curve in the operating conditions and, from the other, to validate and improve analytical calculation models of structural response. Improvements on these aspects could make them more attractive for an extensive use in urban environment.

Starting from the experience gained in an experimental monitoring campaign over a vertical axis wind turbine located over the dam in the Savona Harbour (Northern Italy), the power production in this urban environment has been investigated, pointing out the detrimental effect of turbulence and gusty wind [2]. This paper carries out structural analysis and fatigue assessment considering the operational conditions of the turbine, availing of measures of the structural response and of the actual wind speed.

[1] Associate Professor, Department of Civil, Chemical and Environmental, University of Genova, Via Montallegro 1, Genova, Italy. E-mail: repetto@dicca.unige.it
[2] Assistant Professor, Department of Civil, Chemical and Environmental, University of Genova, Via Montallegro 1, Genova, Italy. E-mail: luisa.pagnini@unige.it

Figure 1. Fatigue damage to the steel supporting pole of a 20kW horizontal axis wind turbine

EXPERIMENTAL FACILITY AND MONITORING EQUIPMENT

The investigated wind turbine is a 20 kW H-rotor turbine, having 8 m diameter and 5.8 m height; it is provided with 5 aluminum, steel and fiberglass blades. The control system provides a regenerative braking; the rotor is slowed by a hydraulic and electrical brakes too. It is supported by a 10.5 m high steel pole, placed upon the dam, at 4.5 m above the ground. Figure 2 shows the location (upon the dam of the Savona Harbour) and the wind rose.

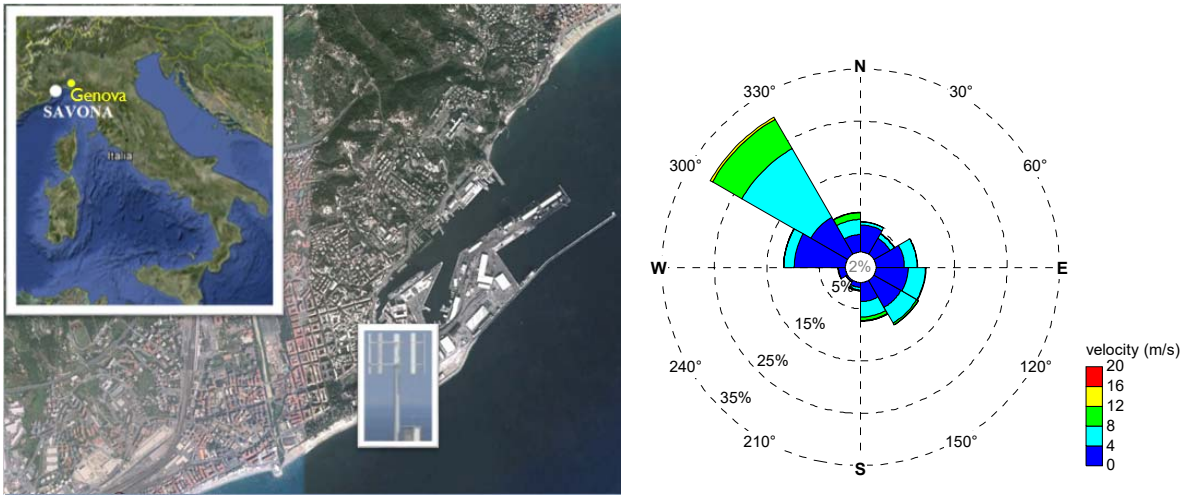

a) b)

Figure 2. Wind turbine location (a) and wind rose (b).

The monitoring system registers the wind field, power production and the rotating speed of the rotor; two couples of servo-accelerometers continuously record the structural response within an operating range of ± 2 g. Two sensors are positioned at the top of the steel pole acquiring the two horizontal acceleration components; two sensors are positioned at an intermediate level to acquire the motion amplitudes related to the second vibration mode. Two couples of uni-axial strain-gages are placed at two different levels of the pole, measuring the nominal strain in the lower part of the structure in both directions. Moreover, one tri-axial strain gage measures a control point in the part of the tower characterized by local structural details. Figure 3a, b shows the wind turbine and the position of the sensors. Major details are given in [3].

With the support of a finite element model and referring to the record in Figure 4 (turbine rotating at the rated power, rotational speed is 48 rpm), we can identify the frequency of the first vibration mode, which involves the sole oscillations of supporting pole, n_1=1.47 Hz. The vibration mode at n_2=2.53 Hz originates from the vertical oscillations of the horizontal beams that support the blades. The vibration mode at n_3=7.28 Hz originates from a torsional vibration mode of the structure. Damping ratio of the first vibration mode has been estimated as ξ_1=0.7%. Due to the aerodynamic dissipation of the rotating blades, damping ratio grows up to 1.5% at the rotating velocity 48 rpm. Straight lines in Figure 4 highlight the harmonic rotor loads that occur at multiple of the rotor speed according to the number of the blades; lines are labeled as 1P (one-per-revolution), 5P (five-per-revolution), 10P (ten-per-revolution). A number of further resonant frequencies are assignable to turbine components.

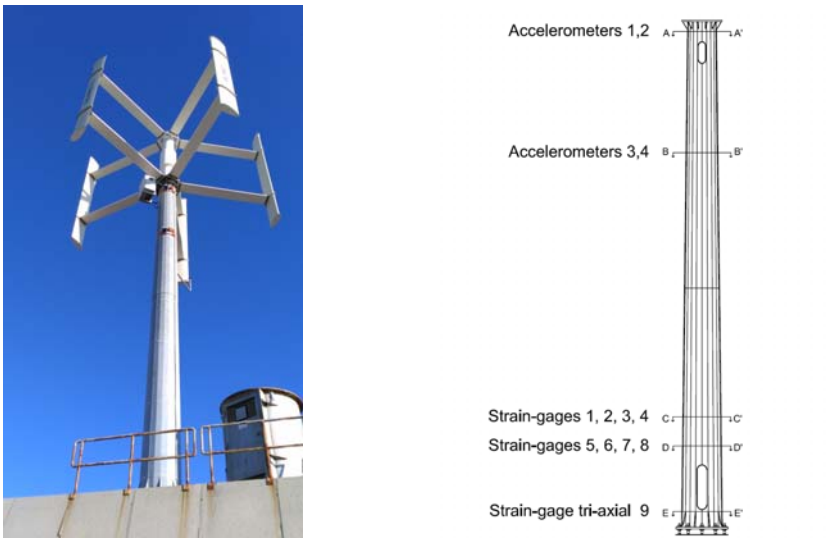

Figure 3. Monitored wind turbine (a) and tower scheme with positions of accelerometers and strain-gages (b).

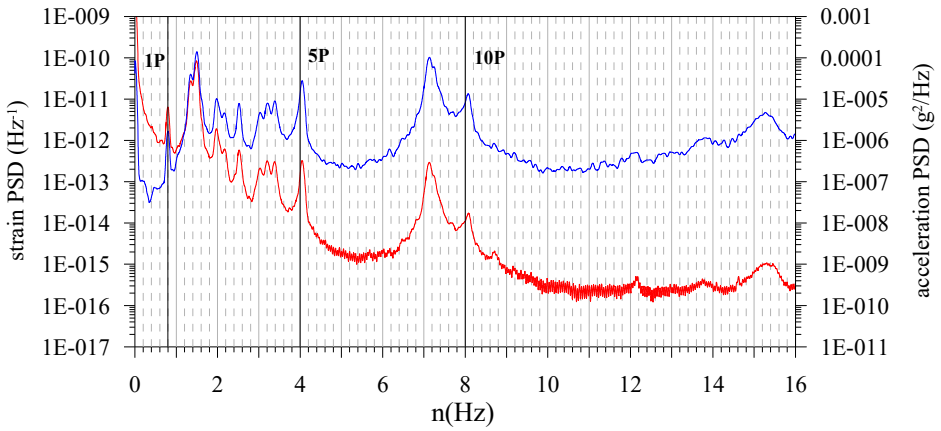

Figure 4. Power spectrum of the top acceleration and base strain of the turbine operating at the rated power.

FATIGUE ASSESMENT

Fatigue analysis requires, from one hand, the estimation of the stress time-histories due to the wind-induced dynamic response of the structure representatives of the loading conditions of the turbine during its structural life; from the other hand, the definition of the fatigue resistance of the critical points that can be potentially affected by fatigue damage. Both these aspects are very critical and can induce relevant uncertainties on the fatigue estimation [4]. The fatigue resistance based on nominal stress values using the classified S-N curves may yield to unrealistic estimation of the load effects when technical standards do not classify details to be compared with. Therefore, finite element solid models of the shaft are developed suitable to identify the critical parts subject to the phenomenon of fatigue and to define the S-N curve for the evaluation of fatigue resistance of the related details. Figure 5a shows the finite element model of the lower part of the supporting pole subjected to a wind loading that engages the fairlead openings, Figure 5b shows the base detail, highlighting possible critical stress levels around the openings, the base stiffener and the base joint. According to the Hot Spot procedure [5], the S-N curve is based on the evaluation of the geometric stress, inclusive of local effects due to the geometry of the joint, excluding the effects of the welding itself. Availing of the data recorded by the monitoring network, this approach will be carefully validated case by case, since the two stress fields, local and structural, are overlapped in real situations, making its definition and evaluation a very critical issue.

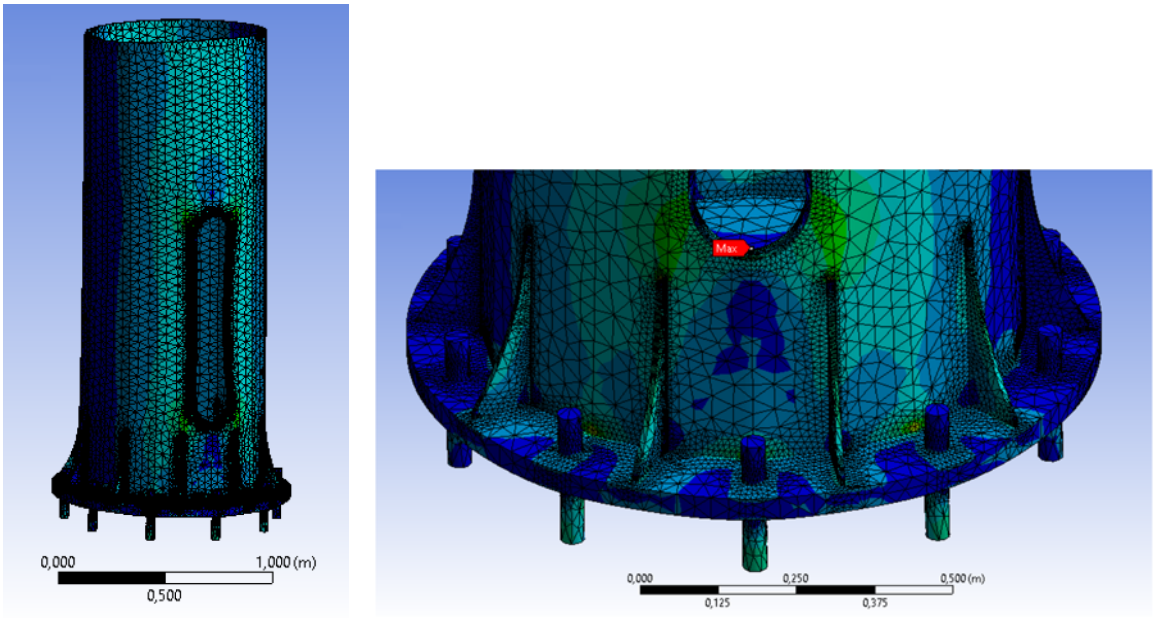

a) b)

Figure 5. Fem model of the lower part of the supporting pole (a) and of the base detail (b)

CONCLUDING REMARKS

This paper uses results from the experimental activity carried out over a vertical axis small wind turbine. Detailed information concerning the wind field are available; long term monitoring collects power production, rotating wind speed and structural response.

The study investigates the effect of the turbulent wind on the structural behavior, pointing out possible critical situations of fatigue. Availing of accurate finite element models of the structural details, and of the experimental measures of stress and strain, this paper outlines the procedure for the fatigue life assessment in these structural typology.

ACKNOWLEDGEMENTS

The authors acknowledge with thanks the support of the TU1304 COST Action “WINERCOST”

REFERENCES

[1] IEC 61400-12-1, “Wind turbines: Part 12.1 - Power performance measurements of electricity producing wind turbines”. International Electrotechnical Commission, Geneva, Switzerland, 2005.

[2] Pagnini, L.C., Burlando, M., Repetto, M.P., “Experimental power curve of small-size wind turbines in turbulent urban environment”, Applied Energy, 154, 2015, pp. 112-121.

[3] Pagnini, L.C., Repetto, M.P., Freda, A., Piccardo, G., Rosasco, M. (2016). “Structural monitoring of a small size vertical axis wind turbine”, IN-VENTO 2016, XIV Conference of the Italian Association for Wind Engineering, 25-28 September 2016, Terni, Italy

[4] Pagnini L.C., Repetto M.P. (2012) The role of parameter uncertainties in the damage prediction of the alongwind-induced fatigue. Journal of Wind Engineering and Industrial Aerodynamics, Elsevier, 104–106 (2012) 227–238

[5] International Institute of Welding, Recommendations for fatigue design of welding joints and components, IIW document XIII-1965-03/XV-1127-03, 2004

THE INTERNATIONAL CONFERENCE ON
WIND ENERGY HARVESTING 2017
20-21 April 2017
Coimbra, Portugal

Paper 308

FOUNDATION STIFFNESS AND DAMPING INFLUENCE ON DYNAMIC RESPONSE AND FATIGUE OF OFFSHORE SUPPORTING STRUCTURES

Mohammad Reza Shah Mohammadi[1]
ISISE, Department of Civil Engineering,
University of Coimbra, P-3004 516,
Coimbra, Portugal

Paul Thomasson[2]
Simis AS
Leonardvegen 3, 7790
Malm, Norway

Carlos Alberto Silva Rebelo[3]
ISISE, Department of Civil
Engineering, University of Coimbra,
P-3004 516,
Coimbra, Portugal

Luís Simões da Silva[4]
ISISE, Department of Civil
Engineering, University of Coimbra,
P-3004 516,
Coimbra, Portugal

Milan Veljković[5]
Faculty of Civil Engineering
and Geosciences, Delft
University of Technology,
Delft, Netherlands

ABSTRACT

The influence of foundation damping in soil geotech model for the offshore wind turbines is not well investigated. The offshore wind turbines are highly dynamically loaded and they operate in a narrow range of frequency close to the excitation frequency. Therefore, the foundation stiffness and damping is very important in order to have a reliable estimation of the dynamic behavior and cost effective design of the wind turbines.

However, there is several models such as static condensation methods, spatial reduction methods, cone models or lumped-parameter models, few of them have been developed in aeroelastic tools to consider the soil stiffness and damping in the simulations. In addition, design guidelines for offshore structures usually ignore any structural damping.

This paper is devoted to the development of simple geotech model in ASHES which is a servo-hydro-aeroelastic analysis software for the wind turbine simulation. In order to investigate the model and the significance of foundation damping, two monopile-supported and jacket offshore wind turbines were considered as the case studies. The offshore wind turbines were subjected to extreme wind and wave loading and were calculated using a linear elastic two-dimensional finite element model. The 5 MW reference wind turbine with monopile and jacket substructure were simulated in ASHES and the loads and dynamic response of the wind turbine supporting structure were obtained. The monopile and jacket structure were designed for 20 m mean sea level depth and deep sea application with 60 m height respectively. The mudline fore-aft moment was calculated for turbine shutdown and idling wind turbine. Furthermore, rain flow counting results estimate the fatigue life with and without considering the soil damping.

It is expected that the soil damping increases the lifetime of the supporting structure and also decreases the loads on the structure. Moreover, improved dynamic response of the supporting structure due to the foundation damping can be observed.

[1] PhD Candidate, ISISE, Department of Civil Engineering, University of Coimbra, P-3004 516, Coimbra, Portugal /mrsm@uc.pt
[2] PhD, Simis AS, Leonardvegen 3, 7790, Malm, Norway / paul.thomassen@simis.io
[3] Associate Professor, ISISE, Department of Civil Engineering, University of Coimbra, P-3004 516, Coimbra, Portugal /crebelo@dec.uc.pt
[4] Professor, ISISE, Department of Civil Engineering, University of Coimbra, P-3004 516, Coimbra, Portugal / luisss@dec.uc.pt
[5] Professor, Faculty of Civil Engineering and Geosciences, Delft University of Technology, Stevinweg 1, NL-2628 CN Delft, The Netherlands / M.Veljkovic@tudelft.nl

NOMENCLATURE

OWT	=	Offshore wind turbine
NREL	=	National Renewable Energy Laboratory
k	=	Stiffness coefficient
c	=	Damping coefficient (Ns/m)
z	=	Local angle of attack (rad)
G_0	=	Initial Shear Modulus (MPa)
S_u	=	Undrained shear strength (kPa)
v	=	Poisson ratio

INTRODUCTION

Offshore wind energy has two main impediments, economics and deep waters. The offshore farms can provide more renewable energy than onshore parks due to higher and more consistent wind speeds. However, the cost of design, maintenance, operation, installation, and the material is much more than the onshore parks [1]. The monopile with 80% of the market is the most common supporting structure for the average water depth of 27 m. As more deep waters are pursued, jacket structures as alternatives are getting more attractive in the market [2], [3].

The wave loads govern the design for the monopile structures in deeper water, therefore, the soil and structural stiffness and the damping play a sensitive role in the design. The foundation and supporting structure has almost 20% of the overall cost of the offshore wind turbine. Therefore, considering the soil and material damping in the design as they might lead to less estimated loads and consequently less material for the same life time, is crucial.

There is different source of damping in the wind turbine analysis including aerodynamic damping, hydrodynamic damping, soil and structural damping. Furthermore, the tuned mass dampers are often installed under the generator in the nacelle. Aerodynamic damping happens when the tower top is in a motion. As it moves fore and aft, the relative wind speed changes which leads to less total tower top excursion [4], [5]. Nevertheless, other source of damping platy more significant roles on the design of the structure. The International Electromechanical Commission stated that the soil damping modelling is the most complex parameter to investigate[6] and Germanischer Lloyd noted the uncertainty of the soil damping contribution to the wind turbine damping[7].

There is two radiation damping and the material damping which the first one comes from geometric dissipation of the waves and the second one is to hysteretic material. The radiation damping effect is negligible due to low loads frequencies (<1 Hz)[5], [8]. Several researchers have used the experimental data from wind turbine special events like emergency shutdown or overspeed stops to estimate the OWT natural frequency. Moreover, they concluded that 0.25 to 1.5% of the overall damping relates to the foundation damping[5], [9], [10].

Previous analytical and numerical methods have estimated the foundation damping using Rayleigh damping function, loading and unloading p-y curves and two dimensional finite element model which included the added hydrodynamic mass, Rayleigh structural damping and foundation damping[5], [11], [12]. In this paper, foundation damping is introduced for all bottom-fixed offshore foundations and other types of damping is neglected as the influence of the foundation damping was the main interest.

The primary objective of this study is to determine the influence of OWT foundation damping and stiffness on lifetime and dynamic response. Section 2 describes the methodology and how the damping is implemented in the ASHES software[13], Section 3 describes the monopile, jacket structures and the design load cases, and Section 4 describes the fatigue and dynamic response for case studies and the influence of the foundation damping is determined.

METHODOLOGY

The p-y model with linear springs and dampers is used in ASHES to model the stiffness and the damping of the foundation. For every node along a pile (monopile of jacket leg pile) two horizontal springs - normal to each other - and two horizontal dampers - normal to each other - are applied. At the bottom node a vertical spring is applied. This means that the stiffness coefficient k and the damping coefficient c are needed to be calculated or known from experiments. Figure 1 shows a pile with the springs and dampers configuration.

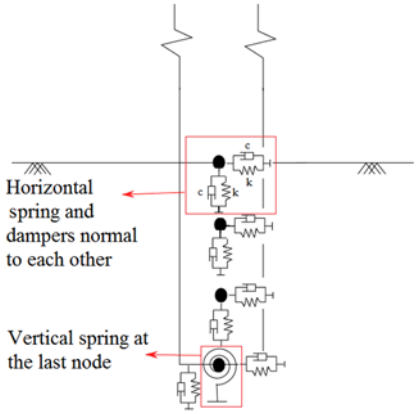

Figure 1: Pile-Soil springs and dampers model

Furthermore, 10 minutes time domain simulation should be performed to study the effect of the stiffness and the damping of the foundation. Then, the rainflow counting method and miner rule are applied to calculate the number of cycles and supporting structures lifetime respectively.

MODEL DESCRIPTION

The NREL 5 MW reference wind turbine is used for the analysis[14], supported by two monopile and jacket structures for 20 and 50 m of water depth.(Table 1)

Table 1: The tower and the supporting structures properties

Property	Value
Hub Height	90 m
Rotor Diameter	126 m
Diameter of Tower Base, Top	6, 3.87 m
Thickness of Tower Base, Top	0.035, 0.025 m
Tower Mass	348 t
Monopile Supporting Structure	
Pile Diameter, Wall thickness	6, 0.07 m
Pile Embedment Depth	34 m
Tower Natural Frequency	0.3 Hz
Jacket Supporting Structure	
Column Diameter, Thickness	0.92, 0.032 m
Max., Min. Brace Diameter	0.57, 0.36 m
Max., Min. Brace Thickness	0.018, 0.014 m
Base, Top Circumcircle Diameter	30, 8 m
Jacket Mass	900t

The ASHES software uses a combination of rigid and flexible bodies to perform time domain analysis for the wind turbine. Moreover, it is able to model the offshore foundation as fixed or flexible with and without damping. However, it does not consider the material nonlinearity as the computational costs greatly increase due to complexity. In this paper, ASHES is used to model both case studies under 50-year extreme wind and wave loading and Normal shutdown using feathering. Table 2 shows the environmental site condition for the simulation.

Table 2: The site condition for monopile and jacket supporting structure

Conditions	Value
Water Depth	20, 50 m
10-min Average Hub Height Wind Speeds	25, 34 m/s
Significant Wave Height	8.5 m
Peak spectral Wave period	10.3 s

The wind and wave loads were consider directionally applied on the structure. Figure 2 shows the jacket model for 50 m of water depth with directionally applied wind and wave regimes.

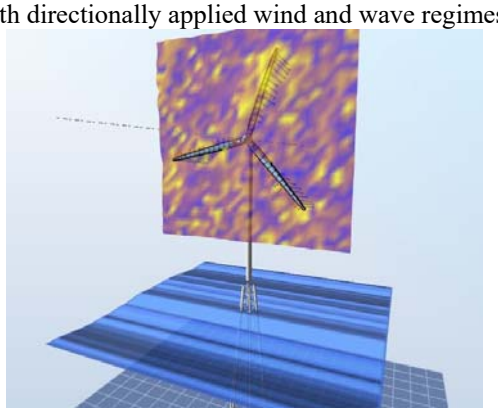

Figure 2: The jacket model under wave and wind loading in ASHES

The three layer soil profile is used in this paper which has different shear modulus, undrained shear resistance, and the Poisson's ratio as Table 3.[8]

Table 3: Site's Soil Properties

$z\,(m)$	$G_0\,(MPa)$	$s_u\,(kPa)$	ν
0-14	20	33	0.498
14-24	100	125	0.490
24-28	600	500	0.470

RESULTS

Figure 3Figure 2 shows the bending moment for the monopile structure with simple fixed flexible ground. As it can be seen, the moment for the flexible mudline with lower stiffness has higher moment. In addition based on rain flow counting method and using amplitude of the moments the number of cycles are calculated and illustrated in Figure 4. The model with lower soil stiffness has more cycles and therefore less lifetime than the higher stifness model.

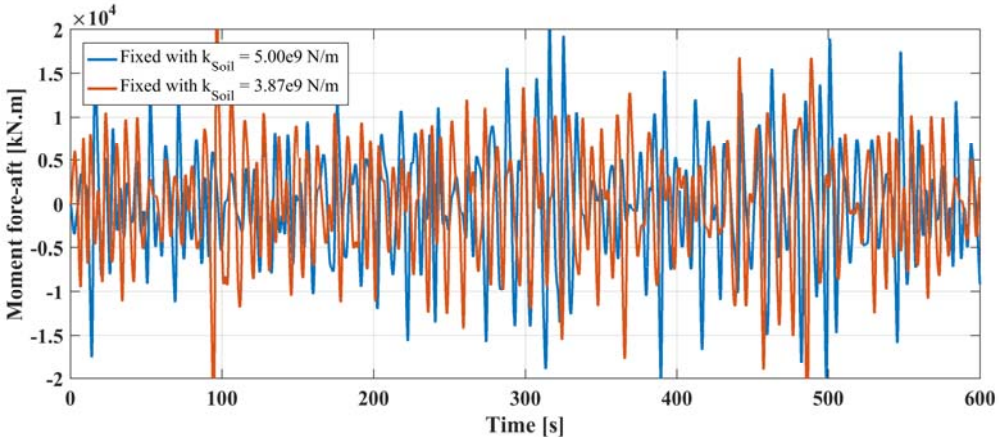

Figure 3: Moment at mudline for a parked turbine under loading

It is expected that the damping model has even more effect in the mudline moment reduction which leads to higher lifetime. Consequently, less material can be used for the same lifetime which means lower cost.

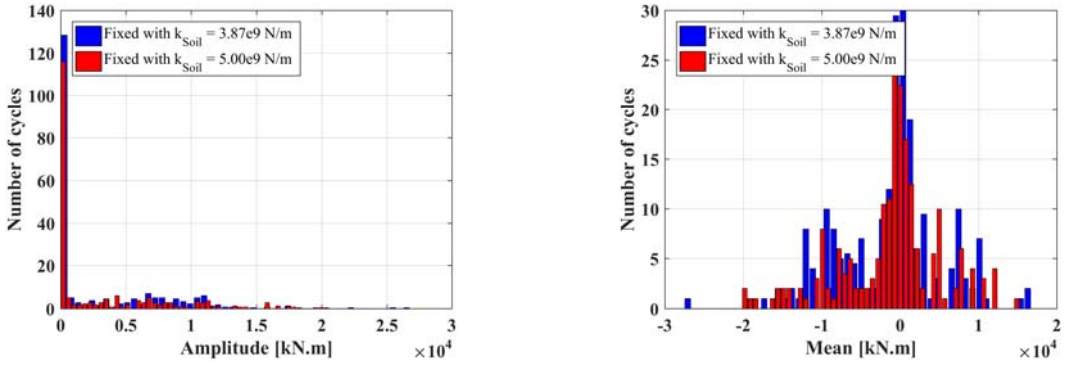

(a) (b)

Figure 4: Number of cycles versus (a) Amplitude and (b) mean value for mudline moment

CONCLUSIONS

The main purpose of this paper was to investigate the effect of mudline foundation stiffness and damping in aeroelastic time history analysis and fatigue life time. Offshore wind turbines (OWTs) are typically designed and analyzed using aeroelastic programs which can efficiently analyze OWT response to stochastic wind and wave loads in the time domain. Because time history analysis is computationally demanding, OWTs are typically modeled with linear material properties and reduced-order foundations. The simplest and most common reduced-order foundation for aeroelastic programs is the mudline stiffness matrix, which condenses soil-structure interaction to a single node. Currently there are no methods recommended by design guidelines for calculating the contribution of foundation damping to OWTs. In this paper, a simplified approach was implemented in ASHES software to the mudline stiffness matrix and damping associated with the NREL 5MW Reference Turbine [14] supported by a 6 m-diameter monopile embedded in 34 m of clay and a jacket supporting structure for 50 m deep water. The mudline stiffness and damping for the NREL 5MW was taken from [8]. The aeroelastic tool ASHES [13] was used for stochastic OWT time history analysis of IEC design load case 6.1a, considering two different supporting structures and various mudline condition including soil stiffness and damping. Mean mudline shear and moment from the fixed mudline ASHES results were used to determine the fatigue lift time and the dynamic responses. Significant influence of damping and stiffness is expected in the simulation and optimized design of the supporting structures.

ACKNOWLEDGEMENTS

The first author acknowledges with thanks the support of the support from European Union's research and innovation program H2020-MSCA-ITN-2014 under grant agreement No 643167 (AEOLUS4FUTURE) is kindly acknowledge.

REFERENCES

[1] W. Musial and B. Ram, “Large-Scale Offshore Wind Power in the United States,” no. NREL/TP-500-40745, 2010.

[2] M. Seidel, “Substructures for offshore wind turbines Current trends and developments,” 2014.

[3] European Wind Energy Association (EWEA), “The European offshore wind industry key 2015 trends and statistics,” 2015.

[4] D. J. C. Salzmann and J. Van der Tempel, “Aerodynamic Damping in the Design of Support Structures for Offshore Wind Turbines,” in *Proc Copenhagen Offshore Conf, Copenhagen*, 2005, p. 9.

[5] W. Carswell *et al.*, “Foundation damping and the dynamics of offshore wind turbine monopiles,” *Renew. Energy*, vol. 80, pp. 724–736, 2015.

[6] International Electrotechnical Committee, “IEC 61400-3. Wind turbines - Part 3: Design requirements for offshore wind turbines,” Brussles, 2009.

[7] Germanischer Lloyd WindEnergie, “Overall damping for piled offshore support structures, guideline for the certification of offshore wind turbines,” 2005.

[8] W. Carswell, J. Johansson, F. Løvholt, S. R. Arwade, and D. J. DeGroot, “Dynamic mudline damping for offshore wind turbine monopiles,” in *Proceeding of the ASME 2014 33rd International Conference on Ocean, Offshore and Arctic Engineering (OMAE2014)*, 2014, pp. 1–8.

[9] M. Damgaard, V. Zania, L. V. Andersen, and L. B. Ibsen, “Effects of soil-structure interaction on real time dynamic response of offshore wind turbines on monopiles,” *Eng. Struct.*, vol. 75, pp. 388–401, 2014.

[10] R. Shirzadeh, C. Devriendt, M. A. Bidakhvidi, and P. Guillaume, "Experimental and computational damping estimation of an offshore wind turbine on a monopile foundation," *J. Wind Eng. Ind. Aerodyn.*, vol. 120, pp. 96–106, 2013.

[11] M. Damgaard, J. K. F. Anderson, L. B. Ibsen, and L. V. Anderson, "Time-Varying Dynamic Properties of Offshore Wind Turbines Evaluated by Modal Testing: Des propriétés dynamiques d'éoliennes offshore dépendant du temps évalué par des tests," in *Proceedings of the 18th International Conference on Soil Mechanics and Geotechnical Engineering*, 2013, pp. 2343–2346.

[12] N. Tarp-Johansen and L. Andersen, "Comparing sources of damping of cross-wind motion," *Eur. Offshore*, 2009.

[13] P. E. Thomassen, P. I. Bruheim, L. Suja, and L. Frøyd, "A Novel Tool for FEM Analysis of Offshore Wind Turbines With Innovative Visualization Techniques," in *Proceedings of the Twenty-second (2012) International Offshore and Polar Engineering Conference*, 2012, vol. 4, pp. 374–379.

[14] J. Jonkman, S. Butterfield, W. Musial, and G. Scott, "Definition of a 5-MW Reference Wind Turbine for Offshore System Development," 2009.

THE INTERNATIONAL CONFERENCE ON
WIND ENERGY HARVESTING 2017
20-21 April 2017
Coimbra, Portugal

Paper 309

MAGNETO-MECHANICAL SIZING OF MAGNETIC GEAR LAMINATED POLE PIECES FOR WIND TURBINE APPLICATIONS

Melaine Desvaux[1]
SATIE Laboratory, ENS Rennes
Université Bretagne Loire, CNRS
35170 Bruz, France

Bernard Multon[2]
SATIE Laboratory, ENS Rennes
Université Bretagne Loire, CNRS
35170 Bruz, France

Hamid Ben Ahmed[3]
SATIE Laboratory, ENS Rennes
Université Bretagne Loire, CNRS
35170 Bruz, France

Stéphane Sire[4]
Université de Bretagne Occidentale
FRE CNRS 3744, IRDL
29238 Brest, France

ABSTRACT

This article deals with the magneto-mechanical sizing of magnetic gear pole pieces for wind turbine applications. Magnetic gears are subjected to be integrated in a wind turbine conversion chain. However, magnetic gear pole pieces seem to have weaknesses in terms of mechanical strength. To ensure the mechanical strength, we propose a definition of a support bar geometry which does not lessen magnetic properties and which correctly maintain the laminated pole pieces. An example is made with this support bar design and with this sizing methodology for a 3.9MW magnetic gear for wind turbine conversion chain.

INTRODUCTION

Mechanical gearboxes, currently used in indirect drive electro mechanical conversion chain (Fig.1a), provide a lower capital expenditure and a lower masses than the direct drive conversion chain [1] (Fig.1b). In return, mechanical gearboxes induce production interruptions and repairs, which increase operating costs [2]. In this context, an interesting solution is to develop a conversion chain with a semi-fast generator and a magnetic gear [3] (with non-contact power transmission) (fig.1c). The most attractive topology of magnetic gears has been proposed by Martin [4] and was the subject of different behaviour studies proposed by Atallah [5].

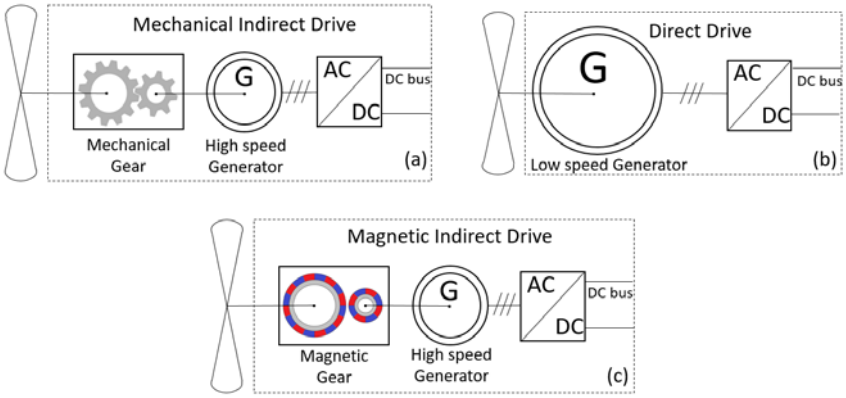

Figure 1. Wind power conversion chains which contain (a) mechanical indirect drive, (b) direct drive, and (c) magnetic indirect drive

1 PhD Student, Dpt. Mechatronics, ENS Rennes, 35170 Bruz, France /melaine.desvaux@ens-rennes.fr
2 Professor, Dpt. Mechatronics, ENS Rennes, 35170 Bruz, France /bernard.multon@ens-rennes.fr
3 Doctor, Dpt. Mechatronics, ENS Rennes, 35170 Bruz, France /hamid.benahmed@ens-rennes.fr
4 Doctor, Dpt. Mechanical, Univ. Bretagne Occidentale, 29238 Brest, France /stephane.sire@univ-brest.fr

This magnetic gear shown in Fig.2 includes an internal ring of permanent magnets, an external ring of permanent magnets and a ring of ferromagnetic laminated pole pieces between the permanent magnets rings. This topology potentially offers high performance with an high torque density and an high reliability than mechanical gearboxes [6] and even more for high torque application like high power wind turbine (of the order of a few MN.m and a few MW) with only magnetic part consideration [7]. However, no magneto-mechanical sizing has been done on this magnetic gear (with an approach similar than [8] for a wind turbine generator) and it seems to have weaknesses in terms of mechanical strength which are subjected to radial and tangential loads from the magnetic field. Indeed, ferromagnetic pole pieces are very elongated structures, laminated perpendicular to the axis of rotation (to minimize iron losses and conserve a high efficiency of the system) and then subjected to magneto-mechanical loads. The weaknesses of the poles pieces raises the question of the possibility to maintain mechanically this laminated pole pieces without lessening the magnetic properties (therefore without increasing air gaps and modifying magnetic field) in high power wind turbine applications (i.e high dimensions of the magnetic gear). This is shown in Fig 3 which represents a part of the magnetic gear developed in a wind turbine context [3].

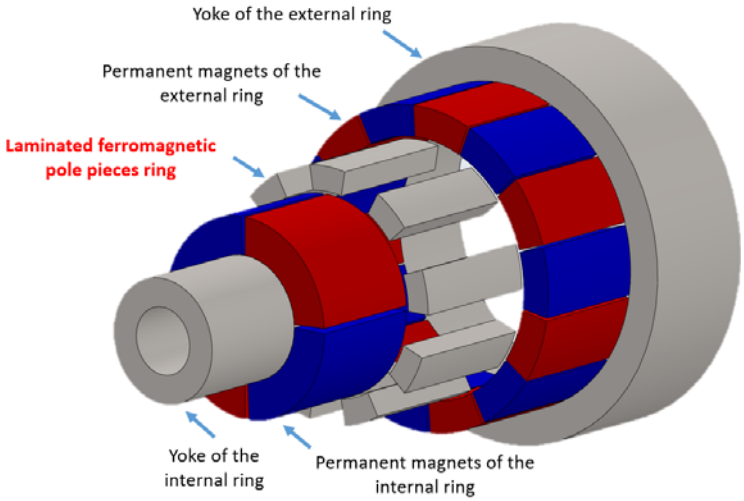

Figure 2. Magnetic gear architecture in an exploded drawing with low pole numbers (in this example: p_{int} = 2, p_{ext} = 7 and Q = 9).

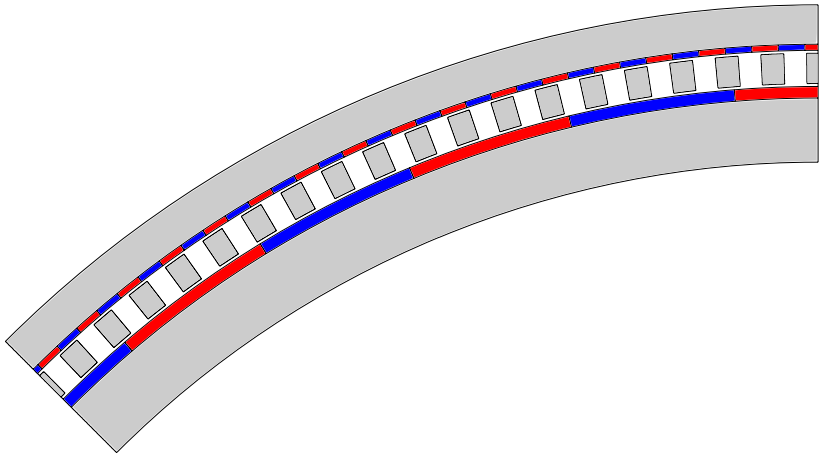

Figure 3. Dimension of the magnetic part of the 3.9 MW 15 rpm magnetic gear with p_{int} = 20, p_{ext} = 131 and Q = 151, an external diameter of 3.8 m and a length of 2 m.

The major contribution of this work is a global static analysis of the variable radial and tangential loads supported by the laminated pole pieces. This static analysis includes the definition of the geometry of dedicated bars which support the pole pieces without lessening magnetic properties.

SUPPORT BAR GEOMETRY OF THE LAMINATED FERROMAGNETIC POLE PIECES

The magnetic gear topology is composed of three rings:

- An internal ring with p_{int} pole pairs of permanent magnets and a ferromagnetic yoke,
- An external ring with p_{ext} pole pairs of permanent magnets and a ferromagnetic yoke,
- A ring with Q ferromagnetic laminated poles between both permanent magnets ring (an example is given in Fig. 2 with low pole numbers, to improve readability: p_{int} = 2, p_{ext} = 7 and Q = 9).

Each permanent magnets rings generates in air gaps a wave of magnetomotive force. Ring with ferromagnetic pole pieces aims to modulate the magnetic field in the two air gaps to obtain common harmonics. The result is a magneto-mechanical torque with an average different from zero and a transmission of power with a synchronism between fundamental magnetic field frequencies in both air gap. To achieve this power transmission, three rings pole numbers must respect equation (1). Then, it is possible to define the ratio λ (2) and the Willis relation for a magnetic gear (3) like a planetary gear where $\omega_{int/0}$, $\omega_{ext/0}$ and $\omega_{Q/0}$ are the speed rotation of the internal ring, the external ring and the pole pieces ring respectively. In function of the fixed ring, the gear ratio G_m is given by (4). For high power applications (for instance wind turbine), the number of pole increases with the diameter. A consequence can be a decrease of their rigidity.

$$p_{int} + p_{ext} = Q \tag{1}$$

$$\lambda = \frac{\omega_{int/0} - \omega_{Q/0}}{\omega_{ext/0} - \omega_{Q/0}} = -\frac{p_{ext}}{p_{int}} \tag{2}$$

$$\omega_{int/0} - \lambda.\omega_{ext/0} + (\lambda - 1).\omega_{Q/0} = 0 \tag{3}$$

$$\begin{cases} \omega_{int/0} = 0 \rightarrow G_m = \dfrac{\omega_{ext/0}}{\omega_{Q/0}} = \dfrac{(\lambda - 1)}{\lambda} \\ \omega_{Q/0} = 0 \rightarrow G_m = \dfrac{\omega_{int/0}}{\omega_{ext/0}} = \lambda \\ \omega_{ext/0} = 0 \rightarrow G_m = \dfrac{\omega_{int/0}}{\omega_{Q/0}} = -(\lambda - 1) \end{cases} \tag{4}$$

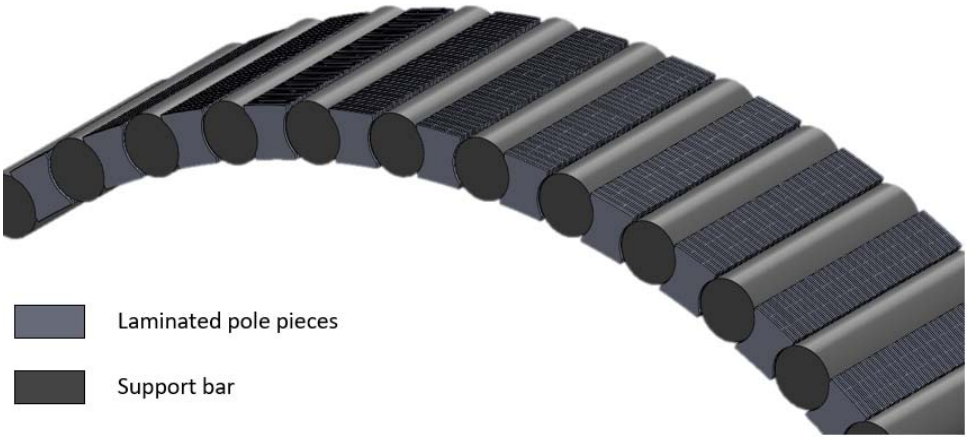

Figure 4. Presentation of the geometry of the supporting bars

To support the laminated pole pieces of the magnetic gear, the support bar geometry shown in Fig.4 is proposed. The support bar is composed of a massive magnetic insulator steel and a magnetic and electrical insulator skin. These support bars do not lessen the magnetic properties; they also do not modify the magnetic field and air gaps. Support bar will then transmit to the structural parts the magneto-mechanical load of the laminated pole

pieces. Support bars are thus subjected to variable radial and tangential magneto-mechanic pole pieces loads; their induced stresses must be then taken into account for their sizing (see [9]). Considering a 1D model of the support bar with fixed ends, it is possible to determine a first approximation of deformations and stresses of the support bars depending on the static magneto-mechanical load. To determine the support bar displacement, it is necessary to evaluate preliminary the radial and tangential pole pieces loads (shown in Fig. 5 for the magnetic gear [3]). The model (hypothesis and constraints) will be presented in the final paper. This paper will also present the sizing example with the 3.9MW magnetic gear [3] for wind turbine conversion chain (dimensions are given in appendix).

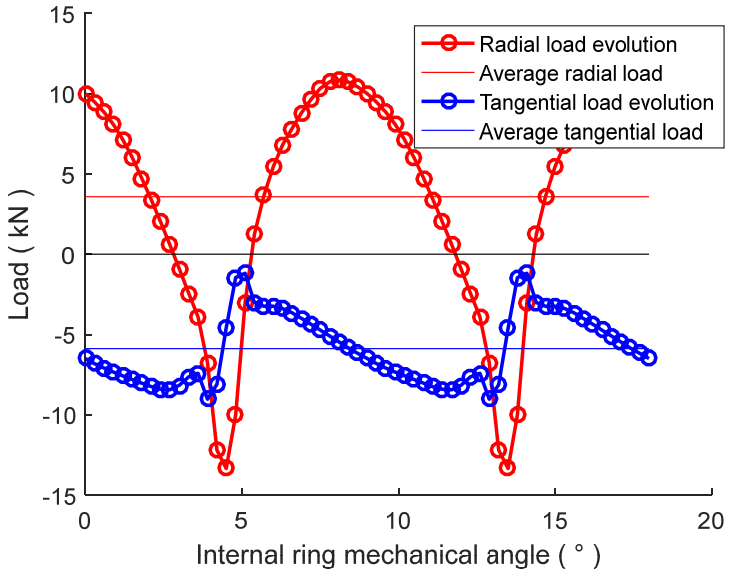

Figure 5. Evolution of the static magneto mechanical radial and the tangential load of laminated pole pieces

CONCLUSIONS

The study is underway. Our first results show that this simplified model is able to evaluate displacements and stresses of the supporting bars. For the 3.9W magnetic gear case study, it is possible to maintain mechanically the laminated pole pieces with air gaps variations lower than 5%.

APPENDIX

Table 1. Wind turbine conversion chain dimension

Symbol	Quantity	Value
P_{rated}	Rated power of wind turbine	3.9 MW
N_{rated}	Rated speed of wind turbine	15 rpm
T_{rated}	Rated torque of the wind turbine	2.5 MNm
T_{Gmax}	Maximal gear torque of the first stage of magnetic gear	2.7 MNm
D	External diameter of the magnetic part of the two stage magnetic gear	4 m
δ_{int}	Internal airgap of the magnetic gear	5 mm
δ_{ext}	External airgap of the magnetic gear	5 mm
G_m	Gear ratio	6.5

REFERENCES

[1] R. Lacal Arántegui and J. Serrano Gonzáles, *2014 JRC wind status report: Technology, market and economic aspects of wind energy in Europe*. 2015.

[2] J. Keller, Y. Guo, and L. Sethuraman, "Gearbox Reliability Collaborative Investigation of Gearbox Motion and High-Speed-Shaft Loads," *NREL, Tech. Rep. TP-5000-65321*, 2016.

[3] M. Desvaux, R. L. G. Latimier, B. Multon, H. Ben Ahmed, and S. Sire, "Design and optimization of magnetic gears with arrangement and mechanical constraints for wind turbine applications," in *2016 11th International Conference on Ecological Vehicles and Renewable Energies, EVER 2016*, 2016.

[4] T. B. Martin, "Magnetic transmission," *Pat. US3378710*, 1968.

[5] K. Atallah and D. Howe, "A novel high-performance magnetic gear," *IEEE Trans. Magn.*, vol. 37, no. 4, pp. 2844–2846, 2001.

[6] E. Gouda, S. Mezani, L. Baghli, and A. Rezzoug, "Comparative study between mechanical and magnetic planetary gears," *IEEE Trans. Magn.*, vol. 47, no. 2, pp. 439–450, 2011.

[7] D. Matt, J. Jac, and N. Ziegler, "Design of a Mean Power Wind Conversion Chain with a Magnetic Speed Multiplier," in *Chap. 10 of InTech book "Advances in Wind Power*, 2012, pp. 247–266.

[8] A. Zavvos, A. S. Mcdonald, and M. Mueller, "Structural optimisation tools for iron cored permanent magnet generators for large direct drive wind turbines," in *IET Conference on Renewable Power Generation (RPG 2011)*, 2011.

[9] A. S. McDonald, M. A. Mueller, and H. Polinder, "Structural mass in direct-drive permanent magnet electrical generators," *IET Renewable Power Generation*. 2008.

THE INTERNATIONAL CONFERENCE ON
WIND ENERGY HARVESTING 2017
20-21 April 2017
Coimbra, Portugal

Paper 310

SHOWTIME: STEEL HYBRID ONSHORE WIND TOWERS INSTALLED WITH MINIMAL EFFORT – DEVELOPMENT OF LIFTING PROCESS

Carl Richter [1]
RWTH Aachen University
Aachen, Germany

Mohammad Reza Shah Mohammadi [2]
ISISE, Department of Civil Engineering,
University of Coimbra, P-3004 516
Coimbra, Portugal

Daniel Pak [3]
University of Siegen
Siegen, Germany

Carlos Rebelo [4]
E, Department of Civil Engineering,
niversity of Coimbra, P-3004 516
Coimbra, Portugal

Markus Feldmann[5]
RWTH Aachen University
Aachen, Germany

ABSTRACT

In recent years, wind energy becomes more competitive with fossil fuels and lots of researches have been done to develop alternatives for supporting structures, controllers and new concepts. In this paper, the focus is the use of a state-of-the-art technology for lifting a very high (over 180 m) hybrid wind turbines. The lower part is the lattice part and the upper part is the tubular part. The connection of these two is the transition piece, which has to be designed very mindful. In this work, the lifting process and the calculation of the loads and different steps for designing the lifting process and the transition piece are presented.

NOMENCLATURE

TP	=	Transition piece
D	=	Drag force (N)
r	=	Radius of the rotor (m)
α	=	Local angle of attack (rad)
ρ	=	Density of air (kg/m^3)

INTRODUCTION

In recent years, wind energy becomes more competitive with fossil fuels and lots of researches have been done to develop alternatives for supporting structures, controllers and new concepts. The offshore wind energy is more economic than onshore, however, it cannot be a solution in many countries. Moreover, several onshore wind turbines already have been installed since the 1980's or even before. Therefore, European countries have been started repowering the onshore wind farms since 2002 [1]. For repowering new wind turbines with higher power capacity are needed. These turbines have to be installed in higher altitudes or in places with high wind velocities.

1 Scientific researcher, Institute of Steel Construction, RWTH Aachen University, Mies-van-der-Rohe-Str. 1, 52074 Aachen, c.richter@stb.rwth-aachen.de
2 PhD Candidate, ISISE, Department of Civil Engineering, University of Coimbra, P-3004 516, Coimbra, Portugal/ mrsm@uc.pt
3 Professor, Institute of Steel Construction, University of Siegen, Paul-Bonatz-Str. 9-11, 57076 Siegen, pak@bau.uni-siegen.de
4 Professor, ISISE, Department of Civil Engineering, University of Coimbra, P-3004 516, Coimbra, Portugal / crebelo@dec.uc.pt
5 Professor, Institute of Steel Construction, RWTH Aachen University, Mies-van-der-Rohe-Str. 1, 52074 Aachen, stahlbau @stb.rwth-aachen.de

Since increasing the height of the tower needs higher and heavier cranes and lifting accessories, the cost of a single turbine via cranes increases. The cost of using cranes is compared with two other ideas, introduced in the following, in Figure 1.

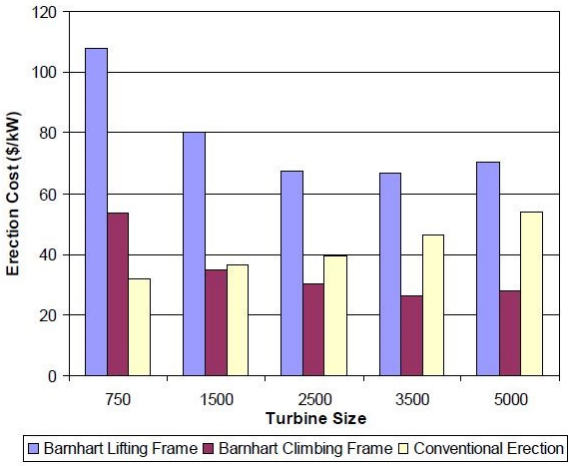

Figure 1: Cost analysis of erecting options for different turbine sizes[7]

Nevertheless, previous self-erection mechanism design, load and cost analysis has documented in industrial and academic reports and patents. An extensive research was done by NREL on several self-erecting concepts in 2001 [2]. Several industries already started to develop a self-erecting concepts mentioned in the NREL report since 1981. The German's Growian wind turbine was constructed and pulled-up the tower with winch. The WTS-3 a large Swedish wind turbine was erected with pair of lifting columns besides the tower and the blade and the nacelle were assembled separately. The Aeolus II used a set of tracks into the tower and nacelle to utilize the lifting process. The Wind Eagle was assembled on the ground and tilted up [3].

More research has been done by T&T engineering as an expert in the drilling and the oil industries. They recommended four concepts using their experiences which might be applicable in the field of wind energy. The concepts can be summarized as, Tilted-Up Method with Self-Supporting Frame, Jack-Up with Offshore Platform Towers for Lifting, Slip-Form Approach, and Telescoping Tower [2].

Barnhart Crane & Lifting is an active company in heavy lifting and transport sector. As they have expertise in lifting, their lifting frame for the chimneys can be adaptable for the wind turbine towers, however, the 5MW wind turbine tower is much heavier than a chimney. Lifting frame has a tower which is mounted to chimney's straddle. The chimney is lifted up with trunnions and raised with a set of strand jacks.

Moreover, they developed methods to erect the wind turbine towers specifically. They proposed several methods which can be listed as, A Slip Form for Non-Tapered Towers, Climbing Frame with The Boom and Mast, Climbing Frame with Boom, Mast, and Counterweight, and Climbing Frame with Lifting Tower and Strand Jacks.

Ederer proposed a new self-erecting mechanism with telescopic lifting tower. Moreover, they used two telescopic tower in the opposite sides of the tower to tilt it up. However, they stopped developing their mechanism further evaluation due to some changes in their company.

In this paper, the installations problem of the high rise wind turbine is addressed. In order to ensure reliability for land-based wind farms, new lifting process for a hybrid supporting structure is designed. The hybrid concept consists of a lattice structure and a tubular part which are connected by a transition piece. The lattice structure was utilized to be a support for a new lifting process. Moreover, the design of the transition piece varies according to the specifications for each project including loading conditions, connections, material properties and the lifting process especially in this research.

METHODOLOGY

There are some common design assumptions which should be taken into account for designing the lifting process and the transition piece. Design assumptions are important for the outcome assessment. Furthermore, possible further discussion highly depends on the initial and boundary conditions of the analysis.

The common assumptions relate to geometry and topology of the supporting structure and the aeroelastic simulation and inertia loads in transition piece level. Therefore, the following tower properties are chosen:

- 5MW NREL reference wind turbine
- 6-legged lattice structure

- Polygon cold-form cross section of legs
- Height of Lattice part 120m
- Height of Tubular Part 65 meters (slightly larger than the blade used in calculations 63 meters)
- Lattice height to spread ration of 4/1 without secondary bracings
- Constant diameter for tubular part with 4.3 m

The structural weight of the burden, the number and location of pivots used for the heave, the angle between each sling and the vertical axis on pivot and the environmental conditions under which the lift is performed characterise the lifting loads. Therefore, every single lifting should be planned individually with considering hazards and the risks. Moreover, all members and connections of a lifted component must be designed corresponding the static equilibrium of the lifted weight and the sling tensions.
Based on DNV-Os-H102, there are different permanent, variable functional, deformation, environmental, and accidental load categories. They are used for different limit state analysis of the lifting process. **Error! Reference source not found.** shows the factor approach for the lifting load calculation based on API standard. Several dynamic amplification, skew effect, centroid shift and others should be considered and multiply to the calculated weight to find out the design loads. On the other hand, the numerical method can be applied to calculate and estimate the lifting loads.

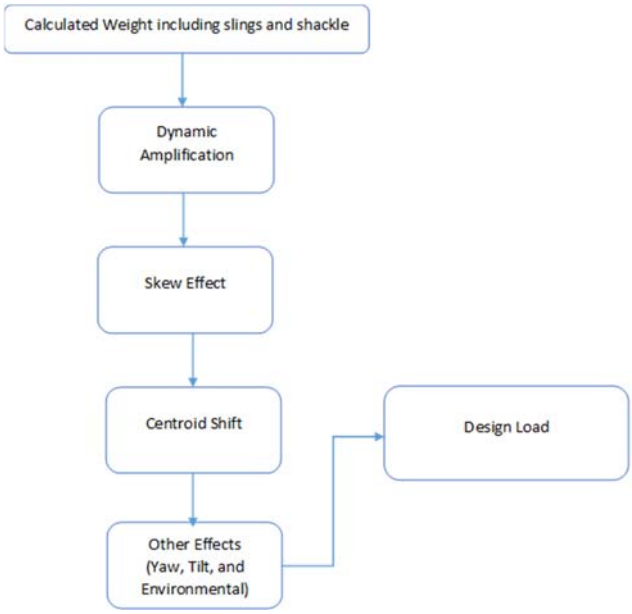

Figure 2: Factor approach for lifting load calculation

The two lifting loads were calculated for two stages of the new lifting process. The first stage is the lifting of the whole tubular tower, then, lifting of the tubular tower with assembled RNA.

RESULTS

The building steps for the new lifting process is as follows based on existing mechanism [4]: the 120 m high lattice tower is separated into six units. First of all unit one of the lattice is mounted and fixed to the foundation by means of a mobile crane. Besides the final construction side, unit-six of the lattice structure is set up and the transition piece is fixed to this last unit, cf. Figure 3 (a). Afterwards, the other sections of the lattice part are assembled one above the other next to the real construction site, cf. Figure 3 (b). A bottom plate for the tubular tower has to be positioned in the middle of the lattice tower. Probably there has to be a foundation arranged beneath the tubular erection place. Then the tubular tower can be temporarily attached to the foundation to provide an overturning during its mounting. The lower segment of the tubular tower is transported to the construction side and is lifted inside the first lattice unit. It is fixed to the bottom plate and a flange is welded to the tubular segment in a certain distance to the bottom plate, cf. Figure 3 (c). Then the second lattice unit is lifted by mobile crane and is mounted to the first unit, see Figure 3 (d). Alternating lattice and tubular segments are lifted and fixed until unit-three of lattice and the third and last part of tubular are on its position, Figure 3 (e)-(g). Unit-four and after that unit-five are mounted to the lattice tower. Before the sixth unit is lifted, the strand jacks and strand guidance are installed to the transition piece, Figure 3 (h). After the last unit is connected to the lattice tower, the strands are arranged to the

strand jacks and guidance and led down to the ground. The strands are connected to the bottom plate. A strand carrousel is established on the ground into the inner hexagon of the lattice to wind up the strands while they are led down, cf. Figure 4.

Depending on the chosen connection type for the tubular segments, there are different possible connections to the mobile crane. If the tubular segments are connected with flange connections the mobile crane can lift them by means of the pre-cut bolt holes and a lifting tool used for the assembly of tubular steel towers

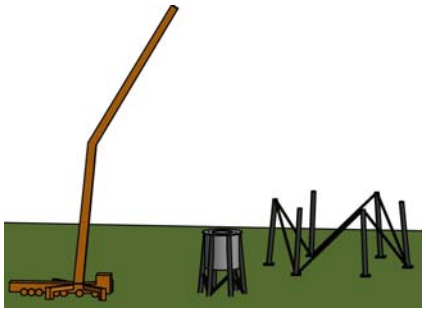

(a)

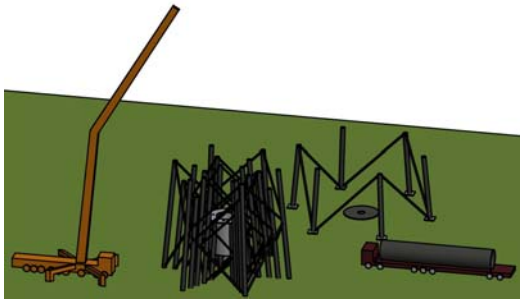

(b)

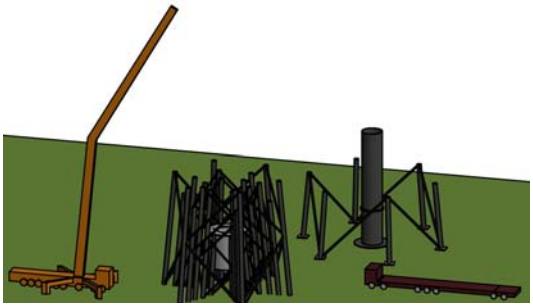

(c)

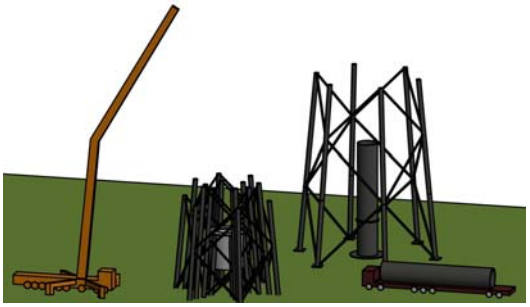

(d)

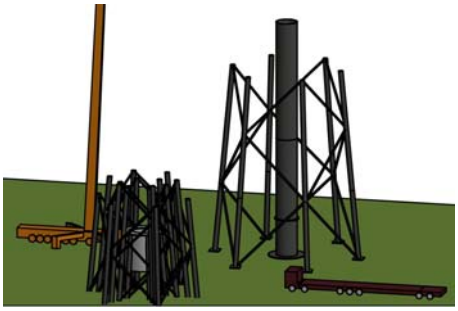

(e)

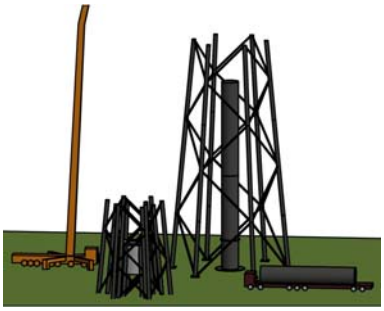

(f)

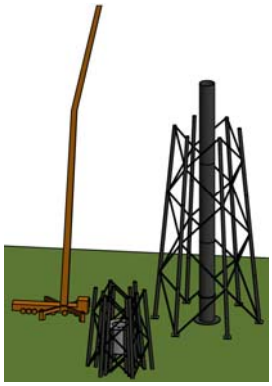

(g)

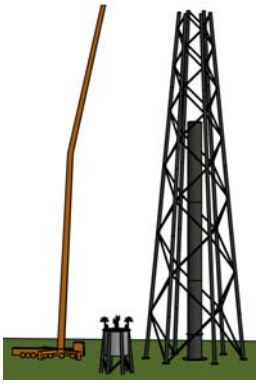

(h)

Figure 3: Alternating erection process

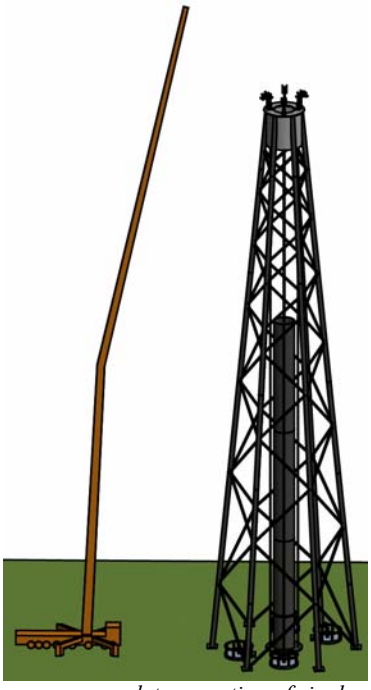

Figure 4: Alternating erection process: complete mounting of single parts and installation of strands

The building steps will be completed with the RNA assembly steps.

CONCLUSIONS

The alternating erection of tubular and lattice part is chosen because it leads to lower loads applied to the transition piece and following smaller dimensions and material costs. For the inserting erection procedure, lots of problems had shown up which are not solved completely. Furthermore, the alternating erection is based on a state of the art technique and is according to the feasibility of the procedure. Therefore, a foundation for the tubular part during assembly has to be arranged. The above-mentioned horizontal support during the lifting process is necessary and has to be chosen and designed further. For the erection and lifting process a large mobile crane, strand jacks, strand guidance and strand carrousels are needed. This erection process outlines also requirements for the transition piece.

At the top of the transition piece a support area for the strand jacks is necessary. In this support area holes has to be arranged beneath the strand jacks. In the inside of the transition piece has to be enough free space for the strands. The top plate has to be large enough to carry the strand guidance also. The transition piece serves also as connection element to the lattice tower.

In conclusion, the new installation process shows promising results so far for the lifting of the tubular tower through the transition piece with the support of the lattice structure. The proposing concept will be fully developed, however, it showed a feasibility from construction and load analysis point of view.

ACKNOWLEDGEMENTS

This article is based on the work within the European research project SHOWTIME “STEEL HYBRID ONSHORE WIND TOWERS INSTALLED WITH MINIMAL EFFORT” in close cooperation of University of Coimbra, Luleå University of Technology; Institute of Steel Construction; University of Birmingham, RWTH Aachen University, Sidenor, Martifer and Friedberg GmbH. This project is funded by the European Commission through the research Fund for Coal and Steel (RFCS) under Grant Agreement No. RFCR-CT-2015-00021 which

is gratefully acknowledged. Sincere thanks are given to the EU, particularly to the RFCS and to the research partners (academic and from industry) for their good cooperation.

REFERENCES

[1] Baniotopoulos, C. C. et al. 2015. Trends and Challenges for Wind Energy Harvesting. Coimbra.
[7] A. Laxson, "WindPACT Turbine Design Scaling Studies Technical Area 3-Self-Erecting Tower and Nacelle Feasibility", National Renewable Energy Laboratory (NREL), March 2001
[8] J. Carter, "Free-Yaw, Free-Pitch Wind-Driven Electric Generator Apparatus", U.S. Patent No. 5,178,518 (January 1993)
[2] Dr. Peter Schäfer, Donges SteelTec GmbH, "The Donges Steel Hybrid Tower for high hub heights" Presentation at SHOWTIME meeting

THE INTERNATIONAL CONFERENCE ON
WIND ENERGY HARVESTING 2017
20-21 April 2017
Coimbra, Portugal

Paper 311

STANDARDIZED STEEL JACKET – FROM OFFSHORE TO ONSHORE

Susanne Höhler[1]
Salzgitter Mannesmann Forschung GmbH
Duisburg, Germany

Hossein Karbasian[2]
Salzgitter Mannesmann Forschung GmbH
Duisburg, Germany

Georg Michels[3]
Salzgitter Mannesmann Renewables
Gladbeck, Germany

ABSTRACT

With the increasing demand to use wind energy new challenges are set to wind energy plants, offshore and onshore. Having to deliver more output, wind energy turbines need to be of greater sizes, have greater hub heights and –in case of offshore turbines- in greater water depths. This sets clear tasks for the structural design of the tower and its foundation. Conventional monopiles are successively substituted by jacket structures, which still have many challenges to face in terms of manufacture and assembly.
Economic jacket solutions take into account material and weight reduction, limiting production and installation costs by still guaranteeing integrity performance for high loads. Targeting this, a modern jacket structure for offshore wind energy towers has been developed that is suitable for serial standardized production. The octagonal jacket structure of tubular legs and braces has then, in a second step, been modified and re-designed for onshore application. This paper presents both layouts and their characteristic features.

INTRODUCTION

Wind energy will play a decisive role in the turnaround of energy supplies for years to come. In Europe the main share in the market (approx. 85 %) is held by offshore wind farms. By 2020, more than 5,000 wind turbines are planned in the North Sea and the Baltic Sea alone. One of the special challenges in such projects is the construction of offshore foundations. Up to now, monopiles hold the largest market share by far. This will very probably change over the next few years. Especially at greater water depths, innovative and economically viable solutions are needed that can withstand the harsh offshore conditions and the loads involved as turbine outputs rise to 10 MW and rotor diameters to 200 m.

For the foundation of offshore wind turbines lattice towers have increasingly been used. These jacket structures have become the state of the art besides tripods and monopiles. A jacket is a truss tower which in general is assembled by legs and braces from circular hollow sections. The connections are welded nodes in different configurations, e.g. X-node or K node. The top of the jacket consists of a transition piece to allow the connection with the turbine tower. Designing a jacket various aspects must be considered, such as material costs and material availability, manufacture, transport and installation, as well as structural integrity and durability over its lifetime. In order to achieve a competitive solution one approach is to use series-produced standard steel products and components, since serial production generates significant cost savings, as can be seen for example in the automotive industry.

The following report presents a jacket design concept which is based on standard components and which shall be suitable for serial production. The concept targets offshore wind energy foundation. Subsequently, since

1 Expert Structural Integrity, Salzgitter Mannesmann Forschung GmbH, Ehinger Str. 200, 47259 Duisburg, Germany, s.hoehler@du.szmf.de
2 Expert Structural Integrity, Salzgitter Mannesmann Forschung GmbH, Ehinger Str. 200, 47259 Duisburg, Germany, h.karbasian@du.szmf.de
3 Director Salzgitter Mannesmann Renewables, Beisenstrasse 53, 45964 Gladbeck, Germany, michels.g@salzgitter-ag.de

the demand for higher performance and increased hub heights also becomes relevant for onshore application and jackets therefore are an alternative to monopiles also onshore, the concept is redesigned for an onshore jacket as well.

DESIGN FOR STANDARDIZED JACKET STRUCTURE - OFFSHORE

Following the idea of a standardized jacket production Salzgitter Mannesmann Forschung (SZMF) has developed a jacket design for offshore wind turbines. While the general jacket layout was developed at SZMF, the detailed design calculations were carried out by SKI Ingenieurgesellschaft mbH, Hannover, Germany. Some basic design assumptions are made:

Basic Design Assumptions

- The jacket is planned for a fictive reference position in the offshore-field "Alpha Ventus" in the German North Sea. Accordingly, wind data and wave data are defined as well as water levels. The water depth with reference to the lowest astronomical tide (LAT) results to 28 m.
- Lifetime of the jacket and wind tower is 20 years.
- A 5 MW wind turbine is considered of type NREL. Technical data is taken from [1], providing speeds and weights, and a hub height of +90.4 mLAT.
- Design Standards and regulations are mainly EN 1990 and EN 1991 for load actions and load combinations, EN 1993 for steel structures, NORSOK Standard N-00 and common DNV Guidelines.

General Layout

The jacket outline is octagonal, comprising eight tubular legs stiffened by four horizontal levels of braces also tubular, see **Fig. 1**. The upper section of the jacket structure is connected with a tubular tower. Due to torsional stiffness and fatigue requirements the layout is revised and additional diagonal stiffeners are inserted. The diagonal tubes are installed in every other jacket section in a helical arrangement around the structure from the top to the bottom level. **Fig. 2** displays the revised design along with characteristic features.

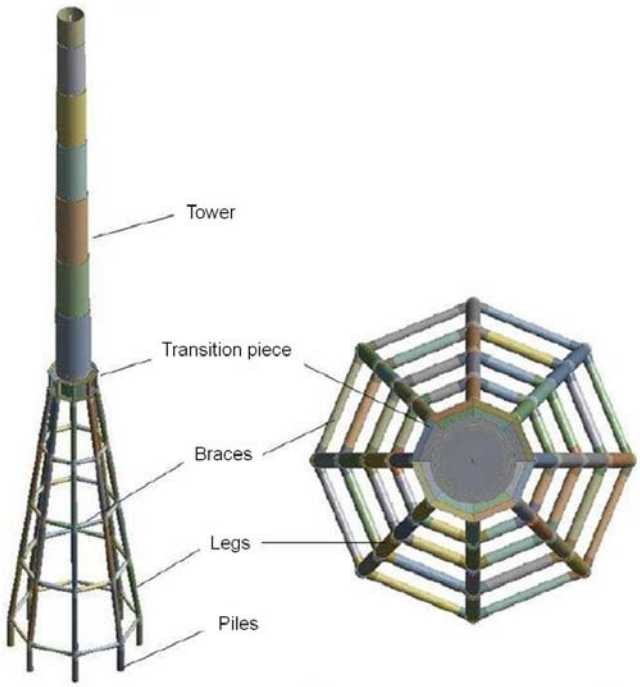

Figure 1 First outline of octagonal offshore jacket with tubular legs and braces

The advantages of this jacket design are that, at first, standardized semi-finished products can be applied. Tubes have uniform dimensions and only a small variety of tube dimensions must be made available. High reproducibility and close tolerances can be guaranteed. The welding of joints, which is a main cost driver for the assembly, can be realized automated, especially since only a limited number of diagonal braces and connections exist. The design concept has been filed for patent and published in a laying open application [2].

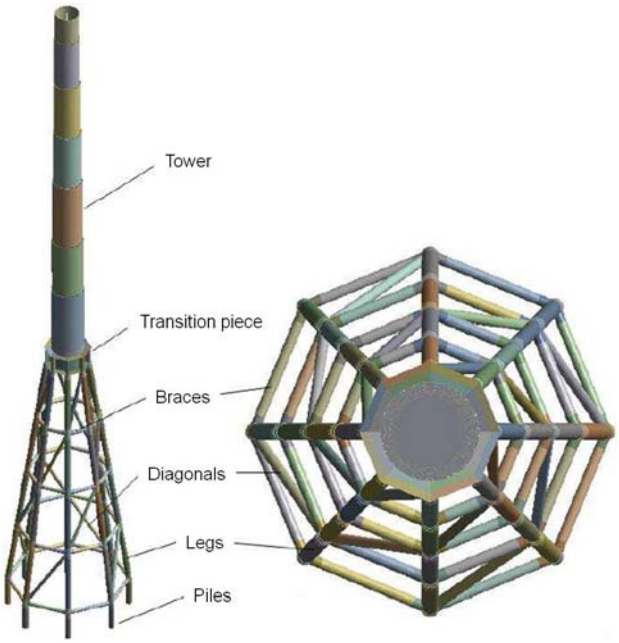

Turbine capacity	2 – 6 MW
Tower head mass	150 – 350 t
Hub height	up to 140 m
Turbine capacity	2 – 6 MW
Jacket height	variable
Steel tube length	variable
Legs – Ø tubes	700 – 1000mm
Braces – Ø tubes	500 – 700mm
Jacket weight	up to 250 t
Steel grade	S355 (variable)

Figure 2 Final outline of the octagonal offshore jacket and features

FROM OFFSHORE TO ONSHORE JACKET

Next to coastal areas also average mountain areas are predestined for wind farms. Despite the significant contribution of onshore wind energy to a sustainable energy mix, its potential is far from being exhausted. All scenarios of future energy supplies forecast a continued expansion of onshore energy capacities. This makes it clear that, for some time to come, wind may be the driving force as an energy source in the turnaround to sustainable energy production. In the further development of onshore wind power plants with greater heights and higher turbine outputs, onshore jacket solutions become an alternative compared to conventional monopiles. Substitution of monopiles of steel or concrete will entail advantages concerning weight and transport costs, manufacture and installation.

Starting from the offshore jacket as shown in Fig. 2, this concept is redesigned for an onshore wind tower. Evidently the load actions are revised for onshore jackets, leading to a much more slender structure with significant mass reduction. Other aspects for the redesign are transport and assembly possibilities for the components. The jacket must be very “easy” to install, therefore a modular system of segments is envisaged. The segments themselves have limit sizes for transport reasons. Their connection via cables or slim rods is considered to avoid field welding and weight.

The final paper presents an onshore jacket design that is based on the offshore layout described above. It is designed for a 2 – 3 MW turbine for an onshore reference position.

CONCLUSIONS AND OUTLOOK

A design concept of a jacket structure for a wind turbine for offshore application has been presented. The octagonal layout has eight tubular legs and horizontal tube braces stiffened by diagonal braces. The solution developed fulfills the demand of possible standardized serial production. Following this approach the structural design has been re-evaluated and modified for onshore application, fitted to onshore scenarios. Thus, two promising concepts are available for offshore and onshore wind turbines.

Future work is focused on the standardized serial fabrication of welded hollow section nodes for offshore and onshore jackets. It requires the application of innovative technologies, such as automated welding via high performance welding processes, intelligent weld preparation and non destructive testing methods. The challenges are the fabrication of the very complex geometries (K-nodes, X-nodes) and the verification of dimensional accuracy. The potential cost reduction by using prefabricated components is estimated as 18% in comparison to the conventional state of the art.

ACKNOWLEDGEMENTS

The offshore jacket design was carried out with contribution of SKI Ingenieurgesellschaft mbH, Hannover, Germany. All project work has been performed in collaboration with Salzgitter Mannesmann Renewables, Gladbeck, Germany.

REFERENCES

[1] Jonkman, J. et al, "Definition of a 5-MW Reference Wind Turbine for Offshore System Development", Technical Report, NREL/TP-500-38060, Nat. Renewable Energy Lab., USA, 2009

[2] Karbasian, H. et al: "Tragstruktur eines Bauwerks, insbesondere Offshore-Windenergieanlage und Verfahren zur Herstellung einer solchen Tragstruktur", Patent DE 10 2013 009 024 A1 2014.12.11

THE INTERNATIONAL CONFERENCE ON
WIND ENERGY HARVESTING 2017
20-21 April 2017
Coimbra, Portugal

Paper 312

NUMERICAL STUDY OF VIBRATIONS IN A STEEL BUILDING INDUCED BY ROOF MOUNTED SMALL SCALE HAWT

Nina Gluhović[1]
Teaching assistant
Belgrade, Serbia

Milan Spremić[2]
Assistant Professor
Belgrade, Serbia

Marko Pavlović[3]
Assistant Professor
Delft, Netherlands

Zlatko Marković[4]
Professor
Belgrade, Serbia

ABSTRACT

One of the most important acceptance issues regarding implementation of the small-scale wind turbines in urban environments is related to the people's quality of life. Human perception of vibrations is very sensitive and therefore turbine induced vibrations can have big influence on the implementation of urban wind harvesting by small-scale turbines at the top of buildings. The aim of this work is to investigate increase of vibrations in a steel building after installation of small-scale turbine at the roof. Comparison is made between floor vibrations influenced by wind action on the building only and together with the roof mounted turbine. Five storey steel building with regular shape is analysed with horizontal axis wind turbine (HAWT) on top with rotor diameter of 5 m. Turbulent wind profile is generated and used in time-history analysis of the building. Results of the analysis in terms of accelerations are compared to the requirements in relevant design codes.

INTRODUCTION

Demands for higher energy efficiency and use of renewable energy resources are constantly increasing. Harvesting of wind energy as a renewable energy resource tends to installation of small-scale wind turbines in urban environments. Installation of small-scale wind turbines in urban regions can gain higher energy efficiency, considering that energy production takes place at the place of its consumption.

Implementation of wind turbines in urban environments has often been compromised by public resistance. Some of the most important issues regarding implementation of wind turbines in urban environments are related to the noise pollution and increased vibrations in buildings. Due to the lack of open free areas in urban regions, installation of wind turbines at buildings is the most possible solution. In case of installation of small-scale wind turbines on existing facilities the increase of floor vibrations can compromise their installation. Human perception of floor vibrations and uncompromised serviceability of equipment in buildings are the two most important acceptability criteria considering increased floor vibrations. Human response to floor motion is very complex phenomenon and it is often related to the combination of factors such as: magnitude of motion, the surrounding environment and the type of human activity which takes place at that moment.

Analysis of relative increase of floor vibrations in a steel building after installation of a small-scale wind turbine on the building's roof is presented in this paper. Five storey steel building with steel-concrete composite floor deck structure is analysed with and without 5 m rotor diameter HAWT considering turbulent wind profile with mean flow speed of 7 m/s. Also, possible increase of floor vibrations is compared with current design requirements for floor vibrations, given in ISO 10137:2007 [4].

[1] Teaching assistant - PhD student, Faculty of Civil Engineering - Department of Material and Structures, University of Belgrade, Bulevar kralja Aleksandra 73, Belgrade, Serbia/ nina@imk.grf.bg.ac.rs
[2] Assistant Professor, Faculty of Civil Engineering - Department of Material and Structures, University of Belgrade, Bulevar kralja Aleksandra 73, Belgrade, Serbia / spremic@grf.bg.ac.rs
[3] Assistant Professor, Faculty of Civil Engineering and Geoscience – Structural Engineering, Delft University of Technology, Stevinweg 1,2600 GA Delft, The Netherlands / m.pavlovic@tudelft.nl
[4] Professor, Faculty of Civil Engineering - Department of Material and Structures, University of Belgrade, Bulevar kralja Aleksandra 73, Belgrade, Serbia /zlatko@grf.bg.ac.rs

METHODOLOGY

The time-history response of the building to the dynamic load excitation by the wind action is analysed in Sofistik FE software. Dimensions of the building's base are 24x40 m and the height of the building is 18 m, as shown in Figure 1. Steel-concrete decks are composed by 330 mm high steel I beams connected by shear connectors to the 160 mm thick concrete deck. Horizontal stability of the building in longitudinal and transversal direction is achieved by moment resisting frames and vertical bracing, respectively, as shown in Figure 1. Design of the case study building is performed according to requirements given in EN1994:2004 [1] and EN1993:2005 [2] in order to provide a real case design and mass vs. stiffness properties of the structure.

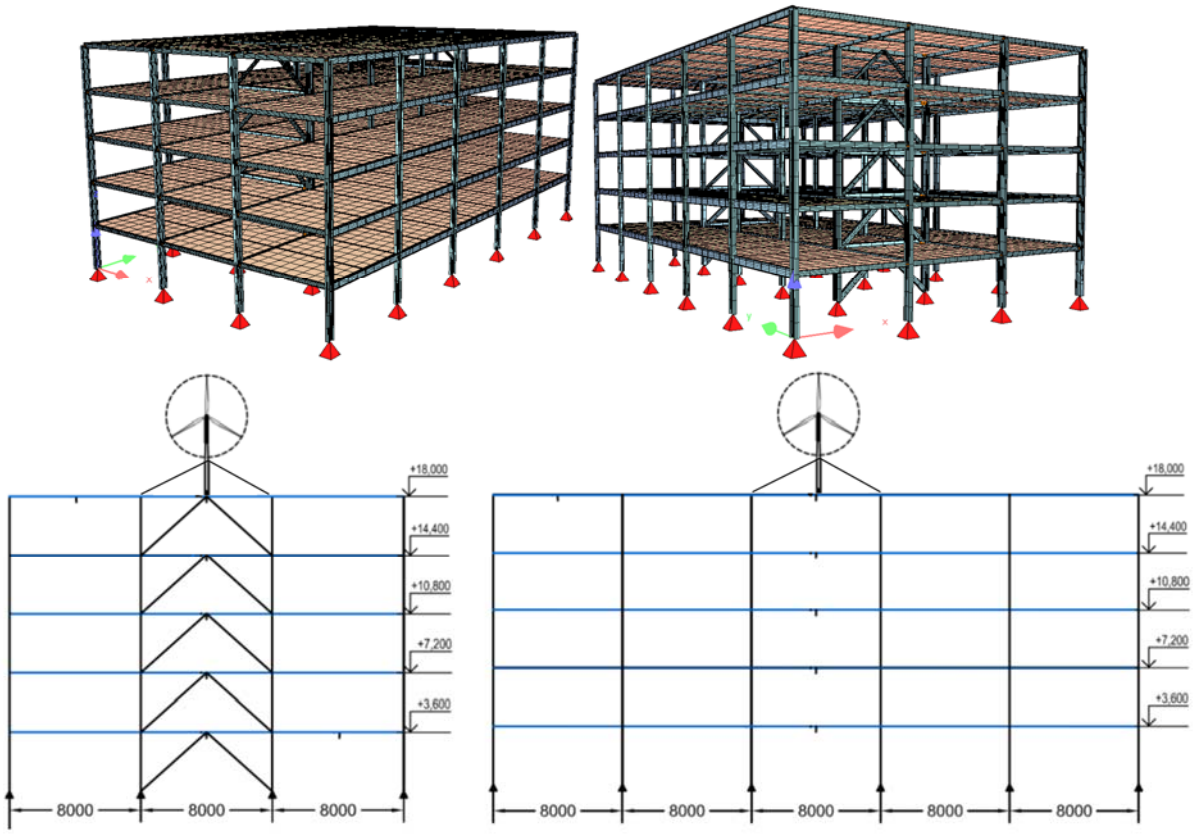

Figure 1. Dimensions of steel building and arrangement of constructive elements

Turbulent wind profile and aerodynamic loads analysis of the turbine is done in a multi-body analysis software package Ashes, see Figure 2. Ashes software integrates finite element analysis (FEA) and blade element momentum (BEM) theory.

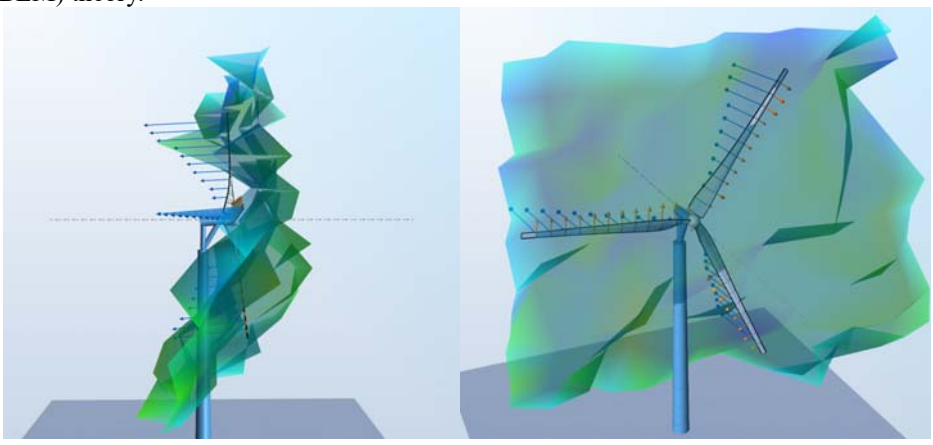

Figure 2. Model of the turbine and the tower in Ashes software.

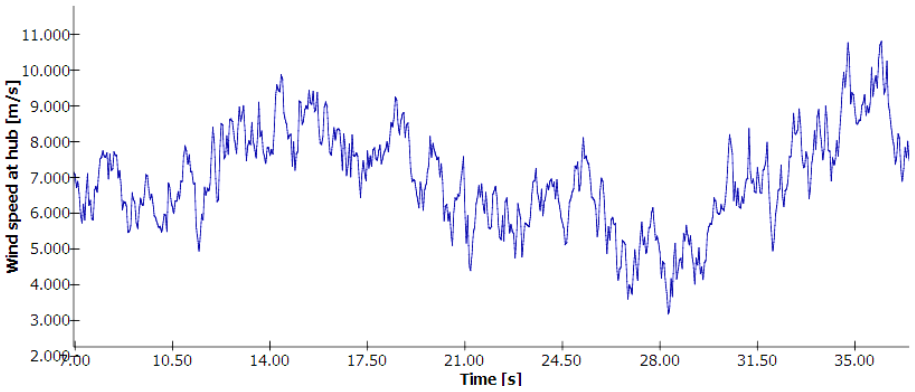

Figure 3. Turbulent wind time history loading generated by TurboSim in Ashes software.

The wind action on the building in two orthogonal directions shown in Figure 1 is applied as a time-history loading of uniform wind pressures corresponding to wind speed shown in Figure 3. External and internal pressure coefficients for building's walls and roof are adopted according to the recommendations given in EN1991:2005 [3], as shown in Figure 4. Loads arising from operation of the turbine are applied as time-histories of forces and bending moments calculated in time-history analysis of the tower and the turbine in Ashes software using spatial wind profile as loading having the mean wind flow identical as shown in Figure 3.

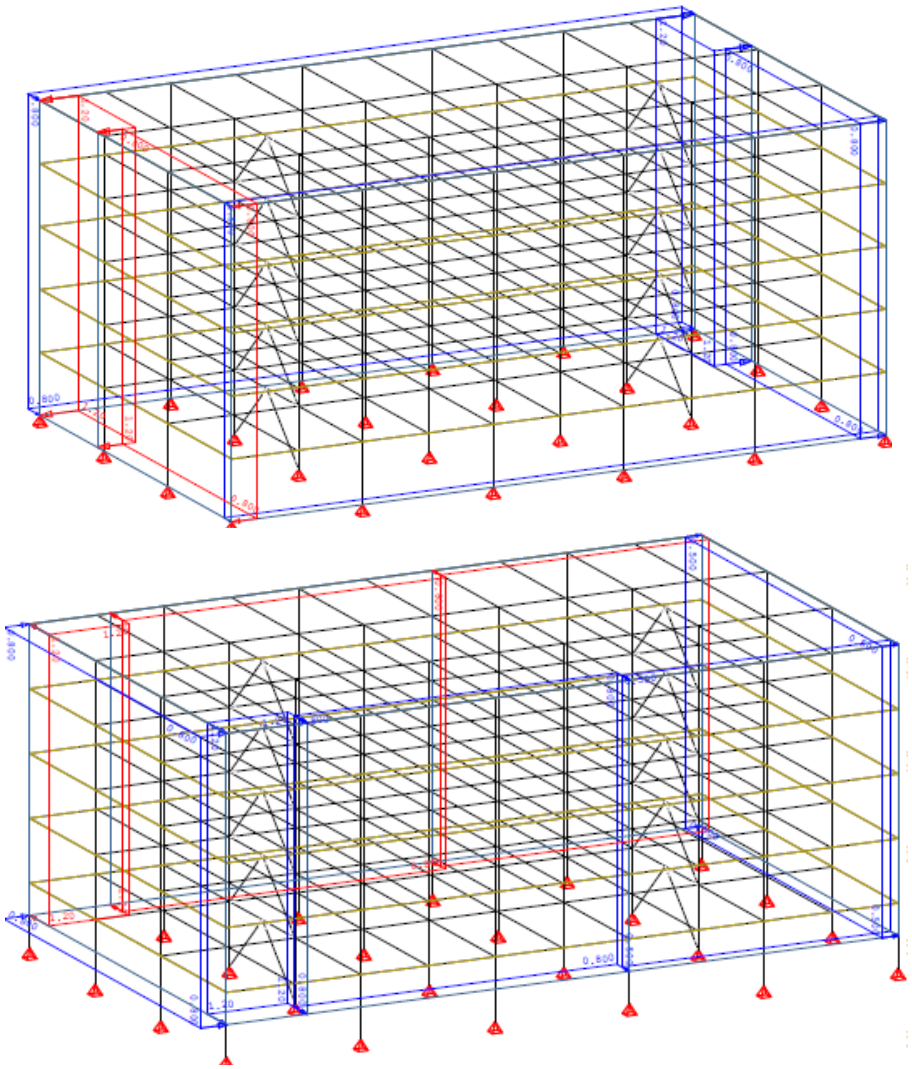

Figure 4. External and internal pressure coefficients for wind actions

RESULTS

Analysis of vibrations for each floor induced by wind action is performed through time-history analysis and extreme accelerations and displacements are obtained. Frequencies of oscillations of each floor are also obtained, which is very important for comparison with design requirements for floor vibrations, e.g. ISO 10137: 2007 [4].

CONCLUSIONS

Increasing demands for installation of wind turbines on the building's roof in urban regions can be compromised due to increase of floor vibrations in buildings. Because of very sensitive human perception of floor vibrations, a detailed analysis of floor vibrations increase caused by installation of wind turbines for urban wind harvesting is required. The level of increase of floor vibrations after installation of small-scale wind turbines at the building's roof is determined in this paper and compared to design code requirements.

REFERENCES

[1] EN1994-1-1: Eurocode 4 - Design of composite steel and concrete structures. Part 1-1: General rules and rules for buildings. Brussels, Belgium: European Committee for Standardization (CEN), 2004.
[2] EN1993-1-1: Eurocode 3 - Design of steel structures. Part 1-1: General rules and rules for buildings. Brussels, Belgium: European Committee for Standardization (CEN), 2005.
[3] EN1991-1-4: Eurocode 1 – Actions on structures. Part 1-4: General actions- Wind actions. Brussels, Belgium: European Committee for Standardization (CEN), 2005.
[4] International Standard ISO 10137- Bases for design of structures- Serviceability of buildings and walkways against vibrations, International Standard Organization (ISO), Switzerland, 2007.

THE INTERNATIONAL CONFERENCE ON
WIND ENERGY HARVESTING 2017
20-21 April 2017
Coimbra, Portugal

Paper 313

PIEZOCOMPOSITES FOR ENERGY HARVESTING

Ioannis Fournianakis[1]
Technical University of Crete
Chania, Greece

Panagiotis Koutsianitis[2]
Technical University of Crete
Chania, Greece

Georgia Foutsitzi[3]
Technological Educational
Institute of Epirus
Arta, Greece

Georgios K. Tairidis[4]
Technical University of Crete
Chania, Greece

Georgios E. Stavroulakis[5]
Technical University of Crete
Chania, Greece

ABSTRACT

In the present paper a smart cantilever beam and two vertical beams of different dimensions with embedded piezoelectric componentsare used for energy harvesting. The mechanical models of the composite smart structure with bonded piezoelectric materials are tested in order to investigate the maximum amount of energy that can be produced. Consequently, piezoelectric elements placed at selected positions of a submerged offshore construction are used. External forces vibrate the system, resulting in energy harvesting. Both beams are modelled by using finite element methods and modal analysis tools. The investigation reveals the feasibility of the proposed harvester, as well as hints for their optimal design.

NOMENCLATURE

f_I	=	Inertia force (N)
f_D	=	Drag force (N)
L	=	Beam length (m)
A	=	Cross-sectional area (m^2)
P	=	Mass density of the beam(kg/m^3)
Y	=	Elastic Modulus
V	=	Volume of the beam (m^3)

INTRODUCTION

Piezoelectric materials have the ability to produce electric charge when subjected to mechanical stresses. These materials can be both natural and synthetic, usually ceramics and are widely used for the formation of sensors and actuators in smart composite structures [1]-[3] as well as for mechanical energy harvesting from vibrations [4]-[5]. The behavior of the interface between the different layers of a laminate composite structure in order to transfer energy from the structure body to the energy harvester is an object of study. The design of the

1 Research Associate, Dipl. Eng., MSc., School of Production Engineering and Management, Technical University of Crete, GR-73100 Chania, Greece / ifournianakis@isc.tuc.gr
2 Graduate Student, Dipl. Eng., School of Production Engineering and Management, Technical University of Crete, GR-73100 Chania, Greece / panoskout@gmail.com
3Professor, Department of Accounting and Finance, Technological Educational Institution of Epirus, TEI Campus−Psathaki, GR-48100 Preveza, Greece / gfoutsi@teiep.gr
4 Dr, Dipl. Eng., MSc., Ph.D., School of Production Engineering and Management, Technical University of Crete, GR-73100 Chania, Greece / tairidis@gmail.com
5 Professor, School of Production Engineering and Management, Technical University of Crete, GR-73100 Chania, Greece / gestavroulakis@isc.tuc.gr

harvester, which is based on the usage of piezoelectric elements, is performed in such a way as to be able to obtain the maximum amount of energy [6].

For the same reason, the piezoelectric elements are placed in the locations that present the maximum strain for given vibrations. It is obvious that bond points should be avoided, due to the fact that no information is given at such positions.Furthermore, the ability of the proposed models to provide satisfactory results, for a large width of different frequencies that described various phenomena i.e. wind excitations, random vibrations, ocean waves etc. is investigated. The design of an energy harvester, in order to exploit wave energy, requires the full knowledge of the wave and the piezoelectric phenomenon. The main purpose of this study is to obtain electric potential by converting the mechanical energy into electricity using piezoelectric elements.

METHODOLOGY

Let us consider a smart beam, which has been used in various investigations of our group [7]-[8], with total length *(L)* is 0.8m with cross-sectional area (*A*) of the beam 0.02x0.02 m^2. The elastic modulus (*Y*) of structure is $73x10^9$ N/m^2 and the shear modulus (*G*) is $40x10^9$ N/m^2. The mass density (ρ) of the beam is 2700 kg/m^3. In the present example the beam is discretized into 32 elements yielding to a system with 64 degrees of freedom. The beam is a cantilever, which means that it is fixed at the left end. In the finite element model, the degrees of freedom of the system are quite large therefore it is required to model the system in modal form.

Therefore the governing system dynamics equation is expressed in modal space by introducing a new variable derived by modal transformation (1

$$\{X\} = \sum_{i=1}^{N} \Phi_i \eta_i(t) = [\Phi]\{\eta\} \tag{1}$$

Where $[\Phi]$ is the modal matrix and $\{\eta\}$ is the modal coordinate vector. The final equation reads:

$$\{\ddot{\eta}\} + [\Omega^2]\{\eta\} = [\Phi]^T \{F_m\} - [\Phi]^T \{F_{el}\} \tag{2}$$

where $\{F_m\}$ is the global mechanical force and $\{F_{el}\}$=-$[K_{u\varphi}]V$ is the electrical force vector due to the actuation and $[\Omega] = diag(\omega_1, \omega_2, ...\omega_N)$ with ω_i the undamped natural frequency of the *i*-th mode.

The amount of energy produced from every piezoelectric element in each eigenvector is given by:

$$E = \frac{1}{2} Y \left(\frac{\Delta\varphi}{L} \right) V_{vol} \tag{3}$$

The quantity $\Delta\varphi$ is given by the following equation:

$$\Delta\varphi = \left(\varphi_i^j - \varphi_{i+1}^j \right) \frac{h}{2} \tag{4}$$

Whereφ_i^j is the i^{th}element of the j^{th} eigenvector and *h* is the height of the beam.

For the design of the offshore energy harvester let us consider a beam vertically positioned and fixed at the bottom end [9]. The total height (*H*) is 3.0m and width (*W*) is 0.30m placed on submerged structure at 3.0m depth. The piezoelectric materials have the form of thin plates that are placed longwisel.The piezoelectric material selected is PZT-4 with the following properties:Crystal symmetry class, uniaxial and density7500 kg/m3. More specifically, for the first model piezoelectric material is placed on the outer side of the beam[10]-[11], while for the second model inside the beam.The force applied along the surface of the beam *f(z, t)*, by the wave phenomenon is given by the Morison equation:

$$f(z, t) = f_I(z, t) + f_D(z, t) \tag{5}$$

where f_I is the inertia force and f_D is the drag force, see e.g. [12].

RESULTS

For the first structure Table 1 showns the finite element where the extra mass is placed, along with the amount of the maximum energy produced and the node where this amount is produced. Note 1 is the fixed (left) end of the cantilever, while node 32 is the free end. The energy is given in Joules. The value of the maximum energy that produced by the structure without the extra mass is 1562.6 J and it appeares at the fixed end of the beam. From the results of Table 1, one can observe that the total energy is not transferred to other elements of the structure when the extra mass is placed. This means that in any case the maximum energy is given at the fixed end of the beam.

In addition, we observe a slight increase when the extra mass is placed at the 9th node. Namely, this amount is 1640.8 J., instead of 1562.6 J, which means that a 5% increase was achieved.

Table 1. Numerical results for the 1st eigenvector

Element of extra mass	Node of max energy	Amount of max energy (J)	Element of extra mass	Node of max energy	Amount of max energy (J)
1	1	1562.80	17	1	1149.20
2	1	1562.80	18	1	1052.10
3	1	1571.60	19	1	957.84
4	1	1582.10	20	1	868.25
5	1	1596.20	21	1	784.51
6	1	1612.30	22	1	707.24
7	1	1627.50	23	1	636.60
8	1	1638.40	24	1	572.49
9	1	1640.80	25	1	514.61
10	1	1630.80	26	1	462.56
11	1	1605.00	27	1	415.89
12	1	1561.90	28	1	374.10
13	1	1501.80	29	1	336.75
14	1	1426.70	30	1	303.39
15	1	1340.20	31	1	273.59
16	1	1246.40	32	1	246.98

In figure 1 the energy at each element before (blue line) and after (red line) addition of the extra mass are shown.

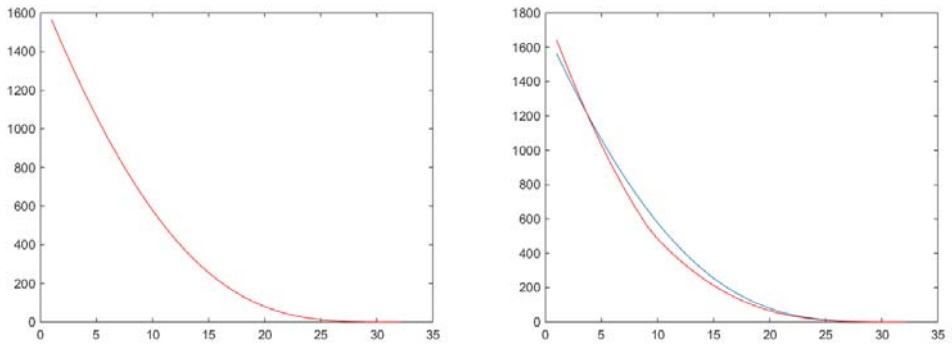

Figure 1. Total energy at each node when extra mass placed at elements 1and 9

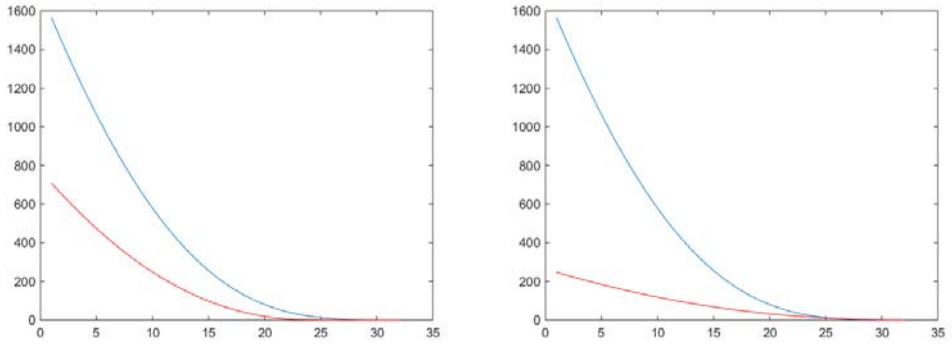

Figure 1. Total energy at each node when extra mass placed at elements 22 and 32

In figure 2 one can observe that the measure of the force (*N*) increases accordingly to the value of 'Z', which represents the depth. Higher amounts of force applied on the free end. Figure 3 illustrates the models during the meshing procedure. The elements used for the mesh follow 3D symmetry. Finally in figure 4 the vertical displacement and the total electric potential of each beam separately, is presented by the colour variations.

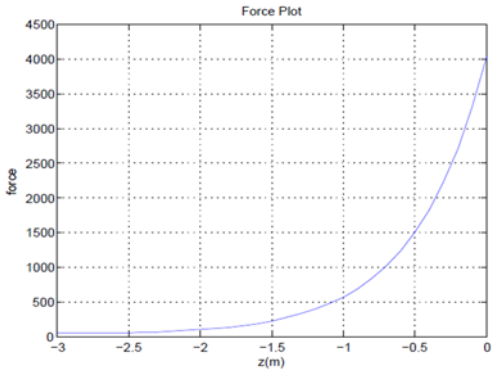

Figure 2. Force along the submerged beam

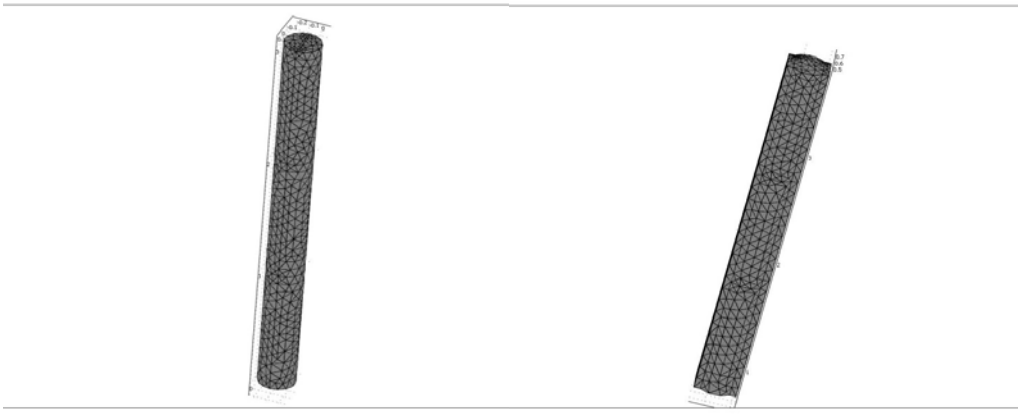

Figure.3 Meshing for both models

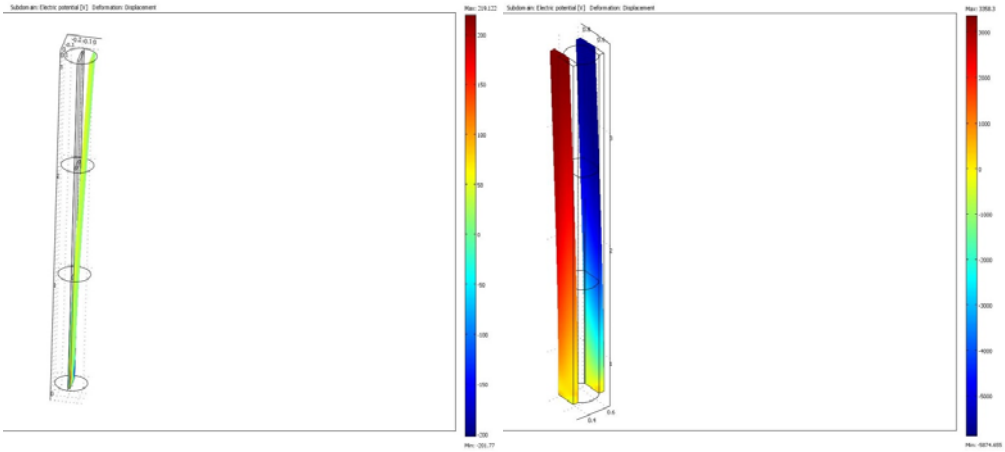

Figure 4. Vertical displacement and electric potential for both models

One may propose different configurations of piezocomposites suitable for energy harvesting. For example a smart layerwise plate with piezoelectric patches can also be used. The structure consists of three discrete layers, that is, the elastic core in the middle, along with two piezoelectric layers at the upper and the lower side of the host structure respectively. Twelve-node rectangular bilinear isoparametric elements, i.e. 4 nodes per element for each of the three layers, with five degrees of freedom per node can be used. See figure 5.

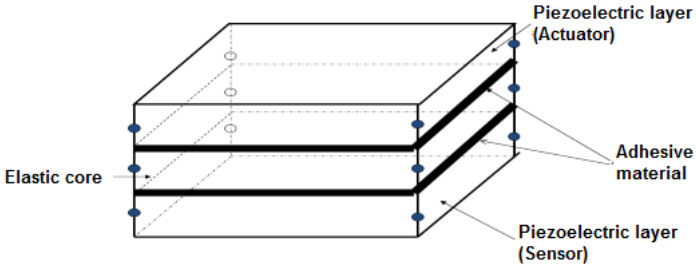

Figure 5. Isoparametric finite element with 4 nodes for each of the three layers of a smart layerwise plate

Eigenvectors of plates in bending, like the one shown in figure 6 can be used in a similar way.

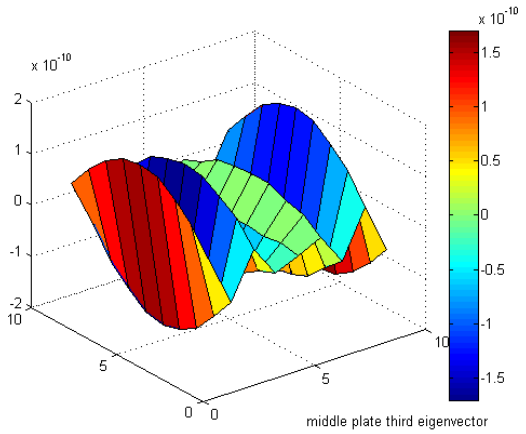

Figure 6. Third eigenmode of the elastic core of a layerwise plate

CONCLUSIONS

The criteria of the harvester, that is, the location, the shape and the size of the piezoelectric components, could be properly quantified within an optimization process for the fine tuning of the properties of the harvesters. Structural optimization for dynamic problems, involving modal characteristics, is a challenging task. Optimization algorithms inspired by nature and especially Evolutionary Algorithms (EAs) can provide very powerful tools for this purpose. Moreover, the ability of the proposed model to provide satisfactory results for a large width of different frequencies that described various phenomena i.e. wind excitations, random vibrations, ocean waves etc. may be part of future investigations.

REFERENCES

[1] G. Tairidis, G. Foutsitzi, G. Tsagkaris, G.E. Stavroulakis, "Fuzzy Control for Vibration Suppression of Smart Plates", in B.H.V. Topping, P. Iványi, (Editors), "Proceedings of the Twelfth International Conference on Computational Structures Technology", Civil-Comp Press, Stirlingshire, UK, 2014, Paper 60

[2] G.K. Tairidis, G.E. Stavroulakis, D.G. Marinova and E.C. Zacharenakis, "Classical and soft robust active control of smart beams", in: M. Papadrakakis et al. eds, "Computational Structural Dynamics and Earthquake Engineering", CRC Press, Balkema and Taylor & Francis, London,, 2009, Ch. 11, 165-178.

[3] G. A. Foutsitzi, Ev. P. Hadjigeorgiou, Ch. G. Gogos and G. E. Stavroulakis, "Modal shape control of smart composite beams using piezoelectric actuators" in Proceedings of 10th HSTAM International Congress on Mechanics, Chania, Crete, Greece, 25 – 27 May, 2013.

[4] Y. Liao, H.A. Sodano, "Optimal placement of piezoelectric material on a cantilever beam for maximum piezoelectric damping and power harvesting efficiency" Smart Mater. Struct. 21,2012, 105014,

[5] G. Park, T. Rosing, M. Todd, C. Farrar, W. Hodgkiss, "Energy Harvesting for Structural Health Monitoring Sensor Networks." J. Infrastruct. Syst. 14, SPECIAL ISSUE: New Sensors, Instrumentation, and Signal Interpretation, 2008, 64–79

[6] G. K Tairidis, G.. A. Foutsitzi, P. Koutsianitis, G. Drosopoulos and G. E. Stavroulakis, Energy Harvesting using Piezoelectric Materials on Smart Composite Structures, The Fifteenth International Conference on Civil, Structural and Environmental Engineering Computing,Prague, Czech Republic 1-4 September 2015.

[7] E.P. Hadjigeorgiou, G.E. Stavroulakis, G.E., C.V. Massalas, "Shape control and damage identification of beams using piezoelectric actuation and genetic optimization" Int. J. Eng., 2006, Sci., 44, 409–421.

[8] G.E. Stavroulakis, G.Foutsitzi, V.Hadjigeorgiou, D.G.Marinova, C.C.Baniotopoulos, "Design andRobust Optimal Control of Smart Beams with Application on Vibrations", Suppression, Advances in Engineering Software,2005, 36, 806–813.

[9] G. E.Stavroulakis, I. S. Fournianakis Design of an Offshore Piezoelectric Energy Harvester and Finite Element Method analysis,Techincal University of Crete, August 2015,Greece.

[10] Heung Soo Kim, Joo-Hyong Kim and Jaehwan Kim, A Review of Piezoelectric Energy Harvesting Based on Vibration, *Int J of Precision Engineering and manufacturing,* 12, No. 6, South Korea, November 2011,pp. 1129-1141.

[11] X.D Xie, Q.Wang, N.Wu, Potential of a Piezoelectric Energy Harvester from Sea Waves, ELSEVIERJournal of Sound and Vibration, Hubei University, ChinaNovember 2013, 1421–1429.

[12] N. Haritos EJSE Special Issue: Introduction to the Analysis and Design of Offshore Structures- An Overview, Electronic Journal of Structural Engineering International, University of Melbourne, Australia, 2007.

THE INTERNATIONAL CONFERENCE ON
WIND ENERGY HARVESTING 2017
20-21 April 2017
Coimbra, Portugal

Paper 314

STATIC ANALYSIS OF DIFFERENT TYPE OF WIND TURBINE TOWERS

Anil Ozdemir [1]
Ankara, Turkey

Fethi Sermet [2]
İzmir, Turkey

M. Ensari Yigit [3]
Manisa, Turkey

Bengi Arisoy [4]
İzmir, Turkey

Emre Ercan[5]
İzmir, Turkey

ABSTRACT

In this paper, behavior of three different types of wind turbine towers under effect of static loads is presented. It is well known that renewable energy requirements over the world increase. The wind is one of the cleanest and economical energy sources. In order to produce larger amount of energy by using wind turbines, the length of the turbine blades is increased. By increasing length of blades, weight of the turbine is increased, so does effect of turbine as static load to the turbine tower. Thus, it becomes necessary to optimize types of turbine towers and dimensions as well as the materials. In this paper, three different wind turbine towers: steel, reinforced concrete and hybrid (reinforced concrete and steel) turbine towers are analyzed using finite element analysis. The finite element model of towers with 10m height is completed and analyzed by using ABAQUS. The deformations and stresses are gathered and compared for different types of towers. Analysis indicates that reinforced concrete tower has lowest displacement, the effect of torsion is dominant in steel tower, and the hybrid tower is vulnerable in connection concrete and steel parts.

INTRODUCTION

The world population has increased exponentially in the last few centuries. Due to this rapid growing in population, the energy demand is also increased. In recent years researches about sustainable, renewable and environmentally friendly energy sources have priority in order to meet the energy demand in the world. Recent years, a significant amount of research has been conducted to formulate the design of various tower structures as optimization problems. Optimization strategies were studied according to minimization of the tower's mass, maximization of the tower's stiffness, minimization of vibrations and maximization of the system natural frequency [1]. In addition to the modal parameters, geometrical properties are also considered optimization parameters. Especially, diameter of the pole is an important parameter [2]. On the other hand, using geometrically nonlinear analysis vs. linear analysis differed very little due to other design constraints, the towers analyzed stay in the elastic range at the final design analyzing method [3-4].

In presented study, linear analysis of geometrically identical three different types of tower is performed. Results are compared regarding deformations and stress distributions.

TYPES OF WIND TURBINE TOWERS

Wind turbine towers are constructed with different materials and different construction systems: Steel lattice towers, steel cylinder towers, reinforced concrete towers and hybrid towers. For example, Fuhrländer Wind Turbine Laasow, built in 2006, in Laasow, Brandenburg, Germany is the world's tallest lattice tower wind turbine with a length of 160 meters. Wind towers intentionally built taller, because, increased production capacity in wind turbine systems has been achieved by achieving higher wind speeds [5], so higher wind speed is gathered at higher levels.

Steel frame type towers: Today, the most preferred type of tower is steel cylinders. Buildings towers in this way show light and high strength properties [6]. It is also preferred because it provides a safer climbing area and lower maintenance costs compared to other tower types.

1 Research Assistant, Civil Engineering Department, Gazi University, Turkey/anilozdemir@gazi.edu.tr
2 Research Assistant, Civil Engineering Department, Ege University, Turkey/fethi.sermet@ege.edu.tr
3 Research Assistant, Civil Engineering Department, Celal Bayar University, Turkey/ensar.yigit@cbu.edu.tr
4 Associate Professor, Civil Engineering Department, Ege University, Turkey/bengi.arisoy@ege.edu.tr
5 Lecturer, Civil Engineering Department, Ege University, Turkey/emre.ercan@ege.edu.tr

Reinforced concrete towers: The most widely used methods in the world construction industry are reinforced concrete systems. Reinforced concrete systems are most widely used methods in the world construction industry. These systems are used extensively in almost every country. Likewise, this system is used in wind turbine tower constructions. The resonance tendency in other turbine towers with increasing tower heights leads to the design of reinforced concrete towers [7]. The greatest advantage of this type of towers is the prevention of local buckling.

Hybrid towers: Hybrid towers are used together with steel and reinforced concrete construction systems. Wind turbine towers are required to be light and extremely durable. In some high tower designs, the reinforced concrete system come out to be advantageous, resulting in the formation of aesthetically unstable structures made very heavy and difficult to maintain. Hybrid towers also benefit from the advantages of the two construction systems. In addition to these advantages, it will also reduce the earthquake loads on the tower.

DESIGN AND ANALYSIS OF AN INDUSTRIAL WIND TURBINE TOWERS

In this section; reinforced concrete, steel and hybrid (reinforced concrete and steel) wind turbine towers with a cylindrical form and with a diameter of 45 cm and of 10 m high are designed. The thickness of steel tower is 5 mm. The steel type is S-335. The compressive strength and density of concrete mixture were 35 MPa and 2400 kg/m^3 respectively and the ratio of poisson of concrete is 0.3. 16Ø16 reinforcement was used in design reinforced concrete tower. These designs is selected because of their costs are very close to each other. Analysis of the wind turbine towers is performed using ABAQUS [8]. Then the deformations and strains that will occur in the wind turbine tower will be examined.

Wind turbine tower designs: The reason to choose the industrial wind turbine tower is due to large demand of smaller power plants. Because, smaller power plants are enough to provide energy necessary to be use small towns or establishment. The greatest advantage of this type of production is that it is realized at the moment of consumption, the transmission and storage losses are almost reduced to zero. The details of the designs of the towers are given in Fig. 1.

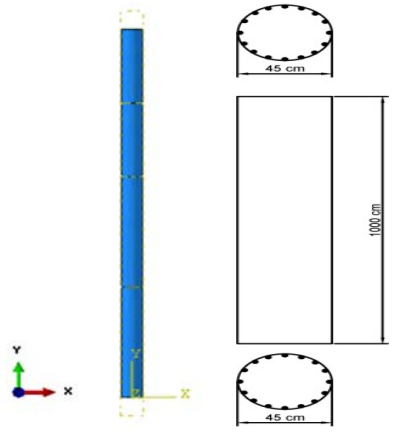

Fig .1 The section and model of the columns of reinforced concrete tower

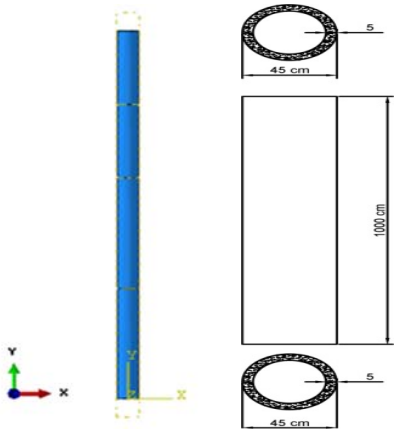

Fig. 2 The section and model of the columns of steel tower

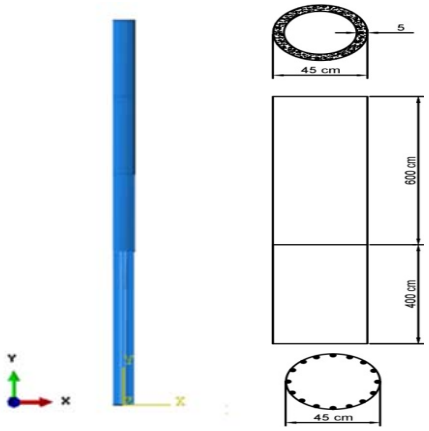

Fig. 3 The section and model of the columns of hybrid tower

Loading Conditions: Loads to be applied to wind turbine towers are made according to TIA/EIA-222-F [9] code calculation methods. The loads and load combinations are given in Table 1 and 2. These loads were applied and analyzed in the same way as the same points in all types of towers presented in this study. Kocaeli earthquake records were taken as earthquake loads.

Table 1. Loads on the tower

Load Direction	TIA/EIA-222-F	
	Load Type	**Load**
x-x	Wind Load (Turbine)	12890.81 N
y-y	Turbine Weight	456.16 N
y-y	Ice Load (Tower)	2302.6 N
x-x	Wind Load (Tower)	2909.64 N/m

Table 2. Load Combinations

Load Combination	Dead Load	Ice Load	Wind Load	Quake Load
1	1	0	1	0
2	1	1	0.75	0
3	1	1	0.75	0.1

The load distributions for Reinforced Concrete, Steel and Hybrid Tower are shown in Fig. 4, on the deformed model of the tower.

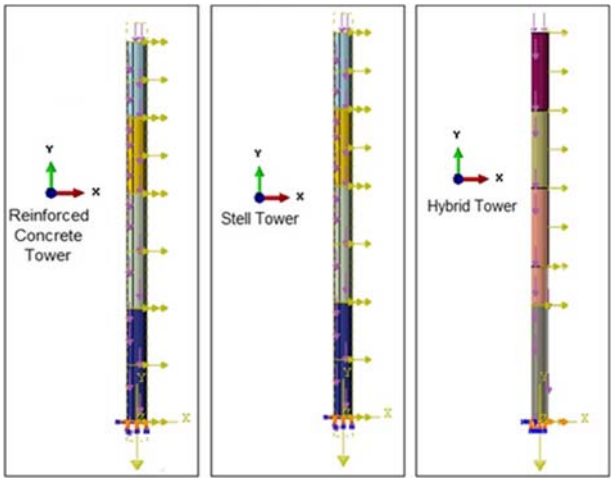

Fig. 4 Load distributions

RESULTS

Displacement: The maximum displacements for reinforced concrete, steel and hybrid towers are shown in Fig. 5. The regions shown in red indicate the largest displacements. According to the displacement contours, the maximum displacement at the tip of the tower is 0.120 cm.

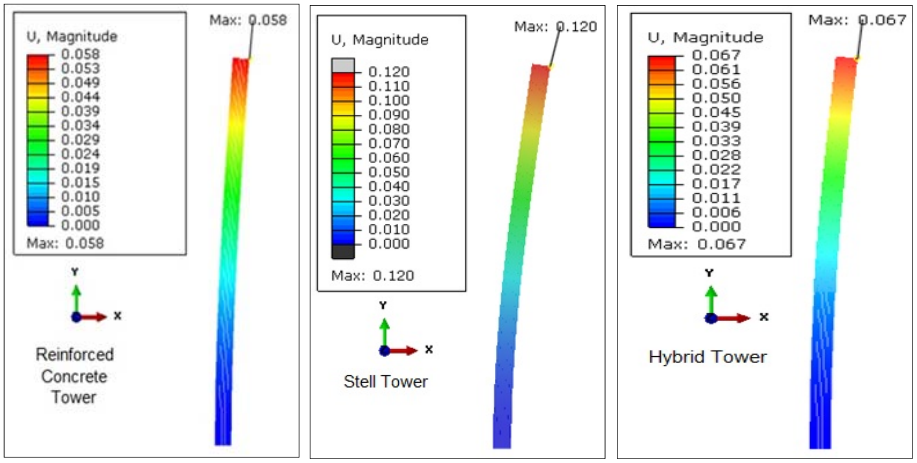

Fig. 5 Displacement of the towers under loading

Stresses: The maximum stresses for reinforced concrete, steel and hybrid towers are shown in Fig. 6. The regions shown in red indicate the largest stresses. According to the stresses contours, the maximum principal stress is 168 MPa, at the bottom of the tower.

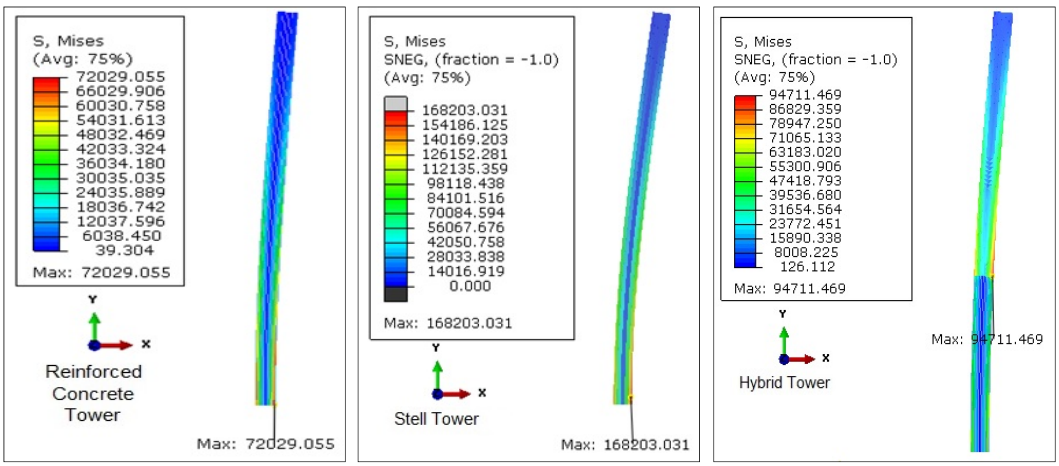

Fig. 6 Stresses of the towers under loading

CONCLUSIONS

Based on the ABAQUS analysis results, it was found that all types of towers perform reasonable well under loads given in Table 1 and 2. None of the towers exhibit damage.

It is seen that the largest stress in reinforced concrete tower design is formed in the lower-outer periphery of the tower. In the steel tower design, the torsion effect was dominant. Torsion effect is a consideration in steel tower design. In the case of hybrid tower design, it is seen from the analysis that the connection of reinforced concrete and steel parts is subjected to the greatest stress.

Maximum stresses and displacement are observed on steel tower design. As it can be seen from analysis results, compared to the steel tower design, the displacement of reinforced concrete tower design decreased 51.6%.

However, the decreasing displacement value for hybrid tower design was recorded as 44.16% compared to the steel tower design.

REFERENCES

[1] Negm, H. M. and Maalawi, K. Y., "Structural Design Optimization of Wind Turbine Towers", Computers and Structures, 74: 649-666, 1999.

[2] Kocer, F.Y. and Arora, J.S., "Design of Prestressed Concrete Transmission Poles: Optimization Approach", Journal of Structural Engineering 122, no. 7 (July): 804-814, 1996.

[3] Kocer, F.Y. and Arora, J.S., "Optimal Design of H-Frame Transmission Poles For Earthquake Loading", Journal of Structural Engineering 125, no. 11 (February): 1299-1308, 1999.

[4] Lewin, T, J., "An Investigation of Design Alternatives for 328-ft (100-m) Tall Wind Turbine Towers", The Degree of Master Thesis, Iowa State University, Iowa, USA, 2010.

[5] Kanbur, F. A., "Steel Tower Design for a 500 KW Wind Turbine", İstanbul Technical University, Graduate Scholl of Natural, The Degree of Master Thesis, İstanbul, Turkey, 2014.

[6] Manwel, J.F., Mcgowan, J.G. and Rogers, A. L., "Wind Energy Explained Theory", Design and Application Secon Edition, John Wiley & Sons, Ltd.U.K, 2009.

[7] Harte, R., G.P.A.G. and Zijl, V., "Structural Stability of Concrete Wind Turbines and Solar Chimney Towers Exposed to Dynamic Wind Action", Journal of Wind Engineering and Industrial Aerodynamics 95, 2007, pp. 1079–1096.

[8] Simulia ABAQUS FEA, Dassault Systèmes, Vélizy-Villacoublay, France, 2016.

[9] TIA/EIA-222-F, "Structural Standards For Steel Antenna Towers And Supporting Structures", 2013.

THE INTERNATIONAL CONFERENCE ON
WIND ENERGY HARVESTING 2017
20-21 April 2017
Coimbra, Portugal

Paper 315

THE USE OF WIND DESIGN SPECTRA FOR ESTIMATING STRUCTURAL PERFORMANCE OF WIND TURBINE TOWERS

P Martinez-Vazquez[1]
School of Civil Engineering, The University of Birmingham
Birmingham, United Kingdom

ABSTRACT

The dynamic performance of wind turbine towers is calculated by using wind design spectra in order to critically evaluate the suitability of this newly developed tool for structural analysis. Wind design spectra are analogous to those used in seismic engineering applications. They are formed based on the response acceleration of single oscillators characterised by their mass, stiffness, damping, and areas exposed to wind, and are suitable for modal analyses. In this paper, results from spectral analyses are compared with those determined through generalised loading acting on the towers that is derived from a simulated wind field. The overall results show consistency between the spectral approach and classical theory and therefore is suggested that wind design spectra can be used to cover wider range of engineering applications.

NOMENCLATURE

A	=	Area exposed to wind	m	=	Structural mass
C_D	=	Drag coefficient	n	=	Gust frequency
C_w	=	Decay constant in the *w*-direction	n_0	=	Fundamental frequency
F^*	=	Generalized force	p_k	=	*k-th* force for num. integration
$H(J)$	=	Transfer function (Displacement)	q	=	Force factor
$J(n)$	=	Transfer function (Acceleration)	z_r	=	Reference height
K	=	Structural stiffness			
M^*	=	Generalized mass	Δ_w	=	Distance in the w-direction
$S_{Aij}(n)$	=	Cross-spectrum of acceleration	ρ	=	Density of air
$S_{cu}(n)$	=	Generalised input acceleration	σ_a	=	Rms of acceleration
$S_F(n)$	=	Force spectrum	ω_0	=	Fundamental (circular) frequency
$S_u(n)$	=	Wind power spectrum	ω_D	=	Damped frequency
U	=	Average wind velocity	ξ	=	Structural damping
$X(n)$	=	Aerodynamic admittance			

INTRODUCTION

Classical theory enables to calculate wind forces and their effects on structures through time or frequency domain analyses. The former can be done for example through wind tunnel simulations or numerical modelling in which the wind flow is represented by real or synthetic wind fields reflecting the spatio-temporal nature of wind gusts. Examples of those are given in [1-4]. On the other hand, frequency domain analyses are typically based on the transformation of the wind power spectrum into a force spectrum which once filtered through a suitable transfer function allows to estimate dynamic effects on structures as in [5-6] although these can also lead to the estimation of equivalent static load as demonstrated in [7-8]. All these methods would be consistent with the Gust Load Factor proposed around four decades ago in [12]. The use of wind response spectra would be more suitable to use in the modal domain where the decomposition of the displaced configuration of multiple degrees of freedom systems can take place. The spectral approach is thus compatible with modal analyses and it has the advantage of reducing

1 Lecturer, School of Civil Engineering, Birmingham University, Edgbaston B15 2TT, United Kingdom, p.vazquez@bham.ac.uk

the computational effort that is often associated to the estimation of wind dynamic response of structures. The idea of generating wind response spectra was first introduced in [9]. The purpose was to establish a formulation which enabled addressing the implications of the uncorrelated nature of wind to the dynamic motion of single and multiple-degree of freedom systems through the use of differential equations. This resulted in the so-called Equivalent Wind Spectrum Technique (EWST). Although wind design spectra were not actually realised in [9] the discussion highlighted the possibility of calculating response spectra analogous to those used in seismic engineering. The present research builds on those ideas although it does not follow the EWST. It maintains cross-correlation functions such as those proposed in [10-11] to describe the structure of turbulent wind and to formulate equations to calculate the response acceleration of single degree of freedom systems. In this way the wind design spectra i.e. charts containing pseudo-spectral acceleration associated to a range of natural frequencies or periods of vibrations, are inferred. In this paper wind design spectra are used to calculate the response of cylindrical towers that resemble those used to support wind turbines. These structures are also subjected to a simulated wind field through the use of generalised forces. The results of both approaches are then compared whilst suitable conclusions are drawn.

METHODOLOGY

The objectives of the research are fulfilled through the following steps: (i) Estimation of wind design spectra; (b) Derivation of generalised forces from a simulated wind field acting along the height of the towers; (c) Identification of steel towers with prismatic shape and estimation of their dynamical properties; (d) Application of spectral and generalised load to the towers; (e) Analysis of results and formulation of conclusions. The following sections address each one of these steps in the order given.

Wind Design Spectra: General Formulation

The wind forces acting on a point-like structure can be generated by using Eq. (1) where $S_F(n)$ represents the force spectrum, n is the gust frequency, q is a force factor, m is the mass excited by the wind, and $S_u(n)$ is the wind power spectrum. The force factor is given by $q = \frac{1}{2}\rho C_D A (1+2U)$ - where C_D represents the drag coefficient, A, ρ, and U are the area exposed to wind, air density, and the average along-wind velocity component. A mathematical definition of the factor q is given in [13].

$$S_F(n) = q^2 S_u(n) \tag{1}$$

$$S_A(n) = \left(\frac{q}{m}\right)^2 S_u(n) \tag{2}$$

$$H(n) = \frac{1}{K\sqrt{(1-r^2)^2+4\xi^2 r^2}} \tag{3}$$

$$J(n) = \frac{1}{\sqrt{(1-r^2)^2+4\xi^2 r^2}} \tag{4}$$

The force spectrum is translated into input acceleration for the system through Eq. (2) whereas the square modulus of Eq. (3)-(4) transform $S_F(n)$ and $S_A(n)$ into response displacement and acceleration, respectively. In these equations r represents the ratio n / n_0 where n_0 is the fundamental frequency of the structure, K represents the structural stiffness and ξ represents the fraction of critical damping defined as $\xi = c / 4m\pi n_0$ – being c the viscous damping. For loaded surfaces it is required to consider the aerodynamic admittance, $X(n)$, that reflects the cross-correlation of wind gusts. This scheme is given by Eq. (6)

$$\sigma_a^2 = \int J^2(n) X^2(n) S_A(n)\, dn \tag{6a}$$

$$|X(n)| = \frac{1}{1+\left(\frac{2n\sqrt{A}}{U}\right)^{4/3}} \tag{6b}$$

$$S_{cu}(n) = \iint_A \phi(z_i)\phi(z_j) S_{A_{ij}}(z,n) dy_i dy_j dz_i dz_j \tag{7a}$$

$$S_{A_{ij}}(z,n) = \frac{S_A(n)}{A^2}\psi(z) e^{-\frac{n_x}{U(z)}\sqrt{(C_y\Delta_y)^2+(C_z\Delta_z)^2}} \tag{7b}$$

$$\sigma_{a,b}^2 = \int J^2(n) S_{cu}(n) dn \tag{8}$$

$$\sigma_{a,r}^2 = \frac{\pi n_0 S_{cu}(n_0)}{4\xi} \quad (9)$$

For multiple-degree of freedom systems Eq. (6) can be expressed in terms of the cross power spectrum, S_{Aij} *(n)* in order to determine the spectral density of the generalised input acceleration S_{cu} *(n)* as in Eq. (7). In this set of equations ψ *(z)* accounts for the variation of turbulence with height, Δ_y and Δ_z give the horizontal and vertical distances between the points *i, j* located at coordinates $\{y_i, z_i\}$ and $\{y_j, z_j\}$, $\Phi(z)$ stands for the modal ordinate at the height *z,* and C_k represent a decay constant in the *k*-direction. Eq. (7) can be applied to a collection of single oscillator with fundamental frequency n_0 in order to obtain the mean square background ($\sigma_{a,b}^2$) and resonant ($\sigma_{a,r}^2$) response accelerations given by Eq. (8) and (9) respectively. The design spectra are assembled by combining $\sigma_{a,b}^2$ and $\sigma_{a,r}^2$ to form a graph with pairs $\{T, S_a(T)\}$ where $S_a(T) = \sigma_{a,b} + \sigma_{a,r}$ and $T = 1/n_0$ represents the fundamental period oscillation.

Generalised Forces and Simulated Wind Field

A simulated wind field covering a height up to 250 m above the ground was generated by using the algorithm suggested in [14]. The details of the simulation have been provided elsewhere - see for example [13-16], therefore only statistics of the simulated time series and cross-correlation results are provided in Tables 1-2.

Table 1. Calculated statistics of simulated wind time series

Stats \ z (m)	10	40	75	100	140	170	200	210	220	240	250
U_t	20.00	30.21	36.21	39.79	42.95	45.39	47.77	48.53	49.15	50.18	50.87
U_s	19.86	29.88	35.14	38.62	41.69	44.05	46.32	47.08	47.69	48.69	49.35
$I_{u,t}$	0.295	0.270	0.244	0.221	0.195	0.172	0.146	0.137	0.129	0.116	0.107
$I_{u,s}$	0.295	0.206	0.173	0.153	0.135	0.122	0.108	0.103	0.099	0.093	0.088

Table 2. Cross correlation results

	1	2	3	4	5	6	7	8	9	10	11
1	**1.0000**	0.4737	0.4100	0.2255	0.2134	-0.0052	-0.0591	-0.1249	-0.1843	-0.1688	-0.0237
2	0.4237	**1.0000**	0.6224	0.3814	0.2928	0.1594	0.0892	0.0231	-0.0493	-0.0151	0.0716
3	0.2090	0.4767	**1.0000**	0.6510	0.5322	0.2694	0.2860	0.2238	0.1078	0.1387	0.2322
4	0.1176	0.2605	0.5419	**1.0000**	0.7333	0.4118	0.4189	0.3157	0.2204	0.2723	0.2803
5	0.0653	0.1408	0.2895	0.5322	**1.0000**	0.6122	0.5377	0.4465	0.3681	0.3842	0.3309
6	0.0394	0.0831	0.1690	0.3092	0.5798	**1.0000**	0.5934	0.5431	0.5346	0.4584	0.3253
7	0.0231	0.0479	0.0961	0.1748	0.3265	0.5625	**1.0000**	0.8046	0.7388	0.6270	0.5227
8	0.0192	0.0394	0.0788	0.1429	0.2665	0.4588	0.8155	**1.0000**	0.8113	0.6355	0.5248
9	0.0164	0.0336	0.0669	0.1210	0.2255	0.3879	0.6893	0.8453	**1.0000**	0.7276	0.5858
10	0.0127	0.0257	0.0508	0.0917	0.1705	0.2929	0.5200	0.6376	0.7543	**1.0000**	0.7524
11	0.0106	0.0213	0.0420	0.0756	0.1403	0.2408	0.4274	0.5240	0.6198	0.8217	**1.0000**

Table 1 shows the variation of target *(U_t)* and simulated wind speed *(U_s)* along a vertical coordinate z together with the corresponding turbulence intensity which is defined as $I = \sigma_u / U$ – where σ_u is the rms of the fluctuating wind speed. The average ratio U_t / U_s is of 1.028 whereas the mean square error associated to the simulated turbulence intensity is of 0.002. Table 2 shows the target and calculated cross-correlation in the lower and upper triangular matrices respectively whilst Point 1 corresponds to that located at z = 10 m. It can be seen in the table that the accuracy of the simulation increases with the proximity between points – see for example the values around the main diagonal. The overall mean square error across cross-correlation results is of 0.0073 which was considered acceptable for the purpose of this research.

Geeralised force *(F^*)* and mass *(M^*)* – were calculated by using Eq. (10) - where Υ (z) represents force or mass per unit length and ϕ is the fundamental modal shape which was approximated by $\phi(z) = (z/H)^{\beta}$ – with β = 1.5. The generalised stiffness was obtained with $K^* = 4\pi^2 n_0^2 M^*$.

$$\Upsilon^* = \int_0^H \phi(z)^2 \Upsilon(z)\, dz \tag{10}$$

The static displacement was derived from the relationship $\Delta = F^*/K^*$ whereas the dynamic response was estimated via numerical integration of Eq. (12), which gives the solution to Eq. (11). The latter representing the dynamic equilibrium of one underdamped oscillator subjected to random load. The numerical integration is done over each time step Δt where the initial and end forces - p_i and p_{i+1}, define the gradient s. The natural and damped frequencies are ω_0 and ω_D - where $\omega_D = \omega_0 \sqrt{(1-\xi^2)}$.

$$m\ddot{d} + c\dot{d} + kd = p(t) \tag{11}$$

$$d(t) = e^{-\xi\omega_0\Delta t}\left[\left(d(0) - \frac{p_i}{k} + \frac{2s\xi}{\omega_0 k}\right)cos(\omega_D\Delta t) + \left(\dot{d}(0) + d(0)\xi\omega_0 - \frac{p_i\xi\omega_0}{k} + \frac{2s\xi^2}{k} - \frac{s}{k}\right)\frac{sin(\omega_D\Delta t)}{\omega_D}\right]\frac{p_i}{k} + \frac{s\Delta t}{k} - \frac{2s\xi}{\omega_0 k} \tag{12}$$

Wind Turbine Towers

The characteristics of three wind turbine towers under study are presented in Table 3. These include generalized properties inferred by using the generalized static load F^* defined in Eq. (10). In this table D_t is the diameter of the tower's section, t_w the thickness of the walls, and m_v is the volumetric mass.

Table 3. Geometry and natural frequencies of the towers

H (m)	D_t m	t_w m	m_v kgm^{-3}	K^* Nm^{-1}	M^* Kg	n_0 Hz
250	25	0.075	94.2	7.32x10^6	3.22x10^6	0.24
150	15	0.044	92.1	5.57x10^6	8.83x10^5	0.40
100	10	0.032	100.5	4.06x10^6	2.85x10^5	0.60

These structures were subjected to static and dynamic load corresponding to a mean velocity U_{10} = 20 ms^{-1} measured at a height of 10 m above the ground and assuming these are located in a suburb. The dynamic actions considered synthetic load and the spectral approach described above. In both cases generalised actions were considered thus assuming that the total response of the towers is based on the fundamental mode of vibration.

RESULTS

The static and dynamic displacements calculated at the top of the towers is shown in Table 4. In this table the spectral ordinate S_a *(T)* associated to the response acceleration of each tower is provided. The values of S_a *(T)* are different for the three structures because the overall area exposed to wind is taken into account when estimating the wind design spectra, as shown in Eq. (7)

Table 4. Static and dynamic displacements

Tower \ Δ (m)	Static (0)	Wind Simulation (1)	Spectral Method (2)	Total (0) + (1)	Total (0) + (2)	Spectral Ordinate S_a *(T)* in ms^{-2}
H = 100 m	0.095	0.030	0.041	0.125	0.136	0.397
H = 150 m	0.195	0.103	0.081	0.298	0.276	0.349
H = 250 m	0.441	0.131	0.137	0.572	0.578	0.213

The results of the dynamic analyses report difference of 0.011 m, 0.022 m, and 0.006 m, for the towers of height 100, 150, and 250 m, respectively. This represents a ratio between columns (1) and (2) in Table 4 of 0.73, 1.27, and 0.96, in the same order. However note that, since the physical difference in these displacements is small, such a ratio should be interpreted with care. The differences obtained could also be referred to the total height of the towers in order to obtain a qualitative measure of the differences. In that case the relative differences between columns (1) and (2) in Table 4 represent 0.011% (H=100m), 0.015% (H=150m), and 0.002% (H=250m) of the height of the towers. Thus the higher and lower accuracy corresponds to the towers of height 250 m and 150 m, respectively. In any case the relative differences encountered in these analyses are encouraging however the two

approaches used are rather different, one is based on the direct application of wind load histories on the structures whereas the other is based on spectral response accelerations i.e. the load been indirectly applied to the towers - yet the results obtained seem fairly consistent. Also note that *true* displacement responses are considered to be those derived from the wind simulation. However a different set of values - for example obtained through full-scale or wind tunnel measurements, would have been preferred. Such sets of values were not available for the present investigation.

CONCLUSIONS

This paper presents a recently developed tool for structural analysis which is currently being tested. The method considers variations in damping levels and types of terrain as well as changes in the width and height to width ratio of structures. Those variations can lead to spectral ordinates which vary from one structure to the other however these were located in the same place. A limitation that derives from this is that the design spectra have to be tailored to specific geometric characteristics. Geometry and aerodynamic properties define the attenuation of the input energy which is applied to the oscillators used to assemble the design spectra. In this investigation it was therefore necessary to calculate the spectra that is related to each of the cases studies. This suggests the need to develop a methodology for non-dimensionalising the parameters that are involved in producing the wind design spectra.

ACKNOWLEDGEMENTS

The author wishes to thank the School of Civil Engineering at the University of Birmingham for the funding granted to disseminating the present research.

REFERENCES

[1] Melbourne WH, 1980. “Comparison of measurements on the CAARC standards tall building model in simulated model wind flows”. J. Wind Eng. Ind. Aerodyn. 6: 73-88.
[2] Holmes J D, 2004. “Along- and cross-wind response of a generic tall building: comparison of wind tunnel data with codes and standards". J. Wind Eng. Ind. Aerodyn. 132: 136-141.
[3] Davenport A, 2008. “Wind tunnel testing: a general outline”. The University of Western Ontario, Faculty of Engineering Science
[4] Martinez-Vazquez P, Rodrigues-Cuevas N, 2007. “Wind field reproduction using neural networks and conditional simulation. Egineering Structures 29: 1442-1449.
[5] Davenport A G, 1967. “Gust loading factors”. American Society of Civil Engineering Journal Paper 5255: 11-34
[6] Gould P L, Abu-Sitta S, 1980. Dynamic response of structures to wind and earthquake loading. Pentech Press
[7] Chen X, Kareem A, 2004. “Equivalent static wind loads on buildings: New Model”. ASCE - Journal of Structural Engineering, 130(10): 1425-1435
[8] Chen X, Zhou N, 2007. “Equivalent static wind loads on low-rise buildings based on full-scale pressure measurements”. Engineering Structures 29: 2563-2575.
[9] Solari G, 1989. “Wind response spectrum”. J Eng. Mech. 115(9): 2057-2073
[10] Vickery B J, 1970. “On the reliability of gust loading factors”. Proc. Technical Meeting Concerning Wind Loads on Buildings and Structures. Build. Sc. Ser. 30. National Bureau of Standards, Washington DC 93-104.
[11] Tanaka H, Lawen N, 1986. Test on the CAARC standard tall building model with a length scale of 1:1000. J. Wind Eng. Ind. Aerodyn. 25: 15-29.
[12] Davenport A G, 1967. “Gust Load Factors”. J. Struct. Div. ASCE 93(3): 11-34.
[13] Martinez-Vazquez P, 2015. “Wind induced vibrations of structures by using wind design spectra”. Int. J. Advanced Str. Eng. Paper under review.
[14] Vanmarcke E, Heredia-Zavoni E, Fenton G, 1993. Conditional simulation of spatially correlated ground motion. J. Eng. Mech. 119(11): 2333-2352.
[15] Rodriguez-Cuevas N, Martinez-Vazquez P, Marquez-Dominguez S, 2006. Dynamic interaction between turbulent wind, and a slender tower. XV Mexican Congress in Structural Engineering (In Spanish)
[16] Martinez-Vazquez P, Sterling M, 2011. Predicting wheat lodging at large scales. Biosystems Engineering. 109: 326-337

THE INTERNATIONAL CONFERENCE ON
WIND ENERGY HARVESTING 2017
20-21 April 2017
Coimbra, Portugal

Paper 316

WIND INDUCED FATIGUE IN WIND TURBINE JOINTS

Stavridou Nafsika[1]
Aristotle University of Thessaloniki
Thessaloniki, Greece

Efthymiou Evangelos[2]
Aristotle University of Thessaloniki
Thessaloniki, Greece

Baniotopoulos Charalampos[3]
University of Birmingham
Birmingham, United Kingdom

ABSTRACT

Tubular steel wind turbine towers are nowadays considered as the standard approach to boost the wind energy production sector expansion within a sustainable energy development. The elevated initial construction cost along with the not so frequent, but catastrophic tower accidents, being the main drawbacks of this sustainable development solution, challenge the engineering community towards more robust structures with minimized initial cost. As a matter of fact wind towers are designed to withstand a variable and complex loading field; therefore, collapse often does not occur due to extreme weather conditions, but with normal wind and stresses still within the elastic range. It has been proved that wind induced fatigue phenomena affect the structural detailing design of such structures subjected to the resonant motion of wind resulting in the repeated loading and unloading of the structure. Recent wind tower failures have highlighted the importance of fatigue design in structures subjected to wind loading and more specifically, in the wind generator tower. These structures are constructed by mounting and joining prefabricated steel tubes on site by means of bolted flanges.Their structural details investigated here are the circumferential welds between the subsequent tower parts, the circumferential welds between the tower shell and the flange and the bolted connections of the tower to the concrete foundation. In order to assess the efficiency of such connections, two identical towers in shape and height are considered for the comparative study only differing in shell thickness and connection bolt size. In both towers, the damage accumulation methodology is used for the fatigue life calculation of the structure, and valuable outcomes on the effect of shell thickness and bolt size to the overall structural behavior of the structure are obtained.

NOMENCLATURE

D_d	=	Cumulative damage
n_{Ei}	=	Number of cycles
N_i	=	Endurance(cycles)
σ_{zz}	=	Normal stresses (MPa)

INTRODUCTION

The aim of the present study is the fatigue life investigation of horizontal axis steel tubular wind turbine towers using numerical methods. Refined full-size numerical models along with detailed micro models have been

[1]Dr Civil Engineer, Department of Civil Engineering, Aristotle University of Thessaloniki, Institute of Metal Structures, University Campus, GR-54124, Thessaloniki, Greece, nstavrid@civil.auth.gr
[2]Lecturer, Dr Civil Engineer, Department of Civil Engineering, Aristotle University of Thessaloniki, Institute of Metal Structures, University Campus, GR-54124, Thessaloniki, Greece, vefth@civil.auth.gr
[3] Professor, School of Civil Engineering, University of Birmingham, Birmingham, B15 2TT, United Kingdom, c.baniotopoulos@bham.ac.uk

proved to be a valuable tool for wind turbine tower structural behavior analysis in the work performed by Bazeos et al. [1] and Lavassas et al. [2]. The loading of the structures that has been used for their numerical investigation is the governing loading of wind turbine towers that is according to Dimopoulos and Gantes [3] the bending moment and the lateral loading caused by the operation of the rotor.

Contemporary energy needs impose the construction of constantly taller wind turbine towers in order to take advantage of the increased wind energy potential existing in higher altitudes and more constant wind speed. Meticulous structural detailing saves material and initial construction costs; therefore, guidelines have been incorporated in relevant design codes exclusively made for wind turbines. Despite the complex loading conditions of such structures, very limited reference for the fatigue assessment of wind towers has been included in relevant design codes, leading to the use of more generalized calculation tools (like Eurocode EN 1993-1-9) and equations by the designers. Recently a series of accidents related to structural failures associated with wind induced fatigue phenomena, happening both on the tower and the tower foundation have been reported.

The collapse of two slender structures has been analyzed in the work performed by Repetto and Solari [4], taking into account damage associated with all wind induced loading conditions. The two structures were designed to satisfy appropriate Structural Codes criteria as far as ultimate limit state is concerned, but the results of site inspection and fatigue life estimation, proves that even well designed and correctly assembled structures can fail within the elastic stress range due to wind induced fatigue damage. From the very early steps of fatigue analysis, the complex stress histories deriving from wind loading were transformed into pressure cycles following the rainflow method and the Miner's law was implemented for the fatigue life estimation through cumulative damage calculation [5].

Tubular steel wind turbine towers, constituting the framework of the present investigation, are constructed by on-site mounting and joining of tubular subsections by means of bolted flanges with the use of pre-tensioned bolts. These subsections are prefabricated by circumferentially welding subsequent circular rings. The tower is usually mounted on the concrete foundation by means of pre-stressed anchor bolts embedded in concrete and bolted to the lower tower flange. In Nussbaumer et al. [6] design guidelines, it is stated that discontinuities in the material and joint geometry, holes, bolts and welds lead to concentration of stresses and potential fatigue problems, while the mother material very rarely experiences fatigue failures.. Applying a nonlinear dynamic analysis the fatigue life assessment of tubular structures has been has been studied by Jia [7]. Again the rainflow method and Miner's rule have been used to assess the cumulative damage of the structure and to calculate the fatigue life of the structure. The significant contribution of this work is that in the procedure of fatigue life calculation of the structures, material nonlinearities, effects due to wind direction and design particularities due to different structural details are all taken into account. As far as structural details are concerned and according to Lacalle et al. [8],fatigue loading ,inadequate weld design and poor welding execution is in most cases the reason of remarkable stress concentrations around the weld seams and several analyses using different methods have been performed in order to assess the reliability of each method., It is proved by Thanassoulas et al.[9] that pretension is necessary in bolted connections in order for the bolts to develop a constant response throughout their life time, irrelevant of the wind loading intensity.

Inspired by the fact that a big number of welded and bolted joints existing in wind turbine towers are potential sources of fatigue failure and the significant number of catastrophic incidents of wind turbine tower collapses due to fatigue phenomena, the present work aims to enlighten welded and bolted joints design detailing. This is realized through the comparison of the fatigue life of two identical towers whose structural detailing differs, based on the calculation of damage accumulation on three different joints. The first is the circumferential weld connecting the tower shell to the circular flange, named as detail F hereafter, the second is the circumferential weld connecting consequent tower rings in order to constitute a tower module, named as detail W hereafter and the third is the anchor bolt connecting the bottom tower flange to the concrete foundation, named as detail A. For this investigation, finite element analysis of the towers is performed with the aid of the commercial software ABAQUS [10]. The fatigue life of the structures is calculated with the damage accumulation method and more specifically the Palmgren-Miner rule. The comparative results of the tower models are presented and special remarks on the effect of the fatigue design on tower shell thickness and bolt size used are made.

METHODOLOGY

The damage accumulation method constitutes one of the basic methods implemented for the fatigue assessment. The loading events used for this method, as analyzed in Annex A of Eurocode 1993-1-9 [11], are based on prior knowledge obtained from similar structures, in order to represent a credible upper bound of the expected loading that the structure is going to be subjected to. Since the loading type that wind energy converter supporting towers are subjected to is mainly wind, it means that wind loading sequences from similar size prototype structures or site data from existing structures can be used for the fatigue life assessment of similar towers. Since this kind of data is hard to be selected and may also dramatically differ even between seemingly same structures and

geographical areas, the current work proposes the use of artificial loading histories produced by TurbSim [12], Aerodyn [13] and FAST [14] the well-known NREL [15] and NWTC [16] software. The production of artificial loading sequences is thus a cheap and accurate task since well-established software from aerodynamics is used. The wind loading histories are obtained at the tower hub height, for certain terrain roughness category according to the Kaimal frequency spectrum. The loads taken into account in the present study are only the main bending moment and lateral loading caused by the upwind direction.

For the purposes of the present scientific work, the damage accumulation method with determination of fatigue load parameters and verification formats described in Annex A [11] is implemented in three types of structural details that exist in all conventional wind turbine towers. Following this methodology, a preliminary static analysis is first conducted in order to determine which one of the same category structural details is more vulnerable to fatigue failure. The purpose of this method is to obtain the stress history developed in the structural details under consideration that are the most vulnerable to fatigue failure. As prescribed in Eurocodes this stress history is determined from measurements on similar structures or from dynamic calculations of the structural response. In the method presented in the work at hand, the stress histories are determined from the artificial wind loading events applied on the numerical model. There are multiple loading histories applied in each tower, covering the range of operational mean wind speeds. After obtaining the developing stress histories in the structural details under consideration, the rainflow cycle counting method is chosen to convert the complex stress time histories into stress range spectra. The stress range spectra for each mean wind speed are combined in order to constitute the spectrum of amplitudes of stress cycles in one year. Having associated the detail category under investigation with the relevant S-N curve provided in Eurocode tables [11], the damage of the structures can be calculated by applying the linear damage accumulation method, called Palmgren-Miner rule. The accumulated damage is:

$$D_d = \sum_i^n \frac{n_{Ei}}{N_i} \tag{1}$$

where:

n_{Ei}= The number of cycles associated with the stress range $\gamma_{Ff}\Delta\sigma_i$ for band i in the factored spectrum

N_i= The endurance (in cycles) obtained from the factored curve.

In the present case, n_{Ei} is obtained from the design stress range spectrum, whereas the reciprocal value of the damage D_d equals the approximated lifetime of the wind turbine towers.

RESULTS

Taking into account the previously presented methodology, the fatigue life assessment is based on the calculation of the stress histories σ_{zz} at the structural details under consideration. The normal stresses of the three structural details, for each tower and for each one of the six loading time histories are calculated. These normal stresses correspond to the main wind loading that the structure is subjected to; the main rotational moment and lateral force due to wind. The stress histories obtained, are converted to stress range spectra, of stress ranges over number of cycles, by applying the rain-flow cycle counting method with the aid of Matlab software.

The stress range spectra are obtained for six loading time histories of 6, 10, 14, 18 and 22 m/sec mean wind speed, covering the range of any possible operational wind speed. For the fatigue check, the first 10 seconds of the loading time histories are neglected in the analysis due to the presence of signal noise deriving from the launching of the machinery. The stress range histograms of one structural detail of one tower and for all the six time histories are combined in order to constitute the annual stress range histogram, where the annual number of cycles for each stress level is presented. The annual number of cycles of the histogram derives from the sum of the cycles of each 10 min wind multiplied by the relevant probability of occurrence, multiplied by the number of 10 minute durations in one year. According to IEC 61400-1 [17], the distribution of wind speeds over an extended period of time can be simulated following the Rayleigh or the Weibull distribution. In the present study the Rayleigh distribution is used in order to calculate the probability of occurrence of each stress level.

Taking into account the probability of occurrence calculated from the Rayleigh distribution and the annual stress range histograms for each wind mean speed, the annual stress range spectrum for each tower and for each structural detail under consideration is calculated (Fig. 1-3).

As already explained in the introduction, damage due to fatigue is cumulative and the linear damage accumulation assumption is made where stress ranges, occurring n_i times, result in a partial damage that is represented by a ratio n_i/N_i where N_i is the number of cycles to failure. The accumulating damage D_d and its reciprocal value for each structural detail of each tower is presented in Table 1.

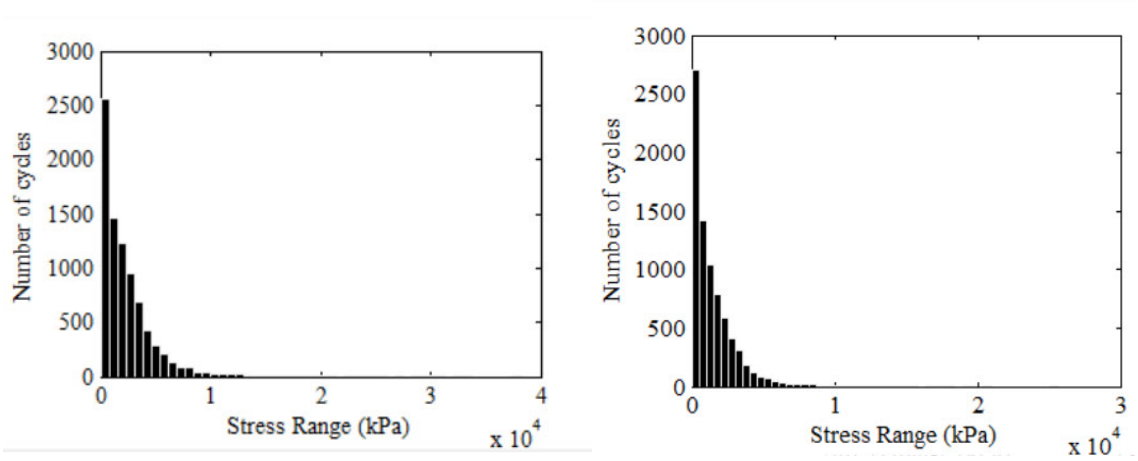

Fig. 1 Design stress range spectra for W detail presented separately for Tower 1 and Tower 2.

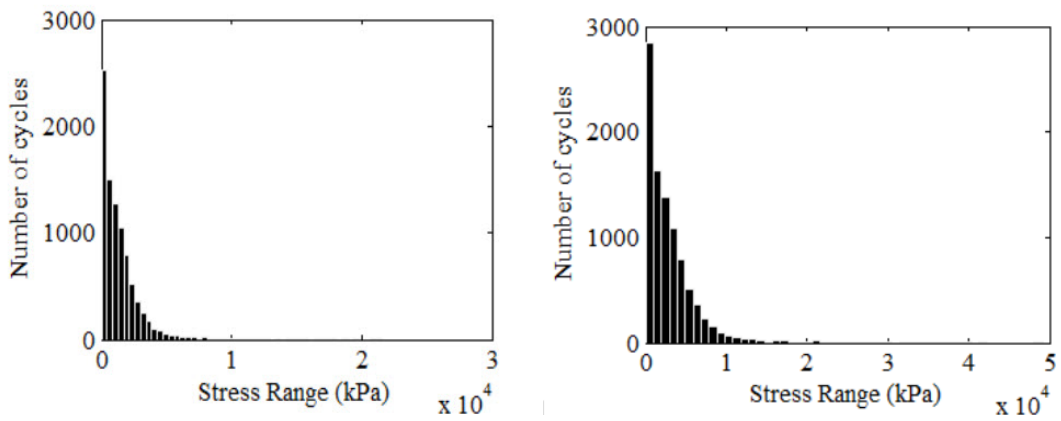

Fig. 2 Annual stress range spectra for F detail presented separately for Tower 1 and Tower 2.

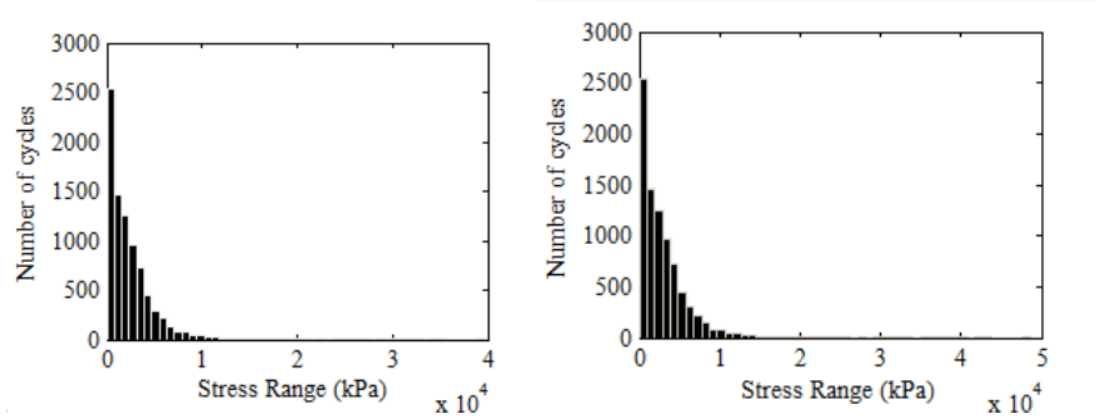

Fig. 3 Annual stress range spectra for A detail presented separately for Tower 1 and Tower 2.

Table 1. Damage and fatigue life of the towers

	Tower 1		Tower 2	
Detail Type	D_d	Fatigue Life	D_d	Fatigue life
W (weld)	0.0007	1428 years	0.0019	526 years
F(flange)	0.0028	357 years	0.0082	122 years
A(anchor)	0.0124	80 years	0.0323	35 years

CONCLUSIONS

The present study evaluates the effect of the shell thickness and bottom diameter increase on the fatigue life calculation of steel tubular wind turbine towers. In the methodology proposed in this work, artificial wind loading histories are used instead of, real wind data. The loads taken into account are derived from the wind action and the assessment of the fatigue effects is conducted by the comparison of the fatigue life of two similar wind turbine towers with same height and bearing capacity but different shell thickness along the tower height and bottom flange diameter. Assessing all structural details, the initial tower (Tower 2) with thinner shell thickness and smaller bottom diameter, appears to have a shorter fatigue life compared to Tower 1. Shell thickness is an important factor in the determination of the tower behavior against wind induced fatigue loading and while the two towers differ in terms of total material used only about 20%, their fatigue life differs about50-65%.Taking into account details W and F, Tower 1 appears to have a longer fatigue life compared to Tower 2 with an increased amount of material used. Despite that fact, both shell thickness solutions appear to have a satisfactory fatigue life exceeding 100 years. When examining the structural detail A, Tower 1 with only 11% longer bottom flange diameter appears to have 60% longer fatigue life. The fatigue life of Tower 2 appears to be low and therefore, for towers with identical shell thickness solutions, greater bottom flange diameters are preferred since their capacity against fatigue loading is higher. Fatigue problems in wind turbine towers are usually solved by increasing shell thicknesses along the tower that obviously results to non-economic structures, whose satisfactory fatigue behavior is possible to be achieved with thinner shells. On the other hand, greater bottom diameters lead to the construction of more robust structures with the same material used.

ACKNOWLEDGEMENTS

The support of the COST TU1304 Action “Wind Energy Technology Reconsideration to Enhance the Concept the Concept of Smart Cities (WINERCOST) is gratefully acknowledged by the authors. The first author expresses with thanks her gratitude to IKY for financial support of the research activities on performing her PhD thesis through the IKY Fellowship of Excellence for Postgraduate Studies in Greece – SIEMENS Program.

REFERENCES

[1] Bazeos, N., G.D. Hatzigeorgiou, I.D. Hondros, H. Karamaneas and D.L. Karabalis et al., “Static, seismic and stability analyses of a prototype wind turbine steel tower”, Engineering Structures, Vol.24, 2002, pp. 1015-1025

[2] Lavassas, I., G. Nikolaidis, P. Zervas, E. Efthimiou , I.N. Doudoumis and C.C. Baniotopoulos, “Analysis and design of the prototype of a steel 1-MW wind turbine tower”, Engineering Structures, Vol.25, 2003, pp. 1097-1106

[3] Dimopoulos, C. and C. Gantes, “Experimental investigation of buckling of wind turbine tower cylindrical shells with opening and stiffening under bending”, Thin-Walled Structures, Vol.54, 2012, pp. 140-155

[4] Repetto, M.P. and G. Solari, “Wind-induced fatigue collapse of real slender structures”, Engineering Structures, Vol.32, 2010, pp. 3888-3898

[5] Suresh Kumar, K. and Stathopoulos T., “Fatigue analysis of roof cladding under simulated wind loading”, Journal of Wind Engineering and Industrial Aerodynamics, Vol.77&78, 1998, pp. 171-183

[6] Nussbaumer, A., L. Borges and L. Davaine, “Fatigue Design of Steel and Composite Structures, Wiley, Germany, 1st Edition, 2011, pp. 334

[7] Jia J., “Wind and structural modeling for an accurate fatigue life assessment of tubular structures”, Engineering Structures, Vol.33, 2011, pp.477-491

[8] Lacalle, R., S. Cicero, J.A. Alvarez, R. Cicero and V. Madrazo, “On the analysis of the causes of cracking in a wind tower”, Engineering. Failure Analysis, Vol. 18, 2011, pp. 1698-1710

[9] Thanasoulas, I., K.G. Koulatsou and C.J. Gantes, “Nonlinear numerical simulation of the response of bolted ring flanges in wind turbine towers”, Proceedings of the 8th Hellenic National Conference of Steel Structures, Oct. 2-4, Metal Structures Research Society, Greece, 2014, pp. 159-169.

[10] DS, “Abaqus analysis user's manual”, Dassault Systemes, Abaqus 6.12, Providence, RI, 2012, USA. http://www.maths.cam.ac.uk/computing/software/abaqus_docs/docs/v6.12/books/usb/default.htm

[11] CEN, “Eurocode 3: Design of steel structures – Part1-9: Fatigue”, European Committee for Standardization, Belgium, 2005

[12] Kelley, N. and B. Jonkman, TurbSim. Department of Energy, NWTC Information Portal, U.S., 2012, https://nwtc.nrel.gov/TurbSim
[13] Laino, D.J., AeroDyn. Department of Energy, NWTC Information Portal, U.S., 2013, https://nwtc.nrel.gov/AeroDyn
[14] Jonkman, J., FAST. Department of Energy, NWTC Information Portal, U.S., 2005, https://nwtc.nrel.gov/FAST
[15] NREL, "National Renewable Energy Laboratory", Department of Energy, U.S.A., 2015
[16] NWTC, "National Wind Technology Center", Department of Energy, U.S.A., 2015
[17] International Electrotechnical Commission, "Wind Turbines-Part 1:Design Requirements", IEC, Geneva, Switcherland, 2005

THE INTERNATIONAL CONFERENCE ON
WIND ENERGY HARVESTING 2017
20-21 April 2017
Coimbra, Portugal

Paper 317

AEROELASTIC RESPONSE ASSESSMENT OF BEND-TWIST COUPLED ROTOR BLADES

Mohammad Reza Shah Mohammadi[1]
ISISE, Department of Civil Engineering, University of Coimbra, P-3004 516,
Coimbra, Portugal

Carlos Alberto Silva Rebelo[2]
ISISE, Department of Civil Engineering, University of Coimbra, P-3004 516,
Coimbra, Portugal

ABSTRACT

The main purpose of this research is devoted to the design of new evaluation procedure for the bend-twist elastic coupling which is efficient and precise with relatively low computational time. Moreover, three coupled blade designs based on SmartBlades reference blade are designed and assessed for the first time for the full scale rotor blades. The evaluation process used a 2D cross sectional analysis to divide the rotor blade into several cross sections and derive their properties. Subsequently, the 1D anisotropic finite element method was used to create the beam model from the cross sections and calculate the element stiffness. To analyze this beam model, the aerodynamic loads on the blade were calculated based on the blade element momentum method. The procedure was initiated with load calculation by Blade Element Momentum and then iterative process due to change of angle of attack caused by bend-twist coupling. The deflection responses, root bending moment, load mitigation and power generation are studies in the post-processing phase. In conclusion, low computational cost and responses precision compared to the conventional 3D finite element models shows that the new evaluation process is promising. Moreover, it can be used as a preliminary analysis tool for the coupled blades assessment.

NOMENCLATURE

BEM	=	Blade Element Momentum
BTC	=	Bend Twist Coupling/Coupled
CFD	=	Computational Fluid Dynamic
FE	=	Finite Element
FEM	=	Finite Element Method

INTRODUCTION

The bend twist stiffness coupling can be introduce in the blade structure as a passive controlling approach. Basically, bend twist coupling causes the blade twist towards feather or stall. So, angle of attack changes to mitigate the load or produce more power.

Aeroelastic tailoring is not a young concept. Initially, Botterell designed a mechanism called balanced pitch rotor in 1981[1]. This mechanism reacts against unbalanced pitching moments with the passive cycle pitch. One of the early research on passive torsional deformation has been done by Koijman in 1996 [2]. The main objective of his study was to develop an analysis for bend-torsional material coupling in wind turbine rotor blade. Lobitz et al. investigated the application and the behavior of twist coupled blades. They claimed around 25% of energy gain in stall control method. Besides, passive twist coupling improves reliability and lowering the installed cost [3].

[1] PhD Candidate, ISISE, Department of Civil Engineering, University of Coimbra, P-3004 516, Coimbra, Portugal /mrsm@uc.pt

[2] Associate Professor, ISISE, Department of Civil Engineering, University of Coimbra, P-3004 516, Coimbra, Portugal /crebelo@dec.uc.pt

A series of research has been done since 2004 to 2010 by SANDIA which leads to a 9 meter research size wind turbine blade called TX-100. The bend-twist coupled prototype extended to mitigate the load at the peak loads during wind turbines operation conditions [7]. Maheri developed a design code to analyze the smart blades in order to maximize the power yield and minimize the maximum loads on the blade [10]. Bottasso et al investigated an optimization on bend-twist coupling parameters. They try to suggest the best fiber layout for their 19 meter blades [11]. Fedorov and Berggreen describe the potential of bend-twist coupling of wind turbine blades. They presented that in commercial blades the magnitude of 0.2 is feasible for carbon fiber rotor blades. Furthermore, by substituting the glass fibers it can be reached to 0.4 [12].

As it explained before, the cost of wind turbines are high and extra process on bend-twist coupling evaluation in rotor blades will increase this cost. Therefore, the absence of fast, robust, and precise tool chain can be sensed. The current research connects BEM and Anisotropic Finite Element Method methods for the load estimation and the structural analysis to evaluate the bend-twist coupling in the commercial size rotor blade. All similar research has been done on research size rotor blades and they used 3D FE or complex algorithm which cost a lot computationally and economically.

In this paper, the baseline blade structure and the new innovative tool chain for analysis the blades are explained in detail first. Then, the designed coupled rotor blades are described. Finally, the deflection response of the blades, root bending moments, and load mitigation are presented.

METHODOLOGY

The baseline blade is IWT-7.5-164 wind turbine rotor blade [13]. As it can be seen in Figure 1 the blade consists of main body with the Balsa, Biax and Triax materials, the shear webs and split spar caps from carbon fibers, Balsa and Foam material, and the steel root.

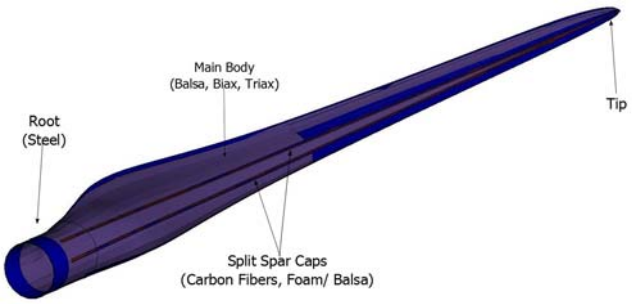

Figure 1: Composite Blade Structure

Moreover, each blade consists several airfoils with different aerodynamics properties, however, the airfoil material and structure are almost the same all along the blade. In this study innovative split spar cap structure and the material is introduced and illustrated in **Error! Reference source not found.**[14].

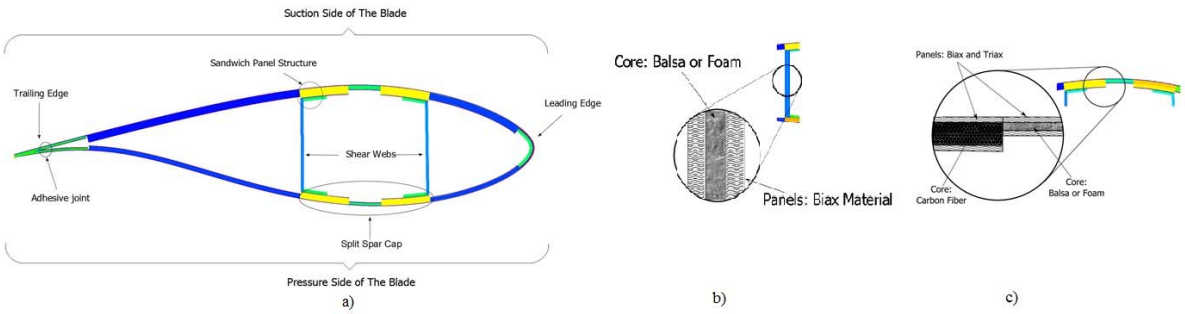

Figure 2: (a) The airfoil structure with the split spar cap, (b) The material layout in the shear web, (c) The material layout in spar caps

In order to be able to design the blade a tool chain is designed based on existing tools and in-house codes. The General layout of the tool chain is presented in Fig.3-a. The tool chain can be divided to four geometry creation, material layup and mesh generation, processing, and simulation blocks. The main contribution of this research has been done in the simulation and the processing blocks. In the simulation block, CCBlade from NREL which uses the BEM method is utilized to estimate the wind loads with the respect to the input data from the geometry creation block [15]. In the processing section, cross sectional analysis is applied on the blade and the properties of the

sections are calculated based on anisotropic FEM theory with BECAS from DTU [16]. Eventually, the in-house FE model is created based on the sections and their properties. Therefore, the blades can be analyzed in FE model with having the stiffness properties and the loads. Finally, the results are sent for the post processing.
In Fig.3-b, the evaluation procedure and the connections between codes are presented more in detail.

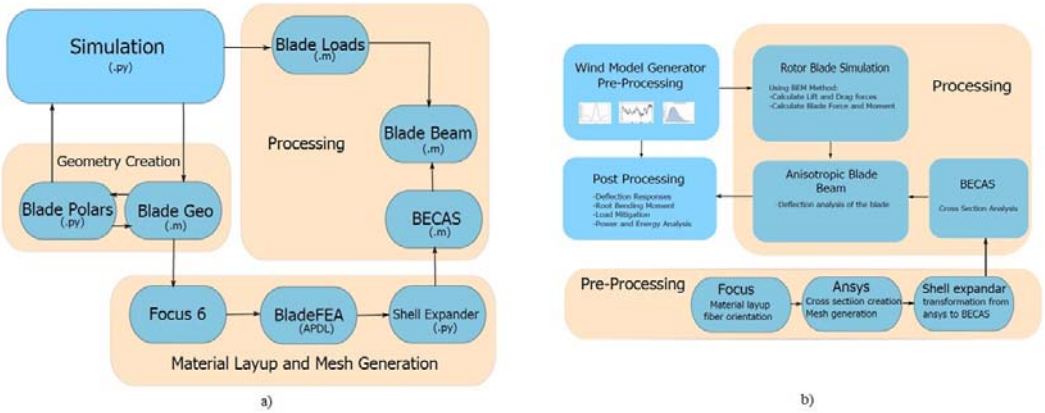

Figure 3: (a) The schematic view of the tool chain, (b) The illustration of the evaluation procedure

To evaluate several wind profile and capturing the load mitigation and calculating root bending momentum with consideration of bend-twist coupling influence, an iterative procedure runs between simulation block and FE model. The bend-twist coupling causes a change in the angle of attack at each step when the new wind loads are calculated. Therefore, the new angle of attack which means additional induced rotation plus the angle of attack is sent back to the aerodynamic part. The simple schematic of evaluation algorithm is shown in Figure 4.

The new evaluation process in this research is applied on the baseline rotor blade and three coupled rotor blade. The baseline blade is 80m split spar cap design as it presented in [14]. The baseline model properties are presented in Table 1. The initial coupled blade are designed based on the work in [11]. The coupled blades specifications and layout are listed in Table 2 which has been done in [17] at IWES.

Table 1: Reference Blade Parameters

	Unit	Value
Blade Length	m	80
Total Blade mass	Kg	30989
Blade Surface	m^2	646.6463
Max. Tip deflection	m	11.86
Design tip speed ratio	-	84

Table 2: Coupled Blade Specifications

Coupled blade	Skin Fiber	Spar cap Fiber	Starting length [m]
20sk-5sc	20º	5º	2
20sk5sc	20º	5º	55
20sk-7.5sc	20º	7.5º	55

As the bending stiffness is reduced by implementing the BTC over the entire length of the blade, the fibers rotation was performed only after 55m of blade length in two blades. The influence of spar cap fiber rotation is much higher in stiffness reduction.

The normal forces are higher at the tip of the blade, so it is reasonable to mitigate only the most effective loads which cause the higher moments at the root. In Fig. 5, different fiber rotation in spar cap and skin is illustrated.

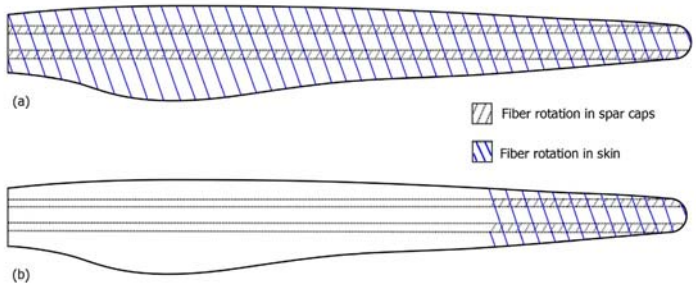

Figure 4: Fiber rotation changes in (a) complete blade length (b) after 55m of blade length[17]

RESULTS

In the following section the simulation results for different load cases. Moreover, the root bending momentum and load mitigation are discussed. The blades deflection and induced rotation for the 8 m/s wind speed are shown in Fig.4 which blade characteristics are also can be obtained. If the wind load is exerted on the blade in a single step is compared with the non-linear steps loading. In this case, the deflection responses are compared together and the results are illustrated in Table 3.

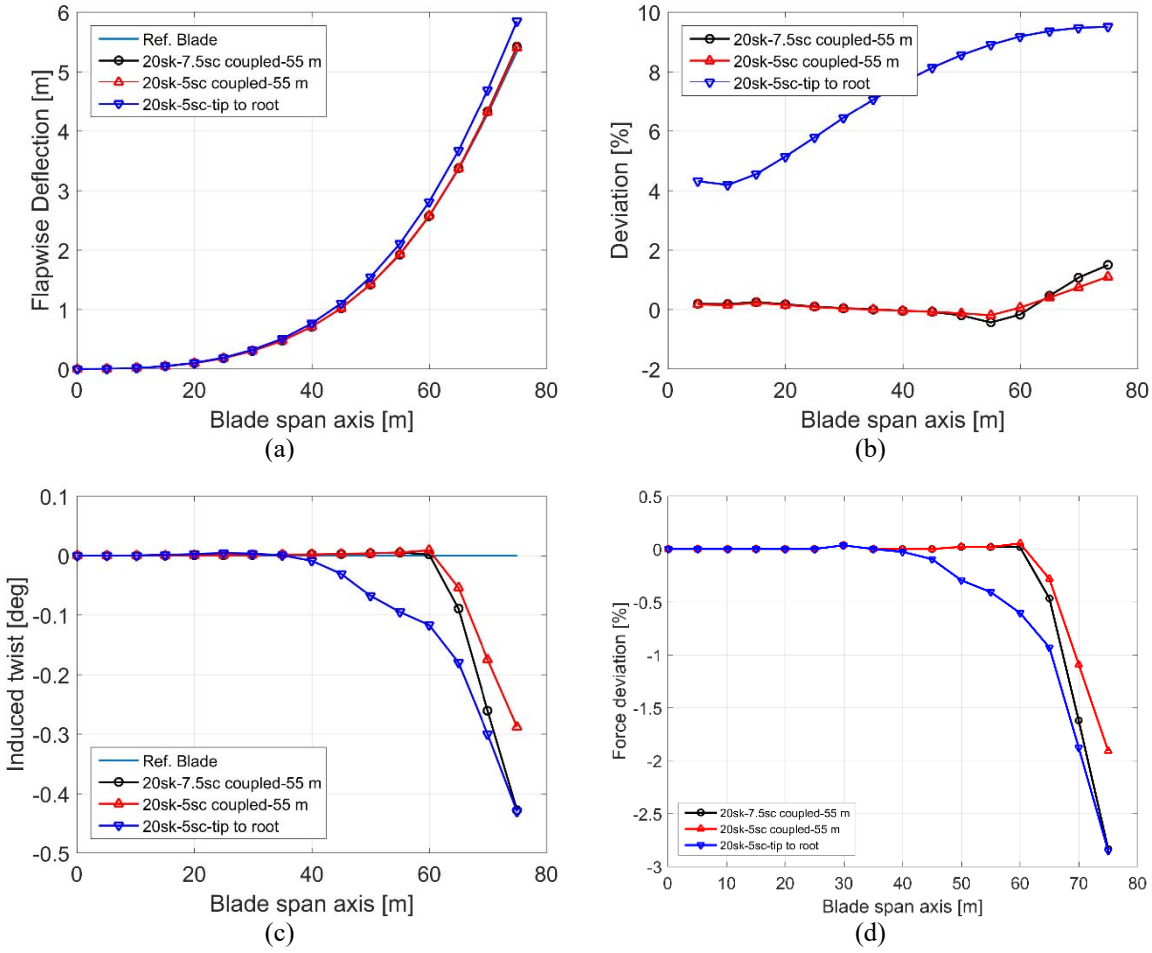

Figure 5: (a) Deflection responses due to 8m/s wind speed for different blade models, (b) Blade deflection along the blade, (c) Induced rotation along the blade due to the coupling, (d) Load reduction along the blade by induced rotation

Table 3: Tip deflection of the blades due to static linear and non-linear 8m/s wind load

Blade Model	Tip Deflection for the Linear Loading[m]	Tip Deflection for the Non-Linear Loading[m]
Ref. Blade	6.132	6.132
Partially coupled 20sk-7.5sc	6.3036	6.2275
Partially coupled 20sk-5sc	6.2811	6.231
Fully coupled 20sk-5sc	6.7146	6.6235

A simulation is run from 1m/s to 11 m/s and in each step root bending moment is calculated. The results for different coupled blades and reference blade are listed in Table 4. Furthermore, the load mitigation is observed in all bend-twist coupled blades. The maximum of 1.43%, 1.1%, and 0.72% can be mentioned respectively for F20sk-5sc, P20sk-7.5sc, and P20sk-5sc coupled blades in comparison with the reference blade.

Table 4: Root bending moment experienced in each wind speed by blades in MNm

Wind Speed (m/s)	Ref. Blade	P.20sk-7.5sc	P20sk-5sc	F20sk-5sc
1	0.174	0.174	0.174	0.174
2	0.703	0.703	0.703	0.703
3	1.583	1.583	1.583	1.582
4	2.816	2.813	2.814	2.812
5	4.401	4.392	4.395	4.389
6	6.339	6.318	6.6325	6.6311
7	8.629	8.588	8.601	8.575
8	11.270	11.198	11.222	11.176
9	14.262	14.145	14.186	14.108
10	17.611	17.424	17.487	17.367
11	21.309	21.032	21.126	20.946

The overall simulation time is calculated around 71 seconds for each wind speed interval while it is more than an hour for the 3D FEM models. Moreover, the deflection of the reference blade out of ANSYS and 1D FE model are compared and the maximum error at the tip of the blade is less than 5%.

CONCLUSIONS

To evaluate and select the preliminary coupled blade designs, the described tool chain is proposed. Using BEM method for estimation of the aerodynamic loads on the blade and accordingly the anisotropic FEM method for the cross sectional analysis, make the evaluation process robust and provides the precise results with the low computational cost. Many other evaluation tools using 3D FEM/CFD were existed as it explained before which are highly computational expensive and complex in the sense of aerodynamic loads calculations. Therefore it is considered that the proposed tool is an efficient compromise between numerical calculation precision and computational time costs. The favorable bend-twist coupled blade design can be proposed based on this evaluation process.

Moreover, calculating damage equivalent load, developing more bend-twist coupled design samples, and cost analysis due to load reduction and the less power generation can be considered for the future work.

ACKNOWLEDGEMENTS

The first author acknowledges with thanks the support of Fraunhofer-Institut für Windenergie und Energiesystemtechnik IWES and the opportunity to develop work in the SmartBlades project on the industrial bend-twist coupled rotor blades. The support from European Union's research and innovation program H2020-MSCA-ITN-2014 under grant agreement No 643167 (AEOLUS4FUTURE) is kindly acknowledge.

REFERENCES

[1] Bottrell G.W. "Passive cyclic pitch control for horizontal axis wind turbines". Proceedings of a Workshop on Wind Turbine Dynamics, NASA Conference Publication 2185, DOE Publication CONF-810226, Cleveland, OH, February 1981; pp.271–276.

[2] Kooijman H.J.T., "Bending-Torsion Coupling of a Wind Turbine Rotor Blade." Basic Research Program Report, ECN, 1996

[3] Lobitz D.W., Veers P.S.,"Aeroelastic Behavior of Twist-Coupled HAWT Blades". American Institute of Aeronautics and Astronautics, AIAA-98-0029, 1998.

[4] Veers P.S., Bir G., Lobitz D.W. "Aeroelastic tailoring in wind-turbine blade application". Wind power '98, AWEA Annual Conference and Exhibition, Bakersfield, CA, April 27 - May 1, 1998.

[5] Lobitz D.W., Veers P.S., et al. "The Use of Twist-Coupled Blades to Enhance the Performance of Horizontal Axis Wind Turbines". Sandia Report SAND 2001-1303, Sandia National Laboratories, Albuquerque, NM, May 2001.

[6] Lobitz D.W., Veer P.S. "Load Mitigation with Bending-Twist-coupled Blades on Rotors Using Modern Control Strategies" Journal of Wind Energy. 6, 2003, p. 105-117.

[7] Locke J., Valencia U., "Design Studies for Twist-Coupled Wind Turbine Blades". SAND 2004- 0522, Sandia National Laboratories, June, 2004.

[8] Berry D. "TX-100 Manufacturing Final Project Report." Sandia Report SAND 2007-6066, Sandia National Laboratories, Albuquerque, NM, November 2007.

[9] Ashwill T.D. "Passive load control for large wind turbines". 51st AIAA/ASME/ASCE/AHS/ASC Structures, Structural Dynamics, and Materials Conference, Orlando, Florida, April 12-15, 2010.

[10] Maheri A, Noroozi S, Vinney J. "Application of combined analytical/FEA coupled-aerostructure simulation in design of wind turbine adaptive blades". Renewable Energy, 32(12), pp 2011-2018, 2006.

[11] Bottasso CL, Campagnolo F, Croce A, Tibaldi C. "Optimization-based study of bend-twist coupled rotor blades for passive and integrated passive/active load alleviation". Wind Energy 2013, 16:1149-1166, 2013.

[12] Fedorov V.A., Berggreen C., "Bend-twist coupling potential of wind turbine blades". Journal of Physics: Conference Series 524, The Science of Making Torque from Wind 2014 (TORQUE), 2014.

[13] Sevinc A., Rosemeier M., Bätge M., et al. IWES Wind Turbine IWT-7.5-164. Specification Revision 00, Leibniz Universität Hannover and Fraunhofer IWES, Hannover, Germany, December 30, 2013.

[14] Rosemeier M, Bätge M "A Concept study of a carbon spar cap design for a 80m wind turbine Blade" The Science Making Torque from Wind, Copenhagen, Denmark, 2014.

[15] NWTC Information Portal (CCBlade). https://nwtc.nrel.gov/CCBlade. Last modified 21- September-2014; Accessed 07-October-2014

[16] Blasques J.P.A.A., Bitsche R., Fedorov V., EderM.A. Applications of the BEam Cross section Analysis Software (BECAS) Proceedings of the 26th Nordic Seminar on Computational Mechanics, pp. 46-49433-456, 2013.

[17] Velichappattuparambil J. S., (2014) "Application of Bend-Twist Coupling on a Wind Turbine Blade", Master Thesis, Fraunhofer IWES, Bremerhaven, Germany.

THE INTERNATIONAL CONFERENCE ON
WIND ENERGY HARVESTING 2017
20-21 April 2017
Coimbra, Portugal
Paper 318

BUILT-ENVIRONMENT WIND ENERGY APPLICATIONS- AN INTRODUCTION

Evangelos Efthymiou [1]
Aristotle University of Thessaloniki
Thessaloniki, Greece

Gülay Altay [2]
Doğuş Üniversity
Istanbul, Turkey

ABSTRACT

Urban wind energy represents a modern field in renewables and is basically defined as the integration of small wind energy into the built environment. Differing from rural conditions, where small wind turbines are mostly utilized, the unique features of urban framework set significant issues to be addressed regarding their performance. The present paper summarizes the types of built-environment wind turbine applications and highlights their special characteristics. The work aims to provide a brief introduction of safety aspects regarding the deployment of urban wind systems and outlines the issues to be addressed from structural point of view towards better understanding of their behaviour.

INTRODUCTION

It is widely acknowledged that significant steps have been undertaken from countries, international organizations such as United Nations to promote the use of renewable energy resources towards sustainable energy, reduced greenhouse gas emissions and a lower dependency from oil. Harnessing wind to generate electricity has proved throughout the years as prevailing source of clean energy forms. Due to technological and industrial development along with adopted policies by states, wind energy sector has experienced tremendous growth. Nowa-days, onshore wind energy utilized in rural land and remoted regions has reached maturity and off-shore activity deployed in sea and marine environment is rapidly developing both in re-search and implementation. According to Global Wind Energy Council, the global demand for wind energy is expected to reach 4.2%-5.8% until 2050 [1].

In the last decade, wind energy sector investigated the expansion of its applications into the built environment through exploitation of small wind energy and introduced urban wind energy. As defined in the technical report-roadmap prepared by Smith et al. in 2012 for the US National Renewable Energy Laboratory (NREL), built environment wind turbines (BWTs) are the wind energy production systems located in an urban or suburban environment. Most of these applications are also classified as small wind turbines (SWTs), therefore a more generic description would be “the application of small wind turbines within a built environment framework” [2].

The field of urban wind energy may be still at primary stage, but gradually it exhibits significant growth rhythm and great potentials for wider utilization. Current data from industry as well recent research projects demonstrate that there are promising opportunities to integrate wind energy in the built environment in effectively. Many people are motivated by a desire to be environmentally responsible, and they want clean, renewable energy to help power their homes or businesses.

As the industry is developing and the cost of small wind turbines is reduced, built-environment applications are becoming more attractive and approachable [3]. In pursuit if energy independence and driven by environmental awareness, more and more people who want renewable energy to enhance power for their homes or businesses have nowadays easier access to this technology. A remarkable growth in built-environment wind turbine unit sales has been registered in recent years. Indicatively, 1,074 roof-top units were installed in US market in 2010, representing an increase of 430% related to 2009 [4]. At global scale, according to the 2015 small wind world report summary, the recorded small wind capacity installed worldwide has reached more than 755 MW as of the end of 2013. This represents a growth of more than 12% compared with 2012, when 678 MW were registered [5]. The acknowledged easier consumer access to small wind turbines resulted in boosting sales and accelerating applications.

The present paper summarizes basic aspects of urban wind energy and aims to provide an introductory background regarding respective built-environment applications. Within the framework of the study, current types

[1] Lecturer, Dr Civil Engineer, Institute of Metal Structures, Dept. of Civil Eng., GR-54124/vefth@civil.auth.gr
[2] Professor, Dr Civil Engineer, Dept. of Civil Eng., 34342 Bebek, Istanbul, Turkey/ askarg@boun.edu.tr

of applications are summarized and to highlight the respective built-environment applications. Structural design aspects of these structures need to be further investigated so that both safety and material economy can result in cost-efficient power generators. Despite the wide application of these systems, structural aspects of their behavior and their response under dynamic loadings need to be enlightened.

BUILT ENVIRONMENT WIND ENERGY APPLICATIONS

Wind turbines can be subdivided into different categories: large (>1 MW), medium (40 kW–1 MW), small (40-20 kW) and micro (20-0.4 kW) [8], while in most cases the typical limit for classifying as small wind is the upper limit of 50kW [6]. In view of turbines that are utilized in built environment wind applications, they are two types, namely the horizontal axis wind turbines (HAWTs) and the vertical axis wind turbines (VAWTs). HAWTs are sensitive to the changes in wind direction and turbulence which have a negative effect on performance due to the required repositioning of the turbine into the wind flow. The best locations for HAWTs are open areas with smooth air flow and few obstacles. In Figure 1 some HAWT models are depicted. Much historical developments of wind turbine technology have focused on HAWTs, although VAWT machines may be more appropriate to the urban context [7]. However, the recent ap-plications of VAWTs provide even better results than horizontal ones, as they use all the different directions of wind flow and are quieter in operation. The type designs include Savonius, Darrieus and H-rotor (Fig.2). In general, VAWTs can produce electrical energy in separate units or they can be used as an integrated system for connecting with an electrical network. Although VAWTs have shown to have advantages over HAWTs, their installation heights are limited and their blades are prone to cyclic fatigue. For large-scale turbines, the market has converged on the three-bladed horizontal axis turbine as the right way forward for multi-megawatt turbines. Furthermore, the main manufacturers now only produce these types and so there is little option for most to opt for large scale VAWTs.

a) Swift

b) Eclectic

b) WES Tulipo

Figure 1. Models of HAWTs [8]

a) Turby

b) Windside

b) Ropatec

Figure 2. Models of HAWTs [8]

Regarding the types of built-environment installations, generally there are three basic types:

a) Building mounted (roof, side)

b) Ground mounted- Standalone small scale wind turbines
c) Building integrated-Building augmented

The majority of built-environment wind applications are roof-mounted small wind turbines with a rated power of 10 kW or less, see Figure 3a [9]. In case of a conventional horizontal axis wind turbine (HAWT), the rotor diameter is less than approximately 7m. Besides HAWTs, several horizontal axis wind turbines (VAWTs) have gained public interest, and some manufacturers market their VAWTs for urban and suburban installations. Small wind turbines can be safe and reliable. Installing them on towers tall enough to place them well above any nearby obstacles, increases production and reduces turbulence-induced loads. However, according to Stankovic et al. home-mounted wind turbines require a relatively high level of knowledge and investment in time in order to avoid unnecessary complications and poor energy yields [10]. This includes understanding key issues such as predicting available wind resources, avoiding turbulence, mitigating environmental impacts, preventing structural damage and understanding the economic aspects. It will also often involve applying for grants, obtaining planning permission, dealing with the production of the electricity (e.g. selling to the grid) as well as maintenance issues.

Another option is the erection of a standalone wind energy unit within the urban environment, see Figure 3b. A free-standing urban wind turbine can be a relatively simple option as it can be procured in an 'off-the-shelf' manner suitable for developers, investors, energy service companies and community schemes [9]. If the impacts of installing wind energy are demonstrably low and local wind resources demonstrably high, a stand-alone wind turbine offers a very real means of addressing concerns such as energy security, pollution, and of course cli-mate change while producing an attractive source of income.

One of the approaches being used, and investigated more frequently, is the incorporation of wind turbines into the design of the building (Figure 3c). Wind turbines located at the high wind speed zones in buildings are called Building Integrated Wind Turbines or Building Augmented Wind Turbines (BAWTs), and the wind turbine makes use of buildings as a concentrator of wind. For retrofit applications can only be positioned to invest any augmentation afforded by the existing building [6]. Based on air naturally flows from areas of high pressure to areas of low pressure, the most effective locations for wind turbines will be either in the accelerated shear layers around the edge and top of the building, or in specially developed passages linking the areas of positive and negative pressure.

Building-integrated turbines are limited to new developments in relatively windy areas and will have natural constraints in the size of turbines they can accommodate. The role of the architect is very significant in configuring the building in an aerodynamic, while the value of the possible cultural benefits should not be underestimated as architecture simultaneously reflects and influences culture and cultural changes. Having these powerful dynamic symbols integrated directly into the heart of urban communities could have positive effects in terms of environmental action (e.g. homeowners improving energy efficiency or engaging directly in renewable energy). Despite their limitations that influence their wider applicability, these type of built-environment application are still at primary stage and efforts are ongoing in order to become viable.

a) Roof mounted b) Ground mounted c) Building integrated

Fig. 3. Types of built-environment wind applications [2]

DESIGN ASPECTS-STRUCTURAL ISSUES

To date, most wind turbines installed in the built environment have been sited with limited understanding of or disregard for the unique challenges of urban framework, with some of them to be briefly presented in the

remaining of the text. Most small wind turbines were designed for the open areas common to rural environment. However, built environment is characterized by higher turbulence, lower average wind speed, more frequent wind direction change and potentially higher vertical inflow [2]. These installations are often located in areas where the wind is blocked or diverted by upstream obstacles and may present issues related to safety, turbine durability, effects on the building, and energy production. The shading and turbulence effects of surrounding obstacles may produce com-plex wind patterns that are difficult to predict, while traditional wind resource maps prove inadequate as wind conditions are evaluated at greater altitude of 50m while most small wind turbines do not reach above 30m [5].

One of the major issues relates to the quality of wind resources at rooftop level and despite the common belief that the wind resources on roofs is adequate for these applications, actually they lack effectiveness. They are much slower than in open sites and they are also less uniform. In addition, the swirling turbulent character of low-level urban wind, due to the complex interaction of the wind with buildings, is detrimental to the amount of energy that can be extracted. These swirling flows also exert irregular stresses on the blades and so also reduce the longevity of the turbine. Underperformance is widely reported for many built-environment wind installations, caused basically by a poor understanding of the wind resources. An exam-ple of this situation is the case study of a turbine at the Boston Museum of Science, which was installed primarily inside a roof recirculation eddy. The implementation of CFD analysis revealed that the winds flow on the bottom part of the turbine, opposed to the prevailing winds and the wind through the top part of the turbine [11].

There are a number of concerns frequently expressed in relation to home-mounted wind tur-bines. Most relate to manufacturers encouraging homeowners, who do not fully understand all of the key issues, to erect small turbines on their roofs (which can lead to disappointment and frustration). It is clear that, standard walls and chimneys are not built to withstand the types of prolonged stresses originating from a turbine mast. Therefore, these structures, unless specifically designed for the purpose, or assessed by structural experts, should not be used as they could present a real safety threat, e.g. from falling bricks, tiles or turbines.

Differing from small wind systems, which are mostly located in rural settings, built-environment wind turbines are designed to be in close proximity to people, businesses and other property. The issues of appropriate siting and operation is of extreme importance, since poor siting and improper use could lead to turbine failure and possible resulting in injury, property damage and potential liabilities.

From structural point of view, built-environment wind turbines have not yet been thoroughly investigated, therefore the need to address safety issues is imperative, as outlined in the most recent report prepared by National Renewable Energy Laboratory [2]. According to the latter, the objectives of fatigue resistance, braking redundancy, fail safe mechanisms and ice-and part-shedding containment were identified as critical barriers to overcome in order to provide reliable and structurally viable applications.

With respect to fatigue life of the turbines, better understanding of the fatigue issues in the built environment is required to remedy safety concerns. Lower average wind speeds in the built environment may reduce one aspect of fatigue loads on BWTs. However, increased turbulence intensity and directional variability will increase another aspect of fatigue loads on a turbine, reducing its design life. Moreover, special consideration shall be given in order to prevent failure in a catastrophic manner, in case of a possible failure. The system should in-corporate fail-safe mechanisms and design philosophies

BWTs require a redundant braking method to stop the rotor even if the turbine has partially failed, leaving the primary brake inoperable. A BWT must not be allowed to operate without control or load (a condition in which the rotor spins uncontrollably fast and may lead to catastrophic failure). If an SWT in a rural environment enters rotor overspeed, the owner typically protects himself and others by staying away until the winds calm and the rotor can be stopped by other means. In a built environment, waiting for calm winds is not an option.

Ice-shedding and part-shedding incidents have been infrequent, but risks are present, and in-creased numbers of built-environment installations also increase the magnitude of these concerns. It is worth noting that parts and ice can be tossed long distances, and it is difficult to predict where they may land. Part-shedding cannot be predicted, but there must be a way to contain this safety hazard. Ice-shedding can be expected after an icing event, but no small wind turbines on the market automatically respond to ice build-up.

CONCLUSIONS

The objective of integration of wind turbines into the built environment is not a simple issue. Besides technical aspects that are still at primary stage, namely not yet identified, defined and studied, there are also socio-economic parameters as well as public acceptance that need to be addressed before wider implementation. Most small wind turbines were designed for rural areas, not the built environment with its high turbulence, lower average

wind speed and more frequent wind direction changes, and potentially higher vertical inflow. Nor were turbines de-signed to be in close proximity to people, businesses, and other property. Poor siting and improper use of BWTs not only results in underperformance, which is widely reported, but also could lead to turbine failure, possibly resulting in injury, property damage, and potential liabilities. In view of safety aspects, the process of structural treatment of these applications, namely understanding the loads, considering the special features of urban terrain, analyzing the interaction with buildings, assessing resonance phenomenon, is imperative in order to achieve better understanding of their behavior, conferring to reliable urban wind energy units.

ACKNOWLEDGEMENTS

The support of the COST TU1304 Action "WINERCOST- Wind Energy Technology Reconsideration to Enhance the Concept the Concept of Smart Cities" is gratefully acknowledged by the authors.

REFERENCES

[1] GWEC-Global Wind Energy Council, "Global Wind Report 2014 - Annual market up-date", Global Wind Energy Council, Brussels, 2015.
[2] Smith J, Forsyth T, Sinclair K, Oteri F., "Built-Environment Wind Turbine Roadmap", NREL-National Renewable Energy Laboratory, NREL/ TP-5000-50499, Colorado, USA, 2012.
[3] James PAB, Sissons MF, Bradford J, Myers LE, Bahaj AS, Anwar A, Green S, "Sea-water Implications of the UK Field Trial of Building Mounted Horizontal Axis Micro-Wind Turbines", Energy Policy, Vol.38, Issue 10, 2010, pp. 6130-6144.
[4] AWEA-American Wind Energy Association, "2010 U.S. Small Wind Turbine Market Report", Washington, DC, 2011.
[5] WWEA-Word Wind Energy Association, "2015 Small Wind World Report Summary", WWEA, Bonn, Germany, 2015.
[6] Megahed NA. "Welcoming the wind: Potential for urban wind turbines to reshape the built environment", Proc. of the 2nd International Conference on Energy Systems and Technologies, 18-21 Feb, Cairo, Egypt, 2013, pp. 257-268
[7] Walker SL. "Building mounted wind turbines and their suitability for the urban scale- A review of methods of estimating urban wind resource", Energy and Buildings, Vol. 43, Issue 8, 2011, pp. 1852-1862.
[8] Cace J, Ter Horst E, Syngellakis K, Niel M, Clement P, Heppener R, Peirano E, Urban wind energy-Guidelines for small wind turbines in the built environment, accessed in 2015. (available at http://www.urban-wind.org/pdf/SMALL_WIND_TURBINES_GUIDE_final.pdf)
[9] Wineur, "Urban wind turbines: Technology review", Work performed by Wineur. Europe: Intelligent Energy Europe, 2005.
[10] Stankovic S, Campell N, Harries A., "Urban Wind Energy", 1st Edition, BDSP Part-nership Ltd, Earthscan, UK, 2009.
[11] Viti V, DesAutels C, Schulman L, "Computational Model of the Flowfield around the Museum of Science, Boston", Proc. of the Conference on Small-Scale Urban Wind Turbines: Lessons from the Museum of Science Wind Turbine Lab, 19 May, Boston, USA, 2010.

Grid Integration, Operations and Control

THE INTERNATIONAL CONFERENCE ON
WIND ENERGY HARVESTING 2017
20-21 April 2017
Coimbra, Portugal

Paper 401

DYNAMIC MODELLING OF A VARIABLE SPEED HAWT

A. Hazal Altug[1]
METUWIND
Ankara,TURKEY

Ilkay Yavrucuk[2]
METUWIND
Ankara,TURKEY

ABSTRACT

In this paper a generic dynamic model for a variable speed horizontal axis wind turbine is developed for an upwind configuration using the MATLAB/Simulink environment. Blade Element Momentum Theory is used to model the rotor in flow. Rigid blade and uniform wind assumptions are made. Aerodynamic and gravitational forces are calculated as distributed loads. The generator torque controller is designed to maximize power conversion at the below-rated regime. For the above-rated regime, a pitch controller is designed to keep generator speed at rated value. First, a fixed speed and fixed pitch turbine data is used to verify the aerodynamic properties of the blades, sectional loads and moments acting on the blades sections and performance outputs. Verification is done by comparing the outputs of the model with the outputs of the LMS Samtech, Samcef for Wind Turbines (S4WT) software. Then the variable speed model of the NREL 5 MW wind turbine data is applied to the model and verification is done by comparing the steady state results with the NREL 5 MW wind turbine.

NOMENCLATURE

S4WT = Samcef for Wind Turbines

INTRODUCTION

Development of an accurate real-time running dynamic model plays a crucial role for wind turbine studies [1]. In this paper a dynamic model for a variable speed horizontal axis wind turbine is developed using Blade Element Momentum (BEM) Theory. A generator torque controller is designed to maximize power extracted from wind for wind speeds below the rated values and a pitch controller is designed to maintain rated generator speed value for wind speeds above the rated values.

METHODOLOGY

The BEM Theory is used to model aerodynamic forces and moments acting on blades as distributed loads. The effect of hub and tip losses are included [2]. Axial and tangential induction factors are calculated through iteration [3]. The relative wind velocity and angle of attack of an element are calculated to find aerodynamic forces. The moments affecting each element are found by the cross product of displacement and force vectors. This is done for each element on a blade and by integration the total moments acting on the blade are calculated. The process is repeated for all three blades while changing the azimuth angle defined for that blade. Total aerodynamic torque acting on the rotor shaft is then calculated from total aerodynamic moments on blades by making necessary axis transformations.

[1] Research Assistant, METUWIND, Department of Aerospace Engineering, Middle East Technical University Ankara/TURKEY/haltug@metu.edu.tr
[2] Assoc. Prof. Dr., METUWIND, Department of Aerospace Engineering, Middle East Technical University Cankaya Ankara/TURKEY/yavrucuk@metu.edu.tr

For a variable speed wind turbine it is necessary to add controllers to the model in order to adjust and limit the rotor speed. A proportional controller is designed to adjust the generator torque for the below-rated operating region seen in Figure 1. Using the generator torque controller the power production is maximized. In order to limit the aerodynamic forces and the rotor speed a PID controller is designed to control the pitch of the blades for the above-rated region, seen in Figure 2.The controllers are also tested for non-uniform winds.

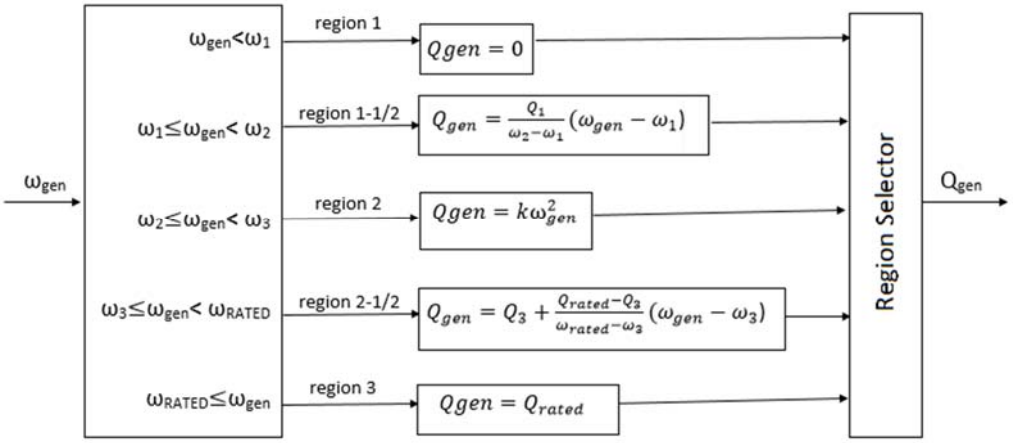

Figure 1. Generator torque controller scheme

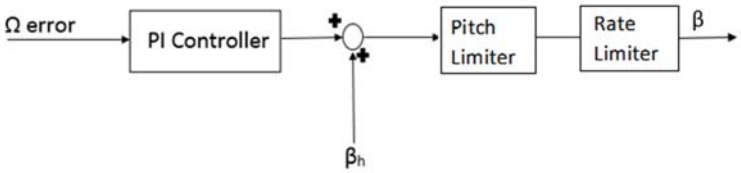

Figure 2. Pitch controller scheme

The aerodynamic power output of the model is calculated using aerodynamic torque. Also the power coefficient is calculated to confirm that the model does not exceed the Betz limit. The dynamic model is developed in the MATLAB/Simulink environment.

RESULTS

The verification of the model is firstly done for a fixed speed fixed pitch wind turbine using S4WT [4],[5]. Firstly, the simulation is performed using the Samcef software. Then, the same wind scenario is applied to the model using same turbine properties. For each blade section, axial and tangential induction factors, tip hub losses, angle of attack, inflow angle, lift and drag coefficients and normal and tangential forces are collected at each blade element. Total aerodynamic torque, power and power coefficients of rotor are calculated for each wind load case. Three different load cases were used; below-rated, rated, and above-rated. Figure 3 shows the comparison results for the rated load case.

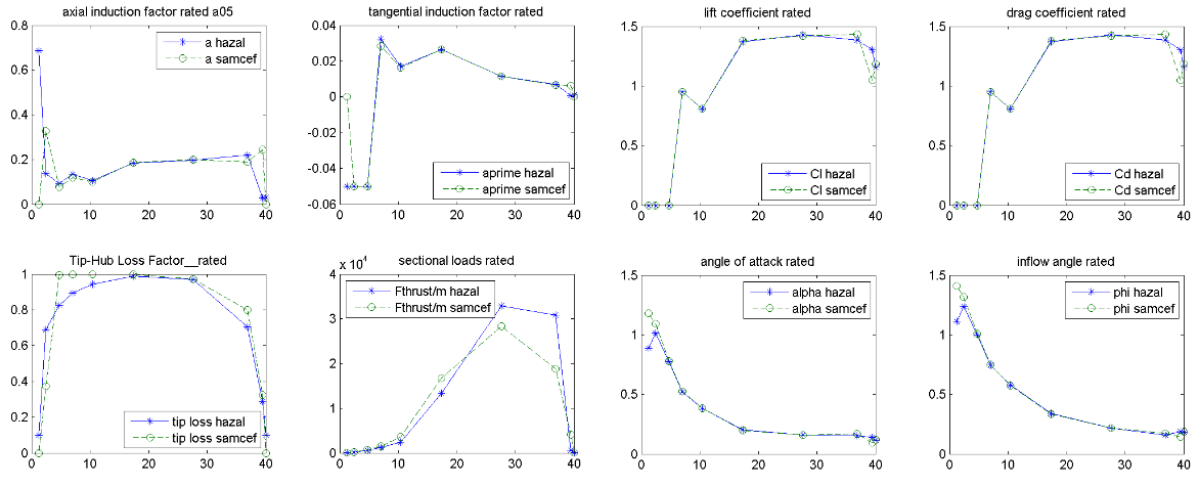

Figure 3. Sectional aerodynamic properties comparison for rated load case

In order to demonstrate the variable speed, wind turbine controllers are activated. NREL 5-MW wind turbine data are implemented to the model and the steady state responses are compared [6]. In Figure 4 the generator torque values, and in Figure 5 the pitch angle values are shown as a function of wind speed. The power outputs of the model and the NREL 5-MW wind turbine are compared in Figure 6 and seen that they follow a similar pattern.

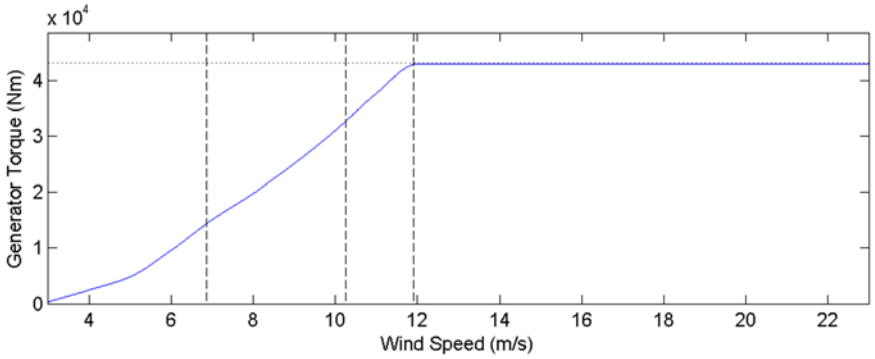

Figure 4. Generator torque as a function of wind speed

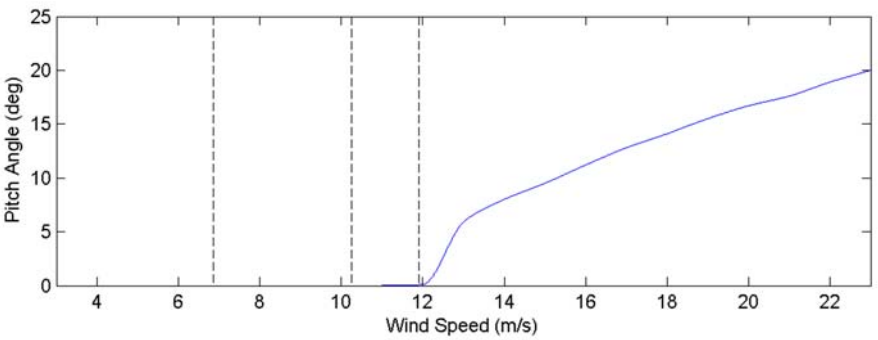

Figure 5. Pitch angle as a function of wind speed

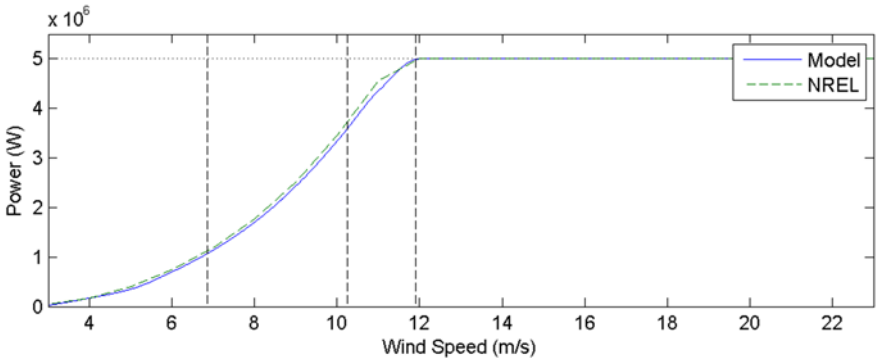

Figure 6. Power as a function of wind speed

CONCLUSIONS

A dynamic model for a variable speed horizontal axis wind turbine is created in the MATLAB/Simulink environment and the verification of the model by using Samcef Software and NREL 5-MW wind turbine steady state power production data. It is seen that the models agree for both fixed speed and variable speed wind turbines.

Details used to create the dynamic model, results from verification and controller performances will be explained in the final paper.

ACKNOWLEDGEMENTS

This study is supported by METU Center for Wind Energy (MetuWind)

REFERENCES

[1] Moriarty P. and Butterfield S. B., Proc. American Control Conf, 2009, pp 2090-2095
[2] Moriarty P. J. and Hansen A. C., "AeroDyn theory manual", National Renewable Energy Laboratory Golden,Colorado, USA, 2005
[3] Manwell J. F., McGowan J. G. and Rogers A. L., "Wind energy explained: theory, design and application", John Wiley & Sons, 2010
[4] S4WT, "Lms samtech samcef wind turbines", 2015, http://www.plm.automation.siemens.com/en_us/products/lms/samtech/samcef-wind-turbines.html
[5] Bonnet, "SWT V3.302 Stationary Aerodynamics Validation", 2013
[6] Jonkman J. M., Butterfield S., Musial W. and Scott G., "Definition of a 5-MW reference wind turbine for offshore system development", National Renewable Energy Laboratory Golden, CO, 2009

THE INTERNATIONAL CONFERENCE ON
WIND ENERGY HARVESTING 2017
20-21 April 2017
Coimbra, Portugal
Paper 402

EVALUATION OF TRANSMISSION SOLUTIONS FOR WIND TURBINES/FARMS

Jovan Todorovic[1]
Power Transmission Company
of Bosnia and Herzegovina
Banja Luka, Bosnia and Herzegovina

ABSTRACT

The electric power produced by wind turbines need to be injected into transmission/distribution grid in the most efficient way to fulfil technical, economic and environmental requirements. Such demands is being made a grid integration of wind turbines very complex task. An optimal grid integration solution is very case dependent, so each project has to be evaluated individually. An onshore/offshore wind turbines/farms grid connection depends on its size and proximity to existing transmission lines, mostly.
This paper describes the most common solutions for the grid integration of onshore/offshore wind power utilization cases. Transmission losses for large offshore wind farms are evaluated, using high voltage alternating current (HVAC) connection solution, for various wind farms sizes and distances to shore.

INTRODUCTION

Unlike conventional sources, power production from wind generation can not be predicted precisely either in short or long term. Although nowadays, the weather forecast has reached very high level of forecast accuracy, Transmission System Operators (TSOs) monitor wind farms operation with special attention in order to keep a power transmission system operation on a safe side. Probability to lose renewable generation production is much higher in compare with production from conventional sources. Wind power fluctuations affects directly on a wind power production and consequently on a power transmission system stability. In order to keep a power transmission system in a stable operating point, the production/consumption balance have to be fulfilled. That is reason why responsible TSO requires from wind power producers to provide certain amount of power reserves in conventional sources.

Besides the high demanding grid integration conditions imposed by responsible TSOs, a spatial dimension of integration stands as one of a serious barrier. Nowadays, in some European countries with high percent of wind turbines/farms penetration into power system, permissions from local authorities for new transmission line corridor or new transformer station are jobs which should not be taken as granted. No matter how short connecting lines should be, it is necessary to be: planned in long term spatial planning of local community, obtained permissions from land owners eventually, environmental and/or ecological permissions, etc.

Onshore windy locations, with high wind power potential, are not urban regions and not close to power transmission lines, usually. Generally, in such locations, wind power is utilized by large size wind turbines/farms requiring overhead power transmission line(s) and power transformer station to be integrated into power system. Within wind farm, wind turbines are interconnected by MV underground cables. When deciding how a large size wind farm should be connected to power system, a whole project should be techno economic evaluated. If decide to use underground cable, such large wind farm needs 110 kV transmission voltage and higher, what increases investment costs, significantly. Mostly, using high voltage underground cables increases investment costs but such solution has minor visual impact onto environment. So, each project has to be treated individually and one part of result is a compromise between investment costs and technical feasibility.

In urban regions/cities, installation of a large size turbine/farm is not convenient from many point of view. Small size wind turbines could be integrated into MV and LV distribution grid. A distribution grid in urban region is installed underground, in most of cases. A power cable from wind generator is in turbine tower and connected to local distribution grid to underground cable. So, a connection line is not visible at all and no any visual impact onto environment. Well developed distribution network within an urban region/city could be advantage for efficient integration of wind turbines (renewable sources). Furthermore, efficient grid integration of renewable sources

[1] Senior engineer for power system analyze and development, "ELEKTROPRENOS BiH, a. d. Banja Luka", Marije Bursac 7a, 78 000 Banja Luka, Bosnia and Herzegovina, jovan.todorovic71@gmail.com

within urban region is one of the preconditions for the successful transformation of existing power grid toward smart grid concept, i.e. smart cities concept.

LARGE OFFSHOREWIND FARMS

Offshore wind turbines/farms are large size turbine/farms and connected to onshore power system by submarine cables. A submarine connection is buried in a sea bottom with no visual impact on environment. A part of connection from a shore to power system connection point could be underground or switched to overhead lines what has to be evaluated for each project individually.
Total power of a great number of wind turbines onto wide area cannot be just summed up to present total output power. In order to simulate a wind farm in proper way an aggregated wind farm model is developed.[1][2]. Thus an aggregated model based on Holttinne and Norgaard ([3]) has been considered.

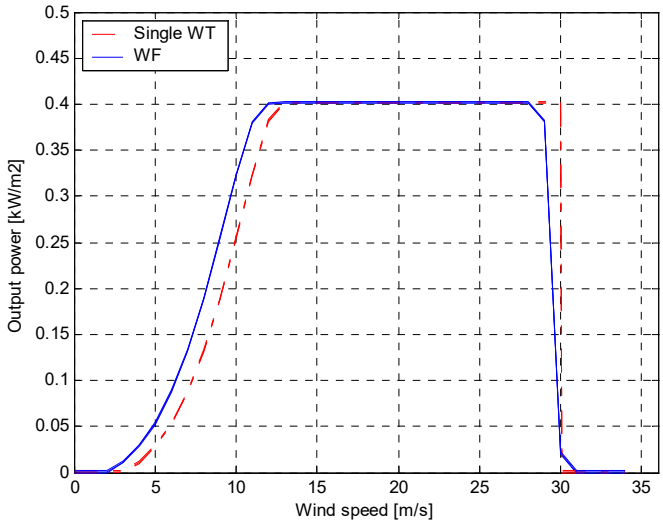

Figure 1. Comparison between normalized single wind turbine power curve and the wind farm power curve for a 1000 MW wind farm and an average wind speed in the area of 9 m/s.

In *Figure 1* the power curve for the wind farm as well as for a single 5 MW wind turbine are compared.
The actual aggregated power curve for the area can be obtained by up-scaling the normalized multi – turbine power curve to match the total installed wind power capacity (multiplting with the number of the turbines). The power curve obtained is used in all the further calculations for losses issues varying the size of the wind farm and the average wind speed in the area.

HVAC TRANSMISSION SYSTEM

Production of large amounts of reactive power can be considered the main limiting factor of HVAC cable utilization in transmission systems for long distances. Choice of a proper transmission system, for large wind offshore farms with hundreds MW of rated power, can be a decisive part of the overall project feasibility. Small differences in transmission losses between transmission solutions could cause large differences in energy output over a project time of 20 years.

A comparison of the transmission capacity of cables with different voltage levels (132 kV, 220 kV and 400 kV) and different compensation solutions (only onshore or at both ends) is presented in *Figure 2*. Cables' limits, as maximal permissible current, voltage swing of receiving end between no-load and full load (< 10%) and phase variation (< 30^{o}) should not be exceeded, according to Brakelmann in [4]. For these cables, the maximal current is the only limit that is reached, while the other two are not critical constraints.

Cable loss calculations are performed based on Brakelmann [5]. Loss calculations take into account the current distribution along cable line and temperature dependence. For 132 KV and 220 KV voltage transmission levels, three core XLPE insulated submarine cables are used while for 400 KV level three single core XLPE submarine cables are considered in trefoil formation.

This paper presents results of transmission losses evaluation for different wind farm size (up to 1000 MW), different transmission voltage levels (132 kV, 220 kV and 400 kV), for average wind speed of 9 m/s in the area and different distances from shore (up to 200 km).

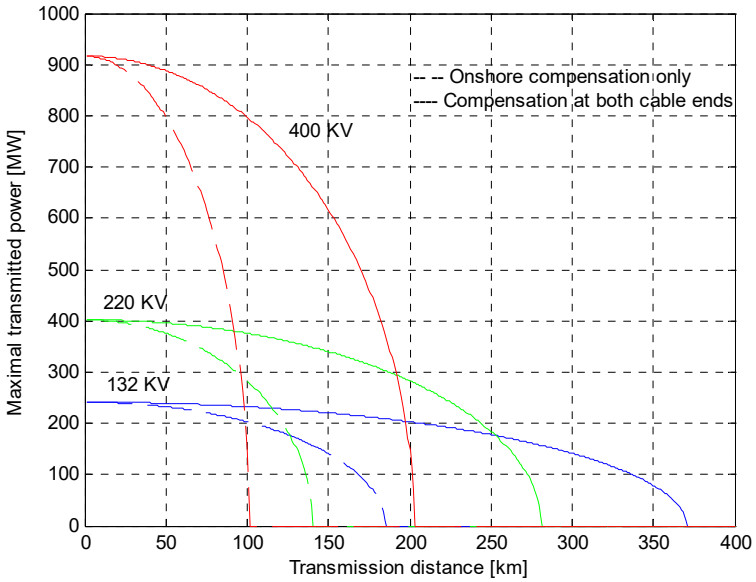

Figure 2. Limits of cables transmission capacity for three voltage levels, 132 KV, 220 KV and 400 KV

System losses for average wind speed of 9 m/s, for three transmission voltage levels (132 KV, 220 KV and 400 KV) and for two wind farm configurations of 500 MW and 1000 MW are presented in *Table 1* and *Table 2*, respectively [2].

Table 1. Transmission Losses of a 500 MW wind farm, with 9 m/s of average wind speed in the area in % of Annual Wind Farm Production.

%	500 MW		
Cable length	132 KV:3 cables	220 KV:2 cables	400 KV:1 cable
50 km	2,78	1,63	1,14
100 km	4,77	3,07	2,54
150 km	7,53	5,05	4,98
200 km	11,09	7,76	17,59

Table 2. Transmission Losses of a 1000 MW wind farm, with 9 m/s of average wind speed in the area in % of Annual Wind Farm Production

%	1000 MW		
Cable length	132 KV:5 cables	220 KV:4 cables	400 KV:2 cables
50 km	3,15	1,96	1,14
100 km	5,7	3,67	2,32
150 km	8,75	5,85	4,3
200 km	12,36	7,58	15,14

Shaded cells in *Table 1* and *Table 2* represents the best transmission solutions with the lowest losses, while number of cables indicates number of cables required for that chosen solution. In the 132 KV columns, number of cables presents the number of cables required for the 200 km. From *Table 1* and *Table 2*, it can be seen that only 220 KV and 400 KV solutions are considered. However, these two submarine XLPE cable designs are still under

development [6]. Considering distances longer than 200 km, 132 KV solutions prevail [1], since at such long distances, 220 KV and 400 KV cables generate large amounts of reactive power.

CONCLUSIONS

Power system integration of wind power imposes to TSOs complex task of keeping power system stability. A grid connection of wind turbines/farms requires interconnection transmission line(s) and power transformer station(s) with significant visual impact onto environment.

Production of large offshore wind farms, connected to grid by HVAC cables, is limited by excessive cables' reactive power generation at long distances. Reactive power compensators are required at both submarine cables ends in order to achieve maximal active power transmission capacity. Transmission losses in high voltage submarine cables dominate over losses in onshore/offshore stations and compensators. Increasing a wind farm distance to shore (over 200 km), the lower voltage transmission levels (220 and 110 kV) stand as the efficient connection solutions.

REFERENCES

[1] Todorovic J., "Losses Evaluation of HVAC Connection of Large Offshore Wind Farms", Master Thesis, Royal Institute of Technology, Stockholm, Sweden, December 2004.
[2] N. Barberis Negra, J.Todorovic and T. Ackermann., "Losses Evaluation of Transmission System for Large Offshore Wind Farms", *Fifth International Workshop on Large-Scale Integration of the Wind Power and Transmission Networks for Offshore Wind Farms*, April 2005, Glasgow.
[3] H. Holttinne, and P. Norgaard, 'A Multi-Machine Power Curve Approach', presented at Nordic Wind Power Conference 1-2 March 2004, Chalmers University of Technology, Göteborg, Sweden, 2004.
[4] Brakelmann H., "Efficiency of HVAC Power Transmission from Offshore-Windmills to the Grid", IEEE Bologna PowerTech Conference, Bologna, Italy, June 23-26, 2003.
[5] Brakelmann H., "Loss determination for long three-phase high-voltage submarine cables", ETEP, 2003, pp 193-198.
[6] Rudolfsen F., Balog G.E., Evenset G., "Energy Transmission on Long Three Core/Three Foil XLPE Power Cables", JICABLE – International Conference on Insulated power cables, 2003.

THE INTERNATIONAL CONFERENCE ON
WIND ENERGY HARVESTING 2017
20-21 April 2017
Coimbra, Portugal

Paper 403

HOSTING CAPACITY OF THE NETWORK FOR WIND GENERATORS SET BY VOLTAGE MAGNITUDE AND DISTORTION LEVELS

Snezana Cundeva[1]
University Ss Cyril and Methodius, FEIT
Skopje, Macedonia

Math Bollen[2] **and Daphne Schwanz**[3]
Electric Power Engineering Group, Luleå
University of Technology, Skellefteå, Sweden

ABSTRACT

The amount of wind generation that can be connected to a certain location without resulting in an unacceptable quality or reliability for other customers is limited. To know how much wind generation can be connected it is important to define appropriate performance indicators. The hosting capacity of networks for wind power generation has been studied. Voltage rise is the performance indicator used to calculate the hosting capacity of low voltage networks for windpower generators. Harmonic and interharmonic spectra from four modern wind turbines were compared with available emission standards. This comparison is used to determine the hosting capacity of the network set by distortion level.

INTRODUCTION

According to the recent International Energy Agency Report [1], the share of renewable energy in global power generation will rise to over 26% by 2020 from 22% in 2013. The generators powered from renewable energy sources are typically much smaller than the conventional generators that dominate today's large power systems. Adding new production or consumption in a distribution grid will affect different properties of the grid such as power flow, voltage quality, short circuit currents etc.

After a brief introductory part on some of the basic electric power system issues, the paper will give two different approaches for finding the hosting capacity for wind generation. In the first example the overvoltage due to distributed generation will set the hosting capacity. In the second example the harmonic emission limits will be considered.

DISTRIBUTED GENERATION AND HOSTING CAPACITY

The impact of distributed generation (DG) strongly depends on the local properties of the distribution system, on the properties of the energy source and on the kind of interface used. The potential adverse impact at distribution level includes:

- Overload of feeders and transformers could occur due to large amounts of production during periods of low consumption.
- The risk of overvoltages increases due to production at remote parts of a distribution feeder.
- Due to the introduction of distributed generation, the level of power-quality disturbances may increase beyond what is acceptable for other customers.
- Incorrect operation of the protection is another potential consequence of large amounts of distributed generation.

The maximum amount of distributed generation that can be connected to the grid at a certain location, without resulting in an unacceptable quality or reliability for other customers, is called hosting capacity [2]. It was first used in order to determine allowable grid penetration of distributed generation and was further developed. To emphasis the role of hosting capacity as a regulation framework [3] proposes an alternative definition: "The hosting capacity is defined as the maximum distributed generation (DG) penetration for which the distribution network

1 Professor, Faculty of Electrical Engineering and IT, University Ss Cyril and Methodius, scundeva@feit.ukim.edu.mk
2 Professor, Electric Power Engineering Group, University of Technology, Skellefteå, Sweden math.bollen@ltu.se
3 PhD Student, Electric Power Engineering Group, University of Technology, Skellefteå, Sweden, daphne.schwanz@ltu.se

still operates according to design criteria and network planning practices based on the European standard EN50160". The hosting capacity varies a lot between different locations in the grid. At some locations, the grid can accept almost no distributed generation without additional investments, whereas it can accept large amounts at other locations.

HOSTING CAPACITY SET BY VOLTAGE MAGNITUDE

The voltage rise resulting from connection of DG can be a major barrier to their connection at the lower voltage levels. Although in practice most of the wind power generation is connected to medium voltage level, the small sized generation units, such as the built environment wind energy technology (BWT), are integrated at low voltage level.

The hosting capacity has been calculated for low-voltage feeders with 400V nominal voltage. The specific conductivity of 1.68×10^{-8} Ωm for copper is used. The hosting capacity per phase, with 1% overvoltage margin, is shown in Table I. The margin of 1% was chosen as this is the usual requirement for generators connected to LV networks [4].

Table 1. Hosting capacity per phase for 400V feeders with 1% overvoltage margin.

Cross section	Cable length				
	50m	200m	500m	2km	Thermal capacity
25mm^2	16kW	3.9kW	1.6kW	390W	33kW
50mm^2	32kW	7.9kW	3.2kW	790W	47kW
120mm^2	76kW	19kW	7.6kW	1.9kW	80kW
240mm^2	150kW	38kW	15kW	3.8kW	120kW

For shorter feeders more than 100 kW can be connected before the voltage rise becomes bigger than 1%. With an average capacity of 3 to 5 kW this equals to more than 20 small wind turbines for the built environment. For cables longer than 2 km the hosting capacity gets less than 1 kW, especially for small cross sectional cables. The thermal capacity of a three phase XLPE cable is shown in the last column. For short cables i.e. 50 m, the maximum load will limit the hosting capacity. For longer cables the voltage rise will set the amount of power that can be connected.

If a margin of 2% is considered, the hosting capacity would be twice bigger.

HOSTING CAPACITY SET BY DISTORTION LEVELS

The emission of disturbances by the generator units may result in increased emission levels. This concerns especially harmonics, voltage fluctuations and unbalance, but also disturbances due to switching of the generators. Modern, MW-size, wind turbines contain power-electronic converters as an interface to the grid. The presence of power-electronic converters distorts the current and the network operators are concerned that the distortion levels in the grid will increase with increased penetration of windpower. Harmonic studies are therefore a common requirement as part of the connection agreements for individual turbines as well as wind parks.

Measurements have been performed of the emission from four individual turbines of 1.8 to 2.5 MW size, equipped with power-electronics. The average spectra for these turbines, obtained over a period of one to four weeks, are shown in Figure 1. Measurements have shown that the emission of wind-power installations is relatively small for the characteristic harmonics (5, 7, 11, 13, etc) but relatively large for non-characteristic harmonics. Next to the characteristic harmonics, these converters inject even harmonics, interharmonics, and high-frequency harmonics. Even harmonics are frequency components at even multiples of the power-system frequency; interharmonics are frequency components that are not an integer multiple of the power-system frequency; high-frequency harmonics are frequency components in the range from 2 to 150 kHz.

The emission of the turbines at harmonic frequencies is much smaller than for other industrial installations or other loads at medium-voltage levels; however the emission at interharmonic frequencies is not present with most other installations.

Currently, there are no voltage-distortion limits in place for interharmonics, so the interharmonic emission is not seen as a concern. Compatibility levels for interharmonics are proposed in an informative annex with IEC 61000-2-2. These levels are very low and can easily be exceeded when larger amounts of wind turbines are

connected. Because these "new harmonics" were absent from the grid before, acceptable limits ("planning levels", "compatibility levels" and "voltage characteristics") have been chosen very low.

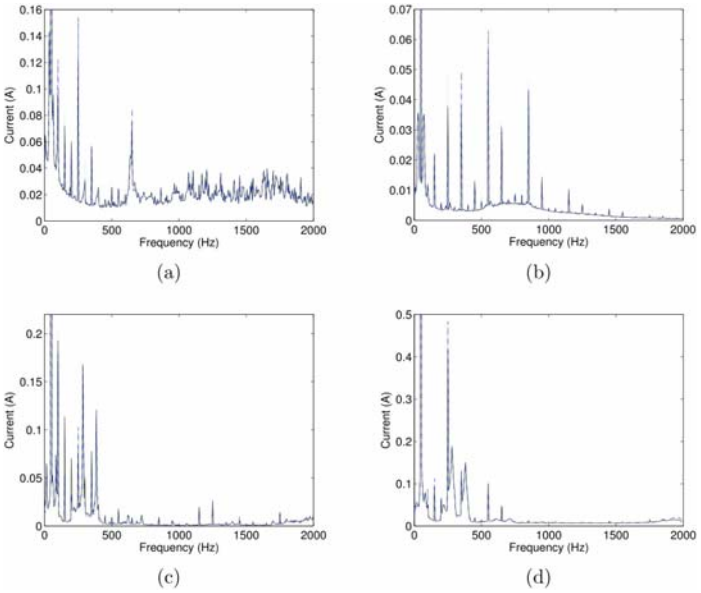

Figure 1 Emission spectrum from four individual turbines

The results from Fig.1 show the emissions from the wind turbines. The harmonic hosting capacity is the maximum amount of wind power generation which can be connected to the network without exceeding the limit for each harmonic voltage component. A methodology for determining the hosting capacity regarding harmonic distortions for a specific point of the power system network is presented in [5].

CONCLUSION

To increase the percentage of distributed generation in the power grid it is essential to know the maximum permissible feed-in power that will not deteriorate the quality and reliability of the supply for other costumers.

In this paper the hosting capacity of the network for wind power generation has been calculated for different power quality phenomena.

Generally for short feeders, integration of more than 100 kW will not result in a voltage rise more than 1%. For such short feeders, the thermal capacity of the cables will limit the hosting capacity. For longer cables the maximum-permissible voltage rise will set the amount of micro generation that can be connected.

Emission measurements have been performed from four modern wind turbines equipped with power-electronic converters. The emission from these wind turbines has been found to be moderate. At harmonic frequencies the emission is much smaller than the emission from industrial, commercial or domestic installations. This means that when the hosting capacity of the network is set by the harmonic emission these turbines can be connected to medium-voltage network without any additional measures. However at interharmonic frequencies their emission is larger than for other installations.

REFERENCES

[1] Renewable Energy Medium Term Market Report, Market Analysis and Forecasts to 2020, International Energy Agency, 2015

[2] M. Bollen, F. Hassan, "Integration of distributed generation in the power system", Wiley – IEEE Press, 2011.

[3] European Regulators Group for Electricity and Gas, "Position paper on smart grids", European Regulators Group for Electricity and Gas, Brussels, 2010.

[4] EN 50438:2007, "Requirements for the connection of micro-generators in parallel with public low-voltage distribution network"

[5] Nunes Santos I., Bollen M.H.J., Ribeiro P.F., "Methodology for Estimation of Harmonic Hosting Capacity", 2014 IEEE 16th International Conference on Harmonics and Quality of Power (ICHQP), Bucharest, 2014

THE INTERNATIONAL CONFERENCE ON
WIND ENERGY HARVESTING 2017
20-21 April 2017
Coimbra, Portugal

Paper 404

A SMALL-SCALE WIND-HYBRID SYSTEM FOR APPLICATIONS IN THE FISH-FARMING INDUSTRY

Pål Preede Revheim[1]
National Wind Energy Center AS
Smøla, Norway

ABSTRACT

This paper studies how wind power based hybrid energy systems can help reduce the diesel consumption of fish farming facilities. It is shown that a wind-battery hybrid energy system can reduce the diesel consumption of an average-size fish farming facility by 70-80 %, reducing annual diesel costs by € 100 000 – € 120 000 and CO2e-emissions by approximately 350 tons/year. The energy cost is comparable to the energy cost from diesel generators, but there is a large potential for cost savings through optimization of wind turbine and battery sizes and improved system integration.

INTRODUCTION

In a large and sparsely populated country like Norway, there will always be places where it is either not possible or not profitable to develop power grids. Some of these places will still be well-suited or even desirable locations for various industries. One current, important example of such an industry is fish farming, at present one of Norway's largest export industries (annual exports of approximately € 5 billion [1]) and with political targets of a fivefold increase by 2050.

As of today, the majority of fish farms operates with diesel generators. From a climate point of view, it would be desirable to replace as much as possible of diesel usage with renewable energy sources. For such a transition to be a realistic alternative, it must also be economically competitive. In large parts of Norway, the potential for solar energy is limited and with large seasonal variations. On the contrary, many potential locations have excellent wind resources, with mean wind speeds exceeding 7 m/s at 10 m. a.g.l. being common. It therefore appears sensible to examine whether exploitation of the wind resources can serve as an alternative to diesel generators.

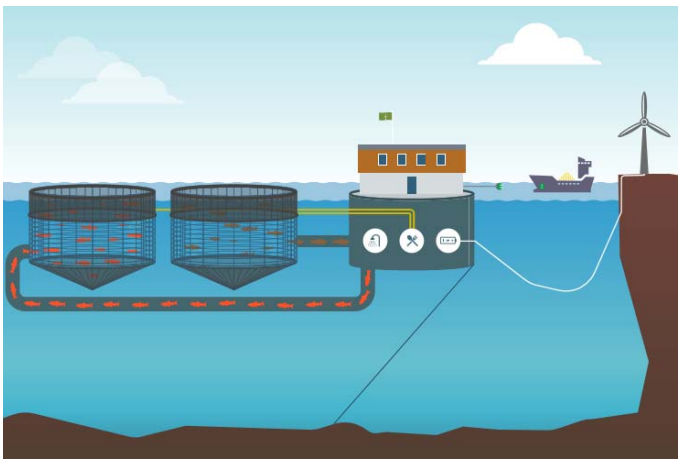

Figure 1. Sketch of fish-farming facility powered by wind energy. The turbine is placed on a nearby islet or in shallow water, and the energy storage and diesel back-up systems on the floating raft itself.

[1]Project manager (PhD), Smøla vindpark, 6570 Smøla, pal@nves.no

A number of studies on wind-diesel hybrid systems is found in the literature (see e.g. [2], [3] and [4]), but the vast majority of these differ from the demands of a fish-farming application both in terms of installed capacity, temporal consumption profile and spatial limitations. A few studies have also been performed on the use of renewable energy sources in fish farming (see e.g. [5], [6] and [7]), but all of these are either concerned with applications on a much smaller scale or the inclusion of fish-farming functionalities in existing offshore wind-farms. The present work constitutes the first step towards designing a functional wind-battery-diesel hybrid energy system tailored for modern fish farming.

METHODOLOGY

The amount of diesel generated power that can be replaced by power generated from the wind by the use of a wind-battery-diesel hybrid system is studied through Monte-Carlo simulations and simulations in HOMER based on an assumed load profile and empirical data on the wind resource at a potential location for a fish-farming facility.

A load consumption profile is obtained from a fish-farming facility operating on diesel generators are used as the basis for simulation studies of wind-hybrid systems. The facility has a diesel consumption of 170 000 liters per year, which corresponds to an annual expenditure of € 180 000. For the facility, peak load is reached during daytime at approximately 150 kW and minimum load at nighttime at approximately 45 kW. This diurnal pattern repeats throughout the year. The annual energy consumption is approximately 450 MWh/year.

Wind data is obtained from a synoptic weather station run by the Norwegian Meteorological Institute. Wind speed and direction is measured at an hourly basis at 10 meter a.g.l. and transformed to hub height at the assumed turbine site by the use of WAsP. The wind resource is summarized in Table 1:

Table 1 – Wind resources at measurement site and turbine site

	Mean wind speed	Power density	Weibull-A	Weibull-k
Measurement site	6.91 m/s	485 W/m^2	7.7	1.64
Turbine site	8.70 m/s	831 W/m^2	9.8	1.86

In the simulations it is assumed a turbine size of 500 kW and a battery with capacity 200 kW/ 400 kWh. The choice of turbine and battery size is based on a qualitative assessment of the requirements of the application as well as on what turbine sizes are available on the market, hence has there not been done efforts to optimize turbine or battery sizing.

RESULTS

The Monte-Carlo simulations show that the reduction in diesel consumption vary over the year, with highest savings in winter (around 80 %) and lowest in summer (around 50 %). Annual reduction is approximately 70 %, which equals to a reduction in annual diesel costs by € 100 000 – € 120 000 and CO2e-emissions by approximately 350 tons/year. The HOMER simulations show an annual reduction of diesel consumption of 82 %, which equals to a reduction in diesel costs by approximately € 140 000 and CO^2 emissions by approximately 400 tons/year. The discrepancies between the simulations is believed due to differences in the assumptions on how the battery and generator are operated.

Both simulations show a general over-production of wind power and a demand for heavy curtailment in high-wind periods. This is obviously caused by the relatively high capacity of the wind turbine. However, a very limited number of wind turbines in the range 250 kW to 500 kW is on the market, and the additional costs of a higher capacity turbine is small compared to an increased storage capacity, so it is not obvious that reducing the capacity of the turbine will be the best strategy for limiting the curtailment.

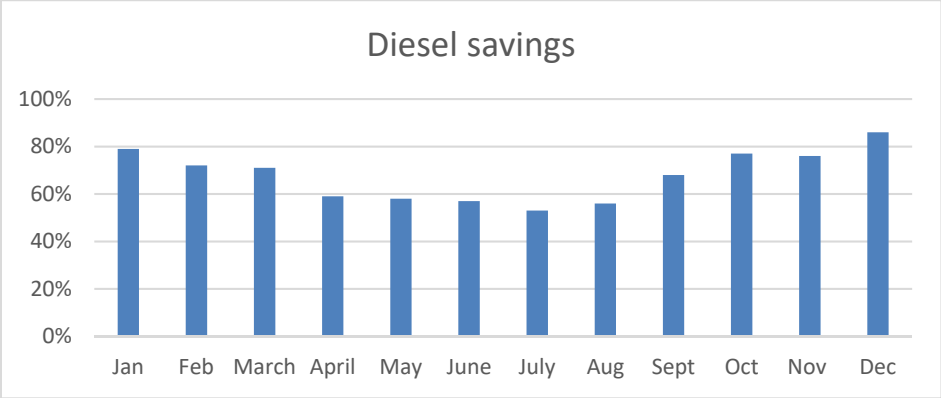

Figure 2. Monthly diesel savings from Monte-Carlo simulations

CONCLUSIONS

Wind power proves to be a promising option for replacing diesel with renewable energy within the fish-farming industry. It has been shown that at locations with good wind resources a win-battery hybrid system can reduce diesel consumption by 70-80 %. For an average-size fish-farming facility this means a reduction of annual diesel costs by € 100 000 – € 120 000 and CO2e-emissions by approximately 350 tons/year. The energy cost is approximately 300 €/MWh, which is comparable to the energy cost from diesel generators. The diesel savings varies significantly over the year, from around 80 % in winter to 50 % in summer, caused by a combination of lower consumption and better wind resource in winter and vice versa.

Future work will focus on decreasing the need for curtailment. Two main strategies will be applied; efforts will be put into optimization of wind turbine and battery sizing, and the potential for alternative use of excess energy (e.g. as fuel for boats, to produce freshwater and O^2 used for disease control locally etc.) will be investigated. The potential for further improvements through efficient utilization of production- and consumption forecasts will also be studied.

ACKNOWLEDGEMENTS

The work has been supported by Smøla Municipality and by the Research Council of Norway through the SkatteFUNN scheme.

REFERENCES

[1] SSB 2015. Akvakultur, 2014, foreløpige tall. https://www.ssb.no/jord-skog-jakt-og-fiskeri/statistikker/fiskeoppdrett/aar-forelopige [23.09.15]
[2] Baring-Gould, E. Ian 2004. Wind/Diesel Power Systems Basics and Examples. NREL. http://apps1.eere.energy.gov/tribalenergy/pdfs/wind_akwd04_basics.pdf [30.09.15]
[3] Rehman, Shafiqur et al. 2012. Feasibility study of a wind–pv–diesel hybrid power system for a village. Renewable Energy 38 (2012), pp. 258-268
[4] Ngan, Mei Shan & Chee Wei Tan 2012. Assessment of economic viability for PV/wind/diesel hybrid energy system in southern Peninsular Malaysia. Renewable and Sustainable Energy Reviews 16 (1), pp. 634-647
[5] Buck, Bela H, Gesche Krause & Harald Rosenthal 2004. Extensive open ocean aquaculture development within wind farms in Germany: the prospect of offshore co-management and legal constraints. Ocean & Coastal Management 47 (2004), pp. 95–122
[6] Lai, Chi-ming & Ta-hui Lin 2006. Technical assessment of the use of a small-scale wind power system to meet the demand for electricity in a land aquafarm in Taiwan. Renewable Energy 31 (2006), pp. 877-892
[7] Toner, Damien & Mo Mathies 2002. The Potential for Renewable Energy Usage in Aquaculture. Technical report. http://www.aquacultureinitiative.eu/Renewable%20Energy%20Report.pdf [23.09.15]

Markets, Strategies, Policies and Socio-economics

THE INTERNATIONAL CONFERENCE ON
WIND ENERGY HARVESTING 2017
20-21 April 2017
Coimbra, Portugal

Paper 501

SITING WIND ENERGY IN THE BUILT ENVIRONMENT: ADVANCES IN PLANNING AND REGULATION

Na'ama Teschner[1]
Post-Doctorate Fellow
Haifa, Israel

Rachelle Alterman[2]
Professor (emerita)
Haifa, Israel

ABSTRACT

Traditionally, energy infrastructures operate on a national or even transnational scales. Recently, with waves of deregulation and privatization, a discussion developed surrounding benefits of using spatial planning and regulation as tools, enabling decentralized forms of energy production and consumption, also on the base of renewable energy (RE) sources. Tendencies toward a distribution of energy mega-infrastructure from centralized to small technologies at urban or household scales, might reveal important spatial implications, especially in land-scarce countries.

Spatial considerations (e.g. scale of land consumption, location, proximity), are considered fundamental in constraining siting of wind energy, though it is not always clear how can planning institutions play a more active role in directing policy in this sphere. Zooming on the similar and different characteristics of Spain and Israel, this study was conducted with the aim of initiating a comparative study of the regulatory planning and land/building -related constrains and incentives of small-scale wind turbines (SSWT) facilities siting. In different countries, diverse approaches are combined to promote or constrain renewable energies according to national targets or environmental goals, but they are often not sufficient to achieve either of these. As has been argued by comparative planning research, each country has been developing its own planning, regulative and public-policy approach [1]. Yet, while countries differ both in their administrative structure and cultures, these institutions are crucial to understanding how wind energy (or other REs) and other spatial-related consideration - can better reconcile [2]. Comparative study of the ways different planning systems regulate small scale wind turbines may yield interesting models or some "good practices".

In a previous WINERCOST workshop entitled "Trends and Challenges for Wind Energy Harvesting", that took place in Portugal, several researchers, [3,4, and 5] among them, have laid down some of the main non-technical knowledge gaps existing with relation to the installation of SSWTs in the built environment. According to this theoretical mapping, while the potential installation of small scale wind turbines in cities co-exist well with current trends urban transition ("smart cities"), they might also face technic, economic, environmental, and social challenges. Many questions, broadly related to sustainability and planning factors, require further research and more case-studies would further deepen our understanding of these challenges.

This paper, therefore reports on the study conducted in Catalonia (Spain) and in Israel with the aim of contributing to the policy and planning perspectives with respect to siting SSWTs in the built environment. The results indicate that small scale wind turbines may require an experimental approach of planning laws and regulations systems and a greater flexibility by planning institutions in order to encourage more installations.

[1] Post Doctorate Fellow, The Center for Urban and Regional Studies, Technion – Israel Institute for Technology, Haifa 32000 Israel, +972-507209080, naamate@technion.ac.il

[2] Chair, Graduate Program in Real Estate. The Center for Urban and Regional Studies, Technion - IIT, Haifa 32000, Israel. +972-505292917, alterman@technion.ac.il

NOMENCLATURE

RE	=	Renewable Energy
SSWT	=	Small Scale Wind Turbine

Figure 1. Street light powered by solar panels and SSWT in Barcelona northern beach. Source: Reuters link here (retrieved: 10.3.2016)

ACKNOWLEDGEMENTS

We thanks the EU's COST action TU1304 WINERCOST for supporting the research. The first author also thanks the Israeli Science Foundation. Prof. Montserrat Pallares-Barbera of the Universitat Autònoma de Barcelona deserves special thanks for her crucial guidance and help regarding Catalonia and Spain in general. We deeply thank the interviewees who generously contributed their time and knowledge. Safira De La Sala has kindly provided help with the non-English material.

REFERENCES

[1] Alterman R. (2001). *National-level planning in democratic countries: an international comparison of city and regional policy-making*. Liverpool University Press.
[2] Terrados, J., Almonacid, G., & Pérez-Higueras, P. (2009). Proposal for a combined methodology for renewable energy planning. Application to a Spanish region. Renewable and Sustainable Energy Reviews, 13(8), 2022–2030.
[3] Paul-Borg, R., & Huber, S. E. (2015). Social, environmental and planning consideration of wind energy technology in the built environment. Work group 3: Introduction. In *Trends and Challenges for Wind Energy Harvesting: Workshop*, Coimbra, Portugal: WINERCOST, pp. 191-195
[4] Norton, C. (2015). Planning and environmental consideration for the development of energy in the urban environment. In *Trends and Challenges for Wind Energy Harvesting: Workshop*. Coimbra, Portugal: WINERCOST, pp. 215–226.
[5] Efstathiades, C. (2015). Smart cities – The role of local authorities in the engagement of small wind turbines in urban areas. In *Trends and Challenges for Wind Energy Harvesting: Workshop,* Coimbra, Portugal: WINERCOST, pp. 227–238.

THE INTERNATIONAL CONFERENCE ON
WIND ENERGY HARVESTING 2017
20-21 April 2017
Coimbra, Portugal

Paper 502

CHALLENGES AND OPPORTUNITIES FOR THE OFFSHORE WIND EXPLORATION IN PORTUGAL

Mário Vieira[1]
IDMEC, IST
Lisbon, Portugal

Elsa Henriques[2]
IDMEC, IST
Lisbon, Portugal

Miguel Amaral[3]
IN+, IST
Lisbon, Portugal

Nuno Oliveira[4]
IN+, IST
Lisbon, Portugal

Luís Reis[5]
IDMEC, IST
Lisbon, Portugal

ABSTRACT

Offshore wind is, nowadays, an emerging renewable source on Europe, with strong capacity potential due to the generalized high wind-levels on the open sea. Because solutions for this wind energetic extraction are highly complex, its implementation differs from other renewable energy technologies as it requires synergies between different industries. Portugal natural resources have been used by two different EU funded projects on the deployment of demonstration prototypes for innovative foundation solutions. Offshore Wind deployment has promoted economic, social and environmental development on other countries; economic benefits, such as the reduction of energy imports, the promotion of technology exports and the development and revive of several industries, such as the offshore, harbor and shipyard ones, have been obtained. Social benefits may also arise, such as the diversification of the energetic system and the generation of energetic independency, thus promoting further security of supply. Environmental benefits arise from lower gas pollutant emissions and the creation of sanctuaries for marine life. In this document, the strategy that better fits the Portuguese socio-economic environment is discussed, the challenges and opportunities are described and the formation of an Innovation System to sustain the chosen strategy is suggested. The government role is essential to create stable conditions for OSW actors, which may be achieved by solid and interconnected public policies. The promotion of an OSW Innovation System should be focused on the generation of technologic and industrial exportations through a Demonstrational Showcase strategy, which is considered to be the most interesting opportunity for the fragile Portuguese economy.

NOMENCLATURE

OSW	=	Offshore Wind
LCOE	=	Levelized Cost of Energy
GDP	=	Gross Domestic Product
EU	=	European Union
O&M	=	Operation and Maintenance

INTRODUCTION

The energetic paradigm is currently changing, and Europe is the leading force pushing this transition. The Kyoto Protocol, signed in 1997 [1],[2], has promoted the commitment of the partaker countries on reducing green-house gas emissions. Instability on the Middle East, and more recently in Russia and Ukraine, has brought adrift the high dependency of the European electric system on foreign and unpredictable players, which ultimately raises supply insecurity [3]. European leaders and actors have, since then, produced strong efforts towards green-house gas emission reduction and energetic independency. In fact, green-house gas emissions have reduced 23% from 1990 to 2012, while at the same period, the global European Union Gross Domestic Product (GDP) rose 46 % [2]. The EU has defined a 20% global quota for renewable energy sources by 2020 and 27% by 2030 [4]. Furthermore, the Paris Agreement, the world's first comprehensive climate agreement, has been signed by 191 countries, including the three greatest green-house gas issuers – China, India and the USA, and will be entered into force on 6 of

1 PhD Candidate, IDMEC, Instituto Superior Técnico, Av. Rovisco Pais nº1 1049 Lisboa, mario.vieira@ist.utl.pt
2 Associate Professor, IDMEC, Instituto Superior Técnico, Av. Rovisco Pais nº1 1049 Lisboa, elsa.h@ist.utl.pt
3 Auxiliar Professor, IN+, Instituto Superior Técnico, Av. Rovisco Pais nº1 1049 Lisboa, miguel.amaral@ist.utl.pt
4 Invited Professor, IN+, Instituto Superior Técnico, Av. Rovisco Pais nº1 1049 Lisboa, nuno.arantes@mitportugal.org
5 Associate Professor, IDMEC, Instituto Superior Técnico, Av. Rovisco Pais nº1 1049 Lisboa, luis.g.reis@ist.utl.pt

November, 2016 [5]. Taking this into account, the existent renewable capacity is not sufficient to guarantee the accomplishment of these goals, which means more capacity needs to be installed in the upcoming years.

The European Union (EU) has defined a 20% global quota for renewable energy sources by 2020, and 27% by 2030 [6] amongst the accumulated energy mixes of its members. In between the installed renewable capacity, Europe as strongly focused on wind dissemination over the last years, with already 129 GW installed by the end of 2014, more than the current nuclear capacity [7]. Onshore wind is now, in fact, commercially competitive against gas and coal: this strong campaign towards wind industry has brought economic benefits, with 2.5 B€ in exports by 2012 [7]. Offshore exploration is the next natural step of this wind power development, since Europe has at its disposal a large marine space with strong wind potential, which is evaluated to be worth at least 350 GW [8]. The installed capacity at the end of 2015 was rated at 11 GW (which represents 92% of the world capacity) [7], with 20 GW predicted by 2020, 150 GW by 2030 and 460 GW by 2050 [9]. 3019 MW were installed in 2015, corresponding to, approximately, 750 new turbines; moreover, 13 billion € worth in financing were granted to new Offshore Wind (OSW) farms, plus 1.8 million € for the respective transmission grids [7]. Still, almost all the capacity is confined to the north European seas, as the winds are quite strong and sea levels are relatively shallow. For the Atlantic sea, 8 to 22 GW are predicted by 2030, with only 27 MW addressed for Portugal [10]. This is mostly explained by the technical challenges imposed by the Atlantic Ocean, which are different from those found on the north-seas, especially because of the higher depths, bigger distances to shore and harsh sea conditions. In fact, for different depths, different solutions for turbine towers installation have arisen. For low depths, the monopile solution is the most affordable, accounting for 74% of the total turbines installed in Europe [9]. Still, for bigger depths, monopile cost surpasses the cost for other solutions, namely jacket or floating structures [11],[12]. In fact, distance and depth are determinant factors for the initial investment on a new farm [13],[14], which can be up to 50% greater than the equivalent onshore [15]. The levelized cost of energy (LCOE) for offshore wind is now evaluated between 115 e 190 €/MWh, which contrasts with cheaper solutions, like coal or gas (respectively 70 and 85 €/MWh) [17].

Because it is served by an extensive marine exclusive economic zone with strong OSW capacity, Portugal appears as a plausible geostrategic location for the development of an Innovation System which focus on the development of Offshore Wind Exploration technologies. However, since it has generically higher depths than the traditional ones found in the north European countries, the technical solutions for this energetic extraction are considerably different, notably on the foundations. Furthermore, these solutions designed for bigger depths are not yet on commercial phases, but still on demonstration or even earlier stages. While this represents a problem for effective commercial extraction, it represents, on the other side, an opportunity for the development of new solutions and for the generation of offshore wind innovation systems.

Due to its intrinsic nature, OSW Exploration brings behind a panoply of different separated industries which must be joined together in the process of building a new Innovation System. In fact, Offshore Wind relies not only on turbine design and manufacturing and on logistic processes, but as well on foundation design, complex manufacturing procedures, expensive installation and logistics, electric transmission and complex operation and maintenance (O&M). It is of crucial relevance the way the connections between these different processes are processed: successful interconnections can promote the construction of an efficient and profitable cluster. The government plays a tremendous role on these processes; a robust policy system which allows investors and stakeholders to operate on an easy-licensing and bureaucracy-free environment, with financial support and robust technology legitimacy needs to be applied. Still, Portugal has economic weaknesses which may threaten the generation of this new Technologic Innovation System for OSW.

METHODOLOGY

The research presented on this article was initially supported by a methodology that was based on the literature review of related high-ranked scientific papers, published books and relevant news available on media resources – both generic and renewable related.

The authors have also enrolled in a series of events which are directly related to this topic, such as the WindEurope Summit Conference and Exhibition, held in Hamburg in September 2016, the WavEC Seminar 2016, and the Final Report presentation for the EU-funded JRC-EASAC joint report presented in November 2016, within the topic of *Marine sustainability in an age of changing oceans and seas*. Within these events, relevant actors and stakeholders for the OSW exploration have been contacted, several projects were acknowledged and a broader and more sustained vision of the topic was acquired.

In the end, a set of interviews was produced to relevant actors, in which their settled experience was used to discuss the today's conditions and the future opportunities for the Portuguese dissemination, specifically addressing all

the dimensions of the considered framework. Interviews to key agents are essential in order to understand the institutional, sectorial and spatial contexts which affect a certain technology development.

STRATEGY DEFINITION

It is necessary to understand, beforehand, which strategy better fits the national energetic and industrial interests and needs, as far as the OSW system implementation is concerned. Two different strategies may be immediately suggested: the first one is based on the current business plan used by the pioneers of OSW implementation: mass capacity addition. The second strategy does not imply mass capacity addition but, instead, focuses on using the industrial and logistic competences of the country to use its offshore resources as a demonstration testing site.

One of the possible strategies for the OSW implementation would be to massively install OSW capacity in the Portuguese ocean areas, following the examples of other countries, such as the world leader UK or the follower Germany. This would not be, however, effectively smart. Both the UK and Germany have huge offshore areas where shallow waters allow for the installation of wind turbines using the monopile foundation solution. This monopile solution is, now, very reliable and is, in fact, the cheapest foundation solution for the OSW industry, being also the number one technology for most of the OSW installed capacity in the world. On the other hand, Portugal does not possess ocean areas where these monopile solutions could be used.

Briefly speaking, Portugal possesses the natural resources, the necessary industry and most of the needed infrastructures, but it does not possess the necessary political will for a massive OSW addition, the financial capacity to back up such money-extensive project, or even, the necessity for such capacity addition, as both solar power and onshore wind can still see their portfolio grow on the country as locations for more capacity are not yet saturated – plus, they are considerably cheaper than OSW, and already fit to compete on the electricity market.

However, and considering the natural, industrial and infrastructural resources that the country has to offer, an opportunity to use them in order to develop a demonstrational showcase of OSW solutions arise. In fact, this has already been done with the Windfloat and the Demogravi3 projects. These projects, although not containing full national incorporation, incorporate a big part of their supply chain asset from national providers – the turbine was not developed in the country, as well as the mechanical design of the foundation, which is, on both cases, foreign made.

CHALLENGES AND OPPORTUNITIES

Portugal may need to install further renewable capacity, but with the end of feed-in tariffs and considering that the economic status of the country is yet weak, only the cheaper solutions will have the opportunity to contribute for more capacity addition. On the other hand, Portugal does have the necessary resources to support prototype deployment, as it has been shown on Windfloat and Demogravi3 projects. Still, Windfloat was decommissioned in 2016 and only Demogravi3 is expected to be installed as a demonstrational prototype, by 2017.

Figure 1. Generic opportunities raised by the development of an OSW Innovation System (modified from [18]).

Portugal already possesses many industries which may be a part of a new industrial cluster integrated on an innovation system focused on OSW development for demonstration purposes. For example, the port of Sines was used for the deployment and decommissioning of the Windfloat prototype and has shown interest in participating in future projects. Lisnave, a shipyard company, participated on the Windfloat assembly. ASM is specialized in turbine tower manufacturing and is currently building a new facility near the Port of Aveiro to build offshore

foundation structures and turbine towers for offshore wind. This new facility is to be installed at the Aveiro Port with the intention of facilitating exportations, on the logistic and, consequently, cost levels. The current factory is held at Sever do Vouga, a village on the countryside, which makes transportation logistics quite complex. Riablades Company, responsible for the manufacturing of turbine blades for Senvion, raised its manufacturing capacity, in 2014, on a 10 million investment that generated 400 jobs. These are a few examples that show how certain industries are committed on contributing for the generation of an Innovation System related with the Wind development. Hopefully, others will follow. The identified opportunities which may rise through the generation of an Offshore Wind Energy Innovation System are described on Figure 1.

CONCLUSIONS

As solutions for deeper waters become commercially available in the following years, possessing a technical showcase of real-scale tested solutions may result in a positive outcome for the Portuguese economy. To provide the Portuguese industry with the capacity to acquire relevant experience and knowledge on the field, as well as to promote the generation of an effective innovation system on the sector, strong, coherent national policies need to be implemented as to ease licensing, installation processes, and to foster R&D capacity on the field.

The generation of the Innovation System which is recommended during this report represents the necessary step in order to obtain all the enounced opportunities. Such Innovation System has already shown signs of being built, mainly with the two European funded projects and with the pre-commercial phase of the Windfloat Atlantic farm. The national agencies and, particularly, the government, should create the necessary conditions to use the already formed industrial and institutional interconnections to generate a sophisticated and effective innovation system, preferable with strong connections to R&D agencies and institutes, with the Academia and with the governmental decision makers.

REFERENCES

[1] United Nations, Kyoto Protocol to the United Nations Framework Convention on Climate Change, 1998
[2] European Environmental Agency, Why did greenhouse gas emissions decrease in the EU between 1990 and 2012?, 2014
[3] Simona O. Negro, Floortje Alkemade, Marko P. Hekkert, Why does renewable energy diffuse so slowly? A review of innovation system problems, Renewable and Sustainable Energy Reviews 16 3836 – 3846, 2012
[4] The European Parliament and Of the Council, Directive 2009/28/Ec, 2009
[5] United Nations, Framework Convention on Climate Change, Adoption of the Paris Agreement, FCCC/CP/2015/L.9/Rev.1, 2015
[6] Directive 2009/28/Ec Of The European Parliament And Of The Council
[7] EWEA, Aiming High, Brussels, 2015
[8] Pérez-Collazo C,Greaves D,Iglesias G. A review of combined wave and offshore wind energy. Renewable Sustainable Energy Rev 2015; 42: 141–53.
[9] EWEA, Deepwater, Brussels, 2013
[10] EWEA, Wind Scenarios, Brussels, 2015.
[11] Eric Rosenauer, Investment Costs Of Offshore Wind Turbines, University of Michigan, 2014
[12] W. Musial, S. Butterfield, B. Ram, Energy from Offshore Wind, NREL, 2006
[13] Prassler, T., Schaechtele, J., Comparison of the financial attractiveness among prospective offshore wind parks in selected European countries, Energy Policy, 2012
[14] Green, Richard, Vasilakos, Nicholas, The economics of offshore wind. Energy Policy 39(2), 496–502, 2011
[15] EWEA, The Economics of Wind Energy, Brussels, 2009
[16] Nikolaus Ederer, The market value and impact of offshore wind on the electricity spot market: Evidence from Germany, Applied Energy, 2015
[17] Fraunhofer, 2013. Levelized Cost of Electricity Renewable Energy Technologies. Fraunhofer Institute for solar energy systems ISE, Freiburg, Germany.
[18] Neven Adzic, et al., Offshore renewable energy in the Adriatic Sea with respect to the Croatian 2020 energy strategy, Renewable and Sustainable Energy Reviews, 2014

THE INTERNATIONAL CONFERENCE ON
WIND ENERGY HARVESTING 2017
20-21 April 2017
Coimbra, Portugal

Paper 503

DEVELOPING AN HOLISTIC POLICY FRAMEWORK TOWARDS PROMOTION OF URBAN WIND ENERGY

Christos O. Efstathiades[1]
Limassol Municipality
Limassol, Cyprus

Öget N. Cöcen[2]
Öget N. Cöcen Mimarlik
Izmir, Turkey

Evangelos Efthymiou[3]
Aristotle University of Thessaloniki
Thessaloniki, Greece

ABSTRACT

In the last decade, wind energy sector investigated the expansion of its applications into the built environment through exploitation of small wind energy and introduced urban wind energy. Despite the recorded technological and scientific progress, considering the multidisciplinary and intersectoral character of this technology, there are still a lot of issues to be addressed. The present paper aims to develop a policy pathway capable to promote effectively the application of wind energy to urban environment. Considering the multifaceted barriers that need to be overcome, ranging from societal acceptance to structural safety topics, the adoption of an holistic approach is proposed to define a suitable policy that can meet the challenges in terms of sustainability and increased. Within the framework of the study, significant factors such as academy and research organizations, local authorities, industry and financial sector are presented and their crucial role in configuring a policy scheme that contributes effectively to deeper penetration of this renewable technology to society, facilitating thus the wider use of built environment win energy applications is highlighted.

INTRODUCTION

According to European Commission's report on "Energy Policy for Europe", the 20% share of renewable energies in overall Community energy consumption, as well as an increase of energy efficiency by 20% must be accomplished until the year 2020 [1]. Moreover, in accordance with European Commission Report "EU Energy, Transport and GHG Emissions Trends to 2050", for electricity generation, renewable energy sources (RES) will provide 35% of the total energy by 2020 [2]. The share will increase up to 50% in 2050 provided that current support schemes, financial instruments and enabling policies will continue and that authorization procedures together with priority access will enable local population to have benefits from investing in local renewable energy sources.

These targets are considered necessary so that a more sustainable energy future for the European Union and for future generations can be achieved. Towards realizing these goals, wind resources can clearly have a vital role, as a proven source of clean, affordable energy which has been developed exponentially throughout recent years. In the field of renewable energy sources, the wind power represents the most dynamic part and the potential of its growth is globally acknowledged. The wind energy field is characterized by improvements throughout the years which are being made in order to generate as much energy as possible at the lowest cost. In the last decade, wind energy sector investigated the expansion of its applications into the built environment through exploitation of small wind energy and introduced urban wind energy. As defined in the technical report-roadmap prepared by Smith et al. in 2012 for the US National Renewable Energy Laboratory (NREL), built environment wind turbines (BWTs) are the wind energy production systems located in an urban or suburban environment. Most of these applications are also classified as small wind turbines (SWTs), therefore a more generic description would be "the application of small wind turbines within a built environment framework" [3].

The field of urban wind energy being still at primary stage, is characterized by a lot of uncertainties both in view of technological and societal aspects. Current data from industry as well recent research projects demonstrate that there are promising opportunities to integrate wind energy in the built environment effectively. Many people are motivated by a desire to be environmentally responsible, and they want clean, renewable energy to help power their homes or businesses. However in order to accomplish higher growth rhythm and exploit the great potentials

1 Dr Civil Engineer/chefst@cytanet.com.cy
2 Architect, PhD, M. Arch in Restoration, 159 sok no5: d:2 35040, Bornova, Izmir/ogetcocen@gmail.com
3 Lecturer, Dr Civil Engineer, Institute of Metal Structures, Dept. of Civil Eng., GR-54124/vefth@civil.auth.gr

for wider utilization, the need for defining the appropriate policy towards this direction is essential. Furthermore, within the smart cities concept, the prime requirement for "smartness" in cities and communities is interoperability, i.e. the ability for things to communicate effectively, and for systems to be integrated in such a way that they operate coherently in response to the users' requirements. For Europe to generate 30% of its electricity requirements from wind technology by 2030, strong support from the general public will be needed. The majority of this production will come from large commercial wind projects installed, both land-based and offshore.

The present paper aims to propose a strategy pathway based towards a more effective promotion of the urban wind energy taking into account the aforementioned parameters. Holistic approach must be a core element of all initiatives related to facilitating interoperability and contributing to the respective market development across Europe. Through a combined action of research, academy, industry and financial sector the knowledge on urban wind energy can be transferred to wider public, familiarity on respective renewable utilizations can be increased and transition to new economy that is based on low carbon technology can be accomplished. This way, the adopted approach can be beneficial in terms of requirements, scope aiming at urban wind energy technology acceleration.

BARRIERS TO OVERCOME

Despite the recorded technological and scientific progress, there are still a lot of issues to be addressed. Some of the key parameters to be clarified are the unique wind resources at urban terrain and their effect on their effect on energy yield, along with social acceptance and financial aspects. There are many areas in which there are concerns for the use of small wind turbines in urban environment. Concerns, not only for financial and technical aspects but also for environmental, social, safety and other reasons [4].

A main concern about the installation of small wind turbines in the urban environment is safety issues. Since such turbines are to be installed in the urban environment and because of the proximity of them with main people activities, neighbors feel a kind of uncertainty regarding potential projects. Safety issues arise also from lightning strikes that can be a problem for urban turbines, because in a case of a strike the turbine may be destroyed and parts of it may fall adjacent to turbines Furthermore, the proximity of small urban wind turbines with the daily activities of many people, make noise levels a critical issue for discussion. Noise is related to tip speed, thus vertical axis small wind turbines are much quieter than horizontal ones because of their lower moving speed [5]. In most countries, especially in South Europe, the most popular urban renewable energy systems are photovoltaic panels [6]. Even if in some locations small wind turbines can produce the same or even more energy with lower investment cost, there is no extensive experience and technical data for this.

Another concern for the installation of build environment wind energy technology (BWT) and one of the main factors regarding the financial feasibility of such installations is wind resource in the certain spot of installation In most countries or even for the whole Europe (Figure 1) there are wind maps for extensive areas but not for the microscale of urban environment [7]. Because of the complexity of the building terrain, it is not feasible to have detailed wind maps for an urban area below a certain height (e.g. 30m).

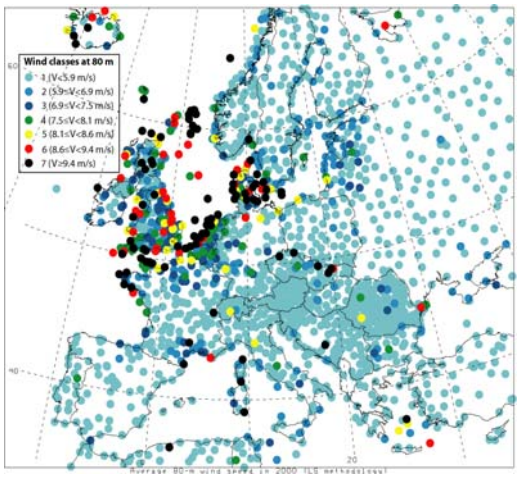

Figure 1. Mean Wind Speed in Europe at 80m height [7]

HOLISTIC APPROACH TOWARDS PROMOTION

In order to promote widely the application of wind energy within urban field, an holistic approach is proposed rather than a monodimensional one, since the challenges that need to be addressed are multifaceted. A policy scheme composed by significant factors like academy, local authorities, industry and financial sector can be effective towards establishment and social acceptance of small wind energy in cities. Universities can transfer the knowledge produced through research activities to general public and act in several ways towards community acceptance of urban wind energy. In particular, significant efforts can be put in explaining the differentiation, explanation of advantages of built environment wind energy technology against large wind parks and for explaining the necessity of the combination of several renewable energy sources, like wind energy combined with solar energy. Another, interesting aspect can be promoting "lessons learned" or "success stories" from BWT projects as well as experience from other countries. In particularly, for BWT a possible implementation of an overall development program that will include certain guidelines not only for owners but also for architects/engineers, will be a very useful tool in order to help them have a clear perspective. Such a plan shall include wind data, preliminary environmental impact study and suggestions about spots of potential placement of urban wind turbines. For this scope, and since it is not feasible to have detailed wind maps for an urban area because of the overall building landscape and the best way to collect useful data are anemometers, local authorities can collect data for certain potential locations of urban wind turbines installation and make them available to the public.

Moreover, the research activities carried out at universities can attract small/ urban wind industry. Establishing a constant dialogue among them, can contribute to increase of research funds while setting up projects that can lead to commercialization of the correspondent outcomes. Within a development procedure of a product, significant time and scientific effort is required for conceptual design, tests and validation processes before marketing it. Achieving a sustainable relationship can prove to be equally beneficial towards advancing urban wind energy technology. In this context, financial sector is necessary to participate in this cooperative network through investments on development of urban wind industry or on research project plans. Providing financial assistance/motivation packages to individual or small companies can facilitate wider deployment of built environment wind energy and contribute to growth of the economy.

Local and regional authorities can encourage the use of BWT by informing and motivating residents, businesses and other local stakeholders on how they can use energy more efficiently. Awareness-raising activities are important to engage the whole community to support sustainable energy policies. In 2008, the EU Climate and Energy Package, the European Commission launched the Covenant of Mayors (CoM) [8]. Considering that 80% of energy consumption and carbon dioxide emissions is associated with urban activity local authorities involvement is critical. Figure 2 presents CoM signatories across Europe over time. For the local authorities that signed the CoM, administrative promotional and technical assistance is provided by the Covenant of Mayors Office, whereas further support is provided by Joint Research Centre and other EU institutions (Committee of the Regions, European Parliament, European Investment Bank, etc.). It is very important that local authorities should lead by example, and play a leading role in sustainable energy activities [9].

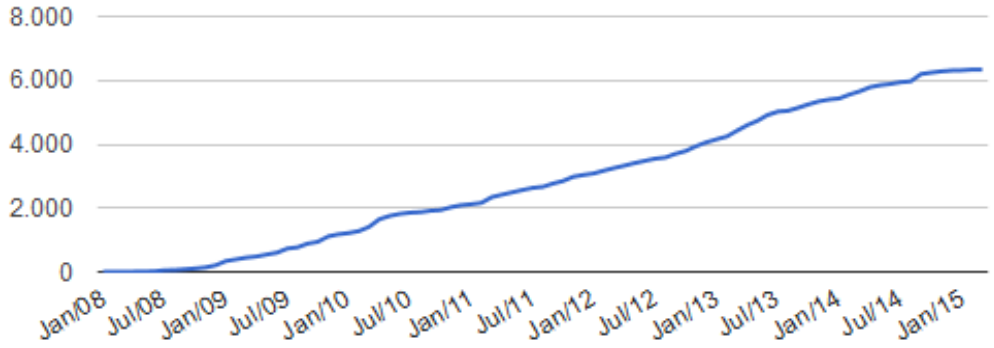

Figure 2. Increasing trend for Covenant of Mayors signatories by local authorities [8]

CONCLUSIVE REMARKS

In this paper, an attempt to define an holistic strategy towards promoting urban wind energy is presented As Francis Bacon said, knowledge is power and the role of academy is essential referring to creating new knowledge on this field, which can be transferred to wider audience through local authorities. Public acceptance of a project or infrastructure is considered to be positive when the majority of citizens are convinced that there are more positive effects in the community than negative. Local authorities have to act in such a way that they will inform citizens not only for the negative but also for positive aspects of the project. In the case of BWT positive aspects are minimization of CO_2 emissions, local production and control of clean energy, etc. For the fulfilment of the above scope local authorities have to lead the right path as planners and regulators, educate and inform citizens as advisors, behave as motivators but also act as producers, suppliers and even consumers

In addition, industry can cooperate with academic and research units in order to advance the related small wind energy systems in terms of manufacture and efficiency. This could lead to commercialization of research outcomes, which could attract the financial sector and invest in this technology. All aforementioned parameters, must be combined and coordinated under a common platform to provide the incentive to end users to understand and eventually apply built environment technology, see in Figure 3 the graphical presentation.

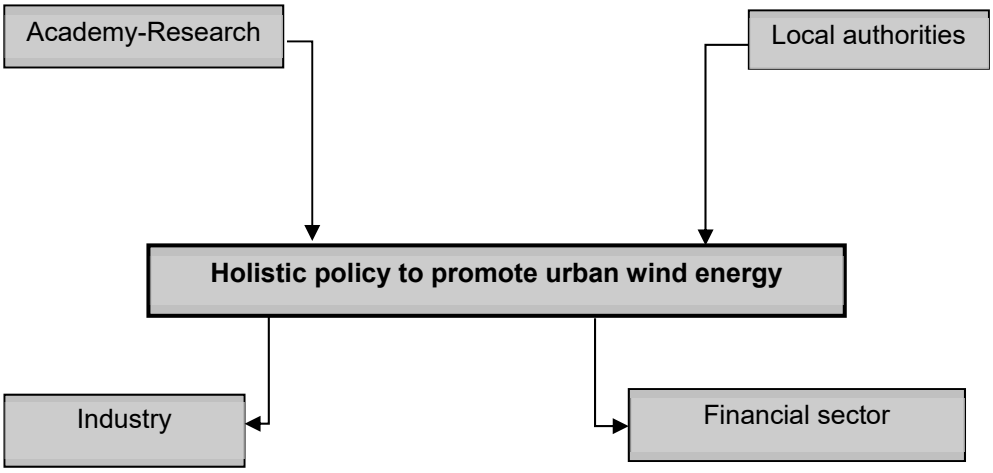

Figure 3. Holistic policy framework towards effective promotion

ACKNOWLEDGEMENTS

The support of the COST TU1304 Action "WINERCOST- Wind Energy Technology Reconsideration to Enhance the Concept the Concept of Smart Cities" is gratefully acknowledged by the authors.

REFERENCES

[1] EC- European Commission, "COM (2007) 1 final: An energy Policy for Europe, Communication from the commission to the European Council and the European Parliament", European Communities: Brussels, 2007.

[2] European Commission, Directorate General for Energy, Directorate General for Climate Action and Directorate General for Mobility and Transport, "EU Energy, Transport and GHG Emissions Trends to 2050", Luxemburg, 2014.

[3] Smith J, Forsyth T, Sinclair K, Oteri F., "Built-Environment Wind Turbine Roadmap, NREL- National Renewable Energy Laboratory", NREL/ TP-5000-50499, Colorado, USA, 2012.

[4] Government of Cyprus, "Renewable Energies - Wind Energy", Ministry of Energy, Commerce, Industry and Tourism, 2005.

[5] Queen University Belfast,"A review of the context for enhancing community acceptance of wind energy in Ireland", Queen University Belfast, SQW Ltd, 2012.

[6] Kasinis, S., "Wind and PV systems in Cyprus", Government of Cyprus, Minis-try of Energy, Commerce, Industry and Tourism, Nicosia 2008.
[7] Jacobson, M. Z., "The Macro View of Wind Power Potential in the United States", Stanford University, Civil & Environmental Engineering, Atmos-phere / Energy Program, 2007.
[8] European Commission / Joint Research Centre / Institute for Environmental Sustainability. "The Covenant of Mayors in Figures 5-Year Assessment", Pub-lications Office of the European Union, Luxembourg, 2013
[9] EC-European Commission, "The Covenant of Mayors", website: http://www.eumayors.eu/agenda_en.html?archive&country=bg&id_event=921, Retrieved March 201

THE INTERNATIONAL CONFERENCE ON
WIND ENERGY HARVESTING 2017
20-21 April 2017
Coimbra, Portugal

Paper 504

THE DEVELOPMENT OF THE ENERGY MATRIX THROUGH PURLIC-PRIVATE PARTNERSHIPS IN CABO VERDE: A CASE STUDY OF WIND POWER

Mário Fernandes Biague[1]
IEDS-UNILAB
Redenção, Ceará, Brasil

Rui Cunha Marques[2]
IST-UL
Lisboa, Portugal

Lidiana R. Fortes Sabino[3]
IEDS-UNILAB
Redenção, Ceará, Brasil

Rejane Felix Pereira[4]
IEDS-UNILAB
Redenção, Ceará, Brasil

Raphael B. Heideier[5]
EPUSP-USP
São Paulo, São Paulo, Brasil

ABSTRACT

This article analyzes the development of the energy matrix in Cabo Verde, diagnosing the possibilities of inserting wind power into the existing system. Among the problems addressed are the restructuring and operation of the electric power sector and the contribution of this energy to mitigate environmental impacts due to the predominant use of fossil fuels to generate electricity throughout the country. We also examine the social, political and technical-economic impacts, seeking to evaluate, through the integrated energy resource planning (IRP) method, the modern concepts of sustainability applied to energy supply and security. In this particular, we selected the existing public-private partnerships (PPPs) as the unit of analysis. These have been established for the purpose of promoting the contribution of wind power to the national energy matrix. For this analysis, we adopted two premises related to the consumption of fossil fuels in the national energy sector, which allowed analyzing the perspective for insertion of wind power. The results obtained show that Cabo Verde is highly dependent on fossil fuels, and that increased use of wind power, which has strong potential, will also help reduce the emission of greenhouse gases, especially CO_2, to the atmosphere. Besides this, it can also lead to emancipation of the country's electric sector, significantly reducing the consumption of fossil fuels and consequently providing social, environmental, financial and political gains, in particular related to energy security and sustainable development of the country. Therefore, according to the results, it can be concluded that strengthening public-private partnerships and the adoption of a policy to encourage the use of wind power in Cabo Verde in the medium and long run will uncontestably increase the security of energy supply and have extremely positive social, political and environmental impacts, besides the considerable reduction of the outflow of capital to pay for imported fossil fuels.

Key Words: Cabo Verde, PPP, IRP, Wind Power, Fossil Fuels, Energy Security, Economic Development, Environment.

NOMENCLATURE

1 Professor, Institute of Engineering and Sustainable Development (IESD), Unilab, Acarape-Ceara-Brazil/mbiague8@gmail.com
2 Professor, Instituto Superior Técnico (IST), University of Lisbon, Lisboa-Portugal/ rcmar@civil.ist.utl.pt
3 Graduate student in Energy Engineering, Institute of Engineering and Sustainable Development (IESD), Unilab, Acarape-Ceará-Brasil/ lidianasabino@hotmail.com
4 Professora, Institute of Engineering and Sustainable Development (IESD), Unilab, Acarape-Ceara-Brazil/ rejanefp@gmail.com
5 PhD student, Department of Electrical Energy and Automation, Polytechnic School of the University of Sao Paulo, Sao Paulo-Brazil/ rbheideier@gmail.com

E (CO2)	=	Emission of CO_2 in tons (t);
FE	=	Emission factor of CO_2 in KgCO2/TJ;
DA	=	Energy generation by fuel (TJ);
Mc	=	Mass of fuel consumed in Gg (Gg = 106 kg) t or kg for energy purposes;
PCI	=	Lower calorific value expressed as TJ / Gg;
Cp	=	Fuel consumption in liters (L);
C_{ant}	=	Previous fuel consumption in liters (L);
TR	=	Reduction rate (10%);
P_{int}	=	Installed power (KW);
E	=	Energy generated (KWh);
t	=	Time expressed in hours (8760 hours per year).

INTRODUCTION

Cape Verde is a country located in the west of the African continent, between parallels 15 and 17 degrees north latitude and longitudes 22º 41 'and 25º 22' West of Greenwich. Located in the middle of the Atlantic Ocean, off Senegal and Mauritania, it is at a distance of about 460 km from the African coast. Cape Verde has an area of 4,033 km² with a population of 526,249 inhabitants and is composed of ten islands, of which only nine are inhabited.

In the socioeconomic context, Cape Verde has a wide dependence on the exterior, both for its supplies in basic needs and capital goods, as well as for the obtaining of financial resources, but especially for the development of the energy sector, (NEW BANK , 2015).

The energy consumption increase poses strategic and infrastructure planning challenges for Cape Verde due to the fact that Cape Verde does not have fossil fuels, mainly depending on imports of petroleum products for energy production (COSTA, 2014). This factor, coupled with the cost of insularity and inadequate capacity to produce and distribute electricity and water, are obstacles to the development of the country, which results in a high cost of electricity in Cape Verde, about 70% higher than that of the European Union (PERCV, 2011).

The energy demand increasing, rising oil prices and their volatility and climate change, to provide security in the electricity supply, it became clear that the Government needs to promote the diversification of energy generation to minimize energy dependence, (MONTEIRO, 2012).

As wind is one of the most abundant natural resources in Cape Verde, the production of wind energy is a viable option, even being considered one of the best alternatives (COSTA, 2013). The energy policy of Cape Verde Government aim to reduce the cost and increase efficiency of this sector encouraging the exploitation of renewable resources. The objective is to cover 50% of electricity demand by 2020 through renewable sources and to have at least one island with 100% renewable energy, in order to respond to the growing demand for energy without compromising the environment (AGENDA FOR ACTION OF ENERGY POLICY, 2015).

Linked to these factors, a dynamic Public-Private Partnership (PPP) was established in 2008 between Infraco Africa Limited, a UK-based infrastructure development company, the Government of Cape Verde and Electra - Electricity and Water Company, SARL (Electra, SARL), the local concessionaire company. The PPP had target the development of four wind farms in Cape Verde, with a total installed capacity of 25.5 MW, distributed in the islands of Santiago (9.35 MW), São Vicente (5.95 MW), Sal (7 , 65 MW) and Boa Vista (2.55 MW)

By creating an independent power producer (CABEÓLICA) to produce electricity for the national grid using wind source, the project was presented as a solution to mitigate the problems resulting from the increasing demand for energy, also working to reduce the import of fossil fuels, financially penalizing and environmentally polluting. Since the inception of wind farms, the company is currently contributing about 24% of the country's total electricity production. Another existing private company is the ELECTRIC WIND that developed and operates a wind farm on the island of Santo Antao, (CABEÓLICA, 2015).

This work is justified in order to analyze the evolution of the Cape Verde energy system with the penetration of wind energy, focusing on its restructuring and operation, as well as its socioeconomic, political and environmental contribution to Cape Verde in a Context of PPP.

METHODOLOGY

A study of the state of the energy sector in Cape Verde was carried out, analyzing the technical, economic, social, political and environmental dimensions of the Integrated Resource Planning (PIR) methodology. Projections were made of wind energy growth, evaluation of its impact on the reduction of greenhouse gases - GHG, as well as evaluation of the impacts due to PPP. The projections were based on two assumptions: one that assesses the trend of fossil fuel consumption growth in the country, its economic, social and environmental impacts; And the other that evaluates the prospects of the insertion of wind energy in the energy matrix through the PPP, proposing an annual increase of 10% according to the goals of the Cape Verde Government. For the evaluation of the environmental impacts resulting from the consumption of fossil fuels, the methodology of the IPCC (1995) was used, taking into account the conversion factors suggested by this organization. For the calculation of the emissions was used Equation 1.

$$E(CO_2) = DA.FE \quad \textbf{(1)}$$

Where,

E (CO2) – emission of CO_2 in tons (*t*);
FE- Emission fator of CO_2 in KgCO2/TJ
DA- Energy generation by fuel (TJ);

It then determined the DA, determined according to Equation 2. The FE factor was also converted from tC / TJ to KgCO2 / TJ. And finally, the emission of CO2 emitted in tCO2 according to Equation 1 was determined.

$$DA = M_C \cdot PCI \quad \textbf{(2)}$$

Where,
Mc- mass of fuel consumed in Gg (Gg = 106 kg) t or kg for energy purposes;
PCI- lower calorific value expressed as TJ / Gg

In addition to determining the amount of CO_2 emission generated by fuel consumption in the current state of the industry, the amount of emissions generated based on projections of consumption over a 10-year period was also calculated, assuming two assumptions:

- Assumption 1: Projection of fuel consumption over this defined period, based on the average growth rate relative to consumption (2006 to 2012). And then determined the CO2

emission generated by this projected consumption, based on the methodology of the IPCC (2006), as described above.

- Assumption 2: Adoption of a reduction rate of 10% of fuel consumption, considering the contribution of wind energy to the generation of electricity.

In order to carry out this calculation, the following procedure was carried out: first, it was based on the last fuel consumption, given for the year 2012, then the calculations were carried out until the year 2022 (projection of 10 years), of According to Equation 3.

$$Cp = C_{ant} - (T_R * C_{ant}) \tag{3}$$

Where,
Cp - fuel consumption in liters (L)
C_{ant} - previous fuel consumption in liters (L)
TR - reduction rate (10%)

After doing so, it also determined the emission of CO2 referring to this projected consumption, using equations 1 and 2. Then, the evolution of the installed power (KW) of wind energy was determined, considering this rate of reduction of the Consumption of fuels and increase of the wind potential for power generation, used in the electric sector of Cape Verde. The installed power was determined according to Equation 4.

$$P_{\text{int}} = \frac{E}{t} \tag{4}$$

Where,
P_{int} - installed power (KW)
E - generated energy (KWh)
T - time expressed in hours (8760 hours)

The power was determined for the two assumptions, and the growth curve was then elaborated based on the power difference of these two assumptions.

RESULTS

It can be observed that the average annual wind power capacity in Cape Verde is around 36%, much higher than the global average annual wind power capacity of 25%. With this, wind energy costs 50% less than the cost of fossil fuels. Therefore, the strong penetration of wind energy in 2011 and 2012 influenced the fall in electricity prices (CABEÓLICA, 2015).

Considering assumption 1 and 2, it was estimated that the GHG emission reduction for the Cape Verde electric sector would be 66% in relation to the base year of 2012. However, the current value of carbon credits does not contribute to promote the expansion of renewable generation.

Still considering assumptions 1 and 2, the potential for expansion of installed capacity of wind power by 2022 was calculated at 60 MW. Even given the large installed capacity of fossil fuel generation, highly idle and flexible, it is believed that the expansion of wind generation would be accompanied by expansion of flexible thermal generation.

CONCLUSIONS

Cape Verde is heavily dependent on fossil fuels, which makes the country's electricity supply very expensive, a barrier to the country's development.

Given the high wind potential with high capacity factors, this energy costs less than conventional thermal generation and its exploration can reduce electricity costs, promoting economic development.

The results show that the exploitation of the wind resource in the country would reduce the cost of electricity by increasing supply and, at the same time, significantly reduce GHG emissions.

ACKNOWLEDGEMENTS

This template was written at the METUWIND Center for Wind Energy. The document is based on the template of the RUZGEM 2013.

REFERENCES

[1] AGENDA DE AÇÃO DE POLÍTICA ENERGÉTICA, “Sustainable Energy For All”, 2015. 62 p. Disponível em: <http://www.se4all.org/sites/default/files/Cape_Verde__AA_PT_Released.pdf>. Acesso em: 20 jul. 2016.

[2] CABEÓLICA. “Relatório e Contas”, 2015. 56 p. Disponível em: <http://cabeolica.com/site1/docs/Relatorio_e_Contas_2015 website.pdf>. Acesso em: 15 jul. 2016.

[3] COSTA, Luís Monteiro. “Previsão da energia eólica – Santiago/cabo verde”, 2013, 69f. Dissertação (Mestrado em Engenharia, Departamento de Faculdade de Economia) - Universidade do Porto, Porto, 2013. Disponível em: <http://www.portaldoconhecimento.gov.cv/bitstream/10961/3538/1/TESE%20Vers%C3%A3o%20Finalpronto.pdf>. Acesso em: 07 jul. 2016.

[4] COSTA, Anildo. “Relatório de Base para Cabo Verde”, 2014. Disponível em: <http://www.cermi-cv.net/uploads/documentos/PT_Relatorio_de_Base_para_Cabo_Verde_1_draft.pdf>. Acesso em: 20 jul. 2016.

[5] ELECTRA. “Relatório Anual Electra”,Electra-Empresa de Eletricidade e Água, 2014. Disponível em: < http://www.electra.cv/index.php/2014-05-20-15-47-04/relatorios-sarl>. Acesso em: 08 jul.2016.

[6] JANNUZZI, Gilberto de Martino et al. Uso Eficiente de Energia e Desenvolvimento Regional. [1995?]. Disponível em: <http://www.fem.unicamp.br/~jannuzzi/documents/PIR-regional.pdf>. Acesso em: 20 set. 2016

[7] MONTEIRO, Ana David. O Impacto das Energias Renováveis na Economia dos Países Emergentes: o caso de Cabo Verde. 2012. 77 f. Dissertação (Mestrado em Gestão de Empresas) - Instituto Universitário de Lisboa, Lisboa, 2012. Disponível em: <http://www.portaldoconhecimento.gov.cv/bitstream/10961/136/1/TRABALHO_DE_MESTRADO_Ana David.pdf>. Acesso em: 02 jun. 2016.

[8] NOVO BANCO. “Contexto Econômico de Cabo Verde”, 2015. Disponível em: <https://www.novo-banco.pt/site/images/documentos/research/research_sectorial/internacional/2014_novembro/caboverde.pdf>. Acesso em: 10 ago. 2016.

[9] PERCV, “Plano Energético Renovável de Cabo Verde”, 2011. Disponível em: <http://www.cermi-cv.net/uploads/documentos/PT_Plano-Energetico-Renovavel-CV-ZDER.pdf>. Acesso em: 25 jun. 2016.

Smart Cities and Environmental Aspects

THE INTERNATIONAL CONFERENCE ON
WIND ENERGY HARVESTING 2017
20-21 April 2017
Coimbra, Portugal

Paper 601

ADVANTAGES AND DISADVANTAGES OF DIFFERENT TYPES OF WIND TURBINES AND THEIR USAGE IN THE CITY

Dr. Ferenc Szlivka[1]
Obuda University
Budapest, Hungary

Dr. Ildikó Molnár[2]
Obuda University
Budapest, Hungary

Gábor Sándor[3]
Obuda University
Budapest, Hungary

ABSTRACT

The wind conditions of a given settlement are significally affected by the features of the ground and different natural and physical obstacles. This is particularly true for residential areas where the volume of turbulence is high. In many cases, if the average annual wind velocity is appropriate, wind turbines or even off-shore parks are established on the outskirts of cities. In both cases, the overall impression of the landscape deteriorates and the public reception is usually negative as well.
Small wind energy systems (<100 kW) are designed to enable the transportation of energy to longer distances. They are connected to the electricity network while micro turbines (>100 kW) are usually used to supply energy for caravans or boats (island mode) as they emit low carbon dioxide. In the case of the systems connected to the electricity network, the consumer gives or takes certain amount of electricity through the counter depending on the wind conditions. The national network in this case acts as a buffer storage. Micro turbines are able to supply energy for flats while small systems are better to supply energy for blocks of flats, companies and whole communities. There are many examples of energy supply with the help of wind turbines: in schools, sport centres, industrial parks and rural flats but they are less present in densely populated urban areas for two reasons: the noise and the overall view. There is no evidence that proves that wind turbines would reduce the value of estates or would harm the features of the neighbouring estates.

In the case of turbines with horizontal axis, usually two or three wooden or plastic impellers are placed on the axis, and the generator is driven by a wheel. Electricity can be directly transmitted into the system or it can be used to charge batteries. Alternative current (AC) is generated by small turbines which can be transformed to direct current (DC). The alternative current is transformed to direct current with the help of an inverter (230V 50Hz Europe) used in Europe.

In the case of wind turbines located on buildings, there can be problems of vibration and the local turbulence can also affect them. It is advised to put the turbines on higher towers (10 m from the structure) in particularly stormy regions, thus the volume of turbulence can be reduced and the life span of impellers can be increased. Higher towers enable a better use of wind velocity. Hybrid systems which combine wind turbines and solar panels are more and more popular.

Micro wind turbines are available on the market although only a few companies provide complex services including planning, installation, maintenance. It is hard to find a service provider who employs certified skilled technicians and who can give a guarantee. The installation of most small wind turbines is relatively

1 Professor, Institute of Mechatronics and Vehicle Engineering, Öbuda University, 1081 Népszínház utca 8., Budapest, Hungary/szlivka.ferenc@bgk.uni-obuda.hu
2 Associate Professor, Institute of Mechatronics and Vehicle Engineering, Öbuda University, 1081 Népszínház utca 8., Budapest, Hungary/molnar.ildiko@bgk.uni-obuda.hu
3 Student, Institute of Mechatronics and Vehicle Engineering, Öbuda University, 1081 Népszínház utca 8., Budapest, Hungary/rodnas.robag@gmail.com

expensive $3000-6000 per kW, which means 10-15 years recovery time depending on the wind velocity and the energy prices of competitors. Continuous support should encourage mass production and a more extensive introduction of this technology on the market but the installation and investment costs should also be decreased.

The main reasons why this technology cannot be widespread are the high investment costs and the length of the recovery time. In addition, it is hard to sell the generated energy because the electricity provider has to purchase the green energy at a higher price than the traditionally produced energy. The other reason while the electricity provider is reluctant to invest in this technology is because it is difficult to plan the energy production ahead.

To make better use of wind energy, different inventions were conceived. Figure 1. shows a twin wind turbine which is the so- called slow-moving American wind turbine. The two impellers rotate in opposite direction in order not to disturb each other. This principle is very similar to the turbo propellers of airplanes where these two propellers rotate opposite each other. We need to know the volume and the efficiency of the air flowing from the first impeller to the other one for the design.

Fig. 1 Dual wind turbine

Figure 2. shows a horizontal dual wind turbine built on a common axis. In the case of these dual wind turbines, it is inevitable that the turbulence created by the impeller which is located on the windy side hits the other impeller located opposite the wind, thus making its performance worse. In order to define the extent of the reduced performance, measurements are necessary. No data have been found concerning the already existing wind turbines. The disturbing turbulence affecting the impeller opposite the wind direction can be reduced by the appropriate location of impellers, the twist of one from the other, the distance of the two impellers from each other, the modification of the tip speed ratio (λ).

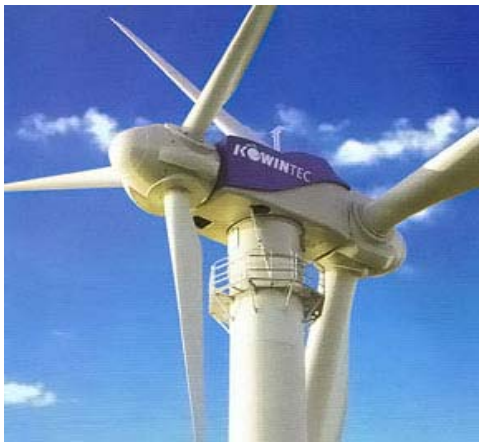

Fig. 2 Horizontal dual wind turbine

The European Commission would like the proportion of renewable energy to increase to 20 per cent in the EU member countries by 2020. This is called the three twenty plan. The new Hungary Development Plan aims at achieving 14 per cent by 2013. An important question in terms of wind energy efficiency is how it is

possible to make use of theoretical energy in practice technically. The cost of electricity per unit is higher in case of unique wind generators than in wind parks. Some investments including the cost of electricity and road networks are lower in wind parks in the case of a wind turbine. The costs of energy per unit can be reduced further if not one but more impellers are installed on a column.
In this article we present some ideas of this type which were put into practice. Before examining them more thoroughly, it is worth comparing the different types of impellers and checking the performance that can be gained from different types of designs. Figure 3. shows the power coefficient in the case of horizontal and vertical impeller types depending on the tip speed ratio (λ)

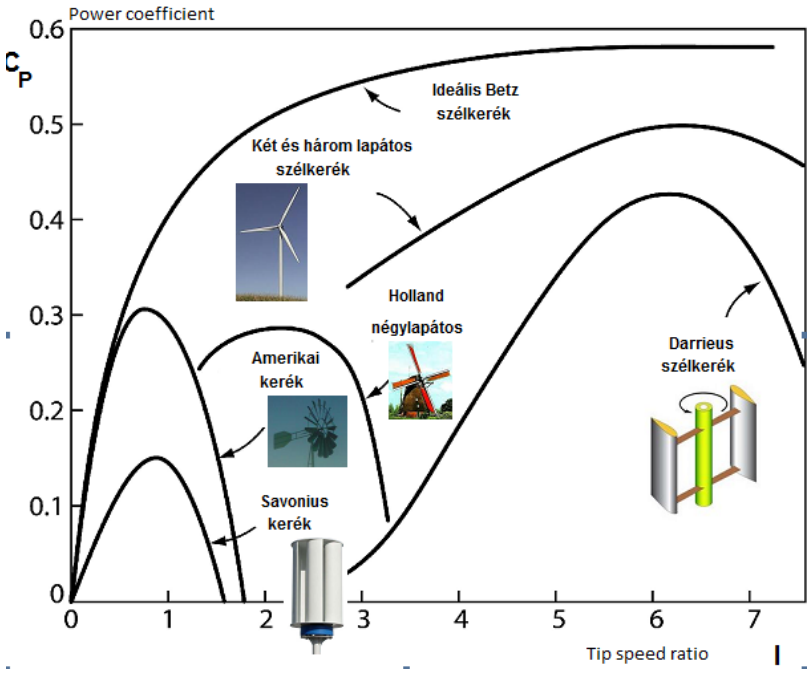

Fig. 3 Performance factor of different impellers

In addition, we present the new structures recommended by us. During our research, we examine the volume of the energy generated from the perspective of fluid flow exclusively. The flow between the blades and the volume of the theoretical performance have been examined with simple experimental methods and with CFD simulation. In further researches we plan to find the optimal parameters of the two impellers using CFD simulation.

REFERENCES

[1] OECD/IEA, International Energy Agency, France, 2009
[2] Molnár, Ildikó Dr. Szlivka, Ferenc: „Eredmények a mezőgazdaságban alkalmazható axiál ventilátorok fejlesztésében” GÉP, LVII. évf., 2006, pp.: 41-44
[3] Tony Burton, David Sharpe, Nick Jenkins and Ervin Bossanyi: „Wind Energy Handbook” JOHN WILEY & SONS, LTD 2001
[4] Dr. Ferenc Szlivka, Dr. Péter Kajtár, Dr. Ildikó Molnár, Dr. Gábor Telekes: CFX Simulation by Twin Wind Turbine, 2011 International Conference on Electrical and Control Engineering (ICECE), China, pp.:5780-5783
[5] (Vad 2001) Vad, János: „Incorporation of Forward Blade Sweep in the Non-free Vortex Method of Axial Flow Turbomachinery Rotor” Periodica Polytechnica ser. Mech. Eng. Vol. 45, No. 2, 2001, pp.: 217–237.
[6] Wissis F. Miller: Dual rotor Wind Turbine US 6,945, 747 B1 Sept. 20, 2005

THE INTERNATIONAL CONFERENCE ON
WIND ENERGY HARVESTING 2017
20-21 April 2017
Coimbra, Portugal

Paper 602

ANALYSIS OF TECHNICAL AND ECONOMIC CHARACTERISTICS OF SMALL WIND TURBINES

Mantas Marciukaitis[1]
Lithuanian Energy Institute,
Kaunas, Lithuania

Giedrius Gecevicius[2]
Lithuanian Energy Institute,
Kaunas, Lithuania

ABSTRACT

The paper provides an analysis of the efficiency of small wind turbines up to 30 kW power. The impact of the rotor size on the annual energy output is analyzed, various factors influencing small wind turbine efficiency are investigated. Capacity factors of a number of operating wind turbines up to 30 kW power are compared and reasons of low efficiency discussed. Technical-economic efficiency evaluation method is proposed for easier selection of small wind turbine model to be installed at a certain location. Results confirm the findings of other studies that performance of small wind turbines in urban environment is poor and the main reason for that is the initial overestimation of the resource and lack of public research based information. Also the results of the survey of public opinion about the urban wind energy development issues are presented.

NOMENCLATURE

P	=	Power (kW)
S	=	Area of the rotor (m^2)
v	=	Wind speed (m/s)
C_{ef}	=	Coefficient of efficiency (%)
ρ	=	Density of air (kg/m^3)
K_{te}	=	Technical-economic parameter

INTRODUCTION

Renewable energy sources are playing an increasing role in modern electric power systems due to their local availability, public acceptance and environment friendliness [1]. Wind power is the renewable source of energy closest to becoming competitive on the market. Due to technological improvements and the implementation scale, wind power makes the largest share of electricity production from renewable sources today, apart from large hydroelectric power plants [2].

Wind energy in the urban environment is a new area and a rather blank page concerning design criteria, aesthetics, concepts, minimizing costs etc. [3]. Even though the wind resource is much higher on the countryside or offshore, wind energy in built environment is attractive for the possibility of direct use of the energy and affordability. A number of studies have been carried out showing that efficiency annual energy yield expectations for small wind turbines in urban area are too high [4-6]. However, investigations of many related aspects like selection of the right location for certain configuration, assessment of local wind resource, impact on the everyday life of the citizens have to be continuously carried out in order to improve the picture of small wind turbines in built environment.

[1] Head of Laboratory for Renewable Energy and Energy Efficiency, Lithuanian Energy Institute, Breslaujos str. 3, Kaunas LT-44403 Lithuania, email: mantas.marciukaitis@lei.lt

[2] Junior research associate, Laboratory for Renewable Energy and Energy Efficiency, Lithuanian Energy Institute, Breslaujos str. 3, Kaunas LT-44403 Lithuania, email: giedrius.gecevicius@lei.lt

METHODOLOGY

Efficiency of several wind turbines in Lithuania was evaluated by using capacity factor formula:

$$C_p = \frac{E_{actual}}{E_{\max}}$$

where E_{actual} represents the energy (kWh) actually generated by a wind turbine over a certain period of time and E_{max} means amount of energy (kWh), which would be generated over the same period of time by the wind turbine operating at nominal power.

Another method for the evaluation of technical and economic efficiency of small scale wind turbines is proposed. This method encompasses relative power and cost parameters of wind turbine. The so called technical-economic efficiency parameter K_{te} is calculated using formula:

$$K_{te} = \frac{P_v / S}{C / P_v} = \frac{P_v^2}{C \cdot S}, \text{ W}^2/\text{EUR m}^2$$

This method is used for the comparison of 13 horizontal axis and 4 vertical axis small scale wind turbines with 1-10 kW installed power.

Typical formula is used for the calculation of the coefficient of rotor efficiency for separate wind speed bins:

$$C_{ef} = \sum_{n=1}^{k} \frac{P_n}{\frac{1}{2} \cdot \rho \cdot v_n^3 \cdot S}$$

where: P – wind turbine power at certain wind speed [W], ρ – density of air [kg/m^3], S – area of the rotor [m^2], v – wind speed [m/s].

RESULTS

The investigation consists of several different analyses covering various issues from wind turbine efficiency and capacity factors to the results of the survey of public opinion about urban wind energy.

Technical data of a number of small scale wind turbines were investigated in order to find out the relations between wind turbine power and efficiency. Results show that average efficiency values increase with wind turbine installed power. According to the official technical data, 1-10 kW wind turbines' average efficiency at 10 m/s wind speed reaches 0.318.

Energy production data of seven wind turbines with installed power 2 to 30 kW operating in Lithuania were analysed to find out their capacity factors under real conditions. The data are publicly available and show that in one year period (2013-2014) the capacity factors didn't exceed 4.3 %.

The efficiency of a 1 kW roof-top wind turbine was analyzed more thoroughly. Simultaneous wind speed and power measurements over one year period have revealed the real power curve (Fig. 1).

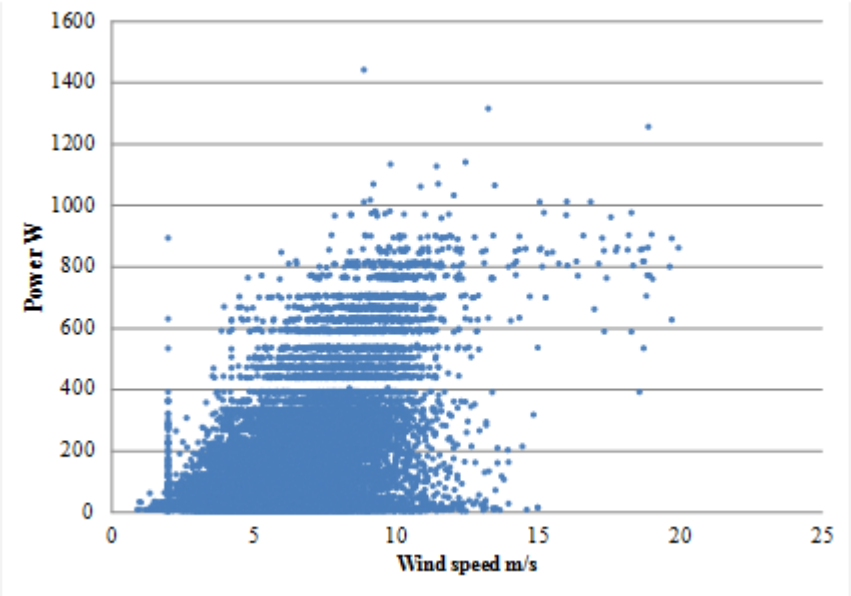

Figure 1. A raw measured power curve of a 1 kW roof-top wind turbine

Various data filtering and approximation methods were applied in order to find the mathematical model of the power curve, but it was concluded that data dispersion is too large. Averaging of data has helped to bring out a clearer view, but a significant part of power curve data at higher wind speeds was lost (Fig. 2), because of the dense time interval (3 s) used for the recording.

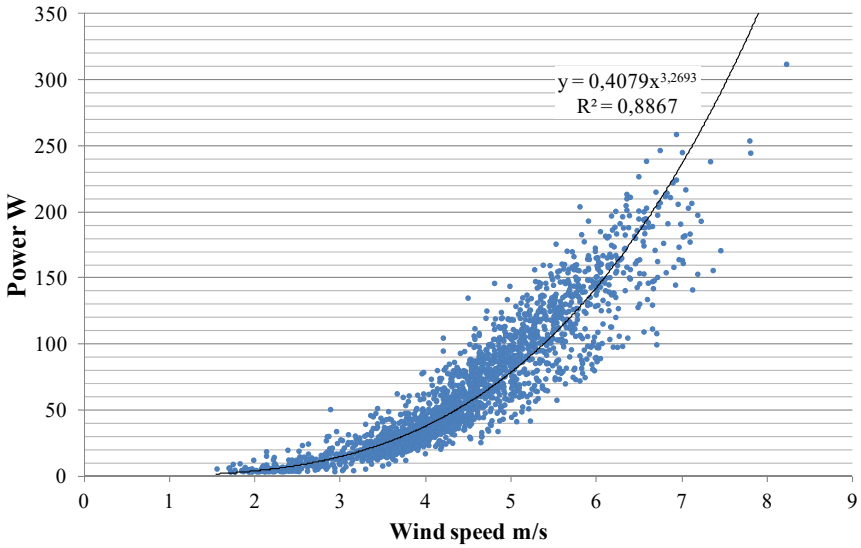

Figure 2. A power curve of 1 kW roof-top wind turbine based on averaged data

The large data scatter is explained by the wind gusts and wind direction variation in obstructed environment which is obviously the main reason for the poor performance of the wind turbine. These results show the potential difficulties and low accuracy in estimating the annual energy yield of wind turbines in urban environment.

Efficiency of the same wind turbine at different wind speeds was investigated. The highest estimated efficiency values (0.208) were found at wind speed of 7-8 m/s (Fig. 3).

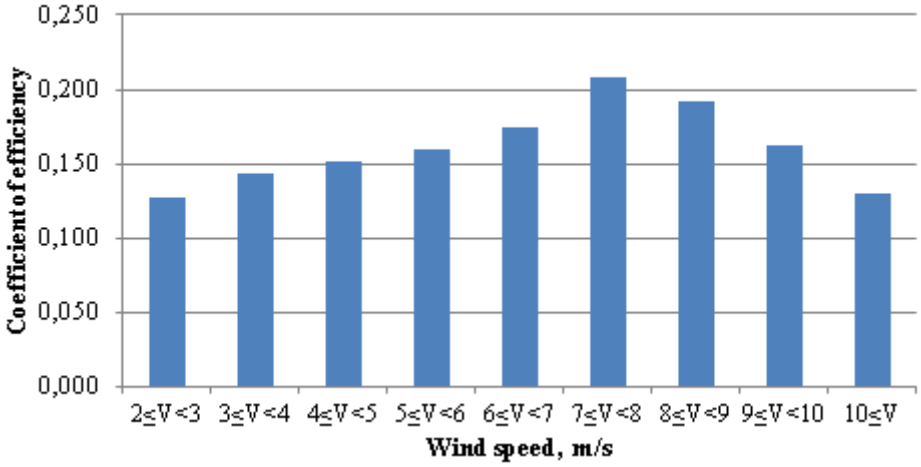

Figure 3. Values of coefficient of efficiency of a 1 kW roof-top wind turbine in different wind speeds

The lowest efficiency values were recorded at wind speeds of 2-3 m/s, and the average for all wind speed bins is 0.161.

In small scale wind turbine market a relation between rotor swept area and turbine power usually falls in the range of 4-6 m^2/kW. Analysis of small wind turbines confirms that relatively larger rotors (>12 m^2/kW) lead to significant increase in annual energy yield in urban environment. However, this fact is rarely taken into account when selecting wind turbines for low wind locations. Larger rotor typically means higher price of the wind turbine, therefore selection of the wind turbine model for a given location should be accompanied by the comparison of its technical and economic parameters.

Technical and economic characteristics of a number of small wind turbines were compared in this work and the results are given in Fig. 4.

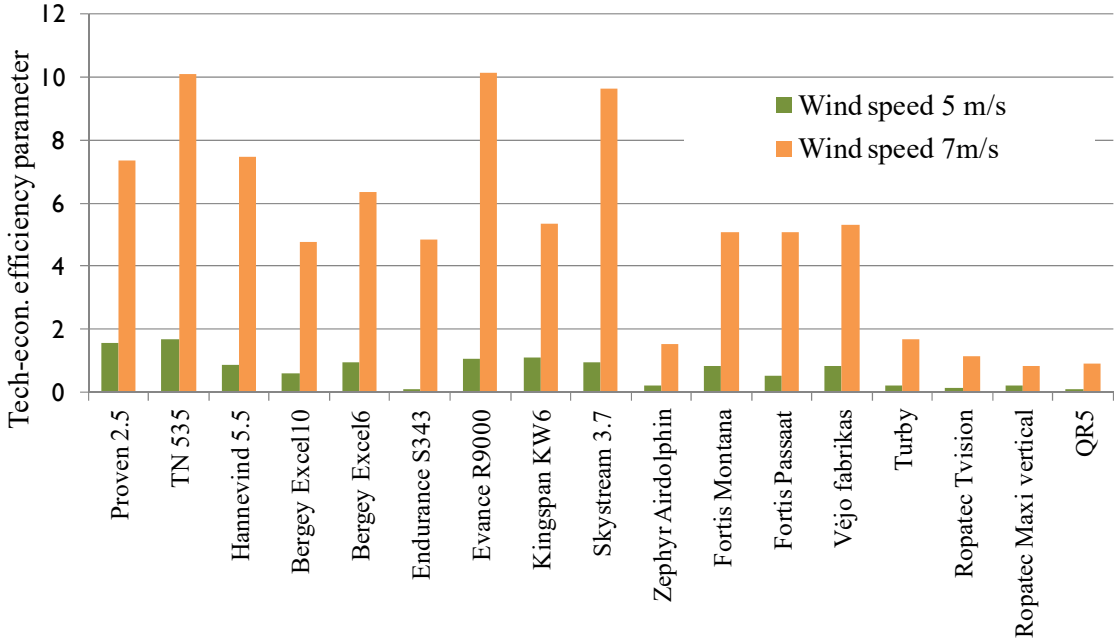

Figure 4. Comparison of several small wind turbines according to the technical-economic parameter K_{et}

Results of the investigation reveal differences between various wind turbine models. The higher the value of the parameter K_{te}, the more reliable and economically efficient wind turbine is at the given wind speed. The last four in the row are vertical axis wind turbine models – 5 times less technically-economically efficient than horizontal axis models.

A special survey was developed by the TU1304 Winercost action's Workgroup 3 and distributed in the participating countries in order to find out people's opinion on wind energy in built environment. It can be judged from the answers that respondents are aware of specific issues related to the development of small wind energy in urban environment. Wind resource seems to be not the main issue when planning the urban wind turbine – other concerns as noise, shadows, visual impact and danger from moving object are of more importance. Most of respondents are in doubt about the economical efficiency of small wind turbines due to low resources and high installation costs. Need for research of urban wind resource and wind turbine reliability and publicity of the results is emphasized.

Another survey of citizens' opinion and attitude to small wind turbines has been carried out by the researchers of Lithuanian Energy Institute. 1809 responses from municipalities and ministries were received and the results show that people are not sure about the efficiency and reliability of small wind turbines, but they agree with the statement that this technology is too expensive. Most of the respondents suggest to install small wind turbines in industrial zones and on the living houses. Only up to 10 % of the respondents consider small wind turbines as potential harm to their health or as a source of irritation and noise. In general statistics of the survey results show positive attitude to the small wind energy technologies in Lithuania.

CONCLUSIONS

Calculations have shown that small wind turbines with relatively larger rotors are more efficient in low wind conditions which are typical in urban areas. Wind turbines with >12 m^2/kW rotor swept area are capable of producing twice more energy comparing to typical turbines with 4-6 m^2/kW rotors.

Efficiency of small scale (1-30 kW) wind turbines installed in Lithuania has been investigated and capacity factors of 1-4 % have been determined. Results of the investigation of an operating 1 kW roof-top wind turbine shows that highest value of the coefficient of wind power conversion efficiency reaches 0.208.

Technical-economic efficiency evaluation method has been proposed for easier selection of small wind turbine model to be installed at a certain location. Investigation has revealed obvious advantages of horizontal axis wind turbines over the vertical axis. This advantage is most significant in the wind speed range of 5-7 m/s.

Surveys of public opinion about the urban wind energy has been carried out which revealed that people are well aware of poor performance problems of urban wind turbines. Most of respondents are in doubt about the economic efficiency of small wind turbines due to low wind resources and high installation costs. Need for research (wind resource also) and publicity of the results is emphasized. The investigation of the urban wind potential is necessary. Most of mistrust in small WTs comes from the lack of information about the winds available at the site, lack of technical knowledge about urban wind resource estimation and the reliability of turbines.

REFERENCES

[1] Simic Z., Havelka J.G., Vhorvcak M.B. "Small wind turbines – a unique segment of the wind power market", Renewable Energy, Vol.50, 2013, pp. 1027-1036.

[2] Olken M. "Windy conditions – integrating this form of power to the grid", IEEE Power & Energy November/December, Vol.9, No.6, 2011, pp. 4-6.

[3] Beller C. "Urban wind energy". PhD thesis, Risoe DTU, Technical University of Denmark, 2011, 168 p. ISSN 0106-2840.

[4] Wang W.-C., Teah H,-Y. Life cycle assessment of small-scale horizontal axis wind turbines in Taiwan. Journal of Cleaner Production, Vol 141, 2017, pp. 492-501.

[5] Al-Hadhrami L.M. Performance evaluation of small wind turbines for off grid applications in Saudi Arabia. Energy Conversion and Management, Vol. 81, 2014, pp. 19-29.

[6] Li Q.S., Shu Z.R., Chen F.B. Performance assessment of tall building-integrated wind turbines for power generation. Applied Energy, Vol. 165, 2016, pp. 777-788.

THE INTERNATIONAL CONFERENCE ON
WIND ENERGY HARVESTING 2017
20-21 April 2017
Coimbra, Portugal

Paper 603

NUMERICAL AND EXPERIMENTAL INVESTIGATION OF AERODYNAMIC LOADS FOR TALL BUILDINGS WITH PRISMATIC AND TWISTED FORMS

Ezgi Orbay [1]
Dept. of Aerospace Engineering,
Middle East Technical University
Ankara, Turkey

Sinan Bilgen [2]
Dept. of Architecture,
Middle East Technical University
Ankara, Turkey

Nilay Sezer-Uzol [3]
Dept. of Aerospace Engineering,
and METUWIND,
Middle East Technical University
Ankara, Turkey

Bekir Özer Ay [4]
Dept. of Architecture,
and METUWIND,
Middle East Technical University
Ankara, Turkey

Yaşar Ostovan [5]
Dept. of Aerospace Engineering,
and METUWIND,
Middle East Technical University
Ankara, Turkey

ABSTRACT

Cantilevered from the ground, tall buildings reaching exceptional heights are inevitably exposed to severe lateral effects, particularly wind loads. As the structures get higher, slenderer and have larger strength-to-weight ratios, their design, both structural and architectural, is principally based on wind rather than gravity or seismic demands. Wind forces acting on this type of structures primarily depends on wind characteristics and the building form. Thus, creating distinctive forms that attract public interest and are aerodynamically efficient is an ambition of architects and engineers for decades. Recently, twisting tall buildings emerged by virtue of such a motivation. This study investigates wind effects on these complex forms through a case study research. Comparisons between wind loads on a twisted building model and those on its conventional prismatic counterpart were performed by making use of both numerical analyses and experimental measurements. The influences of facade texture, wind speed, and wind direction on separated turbulent flow around the model buildings and the aerodynamic loads acting on the buildings have been investigated. Comparisons highlighted that, wind loads around the bluff body of twisting structure is on a lower grade compared to the prismatic counterpart which is valid for both along wind and across wind directions.

INTRODUCTION

There is not a constant definition for the term ‘‘tall building’’ from architectural or technological views. However, when the structural aspect is the subject, the definition particularly comes from the wind loads. In other words, when the design of a building is governed by aerodynamic loads rather than gravity or seismic loads, building can be identified as tall building or high-rise building [1]. Effects of the aerodynamic loads on the tall buildings like towers are focus of researchers in the recent literature [1-9] as the number of tall buildings has been rapidly increasing [2]. Unsteady, 3-D, separated and turbulent flow around the structure creates the wind loads which are the primary design parameter for this kind of structures in terms of occupancy comfort and structural stability [7]. In order to investigate this complex problem, wind tunnel experiments are conducted [4-5, 8] and CFD analyses are performed [6-9] in the recent literature. The wind loads on the 38-storey high-rise building was investigated by Vafaeihosseini in 2011 [6]. Mohotti et al. [7] solved the flow around tall buildings by using k-epsilon turbulence

[1] Research Assistant, PhD Graduate Student, Dept. of Aerospace Engineering, Middle East Technical University (METU), Ankara, Turkey/ezgiorbay@gmail.com
[2] M.S. Graduate Student, Dept. of Architecture, Middle East Technical University (METU), Ankara, Turkey/snnbilgen@gmail.com
[3] Assistant Professor, Dept. of Aerospace Engineering, and METUWIND, Middle East Technical University (METU), Ankara, Turkey/nuzol@metu.edu.tr
[4] Assistant Professor, Dept. of Architecture, and METUWIND, Middle East Technical University (METU), Ankara, Turkey/ozer@metu.edu.tr
[5] PhD Candidate Graduate Student, Aerospace Engineering, and METUWIND, Middle East Technical University (METU), Ankara, Turkey/ostovan@metu.edu.tr

model with a constant velocity profile. Also, he considered the effect of atmospheric boundary layer on the structures. Yılmaztürk and Sezer-Uzol [8-9] performed CFD analyses of a model tall building and also conducted wind tunnel tests to investigate the flow field characteristics and wind loads. Atmospheric boundary layer effects in a short tunnel are also investigated experimentally for the same building [8] by Shojaee et al. [9].

METHODOLOGY

Aerodynamic effects have been analyzed by both wind tunnel tests and numerical analyses. High frequency base balance (HFBB) tests on 3-D building models are performed to evaluate wind load effects on a global scale via wind tunnel tests which is accepted as the most confidential tool all over the world. Moreover, mathematically complex but another confident discipline, named Computational Fluid Dynamics (CFD) is used and comparisons of the results of the CFD simulations are made with the wind tunnel test results.

For wind tunnel tests, experimental models are produced by 3-D printers. In HFBB tests, models are required to have low mass and high rigidity [4], therefore, polyactic acid (PLA) material is preferred to satisfy this necessity. 3-D models can be seen in Figure 1. The scale of the models comes from the dimensions of wind tunnel's test section. Blockage ratio is the maximum cross-sectional area of the model at any cross-section divided by the area of the wind tunnel cross-section [3]. 1/750 scale was used to keep the blockage ratio small enough so that the error introduced is small and no correction is required. Two different design wind speeds of 6.85 m/s and 13 m/s are considered. Influence of angle of attack was investigated for each 15 degrees for each model. Although 10000 Hz is used for data acquisition through the tests, 1000, 100 and 10 Hz of data is also analyzed during post process of data. Data acquisition is implemented for a period of 2 minutes.

(a) (b)

Figure 1. Experimental models during the tests: a) Prismatic b) Twisted

For CFD simulations, unstructured mesh is generated for model scales of prismatic and twisted buildings, since unstructured grids are easy to generate in complex geometries such as twisted towers. The commercial software, Pointwise, is used to generate the computational grid around the towers. In Figure 2, the computational mesh for both cases can be seen. The computational domain of prismatic building and twisted building cases consist of approximately 2600 K cells. In this figure, building positions are according to head wind direction (yaw angle of 0 degree). In Figure 3, mesh around buildings can be seen along the slice at centerline of the domain, which represents zoomed views of the meshes.

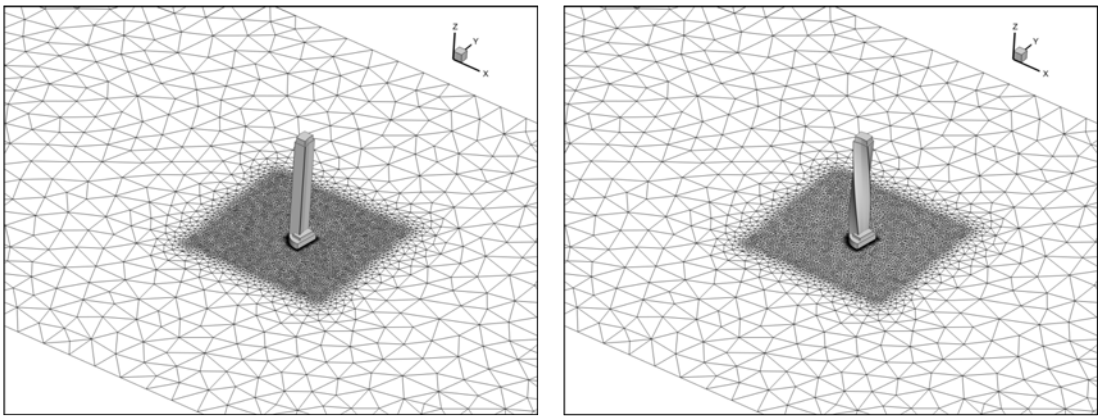

(a) (b)

Figure 2. Computational mesh around a) prismatic building b) twisted building

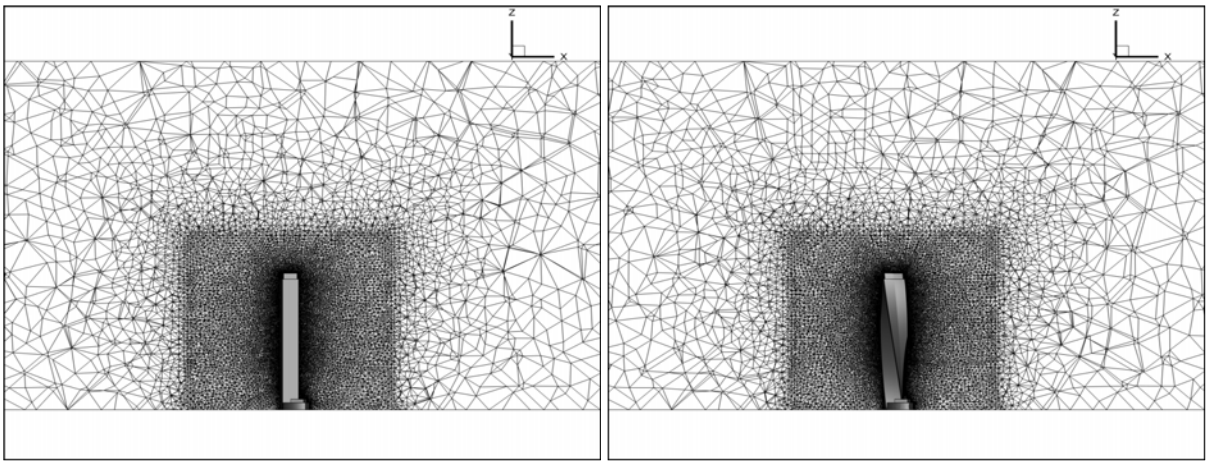

(a) (b)

Figure 3. Unstructured mesh around a) prismatic building b) twisted building

In order to solve the flow field through the computational domain, RANS equations are solved in the computational domain by using the commercial CFD flow solver, CFD++. In CFD analysis, different yaw angles of upcoming wind of ±15, ±75 and ±255 degrees and two different freestream velocities of 6.85 m/s and 13 m/s are considered. Uniform freestream is considered for this study by considering the short wind tunnel used in the tests, while neglecting the atmospheric boundary layer (ABL) effect. For two types of buildings, prismatic and twisted, flow analyses are performed. In the computations, characteristics farfield boundary condition is used in inlet and outlet face of the outer domain. No-slip wall boundary condition is applied at both building and wind tunnel walls. At first, steady-state computations are performed and the forces and moments acting on the building due to aerodynamic loads are compared with the wind tunnel experimental results. Then, unsteady simulations are performed in order to obtain time history of velocities around the building and load fluctuations. The comparison between the computational results and experimental data are also done and discussed.

PRELIMINARY RESULTS

Wind loads obtained from the experimental measurements are presented for the selected wind conditions for both buildings. In CFD analysis, preliminary results are obtained. During the computations, flowfield around the buildings are investigated in terms of velocity and pressure distributions which cause aerodynamic loading at structures. In Figure 4, flow around the prismatic building can be seen showing the pressure variation on the left and velocity magnitude changes on the right. In Figure 5, the preliminary results of the twisted building case are presented.

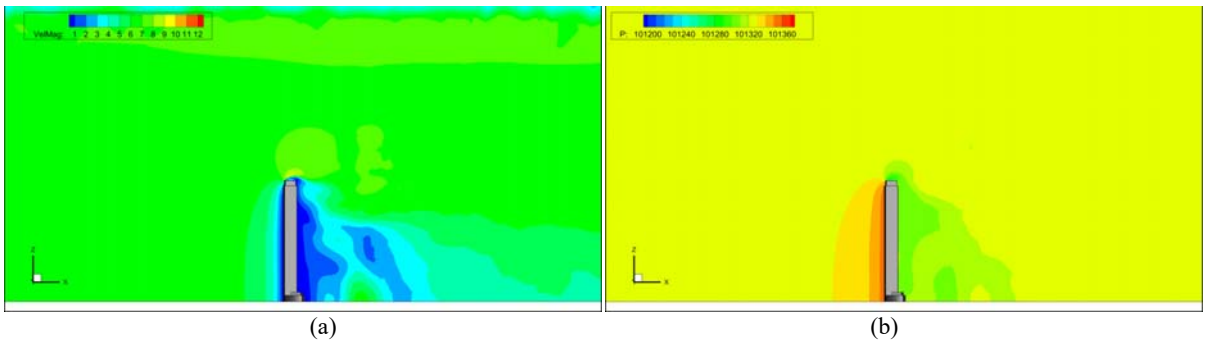

(a) (b)

Figure 4. Flowfield around the prismatic building a) Pressure variation b) Velocity magnitude change

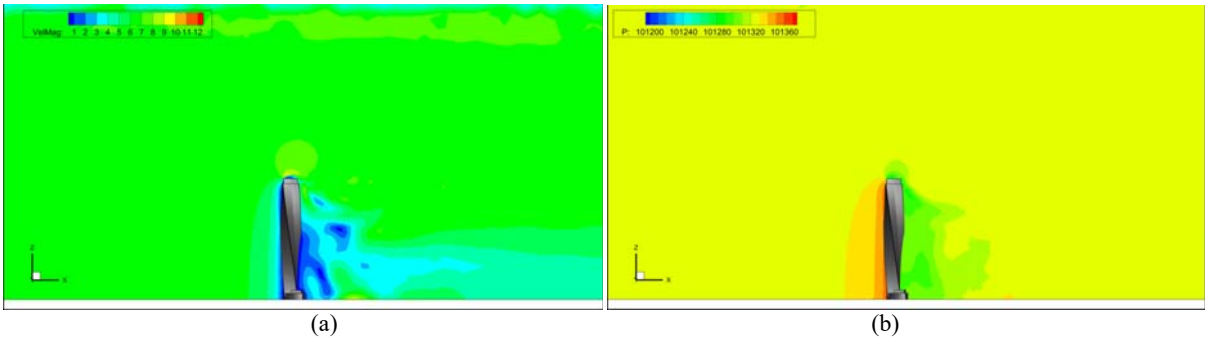

(a) (b)

Figure 5. Flowfield around the twisted building a) Pressure variation b) Velocity magnitude change

CONCLUSIONS

Aerodynamic loads are the primary factors affecting tall building design in terms of structural stability and occupancy comfort. This study mainly investigates aerodynamic effects on the twisting building and on its conventional prismatic counterpart by making use of wind tunnel tests and CFD. The effects of wind characteristics as speed and direction have been analyzed on these forms of building models. Further analyses on the unsteady flow field characteristics will be discussed in the final paper. Comparisons on preliminary results showed that wind loads around the bluff body of twisting structure is on a lower grade compared to the prismatic counterpart which is valid for both along wind and across wind directions.

ACKNOWLEDGEMENTS

This work is a part of the project BAP-08-11-2016-064 supported by METU. The experimental measurements and numerical analyses are performed by using the facilities at the Aerodynamics Laboratory and High Performance Computing Laboratory of METUWIND Center for Wind Energy in METU, respectively. We would like to thank Serkan Ülgen from METU Design Factory, for his technical support and valuable feedbacks during printing process of 3D models.

REFERENCES

[1] Günel, M.H. and Ilgın, H.E., 2014, Tall Buildings: Structural System and Aerodynamic Form, Routledge, Taylor & Francis Group.

[2] CTBUH Year in Review: Tall Trends of 2015, and Forecasts for 2016, The Council on Tall Buildings and Urban Habitat 2015 Year in Review report.

[3] Holmes, J. D., 2015, Wind loading of structures. New York: Taylor & Francis Group.

[4] Gamble, S., Wind Tunnel Testing, STRUCTURE Magazine, 2003, pp. 24-27.

[5] Shojaee, S. M. N., Uzol, O., Kurç, Ö., Atmospheric boundary layer simulation in a short wind tunnel, International Journal of Environmental Science and Technology, February 2014, Volume 11, Issue 1, pp 59–68.

[6] Vafaeihosseini, E., Sagheb, A., & Ramancharla, P. K. (2011). Analysis of Highrise Building using Computational Fluid Dynamics Approach: A Case Study on 38-Storey Highrise Building. Structural Engineering World Congress, India.

[7] Mohotti, D., Mendis, P., & Ngo, T., 2013, Application of Computational Fluid Dynamics (CFD) in Wind Analysis of Tall Buildings.

[8] Yılmaztürk, S., Yüksek Binalar Etrafindaki Akişin Sayisal ve Deneysel İncelenmesi. MS Thesis, Dept. of Mechanical Engineering, TOBB University of Economics and Technology, Sept. 2011.

[9] Yılmaztürk S. and Sezer-Uzol N., "Investigation of Flow Field Around A High-Rise Building Model In Atmospheric Boundary Layer," 6. Ankara International Aerospace Conference, AIAC-2011-094, 14-16 September 2011 - METU, Ankara Turkey.

THE INTERNATIONAL CONFERENCE ON
WIND ENERGY HARVESTING 2017
20-21 April 2017
Coimbra, Portugal

Paper 604

OPTIMAL PLANNING OF THE ENERGY PRODUCTION MIX IN SMART CITIES CONSIDERING THE UNCERTAINTIES OF THE RENEWABLE SOURCES

Stefano Bracco[1]
Univ. of Genova
Genova, Italy

Federico Delfino[2]
Univ. of Genova
Genova, Italy

Luisa Pagnini[3]
Univ. of Genova
Genova, Italy

Michela Robba[4]
Univ. of Genova
Genova, Italy

Mansueto Rossi[5]
Univ. of Genova
Genova, Italy

ABSTRACT

In smart grids and smart cities, the optimal size and location of plants for the production of renewable energy must consider the parameters of the site and the intermittent nature of the resource. The actual behavior of the power units and the load parameters are affected by uncertainties; especially, renewable sources are inherent random due to climatological uncertainty. Using a decision model for the definition of the optimal size and location of plants and using a probabilistic assessment of the parameters involved, the authors intend to formulate the problem according to a probabilistic approach.

NOMENCLATURE

PV	=	Photovoltaic
WT	=	Wind Turbine
CHP	=	Combined Heat and Power

INTRODUCTION

The planning of energy power units in smart grids and smart cities requires the best sizing and combination of the available technologies per each site, according to the end-user needs and in compliance with the network constraints [1]. The use of renewable power generators represents a great advantage in order to reduce primary energy consumptions and greenhouse emissions, however the optimally plan of the mix of power sources has to carefully consider the intermittent nature of the renewable resource and its inherent randomness [2].

The authors of this paper have developed a decision model [3] to find the optimal location and size of different power production systems including renewable energy to satisfy thermal and electrical demands in an urban district. The considered technologies are small size Wind Turbines (*WT*s), solar Photovoltaic (*PV*) and Combined Heat and Power units (micro gas turbines, *CHP*s) that are connected to the same grid. The expected power

1 Assistant professor, Department of Electrical, Electronic, Telecommunication Engineering and Naval Architecture (DITEN), Via Magliotto, Savona, Italy. E-mail: stefano.bracco@unige.it
2 Assistant Professor, Department of Electrical, Electronic, Telecommunication Engineering and Naval Architecture (DITEN), Via Magliotto, Savona, Italy. E-mail: federico.delfino@unige.it
3 Assistant Professor, Department of Civil, Chemical and Environmental Engineering, University of Genova, Via Montallegro 1, Genova, Italy. E-mail: luisa.pagnini@unige.it
4 Assistant Professor, Department of Informatics, Bioengineering, Robotics and Systems Engineering - DIBRIS, Via Opera Pia, Genova, Italy E-mail: michela.robba@unige.it
5 Assistant professor, Department of Electrical, Electronic, Telecommunication Engineering and Naval Architecture (DITEN), Via Magliotto, Savona, Italy. E-mail: mansueto.rossi@unige.it

production is derived according to nominal values of the statistical parameters of the climatic conditions in each hour during the day and in each month during the year. The decision variables are the number of *CHP*s of a given typology, the number of *WT*s and the *PV* surface which are obtained on the basis of the overall costs to be minimized.

Unfortunately, power production from renewable sources is very uncertain due to the inherent randomness of climatic conditions; wind power production of small size *WT*s, in particular, is even more uncertain because turbulence and gusty wind during the operating conditions may have a detrimental effect on the actual behavior of the turbines (Fig. 1, [4]). Moreover, adverse environmental conditions also preclude the use of more efficient technologies that require frequent maintenance interventions, and may result in frequent out of use of the machine and even collapses [5].

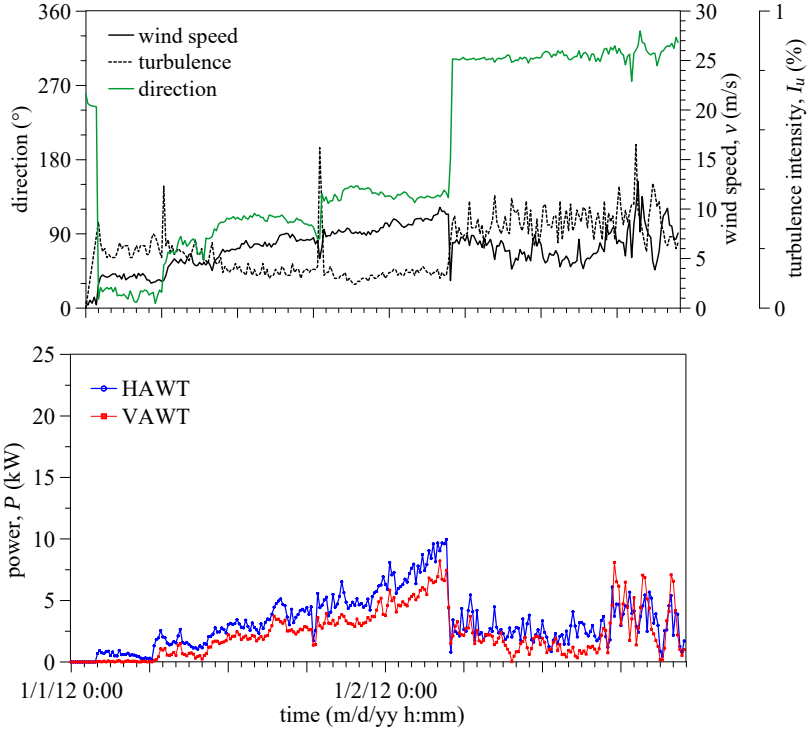

Figure 1. 10-minute averaged values of power output (below) and wind speed (above) recorded over two different 20 kW *WT*s having horizontal (*HAWT*) and vertical axis (*VAWT*).

Starting from these premises, and considering the possible variation of the solar radiation [6], of the wind source [7] and of the turbine performance [4], the present paper intends to analyze the propagation of the uncertainties in the overall power production of the installation, arriving at formulating the mix planning according to a probabilistic viewpoint.

DECISION MODEL

The planning of different energy sources in the electrical grid is a very delicate and strategic issue for the fulfillment of the requisites of smart cities. It requires the best sizing and combination of the available technologies per each site, taking into account the location-dependent properties of renewable sources, the energy demand, the network constraints. The model presented in ref. [4] supplies the optimal choice of sizes (or numbers) of the devices in all the locations which minimize the sum of the overall installation and operative costs, over the considered *Y* time horizon of years. Hourly and seasonally variations of the renewable sources, electrical demand, energy prices, etc., are taken into account by considering, for each month of the year and for each site, the corresponding profile in a typical average day. Hourly prices are considered for the purchasing and selling of electricity.

The smart grid considered avails of Solar *PV* units, small size *WT*s, and *CHP*s, capable of producing both electrical and thermal power. The decision variables of the optimization problem are the surface covered by *PV* panels, the number of *WT*s and *CHP*s, each related to a number of sites, target power and technology fixed in advance.

For each hour t in a representative day of month m, in year y, the electrical power balance of the site s, $P^{Grid}_{s,y,m,t}$, is [5]:

$$P^{Grid}_{s,y,m,t} = D^{el}_{s,y,m,t} - P^{PV}_{s,y,m,t} - P^{W}_{s,y,m} - P^{CHP}_{s,y,m,t} \quad (1)$$

being $D^{el}_{s,y,m,t}$, $P^{PV}_{s,y,m,t}$, $P^{W}_{s,y,m,t}$, $P^{CHP}_{s,y,m,t}$ respectively, the electrical demand, the electric power output of the *PV*s, of the *WT*s, of the *CHP*s, each referred to s, y, m, t; $s = 1,..,S$ is the number of possible sites considered for the installation, $y = 1,..,Y$ is the year number of the expected life considered; $m = 1,..,M$ is the generic month in the year (M=12); $t = 1,..,T$ is the generic hour in the day (T=24).

The annual operating costs of the whole installation, C_y, can be computed as:

$$C_y = \sum_{s=1}^{S}\sum_{m=1}^{M}\left[n_m \sum_{t=0}^{T-1}(C^{GRID}_{s,y,m,t} + C^{PV}_{s,y,m,t} + C^{W}_{s,y,m,t} + C^{CHP}_{s,y,m,t}) \right], \quad y=1..Y \quad (2)$$

being $C^{Grid}_{s,y,m,t}$, $C^{PV}_{s,y,m,t}$, $C^{W}_{s,y,m,t}$, $C^{CHP}_{s,y,m,t}$, respectively, the hourly cost of electricity, *PV*s , *WT*s and *CHP*s in s, y, m, t; n_m is the number of days in month m. Deriving the total capital cost, K, as the sum of the capital costs of all the *PV* fields, *WT*s, *CHP*s, the optimum planning is achieved by minimizing the objective function derived as the sum of installation costs and annual discounted operating costs:

$$\min\left\{ K + \sum_{y=1}^{Y} \frac{C_y}{(1+i)^y} \right\} \quad (3)$$

Constraints apply on decision variables and other quantities. Details of the model are reported in [4].

UNCERATAINTIES IN RENEWABLE SOURCES

The evaluation of the expected power production is usually carried out availing of statistical models of the related climatic parameters recorded in a suitable period of time in the site considered. As a matter of fact, solar radiation and wind speed are a variable resource that is difficult to predict due to meteorological uncertainty. Climatological parameters between the neighboring sites may also vary according to the morphology of the surroundings; the amount of energy that power units will produce with the estimated meteorological resource is uncertain also, *e.g.*, the atmospheric turbulence can have a detrimental effect on the real power curve of the *WT*, making the actual behavior quite different from the power curve supplied by the manufacturer (Fig. 2). Moreover, the choice of the technology to be adopted must be accurately considered for small size *WT*s, in order to preserve the operational activity and the structural safety of the machine. To the authors' experience, in a urban environment, vertical Axis *WT*s reveal less efficient with respect to the Horizontal Axis typology, but the adoption of this technology may prove more advantageous to reduce maintenance and repairing costs.

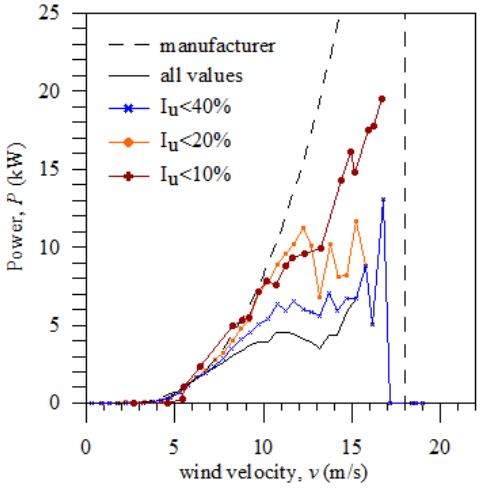

Figure 2. Measured power curve of a 20 kW vertical axis *WT* at different values of the turbulence intensity. Dashed line represents the power curve provided by the manufacturer.

Power production of a *PV* field per square meter, $p^{PV}_{s,y,m,t}$, can be estimated as a function of the conversion efficiency of the *PV* system, η, of the solar radiation, $I_{s,m,y,t}$ and of a parameter related to the outside temperature, γ, dependent on *s, y, m, t*:

$$p^{PV}_{s,y,m,t} = \eta \; I_{s,y,m,t} \; \gamma_{s,y,m,t} \tag{4}$$

The average power delivered by each *WT* is estimated by the integral of the power curve of the turbine and the wind speed distribution. Using a Weibull distribution, it can be obtained as a function of the dimensionless and scale parameter, $k_{s,y,m,t}$, $c_{s,y,m,t}$:

$$p^{W}_{s,y,m,t} = \frac{P_r}{v_r^3}\left\{ c_{s,y,m,t}{}^3 \left[-i\Gamma\left(\frac{3}{k_{s,y,m,t}} + 1, u_{s,y,m,t} \right) \right]_{u_{in}}^{u_r} - e^{-u_{s,y,m,t}} \Big|_{u_r}^{u_{out}} \right\}, \quad u_{s,y,m,t} = \left(\frac{v}{c_{s,y,m,t}} \right)^{k_{s,y,m,t}} \tag{5}$$

where v_{in}, v_{out} are the cut-in and cut-out wind speed, P_r is the rated power at the wind speed v_r; $i\Gamma$ is the incomplete gamma function; each parameter is dependent on *s, y, m, t*.

Availing of uncertainty models of the parameters, derived from available data base of solar radiation and from accurate anemometric measures, considering the discrepancies of the power production with respect to the nominal power curve and using suitable propagation techniques ([8]), the authors intend to propagate uncertainties on the expected power production, formulating the decision model for the definition of the optimal size and location of plants according to a probabilistic approach.

ACKNOWLEDGEMENTS

The authors acknowledge with thanks the support of the TU1304 COST Action “Winercost”

REFERENCES

[1] Mancarella, P., “Distributed multi-generation options to increase environmental efficiency in smart cities”, Proc., 2012 IEEE Power and Energy Society General Meeting, pp. 1-8, San Diego, CA, 2012.

[2] Chicco, G. and Mancarella, P. “Distributed multi-generation: a comprehensive view”, Renewable and Sustainable Energy Reviews, 13, 2009, pp. 535–551.

[3] Bracco, S., Delfino, F., Rossi, M., Robba, M. and Pagnini, L. “Optimal planning of the energy production mix in smart districts including renewable and cogeneration power plants”, IEEE 2nd International Smart Cities Conference: Improving the Citizens Quality of Life, ISC2 2016, Trento, Italy.

[4] Pagnini, L.C., Burlando, M. and Repetto, M.P., “Experimental power curve of small-size wind turbines in turbulent urban environment”, Applied Energy, 154, 2015, pp. 112-121.

[5] Pagnini, L.C., Repetto, M.P., Freda, A., Piccardo, G. and Rosasco, M. “Structural monitoring of a small size vertical axis wind turbine”. Proc., XIII Conference of the Italian association for the Wind Engineering, INVENTO 2016, Terni, 2016.

[6] Espinar, B., Aznarte, J.L., Girard, R., Moussa A.M. and G. Kariniotakis, “Photovoltaic Forecasting: A state of the art”, Proc., 5th European PV-Hybrid and Mini-Grid Conference, Tarragona, Spain. OTTI - Ostbayerisches Technologie-Transfer-Institut, 2010.

[7] Pagnini, L.C. and Solari, G. “Joint modelling and mapping of the parent population and extreme value distributions of the mean wind velocity”, Journal of Structural Engineering, ASCE, 142(2), 2016.

[8] Pagnini, L., Repetto, M.P. “The role of parameter uncertainties in the damage prediction of the alongwind-induced fatigue”, Journal of Wind Engineering and Industrial Aerodynamics, 104, 2012, pp. 106-127.

THE INTERNATIONAL CONFERENCE ON
WIND ENERGY HARVESTING 2017
20-21 April 2017
Coimbra, Portugal

Paper 605

THE URBAN WIND ENERGY POTENTIAL FOR INTEGRATED ROOF WIND ENERGY SYSTEMS BASED ON LOCAL BUILDING HEIGHT DISTRIBUTIONS

Rijk Blok[1]
TU/e Eindhoven University of Technology
Netherlands

Michiel Coers[2]
TU/e Eindhoven University of Technology
Netherlands

ABSTRACT

An Integrated Roof Wind Energy System (IRWES) is a roof mounted structure with an internal wind turbine that uses smart aerodynamics to catch and accelerate wind flow. It has been designed for application on (existing) buildings in the urban environment. To estimate the maximum total wind energy harvesting potential of cities, while using these kind of roof mounted units, a method has been developed. The method analyses actual height measurement data files, estimates surface roughness, and calculates wind energy potential for different building height categories. This wind energy potential is based on theoretical calculated additional building heights for these roof mounted systems, based on building strength and stiffness capacity estimations, local (average) wind velocities as well as the IRWES wind energy efficiency characteristics. The method has been applied to the cities of Amsterdam, Rotterdam as well as Eindhoven, Netherlands, but could also be applied to any City in the World. Results make it possible to compare Urban Wind Energy Potential of whole cities but also to compare height categories of buildings as well as to quickly estimate what an IRWES unit could provide for a single building.

INTRODUCTION

The world's population never grew so fast, combined with our modern energy consuming society the demand for energy is high. The global energy consumption is estimated to increase by 53% between 2008 and 2035 [1] . To catch up with this continuing increase in energy demand and combined depletion of fossil fuels, people have to invest in techniques for generating renewable energy. In Eindhoven, company IBIS Power developed their renewable energy solution "Integrated Roof Wind Energy System", further called IRWES. IRWES is a roof-mounted structure with an internal wind turbine making use of smart aerodynamics to catch and accelerate the wind flow [2] . In comparison to conventional wind turbines, this "elegant" system is designed for application in the urban environment. To see in which Urban Environments the application of these Roof Mounted systems is most useful and to see to what extend these systems in general can contribute a calculation method has been developed to more precisely estimate Urban Wind Energy potential.

METHODOLOGY

Starting from height measurement data files (Actual Heights Netherlands (in Dutch) AHN) [3] that have been acquired using laser-altimetry, a method has been developed to arrive at building dimensions: heights and roof area, through extensive Matlab analysis with density based space clustering methods. Using this analysis the surrounding perimeters of every building is reviewed to calculate the surrounding surface roughness, zero-plane displacement height and wind velocities using data from local nearest wind stations. From strength and stiffness estimates of the building the additional height available for to Integrated Roof Wind Energy System is estimated

[1] Assist. Professor, Structural Design, TU/e, Eindhoven University of Technology, Netherlands, Structural designer W5A Structures, Netherlands R.Blok@tue.nl
[2] Wind specialist and Structural designer, Eindhoven, Netherlands, michielcoers@hotmail.com

(without compromising the structural usability and structural safety). With these available extra height capacity and based on the local average wind velocities the energy potential of the additional IRWES is then calculated.

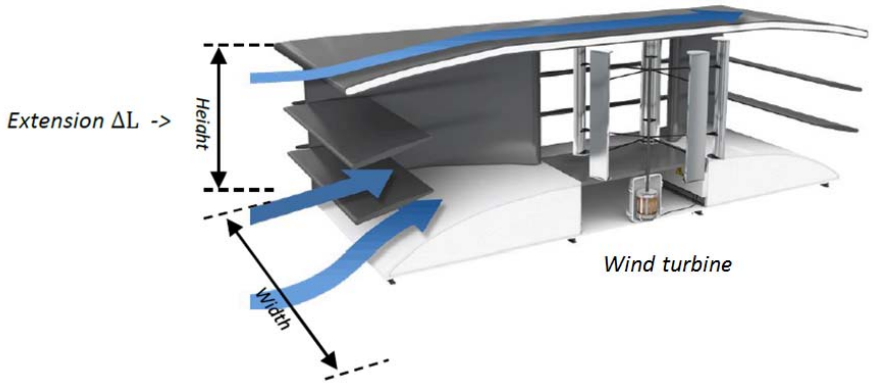

Figure 1. Principle of Integrated Roof Energy System IRWES

RESULTS

The Matlab analysis of the measured height data results in building dimensions: Building heights and building roof area as well as the building's surroundings. The AHN files have been cleaned of 'noise' such as trees, fences, etc. and create a set of data which only consists of buildings, (a statistical method called 'Density-Based Spatial Clustering' [4] has been used.

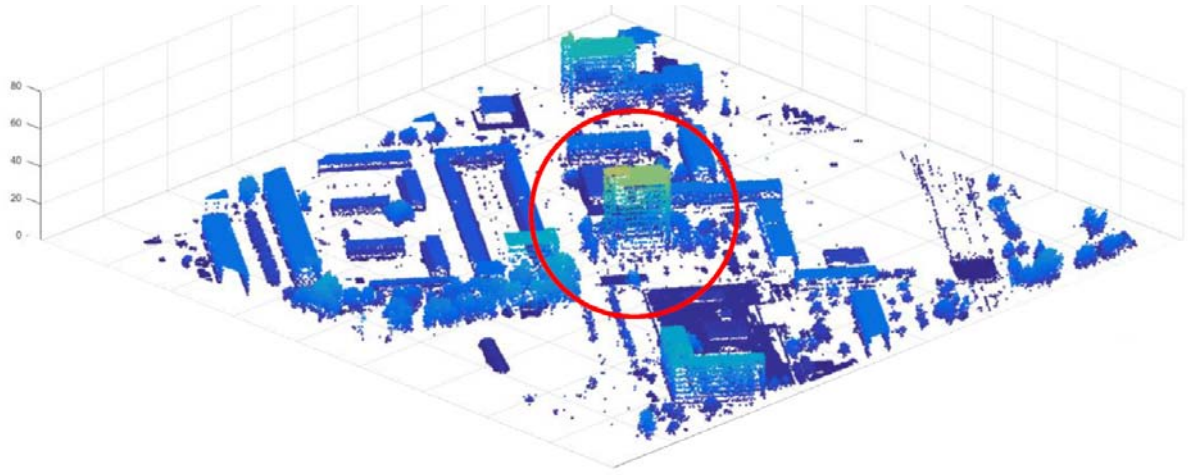

Figure 2. Example of Matlab output: Building and it's surroundings after noise reduction

Every building that has been accounted for thus has its own properties regarding roof surface, height and wind speed. Based on the measured height data the number of buildings in each height category has been established. From the number of buildings and their roof area the theoretical potential for wind energy harvesting has been calculated using the IRWES characteristics. Table 1 shows the yearly wind energy for the city of Rotterdam per building height category.

Table 1. Total yearly energy output of Integrated Roof Wind Energy Systems in city of Rotterdam (5% and 10% category)

Building height [m]	*Number of building [#]*	*Total roof surface [m²]*	*MWh/yr 5%*	*MWh/yr 10%*
150+	3	2861	78	153
140-149	2	3830	65	128
130-139	1	600	13	25
120-129	2	1012	20	40
110-119	1	1709	22	42
100-109	6	3870	76	151
90-99	10	8651	156	309
80-89	9	5668	129	254
70-79	14	9684	164	324
60-69	19	12331	181	358
50-59	55	42783	396	783
40-49	79	55466	430	850
30-39	143	123538	548	1083

The method has been applied to the data of the city of Amsterdam, Rotterdam as well as Eindhoven, Netherlands, but could be applied to any city in the world given that height measurement data are available and local wind characteristics (velocities) are available.

CONCLUSIONS

The method proofs to make more precise estimations on Urban Wind Energy Potential possible taking into account the local Urban building height distributions and local wind characteristics. The method covers the scale of a particular local building to the scale of a whole city. With regard to the buildings overcapacity for each building height category now estimations of 5 and 10% have been used. More research for estimating average structural building overcapacity per building height category is needed.

ACKNOWLEDGEMENTS

This study has been performed as a graduation study and has been co-supervised and also made possible by Dr. Ir. A.B. Suma of Ibis power b.v. producer of IRWES..

REFERENCES

[1] Atanasiu, B., & Bertoli, P. Electricity consumption and efficiency trends in the enlarged European Union, *Institute of Environment and Sustainability, Luxembourg*. (2007).

[2] Suma, A.B., Ferraro, R.M., Dano, B. and Moonen, S.P.G., *"Integrated Roof Wind Energy System."* In 2nd European Energy Conference, Maastricht, The Netherlands, (2012).

[3] AHN, *Het AHN (Actueel Hoogtebestand Nederland*. Retrieved from Actueel Hoogtebestand Nederland: http://www.ahn.nl/pagina/het-ahn/het-ahn.html, (2015).

[4] Ester, M., e.a., A Density-Based Algorithm for Discovering Clusters, Institute for Computer Science, Univ. Munich, from KDD-96 Proceedings, Germany,(1996).

THE INTERNATIONAL CONFERENCE ON
WIND ENERGY HARVESTING 2017
20-21 April 2017
Coimbra, Portugal

Paper 606

WIND TURBINE DESIGNS FOR URBAN APPLICATIONS

Aierken Dilimulati[1]
Concordia University
Montreal, Quebec, Canada

Ted Stathopoulos[2]
Concordia University
Montreal, Quebec, Canada

Marius Paraschivoiu[3]
Concordia University
Montreal, Quebec, Canada

ABSTRACT

The modern day demand for renewable energy and the development of energy independent building designs have motivated significant research into the improvement of wind power technologies that target urban environments. However, the implementation of wind turbines in urban environments is still very limited. There have been some experimental studies concentrating on different designs of urban wind turbines either using computational fluid dynamics (CFD) or wind tunnels tests or field data from existing or new turbine designs. This paper reviews the state-of-the-art of urban wind energy by examining the various types of urban wind turbine designs and their characteristics, with a view to optimize their performance.

NOMENCLATURE

A	=	Rotor blade swept area
A^*	=	Diffuser exit area
U	=	Wind speed
C_p	=	Power coefficient
Lt	=	Diffuser axial length
ρ	=	Air density
P_{wind}	=	Wind power

INTRODUCTION

Wind energy harnessing technologies are a large part of the renewable energy sector, and as such have been the focus of a great deal of research in the last couple of decades. Developing efficient and cost effective wind turbines for urban applications can reduce dependency on fossil fuels for energy demand. In addition, the ability to provide power at the source of the demand can reduce the cost of distribution. Wind power increases with the cube of wind velocity, i.e.

$$P_{wind} = \frac{1}{2}\rho A U^3$$

The velocity and the density of the air flow increase in urban areas, as air is forced to navigate around obstacles such as buildings, structures, buses and trains. This creates an opportunity to take advantage of the locally increased density and velocity of the airflow. However, the unavoidable general reduction of the mean flow, due to the increased ground roughness (friction) and the unpredictable - and often changing - direction of air movement, i.e. wind, within urban areas result in a severely turbulent flow, which is not ideal for use as the driving force of wind turbines. Therefore, the design of efficient and effective wind turbines, which can operate under these conditions, becomes critical for performance optimization.

1 M.A.Sc. student, Dept of Mechanical and Industrial Engineering, Concordia University, Montreal, Canada/arkendilmurat@gmail.com
2 Professor, Dept. of Building, Civil and Envir. Engineering, Concordia University, Montreal, Canada/statho@bcee.concordia.ca
3 Professor, Dept. of Mechanical and Industrial Engineering, Concordia University, Montreal, Canada/marius.paraschivoiu@concordia.ca

PREVIOUS WORK

There are many different types of wind turbine designs today, each with its own unique performance profile. Designs are driven by various requirements specific to the application and location of the device. Some of these design criteria include size constraints, noise limitations, the visual disturbance concerns and the low start up wind speed. Depending on these criteria, one particular wind turbine may be more advantageous in one aspect than the other. Savonius rotors are some of the oldest designs for wind turbines. They have proven to be well suited to micro scaled urban operations due to their simple design and relatively low cut-in wind velocity (Saha et al., 2008). The Darrieus vertical axis wind turbine (VAWT) – see Figure 1 - is one of the most attractive options for rooftop installation, as it is visually unobtrusive and produces low-level acoustic emissions (Balduzzi et al., 2012). In addition, recent designs of Darrieus wind turbines show good self-startup abilities (Batista et al., 2015).

Some wind turbine designs focus more on one particular operational requirement than others. One such example is the Lotus-shaped micro wind turbine that is used almost exclusively for decorative purposes in urban areas due to its aesthetic appeal (Wang and Zhan, 2015). Relative to other designs, the power generated by Lotus turbines is not significant, and is usually not the main reason for deployment (Wang and Zhan, 2015). Vertical axis wind turbines (VAWT) are known to perform well in built environments due to their multidirectional ability in turbulent flow (Elkhoury et al., 2015).

There is an increasing amount of research devoted to urban wind power, however there are still a lot of questions about the performance of wind turbines. The main concern about the feasibility of urban wind turbine applications is the power output. Clearly, there is a need for new designs with high power efficiency. A diffuser augmented wind turbine (DAWT), with a brimmed structure at the exit periphery of the diffuser, has been tested in parks in Japan (Ohya and Karasudani, 2010) – see Figure 2. With a long diffuser length (Lt) the brimmed DAWT produces a power output 4~5 times that of a conventional wind turbine. It is important to acknowledge the difficulties in predicting the power output of a wind turbine as the wind profile may vary with different scales. Therefore, the wind turbine power output data should be used cautiously and further analysis is very important. There has been some preliminary research into the design of a brimmed diffuser structure to envelope a rooftop VAWT for power augmentation. This paper will also serve as a foundation for future design and experiments of such wind turbines.

Figure 1 New Darrieus VAWT design prototype (Balduzzi et al., 2012)

Figure 2 500W wind-lens turbine (Ohya and Karasudani, 2010)

METHODOLOGY

A thorough literature review has been carried out to comprehend the existing urban wind turbine technologies. All relevant sources of information have been compiled in a database with special focus on wind turbines in urban built environments. Different geometric designs have been categorized for comparison of their performances in a thematic analysis. Data collected from CFD analysis, wind tunnel tests, and field experiments will be analyzed to validate the consistency of the reported results about their performance. Data obtained from different sources for similar types of wind turbines and data from different experimental analyses will be compared for traversal analysis. The power coefficient, C_p, will be used as a key indicator of power efficiency when comparing different wind turbines.

RESULTS

Figure 3 shows a comparison of the power output of a brimmed type of DAWT (Wind-lens) with that of a conventional wind turbine. The increase in the power output is mainly due to the increase in the mass flow rate as wind accelerates in the diffuser with the low pressure created by the vortex at the exit. The green dashed curve in the figure is the power curve for a conventional “bare” wind turbine. The blue solid power curve, obtained using wind tunnel test, for C_p value of 1.4, is compared with the field vary from the wind tunnel-curve, with some field data points having significantly higher values. This is due to the fluctuation of the wind speed in the field test (Ohya and Karasudani, 2010).

Skeptics argue that the power coefficient calculated using a smaller rotor blade swept area is misleading. However, the power coefficient is still 38~73% higher for a long diffuser when calculated using the reference area A^*, which refers to the exit brim diameter (Ohya and Karasudani, 2010).

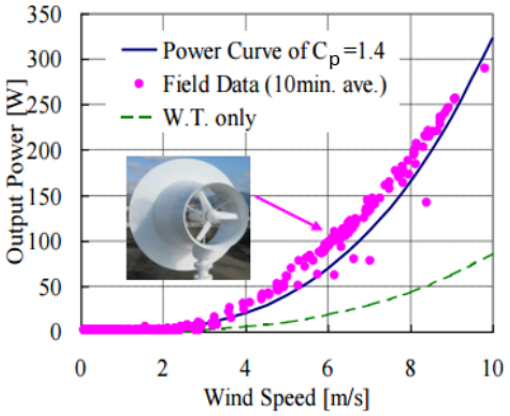

Figure 3. Field experiment of 500W wind turbine with wind-lens (Ohya and Karasudani, 2010)

CONCLUSION

The increasing demand for sustainable building designs and the technological advancement in wind turbine development have created an urgent call for efficient and realistic wind turbine designs for urban applications. There are many designs available, each being advantageous in a particular aspect of design requirements. However, general implementation of wind turbines in urban built environments is not yet very common. As a result, data available about their performance is limited. The overall analysis of existing wind turbines for built environments that will be carried out can provide a better understanding of wind turbine development and guidelines for future research in this area. A low cost and power efficient urban wind turbine for rooftop installation will be examined in the framework of this work, with a view to achieve the best performing power augmented wind turbine.

ACKNOWLEDGEMENTS

The authors gratefully acknowledge the use of the services and facilities of the Faculty of Engineering and Computer Science at Concordia University. This work was supported by funds originated from the Concordia Institute for Water, Energy and Sustainable Systems (CIWESS).

REFERENCES

Balduzzi, F., Bianchini, A., Carnevale, E.A., Ferrari, L., Magnani, S. 2012. Feasibility analysis of a Darrieus vertical-axis wind turbine installation in the rooftop of a building. Applied Energy 97, 921-9.

Batista, N.C., Melício, R., Mendes, V.M.F., Calderón, M., Ramiro, A. 2015. On a self-start Darrieus wind turbine: Blade design and field tests. Renewable and Sustainable Energy Reviews 52, 508-522.

Elkhoury, M., Kiwata, T., Aoun, E.2015. Experimental and numerical investigation of a three-dimensional vertical-axis wind turbine with variable-pitch. Journal of Wind Engineering and Industrial Aerodynamics 139, 111-123.

Ohya, Y., Karasudani, T. 2010. A shrouded wind turbine generating high output power with wind-lens technology. Energies 3, 634-649.

Saha, U.K., Thotla, S., Maity, D. 2008. Optimum design configuration of Savonius rotor through wind tunnel experiments. Journal of Wind Engineering and Industrial Aerodynamics 96, 1359-1375.

Wang, Y., Zhan, M. 2015. Effect of barchan dune guide blades on the performance of a lotus-shaped micro-wind turbine. Journal of Wind Engineering and Industrial Aerodynamics 136, 34-43.

THE INTERNATIONAL CONFERENCE ON
WIND ENERGY HARVESTING 2017
20-21 April 2017
Coimbra, Portugal

Paper 607

WIND TURBINE INTEGRATION TO TALL BUILDINGS

İlker Karadağı
Istanbul Technical University
Istanbul, Turkey

Nuri Serteser2
Istanbul Technical University
Istanbul, Turkey

ABSTRACT

Having a far distance from the ground levels exposed to turbulent wind conditions, tall buildings have the potential of generating wind energy. Unfortunately, rare studies have been conducted on wind turbine integration to tall buildings located in dense urban areas. Within the scope of this study, three tall buildings located in 4th Levent region of İstanbul were investigated with respect to their potential of generating wind energy. For the integration of wind turbines to the tall buildings, it is necessary to know the wind characteristics of the buildings to be able to determine the amount of energy that can be produced. Contrary to the wind characteristics in open spaces, the wind flows around the buildings may be characterized with high turbulence intensity and frequent sudden gusts. For this reason, the determination of the wind flow around the building is not only important for the amount of energy that can be generated, but also for the safety of the turbines exposed to fatigue caused by the flow characteristics.

There are several different ways to determine the wind characteristics around the building. One of these methods is to acquire information on wind direction and speed with using the wind sensors located at different positions and heights. That sensor data can be used to make assumption as to building's wind energy capacity. Data collection with anemometers is a realistic and reliable method, but the data obtained is limited to sensor locations. Except this method, experimental studies ca be also conducted for analyzing wind-building interaction and flow characteristics around the buildings. However, in the wind tunnel studies, the output data is mostly limited with pressure and velocity sensor points, moreover the recent studies on comparing different wind tunnel laboratory studies for the same case showed high differences even reaching up to %40 percent. Besides these two methods, the wind flow characteristics can be determined by simulations of computational fluid dynamics (CFD) too. With these simulations it is possible to obtain high resolution wind data in a very wide area around the building. In particular, numerical analyzes in which the meteorological data are taken as velocity input and the logarithmic wind profile is processed to the boundary conditions can yield close results with the determination of a suitable turbulence model and the sufficient number of iterations. For this reason, in the scope of this study, a CFD simulation software was used. For the simulations, an open source CFD software named OpenFOAM which is widely used both commercially and academically was chosen. The first input of the software is the 3D building geometry. For this input, case buildings were modeled in detail along with their immediate surroundings and with all details that could affect the flow. In the next step, the calculation nodes were defined with using mesh settings. During this process, high density meshing was used at the boundary layers and in the assumed critical regions, and mesh independency studies were conducted. Once the meshing process was complete, boundary conditions were determined (inlet, outlet, etc.) and the appropriate turbulence model and wind velocity profile were selected. After that, simulations were run, then the analysis results were analyzed in a post-process software and the necessary conclusions were derived.

At the last stage, an appropriate wind turbine model was chosen and design proposals were developed to integrate chosen wind turbine system to the case buildings. Then, the amount of energy that can be produced

1 Res. Asst, Dept. of Architecture, Istanbul Technical University, Taskisla/Istanbul/serteser@itu.edu.tr
2 Asst.Prof., Dept. of Architecture, Istanbul Technical University, Taskisla/Istanbul/serteser@itu.edu.tr

with the proposed system was calculated and it's seen that, preliminary comprehensive studies are very important for the efficiency of the wind turbine system, otherwise it wouldn't be possible to benefit from this type of systems sufficiently. It's also concluded that, as to accurate positioning of the wind turbine and the hub height, detailed analyzes should be conducted on determining highly turbulent flow areas which can reduce the amount of energy yielded from the wind turbine. Besides, environmental benefits of using a sustainable energy system were examined. For this purpose, the elimination of carbon emissions which would be released for the equivalent energy yielded from fossil fuels were calculated. It's seen that, using wind turbines leads to significant decrease in carbon emissions.

Special session AEOLUS4FUTURE

THE INTERNATIONAL CONFERENCE ON
WIND ENERGY HARVESTING 2017
20-21 April 2017
Coimbra, Portugal

Paper A4F.01

A STATE-OF-THE-ART REVIEW ON LOCAL FATIGUE DESIGN OF SUPPORT STRUCTURES FOR OFFSHORE WIND TURBINES

Gonçalo T. Ferraz[1]
Institute for Steel Construction - LUH
Hanover, Lower Saxony, Germany

Ana Glišić[2]
Institute for Steel Construction - LUH
Hanover, Lower Saxony, Germany

Peter Schaumann[3]
Institute for Steel Construction - LUH
Hanover, Lower Saxony, Germany

ABSTRACT

The scientific community is devoting more attention to the wide scope of offshore wind turbine structures. Since such structures are subjected to high level of fatigue loads as well as a large number of load cycles caused by wind, waves and turbine operation, the fatigue performance of welded connections is usually a design driving criteria. In this paper, a brief revision on load simulation and strength analysis procedures as well as local fatigue design methods of support structures for offshore wind turbines is presented. In order to face some of the challenges in this area of expertise, a research project is introduced, aiming to exploit residual capacities in the fatigue design of tubular joints of support structures for offshore wind turbines.

NOMENCLATURE

FEA	=	Finite Element Analysis
FM	=	Fracture Mechanics
HSS	=	Hot spot stress
LEFM	=	Linear Elastic Fracture Mechanics
NSA	=	Notch Stress Approach
OWT	=	Offshore Wind Turbine
SCF	=	Stress Concentration Factor
SIF	=	Stress Intensity Factors
SSA	=	Structural Stress Approach

INTRODUCTION

Wind energy has become a mainstream source of energy due to the growing energy demands, the imposed limits of greenhouse gases emissions (Kyoto Protocol) and the desired diversification of energy supply related to the fossil fuels dependence, the aversion to the traditional fission nuclear power and the lack of progression in the application of fusion nuclear power [1].

In the last two decades wind turbines moved offshore due to the limited in-land space for the development of onshore wind farms, the possibility to accommodate even more wind power under significant steadier wind conditions, and the lower environmental impact inherent to an Offshore Wind Turbine (OWT). The support

1 Research Assistant, Institute for Steel Construction, Leibniz University of Hanover, Appelstr. 9a, 30167, Hanover, Germany, e-mail: ferraz@stahl.uni-hannover.de
2 Research Assistant, Institute for Steel Construction, Leibniz University of Hanover, Appelstr. 9a, 30167, Hanover, Germany, e-mail: glisic@stahl.uni-hannover.de
3 Full Professor, Institute for Steel Construction, Leibniz University of Hanover, Appelstr. 9a, 30167, Hanover, Germany, e-mail: schaumann@stahl.uni-hannover.de

structure of an offshore wind turbine has a great contribution to the overall cost-effectiveness of the all system, especially in deep waters. As current practice, monopiles are the preferred type of support structures for water depths up to 30 m [2]. Thus, monopile diameters up to 10 m are subject of latest design concepts, leading to manufacturing, transportation and erection challenges. However, more attention have been payed to the use of jacket structures to larger water depths. The design of jacket substructures for offshore wind turbines is still in an early stage of development although the use of such substructures has the potential to become the dominant solution due to the expected optimization of design methods, fabrication techniques (in particular with respect to the connection between members), transportation and erection [3, 4].

Since OWTs are subjected to high level of fatigue loads as well as a large number of load cycles caused by wind, waves and turbine operation, the fatigue performance of welded connections is usually a design driving criteria. The fatigue behaviour of welded tubular joints is a well-recognised problem in the design of tubular structures [5]. The fatigue strength of such joints depends on the absolute and relative size of its members (size effect), on the load case, on the initial crack-like imperfections, and on the welding residual stress fields [6]. Research addressing these fatigue issues has been carried out during the last 35 years, mainly by the offshore industry [5, 6].

In this paper, a brief revision on load simulation and strength analysis procedures as well as local fatigue design methods of support structures for OWT is made, with the aim of contextualize the fatigue problematic within the entire design process and to emphasize the importance of local fatigue design assessment. Finally, a research plan within the framework of the Innovative Training Network (ITN) AEOLUS4FUTURE is introduced, aiming to exploit residual capacities in the fatigue design of tubular joints of support structures for offshore wind turbines.

LOCAL FATIGUE DESIGN OF OWT SUPPORT STUCTURES

The number of load cycles generated from the rotor of an OWT within its design life time (usually 20 years) may reach more than 1x 10^9 load cycles [7]. Furthermore, geometric discontinuities lead to stress concentrations that must be considered within the fatigue assessment [8].

Tubular joint design is a well-known field of research of the offshore industry. For fatigue verifications, it is common practice to evaluate the calculated damage based on hot spot stresses (HSSs) in combination with related S-N curves [9]. However; the geometrical characteristic of tubular joints, especially with respect to multiplanar joints, has a complicated influence to the HSS. Extensive researches have been undertaken using numerical tools to generate data in HSS distribution, Stress Concentration Factors (SCFs) and Stress Intensity Factors (SIFs) for tubular joints, with focus on the uniplanar tubular joints such as T joints and K joints [10].

Regarding the type of OWT support structure, nominal stress approach may be used to determine the damage values for monopile structures. For tubular joints of jacket structures, the nominal stress approach is not applicable. An alternative method is the Structural Stress Approach (SSA) which can be carried out using parametric formulas or numerical methods [11]. Furthermore, sophisticated concepts like the Notch Stress Approach (NSA) can be used for fatigue assessment [12]. Schematization of this different stress approaches is given in Figure 2, for an exemplificative geometry discontinuity, where a fatigue crack is expect to grow.

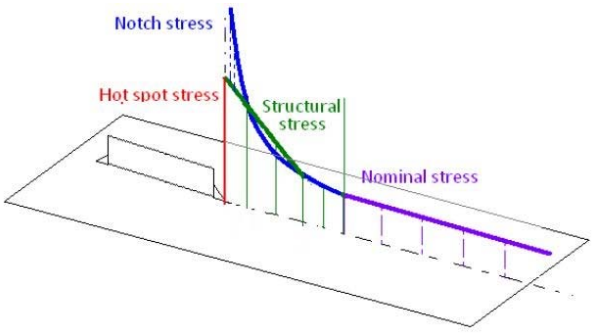

Figure 2. Nominal Stress vs Structural Stress; Hot Spot Stress vs Notch stress [13].

RESEARCH ON WELDED TUBULAR JOINTS

The fatigue performance of welded connections is usually a design driving criteria of support structures for OWTs, due to high level of fatigue loads as well as a large number of load cycles. Components with load cycles of this magnitude can hardly be analysed by means of experimental research and, for that fact, the development of improved numerical models is an important area of fatigue research. In order to push superior risk and cost considerations to a new level, a research project within the framework of the Innovative Training Network (ITN) AEOLUS4FUTURE is under development, in the topic of local fatigue design methods of support structures for OWTs.

The research project proposes an experimental and numerical investigation on the fatigue performance of large scale tubular X joints, with automated Tandem MIG/MAG welds. Automated welding technologies have already been development, for the production of tubular joints [14]. The production automation allows the delivery of standardized components and the application of dual wired welding processes (Tandem MIG/MAG), which can only be applied by robotic welding due to the required precision in positioning. Therefore, there is a need to investigate the fatigue behavior of the assembled joints, as such technology allows welding from both sides of the steel tubes (as strategy to improve fatigue behavior), higher weld deposition rates, lower welding time and overall cost reduction.

Up to now, the large scale experimental investigation is under planning and preliminary numerical models have already been developed by use of SSA, as shown in Figure 9 (a). The aim of these models was to simulate and evaluate the experimental test setup. The finite element model was developed in Ansys© environment, by means of the dedicated tool Falcos©, developed at the Institute for Steel Construction of the Leibniz University Hannover. A 20-node solid element (SOLID95) is used. This element type has a high degree of accuracy as result of midside nodes. The influence of mesh refinement and boundary conditions on SCFs is discussed in the extended version of this paper. The hot spot stresses were located, as shown in Figure 9 (b), and the stress concentration factors were calculated. The maximum SCF equal to 4,10 was estimated for the load case scenario of a unitary axial load (1 N/mm^2).

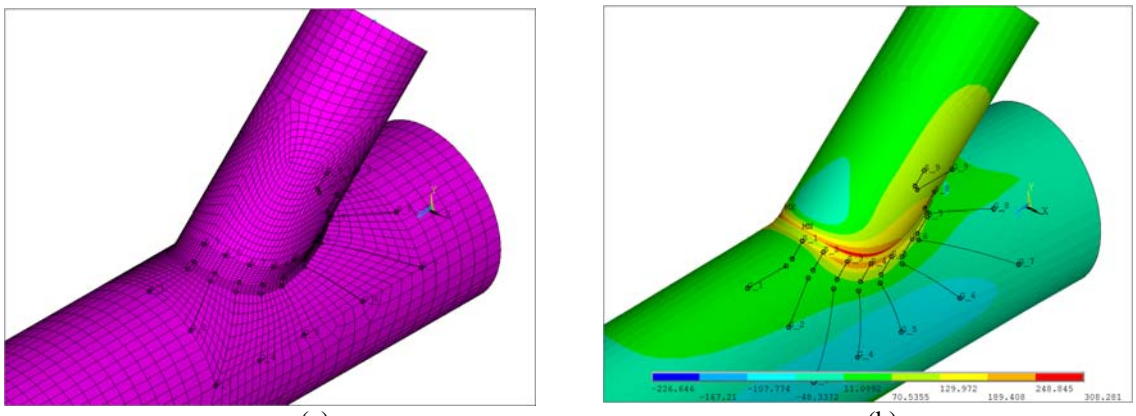

(a) (b)

Figure 9. (a) X-Joint finite element model; (b) Load simulation and hotspot stress location.

CONCLUSIONS

In this paper, a brief revision of the scope of standard fatigue design procedures as well as local fatigue design methods of support structures for offshore wind turbines is made. In order to push superior risk and cost considerations to a new level, a research plan related to the work package 4 of the Innovative Training Network (ITN) AEOLUS4FUTURE was introduced.

The research work developed so far, proved that it is possible to perform fatigue testing of large scale tubular X joints, with automated Tandem MIG/MAG welds. However, there are still challenges to overcome, concerning the experimental planning, in order to make the ambitious experimental investigation possible. If successful, the results of the experimental campaign will be used to validate numerical models. Furthermore, a numerical investigation will be performed by use of local concepts to achieve a deeper understanding of the

damage mechanism. For fatigue verifications, the Structural Stress Approach (SSA) will be applied, combining parametric formulas and numerical methods. Furthermore, global models will be combined with sub-modelled crack regions and more sophisticated concepts like the Notch Stress Approach (NSA) will be used for fatigue assessment. Finally, parametrical studies and differences on fatigue life will be quantified between the standard and the advanced methods. Parameters such as loading, diameter/thickness ratio and steel grades will be investigated.

ACKNOWLEDGEMENTS

The authors acknowledge the support from the European Commission's Framework Programme Horizon 2020, through the Marie Curie Innovative Training Network (ITN) AEOLUS4FUTURE - Efficient harvesting of the wind energy (H2020-MSCA-ITN-2014: Grant agreement no. 643167).

REFERENCES

[1] Esteban M. D., Diez J. J., López J. S., Negro V. “Why offshore wind energy?”, Renewable Energy, Vol. 36, 2011, pp. 444-450.
[2] Dubois J., Thieken K., Schaumman P., Achmus M. “Influence of soil resistance approach on overall structural loading of large diameter monopoles for offshore wind turbines”, Proceedings of the IWEC conference, Amsterdam, Netherlands, 2011, pp. 437-444.
[3] Dong W., Moan T., Gao Z. “Long-term fatigue analysis of multi-planar tubular joints for jacket-type offshore wind turbine in time domain”, Engineering Structures, Vol. 33, 2011, pp. 2002-2014.
[4] Yeter B., Garbatov Y., Soares C. G. “Fatigue damage analysis of a fixed offshore wind turbine supporting structure”, Developments in Maritime Transportation and Exploitation of Sea Resources – Guedes Soares & López e Pena (eds), London, 2014, pp. 415-424.
[5] Schumacher A., Nussbaumer A. “Experimental study on the fatigue behaviour of welded tubular K-joints for bridges”, Engineering Structures, Vol. 28, 2006, pp. 745-755.
[6] Acevedo C., Nussbaumer A. “Effect of tensile residual stresses on fatigue crack growth and S–N curves in tubular joints loaded in compression”, International Journal of Fatigue, Vol. 36, 2012, pp. 171-180.
[8] Dalhoff P., Argyriadis K., Klose M. “Integrated load and strength analysis for offshore wind turbines with jacket structures”, Proceedings of the EOW conference, Berlin, Germany, 2007.
[7] DNV-RP-C203. “Recommended practices, fatigue design of offshore steel structures”, DNV Recommended Practice, 2014.
[9] DNV-RP-F204. “Riser Fatigue”, DNV Recommended Practice, 2010.
[10] Dubois J., Muskulus M., Schaumman P. “Advanced representation of tubular joints in jacket models for offshore wind turbine simulation”, Energy Procedia, No. 35, 2013, pp. 234-243.
[11] Schaumann P., Kleineidam P. “Fatigue design of support structures for offshore wind energy converters”, Proceedings of the Global WINDPOWER conference, Chicago, Illinois, USA, 2004.
[12] Schaumann P., Wilke F. “Current developments of support structures for wind turbines in offshore environment”, Proceedings of the ICASS conference, Vol. II, 2005, pp. 1107–1114.
[13] Guanying L., Yidong W. “A study of the thickness effect in fatigue design using the hot spot stress method”. Master Thesis, Chalmers University Of Technology, 2010.
[14] Salzgitter Mannesmann Renewables, http://www.szmr.de/en/fields-of-activity/offshore-wind.htm.

THE INTERNATIONAL CONFERENCE ON
WIND ENERGY HARVESTING 2017
20-21 April 2017
Coimbra, Portugal

Paper A4F.02

ADVANCED NUMERICAL MODELLING OF WAVE LOADING ON MONOPILE-SUPPORTED OFFSHORE WIND TURBINES

Agota Mockute[1]
University of Florence
Firenze, Italy

Enzo Marino[2]
University of Florence
Firenze, Italy

Claudio Borri[3]
University of Florence
Firenze, Italy

ABSTRACT

This paper introduces a research project on advanced numerical modelling of offshore wind turbines that is being conducted as part of the AEOLUS4FUTURE innovative training network. In anticipation to contribute towards increased renewable energy production and reduced cost of electricity from offshore wind, the research is aimed at improving existing numerical simulation tools to enable more accurate study of novel offshore wind turbine concepts. Following from the state-of-the-art review of present challenges, work is focusing on wave loading on monopile-supported wind turbines in rough seas, with emphasis on nonlinear effects. The numerical model advancement is started with validation of a solver for fully nonlinear wave kinematics and comparison of hydrodynamic loading models – Morison equation and its corrections at this phase.

INTRODUCTION

Climate change, exhaustible fossil fuels and continuously growing energy demand creates the need for the world to shift towards more sustainable power production, and wind is one of the most promising renewable energy sources [1]. With the aims to innovate wind energy systems which would lead to increased generation of clean energy and reduced emissions, AEOLUS4FUTURE training network (H2020-MSCA-ITN-2014-SEP-210161718) was launched in 2015 to train the new generation of wind energy researchers, and the presented research project forms part of the scheme [2].

Offshore wind resources are vast – winds are stronger and less turbulent than onshore, the noise intensity and aesthetics are a lesser issue, thus the turbines can be of greater scale. However, bigger turbines entail more slender towers and blades which are prone to larger displacements, especially when placed in the harsh and complex offshore conditions. Detailed design, production, installation and maintenance of such structures are costly processes; therefore a combination of continuous innovation, appropriate designing and testing is crucial to advance the field and avoid failures [3].

Testing in full-scale is cumbersome, and model tests are too expensive and time-consuming to be carried out on every innovative concept. The cheapest and fastest method to check viability and design turbines is numerical simulation, validated on experimental data to ensure its reliability [4]. Accurate modelling of the loads on the turbine and its response helps to improve both: firstly to avoid overdesigning and therefore reducing the production costs, and secondly to correctly predict the modes of failure, leading to increased life expectancy and more appealing payback period [3]. Therefore this research is focusing on loading models and structural dynamic solvers, aiming to improve existing hydro-aero-elastic numerical solvers which would then model the coupled system response of the offshore wind turbines.

The paper is structured as follows. The first two sections present the state-of-the-art summary. Firstly, offshore code comparison section introduces the international project on the comparison of numerical solvers

[1] Doctoral candidate, Dept. of Civil and Environmental Engineering, University of Florence, Via di Santa Marta, 3, 50139 Firenze, Italy. Email: amockute@dicea.unifi.it
[2] PhD, Post-doc fellow, Dept. of Civil and Environmental Engineering, University of Florence, Via di Santa Marta, 3, Firenze 50139, Italy. Email: enzo.marino@dicea.unifi.it
[3] Prof. Dr. Ing., Dept. of Civil and Environmental Engineering, University of Florence, Via di Santa Marta, 3, Firenze 50139, Italy. Email: cborri@dicea.unifi.it

currently used in offshore wind turbine modelling both in industry and academia, which was a cornerstone for identification of the area of interest for the research project. Then an overview of the main current advances and challenges of this field is presented in the wave load modelling on monopiles section. Subsequently, an outline of current work is given in the section for advancement of numerical solver, followed by outlook on future work and concluding remarks.

OFFSHORE CODE COMPARISON

In order to test and compare the different codes used worldwide for modelling the offshore wind turbines, the Offshore Code Comparison Collaboration (OC3), and its Continuation (OC4) were carried out [5-7]. Multinational participants used various solvers to model NREL offshore 5-MW baseline wind turbine (a representative model developed for the use in conceptual evaluation studies, full details in [8]) on the most common supporting structures, which are illustrated in figure 1. Overall, the collaborations were a successful step in the continuous improvement of offshore wind turbine modelling which provided valuable feedback for the code users and developers.

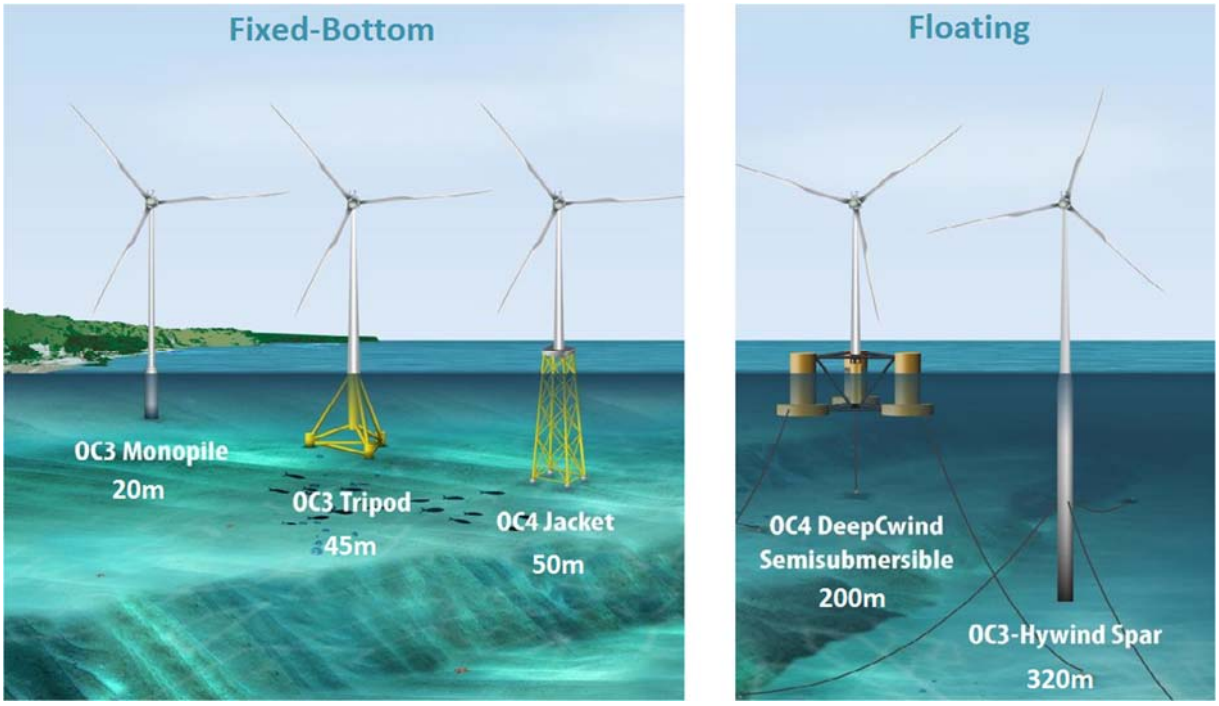

Figure 1. The five support structures studied by OC3 and OC4 project participants, the projects and depths they were modelled in. Courtesy of [9]

A crucial finding of OC4 Phase II was that the most significant discrepancies were observed in different hydrodynamic modelling approaches but due to the complexity of semisubmersible structure it was impossible to investigate the subject at the time [8]. Moreover, it was recognised that even though comparing code-to-code detects some mismatches, it does not distinguish which code represents real-life scenario most accurately [8]. Therefore Offshore Code Comparison Collaboration Continuation, with Correlation (OC5) project followed, where the modelled results were compared to experimental, and in Phase I a vertical cylinder was examined without a wind turbine, focusing solely on hydrodynamic loads and fidelity of their modelling approaches [10]. Consequently, the appropriate wave load modelling on monopile-supported offshore wind turbines has become the interest of this research project.

WAVE LOAD MODELLING ON MONOPILES

The literature review on wave loading of monopile-supported offshore wind turbines presents an increasing interest in nonlinear effects on the structure and appropriate modelling of the environments where they occur. Nonlinear effects, such as springing, ringing and impulsive forcing, are referred to as sudden dynamic amplifications of the turbine response, which generate high stress levels on the structure. They are illustrated in figure 2 and have been observed on monopile-supported offshore wind turbines [11-18], especially in parked state [18-20]. Springing is caused when higher harmonics of the hydrodynamic loading match the natural frequency of

the structure [11,14,17,19-20], while slamming is an impulsive excitation from waves breaking onto a structure [14-15,17,19,28-29]. Ringing has been receiving especially much attention from the scientific community and there is still debate on a single definition of the phenomenon, although it is most commonly associated with resonant response to higher order hydrodynamic loading component or secondary loading cycle [11-12,14-17,19-21].

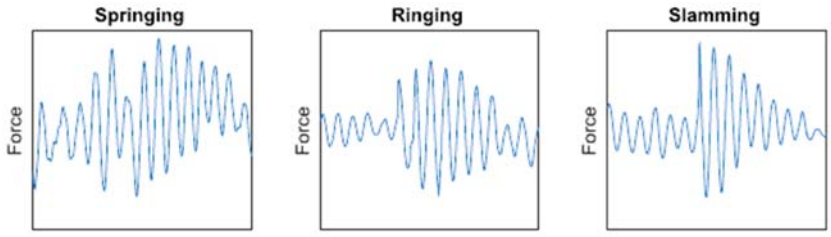

Figure 2. Examples of nonlinear effects – springing, ringing and impulsive excitation. Courtesy of [17].

Nonlinear effects turned out to be the focus of the OC5 Phase I as well, since the main force component, resulting from linear waves, was captured with sufficient accuracy by all participants [10]. Experiment was carried out on a flexible cylinder (scaled version of the OC3 monopile) fixed to the floor of a wave tank with a sloped floor in two sets of depths, measuring shear force at the bottom and displacement at the top of the cylinder. It was found that the second and third peak components of the force signal, responsible for the nonlinear effects on the structure, are much larger in shallower water than in deep water. These peaks were captured best when either measured wave elevation or wave kinematics derived from the fully nonlinear potential flow solver were used. In contrast, linear wave models failed to capture the second and third force peaks, omitting the presence of nonlinear effects, as also seen in literature review [13-14,17-20]. Moreover, fully nonlinear potential flow solver also excelled in capturing the force estimation in shallow water, being the only model that could directly model the influence of nonlinear wave transformation over the sloped seabed. The findings show the importance of fully nonlinear wave kinematics and appropriate hydrodynamic loading modelling, especially in the highly nonlinear conditions that monopile-supported offshore wind turbines are placed – shallow waters and steep or overturning waves.

The most commonly used hydrodynamic loading model for monopiles due to their slenderness is Morison equation. If suitably calibrated, this widely applied semi-empirical equation is normally working well in linear and weakly nonlinear waves, and is therefore implemented in the vast majority of commercial hydro-aero-servo-elastic solvers [10,24]. However, in steeper waves and shallower depths, when nonlinearities are higher and resonant effects take place, the original Morison's model has been found to mispredict the higher-order harmonic force components, responsible for nonlinear effects, thus the suitability of this hydrodynamic model is doubted [11,14,16,21-23]. Consequently, corrections to Morison equation and alternative hydrodynamic loading models are available in literature, e.g. slender-body corrections proposed by Rainey (1989) [21], and perturbation technique-based models, such as FNV theory [22] or Malenica and Molin (1995) [23].

To sum up, the state-of-the-art review points to a need of more accurate hydrodynamic loading modelling for monopile-supported offshore wind turbines, for which an accurate solver with fully nonlinear wave kinematics and most appropriate hydrodynamic loading model are crucial.

ADVANCEMENT OF NUMERICAL MODEL

FAST by NREL [24] is an aeroelastic simulator which interfaces with AeroDyn for simultaneously calculated aerodynamic forces [25], and is one of the most widely used tools for onshore wind turbine design applications. When also coupled with HydroDyn, which computes the hydrodynamic loads for offshore structures in time-domain [26], a hydro-aero-servo-elastic solver for offshore wind turbines is enabled. The tool is of special interest to this research because it is an open-source computer-aided engineering tool, providing possibility to develop a code for only a part of module and then couple it in the hydro-aero-servo-elastic solver.

In order to tackle the issues in hydrodynamic modelling of monopile offshore wind turbines, activity has been started on a two-dimensional fully nonlinear potential flow-based solver, which is to be coupled with hydro-aero-servo-elastic solver FAST for full dynamic response of the system in highly nonlinear waves. The code is based on higher-order boundary element method, and unlike the linear and weakly nonlinear wave theories which are usually employed in commercial solvers, it implies no limitations on wave steepness up to the re-entering of breaking wave [27].

First, a validation study on the ability of the code to recreate highly nonlinear wave behaviour is carried out by comparing the results of the code with available experimental data. The regular wave kinematics and elevations

on a flat-bottom numerical wave tank are validated by comparison with analytical theories and available experimental data.

After the wave kinematics are validated, a systematic study on hydrodynamic loading models is to be conducted. The first phase is to carry out a comparison study between Morison equation and its corrections proposed by Rainey (1989) [21]. The loading is first assessed on three idealised structures: fixed rigid cylinder, hinged rigid cylinder, and fixed flexible cylinder. Subsequently the study will be extended to the real wind turbines and the wave kinematics developed in the code will be inputted to the FAST coupled solver and simulated on the NREL 5MW baseline offshore wind turbine.

FUTURE PLANNED ACTIVITY

The further foreseen stages of the project consist of conducing the hydrodynamic loading model comparison study including more models, such as FNV theory [22]. Then the code is to be advanced with a sloping bottom because the transition to shallow water causes the waves to steepen and nonlinearities to accumulate, and the coastal area where the seabed slopes is a common location monopile wind turbines [10,13,17]. Furthermore, after validation of the capability of the code to grasp the nonlinear wave behaviour on the sloping bed, such comparison study of hydrodynamic models is to be repeated with a focus on nonlinear effects induced by the wave transformation from deep to shallow water.

It is aimed to provide a numerical solver for offshore wind turbines which, without causing an excessive increase in computational time, more accurately captures the nonlinear loading to which monopile-supported offshore wind turbines are subjected in their complex environment of shallow to intermediate depths, uneven seabed and highly nonlinear behaviour of waves. The advanced code could then be applied to study the sensitivity of the dynamic monopile-supported system to nonlinear effects, for example in the case of wind-wave misalignment, and assess their impact on the design loads and turbine lifetime.

CONCLUDING REMARKS

Major development has been carried out in the field of numerical modelling of offshore wind turbines over the past decades and is still ongoing, especially boosted by the international code comparison collaboration projects. The key issue identified is the need to accurately model higher-order wave kinematics and fluid-structure interaction on monopile-supported offshore wind turbines in order to avoid overlooking dangerous resonating and nonlinear effects. Action has been started on advancement of a code for fully nonlinear waves, which is to be coupled with hydro-aero-servo-elastic solvers, and on the assessment of hydrodynamic loading models. A systematic comparison study between Morison equation and its corrections on a flat bottom in regular waves is to be presented as the first stage of the research project. The continuous work on this project is expected to ultimately lead to increased accuracy of the modelling of offshore wind turbines without penalising the computational time, and the enhanced tool would be used to study safer and more economic designs of new generations of offshore wind turbines, hence contributing to the eventual reduction in the costs of the offshore wind turbine production and maintenance.

ACKNOWLEDGEMENTS

The authors acknowledge with thanks the support of the European Commission's Framework Program "Horizon 2020", through the Marie Skłodowska-Curie Innovative Training Networks (ITN) "AEOLUS4FUTURE - Efficient harvesting of the wind energy" (H2020-MSCA-ITN-2014: Grant agreement no. 643167) to the present research project. Furthermore, the COST TU1304 action WINERCOST is gratefully acknowledged.

REFERENCES

[1] GWEC, "Global Wind Report, Annual Market Update, 2014", Technical report, 2014.
[2] "AEOLUS4FUTURE - Efficient harvesting of the wind energy". Call: H2020-MSCA-ITN-2014 - Proposal Number: SEP-210161718.
[3] Karimirad, M., "Offshore Energy Structures: For Wind Power, Wave Energy and Hybrid Marine Platforms.", Springer, Switzerland, 2014.
[4] Baniotopoulos, C.C., Borri, C., Stathopoulos, T., "Environmental Wind Engineering and Wind Energy Structures", Springer Verl., Wien New York, 2010.
[5] Jonkman, J., and Musial, W., "Offshore Code Comparison Collaboration (OC3) for IEA Task 23 Offshore Wind Technology and Deployment", NREL, USA, 2010.
[6] Jonkman, J., Robertson, A., Popko, W., et al., "Offshore Code Comparison Collaboration Continuation (OC4), Phase I – Results of Coupled Simulations of an Offshore Wind Turbine with

Jacket Support Structure", presented at the 22nd Int. Society of Offshore and Polar Engineers Conf., Rhodes, Greece, Jun. 2012.
[7] Robertson, A., Jonkman, J., Vorpahl, F., et al., "Offshore Code Comparison Collaboration Continuation Within IEA Wind Task 30 : Phase II Results Regarding a Floating Semisubmersible Wind System Preprint," presented at the 33rd Int. Conf. on Ocean, Offshore and Arctic Engineering, San Francisco, California, Jun. 2014.
[8] Jonkman, J., Butterfield, S., Musial, W., and Scott, G., "Definition of a 5-MW reference wind turbine for offshore system development", NREL, USA, 2009.
[9] Robertson, A., "Introduction to the OC5 Project", [Internet]. 2015; Available from: http://www.sintef.no/Projectweb/Deepwind_2015/Presentations/
[10] Robertson, A., Wendt, F., Jonkman, J., et al., "OC5 Project Phase Ib: Validation of Hydrodynamic Loading on a Fixed, Flexible Cylinder for Offshore Wind Applications", Energy Procedia, vol. 94, 2016, pp. 82-101.
[11] Chaplin, J. R. R., Rainey, R. C. T., and Yemm, R. W., "Ringing of a vertical cylinder in waves", J. Fluid Mech., vol. 350, 1997, pp. 119–147.
[12] Grue, J. and Huseby, M., "Higher-harmonic wave forces and ringing of vertical cylinders", Appl. Ocean Res., vol. 24, 2002, pp. 203–214.
[13] Schløer, S., Bredmose, H., and Bingham, H. B., "Irregular Wave Forces on Monopile Foundations. Effect af Full Nonlinearity and Bed Slope", in Proceedings of the ASME 30th 2011 Int. Conf. on Ocean, Offshore and Arctic Engineering, 2011, vol. 5, pp. 581-588.
[14] Marino, E., Lugni, C., and Borri, C., "A novel numerical strategy for the simulation of irregular nonlinear waves and their effects on the dynamic response of offshore wind turbines", Comput. Methods Appl. Mech. Eng., vol. 255, 2013, pp. 275–288.
[15] Paulsen, B.T., Bredmose, H., and Bingham, H.B., "An efficient domain decomposition strategy for wave loads on surface piercing circular cylinders", Coast. Eng., vol. 86, 2014, pp. 57–76.
[16] Paulsen, B.T., Bredmose, H., Bingham, H.B., Jacobsen, N.G., "Forcing of a bottom-mounted circular cylinder by steep regular water waves at finite depth", J. Fluid Mech., vol. 755, 2014, pp. 1–34.
[17] Schløer, S., Bredmose, H., and Bingham, H.B., "The influence of fully nonlinear wave forces on aero-hydro-elastic calculations of monopile wind turbines", Marine Structures, vol. 50, 2016, pp. 162-188.
[18] Marino, E., Giusti, A., Manuel, L., "Offshore wind turbine fatigue loads: The influence of alternative wave modeling for different turbulent and mean winds", Renewable Energy, vol. 102, 2017, pp. 157-169.
[19] Marino, E., Lugni, C., and Borri, C., "The role of the nonlinear wave kinematics on the global responses of an OWT in parked and operating conditions," J. Wind Eng. Ind. Aerodyn., vol. 123, 2013, pp. 363–376.
[20] Marino, E., Nguyen, H., Lugni, C., Manuel, L., Borri, C., "Irregular Nonlinear Wave Simulation and Associated Loads on Offshore Wind Turbines", J. Offshore Mech. Arct. Eng., vol. 137, 2015, p. 0221901.
[21] Rainey, R.C.T., "A new equation for calculating wave loads on offshore structures", J. Fluid Mech., vol. 204, 1989, pp. 295–324.
[22] Faltinsen, O.M.; Newman, J.N., and Vinje, T., "Nonlinear Wave loads on a slender vertical cylinder", J. Fluid Mech., vol. 289, 1995, pp.179–198.
[23] Malenica, S. and Molin, B. "Third-harmonic wave diffraction by a vertical cylinder", J. Fluid Mech., vol. 302, 1995, pp. 203–229.
[24] Jonkman, J. M., and Buhl Jr., M., "FAST User's Guide", NREL, USA, 2005.
[25] Hansen, A. C., and Laino, D. J., "User's Guide to the Wind Turbine Aerodynamics Computer Software AeroDyn", Windward Engineering, 2002.
[26] Jonkman, J. M., Robertson, A., and Hayman, G. J., "HydroDyn User's Guide and Theory Manual", NREL, USA, 2014.
[27] Marino, E., "An integrated nonlinear wind-waves model for offshore wind turbines", PhD thesis, Department of Civil and Environmental Engineering, University of Florence, 2010.
[28] Marino, E., Borri, C., and Peil, U., "A fully nonlinear wave model to account for breaking wave impact loads on offshore wind turbines", J. Wind Eng. Ind. Aerodyn., vol. 99, 2011, pp. 483–490.
[29] Marino, E., Borri, C., and Lugni, C., "Influence of wind-waves energy transfer on the impulsive hydrodynamic loads acting on offshore wind turbines", J. Wind Eng. Ind. Aerodyn., vol. 99, 2011, pp. 767–775.

THE INTERNATIONAL CONFERENCE ON
WIND ENERGY HARVESTING 2017
20-21 April 2017
Coimbra, Portugal

Paper A4F.03

INFLUENCE OF WAVE LOAD VARIATIONS ON OFFSHORE WIND TURBINE STRUCTURES

Ana Glišić[1]
Institute for Steel Construction
Hanover, Lower Saxony, Germany

Gonçalo T. Ferraz[2]
Institute for Steel Construction
Hanover, Lower Saxony, Germany

Peter Schaumann[3]
Institute for Steel Construction
Hanover, Lower Saxony, Germany

ABSTRACT

Nowadays, much attention is payed to the development of renewable energy resources. Wind energy plays a major role in this issue. That is why there is a growing interest for improving the design process of wind turbines at many aspects. This study compares two types of offshore wind turbines structures, the monopile and the jacket structure, in their dependency on wave load characteristics' variations. The examined wave characteristics are significant wave height and wave peak period. The jacket structure showed lower influence of increase of wave height to stresses in the cross section at the bottom of the structure compared to the monopile structure. The monopile structure showed slight dependency of stresses on increasing wave frequency, while the jacket structure showed nearly no dependency, due to its more complex geometry and higher stiffness.

NOMENCLATURE

OWT	=	Offshore wind turbine
Ts	=	Wave peak period (s)
Hs	=	Significant wave height (m)
S	=	Stress (MPa)

INTRODUCTION

Renewable energy resources are nowadays a growing industry, aiming to a gradual transition of energy production from fossil fuels to green energy. With respect to Kyoto protocol, many producers turn to renewable energy resources, which leads to a fact that more than 75% of new power capacity installations in EU in the year 2015 are renewable resources. The leading among the new renewable energy resources is wind energy [1]. In the

[1] M.Sc, Institute for Steel Construction, Leibniz Universitaet Hannover, Germany, glisic@stahl.uni-hannover.de, tel. +49 511 762 3712, fax +49 511 762-2991
[2] M.Sc, Institute for Steel Construction, Leibniz University Hannover, Germany, ferraz@stahl.uni-hannover.de
[3] Prof.Dr.-Ing, Institute for Steel Construction, Leibniz University Hannover, Germany, schaumann@stahl.uni-hannover.de

last two decades, even more wind energy is harvested by moving offshore. That brings up a problem of more complicated and expensive installation, but wide available locations for wind farms and higher electricity output justify the decision to go offshore. In addition, the capacity of offshore wind turbines gradually grows, so nowadays the average OWTs' capacity is 4.8 MW [2]. Therefore, there is a growing interest in improving the design process of OWTs at many aspects, but the reduction of costs remains the main challenge.

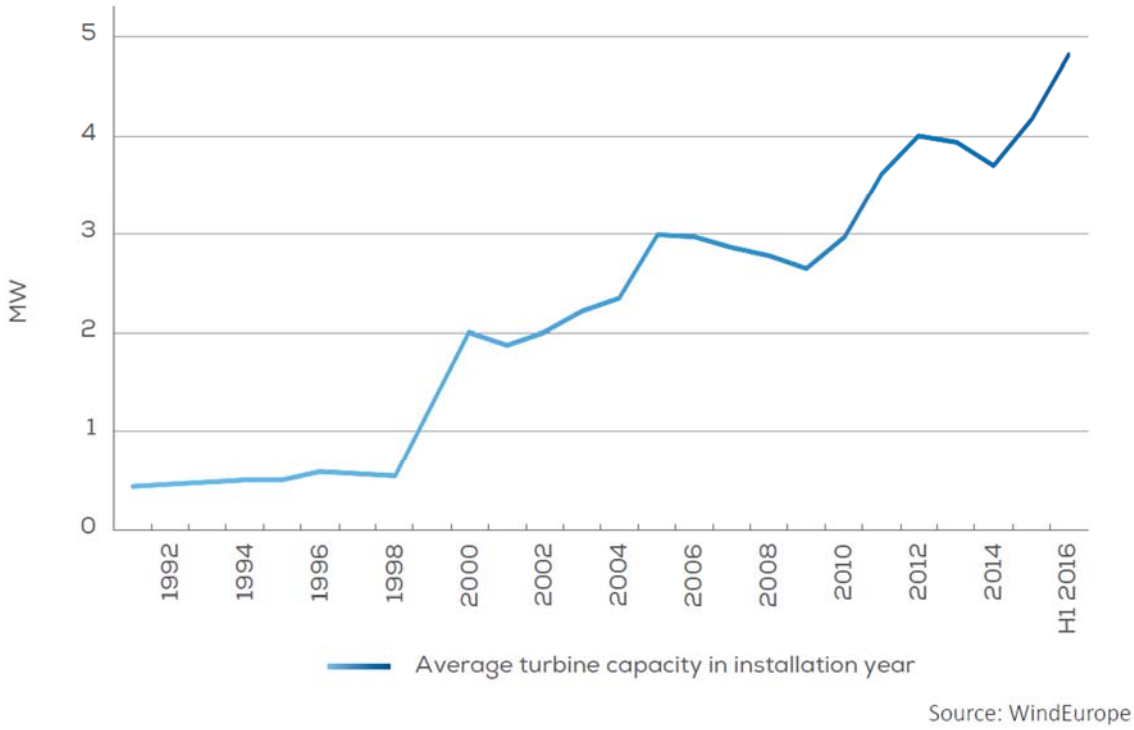

Figure 1. Average annual rated capacity of OWTs installed

The design of OWT support structures contains high number of stochastic variables that influence loads characteristics and structural responses. These variables cause many uncertainties, whose impact on a structural behavior is not obvious without a deeper investigation [3]. This study investigates the dependency of stresses in OWT structures on characteristics of wave loads.

METHODOLOGY

Two types of reference OWT structures are studied and compared: the monopile and the jacket structure. Regarding the supporting structures of OWTs in general, monopile is the most commonly employed structure in shallow and medium water depths (0-30m), due to relatively easy installation and simple design. For higher water depths (20-50m), jacket support structures are employed due to higher stiffness, as well as smaller surface facing the wave movement compared to monopiles [4]. Both structures are modelled in finite element analysis tool, developed at the Institute for Steel Construction of Leibniz University of Hanover, namely Poseidon, specialized for wave-induced loads. Poseidon has an integrated tool for simulation of wave loads, by means of either irregular sea states, or single design waves [5]. Irregular sea states are generated as a superposition of a number of regular waves in order to achieve a very realistic model. However, it is not obvious how every single waveform from the sea state contribute to the caused stress. In order to perceive how sensitive are the structures to different wave characteristics (wave heights, frequencies), sea state is separated into single design waves, and each of them is applied to the structure. The stress results are recorded by the set of sensors positioned on the corresponding spots on the structures with the corresponding angles, and compared. Finally, it is stated which of the observed structural types is more sensitive to specific wave characteristics.

RESULTS

The obtained results show that both of the reference structures stand higher stresses with the increase of wave height, as expected. It is demonstrated that both of dependencies are nearly linear, as the simulations are carried out in the domain of linear deformations without extreme loads. However, the dependency line for monopile is steeper, which shows that monopiles are more sensitive to wave heights compared to jacket structures, due to their geometry.

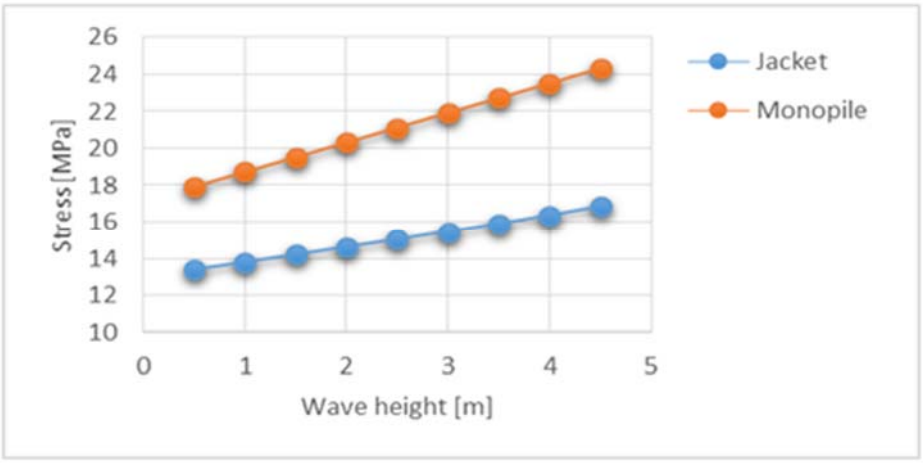

Figure 2. Significant wave height - stress dependency for monopile and jacket structure

Regarding different wave frequencies, the monopile structure shows slight increase of stresses with increase of wave frequency. The gradient of stress increase gets higher as the wave frequency approaches the first eigenfrequency of the structure. The jacket structures shows nearly no dependency on examined wave frequency change.

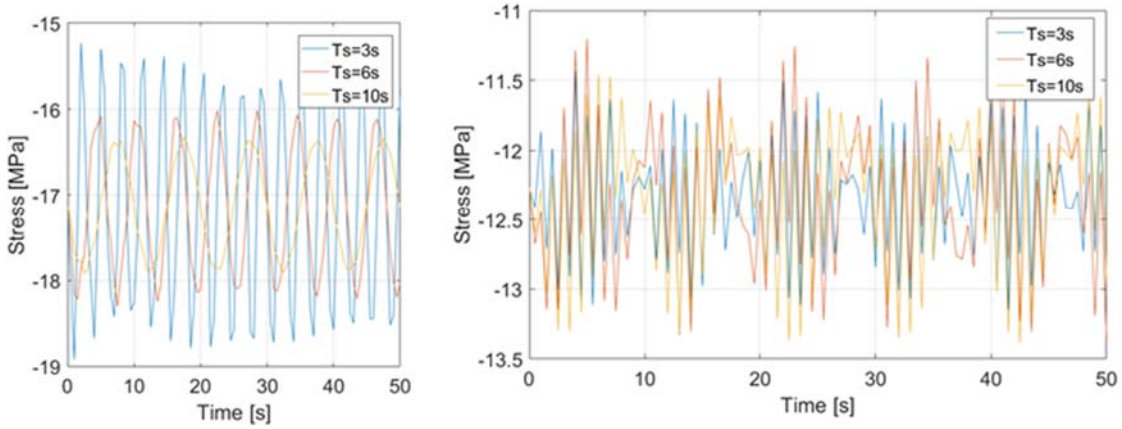

Figure 3. Stress results for monopile (left) and jacket structure (right) for different wave frequencies

CONCLUSIONS

The obtained results show that the jacket structure is in general less sensitive to the change of wave load parameters compared to the monopile structure. Due to its complex geometry and higher stiffness, the jacket structure shows low linear sensitivity to the increase of wave height and nearly no sensitivity to change of wave period, while monopile shows steeper linear sensitivity to wave heights and sensitivity to decrease of wave periods. This research is focused on one, most frequent wind speed. For a complete overview, other wind speeds as well as the extreme load cases must be taken into consideration.

ACKNOWLEDGEMENTS

The authors acknowledge with thanks the support of the European Commission's Framework Program "Horizon 2020", through the Marie Skłodowska-Curie Innovative Training Networks (ITN) "AEOLUS4FUTURE - Efficient harvesting of the wind energy" (H2020-MSCA-ITN-2014: Grant agreement no. 643167), to the present research project.

REFERENCES

[1] The European Wind Energy Association: *Wind in power: 2015 European statistics*, 2016

[2] The European Offshore wind industry: *Key trends and statistics, 1st half 2016,* June 2016

[3] L. Ziegler, S. Voormeeren, S. Schafhirt, M Muskulus: *Sensitivity of Wave Fatigue Loads on Offshore Wind Turbines under varying Site Conditions,* 12th Deep Sea Offshore Wind R&D Conference, EERA DeepWind'2015

[4] DNV-OS-J101: *Design of offshore wind turbine structures*, DNV Offshore Standard, 2014

[5] Böker C.: *Load simulation and Local Dynamics of Support Structures for Offshore Wind Turbines*, PhD Thesis, Leibniz University Hannover, 2010

THE INTERNATIONAL CONFERENCE ON
WIND ENERGY HARVESTING 2017
20-21 April 2017
Coimbra, Portugal

Paper A4F.04

STABILITY ANALYSIS OF NEWLY DEVELOPED POLYGONAL CROSS-SECTIONS FOR LATTICE WIND TOWERS

Gabriel Sabau[1]
Luleå University of Technology
Luleå, Norbotten, Sweden

Efthymios Koltsakis[2]
Luleå University of Technology
Luleå, Norbotten, Sweden

Ove Lagerqvist[3]
Luleå University of Technology
Luleå, Norbotten, Sweden

ABSTRACT

The pursuit for cheaper energy is leading the current wind tower design to increased heights. However, the current wind turbine towers designs would generate unjustified costs for transportation and erection. In order to reduce these costs, several simplified erection methods have been proposed. One of such is the hybrid lattice-tubular steel tower. For economic feasibility, built-up cold-formed polygonal cross-sections have been proposed for the lattice part. This paper investigates the behavior of such cross-sections in order to evaluate their failure modes. The first part contains an introduction and a short presentation of the current state-of-art in the buckling of plates and cold-formed members. The methodology of the study is then presented. A comparative study is performed between several closed sections to validate a simplified model to determine the upper limit of class 3 sections.

NOMENCLATURE

$P_{cr,E}$	=	critical load of a column according to Euler's formula (kN)
E	=	steel elastic modulus (MPa)
I	=	second moment of area (mm^4)
L_{cr}	=	effective member length (m)
σ_{cr}	=	critical stress (MPa)
t	=	plate thickness (mm)
b	=	plate width (mm)
k	=	4 , factor to account for the plate boundary conditions (-)
υ	=	0.3, Poisson coefficient (-)
$P_{cr,J}$	=	critical load of an intermediate length column according to Johnson's formula (kN)
f_y	=	yield strength (MPa)
A	=	total area of the cross-section (mm^4)
r	=	radius of gyration
λ	=	non-dimensional slenderness

INTRODUCTION

1 PhD Student, Department of Civil, Environmental and Natural Resources Engineering, Luleå University of Technology, gabsab@ltu.se
2 Senior Lecturer, Department of Civil, Environmental and Natural Resources Engineering, Luleå University of Technology, eftkol@ltu.se
3 Professor, Department of Civil, Environmental and Natural Resources Engineering, Luleå University of Technology, ove.lagerqvist@ltu.se

In the discussions regarding the erection of on-shore wind turbine towers, with heights above 100m it is commonly agreed among the scientific community that the main limitations of current tubular steel towers are the transportation and erection conditions.

The on-shore wind turbine towers are thus limited by the transportation conditions. To keep the on-shore wind turbines a competitive option, innovative solutions for the tower design are required. By choosing just one type of configuration one are limited by the disadvantages that these bring. As presented by Hau (2013)[2] the conical tubes present a great advantage for heights up 80m, as seen in **Figure 1**. However, from this point on, the mass and the costs increase significantly.

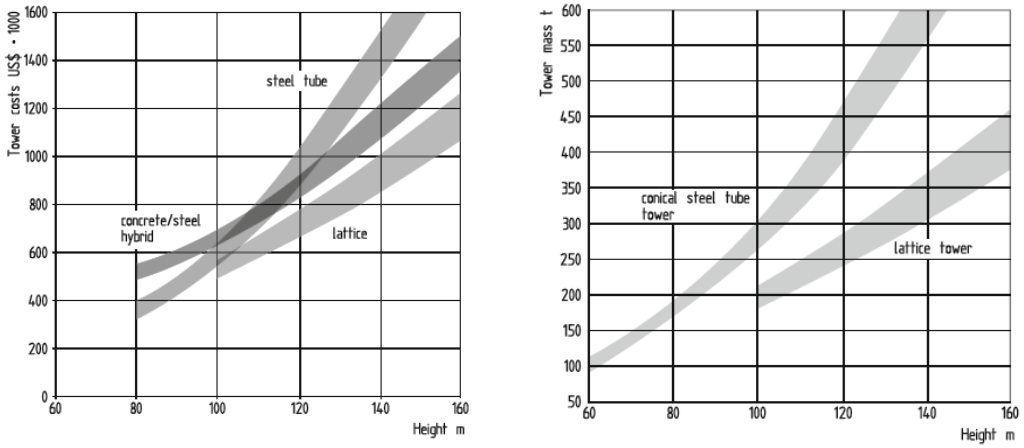

Figure 1. Tendencies of costs and mass for a 3 MW wind turbine with a rotor diameter of 100m (2011 steel prices) **Error! Reference source not found.**

An alternative to conical section was used to build the modular Andersen tower [5]. This tubular tower claimed to have the capacity of reaching heights of more than 150m. One of such was built to the height of 140m. However, it did not have a very high impact on the market. The tower is composed out of u-plates as seen in **Figure 2**.

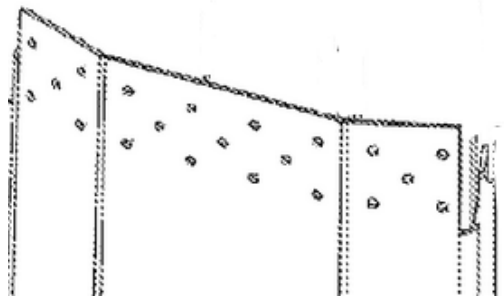

Figure 2. Plate used in the production of Andresen Towers (Langeskov and Middelfart 2013)[5]

The cheapest option in this case would be the use of lattice towers. However, these types of towers have been used in the past and present a series of problems, such as installation and maintenance costs. Regardless of their known issues, the designs can be improved and adapted to the specificity of the wind turbine. Recently, a 80m wind turbine towers was suggested by Husemann and Meiners (2013)[3]. The idea behind the design lies in the ease of installation. It is a structure composed of cold formed polygonal elements for the legs that can easily be connected with the stabilizing diagonal and horizontal struts. This option becomes difficult for higher wind turbine towers due to necessary number of connections. Another disadvantage is that the individual plates of the cross-section are relatively slender and S355 (normal strength steel) is recommended.

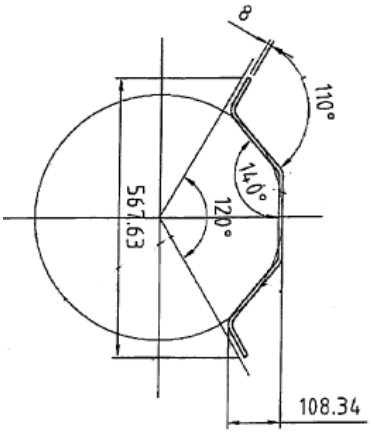

Figure 3. Plate used for the built-up polygonal cross-section [3]

For this purpose the most efficient cross-section needs to be identified. It is hard to decide which criteria define the optimal cross-sections. The optimization can vary based on different factors such as the number of connections required, the total material used, the installation costs and the time needed for installation. The target for investors is normally the total cost. However, this can vary in a very wide range based on the location of the construction and the fluctuation of the material costs. It is assumed that for the tower to be appealing for the manufacturers a fast execution time is required. Therefore, a reduction of the number of connections is recommended. For this reason, it is crucial to have the existing members as long as possible without secondary bracings.

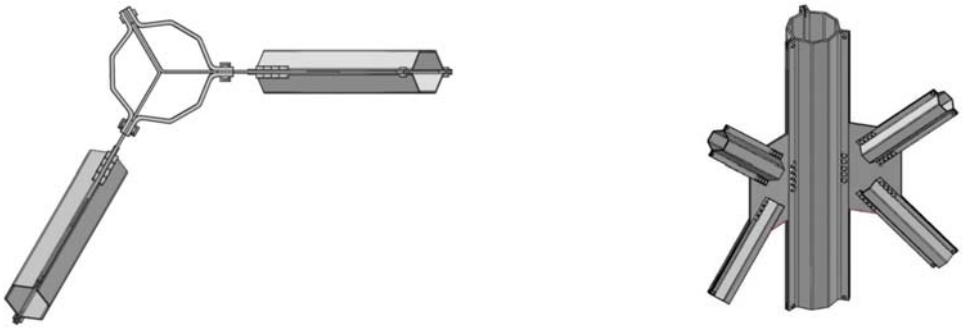

Figure 4. Example of joint for polygonal lattice tower (Jovašević et al. 2016)[4]

A study of the independent plates has been performed by Tran et al. (2016) [6]. The investigated cold-formed plates are made of S500, S700 and S960 high-strength steel. The boundary conditions used in the experiments were considered to be fully fixed. Based on the experimental results, a comparison by means of finite element method was later made (Tran et al. 2016b)[7]. It was concluded that good agreement between ultimate loads can be achieved by considering the imperfections as described in EN 1993-1-1 (2005)[1].

As stated in the EN 1993-1-1 (2005)[1], the verification of the members subjected to pure compression allows for the full use of the cross-section area if it is proven to be in the range of class 1-3. Therefore, the aim would be to use cross-sections at the limit of class 3 to class 4. This paper investigates the behavior of such cross-section considering the plates working as a whole polygonal cross-section, disregarding the contribution of the adjacent plates used for connecting the plates. The methodology for assessing the cross-section class is presented together with the evaluation of the member failure modes. The results are then compared between different cross-sections sizes. Finally, the conclusions are presented and discussed.

METHODOLOGY

As presented in the introduction the first step would be identifying the limit between class 3 and class 4 cross-sections. The classification provided in EN 1993-1-1 (2005)[1] mainly refers to hot-rolled or welded sections, it cannot be applied to cold-formed members without considering several additional factors. A class 4 section is defined by local buckling of the cross-section before reaching the yielding point of the most compressed fiber. Having this as a start point, it assumed that the class 4 limit is defined by the change of the first buckling mode. In this particular case the change would be between the Euler buckling mode and the plate buckling mode.

Considering that the critical load of a double symmetric compressed member with the buckling length, L_{cr}, and a second moment of area, I, is defined by Eq.(1) and the critical load of a compressed plate of a given thickness, t, and width, b, is defined by Eq.(2). The limit of the two buckling modes was discretized using Eq.(4), by varying the radius of the circle circumscribing the cross-section, R and the effective buckling length of the members.

$$P_{cr,E} = \frac{}{L_{cr}^2} \tag{1}$$

$$\sigma_{cr} = k \frac{}{12(1-\upsilon^2)} \cdot \frac{}{b^2} \tag{2}$$

$$P_{cr,J} = f_y A \left[1 - \left(\frac{}{4\pi^2 E} \right) \left(\frac{}{r} \right) \right] \tag{3}$$

$$P_{cr} \geq \sigma_{cr} \cdot A \tag{4}$$

The curve defining the limit between the 2 buckling modes disregarding the imperfections can be seen in **Figure 5**. Euler's formula cannot be applied for intermediate or short members. For that reason it is very important to consider that the critical stress is limited to the yield strength of the material. Johnson's formula, Eq. (3), gives an accurate estimate of this behavior.

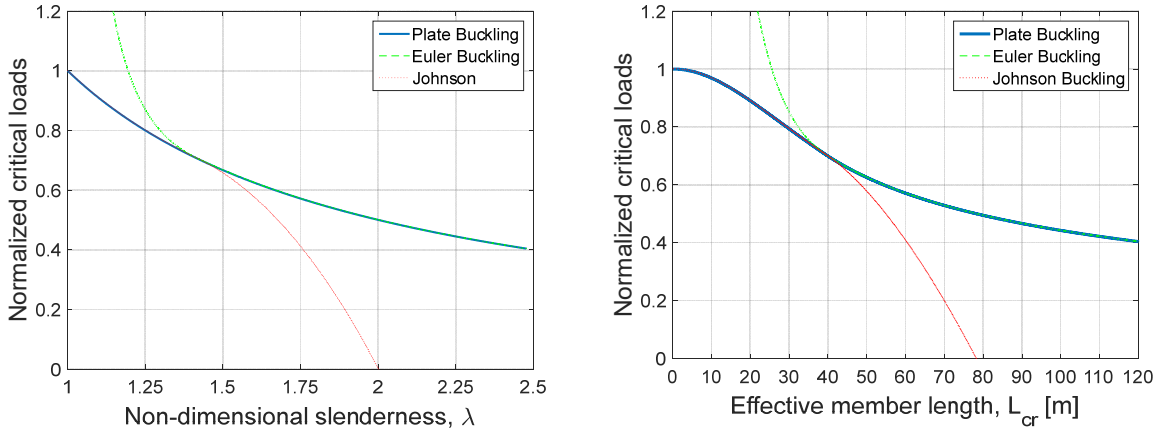

Figure 5. Slenderness curve for a polygonal cross-section with 9 facets considering f_y=355 MPa

The transportation conditions of the profiles are considered to be normal under a length of 14 m, therefore a length of 12 m was considered. The joints and continuity connections are considered to reduce the effective length of the member to approximately 10m. The ultimate purpose would be to determine a cross-section size to which high strength steel can be efficiently used. As seen in **Figure 6**, the advantage of the high strength steel is only displayed for low member slenderness. Afterwards, the potential advantage is gradually lost due to the instability effects.

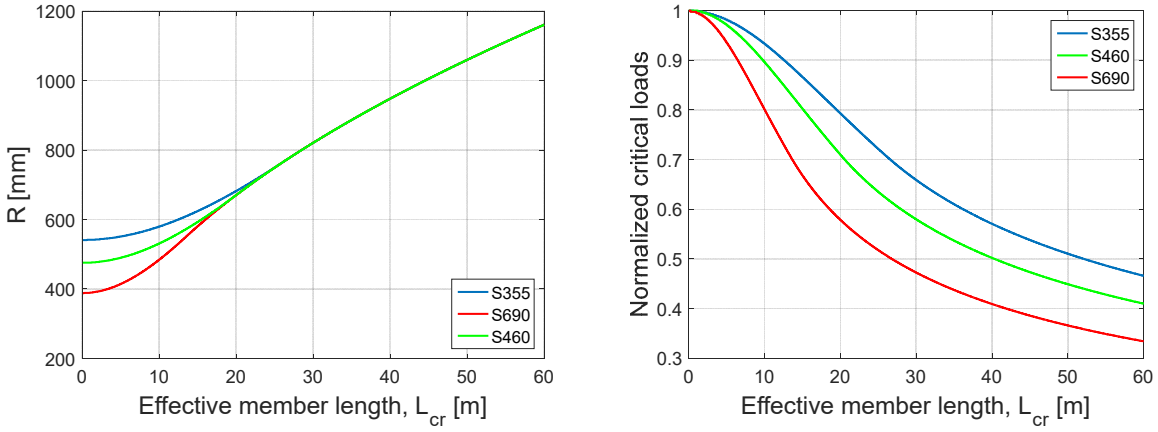

Figure 6. Radius of the circle circumscribing the polygonal cross-section vs. the effective member length for different steel grades

The second part of the study consisted of analyzing a series of selected cross-sections as seen in **Table 1**

Table 1. Geometrical properties of the analyzed struts

R[mm]	L[m]	t[mm]	b[mm]	facets[#]	A[mm^2]
300	10	12	205	9	22163
350	10	12	239	9	25857
400	10	12	274	9	29551
450	10	12	308	9	33244
500	10	12	342	9	36938

A buckling analysis of the members was performed. The purpose was to identify a correlation between the buckling modes and to determine if the two modes will influence each other. The requested number of modes was set to 5, in order to use them as an input for a subsequent GMNIA analysis.

RESULTS

The buckling analysis results show a good agreement between the predicted modes and the results obtained from the FE analysis. If the section is considered to be closed, the buckling mode is defined by the minimum value of the plate and Euler critical load.

Table 2. First buckling modes comparison

R [mm]	b [mm]	P_{cr} [kN]			FEM	EC
		FEM	Euler	Plate		
300	205	18768	**19059**	57536	Global	Global
350	239	29638	**30265**	49317	Global	Global
400	274	42880	45176	**43152**	Local	Local
450	308	38270	64324	**38357**	Local	Local
500	342	34555	88235	**34522**	Local	Local

The first local buckling mode shows an eccentric behavior as can be seen in **Figure 7**. When used as input for the imperfection a combination of modes occurs due to the added eccentricity. Therefore, for future work an imperfection function will be added to account for both local and global imperfection. This way, the identification of modes will not be done by means of eigenvector buckling analysis but by means of minimum critical load.

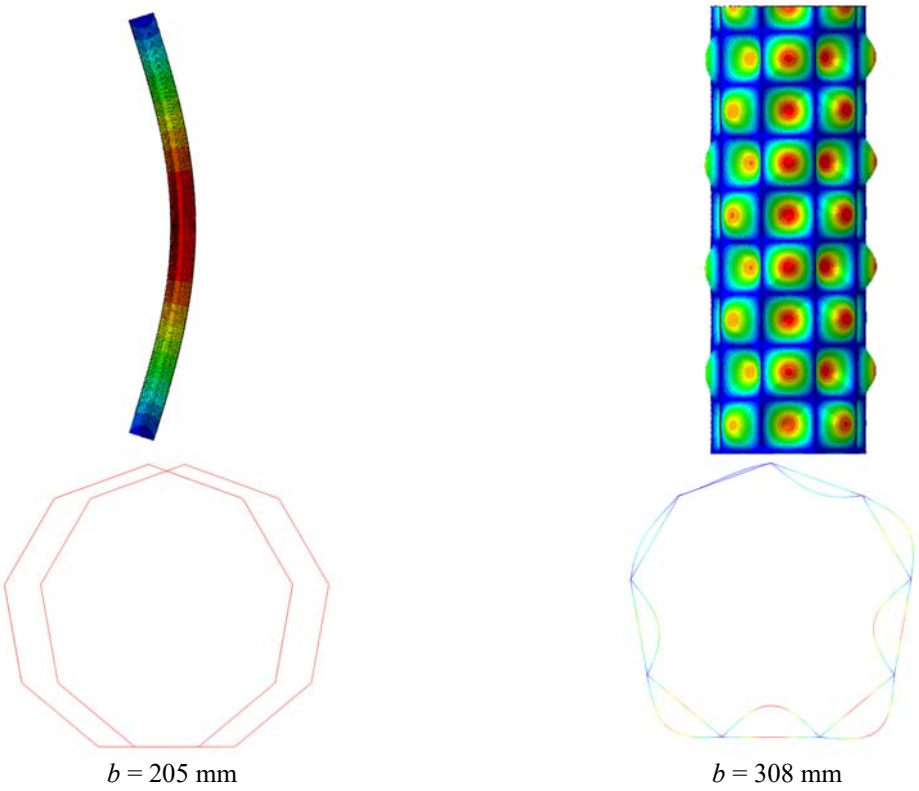

b = 205 mm *b* = 308 mm

Figure 7. First buckling modes

CONCLUSIONS

By limiting the plate buckling of the individual polygonal facets to the Euler buckling mode, a safe estimate can be made to keep the cross-section in class 3. However, the ultimate resistance of the member becomes very sensitive to imperfections. This effect will amplify if a built-up option will be used. In this situation, the combination of modes becomes a higher problem.

Attention needs to be given to the classification methods presented in EC 3. A class 3 section will reach yield stresses in the most compressed fiber, but local buckling is liable to occur. Therefore, it is not enough to limit the buckling mode to a global one, but also to the critical plate stresses to the yield stress of the material.

The paper presents the motivation of choosing to investigate the polygonal cross-sections and the approach of the selected subject. A short introduction and state-of-the art on current steel wind turbine towers structural typologies is presented. The methodology of the analysis is explained and the selected study cases are specified. The results from the buckling analysis are presented and discussed. Finally, the conclusions of the study are being presented together with the future work.

ACKNOWLEDGEMENTS

The authors acknowledge with thanks the support of the European Commission's Framework Program "Horizon 2020", through the Marie Skłodowska-Curie Innovative Training Networks (ITN) "AEOLUS4FUTURE - Efficient harvesting of the wind energy" (H2020-MSCA-ITN-2014: Grant agreement no. 643167) to the present research project.

REFERENCES

[1] EN 1993-1-1.Eurocode 3: Design of steel structures - Part 1-1: General rules and rules for buildings. *Eurocode 3*, 2005 .

[2] Hau, E.Wind Turbines. *Wind Turbines Fundamental, Techonologies, Application, Economics*, 2013 .

[3] Husemann, K., and Meiners, W."Tower for a wind power plant," 2013 2(12).

[4] Jovašević, S., Correia, J. A. F. O., Pavlović, M., Rebelo, C., De Jesus, A. M. P., Veljković, M., and da

Silva, L. S."Global Fatigue Life Modelling of Steel Half-pipes Bolted Connections." *Procedia Engineering*, The Author(s), 2016 160(Icmfm Xviii), 278–284.

[5] Langeskov, A. K., and Middelfart, L. R."Tower Element." United States Patent, 2013 .

[6] Tran, A. T., Veljkovic, M., Rebelo, C., and da Silva, L. S."Resistance of cold-formed high strength steel circular and polygonal sections - Part 1: Experimental investigations." *Journal of Constructional Steel Research*, Elsevier Ltd, 2016a 120, 245–257.

[7] Tran, A. T., Veljkovic, M., Rebelo, C., and da Silva, L. S."Resistance of cold-formed high strength steel circular and polygonal sections - Part 2: Numerical investigations." *Journal of Constructional Steel Research*, 2016b 125, 227–238.

THE INTERNATIONAL CONFERENCE ON
WIND ENERGY HARVESTING 2017
20-21 April 2017
Coimbra, Portugal

Paper A4F.05

STEEL HYBRID TOWERS FOR WEC: GEOMETRY AND CONNECTIONS IN LATTICE STRUCTURE

Slobodanka Jovašević[1]
ISISE/UC
Coimbra, Portugal

Carlos Rebelo[2]
ISISE/UC
Coimbra, Portugal

Marko Pavlović[3]
TUDelft
Delft, The Netherlands

J. A. Correia[4]
INEGI/UP
Porto, Portugal

ABSTRACT

With the increase for renewable energies demand, namely wind energy, the construction of more powerful wind energy converters (WEC) is a matter of great importance. More powerful converters require higher supporting towers. Height of the most commonly used steel tubular towers is limited by manufacturing and transportation logistics. The lattice tower instead of tubular steel towers appears as a possible solution. To overcome a large number of bolts as the major disadvantage of the lattice tower a new solution, which uses steel hybrid tower by assembling a lattice structure for the lower portion and a tubular tower for the upper portion is under investigation. The focus in this work is the development of the lattice structure using low-maintenance preloaded bolted connections and, for the members, new types of cross-sections. The geometry of the lattice portion of the tower is assessed in order to decrease number of the bolts. Experiments on the connections will be carried out and validated by finite element analysis (FEA). Parametric study of production tolerances will be performed and design methodologies will be proposed taking also into account the influence of the joint assembling tolerance.

INTRODUCTION

Wind energy has been used for more than 3000 years. At first used for pumping water or milling grains, and in recent years for producing electricity. Today, when global warming has become one of the most serious environmental issues, the need for renewable energies is increasing. In 2014 the European Union set the target that until 2030 in the total energy consumption at least 27% will be covered from renewable sources [1]. The high demand for wind energy is leading to construction of more powerful wind energy converters that demand higher towers to reach zones of higher speed and less turbulent wind. With the increase of the tower height also transportation, assembly, erection and maintenance of the tower becomes more difficult and more costly. Tower construction costs are up to 30% of the total WEC cost [2]. On the other hand, increase in height rises the generated energy.

At the moment, the most commonly used type of the tower for WEC is steel tubular tower. However, for the heights above 100 m, this type of the tower requires large diameter at the tower base which makes the usual assembling process unfeasible due to public road transportation limitations. To build high towers lattice solution is being proposed by some tower producers. Comparing to tubular tower, current solutions for lattice towers have

1 Early Stage Researcher, ISISE, Department of Civil Engineering, University of Coimbra, P-3004 516 Coimbra, Portugal, s.jovasevic@uc.pt
2 Associate Professor, ISISE, Department of Civil Engineering, University of Coimbra, P-3004 516 Coimbra, Portugal, crebelo@dec.uc.pt
3 Assistant Professor, Department of Structural Engineering , TU Delft, Postbus 5 2600 AA Delft, The Netherlands/ M.Pavlovic@tudelft.nl
4 Post-Doc researcher, University of Porto, INEGI, Faculty of Engineering, Rua Dr Roberto Frias, 4200-465 Porto, Portugal,

many bolted connections posing problems of maintenance during service life.. On the other hand, lattice tower is not affected by transportation limitations [2], [3].

The propose of this research is to develop steel hybrid tower for onshore applications with hub height up to 220 m using a new type of lattice structure for lower portion of the tower and a current tubular structure for upper portion of the tower. The use of tubular tower for upper portion takes all the advantages of optimized technology for tubular steel towers with the diameters within public road transportation limitations, while the lattice portion enables the required extension of height [4]. Another advantage is that the lattice portion can be used to facilitate installation of the upper tubular portion and the turbine, therefore avoiding the need for very high cranes.

For the lattice elements new types of welded and bolted cross-sections and connections are proposed. Cross-section and member performance, together with bolted connections will be investigated. New steel grade for bolts will be applied. The aim of this work is optimization and detailed design of *in-situ* connections with use of preloaded bolts. Parametric study on the geometry of the lattice portion of the tower was done in order to determine the geometry and the cross-sections of the connected members. Experiments on the connections will be carried out in order to obtain moment-rotation relationship and FEA validation of the experimental results along with a parametric study (of production tolerances) will be made. Hand-calculation model of the joint components behaviour and the whole joint will be developed. Fatigue behavior of the connection will be numerically assessed as well.

METHODOLOGY

A set of structural solutions was designed for ULS in order to assess different geometries of the lattice structure. Parameters chosen in the study are mainly targeting the balance between the height of tubular and lattice parts, the balance of base width to height and the number of connections/bolts to be used. Defined case studies have following parameters:

- wind turbine power: 5MW
- lattice part height: 120m
- tubular part height: 100m
- number of 'Legs': 4 and 6
- height/spread ratio of lattice part: H/L=1/1; 2/1; 3/1; 4/1; 5/1; 6/1

In order to determine optimal geometry for the face of the lattice part, four different solutions (Figure 1) were analyzed. For each case the angle of the brace from horizontal plane was varied between 30° and 50° (35° and 55° for 6 "legs" towers) with the increment of 5°. Based on the results, 2nd solution was chosen for parametric study. In case of the lattice with 6 "legs" two solutions were considered, one chosen for 4 "legs" lattice towers and one with K braces (Figure 1). Solution chosen for further investigation was with K braces. In both cases (4 and 6 "legs") the parametric study was carried out with the brace angle of 45°.

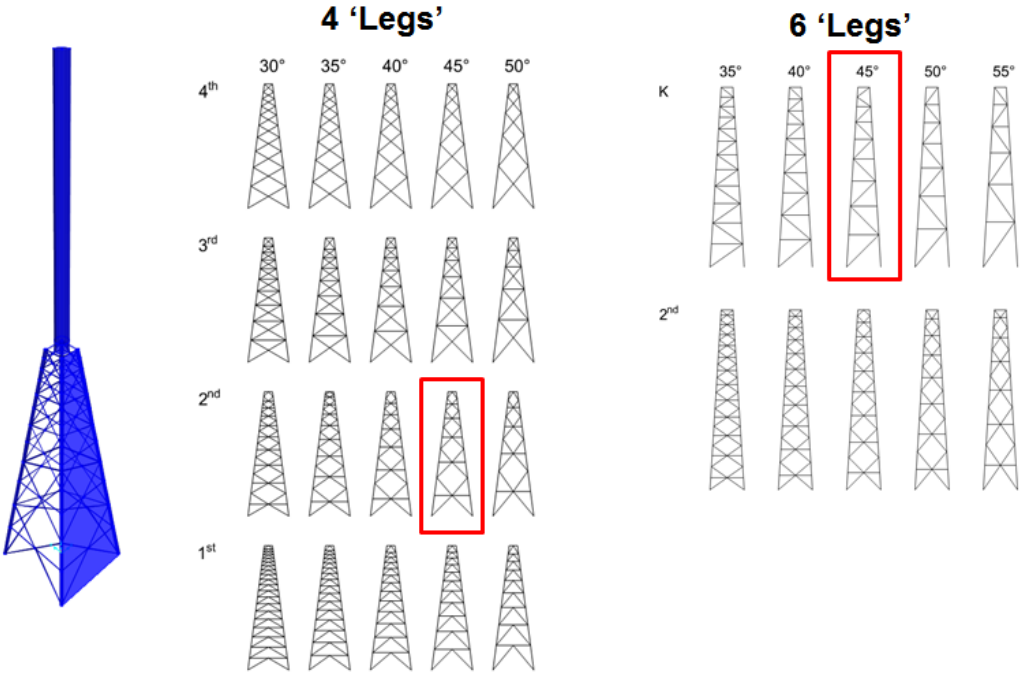

Figure 1. Parametric study – brace geometry

Parameters considered in the comparison of proposed solutions are:
- weight of the lattice structure
- number of the connections in the structure,
- estimated number of the bolts (for N_{Ed} in brace elements)
- reaction force in the foundation

In-situ connections in the lattice portion of the tower, with extensive use of preloaded bolts, will be analyzed in details. Connection with Gusset plates will be used for pylons which are connected in different direction to the bracing system and simple gusset plates for the braces in order to maintain simplicity of the connection bolted *in-situ*. Cross-section of profiles used in connections of lattice portion are given in Figure 2.

Pylon members	
welded pylon	
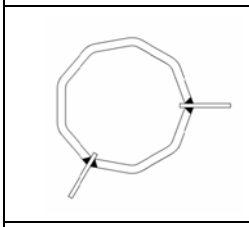	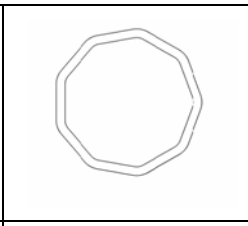
Joint detail	Cross-section
bolted built-up pylon	
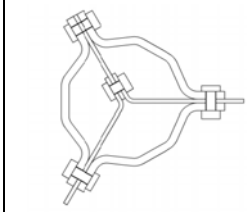	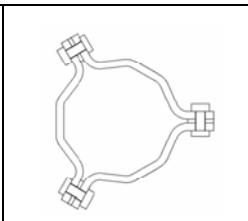
Joint detail	Cross-section

Brace members	
bolted built-up brace	
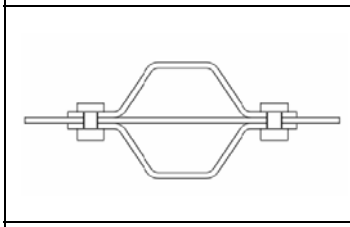	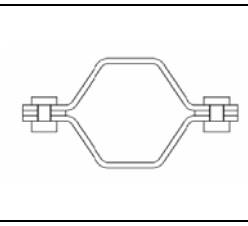
Joint detail	Cross-section

Figure 2. Proposed cross-sections and detailing for pylon and brace with Gusset plates joints

Preliminary parametric study is carried out in order to predict the behaviour of the connections to be tested. The parameters varied are thickness of the brace member, gusset plate thickness and bolts diameter (Table 1). The numerical analysis is performed using the Abaqus FE software package.

Table 1. Numerical study parameters

Pylon		Brace		Bolts	Gusset Plate
D [mm]	t [mm]	D [mm]	t [mm]		t [mm]
			4	M24	10
			5	M27	10
			6	M30	12
325	20	220	8	M36	15
			10	M36	14
			12.5	M42	18
			15	M48	20

Preloaded bolted connections with welded and bolted built-up pylon member alternatives are to be tested. In both case the diagonal is bolted. Specimens to be tested are vertical pylon and diagonal member with pylon to diagonal angle of 90º and 45 º (Figure 3). Three specimens for each parameter will be tested (12 experiments in total). Required capacity for the actuators and ultimate load will be determined from numerical study of the set-

up. Experimental results will be validated by the FE models. Based on experimental and numerical results the design recommendations for hybrid steel towers will be given.

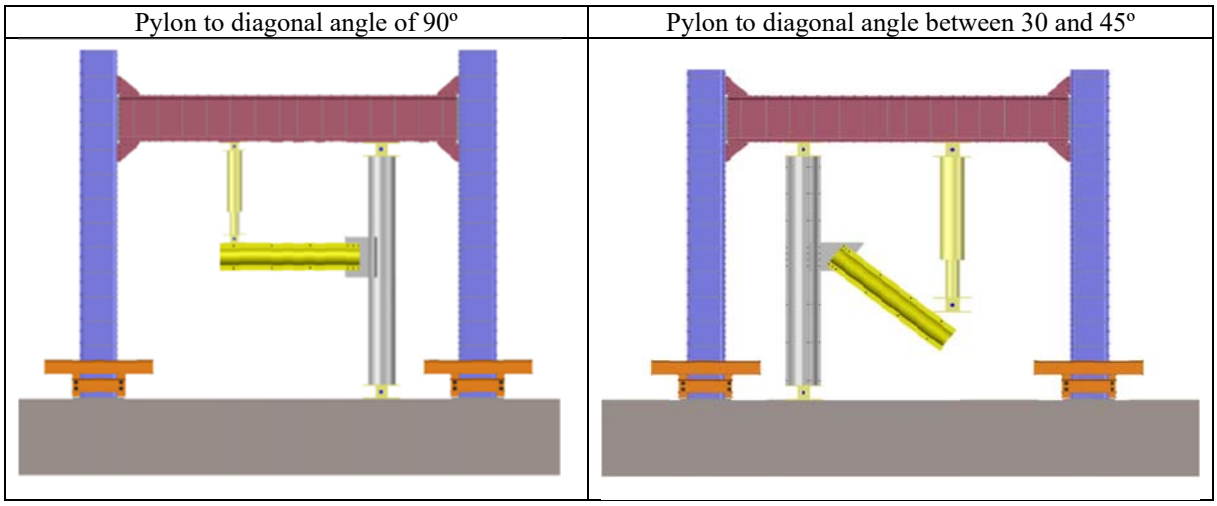

Figure 3. Layout of the connections to be tested

RESULTS

Study on the search of optimal geometry for the lattice structure based on material weight and number of connections and bolts has been performed. Parametric study results for 4 and 6 "legs" structures are shown in Figure 4. Comparison is made for mass of the structure, number of the connections and estimated number of the bolts. In the Figure 4 (left) only lattice portion of the tower was considered in analysis. The lowest mass of the structure was obtained for height/spread ratios 3/1 to 5/1. This three ratios were chosen for further investigation in which the tubular portion is included. Number of the bolts was estimated for each solution. The lowest number of the bolts was obtained for lattice tower with 6 "legs" and K braces without horizontals.

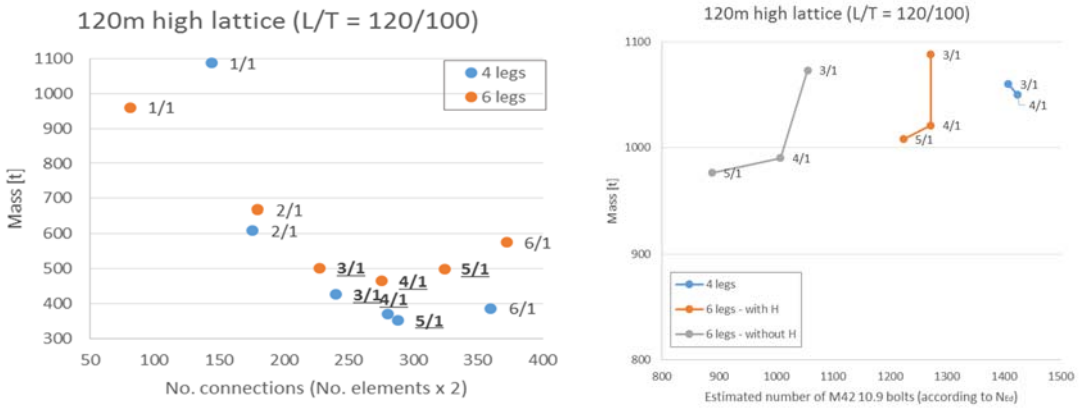

Figure 4. The weight and number of the connections (estimated number of the bolts) for chosen geometries

Taking into account that with the increase of height/spread ratio the reaction forces are increasing, the solution that was chosen as the most optimal one between the proposed cases is for ratio 4/1.

CONCLUSIONS

Numerical and experimental characterization of connection behaviour in the lattice portion of the tower with use of preloaded bolts will be carried out. FE verification of the experimental results and parametric study where production tolerances are varied will proceed. New hand calculation model, taking into account joint tolerance for assembly will be developed. In order to determine the geometry of the connections parametric study on structural optimization was carried out. Between the proposed solutions one for 6 "legs" with K braces (45°) and height/spread ratio 4/1 represents the most suitable balance between the mass of the structure, number of the bolts in the connections and reaction forces in the foundations.

ACKNOWLEDGEMENTS

The authors acknowledge with thanks the support of the European Commission's Framework Program "Horizon 2020", through the Marie Skłodowska-Curie Innovative Training Networks (ITN) "AEOLUS4FUTURE – Efficient harvesting of the wind energy" (H2020-MSCA-ITN-2014: Grant agreement no. 643167) to the present research project. Support of RFCS. This work was also partly financed by FEDER funds through the Competitivity Factors Operational Programme - COMPETE and by national funds through FCT – Foundation for Science and Technology within the scope of the project POCI-01-0145-FEDER-007633 and by the RFCS research program through the SHOWTIME project with Grant Agreement RFSR-CT-2015-00021.

REFERENCES

[1] EWEA, "Wind energy scenarios for 2030", A report by the European Wind Energy Association – August 2015
[2] Hau E, "Wind turbines – Fundamentals, Technologies, Application, Economics" (3rd ed.), Springer, Germany, 2013
[3] J.F. Manwell, J.G. McGowan, A. L. Rogers, "Wind energy explained – Theory, Design and Application", Wiley, USA, 2002
[4] Hüsemann K, "Ruukki Wind towers – High truss towers for wind turbine generators", Ruukki, Finland, 2010
[5] ISO-898-1: "Mechanical properties of fasteners made of carbon steel and alloy steel", International Organization for Standardization, Switzerland, 2013

THE INTERNATIONAL CONFERENCE ON
WIND ENERGY HARVESTING 2017
20-21 April 2017
Coimbra, Portugal

Paper A4F.06

THE HYBRID HIGHRISE WIND TURBINE TOWER CONCEPT

Mohammad Reza Shah Mohammadi[1]
ISISE, Department of Civil Engineering,
University of Coimbra, P-3004 516
Coimbra, Portugal

Carlos Rebelo[2]
ISISE, Department of Civil Engineering,
University of Coimbra, P-3004 516
Coimbra, Portugal

Milan Veljković[3]
Faculty of Civil Engineering and Geosciences
Delft University of Technology
Delft, The Netherlands

Luis Simões da Silva[4]
ISISE, Department of Civil Engineering,
University of Coimbra, P-3004 516
Coimbra, Portugal

ABSTRACT

Tower technology shows convincing potential for the increase of the electric power generation and reduction in the cost of wind energy. By accessing higher altitude, especially important in a forest environment, the high rise towers harvest more energy from the wind. However, the taller tower requires more materials, taller cranes for the execution and they can be trigger for the serious logistic challenges.

In order to achieve the competitive high rise wind turbine tower, a hybrid lattice-tubular steel tower is investigating. Different scenarios and innovations planned to be performed in order to obtain a tower with the height of 120 to 220 meters considering different load cases for the structural design and the optimization. Furthermore, the transition piece which is a connection between the lattice supporting structure and the tubular tower, is designed in detail. The dynamic response of the supporting structure regarding the transition piece concepts and the fatigue lifetime due to the high cyclic moment are investigated

The main issues and initial solutions of the project are discussed and the pathway is presented towards the new design of the hybrid steel tower and appropriate execution system.

NOMENCLATURE

DEL	=	Damage Equivalent Loads
DLC	=	Design Load Case
FEM	=	Finite Element Method
NREL	=	National Renewable Energy Laboratory
LDST	=	Large Diameter Steel Tower
TP	=	Transition Piece

1 PhD Candidate, ISISE, Department of Civil Engineering, University of Coimbra, P-3004 516, Coimbra, Portugal/ mrsm@uc.pt

2Assistant Professor, ISISE, Department of Civil Engineering, University of Coimbra, P-3004 516, Coimbra, Portugal/ crebelo@dec.uc.pt

3 Professor, Faculty of Civil Engineering and Geosciences, Delft University of Technology, Stevinweg 1, NL-2628 CN Delft, The Netherlands/ M.Veljkovic@tudelft.nl

4 Professor, ISISE, Department of Civil Engineering, University of Coimbra, P-3004 516, Coimbra, Portugal / luisss@dec.uc.pt

INTRODUCTION

Wind is known as one of the green source of energy. Nowadays, the wind turbine is getting more competitive compare to the fossil fuels. One way to make the wind energy more economic than fossil fuels is to increase the electric power generation in a wind turbine.

To do so, two interdependent strategies are applied. Increasing the rotor blade diameter and, consequently, increasing the wind turbine tower height, which on its turn allows to take advantage of higher wind speed and more steady wind flow. However, increasing the height of wind turbine tower structure leads to new challenges in different aspects. One of the main issues is the structural strength and fatigue due to increased loads and the logistic feasibility of the structure.

Although wind turbine towers accounts for 30% of the overall investment of an installation, few researches have been conducted in order to improve tower design or to make a cost effective execution process [1].

Figure 1 shows the conventional tower concepts, however, the steel tubular tower is the most common tower which is used in onshore wind parks. The tallest installed wind turbine onshore belongs to Vestas 3 MW wind turbine with 166 m height. The innovative tower design was introduced as large diameter steel tower (LDST) for this wind turbine model with 6.2 to 6.5 m of the tower base diameter. Although road transportation standards limit the allowable tower diameter, tower base segments are built in several pieces to make it possible for transportation. However, it increase the cost of transportation and the installation [2].

Figure 1: The Wind Turbine Tower Concepts

Towers usually are constructed using steel and/or concrete design. Convectional steel tubular towers use the ring flange connection. With the higher tower the fatigue problem gets dominant due to higher loads on flange's weld and higher tensile force on bolts. New friction connection was studied in [3] to avoid use of expensive welded flange connections also prone to fatigue. Moreover, to overcome logistic difficulties, the concrete bottom segment of wind turbines towers are employed which increase the construction complexity [1].

Recently, few other hybrid concepts have been presented. Iowa state university presented a new tower technology, called Hexcrete which refers to hexagon-shape towers made of concrete panels connected to concrete columns. As it uses precast components, it is transportable and has less logistic difficulties [4]. New founded company-Advanced Tower Systems- developed a new concept consisting a 74 meter precast concrete as a lower part and a 55 meter high steel tower [5].

GE also proposed new enclosed lattice space frame goes beyond 130 meters for towers and allows assembly onsite. Furthermore, the new idea make the tower cost effective and utilized standard logistic [6].

In order to calculate the aero-hydrodynamic loads on a wind turbine and also investigate the operational states, several simulation tools are designed. NREL introduced FAST as a servo-hydro-aeroelastic tool which used conventional BEM method to calculate the loads and the finite element method to solve the system. The outcome of several condition of the wind turbine is compared between FAST, ADAMS, and DHAT in [7]. Moreover, several similar tools were developed in DTU and validated by experimental and other simulation tool [8], [9]. Recently, a new software is developed with a real time GUI and detail aeroelastic analysis which is very easy to make any type of supporting structure [10].

The lattice/jacket fatigue and dynamic response is studied in [11]–[13]. The effect of the wind and wave loads were studied in [12] and the effect of added mass and different connection in the jacket structure on the dynamic response was studied in [11]. In [14], the fatigue damage was assessed for different load condition on critical regions of jacket structures. Moreover, different spectral and probabilistic methods were investigated to evaluate

the fatigue damage of wind turbine supporting structures in [15], [16]. The dynamic response and the loads from different DLCs were investigated for a monopile structure and the most critical load case was proposed in [17].

METHODOLOGY

Introduction

The general approach of this PhD research is to design and optimize a new hybrid wind turbine tower which consists of a lattice structure, a tubular part, and a transition piece to connect the lattice and the tubular part. Moreover, the detail analysis of the transition pieces as a connection between lattice and tubular segment will be provided. A new execution process will be designed in detail utilizing the lattice part as the supporting structure for erecting process of the tubular part and the nacelle. Therefore, the transient loads from the lifting process should be taken into account as well.

The lattice structure is designed using an iterative aeroelastic loads approach (Figure 2). Then, the aeroelastic response of the final lattice/tubular hybrid structure under different DLCs regarding the IEC standard will be fully investigated [18]. Afterward, the fatigue and the dynamic response of the whole structure corresponding the transition piece is calculated for different case studies.

In order to fulfill the new tower structure design requirements, following objectives are established:

- Identification of wind loads for different scenarios with servo-hydro-aeroelastic simulation tool.
- Optimization of the properties and the geometry of the lattice and tubular part with the minimum effort for transportation and installation.
- To provide the ultimate state limit and fatigue design of the lattice structure.
- To develop two alternative conceptual solutions for the transition segment and providing the detail design with consideration of the lifting device integration
- Investigate the dynamic response and fatigue lifetime and behavior under cyclic loading.

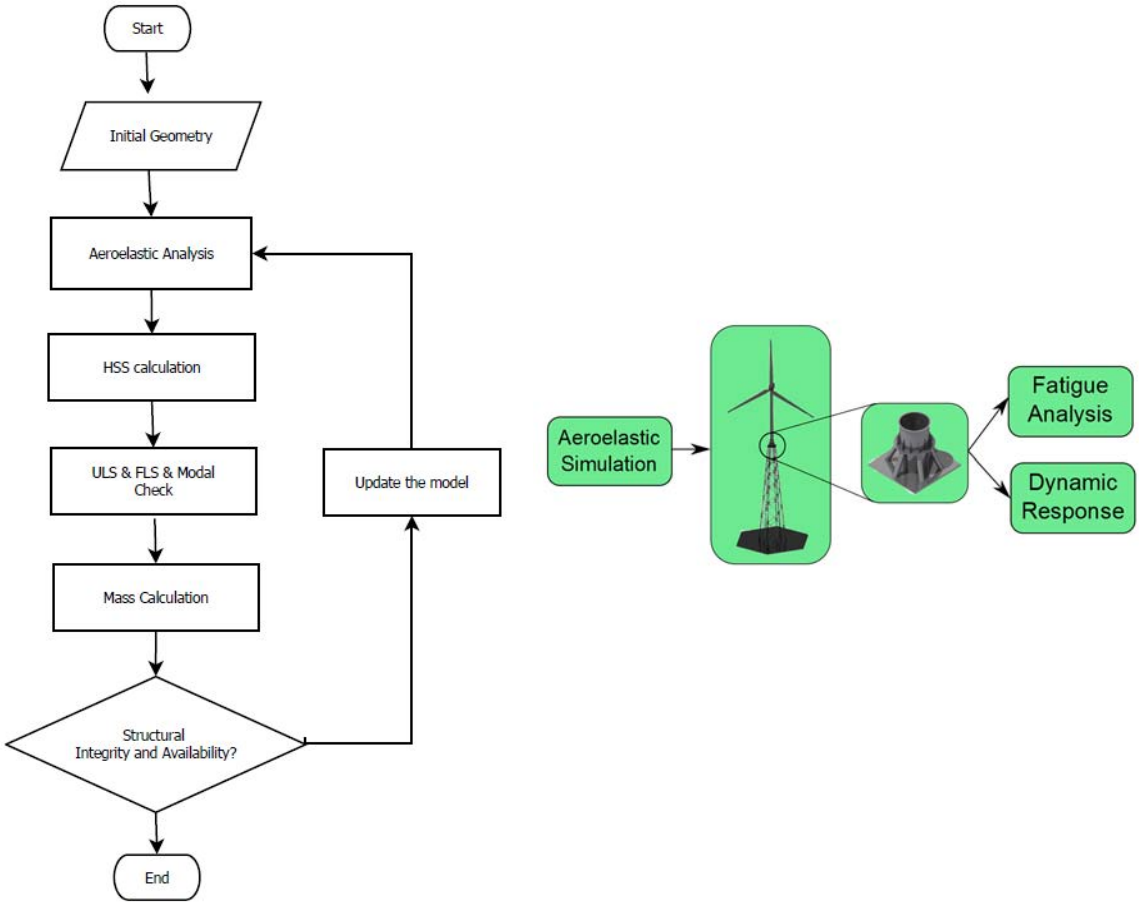

Figure 2: (left) the iterative approach flowchart (right) the work flow of the hybrid structure design and assessment

Iterative design and aeroelastic simulation

In order to design the detail of the wind turbine lattice and tubular part, the forces and the moments exerted on different cross sections are necessary. In the initial phase, extreme wind conditions regarding the IEC 61400 are identified. Due to complexity of the wind turbine behavior, three design load cases (DLC) are considered for initial ultimate state design.

An initial concept of lattice structure was designed and the NREL 5MW RNA and tubular tower structure was used in the initial load analysis. A parametric study has been done on the lattice structure to find out the minimum number of connection and configuration for the lattice structure. The varied parameters are mentioned in Table 1 and Table 2 shows the 5MW NREL wind turbine specification.

Table 1: Lattice structure design parameters

Parameters	Values
Number of Legs	4, 6
H/S (Height/Spread)	1/1, 2/1, 3/1, 4/1, 5/1, 6/1
Bracing Angle (◦)	30, 35, 40, 45, 50, 55
DLCs	1.1, 1.3, 6.1

Table 2: 5MW NREL Wind Turbine Specification

Info	**Value**	**Unit**
Mass	349,606	Kg
Rotor	31,4	%
Main Shaft	16,2	%
Nacelle	68,6	%
Rotor, Hub Diameter	126-3	m

Nevertheless, four structure is proposed in Table 3. Different height is considered for the lattice and tubular part. Moreover, it is possible to study the best combination of tubular and lattice part.

Table 3: Different High-Rise Wind Turbine Height Scenarios

Total Tower Height(m)	Lattice Height(m)	Tubular Height(m)
120	60	60
160	100	60
180	60	120
220	100	120

Dynamic Response

Wind turbines is a dynamic machinery with high bending moments on the supporting structure. Moreover, the operation of the wind turbine is variable speed which means more broad working frequencies. NREL 5MW wind turbine has the minimum rotational speed of 6.9 rpm and the maximum of 12.1 rpm, it means the 1P frequency range is between 0.115-0.202 Hz and 3P is between 0.345-0.605 Hz.

There is different concepts for the design of the overall structural stiffness to avoid the tower frequency and excitation frequency conjunction. The three convectional design approaches can be defined as following:

- Soft-soft, where the tower and blade stiffness are below the 1P frequency. It requires high precision controlling system as the system deflection is highly depended on the rotor rotational speed changes. Moreover, it needs very stiff foundation to overcome the overturning of the whole structure.
- Soft-stiff, where the tower frequency lies between 1P and 3P frequency. It is the most common design of the wind turbine structure.
- Stiff-stiff, where the tower frequency is higher than the blade passing frequency 3P.

Most of the time the soft-stiff is selected for the design of the blade and the supporting structure. Therefore, the tower frequency should be laid between 0.222 and 0.311 Hz (10% safe margin) to avoid the resonance. These ranges and working frequencies are illustrated in Figure 3.

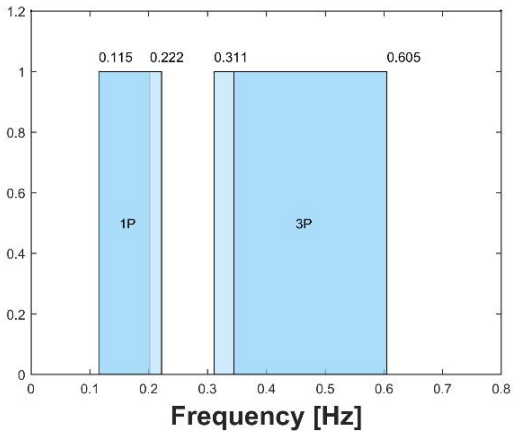

Figure 3: The working frequencies of NREL 5MW wind turbine

Fatigue Analysis

As the economic life time of the wind turbines are generally more than 20 years, the fatigue design of the wind turbine components should be considered in detail. The fatigue failure starts from a tiny crack and grows non-linearly with cyclic loading. To determine how much the wind turbine components can stand against the cyclic loading with different load range due to wind speed changes, there have to be a numerical and experimental test. Simply, the fatigue analysis of a wind turbine can be divided into steps below:

1- Data collection (10-minutes of loads timeseries)
2- Load cycle counting
3- Distribution function definition
4- Palmgren-Miner rule corresponding to the material S-N curve

RESULTS

In this section the results of the project so far are discussed. Initially the forces and moments regarding different load cases are presented and the dynamic response and the fatigue calculation will be discussed.

Structural design

Figure shows the results of parametric study of the lattice structure design. Figure 4-a, b show the bracing inclination angle, estimation of the number of bolts and the structural mass respectively.

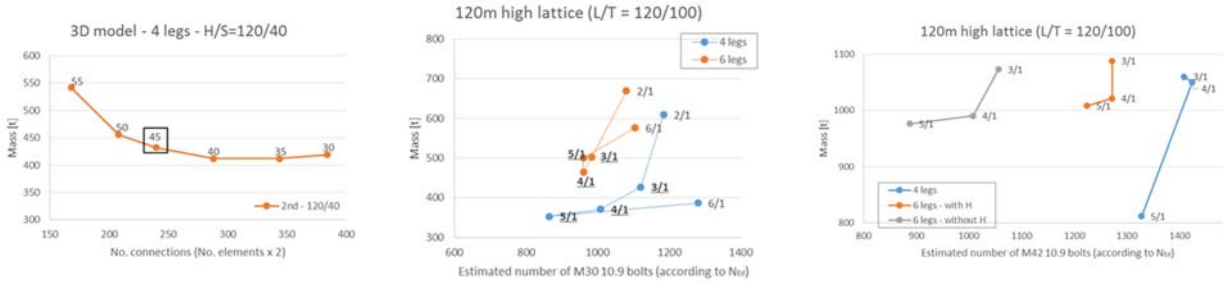

(a) (b) (c)

Figure 4: (a) The bracing inclination angle, (b) Mass-number of bolts for different H/S ratio (c) the mass for lattice structure with and without horizontal bracing and different number of legs

It can be seen that the best angle for bracing system is 45°. Height to spread ratio 4/1 and 5/1 lead to less number of bolts and the 6-legged structure without horizontal bracing provide the least structural mass.

Dynamic response

The modal analysis was performed for the lattice structure and the first 10 modeshape and the frequency was obtained. Moreover, initially the significance of the transition piece weight was investigated on first natural frequency of the supporting structure. Figure 5 shows the influence of two different transition piece on the natural frequency of the different towers.

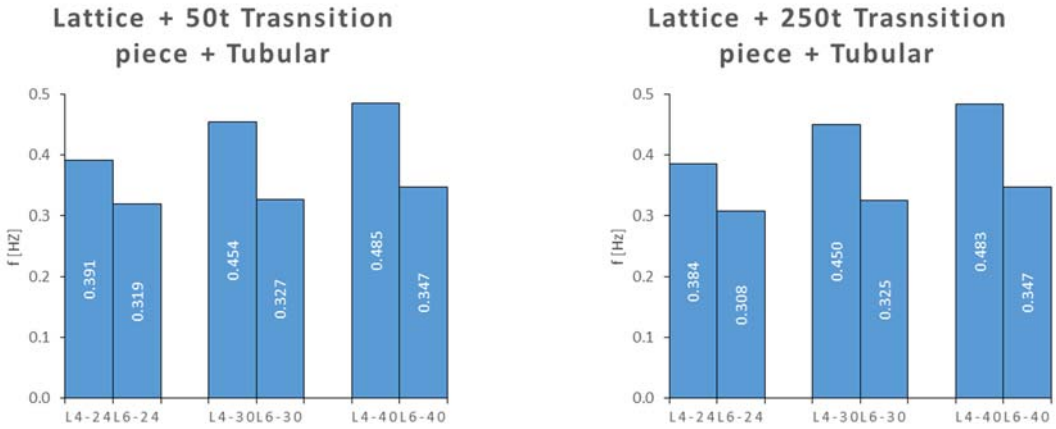

(a) (b)

Figure 5: First natural frequency of the different towers corresponding different transition pieces

It is obvious that the 6-legged lattice can be used as the working frequency will lay between the 1P and 3P frequencies of the wind turbine. However, detail analysis will be performed to capture the effect of the transition piece on the dynamic behavior and general response of the tower.

Fatigue analysis

In order to calculate the overall fatigue lifetime of the wind turbine at the transition piece level, a probability distribution function of the operational condition between cut-in and cut-off wind speed, idling, and special events like extreme wind speed, start-up and shutdown should be defined. Furthermore, all the mentioned conditioned aeroelastic simulation should be performed and the forces and moments at the transition piece should be obtained.

In this research, the procedure above was performed to certificate the new hybrid structure. Moreover, the fatigue lifetime will be calculated based on amplitude, mean and the Markov matrix and the difference in lifetime calculation will be reported. Figure 6-a shows the amplitude and mean value for 12 m/s wind speed and Figure 6–b shows the DEL for each wind speed in operational condition and idling. As it is expected, the 12m/s has the highest influence on the DEL because the controller just involves at the 12 m/s as the rated speed.

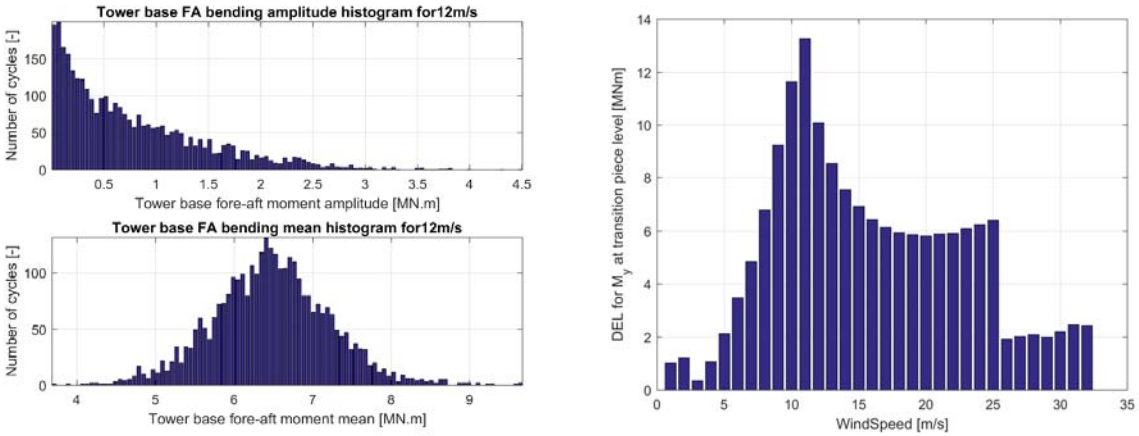

Figure 6: (a) The amplitude and the mean histogram for 12 m/s wind speed, (b) The DEL for 3 to 31 m/s wind speed

CONCLUSIONS

To increase the height of onshore wind turbine, many aspects should be considered. The first issue is the higher wind loads due to the shear profile at the higher altitude that requires more strength structure and higher fatigue life time. The next is the economic execution process with ease for the high rise wind turbine towers.

In order to design the new structure the wind loads were determined with aeroelastic simulation tool. As it was discussed, the new hybrid tower was designed and the new proposed lattice structure was designed to increase the feasibility of higher altitude and smarter installation and transportation. The transition piece a key component FEM analysis was discussed and the influence of transition piece on the dynamic response of the supporting structure was investigated. Moreover, fatigue life time of the turbine at the transition piece level was calculated.

All the design requirement for the tower structure design and the erection process was foreseen to fulfill the optimal and robust design.

As conclusion, this PhD research will be devoted to design and optimization of the hybrid wind turbine towers and providing the ultimate state limit, dynamic response and fatigue analysis of the structure. On the other hand, the new self-erecting procedure will be proposed based on existing self-sliding mechanism. The cost consideration and the time efficiency of the procedure will be taken into account to be minimum.

ACKNOWLEDGEMENTS

The authors acknowledge with thanks the support of the European Commission's Framework Program "Horizon 2020", through the Marie Skłodowska-Curie Innovative Training Networks (ITN) "AEOLUS4FUTURE - Efficient harvesting of the wind energy" (H2020-MSCA-ITN-2014: Grant agreement no. 643167) to the present research project.

REFERENCES

[1] R. McKenna, P. Ostman v.d. Leye, and W. Fichtner, "Key challenges and prospects for large wind turbines," *Renew. Sustain. Energy Rev.*, vol. 53, pp. 1212–1221, 2016.

[2] Vestas Wind Systems A/S, "Large Diameter Steel Flanges (LDST)," 2016.

[3] M. Veljkovic *et al.*, "High-strength tower in steel for wind turbines," 2012.

[4] "http://www.news.iastate.edu/news/2015/11/10/tallertowers." .

[5] "http://www.hybridturm.de/projekte/winterborn.html." .

[6] "http://www.windpowermonthly.com/article/1283941/ge-develops-space-frame-tower." .

[7] M. Buhl and A. Manjock, "A Comparison of Wind Turbine Aeroelastic Codes Used for Certification," in *44th AIAA Aerospace Sciences Meeting and Exhibit*, American Institute of Aeronautics and Astronautics, 2006.

[8] S. Oeye, "FLEX4. Simulation of wind turbine dynamics," in *In B. Maribo Pedersen, editor, State of the Art of Aerolastic Codes for Wind Turbine Calculations*, 1996, pp. 71–76.

[9] J. Thirstrup Petersen, "The aeroelastic code HawC - model and comparisons." Technical University of Denmark. Department of Fluid Mechanics, p. 129–135 BT–State of the art of aeroelastic codes, 1996.

[10] P. E. Thomassen, P. I. Bruheim, L. Suja, and L. Frøyd, "A Novel Tool for FEM Analysis of Offshore Wind Turbines With Innovative Visualization Techniques," in *Proceedings of the Twenty-second (2012) International Offshore and Polar Engineering Conference*, 2012, vol. 4, pp. 374–379.

[11] W. Shi, H. Park, J. Han, S. Na, and C. Kim, "A study on the effect of different modeling parameters on the dynamic response of a jacket-type offshore wind turbine in the Korean Southwest Sea," *Renew. Energy*, vol. 58, pp. 50–59, 2013.

[12] W. Dong, T. Moan, and Z. Gao, "Long-term fatigue analysis of multi-planar tubular joints for jacket-type offshore wind turbine in time domain," *Eng. Struct.*, vol. 33, no. 6, pp. 2002–2014, 2011.

[13] M. Seidel, "Jacket substructures for the REpower5 M wind turbine," in *Proceedings of European offshore wind energy conference and exhibition*, 2007.

[14] B. Yeter, Y. Garbatov, and C. Guedes Soares, "Fatigue damage assessment of fixed offshore wind turbine tripod support structures," *Eng. Struct.*, vol. 101, pp. 518–528, 2015.

[15] J. Ding and X. Chen, "Fatigue damage evaluation of broad-band Gaussian and non-Gaussian wind load effects by a spectral method," *Probabilistic Eng. Mech.*, vol. 41, pp. 139–154, 2015.

[16] L. Ziegler, S. Voormeeren, S. Schafhirt, and M. Muskulus, "Design clustering of offshore wind turbines using probabilistic fatigue load estimation," *Renew. Energy*, vol. 91, pp. 425–433, 2016.

[17] A. Morató, S. Sriramula, N. Krishnan, and J. Nichols, "Ultimate loads and response analysis of a monopile supported offshore wind turbine using fully coupled simulation," *Renew. Energy*, vol. 101, pp. 126–143, 2017.

[18] International Electrotechnical Committee, "International Electrotechnical Committee (IEC) 61400-1," 2006.

THE INTERNATIONAL CONFERENCE ON
WIND ENERGY HARVESTING 2017
20-21 April 2017
Coimbra, Portugal

Paper A4F.07

CONDITION MONITORING OF WIND TURBINES: A REVIEW

Rana Moeini[1]
University of Birmingham
Birmingham, United Kingdom

Pietro Tricoli[2]
University of Birmingham
Birmingham, United Kingdom

Hassan Hemida[3]
University of Birmingham
Birmingham, United Kingdom

Charalampos Baniotopoulos[4]
University of Birmingham
Birmingham, United Kingdom

ABSTRACT

The ever-increasing growth of wind power plants has raised the awareness that high reliability of wind turbines requires an appropriate condition monitoring system. This can have a real impact only if an in-depth understanding of the operations of wind turbines is carried out. This paper focuses on the on-line condition monitoring of electrical components of a wind turbine to diminish the downtime due to maintenance. The state of the art condition monitoring methods of electrical generators and power converters are critically reviewed. The analysis of the technical literature points out that the effect of wind speed variation is not considered for traditional condition monitoring schemes. However, wind speed has a direct correlation with thermal cycling of IGBTs and hence, their residual lifetime. Moreover, other electrical components such as the dc-link capacitors and the generator suffer electrical and temperature stress when the wind is variable. Thus, the paper proposes a novel condition monitoring method based on an artificial intelligent algorithm that includes the measurement of wind speed to analyze the effects on the electrical system of a wind turbine.

INTRODUCTION

Different failures occur during the operations of wind turbines (WTs) such as electrical, electronic, mechanical and hydraulic failures and electronic subsystems faults. According to statistics on data recordings, the electrical subsystem has the highest failure rate, in which power converters, control system and generator account for 17.5%, 12.9% and 5.5%, respectively [1]. Condition monitoring (CM) can be beneficial to anticipate the occurrence of these failures and, hence, minimise the maintenance costs and the unplanned operation halts. CM of electrical systems are divided into diagnosis and prognosis is subsystems, where the first is used to identify the root cause of the fault and the second predicts the health level of each component and highlights incipient faults. A number of failure mechanisms can occur in the electrical components of WTs. However, electrical failures are normally analysed only looking at electrical quantities, so that for example the wind conditions are not directly considered. In addition, since each failure of an electrical component can have adverse effects on other components and, consequently, lead to catastrophic failures, a comprehensive approach for CM is essential.

This paper is structured as follows: section 1 describes the main components of the electrical system of WTs and summarises various types of failures. In section 2, CM methods are critically analysed for each type of WT

[1]Early Stage Researcher & PhD student, School of Engineering, University of Birmingham, Edgbaston, Birmingham B15 2TT, United Kingdom / r.moeini@bham.ac.uk.
[2]Lecturer, School of Engineering, Electrical and Systems Engineering, University of Birmingham, University of Birmingham, Edgbaston, Birmingham B15 2TT, United Kingdom / p.tricoli@bham.ac.uk.
[3]Senior Lecturer, School of Engineering, Edgbaston, Birmingham B15 2TT, United Kingdom / h.hemida@bham.ac.uk.
[4] Professor and Chair, School of Engineering, University of Birmingham, Edgbaston, Birmingham B15 2TT, United Kingdom /c.baniotopoulos@bham.ac.uk.

and compared to highlight the existing gaps of the technical literature. Finally, the directions of future studies on the subject are indicated in the section Progress and Future Work.

REVIEW OF THE ELECTRICAL SYSTEM OF WIND TURBINES

WTs convert the mechanical energy of wind into electrical energy with electrical generators [2]. In fixed speed WTs, the generator is squirrel-cage induction type and it is connected directly to the grid. However, this type of WT can produce power only when the wind speed is within a narrow range above the synchronous speed of the generator. Invariable-speed WTs, a power converter has to be fitted to the electrical system[3]. Both doubly-fed induction generators (DFIG) and synchronous generators can be used for variable speed applications. For the former, the power converter has the function to harmonise the voltage of the rotor windings of the generator with the voltage of the grid, either in terms of magnitude or frequency or both. For the latter, the power converter has the function to harmonise the frequency of the generator with the frequency of the grid.

Squirrel cage induction generators are used for fixed speed WTs and; as mentioned before, are directly connected to the grid [4],[5], as shown in Fig. 1. The drive-train consists of a shaft with blades, a gearbox, a mechanical brake and an electrical generator. The gearbox is present in most WTs, because the rotating speed of the electrical generators is normally significantly higher than that of the shaft. In order to compensate for the reactive power of the generator, a reactive compensation unit is added in parallel at the bus bars. These generators are very cost-effective, especially for micro and medium WTs. Due to the narrow range of operations and the requirements on reactive power, these generators are not preferred for large WTs [1], [6].

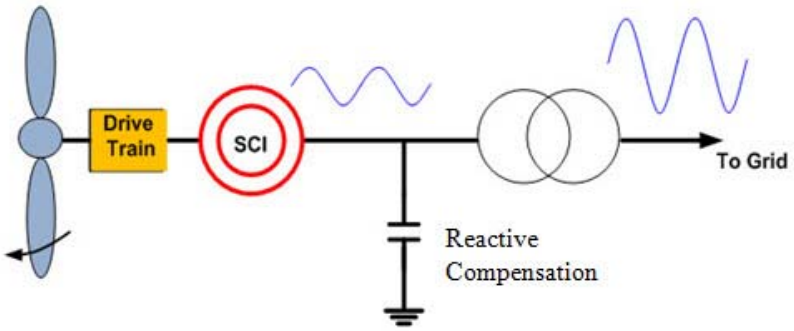

Figure.1. The diagram of Fixed-Speed WT (Squirrel Cage Generator)

The electrical system of a WT with a DFIG is shown in Fig. 2. A back-to-back ac-dc-ac power converter is used to rectify the grid voltage at grid frequency and then convert it into the desired three-phase ac voltage at slip frequency for rotor excitation. A dc-link capacitor is connected between the two converters as energy buffer [7]. A controller is used to regulate separately the real and reactive powers of the stator.

A wound-rotor induction generator has the stator winding which is directly connected to the grid, while the rotor is supplied by a power converter [8]. For this reason, this type of generator is called doubly-fed because both the stator and rotor windings are energised.

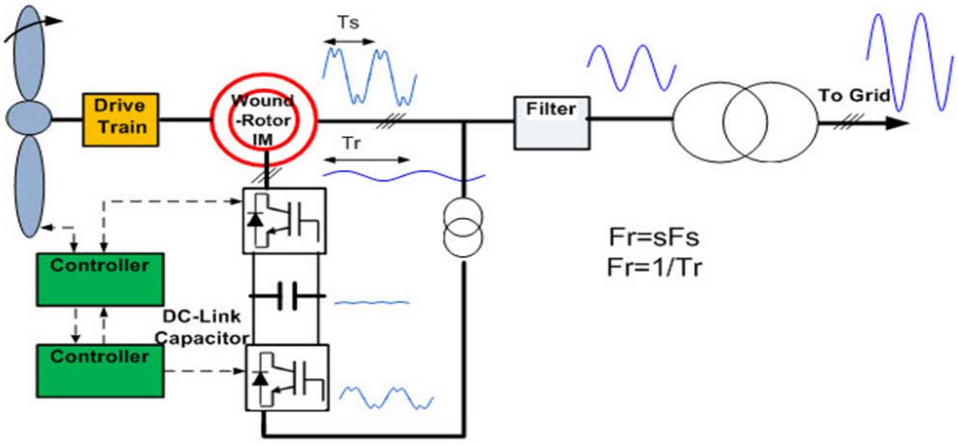

Figure.2. Diagram of doubly-fed induction generator

The electrical system of a WT with a Permanent Magnet Synchronous Generator (PMSG) is shown in Fig. 3. The power converter is connected to the stator winding and the machine is excited by the rotor magnets. The converter has two stages with an intermediate dc-link to convert the variable frequency of the generator into the constant frequency of the grid [9].

It should also be noted that the efficiency and the power density of permanent magnet generators are remarkably higher than those of squirrel cage generators and the DFIGs, because of the lack of excitation current. However, they are more expensive because rare-earth magnets (e.g. NdFeB) are necessary for the rotor.

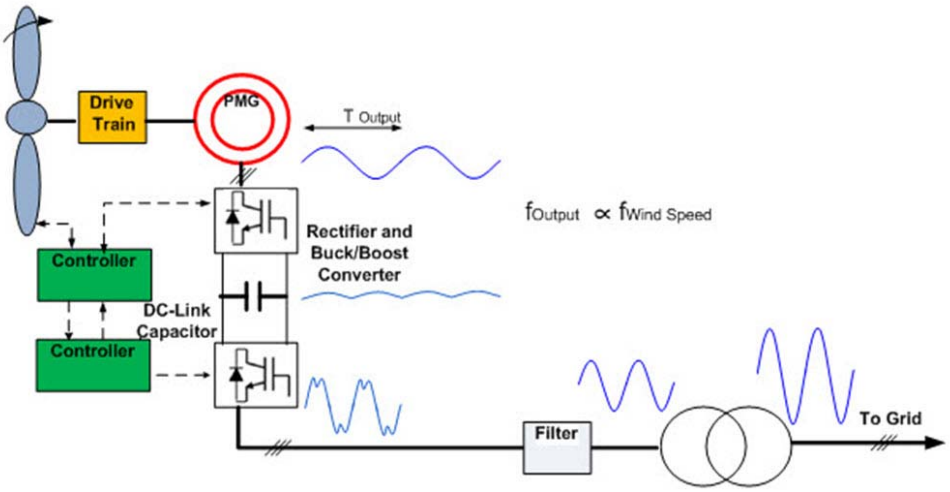

Figure.3. Diagram of permanent magnet synchronous generator

Fig.4. summarises the different types of WTs, classified on the basis of the generator type [5],[10].

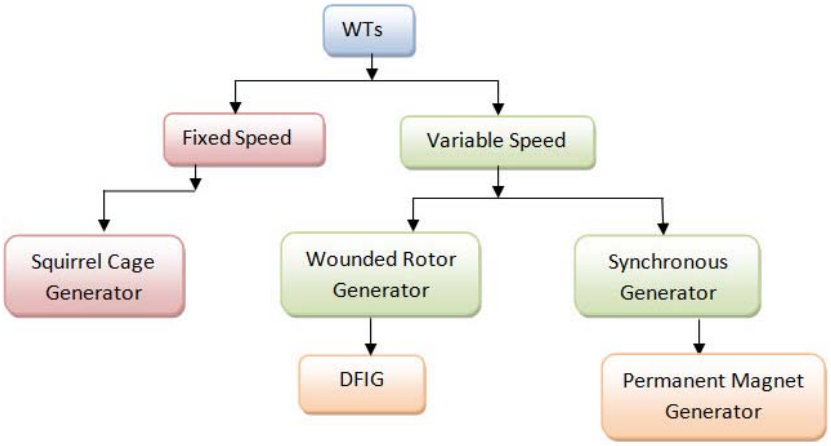

Figure.4. Classification of the electrical generators for WTs.

CM THEORY FOR WTS

WTs are complex systems consisting of a number of critical components. Malfunction of any of these critical components will most likely result in a downtime and high costs due to the loss of production and required maintenance. Depending on the specific component and mode of failure, the effect on the overall downtime, maintenance timescale and financial losses can vary significantly. Thus, the existence of a high-tech and accurate CM system is of paramount importance to diminishing the risk of failure by understanding not only early fault detection, but also the lifetime prediction of components during WTs operations.CM can be divided into two categories, on-line and off-line CM systems. In off-line CM, data are collected on a regular schedule time and the CM equipment is not integrated with the component monitored [6],[11]. The main drawback of off-line CM is that the operation of the components should be halted to undertake measurements during the CM. Thus, the health status of the on-line proposed components is not obvious in real time. On the other hand, in on-line CM, the instantaneous feedback of the operating condition is logged [5],[12]. In other words, providing continues information of system with measuring electrical and thermal vibration of each monitored components is essential for this type of CM. However, due to the fact that those variations do not follow a special profile in WTs, CM can be very complicated. In order to address this hardship, two different kinds of CM methods have been proposed, the sensor based and diagnostic based.

DIFFERENT TYPES OF SENSOR BASED CM TECHNOLOGY FOR WTS

Sensor-based CM techniques require special sensors and an associated signal processing. In order to apply effectively this CM system, the types of sensor and signal processing play a pivotal role. In Fig. 5, WT's parts are categorized according to the associated CM techniques. Nine different types of CM techniques are mostly represented nowadays and widely applied:

- vibration analysis for rotating equipment, such as generators, gearboxes and bearings [13], [14];
- acoustic emissions for bearings, blades, gearboxes, power electronic devices and dc-link capacitors[15];
- ultrasonic testing for towers, blades and power electronic devices [16];
- oil analysis for gearboxes and bearings [17], [18];
- strain measurements for structures[19], [20];
- thermography for electronic components and generators[21];
- shock pulse for bearings [22], [23];
- electrical parameters analysis for power electronic devices, dc-link capacitors and generators [24], [25];

The CM data are analysed by the following signal processing methods:

- trend analysis, collecting data from different sensors, used for pitch mechanisms [26];
- time-domain analysis, studying any variant in signal and trend [27];
- amplitude modulation analysis, extracting low frequency and low amplitude, used for gearboxes[28];
- wavelet transform to monitor vibrations, used for bearings [29];
- fast Fourier transform, analysing vibration signals used for rotating devices[30];

- hidden Markov model (HMV), vibration signal analysis, used for machines and bearings [31];
- artificial intelligence technique, used for mechanical systems [32];

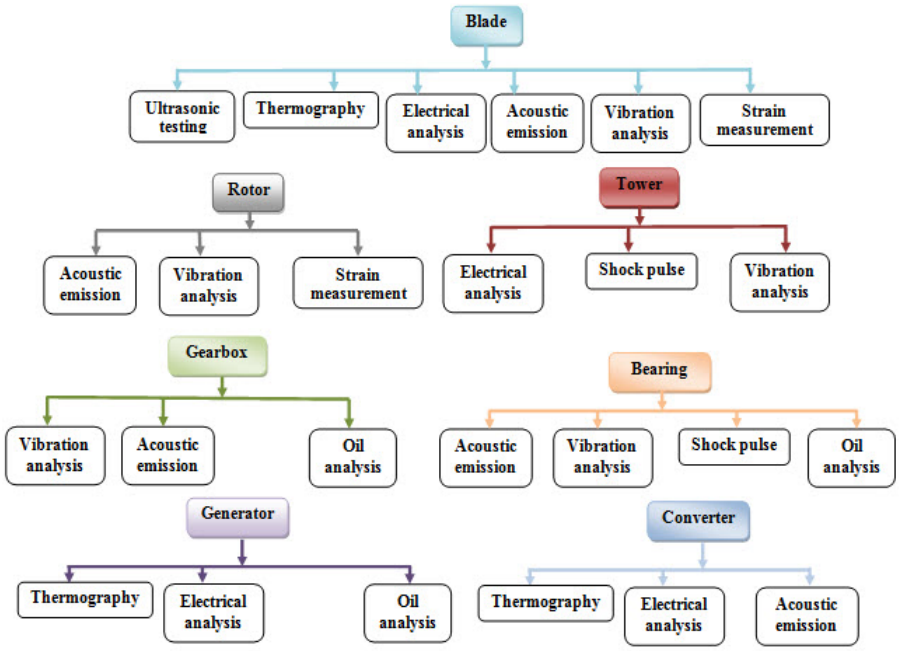

Figure.5. CM methods for WTs

In order to provide an effective CM method for WTs, fault diagnosis and detection are a crucial part. In fact, each WT's components have a potential to face different failure mechanisms, each of which requires specific monitoring techniques. Table.1. shows different failure mechanisms as reported in [33],[34].

Subsystem	Rotor			Drive Train			Electrical system			Generator
Components	Blades	Bearings	Shaft	Main shaft bearing	Mechanical brake	Gearbox	Control system	Power electronics	DC-link	
Faults mechanism	Cracking, Aging, Adjustment error	Wearing, Spalling, Rolling element Defect, Shell defect	Fatigue, Cracking	Wearing, Vibration	Locking position	Wearing , fatigue	Short circuit,	Short circuit, Bond wire lift-off, Solder fatigue, Thermal grease, Aging, Thermal and Electrical over-stresses	Electrolyte solution evaporation, Thermal and Electrical over-stresses	Wearing, Electrical problems, Bar cracking, Over speed, Overheating, Rotor asymmetries, Winding damage,

Table.1. Potential failures of WTs

CM BASED ON FAULTS FOR THE ELECTRICAL DRIVE TRAIN COMPONENTS

The main components of the fixed speed WTs are the squirrel cage generator and gearbox, as shown in Fig. 1. With reference rotor's bars, the health status can be monitored by analysing the spectrum of the stator current, which is modified by additional harmonics in case of geometrical and magnetic imbalance[35]. Thus,

many harmonic detection techniques have been proposed to identify the presence of undesired harmonics in the spectrum of the stator current, based on discrete Fourier transform (DFT) methods.

With reference to the common faults of stator windings, the main reason of failure is the degradation of the windings insulation for high temperature and electrical and mechanical stresses. Some on-line CM algorithms have been proposed based on thermal monitoring, fault detection of winding turns and partial discharge [36].

The main reason of bearing faults is the torque variations due to the variable power, contributing to surface and bending fatigue. Moreover, misalignment and improper lubrication are other significant causes of bearing faults [37].The CM procedures aimed to detect bearing faults are mainly based on vibrations and magnetic, thermal and acoustic emissions.

In variable speed WTs with DFIGs, the rotor winding's faults can be detected by measuring both the leakage flux and the shaft voltage [38]. In the leakage flux test, a detection coil is mounted near to the rotor, so that it can measure induced voltage. Thus, any reduction of the leakage flux in one of the rotor coils can be detected via the decrease of the induced voltage. In the shaft voltage test, the shaft-to-ground voltage is monitored, so that any leakage current flows through the shaft generates a voltage that can be detected by the CM system.

CM OF POWER ELECTRONIC CONVERTERS

Statistically, IGBTs (Insulation Gate Bipolar Transistors)are the most sensitive parts in converters accounting for 30% of failures, followed by dc-link capacitors and IGBT drivers at nearly 20% and 15%, respectively [39]. Thus, both IGBT and dc-link capacitors should be accurately monitored during WTs operation. The semiconductor devices of the converter suffer from thermal stresses due to the switching and the temperature swings related to the variable power generation.

Lifespan of dc-link capacitor is mainly affected by thermal, electrical and mechanical stresses drying the electrolytic capacitor, considered as a common failure because of the electrolyte solution evaporation [40]. A typical method used to monitor capacitors is based on the measurement of the equivalent series resistance, which is an index of their residual lifetime [41]. An alternative method is based on the measurement of the voltage ripple across the capacitor, which is related to current ripple [42],[43],[44]. Nonetheless, the effect of load variations on voltage ripple variations is not considered in this method. Furthermore, acoustic emissions are also utilized to distinguish the discharge of capacitor due to the aging process [45].

Measuring both temperature and frequency play a pivotal role in improving the accuracy of the CM system when WT has a variable load. Temperature and frequency can be measured for stator's winding and they are strictly related wind speed fluctuations [46]. The relation between the stator's winding temperature is shown in equations (1) and (2), where R_s is the stator resistance and T_s is stator temperature, $V_{ak,on}$ is the forward voltage of IGBTs and diodes, Rs0 is the stator resistance at the reference temperature, Ts0 is the reference temperature (normally 75°C) and α is the resistivity temperature coefficient [47]:

$$R_s = \frac{\left[\left(E_{c,dc} - 2V_{ce,on}\right)D + \left(-V_{ce,on} - V_{ak,on}\right)(1-D)\right]}{2I_{as,dc}} \quad (1)$$

$$T_s = T_{so} + \frac{R_s - R_{so}}{\alpha \times R_{so}} \quad (2)$$

The reliability of semiconductor devices is improved using IGBT modules instead of discrete devices, because multiple devices are casted from the same die. Nevertheless, various types of failure mechanisms occur in semiconductor modules, such as bond wire fatigue [48], bond wire lift-off [49], bond wire heel cracking [50], aluminium metallization [51] and solder fatigue [52]. Almost all of them are originated from thermal swings during converter operations and the mismatch of thermal expansion between the different materials of the modules [53]. In fact, thermal stresses are originated from both power and thermal cycling of power switching components. Power cycling losses is generated by load variation, while thermal cycling losses is generated by thermal variation [54].

Different methods can be applied to detect these failures, such as electrical parameters evaluation [55], [56] and estimation of the thermal equivalent resistance of the IGBTs [57],[58]. Some of them are recognized as off-line methods and others as on-line methods. For instance, taking advantages of threshold voltage is ensured for

CM even in low switching frequency. Nonetheless, it is not distinguished as an on-line CM method [59], since tracing is difficult and inaccurate while the system operates in variable high frequency switching speed. In addition to this, measuring the gate-emitter voltage v_{GE} to detect bond wire-lift off is also considered as an off-line method, since it requires injection of external signals to the gate [60]. On the other hand, measuring some parameters such as the junction temperature T_j or thermal impedance or resistance thermal path, t_{on}, t_{off} and $V_{CE\text{-}on}$ should be applied for the on-line monitoring [61]. In order to provide valid online CM methods for WTs it is essential to verify the variation of the most appropriate electrical parameters.

Each CM system of IGBTs has its own practical limitations in terms of reliability, implementation costs, size and accuracy. The main challenge for the next generation of CM system is to reduce at minimum the number of sensors, with consequent reduction of implementation costs. However, the detection of faulty components is extremely difficult in this case and can lead to serious reduction of the accuracy of the fault detection [62]. In fact, the variation of some electrical parameters is correlated. For instance, the junction temperature swings can be also considered as a symptom of bond wire lift-off and solder fatigue. Therefore, multi-fault indicators should be organized and cross-related to obtain an accurate CM method [63], [64]. Thus, in order to effectively monitor the health status of IGBTs and anticipate their residual lifetime, further studies are still required. An artificial control system could be a good candidate to evaluate simultaneously different electrical and thermal parameters affecting the lifetime of IGBTs. Moreover, wind fluctuation imposes additional random thermal, mechanical and electrical stresses to the drive train and, hence, to IGBTs. Thus, wind speed fluctuation should be monitored and included in the CM system of WTs to improve the reliability of the electric drive train.

PROGRESS AND FUTURE WORK

The aim of this research is to investigate the effects of the wind speed and wind turbulence on the electrical components of a WT, with specific focus on the power electronic devices, the dc-link capacitor and the generator. The analysis will lead to the development of a new model that estimates the health degradation of these components. Eventually, a new CM system will be developed to correlate wind speed and turbulence with the variations of electrical parameters. Different electrical quantities of the electrical system (mainly voltage, current and frequency) are monitored by the CM system with the specific objective to correlate wind conditions with the operating frequencies of IGBTs for the generator-side converter and with the collector current for the grid-side converter.

The variable wind conditions cause variations of the electrical parameters and temperature swings and these variations should be analyzed by the new CM system. Due to the non-linear relations between the parameters and the ageing of components, a significant computational effort is expected and, hence, advanced monitoring algorithms based on artificial intelligence (AI) are necessary. Thanks to these algorithms, the detection of faults and the consequent decision-making can be reliably carried out even when multiple factors are playing together. Starting from an initial healthy condition, wind speed, electrical parameters and temperature swings are measured on-line and any variation is analyzed by an AI to provide real-time information of components' operations. In other words, each component faces different fault mechanisms and root causes. For instance, for generators, electrical faults can be originated from short circuits or electrical asymmetry or inductive imbalance. An early detection of faults based on the elaboration of information related to the fault's mechanism is beneficial to enhance significantly the accuracy of the CM system.

The AI monitoring system can be based on a fuzzy controller. This controller is particularly suitable when the mathematical model of the system is unknown or extremely complex to be managed by deterministic controllers like PIDs. In fact, a fuzzy controller is based on empirical rules and can be readily upgraded for more complex system by simply increasing the number of fuzzy rules. For example, to monitor the health status of an IGBT, fuzzy description can prepare the precise capability of analysis of the IGBT's health status via considering variation in electrical parameters (V_{CE}, V_{GE} and $I_{GE,}$) and T_j. Additionally, many other algorithms such as genetic algorithms (GA)[65][66], bee colonies(BC) [66] and neural networks(NN) [67] will be investigated.

The amount of variation of electrical parameters (T_j and V_{CEon}) plays a key role to understand the health status of switching devices. For instance, a 3% increment of V_{CEon} is the symptom of wear-out, whereas an increment between 5% and 10% can be considered an early fault, while a 20% increment can be considered as a critical failure. Similarly, a 5% of increase of T_j indicate the starting of wear-out started, a 10% increment an early fault and a 20% increment a critical failure [68]. These variations can be introduced as fuzzy rules to estimate the health status of the IGBTs.

The CM monitoring of power devices is complicated by the fact that some failure mechanisms are positively correlated with an electrical parameter, while another failure mechanism is negatively correlated to the same electrical parameter. For instance, bond wire-lift off produces an increase trend of V_{CEon}, while die degradation causes a decrease trend of the same parameter. Therefore it is essential to understand the correlation between all the parameter related to each fault mechanism to avoid error in the fault detection.

CONCLUSIONS

This paper has reviewed the main topologies of the electrical system of wind turbines, with a critical revision of condition monitoring systems proposed in the technical literature. Most of the methods for the condition monitoring of electrical components are based on the real-time evaluation of electrical parameters. However, the variation of the wind speed and wind turbulence may have a significant effect on the health of these components. The influences of wind fluctuation and its impact on condition monitoring have received only little attention so far in the technical literature. Therefore, this project will try to fill this gap and integrate the information on wind conditions into the condition monitoring system of the electrical components. This will be achieved through an artificial intelligent condition monitoring system, which can effectively take into account the concurrent presence of different root causes of failures. Artificial intelligent can provide a suitable way to find out not only relations between different causes of faults, but also to evaluate the health status of the components themselves. Due to the complexity of the phenomena involved, an artificial intelligent control algorithm will be developed to infer the data from the sensors with sufficient accuracy and reliability. As a final goal, a dedicated fuzzy controller will be applied to provide a definition of the health status for the electrical drive train components during the operation of wind turbines.

ACKNOWLEDGEMENTS

This research is conducted as a part of “AEOLUS4FUTURE - Efficient harvesting of the wind energy” (H2020-MSCA-ITN-2014: Grant agreement no. 643167), founded by the European Commission’s Framework Program “Horizon 2020”(the Marie Skłodowska-Curie Innovative Training Networks (ITN)). The last two authors acknowledge the support of COST TU1304 Action in their relevant research activity.

REFERENCES

[1] M. Papaelias, S. Kerkyras, S. Hajiabady, P. Tricoli, and S. Hillmansen, “Efficient diagnostic condition monitoring for industrial wind turbines,” in 3rd Renewable Power Generation Conference (RPG 2014), 2014, pp. 8.47–8.47.

[2] C. Baniotopoulos, Claudio Borri, Bert Blocken, Hamida Hassan, Milan Veljkovic, Tommaso Morbiato, Roben Paul Borg, Stefanie Huber and Evangelos Efthymiou “Advances In Wind Energy Technology,” Cost Action TU1304 Winercost International Training School Malta. [Online]. Available: http://www.winercost.com/index.php/activities/training-schools.

[3] E. Hau, Wind Turbines: Fundamentals, Technologies, Application, Economics. Springer Science & Business Media, 2005.

[4] S. M. A. Cruz and A. J. M. Cardoso, “Rotor cage fault diagnosis in three-phase induction motors by the total instantaneous power spectral analysis,” in Conference Record of the 1999 IEEE Industry Applications Conference. Thirty-Forth IAS Annual Meeting (Cat. No.99CH36370), 1999, vol. 3, pp. 1929–1934.

[5] C. Chompoo-Inwai, C. Yingvivatanapong, K. Methaprayoon, and W. J. Lee, “Reactive compensation techniques to improve the ride-through capability of wind turbine during disturbance,” IEEE Trans. Ind. Appl., vol. 41, no. 3, pp. 666–672, 2005.

[6] “Renewable Energy Integration: Challenges and Solutions (Green Energy and Technology): Jahangir Hossain, Apel Mahmud, Available: http://www.amazon.com/Renewable-Energy-Integration-Challenges-Technology/dp/9814585262. [Accessed: 26-Feb-2016].

[7] C. Yingvivatanapong and K. Methaprayoon, “Reactive compensation techniques to improve the ride-through of induction generators during disturbance,” in Conference Record of the 2004 IEEE Industry Applications Conference, 2004. 39th IAS Annual Meeting., 2004, vol. 3, pp. 2044–2050.

[8] T. Tafticht, K. Agbossou, and A. Cheriti, “DC bus control of variable speed wind turbine using a buck-boost converter,” in 2006 IEEE Power Engineering Society General Meeting, 2006, p. 5 pp.

[9] M. Zafarani, T. Goktas, and B. Akin, “A comprehensive analysis of magnet defect faults in permanent magnet synchronous motors,” in 2015 IEEE Applied Power Electronics Conference and Exposition (APEC), 2015, pp. 2779–2783.

[10] R Moeini, P.Tricoli, H.Hemida, C.Baniotopoulos, "Increasing the reliability of wind turbines using condition monitoring of semiconductor devices: a review" renewable power generation conference, 2016.
[11] Z. Hameed, S. H. Ahn, and Y. M. Cho, "Practical aspects of a condition monitoring system for a wind turbine with emphasis on its design, system architecture, testing and installation," Renew. Energy, vol. 35, no. 5, pp. 879–894, May 2010.
[12] T. Wakui and R. Yokoyama, "Wind speed sensorless performance monitoring based on operating behavior for stand-alone vertical axis wind turbine," Renew. Energy, vol. 53, pp. 49–59, May 2013.
[13] N. Tandon and B. C. Nakra, "Comparison of vibration and acoustic measurement techniques for the condition monitoring of rolling element bearings," Tribol. Int., vol. 25, no. 3, pp. 205–212, Jun. 1992.
[14] W. Bartelmus and R. Zimroz, "Vibration condition monitoring of planetary gearbox under varying external load," Mech. Syst. Signal Process., vol. 23, no. 1, pp. 246–257, Jan. 2009.
[15] Li Lin, Wenxiu Lu, and Fulei Chu, "Application of AE techniques for the detection of wind turbine using Hilbert-Huang transform," in 2010 Prognostics and System Health Management Conference, 2010, pp. 1–7.
[16] J. Knezevic, Reliability, maintainability, and supportability: a probabilistic approach. McGraw-Hill, 1993.
[17] Z. Hameed, Y. S. Hong, Y. M. Cho, S. H. Ahn, and C. K. Song, "Condition monitoring and fault detection of wind turbines and related algorithms: A review," Renew. Sustain. Energy Rev., vol. 13, no. 1, pp. 1–39, Jan. 2009.
[18] and A. W. K. Wiesent, B. R., M. Schardt, "Gear oil condition monitoring for offshore wind turbines," 2012. [Online]. Available: www. Machinerylubrication. com/Read/28782/gear-oilcondition-monitoring ,.
[19] K. Papadopoulos, E. Morfiadakis, T. P. Philippidis, and D. J. Lekou, "Assessment of the strain gauge technique for measurement of wind turbine blade loads," Wind Energy, vol. 3, no. 1, pp. 35–65, Jan. 2000.
[20] and J. G. Caselitz, P., "Fault prediction techniques for offshore wind farm maintenance and repair strategies," 2003.
[21] B. M. Smith, "Condition monitoring by thermography," NDT Int. 11, no. 3, pp. 121–122.
[22] L. Zhen, H. Zhengjia, Z. Yanyang, and C. Xuefeng, "Bearing condition monitoring based on shock pulse method and improved redundant lifting scheme," Math. Comput. Simul., vol. 79, no. 3, pp. 318–338, Dec. 2008.
[23] J. Cheng, Y. Yang, and D. Yu, "The envelope order spectrum based on generalized demodulation time–frequency analysis and its application to gear fault diagnosis," Mech. Syst. Signal Process., vol. 24, no. 2, pp. 508–521, Feb. 2010.
[24] Y. Amirat, M. E. H. Benbouzid, B. Bensaker, and R. Wamkeue, "Condition Monitoring and ault Diagnosis in Wind Energy Conversion Systems: A Review," in 2007 IEEE International Electric Machines & Drives Conference, 2007, vol. 2, pp. 1434–1439.
[25] W. J. Staszewski and G. R. Tomlinson, "Application of the wavelet transform to fault detection in a spur gear," Mech. Syst. Signal Process., vol. 8, no. 3, pp. 289–307, May 1994.
[26] D. Scott, P. J. McCullagh, and G. W. Campbell, "Condition monitoring of gas turbines — An exploratory investigation of Ferrographic trend analysis," Wear, vol. 49, no. 2, pp. 373–389, Aug. 1978.
[27] E. Lelarasmee, A. E. Ruehli, and A. L. Sangiovanni-Vincentelli, "The Waveform Relaxation Method for Time-Domain Analysis of Large Scale Integrated Circuits," IEEE Trans. Comput. Des. Integr. Circuits Syst., vol. 1, no. 3, pp. 131–145, Jul. 1982.
[28] T. Adu, "An accurate fault classification technique for power system monitoring devices," IEEE Trans. Power Deliv., vol. 17, no. 3, pp. 684–690, Jul. 2002.
[29] Z. K. Peng and F. L. Chu, "Application of the wavelet transform in machine condition monitoring and fault diagnostics: a review with bibliography," Mech. Syst. Signal Process., vol. 18, no. 2, pp. 199–221, Mar. 2004.
[30] Q. He, F. Kong, and R. Yan, "Subspace-based gearbox condition monitoring by kernel principal component analysis," Mech. Syst. Signal Process., vol. 21, no. 4, pp. 1755–1772, May 2007.
[31] L. Wang, M. G. Mehrabi, and E. Kannatey-Asibu, "Hidden Markov Model-based Tool Wear Monitoring in Turning," J. Manuf. Sci. Eng., vol. 124, no. 3, p. 651, Aug. 2002.
[32] E. Jantunen, "A summary of methods applied to tool condition monitoring in drilling," Int. J. Mach. Tools Manuf., vol. 42, no. 9, pp. 997–1010, Jul. 2002.
[33] S. Nandi, H. A. Toliyat, and X. Li, "Condition Monitoring and Fault Diagnosis of Electrical Motors—A Review," IEEE Trans. Energy Convers., vol. 20, no. 4, pp. 719–729, Dec. 2005.
[34] B. Lu, Y. Li, X. Wu, and Z. Yang, "A review of recent advances in wind turbine condition monitoring and fault diagnosis," in 2009 IEEE Power Electronics and Machines in Wind Applications, 2009, pp. 1–7.
[35] Z. Liu, X. Yin, Z. Zhang, D. Chen, and W. Chen, "Online Rotor Mixed Fault Diagnosis Way Based on Spectrum Analysis of Instantaneous Power in Squirrel Cage Induction Motors," IEEE Trans. Energy Convers., vol. 19, no. 3, pp. 485–490, Sep. 2004.
[36] J. Yang, S. Bin Lee, J. Yoo, S. Lee, Y. Oh, and C. Choi, "A Stator Winding Insulation Condition Monitoring Technique for Inverter-fed Machines," in 37th IEEE Power Electronics Specialists Conference, pp. 1–

7.
[37] A. D. Hansen and G. Michalke, "Modelling and control of variable-speed multi-pole permanent magnet synchronous generator wind turbine," Wind Energy, vol. 11, no. 5, pp. 537–554, Sep. 2008.
[38] Y. Han and Y. H. Song, "Condition monitoring techniques for electrical equipment-a literature survey," IEEE Trans. Power Deliv., vol. 18, no. 1, pp. 4–13, Jan. 2003.
[39] A. Wechsler, B. C. Mecrow, D. J. Atkinson, J. W. Bennett, and M. Benarous, "Condition Monitoring of DC-Link Capacitors in Aerospace Drives," IEEE Trans. Ind. Appl., vol. 48, no. 6, pp. 1866–1874, Nov. 2012.
[40] V. A. Sankaran, F. L. Rees, and C. S. Avant, "Electrolytic capacitor life testing and prediction," in IAS '97. Conference Record of the 1997 IEEE Industry Applications Conference Thirty-Second IAS Annual Meeting, vol. 2, pp. 1058–1065.
[41] M. Kim, K. Lee, J. Yoon, S. Bin Lee, and J. Yoo, "Condition Monitoring of DC Link Electrolytic Capacitors in Adjustable Speed Drives," in 2007 IEEE Industry Applications Annual Meeting, 2007, pp. 237–243.
[42] A. Lahyani, P. Venet, G. Grellet, and P.-J. Viverge, "Failure prediction of electrolytic capacitors during operation of a switchmode power supply," IEEE Trans. Power Electron., vol. 13, no. 6, pp. 1199–1207, 1998.
[43] H. M. Pang and P. M. H. Bryan, "A life prediction scheme for electrolytic capacitors in power converters without current sensor," in 2010 Twenty-Fifth Annual IEEE Applied Power Electronics Conference and Exposition (APEC), 2010, pp. 973–979.
[44] J. Smulko, K. Józwiak, M. Olesz, and L. Hasse, "Acoustic emission for detecting deterioration of capacitors under aging," Microelectron. Reliab., vol. 51, no. 3, pp. 621–627, Mar. 2011.
[45] J. W. Choi, S. Il Yong, and S. K. Sul, "Inverter output voltage synthesis using novel dead time compensation," in Proceedings of 1994 IEEE Applied Power Electronics Conference and Exposition - ASPEC'94, pp. 100–106.
[46] S.-B. Lee and T. G. Habetler, "An on-line stator winding resistance estimation technique for temperature monitoring of line-connected induction machines," in Conference Record of the 2001 IEEE Industry Applications Conference. 36th IAS Annual Meeting (Cat. No.01CH37248), vol. 3, pp. 1564–1571.
[47] Y. Xiong, X. Cheng, Z. Shen, C. Mi, H. Wu, and V. Garg, "A Prognostic and Warning System for Power Electronic Modules in Electric, Hybrid, and Fuel Cell Vehicles," in Conference Record of the 2006 IEEE Industry Applications Conference Forty-First IAS Annual Meeting, 2006, vol. 3, pp. 1578–1584.
[48] Q. Miao and V. Makis, "Condition monitoring and classification of rotating machinery using wavelets and hidden Markov models," Mech. Syst. Signal Process., vol. 21, no. 2, pp. 840–855, Feb. 2007.
[49] R. C. M. Yam, P. W. Tse, L. Li, and P. Tu, "Intelligent Predictive Decision Support System for Condition-Based Maintenance," Int. J. Adv. Manuf. Technol., vol. 17, no. 5, pp. 383–391, Feb. 2001.
[50] O. Schilling, M. Schäfer, K. Mainka, M. Thoben, and F. Sauerland, "Power cycling testing and FE modelling focussed on Al wire bond fatigue in high power IGBT modules," Microelectron. Reliab., vol. 52, no. 9–10, pp. 2347–2352, Sep. 2012.
[51] J. Lehmann, M. Netzel, R. Herzer, and S. Pawel, "Method for electrical detection of bond wire lift-off for power semiconductors," in ISPSD '03. 2003 IEEE 15th International Symposium on Power Semiconductor Devices and ICs, 2003. Proceedings., pp. 333–336.
[52] S. Ramminger, N. Seliger, and G. Wachutka, "Reliability model for Al wire bonds subjected to heel crack failures," Microelectron. Reliab., vol. 40, no. 8–10, pp. 1521–1525, Aug. 2000.
[53] J. R. Black, "Electromigration failure modes in aluminum metallization for semiconductor devices," Proc. IEEE, vol. 57, no. 9, pp. 1587–1594, Sep. 1969.
[54] J. H. L. Pang, B. S. Xiong, and T. H. Low, "Creep and fatigue characterization of lead free 95.5Sn-3.8Ag-0.7Cu solder," in 2004 Proceedings. 54th Electronic Components and Technology Conference (IEEE Cat. No.04CH37546), vol. 2, pp. 1333–1337.
[55] V. Smet, F. Forest, J.-J. Huselstein, F. Richardeau, Z. Khatir, S. Lefebvre, and M. Berkani, "Ageing and Failure Modes of IGBT Modules in High-Temperature Power Cycling," IEEE Trans. Ind. Electron., vol. 58, no. 10, pp. 4931–4941, Oct. 2011.
[56] B. Ji, V. Pickert, W. P. Cao, and L. Xing, "Onboard condition monitoring of solder fatigue in IGBT power modules," in 2013 9th IEEE International Symposium on Diagnostics for Electric Machines, Power Electronics and Drives (SDEMPED), 2013, pp. 9–15.
[57] K. Wang, Y. Liao, G. Song, and X. Ma, "Over-Temperature protection for IGBT modules," pp. 1–7.
[58] N. Patil, J. Celaya, D. Das, K. Goebel, and M. Pecht, "Precursor Parameter Identification for Insulated Gate Bipolar Transistor (IGBT) Prognostics," IEEE Trans. Reliab., vol. 58, no. 2, pp. 271–276, Jun. 2009.
[59] H. Shaukatullah and A. Claassen, "Effect of thermocouple wire size and attachment method on measurement of thermal characteristics of electronic packages," in Ninteenth Annual IEEE Semiconductor Thermal Measurement and Management Symposium, 2003., pp. 97–105.
[60] "Power Electronics: Circuits, Devices & Applications: Amazon.de: Muhammad H. Rashid:

Fremdsprachige Bücher." [Online]. Available: http://www.amazon.de/Power-Electronics-Circuits-Devices-Applications/dp/0133125904. [Accessed: 26-Feb-2016].
[61] I. Bahun, N. Čobanov, and Ž. Jakopović, "Real-Time Measurement of IGBT's Operating Temperature," Automatika – Journal for Control, Measurement, Electronics, Computing and Communications, vol. 52, no. 4. 02-Sep-2012.
[62] E. A. Bossanyi, "The Design of closed loop controllers for wind turbines," Wind Energy, vol. 3, no. 3, pp. 149–163, Jul. 2000.
[63] M. S. Selig and V. L. Coverstone-Carroll, "Application of a genetic algorithm to wind turbine design," Sep. 1995.
[64] M. Held, P. Jacob, G. Nicoletti, P. Scacco, and M.-H. Poech, "Fast power cycling test of IGBT modules in traction application," in Proceedings of Second International Conference on Power Electronics and Drive Systems, vol. 1, pp. 425–430.
[65] M. S. Selig and V. L. Coverstone-Carroll, "Application of a Genetic Algorithm to Wind Turbine Design," J. Energy Resour. Technol., vol. 118, no. 1, p. 22, Mar. 1996.
[66] H. T. Jadhav and R. Roy, "Gbest guided artificial bee colony algorithm for environmental/economic dispatch considering wind power," Expert Syst. Appl., vol. 40, no. 16, pp. 6385–6399, Nov. 2013.
[67] V. Galdi, A. Piccolo, and P. Siano, "Designing an Adaptive Fuzzy Controller for Maximum Wind Energy Extraction," IEEE Trans. Energy Convers., vol. 23, no. 2, pp. 559–569, Jun. 2008.
[68] V. Smet, F. Forest, J.-J. Huselstein, A. Rashed, and F. Richardeau, "Evaluation of V_{CE} Monitoring as a Real-Time Method to Estimate Aging of Bond Wire-IGBT Modules Stressed by Power Cycling," IEEE Trans. Ind. Electron., vol. 60, no. 7, pp. 2760–2770, Jul. 2013.

THE INTERNATIONAL CONFERENCE ON
WIND ENERGY HARVESTING 2017
20-21 April 2017
Coimbra, Portugal

Paper A4F.08

EXPERIMENTS FOR THE DEVELOPMENT OF AN INVERSE WIND LOAD RECONSTRUCTION PROCEDURE FOR WIND ENERGY CONVERTERS

Mirjana Ratkovac[1]
Ruhr-Universität Bochum,
Wind Engineering and Flow Mechanics
Bochum, Germany

Rüdiger Höffer[2]
Ruhr-Universität Bochum,
Wind Engineering and Flow Mechanics
Bochum, Germany

ABSTRACT

Wind power is a cost effective, clean and reliable source of renewable energy. In order to meet the world's growing energy needs, wind turbine technology is continuously upgraded. One of the areas that require improvements is the achieving of more precise information on wind load time histories acting on the structures in order to reduce design uncertainties and consequently optimize the general implementation costs. Since the wind load cannot be measured directly, one of the possible approaches is to reconstruct the load inversely from structural response data based on structural health monitoring measurements. This paper deals with reviewing the state-of-the-art on the inverse wind load identification with the goal of developing a suitable method which is applicable to wind energy converters. For this purpose experiments in the atmospheric boundary layer wind tunnel at Bochum are being carried out, with the goal to apply and validate the developed method. The experiments also assist the investigation of the wind loads acting on a full-scale wind turbine placed in Dortmund, Germany.

NOMENCLATURE

m	=	mass (kg)
c	=	damping
k	=	stiffness (KN/m)
t, τ	=	time (s)
$h(t)$	=	impulse response function IRF
$u, \dot{u}, \ddot{u}$	=	structural response quantities
p	=	external force

INTRODUCTION

Direct measurement of the wind load acting on the civil engineering structures or on their components is often not possible during the life-time of the structure. However, the wind-induced structural response for structural health monitoring is nowadays regularly being measured. In order to get better knowledge on wind load acting on the structure, these known structural response measurements can be used. This becomes then the inverse engineering problem, known for the ill-posedness of the solution, meaning that the solution is either overdetermined, unstable or not unique. Many authors have dealt with this thematic in last decades using different approaches [1,2,3,4]. However, not much research has been done in the field of wind turbines, where extensive research would be preferable [5]. Knowledge on static and dynamic characteristics of the wind turbine structure, as well as on the acting load is crucial when it comes to fatigue assessment, damage diagnosis and life-time forecast, for the whole structure or its components. The better knowledge on the wind load can contribute to

[1] Doctoral researcher, Wind Engineering and Flow Mechanics, Ruhr-Universität Bochum, Universitätsstraße 150, 44801 Bochum, Germany / mirjana.ratkovac@rub.de
[2] Professor, Wind Engineering and Flow Mechanics, Ruhr-Universität Bochum, Universitätsstraße 150, 44801 Bochum, Germany / ruediger.hoeffer@rub.de

lowering the uncertainties in structural design and consequently reduce the costs of the structure. In this paper the overview of methodologies used in the past for solving the inverse problem for wind load identification for different types of structures will be presented. For the purpose of further developing a method suitable for full-scale application, atmospheric boundary layer wind tunnel test at Ruhr University in Bochum will be done. The measurements of the load and the structural response will be conducted. These measurements will later be used for the purpose of validating and applying the procedure for wind load identification.

METHODOLOGIES - STATE-OF-THE-ART REPORT

In 1923 Hadamard [6] proved that load identification inverse process is ill-posed which has caused low interest in this area of research in later years. In 1987 Stevens [7] did an overview of the methods for force reconstruction, which were used by then. Later in 2014 there is overview of methods for inverse problems in engineering done by Sanchez and Benaroya [8]. The most general approach to deal with ill-posed problems is to transform them into a well-posed one, using a regularization method [9,10]. In this area the method which has been most widely used by many authors to solve different types of inverse problems was proposed by Tikhonov in 1977.

In general, methods for inverse load identification can be divided in three categories:
- deterministic methods in frequency or time domain
- stochastic methods
- methods applying artificial intelligence or neural networks

Time domain methods use impulse response functions for different response types, such as displacement, velocity acceleration, or strain and convolution integral (2) to solve the differential equation of motion (1).

$$m\ddot{u} + c\dot{u} + ku = p(t) \tag{1}$$

$$u(t) = \int_0^T h(t-\tau)p(\tau)dt \tag{2}$$

Frequency domain methods use similar approach with frequency response functions that define dynamic characteristics of the structure. Table 1 shows the overview of methods used in the area of wind load identification, which will be discussed in this paper. There is not much research done in the field of wind turbine structures. However, there is a study done by Phan and Rolfes [5] using the Code FAST in order to estimate wind control and aerodynamics influence on wind load estimation. It is desirable to do wind tunnel test and a full scale experiment in order to get more precise results in this field for purposes of application on wind energy converters.

Table 1. Selection of recent research achievements in the area of inverse wind load identification

	Technique	Model	Investigation	Response type	Conclusions
Law et al. [2005]	Tikhonov regularization, L curve method, iteration scheme	50m guyed mast numerical simulation	Limited response, noise	Displacement, strain	Iteration scheme improves results, low noise influence
Hwang, Kareem, Kim [2009]	Kalman filter, Riccati equation	210 rectangular chimney wind tunnel test, numerical simulation	Type of response, noise, dynamic modeling uncertainties	Displacement, velocity, acceleration	Acceleration, frequency affects results more than the damping
Fritzen, Klinkov [2011]	Unknown input observer	Scaled tower laboratory test, numerical simulation	Number of modes influence, noise, collocation problem	Acceleration, strain	Acceleration, frequency influences results more than damping, collocation possible
Pahn, Rolfes, NREL [2012]	Frequency response matrix	Onshore wind turbine Code FAST	Thrust force, aerodynamics, wind turbine control	Acceleration	Low control activity influence, amplified dynamic response
Kazemi [2016]	Tikhonov regularization, L-curve/GCV method	9.1m guyed mast, cantilever beam laboratory test, numerical simulation	AIRM, L-curve/GCV, response type, noise	Displacement, acceleration	Displacement, augmented response matrix advantage, L-curve method

EXPERIMENTS

For the purpose of developing and validation of the method for wind load identification, experiments on the model in the wind tunnel are being carried out. Atmospheric boundary layer wind tunnel of the Ruhr-Universität Bochum has a cross section of 1.6 m x 1.8 m and a test section of 1.6 m length; the boundary layer is generated through a Counihan system and a roughness field of 8 m length. Figure 1 shows the layout of the wind tunnel. In frames of the experiment, the structural response, displacements and strains are being measured at different levels along the height of the model, as well as the moments and forces at the base of the model, in order to get the load time histories at multiple points and comparable results. At the same time the measurement of the surface pressures on the model, caused by wind load, is being conducted. By comparing the results on the wind load time history gained by using the proposed methodology and the surface pressure measurements in the wind tunnel, the validation and accuracy of the proposed method can be determined. Figure 2 shows the schematic view of the pressure sensor and of the force moment balance. Full-scale experiments will be done using the structural health monitoring data gathered since 2010 on a wind turbine in Dortmund, combined with operation modal analysis in order to determine the loads acting on the structure, e.g. rotor thrust.

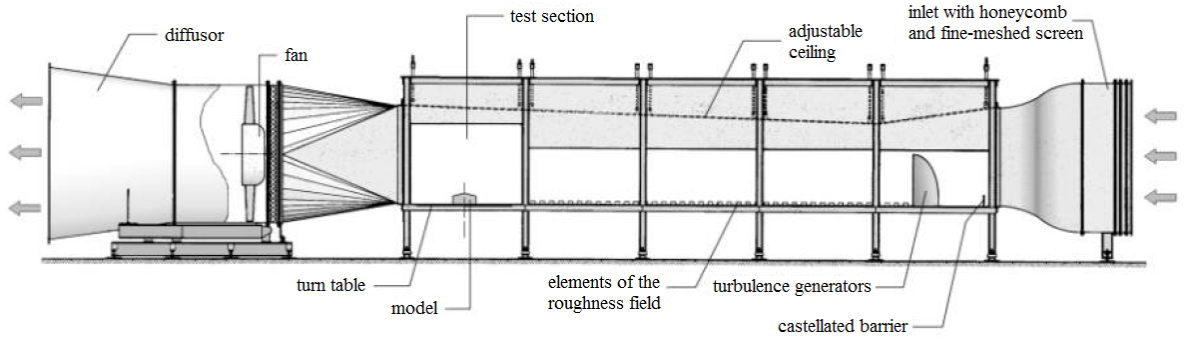

Figure 2. Open section atmospheric boundary layer wind tunnel of the Ruhr-University in Bochum, Germany

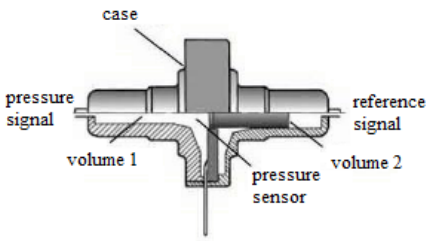

Figure 2. Schematic representation of a pressure sensor (left), and a high-frequency balance for the measurement of the base bending moment as well as of integral shear forces (right)

Figure 3. Wind turbine at Dortmund (equipped with 6 deformation sensors)

FUTURE WORK WITH WIND TUNNEL TEST DATA

Results from wind tunnel tests will be used to validate the method for wind load reconstruction, which will be applied on a full-scale wind turbine structure. A better understanding of the wind load can help to improving the wind load approximation and the design of the structures in general. When it comes to wind energy converters, as they are relatively young constructions with a need of extended data bases for the life-time estimation, more precise information on exact wind load time history acting on the structure would be of great importance for life-time

estimation, as well as for fatigue assessment. Wind load identification methods can also find suitable application for determination of the load acting on the structural parts of interest, equipment of sensitive points on the structure.

ACKNOWLEDGEMENTS

The authors acknowledge with thanks the support of the European Commission's Framework Program "Horizon 2020", through the Marie Skłodowska-Curie Innovative Training Networks (ITN) "AEOLUS4FUTURE - Efficient harvesting of the wind energy" (H2020-MSCA-ITN-2014: Grant agreement no. 643167) and the support of the DEW21 belonging to City of Dortmund/Germany granted to the present research project.

REFERENCES

[1] S.S. Law, J.Q. Bu, X. Q. Zhu, Time-varying wind load identification from structural responses, Engineering structures 27, 2005, 1586-1598
[2] J. Hwang, A. Kareem, H. Kim, Wind load identification using wind tunnel test data by inverse analysis, Journal of Wind Engineering and Industrial Aerodynamics, (326), 2011, 18-26
[3] C.P. Fritzen, M. Klinkov, Load Identification for Structural Health Prognosis, Structural Health Monitoring of Military Vehicles Lecture Series, North Atlantic Treaty Organization, 02.10.2014
[4] Kazemi-Amiri, Inverse reconstruction of wind load and stochastic response analysis from sparse long term response measurements, Doctoral Thesis, Vienna Doctoral Programme on Water Resource Systems, 2016
[5] Pahn, T., Rolfes R., Jonkman J., and Robertson, A., Inverse Load Calculation of Wind Turbine Support Structures – A Numerical Verification Using the Comprehensive Simulation Code FAST, Presented at the 53rd Structures, Structural Dynamics, and Materials Conference Honolulu, Hawaii, April 23 – 26, 2012
[6] Hadamard, J.: Lectures on Coughy's Problem in Linear Partial Differential Equations. Yale University Press, New Haven, 1923
[7] K. Stevens: Force identification problems - an overview, Proc. of SEM, Spring Meeting, Houston, 1987, pp. 838-844
[8] J. Sanchez, H. Benaroya, Review of force reconstruction techniques, Journal of Sound and Vibration, (333), 2014, 2999–3018
[9] Tikhonov, A.N., Arsenin, V.Y.: Solution of Ill-Possed Problems. Winston and Sons, Washington, DC, 1977
[10] Philips, D.L.: A technique for the numerical solution of certain equations of the first kind. J. ACM 9 84–97, 1962

THE INTERNATIONAL CONFERENCE ON
WIND ENERGY HARVESTING 2017
20-21 April 2017
Coimbra, Portugal

Paper A4F.09

WIND TURBINE AEROFOILS: A MESH DEPENDENCY STUDY

Giulio VITA[1]
University of Birmingham
Birmingham, United Kingdom

Yakut Cansev KUCUKOSMAN[2]
Von Kármán Inst. for Fluid Dyn.,
Brussels, Belgium

Hassan HEMIDA[3]
University of Birmingham
Birmingham, United Kingdom

Christophe SCHRAM[4]
Von Kármán Inst. for Fluid Dyn.,
Brussels, Belgium

Jeroen VAN BEECK[5]
Von Kármán Inst. for Fluid Dyn.,
Brussels, Belgium

Charalampos BANIOTOPOULOS[6]
University of Birmingham
Birmingham, United Kingdom

ABSTRACT

A large eddy simulation (LES) study of the flow pattern around a typical wind turbine aerofoil sections is performed. The DU-96-180 is investigated in attached and nearly-stalled conditions (4-20 deg of angle of attack) with two ranges for the Reynolds number ($\mathcal{R}e=1.50\times10^5\div1.13x10^6$). The resulting flow pattern is then compared and validated with available results from the literature.

This configuration has been chosen, because it is a challenging setup to be modelled with accuracy using Reynolds Averaged Navier–Stokes (RANS) technique. Also mesh requirements and transitional behavior constitute a complexity for Large Eddy Simulation (LES), which usually requires large grids and small time-steps. The behaviour of an aerofoil near stall is characterized by the formation of a laminar separation bubble (LSB), which triggers transition or separation due to the adverse pressure gradient which is present because of the enhanced angle of attack α.

In this study the alternative wall-modelled LES (WM-LES) approach is implemented as an alternative to the traditional wall-resolved LES (WR-LES): the two approaches will be using the Smagorinsky technique with vanDriest damping at the wall.

The purpose is to optimize the grid requirements towards a more cost-effective simulation, without losing accuracy.

1 Early Stage Researcher & Ph.D. Candidate, School of Civil Engineering, University of Birmingham, Edgbaston, Birmingham, B15 2TT, United Kingdom / g.vita@bham.ac.uk

2 Early Stage Researcher & Ph.D. Candidate, Environmental and Applied Fluid Dynamics Department, von Kármán Institute for Fluid Dynamics, Brussels, Belgium / yakut.cansev.kucukosman@vki.ac.be

3 Senior Lecturer & Deputy Head of Research, School of Civil Engineering, University of Birmingham, Edgbaston, Birmingham B15 2TT, United Kingdom / h.hemida@bham.ac.uk

4 Associate Professor, Environmental and Applied Fluid Dynamics Department, von Kármán Institute for Fluid Dynamics, Brussels, Belgium / christophe.schram@vki.ac.be

5 Professor, Environmental and Applied Fluid Dynamics Department, von Kármán Institute for Fluid Dynamics, Brussels, Belgium / jeroen.vanbeeck@vki.ac.be

6 Full professor & Chair of Sustainable Energy Systems and Director of Resilience Centre, School of Civil Engineering, University of Birmingham, Edgbaston, Birmingham B15 2TT, United Kingdom / c.baniotopoulos@bham.ac.uk

NOMENCLATURE

c	=	Chord length (m)
LES	=	Large Eddy Simulation
LSB	=	Laminar Separation Bubble
RANS	=	Reynolds-Averaged Navier-Stokes
$\mathcal{R}e$	=	Reynolds number (-)
SGS	=	Sub-Grid Scale
URANS	=	Unsteady RANS
WM-LES	=	Wall-Modelled LES
WR-LES	=	Wall-Resolved LES
α	=	Angle of attack (deg)

INTRODUCTION

Large Eddy Simulation (LES) is accounted as a fast-growing tool to be used also for industrial applications especially when enhanced accuracy for the fluctuating statistics of flows are needed [1]. Among other industrial and aeronautical applications, this also applies to wind turbine aerodynamics [2]. LES was shown to predict accurate statistics for the calculation of the radiated noise from aerofoils [3]. LES is also accurate, when specific fluctuating inlets are investigated [4], in particular regarding the prediction of the decay of turbulence in wakes [5]. Therefore, a large number of application with complex geometries have also been fulfilled successfully [6], [7]. However, using LES for actual industrial flows, still remains an expensive task [8]. This has a twofold reason: (i) the mesh requirements because of the complexity of boundary layers; (ii) the time-stepping requirements, as high-order schemes are often unstable and need for a short time step to be considered.

The research community has been working on the optimization of LES requirements [9]. The main areas of concern are recognized in: (i) the use of wall-functions [10]; (ii) the use of a dynamic mesh local refinement or further computational techniques [11]. The problem is then twofold: on one hand the accuracy of LES is dependent on strict computational setups, which the research is trying to loosen up by proposing improved Sub-Grid Scale models; on the other new computational setups are investigated to overcome the limitations within the dependency of SGS models to grid and time-stepping, however this has a major impact on the accuracy of the simulation.

Nevertheless, LES remains the best technique to reproduce fluctuating statistics [9].

This work is aimed to test the effectiveness of LES to simulate the fluctuating and peak characteristics of the flow pattern around a wind turbine aerofoil, in order to be used on the response under turbulent structures. This work is the outcome of a collaboration between the Department of Civil Engineering of the University of Birmingham (United Kingdom) and the Department of Environmental and Applied Fluid Dynamics of the Von Kármán Institute of Fluid Dynamics (Belgium), under the European Commission Framework Horizon2020, funded by the Marie Skłodowska-Curie Innovative Training Networks (ITN) “AEOLUS4FUTURE - Efficient harvesting of the wind energy” (H2020-MSCA-ITN-2014: Grant agreement no. 643167).

METHODOLOGY

In this study, the ability of LES to produce accurate fluctuating flow statistics will be investigated for a model wind turbine aerofoil in a uniform smooth flow. Both the URANS and the LES technique will be implemented for comparison. The comparison will be based on the fluctuating statistics of the flow pattern, as introduced. The aerofoil to be tested is the DU96w180 of the University of Delft, designed specifically for wind turbine aerofoil. It has a thickness of 18% and a smooth stall behavior [Ref.]. The aerofoil is modelled in two configurations, namely the pre-stalled configuration and the stalled one. The Reynolds number range which is chosen is based on the uniform inflow velocity u and the chord length c and is $\mathcal{R}e=1.5\times10^5\div10^6$.

The computational domain is 2D for both computational techniques, whereas in LES the span-wise dimension is indeed discretized by 5-10-20 cells in order to understand the effect of a quasi 2D computational domain in the accuracy of results. Moreover, a brief evaluation of the discretization schemes is proposed in order

to understand the possibility of having an even more cost-effective computational strategy using hybrid or bounded schemes. The computational Domain is sketched in Fig. 1.

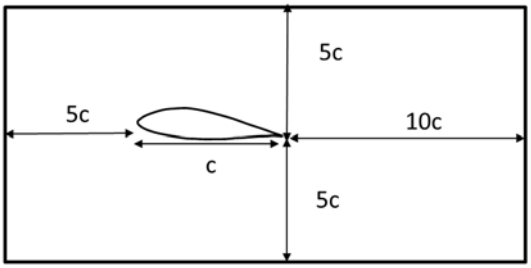

Figure 1. The main domain configuration (Case #1)

A series of LES SGS models is tested, comparing them with RANS technique. Table 1 summarises the computational models to be setup.

Table 1. List of computations

Computational models			
	CFD technique	2D models – DU96w180	
		Pre-stall 4deg	Stall 20deg
1	RANS k-ω SST	×	×
2	URANS k-ω SST	×	×
3	WRLES Smagorinsky y+=1	×	×
4	WMLES Smagorinsky y+=5	×	×

As the aim is to setup a CFD framework to yield accurate fluctuating statistics, different mesh, from hybrid to structured grid, will be implemented and tested with respect of their refinement. This is of extreme importance for the assessment of the separation point and its intermittent behavior as well as the existence of a separation bubble. Fig. 2 shows the structured mesh, with the adjustments undertaken to limit the Courant number in the regions of accelerated flow on the suction and pressure side of the aerofoil.

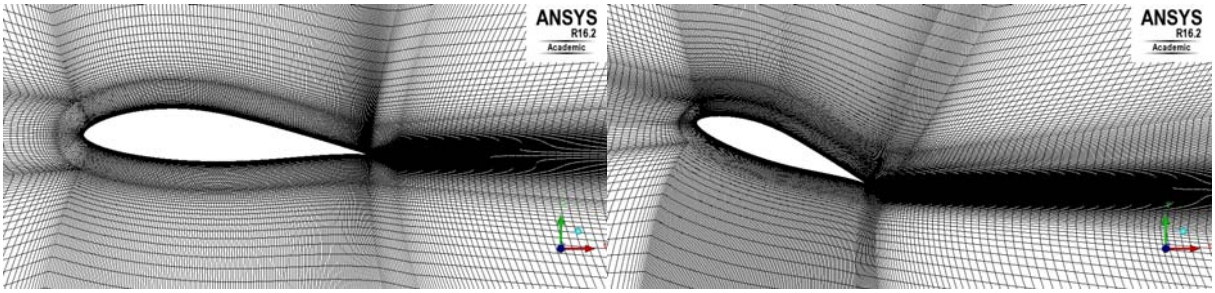

Figure 2. Structured hexa block C-Grid for the pre-stalled (a) and stalled (b) configurations.

ACKNOWLEDGEMENTS

The authors gratefully acknowledge the support of the European Commission's Framework Program "Horizon 2020", through the Marie Skłodowska-Curie Innovative Training Networks (ITN) "AEOLUS4FUTURE - Efficient harvesting of the wind energy" (H2020-MSCA-ITN-2014: Grant agreement no. 643167).

REFERENCES

[1] T. Tamura, "Towards practical use of LES in wind engineering," *J. Wind Eng. Ind. Aerodyn.*, vol. 96, no. 10, pp. 1451–1471, 2008.

[2] D. Mehta, A. H. van Zuijlen, B. Koren, J. G. Holierhoek, and H. Bijl, "Large Eddy Simulation of wind farm aerodynamics: A review," *J. Wind Eng. Ind. Aerodyn.*, vol. 133, pp. 1–17, 2014.

[3] E. Manoha, B. Troff, and P. Sagaut, "Trailing-Edge Noise Prediction Using Large-Eddy Simulation and Acoustic Analogy," *AIAA J.*, vol. 38, no. 4, pp. 575–583, Apr. 2000.

[4] G. R. Tabor and M. H. Baba-Ahmadi, "Inlet conditions for large eddy simulation: A review," *Comput. Fluids*, vol. 39, no. 4, pp. 553–567, Apr. 2010.

[5] Y.-T. Wu and F. Porté-Agel, "Atmospheric Turbulence Effects on Wind-Turbine Wakes: An LES Study," *Energies*, vol. 5, no. 12, pp. 5340–5362, Dec. 2012.

[6] H. Hemida and C. Baker, "Large-eddy simulation of the flow around a freight wagon subjected to a crosswind," *Comput. Fluids*, vol. 39, no. 10, pp. 1944–1956, 2010.

[7] H. Hemida and S. Krajnović, "LES study of the influence of the nose shape and yaw angles on flow structures around trains," *J. Wind Eng. Ind. Aerodyn.*, vol. 98, no. 1, pp. 34–46, 2010.

[8] H. Hemida, C. Baker, and G. Gao, "The calculation of train slipstreams using large-eddy simulation," *Proc. Inst. Mech. Eng. Part F J. Rail Rapid Transit*, vol. 228, no. 1, pp. 25–36, Jan. 2014.

[9] B. Blocken, T. Stathopoulos, and J. P. A. J. van Beeck, "Pedestrian-level wind conditions around buildings: Review of wind-tunnel and CFD techniques and their accuracy for wind comfort assessment," *Build. Environ.*, vol. 100, pp. 50–81, 2016.

[10] U. Piomelli, "Wall-layer models for large-eddy simulations," *Prog. Aerosp. Sci.*, vol. 44, no. 6, pp. 437–446, 2008.

[11] I. Mary and P. Sagaut, "Large Eddy Simulation of Flow Around an Airfoil Near Stall," *AIAA J.*, vol. 40, no. 6, pp. 1139–1145, Jun. 2002.

THE INTERNATIONAL CONFERENCE ON
WIND ENERGY HARVESTING 2017
20-21 April 2017
Coimbra, Portugal

Paper A4F.10

GENERATING TURBULENCE USING PASSIVE GRIDS IN WIND TUNNEL TESTING

Giulio Vita[1]
University of Birmingham
Birmingham, United Kingdom

Hassan Hemida[2]
University of Birmingham
Birmingham, United Kingdom

Thomas Andrianne[3]
University of Liége
Liége, Belgium

Charalampos Baniotopoulos[4]
University of Birmingham
Birmingham, United Kingdom

ABSTRACT

This paper reports on a wind tunnel experiment on a wind turbine aerofoil under turbulent inlet. Urban Wind Energy is considered as a promising way of harvesting wind energy in built areas, hence slashing infrastructural wind energy costs. Effective positioning strategies are needed to maximise the performance; however, the role of turbulent inflows is not clear. In particular, the role of turbulent length scales is difficult to assess. In this work, the DU96w180 wind turbine aerofoil is investigated regarding its aerodynamic performance under varying inflow turbulence structures. Particular attention is given to the stall mechanism, hence the angle of attack of the blade is varied accordingly *0<α<45deg*. Inlet turbulence is created by means of passive grids, with various geometrical setup, in order to obtain a wide range of turbulent structures. In order to test the effect of large scales, two chord length for the model are chosen *c=0.125÷0.025m* in order to maximise the length-to-chord ratio *L/c*.

NOMENCLATURE

α	=	Angle of Attack [deg]
β	=	Porosity [-]
c	=	Chord length of aerofoil model [m] | characteristic length [m]
d	=	Grid bar size [m]
FST	=	Free Stream Turbulence
I	=	Turbulence intensity [-]
L	=	Integral length scale of turbulence [m]
M	=	Grid mesh size [m]
$\mathcal{R}e$	=	uc/ν Reynolds number
UWE	=	Urban Wind Energy
WT	=	Wind Turbine
x	=	Distance between model and grid [m]

1 Early Stage Researcher and phD Student, School of Civil Engineering, University of Birmingham, Edgbaston, Birmingham, B15 2TT, United Kingdom / g.vita@bham.ac.uk
2 Senior Lecturer, School of Civil Engineering, University of Birmingham, Edgbaston, Birmingham B15 2TT, United Kingdom / h.hemida@bham.ac.uk
3 Head of the Wind Tunnel Laboratory, Department of Aerospace and Mechanical Engineering, University of Liége 1, Chemin des Chevreuils, Liége, B-4000, Belgium / t.andrianne@ulg.ac.be
4 Full professor, Chair of Sustainable Energy Systems and Director of Resilience Centre, School of Civil Engineering, University of Birmingham, Edgbaston, Birmingham B15 2TT, United Kingdom / c.baniotopoulos@bham.ac.uk

INTRODUCTION AND BACKGROUND

Urban Wind Energy (UWE) is accounted as a suitable way of harvesting more wind energy in a more cost-efficient way [1]. However, the aerodynamics of wind turbines (WTs) located in built areas is challenging because of several issues, e.g. the statistics of the wind at the inlet and the response of WTs to such turbulent inflows. Based on these issues, the positioning of WTs within built premises is the main concern in UWE [2]. Supposedly, a suitable location for harvesting wind is at those spots of the urban environment, where the mean wind velocity is maximised, while the fluctuating wind is minimised [3]. However, this statement might find its origin in the tendency of replicating standard wind climate conditions [4], rather than reliable results, showing the actual performance with varying position, excluding limited literature focusing on the power output, rather that the aerodynamic performance [5].

This work will focus on the aerodynamic response of WTs to turbulent structures at the inlet. In fact, it is normally agreed that turbulence at the inlet is not a governing parameter for the aerodynamic performance. This important statement is largely accepted in the aeronautical field. Miley [6] pointed out that aerofoils are only sensitive to turbulence, if the inflow integral length scale is comparable with the boundary layer thickness. Wind Turbine aerodynamics has internalized this assumption, then Free Stream Turbulence (FST) supposedly has an effect only on the unsteady variation of the real angle of attack α, therefore turbulence is neglected in experiments and simulations [7]. The integral length scale of turbulence is then accounted as the reason, why atmospheric turbulence, which is characterised by large scales, has no role in the aerodynamic performance.

However, this assumption is invalidated for WTs for a twofold reason: (i) when placed in built premises, but also in clusters or in ducts, the turbulent inflow is not comparable to atmospheric winds, as usually provided with smaller scales; (ii) the understanding of the effects of turbulence on WT blades is directly related to bluff body aerodynamics, as WTs experience stall, which is affected by turbulence.

Numerous experimental studies have been performed to investigate the effect of either turbulence intensity or length scale of inflow turbulence on bluff bodies [8]. Although the literature still shows incongruences, important results are available for various basic bluff bodied shapes, but also for engineering applications as wind turbine blades [9]–[11]. Most works only correlate the aerodynamic performance with the turbulence intensity of the inflow, either disregarding the effect of the length scales, or giving a marginal interpretation of their importance. The reason for that is the difficulty in varying the range of the length scale L to characteristic dimension c ratio, while fixing the other statistics. Moreover, it is difficult to obtain range of scales larger than $L/c \leq 1.5 \div 2$. Therefore, the research is not directly applicable to atmospheric flows, which experience much larger integral scales. Nonetheless, urban flows are rather local flows characterised by signature turbulence in wakes or shear layers of buildings and other obstacles, hence the negligibility of turbulence is not a trivial assumption [12].

Bearman & Morel [8] have shown that free stream turbulence (FST) affects considerably both the mean and unsteady behaviour of separated shear layers of bluff bodies. In particular, the surface pressure is affected by a shift towards the separation point in both the mean, fluctuating and peak pressure statistics. This finding is confirmed also by Nakamura & Ozono [13], who stress out the role of the turbulent length scales. In particular, it seems that turbulence has a noticeable effect for $L/c \leq 5$, then approaching the smooth flow behaviour for higher scales. Li and Melbourne [14] used a large range of grid meshes and distances for a set of square prisms, noting that the effect of length scales is more pronounced for higher turbulence intensities. Haan et al. [15] obtained however that the effect of large integral scales up to $L/c = 7.8$ is still remarkable.

On the wake of the results for bluff bodies, a limited amount of research has been conducted also on the evaluation of the effects of inlet turbulence on typical WT blades [16]. In particular, the stall mechanism is sensitive to turbulence intensities at the inlet, for various Reynolds number regimes [17]. However, it is not clear, whether this is associated will small or large integral length scales. Nevertheless, a twofold effect is noticeable on aerofoils: (i) the triggering of laminar-to-turbulent transition of the boundary layer (decreasing maximum Lift); (ii) the increase of transport of momentum between the boundary layer region and the undisturbed flow, thus increasing the resistance against adverse pressure gradient and delaying separation (increasing maximum Lift). Although the second effect is more pronounced [18], the presence or lack of transition must be carefully accounted [9].

It appears that an increase in turbulence intensity enhances WT blade properties, causing a delay in stall and an increase in maximum Lift and aerodynamic performance [10], [19], [20]. Maldonado et al. [9] add that large scales dampen the actual effect of turbulence, but the limited range of turbulent characteristics tested needs further extension to draw definitive conclusions on this issue.

This work will present the first results of an experimental investigation, which tries to go beyond limitations in the experimental setup, testing a wide range of turbulence scales and intensities and correlating them with the angle of attack and the stall mechanism. University of Liége. The aim of the experiment is to understand the role of the length scale of turbulence in influencing the aerodynamic performance of wind turbine aerofoils.

METHODOLOGY

The aerodynamic behaviour of a Wind Turbine aerofoil is tested in the wind tunnel of the University of Liége. The parameters which govern the behaviour are basically the variation of the angle of attack α and the Reynolds numbers Re_c. In this experiment, the further parameters of the turbulence intensity $I = \sigma_u/\bar{u}$ and the integral length scale L are studied, with particular reference to the pressure distribution along the aerofoil.

The experiment will be fulfilled at the University of Liége. The setup is outlined in Fig. 1.

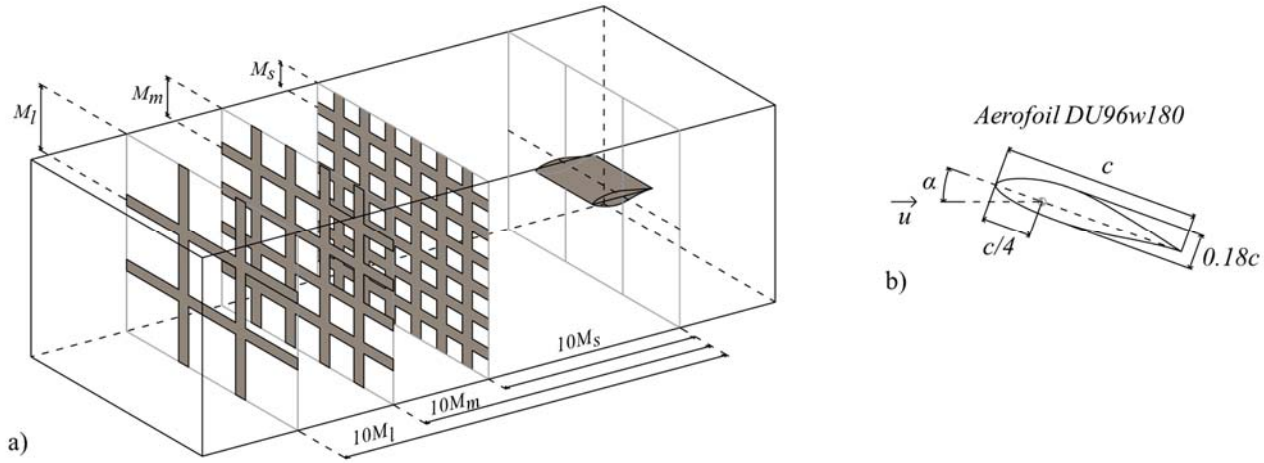

Fig. 1 a) Wind Tunnel Experimental Setup, with the set of three grids; b) the aerofoil model.

The wind tunnel of the University of Liège is a closed loop subsonic boundary layer wind tunnel (*Mach<0.15*), with the possibility of an open-loop configuration. The test-section of *1.80×2.00×2.50m* is placed at *16.00m* from the inlet nozzle. This distance is suitable for the development of a wide range of turbulent inlet structures, which will be generated using the passive grid technique. The generation of vorticity due to the presence of the grid and the consequent drop in the pressure field cause the quiescent upstream flow to develop isotropic turbulent characteristics, which is ideal in order to understand the role of simple turbulence statistics. Various typologies of grids are reported in the literature. However, the square barred grid is accounted as the most reliable geometry of generating an isotropic uniform turbulent flow-field [21].

A set of passive grids, consisting of a mesh of square wooden bars, will be implemented. Various turbulence structures will be obtained by varying bar width d and mesh pace M. The distance x upstream to the model is a parameter to be controlled. In order to have isotropy, a distance of at least $10M=x$ has to be kept.

A preliminary grid setup is proposed in Tab 1.

Table 1. Proposed setup of the set of grids.

Grid	Bar Size		Mesh Size		Min. distance		Porosity
	d [m]	d/c	M [m]	M/c	$10M=x$ [m]	x/c	$\beta=(1-d/M)^2>0.5$
Small, *s*	0.025	0.2	0.125	1	1.25	10	0.64
Medium, *m*	0.0625	0.5	0.375	3	3.75	30	0.69
Large, *l*	0.1875	1.5	0.75	6	7.50	60	0.56

The wind turbine aerofoil to be tested is the DU 96w180, designed at the University of Delft [22]. Regarding the size of the model, following considerations on the choice of the chord length have been made. The use of a passive grid allows for a length scale of $L_{x,max} \cong 15\text{-}20cm$. In order to test the effect of large scales, a model with a rather small chord length $c \cong 0.1\text{-}0.15m$ is necessary. The literature confirms the difficulty in simulating large scales in wind tunnels and the necessity of a small chord [20]. Therefore, for this experiment, two chord lengths are chosen to be tested with the set of three grids. A first model, $c_1=0.125m$, will allow the performation of surface pressure measurements, while a second model $c_2=0.025m$, will allow the estimation of large scales, measuring the aerodynamic forces on the model. The latter will obviously require a correction of the velocity of the wind tunnel in order to match the Reynolds number which is chosen for the c_1 model. Regarding the Reynolds number, two ranges are chosen in particular: 1) low-Reynolds range $\mathcal{R}e \cong 1.5\times10^5$; 2) high-Reynolds range $\mathcal{R}e \cong 1.5\times10^6$. However, the main parameter to be varied throughout the experiment is the angle of attack α (Fig. 1). A large range

is proposed, to understand the role of turbulence with specific regard to the stall mechanism: 0) Zero angle *0deg*; 1) Pre-stall *2-8÷10deg*; 2) Stall *10-15deg*; 2) Post-stall *10-20deg*; 3) Full-stall *20-45deg*.

The following table introduces the experimental campaign to be fulfilled, with an estimation of the number of setups.

Table 2. Experimental setup.

Grid M/c_1, d/c_1, β	Position of the grid x [m]	exp. turb. Intensity I	expected int. length scale L	Range of angles α	Estimated experiments
Undisturbed	-	*<0.1%*	-	*0-45→5* conf.	*4-5*
Small (1, 1/5, 0.64)	$x=10M_s=1.25$	*high*	*Small*	*0-45→5* conf.	*16-20*
	$x=10M_m=3.75$	*normal*	*Small*	*0-45→5* conf.	
	$x=10M_l=7.50$	*low*	*Medium/Small*	*0-45→5* conf.	
	$x=5M_s=6.25$	*low*	*Small*	*0-45→5* conf.	
Medium (3, 0.5, 0.69)	$x=10M_s=1.25$	*high*	*Small*	*0-45→5* conf.	*16-20*
	$x=10M_m=3.75$	*high*	*Medium*	*0-45→5* conf.	
	$x=10M_l=7.50$	*low/normal*	*Medium/Large*	*0-45→5* conf.	
	$x=5M_s=6.25$	*normal*	*Medium*	*0-45→5* conf.	
Large (6, 1.5, 0.57)	$x=10M_l=7.50$	*normal*	*Medium*	*0-45→5* conf.	*12-15*
	$x=5M_s=6.25$	*normal/high*	*Medium*	*0-45→5* conf.	
	$x=7M_s=8.75$	*normal/low*	*Large*	*0-45→5* conf.	

The use of two models allows for a wide range of turbulence characteristics to be related and compared. However, such a wide variability of parameters has to take into account the actual content in small scales, as a growth in integral length scale is usually related to a change in the small scales content.

These results will be used as validation for future test-cases on the flow pattern on aerofoils.

ACKNOWLEDGEMENTS

The authors acknowledge with thanks the support of the European Commission Framework Program "Horizon 2020", through the Marie Skłodowska-Curie Innovative Training Networks (ITN) "AEOLUS4FUTURE - Efficient harvesting of the wind energy" (H2020-MSCA-ITN-2014: Grant agreement no. 643167), to the present research project.

REFERENCES

[1] S. Stankovic, N. Campbell, and A. Harries, *Urban Wind Energy*. Earthscan, 2009.

[2] H. Hemida, A. Šarkic, S. Gillmeier, and R. Höffer, "Experimental investigation of wind flow above the roof of high-rise building," in *WINERCOST Workshop "Trends and Challenges for Wind Energy Harvesting,"* 2014, p. p.25-34.

[3] I. Abohela, N. Hamza, and S. Dudek, "Effect of roof shape, wind direction, building height and urban configuration on the energy yield and positioning of roof mounted wind turbines," *Renew. Energy*, vol. 50, pp. 1106–1118, 2013.

[4] C. C. Baniotopoulos, C. Borri, and T. Stathopoulos, "Environmental Wind Engineering and Design of Wind Energy Structures," *Springer-Verlag*, vol. 531. Springer-Verlag, Wien, p. 352, 2011.

[5] K. Sunderland and M. Conlon, "Estimating the Yield of Micro Wind Turbines in an Urban Environment : A Methodology Estimating the Yield of Micro Wind Turbines in an Urban Environment : A Methodology," pp. 1–6, 2010.

[6] S. Miley, "A catalog of low Reynolds number airfoil data for wind turbine applications," 1982.

[7] D. Simms, S. Schreck, M. Hand, and L. Fingersh, "NREL unsteady aerodynamics experiment in the

NASA-Ames wind tunnel: a comparison of predictions to measurements," 2001.
[8] P. W. Bearman and T. Morel, "Effect of free stream turbulence on the flow around bluff bodies," *Prog. Aerosp. Sci.*, vol. 20, no. 2, pp. 97–123, 1983.
[9] V. Maldonado, L. Castillo, A. Thormann, and C. Meneveau, "The role of free stream turbulence with large integral scale on the aerodynamic performance of an experimental low Reynolds number S809 wind turbine blade," *J. Wind Eng. Ind. Aerodyn.*, vol. 142, pp. 246–257, 2015.
[10] X. Amandolèse and E. Széchényi, "Experimental study of the effect of turbulence on a section model blade oscillating in stall," *Wind Energy*, vol. 7, no. 4, pp. 267–282, 2004.
[11] C. Sicot, P. Devinant, T. Laverne, S. Loyer, and J. Hureau, "Experimental study of the effect of turbulence on horizontal axis wind turbine aerodynamics," *Wind Energy*, vol. 9, no. 4, pp. 361–370, Jul. 2006.
[12] M. W. Rotach, "On the influence of the urban roughness sublayer on turbulence and dispersion," *Atmos. Environ.*, vol. 33, no. 24–25, pp. 4001–4008, 1999.
[13] Y. Nakamura and S. Ozono, "The effects of turbulence on a separated and reattaching flow," *J. Fluid Mech.*, vol. 178, no. 1, p. 477, Apr. 2006.
[14] Q. . Li and W. . Melbourne, "The effect of large-scale turbulence on pressure fluctuations in separated and reattaching flows," *J. Wind Eng. Ind. Aerodyn.*, vol. 83, no. 1, pp. 159–169, 1999.
[15] F. L. Haan and A. Kareem, "Anatomy of Turbulence Effects on the Aerodynamics of an Oscillating Prism," *J. Eng. Mech.*, vol. 135, no. 9, pp. 987–999, Sep. 2009.
[16] G. Vita, H. Hemida, and C. C. Baniotopoulos, "Effect of atmospheric turbulence on the aerodynamics of wind turbine blades: a review," in *Proceedings of the 1st WinerCost International Conference, Ankara, TR*, 2016.
[17] S. Wang, Y. Zhou, M. M. Alam, and H. Yang, "Turbulent intensity and Reynolds number effects on an airfoil at low Reynolds numbers," *Phys. Fluids*, vol. 26, no. 11, p. 115107, Nov. 2014.
[18] R. F. Huang and H. W. Lee, "Effects of Freestream Turbulence on Wing-Surface Flow and Aerodynamic Performance," *J. Aircr.*, vol. 36, no. 6, pp. 965–972, Nov. 1999.
[19] C. Sicot, P. Devinant, S. Loyer, and J. Hureau, "Rotational and turbulence effects on a wind turbine blade. Investigation of the stall mechanisms," *J. Wind Eng. Ind. Aerodyn.*, vol. 96, no. 8, pp. 1320–1331, 2008.
[20] K. E. Swalwell, "The effect of turbulence on stall of horizontal axis wind turbines," pp. 1–307, 2005.
[21] P. E. Roach, "The generation of nearly isotropic turbulence by means of grids," *Int. J. Heat Fluid Flow*, vol. 8, no. 2, pp. 82–92, 1987.
[22] W. A. Timmer and R. P. J. O. M. van Rooij, "Summary of the Delft University Wind Turbine Dedicated Airfoils," in *ASME 2003 Wind Energy Symposium*, 2003, pp. 11–21.

THE INTERNATIONAL CONFERENCE ON
WIND ENERGY HARVESTING 2017
20-21 April 2017
Coimbra, Portugal

Paper A4F.11

WIND TUNNEL TESTING OF SMALL VERTICAL-AXIS WIND TURBINES IN URBAN TURBULENT FLOWS

Andreu Carbó Molina[1]
University of Florence
Florence, Italy

Gianni Bartoli[2]
University of Florence
Florence, Italy

Tim De Troyer[3]
Vrije Universiteit Brussel
Brussels, Belgium

ABSTRACT

The following study presents a wind tunnel approach to evaluate the efficiency of Vertical-Axis Wind Turbines (VAWT) in high turbulence-level flows. The first part of the research consists in studying the design and implementation of turbulence grids in wind tunnels. Such grids allow control of the turbulence inside the tunnel to approximate realistic urban wind conditions. In the second phase, these turbulent grids are used to test a H-Darrieus VAWT into different levels of turbulence. The final goal is to improve the modelling of turbulent urban flows inside the wind tunnel, and determine the influence of high turbulence-level flows in the performance of VAWT. This will contribute to the technology of wind harvesting in the built environment.

NOMENCLATURE

C_P	=	Power Coefficient (-)
D	=	Diameter of the Rotor (m)
H	=	Height of the rotor (m)
I_u	=	Intensity of Turbulence (-)
Q	=	Torque (Nm)
R	=	Turbine Radius (m)
V	=	Wind speed (m/s)
λ, TSR	=	Tip Speed Ratio (-)
ρ	=	Density of air (kg/m^3)
ω, RPM	=	Angular speed (min^{-1})
$VAWT$	=	Vertical Axis Wind Turbines
$HAWT$	=	Horizontal Axis Wind Turbines

INTRODUCTION

Vertical-Axis Wind Turbines (VAWT) differ from the conventional horizontal ones (HAWT) in the orientation of their axis, which leads to differences in their operation. The 3-bladed HAWT, the so called “Danish concept”, presents the highest efficiency and has become the most established technology [1]. However, for urban flows, where the wind is typically slow and complex, HAWTs show poor results. VAWTs, on the other hand, are omni-directional, adapting quicker and better to a changing wind direction, and operate at lower tip-to-speed ratios

[1]PhD Student, Civil and Environmental Engineering Department, University of Florence, andreu.carbo.molina@dicea. unifi.it
[2]Associate Professor, Civil and Environmental Engineering Department, University of Florence, gbartoli@dicea.unifi.it
[3] Assistant Professor, Faculty of Engineering, Vrije Universiteit Brussel, tim.de.troyer@vub.ac.be

(TSR), which makes them less noisier [2]. Thanks to these features, VAWTs have found in small urban wind energy their market during the last decade [3]. Detailed literature is available on large VAWT from research programs in the 80s [4, 5], and several small VAWTs models are under operation and testing. However, there is still few research available about their performance under urban flow conditions.

In built environments, the rotor experiences high levels of turbulence, inclined, reverse and stratified flows. The challenge of finding a desirable location is considerable, and has lead to multiple cases of bad practice. The lack of a detailed wind study of the location leads to turbines with poor energy production, giving bad press for VAWT and renewable energy in general. To avoid this, literature and on-site measurements can be used to determine the best locations for wind turbines in an urban environment: top of buildings, large avenues, canyon effects, etc. [6]. From literature, it can be seen that in these sites there is an acceleration of wind speed, but high levels of turbulence (I_u >20%) are reached [7]. This turbulence level needs to be considered when evaluating the performance of the wind turbine prototypes.

METHODOLOGY

The objective of this work is to experimentally evaluate the behavior of VAWTs in turbulent urban flows. The first part of the research is performed at the CRIACIV facility from the University of Florence, Italy. This is a Boundary Layer Wind Tunnel with a cross section of 2.4m x 1.6m in the test area, that allows to develop stable turbulence intensity and length scale levels (Figure 1).

Figure 1. CRIACIV wind tunnel in Prato, Italy.

The very initial research step is to select the best locations to place a small urban wind turbine from literature and on-site measurements. From literature, the flow conditions in mean wind speed and turbulence intensity are determined. With a careful similarity study, the wind flow conditions in those chosen locations are reproduced inside the wind tunnel.

Most of VAWT wind tunnel measurements up till now do not consider turbulent flow, or keep it at low levels (I_u <5%). To generate high levels of turbulence inside the wind tunnel, turbulence grids are used. These grids modify the free stream present in the wind tunnel, stopping the flow and creating vortexes. CRIACIV wind tunnels possess two grids (10cm x 10cm and 55cm x 55cm mesh), that can be placed at different distances from the test section and combined to obtain a range of turbulence levels and length scales in which to perform the urban flow modeling [8]. With the results of this study, a series of empirical rules will be written down and presented about that issue.

The second part of the research is done at the Vrije Universiteit Brussel (VUB), where the VAWT testing is performed. The boundary layer wind tunnel in the Mechanical Engineering Department has a 2 m x 1 m test section. The experience gathered in the first phase of the research is used to design and build a grid adapted for this wind tunnel, and with that recreate the urban turbulent conditions to test the turbine.

The VAWT is a H-Darrieus design with D=50 cm and H=80 cm, and it was built in lightweight carbon fiber at VUB (Figure 2). The blades' profile is a NACA0018 with 5 cm chord. Its operational characteristics are listed below:

- Aspect ratio H/D=1.6
- Tip speed ratio λ= 2.5 to 3.2
- Incident wind speed V=7 to 12 m/s
- Revolutions per minute ω=900 – 1400 rpm

Figure 2. VAWT model built by the VUB team [9].

The turbine is supported by an aluminum modular frame already tested in other VAWT measurements. The torque is measured by a 2Nm torque meter, and the RPM are measured using variable resistors. The axis of the turbine is coupled to brushed DC motor/generator, that allows the start-up of the turbine.
The parameter to calculate the performance of the turbine will be the Power Coefficient (C_P):

$$C_P = \frac{P_{turbine}}{P_{wind}} = \frac{Q\omega}{\frac{1}{2}\rho DHV^3}$$

The conventional way of representing C_P in wind turbine studies is plotting it against the Tip-Speed Ratio of the turbine, a non-dimensional number that relates the speed of the blade tip with the incident wind:

$$\lambda = \frac{\omega R}{V}$$

RESULTS

The values of C_P of the turbine are measured while changing V and ω within the operational limits, and plotted to obtain the $C_P - \lambda$ curves that represent the wind turbine performance. Special attention should be paid into the effect of Reynolds number, that has been proved to exert a large influence into the performance curves [10].

Three series of experiments are performed. First, the turbine efficiency is evaluated conventionally, with no obstacles in the wind tunnel and therefore very low turbulence (I_u <1%). Then, the tests are repeated at medium (I_u =5-10%) and high turbulence (I_u >15%), according to the capabilities of the built grid. If any interesting phenomena are observed, more values of I_u can be tested.

CONCLUSIONS

The parametric study done in this work should allow to increase the knowledge about how turbulent flows affect the performance of a generic H-Darrieus rotor. With a larger range of turbulent values than the existing work in this field, the results obtained would permit to present some empirical rules about this phenomenon. Those results will also contribute to the application of the VAWT technology in urban environments, by giving some hints about the reasons of the generally-poor behaviour of urban wind turbines. Those results may be applied to correct the power ratings provided by the VAWT manufacturers and to investigate methods to mitigate those effects in future designs.

The first part of the research, moreover, will become an interesting contribution to the wind tunnel testing knowledge. As every wind tunnel presents particular characteristics, applying the same procedures in two of them (CRIACIV and VUB) will provide valuable experience in grid-generated turbulence and how to apply it properly.

ACKNOWLEDGEMENTS

The present research takes part in the European Innovative Training Network (ITN) AEOLUS4FUTURE "Efficient Harvesting of the Wind Energy". The project is funded by the Horizon 2020 research and innovation program under the Marie Skłodowska-Curie grant agreement No. 643167. Furthermore the COST TU1304 action (WINERCOST) is gratefully acknowledged.

REFERENCES

[1] T. Burton. *Wind Energy Handbook*, John Wiley & Sons, 2001.

[2] I. Paraschivoiu. *Wind Turbine Design: With Emphasis on Darrieus Concept*. Presses inter Polytechnique, 2002.

[3] P. Cooper. *Development and analysis of vertical-axis wind turbines*. Appears in *Wind Power Generation and Wind Turbine Design*, edited by Wei Tong. WIT Press, 2010.

[4] T. Price. *UK Large-Scale Wind Power Programme From 1970 to 1990: The Carmarthen Bay Experiments and the Musgrove Vertical-Axis Turbines.* Wind Engineering, Vol. 30, No. 3, 2006.

[5] H. Sutherland. *A Retrospective of VAWT Technology.* Sandia National Laboratories, 2012.

[6] M. C. Runacres, J. J. Vermeir, and T. De Troyer. *BIM E11-359 Final Report—Identificatie Identificatie sites, opzetten windmetingscampagnes en uitvoering van haalbaarheidsstudies in het Brussels Hoofdstedelijk Gewest*. Leefmilieu Brussel, 2014.

[7] I. Janajreha, L. Su , F. Alan. *Wind energy assessment: Masdar City case study*. Renewable Energy 52, 2013.

[8] C. Mannini, A. M. Marra, L. Pigolotti, G. Bartoli. *Unsteady pressure and wake characteristics of a benchmark rectangular section in smooth and turbulent flow*. 14th International Conference on Wind Engineering – Porto Alegre, Brazil, 2015.

[9] T. De Troyer**,** M. Runacres. *Wind Tunnel Testing of a Pair of VAWTs for Offshore Applications*, 2016.

[10] D. W. Wekesa, C. Wang, Y. Wei, W. Zhu. *Experimental and numerical study of turbulence effect on aerodynamic performance of a small-scale vertical axis wind turbine*. J. Wind Eng. Ind. Aerodyn. 157, 2016.

THE INTERNATIONAL CONFERENCE ON
WIND ENERGY HARVESTING 2017
20-21 April 2017
Coimbra, Portugal

Paper A4F.12

BLADE TIP NOISE PREDICTION BY LINEARIZED AIRFOIL THEORY

Yakut Cansev KUCUKOSMAN[1] **Julien CHRISTOPHE**[2] **Christophe SCHRAM**[3] **Jeroen VAN BEECK**[4]

von Karman Institute for Fluid Dynamics, Sint-Genesius-Rode, Belgium

ABSTRACT

In this study, a far-field noise prediction of a wind turbine airfoil section is carried out by using Amiet's semi-analytical model to predict far-field noise emitted at the trailing edge. Two-dimensional steady Reynolds Averaged Navier-Stokes computations are performed for DU-96-180 type airfoil at 4^o angle of attack with a Reynolds number of $Re = 1.13x10^6$. Different wall pressure spectrum based on empirical and statistical models, which are required in the formulation of Amiet, are investigated. The wall pressure spectrum is evaluated by using the boundary layer information obtained from the Reynolds Averaged Navier-Stokes computations, on the other hand, the empirical models are based on the normalization laws obtained by the theoretical or experimental investigation. Therefore, this paper focuses on the comparison of the different wall pressure model approaches.

NOMENCLATURE

RANS	=	Reynolds-Averaged Navier-Stokes
PSD	=	Pressure Spectrum Density
APG	=	Adverse Pressure Gradient
LES	=	Large Eddy Simulation
Re	=	Reynolds Number
DNS	=	Direct Numerical Simulation
RSNM	=	RANS-based Statistical Noise Model
SNGR	=	Stochastic Noise Generation and Radiation
BPM	=	Brooks, Pose and Marcolini
C	=	Chord (m)
ω	=	Angular Frequency
b	=	Span (m)
l_y	=	Spanwise Correlation Length
$\mathcal{L}$	=	Aeroacoustic Transfer Function
ϕ_{pp}	=	Wall Pressure Spectra
U_c	=	Convection Velocity (m/s)
ρ_∞	=	Density (kg/m^3)
U_∞	=	Freestream Velocity (m/s)
α	=	Angle of attack

[1]Ph.D. Candidate, Environmental and Applied Fluid Dynamics Department, von Karman Institute for Fluid Dynamics, Bruxelles/Belgium, yakut.cansev.kucukosman@vki.ac.be
[2] Senior Research Engineer, Environmental and Applied Fluid Dynamics Department, von Karman Institute for Fluid Dynamics, Bruxelles/Belgium, julien.christophe@vki.ac.be
[3] Associate Professor, Environmental and Applied Fluid Dynamics Department, von Karman Institute for Fluid Dynamics, Bruxelles/Belgium, christophe.schram@vki.ac.be
[4] Professor, Environmental and Applied Fluid Dynamics Department, von Karman Institute for Fluid Dynamics, Bruxelles/Belgium, jeroen.vanbeeck@vki.ac.be

INTRODUCTION

The increasing need for sustainable and clean energy resources is a strong incentive in the field of wind engineering. However, a main issue with the implementation of wind turbines is the acoustic annoyance they cause in their immediate environment [1–3] . Therefore, low-cost and precise noise prediction tools are needed in the process of the wind turbine design and the wind farm planning.

The predominant wind turbine noise production mechanism is associated with the turbulence that develops along the blade surface and scatters at the trailing edge as acoustic waves [4,5]. Trailing edge noise prediction approaches can be distinguished along three categories; semi-empirical methods, direct methods and hybrid methods. Semi-empirical methods such as Brooks, Pose and Marcolini (BPM) model [6] and TNO model[7] are based mostly on experimental data. The BPM model expresses the far field noise in 1/3-octave band based on the velocity and scaling laws. The model is tuned based on a generic airfoil profile, which can lead to poor prediction for other airfoil profiles [8]. The TNO model is based on turbulent boundary layer and the wall pressure wavenumber frequency spectrum developed by Parchen [7]. The Blake's equation is used [9] for the prediction of the wall pressure wavenumber frequency spectrum. This model was observed to yield an under-prediction of the noise level compared to some experimental results [10,11] even though it shows a correct behavior with respect to incoming velocity and angle of attack.

In direct methods, the flow and the sound fields are computed together by solving the compressible flow equations. Direct Numerical Simulation (DNS) [12] resolves all turbulence scales, while Large Eddy Simulation (LES) [13] utilizes sub-grid scale to model small eddies. Both can in theory be used to calculate the radiated noise directly. However, in terms of computational cost, DNS or LES techniques are still too costly to be applied for industrial design purposes. These approaches are however well suited to provide a better understanding of surface pressure spectrum behavior, supporting the development of simplified models.

Hybrid methods offer an interesting compromise in terms of accuracy vs. CPU cost, by decoupling the flow and acoustic calculations. Hybrid methods usually consist in the following two steps: first, the unsteady flow field is computed in the region of the source term; secondly, an acoustic propagation method is used to compute the acoustic source radiation towards the far-field. In order to further reduce the computational cost, Reynolds-Averaged Navier-Stokes (RANS) simulations can be preferred over scale-resolved simulations to provide a source model. In that case, complementary stochastic methods are necessary to synthesize the missing unsteady information about the flow. The Stochastic Noise Generation and Radiation (SNGR) [14,15] was developed to this end. Finally, purely statistical methods (not involving any stochastic reconstruction) offer the cheapest solution amongst the hybrid methods. The RANS-based Statistical Noise Model (RSNM)[16] follows this path, the acoustic far field being computed by using semi-infinite half plane Green' s function combined with a model for the turbulent velocity cross-spectrum in the vicinity of the trailing-edge. Alternatively, wall pressure based models compute the acoustic far field using a diffraction analogy technique[17] or Amiet's theory [18]. In this paper, the acoustic far field prediction is performed by theory of Amiet.

AMIET'S ANALYTICAL MODEL FOR TRAILING EDGE NOISE

Amiet's theory provides an analytical model to compute the far-field acoustic noise of an airfoil subjected to a periodic gust [18]. This model was extended to predict trailing-edge noise [19], considering the scattering of a wall pressure gust convected past the trailing edge. The derivation is performed by solving the scattering problem iteratively at the trailing edge. A leading-edge back-scattering correction is performed by considering the finite length chord by Roger & Moreau [20] as the original method assumes that airfoil extends infinity in the upstream direction.

The far-field acoustic PSD (S_{pp}) for trailing edge in the midspan plane at a given observer location, $\boldsymbol{x} = (R, \theta, z = 0)$ can be written as:

$$S_{pp}(\boldsymbol{x}, \omega) = \left(\frac{sin\theta}{2\pi R}\right)^2 (kC)^2 b |\mathcal{L}|^2 \, l_y(\omega) \, \phi_{pp}(\omega)$$

where C is the chord length, b is the semi-span, ω is the angular frequency, l_y is the spanwise correlation length, $\mathcal{L}$ is the aeroacoustic transfer function [20], and ϕ_{pp} is the wall pressure spectrum. The spanwise correlation length based on the convection velocity, U_c, is computed by the Corcos model [21] as:

$$l_y = \frac{bU_c}{\omega}$$

The wall pressure spectra ϕ_{pp} will be computed form Goody [22], Rozenberg [23] and Panton & Linebarger[24] models. The Goody's model considers the effect of Reynolds number and gives good match with experiments with zero-pressure gradient flow. However, the model provides poor estimation in presence of an adverse-pressure gradient (APG). Later, Rozenberg's model, which is the improved version of Goody's model, will be investigated. This model is based on the boundary layer information and takes into the effect of the APG. Panton & Linebarger's statistical model is based on the complete boundary layer profile information.

PRELIMINARY RESULTS

The two dimensional (2D) steady RANS computations are performed by the open source OpenFOAM with DU-96-180 wind turbine airfoil. The operating conditions are chosen from the BANC benchmark[25] as the following; the freestream velocity, $U_\infty = 60\ m/s$, the Reynolds number, $Re = 1.13 \times 10^6$, the density, $\rho_\infty = 1.164\ kg/m^3$, the chord of the airfoil is $C = 0.3\ m$ and the angle of attack, $\alpha = 4^\circ$. The domain and grid dependency tests are performed as preliminary investigation.

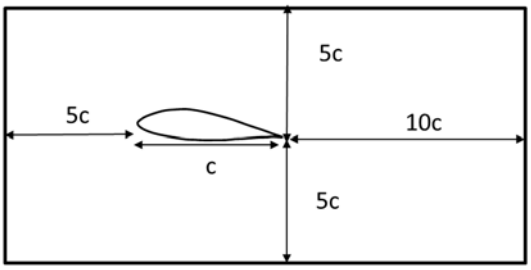

Figure 1. The main domain configuration (Case #1)

The domain dependency is tested with two different configuration, the main case (Case #1) shown in Figure 1 has a 10C length in the wall normal direction and the second is increased to 20C (Case #2), the upstream and downstream dimensions being identical. The pressure coefficient along the airfoil and the velocity profile at the 0.02 % from the trailing edge are shown in Fig. 2a and Fig. 2b. The pressure coefficient distributions ae very similar using both computational domains, and agree reasonably well with results obtained using the XFOIL solver[26], excepted close to the trailing edge. The velocity profiles also confirm the fact that the domain with 10C lateral extent is sufficient.

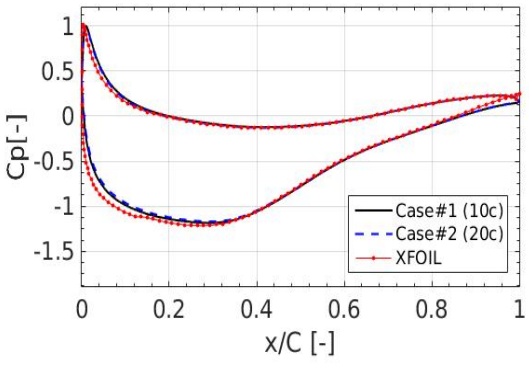

Figure 2a. Cp distribution along the airfoil compared with XFOIL[26] predictions.

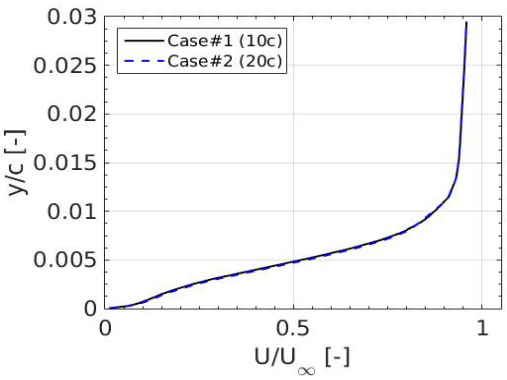

Figure 2b. Velocity profile at the 0.02 % from the trailing edge with different domain configurations.

The mesh dependency check is performed using four different mesh refinements listed in Table 1 where Case #1 is denoted by the main configuration in Fig. 1. From the Fig. 3a. While the pressure distribution appears rather insensitive to the mesh refinement for the investigated cases, the velocity profiles exhibit much more sensitivity, as can be seen in Fig.3b. This is important as the acoustic prediction relies on the details of the velocity profile close to the trailing edge.

Table 1. Grid dependency parameters

	Background Mesh size (m)
Case#3 (finer)	0.05
Case#1 (fine)	0.1
Case#4 (coarse)	0.2
Case#5 (coarser)	0.4

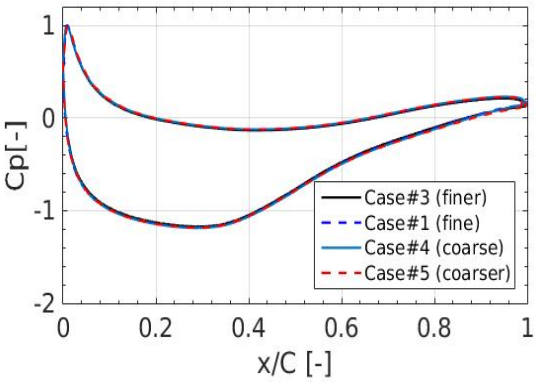

Figure 3a. Cp Distribution along the airfoil with different mesh sizes

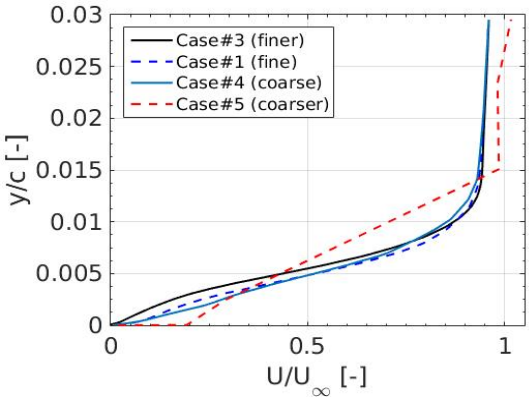

Figure 3b. The velocity profile at the 0.02 % from the trailing edge with different mesh sizes

PRELIMINARY CONCLUSIONS AND PERSPECTIVES

The preliminary results of the numerical simulations permit quantifying the sensitivity of the key flow parameters with respect to the domain size and mesh refinement. The final paper will compare the results of the acoustic predictions obtained using these flow data as an input to different statistical modelling approaches. Two paths will be followed to estimate the wall pressure spectrum near the trailing edge, on the basis of the RANS data. The first approach consist in re-scaling non-dimensional wall pressure models (the Goody and Rozenberg models), which account or not for the effect of pressure gradients. The second approach, the Panton & Linebarger one, is based on an integration of the Poisson equation and involves *a priori* less restrictive assumptions about the flow and should thus be more generally applicable. The methods will be compared on the basis of their accuracy, by comparison with established databases,[25] and of their robustness with regard to inaccurate input RANS data.

ACKNOWLEDGEMENTS

The authors gratefully acknowledge the support of the European Commission's Framework Program "Horizon 2020", through the Marie Skłodowska-Curie Innovative Training Networks (ITN) "AEOLUS4FUTURE - Efficient harvesting of the wind energy" (H2020-MSCA-ITN-2014: Grant agreement no. 643167).

REFERENCES

1. Bockstael, A. *et al.* Wind turbine noise: annoyance and alternative exposure indicators.
2. Waye, K. P., Öhrström, E., Psycho-acoustic characters of relevance for annoyance of wind turbine noise. *J. Sound Vib.* **250,** 65–73 (2002).
3. Schmidt, J. H. & Klokker, M. Health effects related to wind turbine noise exposure: a systematic review. *PLoS One* **9,** e114183 (2014).
4. Barone, M. F. Survey of Techniques for Reduction of Wind Turbine Blade Trailing Edge Noise. (2011).
5. Oerlemans, S., Fisher, M., Maeder, T. & Kögler, K. Reduction of Wind Turbine Noise Using Optimized Airfoils and Trailing-Edge Serrations. *AIAA J.* **47,** 1470–1481 (2009).
6. Brooks, T. F., Pope, D. S. & Marcolini, M. A. NASA Reference Publication 1218 Airfoil Self-Noise and

Prediction. (1989).
7. Parchen, R. *Progress report DRAW : a prediction scheme for trailing edge noise based on detailt boundary layer characteristics*. (1998).
8. Moriarty, P. & Migliore, P. Semi-Empirical Aeroacoustic Noise Prediction Code for Wind Turbines. (2003).
9. Blake, W. K. *Mechanics of flow-induced sound and vibration Volume I, General concepts and elementary sources*. (Academic Press, 1986).
10. Kamruzzaman, M. *et al.* Comprehensive evaluation and assessment of trailing edge noise prediction based on dedicated measurements. *Noise Control Eng. J.* **59,** 54 (2011).
11. Bertagnolio, F. Trailing Edge Noise Model Applied to Wind Turbine Airfoils. (2008).
12. Sandberg, R. D. & Sandham, N. D. Direct numerical simulation of turbulent flow past a trailing edge and the associated noise generation. *J. Fluid Mech.* **596,** (2008).
13. Gloerfelt, X. & Le Garrec, T. Trailing edge noise from an isolated airfoil at a high Reynolds number.
14. Ewert, R., Appel, C., Dierke, J. & Herr, M. RANS/CAA based prediction of NACA 0012 broadband trailing edge noise and experimental validation.
15. Ewert, R. Broadband slat noise prediction based on CAA and stochastic sound sources from a fast random particle-mesh (RPM) method. *Comput. Fluids* **37,** 369–387 (2008).
16. Doolan, C. J., Gonzalez, C. A. & Hansen, C. H. Statistical Estimation of Turbulent Trailing Edge Noise. (2010).
17. Chandiramani, K. L. Diffraction of evanescent waves, with applications to aerodynamically scattered sound and radiation from unbaffled plates. *J. Acoust. Soc. Am.* **55,** 19 (1974).
18. Amiet, R. K. & K., R. Acoustic radiation from an airfoil in a turbulent stream. *J. Sound Vib.* **41,** 407–420 (1975).
19. Amiet, R. K. & K., R. Noise due to turbulent flow past a trailing edge. *J. Sound Vib.* **47,** 387–393 (1976).
20. Roger, M. & Moreau, S. Back-scattering correction and further extensions of Amiet's trailing-edge noise model. Part 1: theory. *J. Sound Vib.* **286,** 477–506 (2005).
21. Corcos, G. M. The structure of the turbulent pressure field in boundary-layer flows. *J. Fluid Mech.* **18,** 353 (1964).
22. Goody, M. Empirical Spectral Model of Surface Pressure Fluctuations. *AIAA J.* **42,** 1788–1794 (2004).
23. Rozenberg, Y., Robert, G. & Moreau, S. Wall Pressure Spectral Model Including the Adverse Pressure Gradient Effects.
24. Panton, R. L. & Linebarger, J. H. Wall pressure spectra calculations for equilibrium boundary layers. *J. Fluid Mech.* **65,** 261 (1974).
25. Herr, M. *et al.* Broadband Trailing-Edge Noise Predictions—Overview of BANC-III Results. in *21st AIAA/CEAS Aeroacoustics Conference* (American Institute of Aeronautics and Astronautics, 2015). doi:10.2514/6.2015-2847
26. Herr, M., Bahr, C. J. & Kamruzzaman, M. Problem Statement for the AIAA/CEAS Second Workshop on Benchmark Problems for Airframe Noise Computations (BANC-II). (2012).

THE INTERNATIONAL CONFERENCE ON
WIND ENERGY HARVESTING 2017
20-21 April 2017
Coimbra, Portugal

Paper A4F.13

PARAMETRIC STUDY OF A STOCHASTIC METHOD FOR TRAILING-EDGE TURBULENCE GENERATION FOR AEROACOUSTIC APPLICATIONS.

A.H. Kadar [1]
Siemens PLM Software
Leuven, Belgium

P. Martinez-Lera [1]
Siemens PLM Software
Leuven, Belgium

M. Tournour [1]
Siemens PLM Software
Leuven, Belgium

W. Desmet[2]
K.U. Leuven
Leuven, Belgium

ABSTRACT

The aerodynamic noise generated from wind turbines is a growing concern with the ever increasing size of the turbine blades. The aerodynamic noise prediction is frequently based on unsteady CFD simulations, which can be expensive for the Reynolds numbers that are characteristic of wind turbines. The Random Particle-Mesh (RPM) method which is a stochastic approach to reconstruct the aerodynamic sources of sound in time domain from a solution to the averaged flow equations (RANS) is a promising alternative to high-fidelity unsteady CFD simulations. Since, trailing-edge noise constitutes a significant source of noise emitted by wind turbines, in this work the RPM method is applied to generate trailing-edge turbulence. The method is applied to a relatively simple Controlled-Diffusion airfoil geometry in 2D. Due to the stochastic nature of the method the choice of the simulation parameters has a significant impact on the statistics of the reconstructed turbulence. In the final paper a parametric study of the stochastic method will be presented with an aim to gain deeper understanding of the method and to propose guidelines for higher accuracy and lower computational cost.

NOMENCLATURE

CAA	=	Computational Aeroacoustics
CFD	=	Computational Fluid Dynamics
RPM	=	Random Particle-Mesh Method
RANS	=	Reynolds-Averaged Navier-Stokes

I. INTRODUCTION

The increasing aerodynamic noise level from large scale wind turbine blades is now a growing concern due to the close proximity of wind farms to human settlements. Research has shown that noise from wind turbines increases the risk of annoyance and disturbed sleep and possibly even psychological distress [1]. Therefore it is important to estimate and mitigate wind turbine noise when planning future wind farms.

The aerodynamic noise generated from a wind turbine is due to the interaction of the incoming turbulent flow with the surface of the turbine blade. There are several aerodynamic noise generation mechanisms from wind turbines that have been identified in the literature [2], including low-frequency noise, inflow turbulence noise and airfoil self-noise. The most prominent source of noise arising from horizontal axis wind turbines is the airfoil self-

[1] Siemens Industry Software N V, Interleuvenlaan 68, 3001 Leuven, Belgium
Email: ali.kadar@siemens.com (A.H. Kadar)
[2] Katholieke Universiteit Leuven, Department of Mechanical Engineering , Celestijnenlaan 300 B
3001 Leuven, Belgium

noise or blade trailing edge noise [3, 4]. The blade trailing edge noise is due to the conversion of local flow perturbations in the turbulent boundary layer into acoustic waves through interaction with the acoustically thin trailing edge.

A widely used method to predict trailing-edge noise is the so called hybrid approach wherein the computational domain is decomposed into different regions namely the source region and the acoustic propagation region. In the source region the transient flow field is first computed using high-fidelity numerical simulation tools like DNS, LES or DES (Detached Eddy Simulation). The transient flow field obtained is then used as a basis to define equivalent sound sources using the acoustic analogy's available in literature. It is found that the hybrid CAA techniques with flow input from LES shows accurate noise predictions [5, 6], it remains however very expensive for industrial applications.

It is possible to accelerate the computation of the hybrid approach by replacing the expensive CFD stage by Stochastic reconstruction approach for generating the turbulent fluctuations. In this framework the Random Particle-Mesh (RPM) method developed by Ewert et. al. [7-11] was introduced recently as a fast and efficient approach to set up fluctuating sound sources in the time-domain. The main idea here is to synthesize a turbulent field by filtering a random stochastic field. The filter is expressed in terms of the energy spectrum and controls the spatial properties of the synthetic turbulence. The generated turbulent flow field is not an exact solution of the flow equations but reproduce very accurately several key features of the sound sources, such as the energy spectrum, the correlation length and the time scales as provided by a RANS simulation of the time-averaged turbulent flow field. The stochastically reconstructed sources can then be used in conjunction with an acoustic solver for calculating the acoustic propagation.

The present work is inscribed in the line of stochastic reconstruction approach for synthesizing turbulent fluctuations around the trailing edge of an airfoil. The outline of this paper is as follows: Section II. presents the theoretical background of the RPM method for aeroacoustic applications, section III. describes the methodology illustrated using the Valeo CD airfoil test case and section IV. and section V. presents some preliminary results and conclusions respectively.

II. THEOREICAL BACKGROUND

Aeroacoustic analogy's governing the propagation of flow generated sound can be formally expressed in the form $\Gamma p'(\vec{x},t) = q_s(\vec{x},t)$, where Γ is the acoustic propagation operator, p' is the acoustic pressure fluctuation and q_s is the source term. The far-field noise caused by the source term q_s is unambiguously defined by the two-point cross-correlation of the source (Ewert et. al. [7]) given by

$$R^{q_s}(\overrightarrow{x_1},\overrightarrow{x_2},t_1,t_2) = \langle q_s(\overrightarrow{x_1},t_1), q_s(\overrightarrow{x_2},t_2)\rangle.$$

A filter based method able to synthesize turbulent velocity fluctuations with the desired two-point cross-correlation has been developed by Ewert et. al. [7-11] and is known as Random Particle-Mesh (RPM) method. The method can be applied in conjunction with an acoustic analogy when the source term q_s can be expressed as a linear function of velocity fluctuations.

Building upon the work of Ewert et. al. a purely Lagrangian approach to the RPM method was proposed by Dieste [12] The method is able to generate two-dimensional, locally homogeneous, isotropic and evolving turbulence. In the present work the RPM solver [13] based on the Lagrangian approach of Dieste is used for generating trailing-edge turbulence.

In the framework of the Random Particle-Mesh method the turbulent fluctuations are stochastically generated by spatially filtering convected white noise. In Dieste's approach the discrete realization of the convected white-noise is by means of Lagrangian particles distributed over the source domain and convected by the RANS mean flow. The method requires as input statistical properties of turbulent flow such as the distribution of turbulent kinetic energy, integral length and time scales of turbulence. In addition the spatial filter is derived by prescribing a model for the turbulence energy spectrum such as Gaussian, Von Karman or Liepmann [12] model spectrum.

The velocity fluctuations obtained by spatially filtering convected white-noise are given by (for detailed derivation refer to Dieste et. al. [12])

$$\acute{\boldsymbol{u}}\,(\boldsymbol{x},t) = \sum_{n=1}^{N} \boldsymbol{G}(r_n, k(\boldsymbol{y_n}), \Lambda(\boldsymbol{y_n}))\, W_n(\mathrm{t},\tau)$$

where $\boldsymbol{G} = \nabla \times (0,0,G)$ is defined by the prescribed Gaussian filter G expressed as:

$$G(r) = \sqrt{\frac{2k}{\pi}}\, e^{-\frac{\pi r^2}{2\Lambda^2}}$$

The filter G is a function of the turbulent kinetic energy (k) and integral length scale (Λ). The velocity fluctuations $\acute{\boldsymbol{u}}\,(\boldsymbol{x},t)$ at an observer point can be obtained by summing over all the N random particles in the source domain on which the white noise field $W_n$is defined. The strength of the random particle at each time can be obtained using the Langevin equation in the Lagrangian frame given by:

$$\frac{\partial}{\partial t} W_n(t) = -\frac{1}{\tau} W_n(t) + \sqrt{\frac{2}{\tau}}\, \varsigma_n(t)$$

where $W_n$and ς_n are zero-mean Gaussian distribution with variance determined by the density of particles. The exponential time correlation of turbulence is prescribed by the Langevin equation which is numerically integrated using higher order Runge-Kutta time integration schemes.

In 2-D the RPM domain is defined as a rectangle enclosing the source region. The dimensions of the rectangle are defined by the maximum distance from the source region where the random particles still contribute significantly to the velocity fluctuations. The RPM domain, grid size (Δ_{RPM}) and no of particles (N) are estimated based on distribution of the turbulent kinetic energy and the integral length scale of turbulence. The sampling time (Δt_S) and the number of samples (N_s) required to accurately reproduce the RANS statistics are determined by the integral time scale of turbulence (τ). The choice of these parameters has an impact on the statistical behavior of the generated turbulence and there are guidelines available in literature [14] to determine them.

III. METHODOLOGY

In the present work the stochastic reconstruction method is applied to the low-speed controlled-diffusion (CD) airfoil derived from the Valeo automotive cooling module. The schematic of the CD airfoil is shown in Figure 1. The airfoil has a chord length (C_L) of 0.134 m and a span length (L) of 0.3 m.

Figure 1. Schematic of the Valeo CD airfoil

The Valeo CD airfoil has been thoroughly investigated both experimentally [15,16] and numerically [17,18,19]. It is therefore a good representative test case for assessing the stochastic reconstruction approach in the context of trailing-edge turbulence generation for aeroacoustic applications. In this work the stochastic method is applied to the CD airfoil geometry in 2D and therefore the statistics of the reconstructed fluctuations can only be compared with the RANS statistics but cannot be compared with the LES numerical results available in 3D [19,20]. This will be accomplished as part of the future work.

The configuration considered in the present work is the Valeo CD airfoil at an angle of attack $\alpha = 8^0$ with free stream velocity $U_\infty = 16\, m/s$ which corresponds to the Reynolds number $Re_C = 1.6\, X\, 10^5$ based on the chord length. The RANS computational domain and mesh are shown in Figure 2. The size of the computational

domain is $4C_L$ in the stream wise direction and $2.5C_L$ in the transverse direction. The domain is discretized using a block-structured mesh with 167,770 predominantly hexahedral cells distributed across 7 levels of refinement.

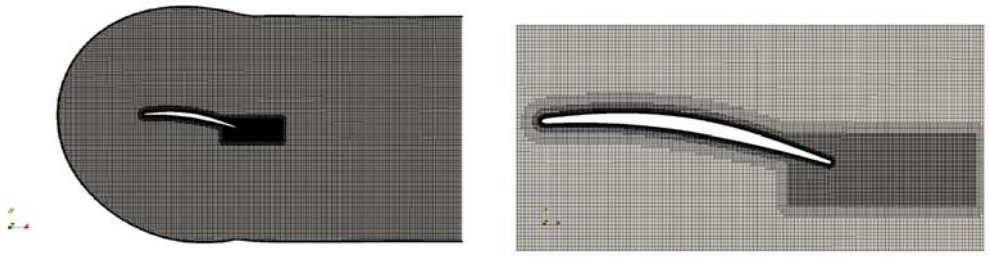

Figure 2. a) RANS Computation domain. b) Mesh refinement in the boundary layer and in the wake of the airfoil.

Incompressible 2-D RANS computation using the k-ω SST RANS turbulence model is performed using the Finite Volume solver OpenFOAM 3.0 [21] The discretization schemes used are second-order accurate in space and time. The flow is non-dimensionalized using airfoil chord length and free stream velocity. The streamline plot of the non-dimensional velocity field is shown in Figure 3. In order to take into account the jet deflection that is observed in the experiments the velocity boundary conditions at the inlet are extracted from a RANS computation performed on a larger domain including the airfoil, nozzle and the jet [20] A no-slip boundary condition on the airfoil surface and a pressure outlet boundary condition at the exit are prescribed. The turbulent kinetic energy (k) at the inlet is calculated from the turbulent intensity I=0.7% provided as a fraction of the mean velocity as $k = \frac{3}{2}(U_\infty I)^2$. The turbulent specific dissipation rate (ω) is calculated via the mixing length $l_m \sim C_L$ as $\omega_t = \frac{k^{0.5}}{C_\mu^{0.25} l_m}$ where $C_\mu = 0.09$ is a model constant.

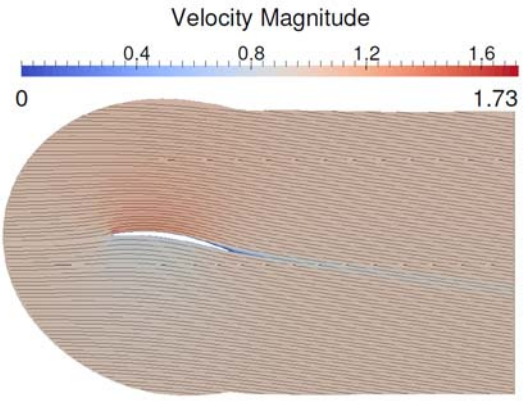

Figure 3. Flow streamlines around the CD airfoil computed using the $\boldsymbol{k-\omega}$ SST RANS turbulence model.

The turbulent kinetic energy is localized close to the trailing-edge and in the wake of the airfoil. The RPM domain is therefore restricted to a rectangular box including the trailing-edge and the airfoil wake as shown in Figure 4. The RANS flow domain is rotated by the angle of attack $\alpha = 8^0$ to align the flow streamlines in the wake with the x-Axis. This is done to facilitate the computation of space and time correlations along the streamline aligned with the x-Axis as shown in Figure 5.a.

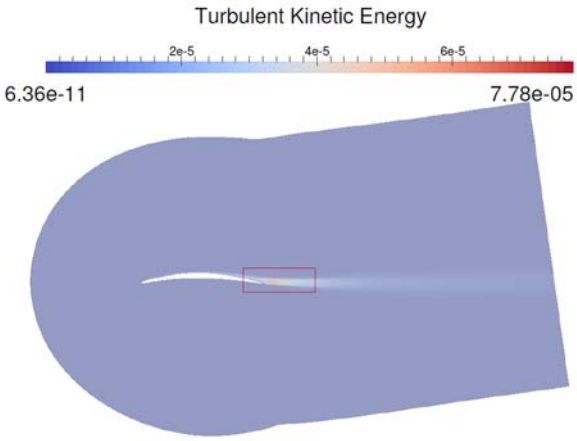

Figure 4. Rotated RANS flow domain and outline of the RPM domain

The RANS simulation results are further non-dimensionalized with the speed of sound $c_0 = 340\, m/s$ for the stochastic source generation and the subsequent acoustic propagation that will be done in future. Henceforth, all the subsequent physical quantities presented in the paper should be considered to be non-dimensionalized with airfoil chord length and speed of sound. The RANS data including the mean flow, turbulent kinetic energy(k), integral length scales(Λ) and integral time scales(τ) are mapped from the block-structured CFD mesh onto the uniform RPM grid using ParaView [22].

IV. RESULTS

Due to the stochastic nature of the method there is no definitive criteria for determining the simulation parameters. However, some preliminary best practice experience has been obtained for the application of RPM method to trailing-edge turbulence generation [14]. The choice of the simulation parameters for the stochastic method are listed in Table 1.

Table 1. Choice of parameters for the stochastic method

Simulation Parameters	Non-dimensional Value
Uniform RPM Grid Spacing Δ_{RPM}	0.001
No of Particles (N)	120000
Turbulence Energy Spectrum	Gaussian
Sampling Interval (Δt_S)	0.02125
No of Samples (N_s)	10000

The quality of the synthetic turbulence generated by the stochastic method is assessed by comparing the statistics of the reconstructed fluctuations with the RANS statistics. The results of the computed statistics with the choice of parameters as listed in Table 1. are presented in this section. The reconstructed turbulent kinetic energy is compared with the RANS turbulent kinetic energy in Figures 5 and 6.

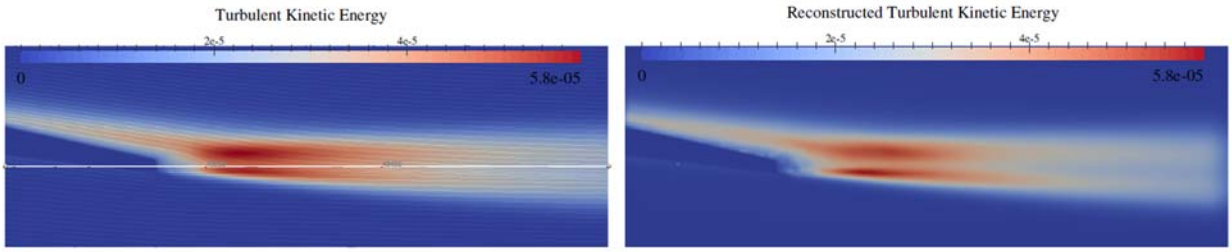

Figure 5. a) RANS turbulence kinetic energy with reference points on the x-Axis behind the trailing-edge. b) Reconstructed turbulent kinetic energy.

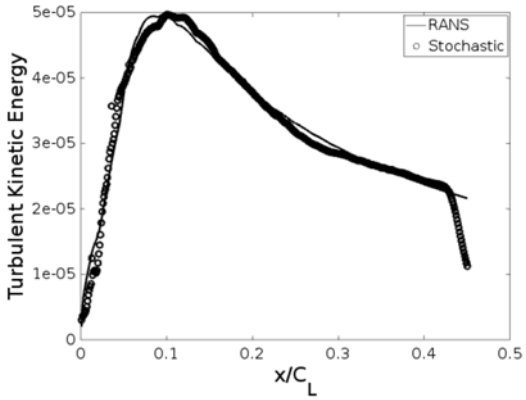

Figure 6. Reconstructed turbulent kinetic energy along the x-Axis behind the trailing-edge.

The statistical properties of the synthetic turbulence are further assessed by comparing numerical two-point cross-correlations $R_{ij}(\boldsymbol{r},t) = \langle \acute{u}_i(\boldsymbol{x_1},t_1)\, \acute{u}_j(\boldsymbol{x_2},t_2)\rangle$ where $\boldsymbol{r} = |\boldsymbol{x_2} - \boldsymbol{x_1}|$ and $t = |t_2 - t_1|$ with the analytical expressions. Assuming a model of the energy spectrum of turbulence it is possible to provide explicit expressions for the two-point cross-correlations $R_{ij}(\boldsymbol{r},t)$. For the Gaussian energy spectrum the numerical two-point cross-correlations are compared with analytical expressions in Figure 7.

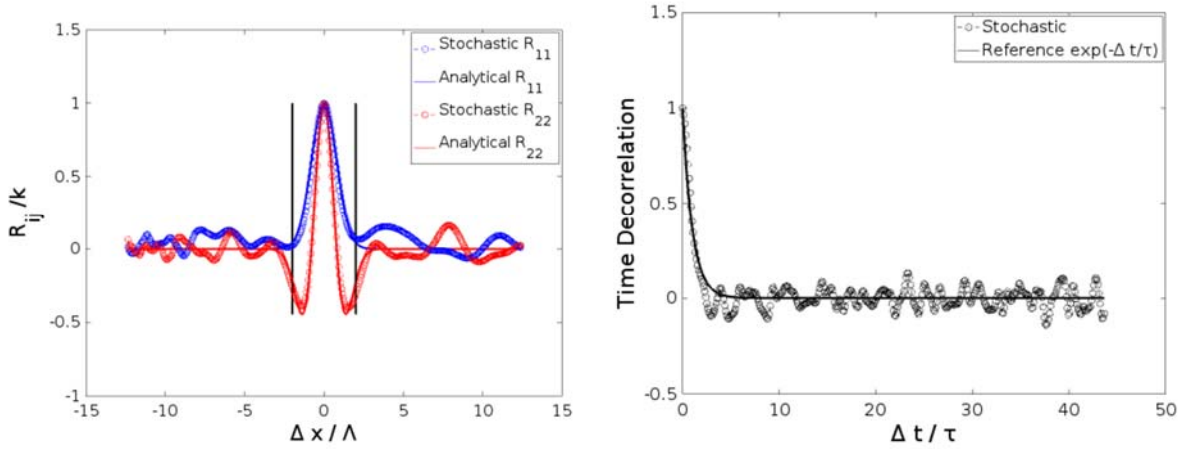

Figure 7. Correlation in space along x-Axis about mid reference point 48455 in Figure 5.a. b) Time correlation of a point moving with the mean flow along the streamline aligned with the x-Axis with respect to the left reference point 48280 shown in Figure 5.a.

From the plots it is concluded that the statistics of the reconstructed turbulence is in good agreement with the RANS statistics. The variance of the reconstructed fluctuations closely reproduces the target variance. Further the method is able to reproduce the two-point cross-correlations for the prescribed Gaussian energy spectrum and the exponential time correlation prescribed by the Langevin model. However due to the stochastic nature of the method the accuracy and computational cost of the method are determined by the choice of the parameters. The next step would be to do accomplish a parametric study to determine guidelines for the choice of the parameters for desired accuracy and minimum computational cost.

V. CONCLUSIONS

This paper presents an application of a stochastic reconstruction method for trailing-edge turbulence generation. The Random Particle-Mesh method first introduced by Ewert et. al. is applied to reconstruct turbulent fluctuations close to the trailing-edge and in the wake of the well investigated controlled-diffusion (CD) airfoil. The quality of the synthetic turbulence generated by the method is assessed by comparing the variance of the reconstructed fluctuations with the target variance obtained from Reynolds-Averaged Navier-Stokes (RANS) computation. The variance of the reconstructed fluctuations is found to be in good agreement with the target variance. Further the method is able to reproduce the two-point cross-correlations for the prescribed Gaussian energy spectrum and the exponential time correlation prescribed by the Langevin model. Due to the stochastic nature of the method, the choice of the simulation parameters viz grid size, number of particles, turbulence energy spectrum model, sampling time and number of samples has an impact on the statistics of the generated turbulence. In the final paper a parametric study of the effect of these parameters on the statistics of the reconstructed fluctuations and the computational cost will be presented. Future work will involve the comparison of two-point cross-correlation of the acoustic source term obtained stochastically with that obtained using LES simulations of a short span in 3D [19,20] .

ACKNOWLEDGEMENTS

The authors acknowledge with thanks the support of the European Commission's Framework Program "Horizon 2020", through the Marie Skłodowska-Curie Innovative Training Networks (ITN) "AEOLUS4FUTURE - Efficient harvesting of the wind energy" (H2020-MSCA-ITN-2014: Grant agreement no. 643167) to the present research project.

REFERENCES

[1] Schmidt, J. H., & Klokker, M. (2014). "Health effects related to wind turbine noise exposure: A systematic review". *PloS one*, *9*(12), e114183.

[2] Brooks, T. F., & Schlinker, R. H. (1983). "Progress in rotor broadband noise research". *Vertica*, *7*, 287-307.

[3] Schlinker, R. H., & Amiet, R. K. (1981, October). "Helicopter rotor trailing edge noise". In *AIAA, Astrodynamics Specialist Conference* (Vol. 1).

[4] Oerlemans, S., Sijtsma, P., & López, B. M. (2007). "Location and quantification of noise sources on a wind turbine". *Journal of sound and vibration*, *299*(4), 869-883.

[5] J. Christophe, S. Moreau, LES of the trailing-edge flow and noise of a controlled-diffusion airfoil at high angle of attack, Center for Turbulence Research, Annual Research Briefs, Stanford University (2008): 305-316.

[6] J. Christophe, J. Anthoine, S. Moreau, Trailing edge noise of a controlled-diffusion airfoil at moderate and high angle of attack., 15th AIAA/CEAS aeroacoustics conference (2009).

[7] R. Ewert, J. Dierke, J. Siebert, A. Neifeld, C. Appel, M. Siefert, O. Kornow, CAA broadband noise prediction for aeroacoustic design, Journal of Sound and Vibration, 330(17), 4139-4160.

[8] Roland Ewert, R. Emunds, CAA slat noise studies applying stochastic sound sources based on solenoidal digital filters., AIAA paper 2862 (2005): 2005.

[9] R. Ewert, RPM-the fast Random Particle-Mesh method to realize unsteady turbulent sound sources and velocity fields for CAA applications, AIAA Pap. 2007-3506 (2007).

[10] M. Siefert, R. Ewert, Anisotropic synthetic turbulence with sweeping generated by random particle mesh method, In Progress in Turbulence III (pp. 143-146). Springer Berlin Heidelberg (2009).

[11] Roland Ewert, Broadband slat noise prediction based on CAA and stochastic sound sources from a fast random particle-mesh (RPM) method., Computers & Fluids 37.4 (2008): 369-387.

[12] Dieste, M. (2011). *Random-vortex-particle methods applied to broadband fan interaction noise* (Doctoral dissertation, University of Southampton).

[13] B. Vanelderen,W. De Roeck,W. Desmet, Flow noise prediction of confined flows using synthetic turbulence and linearized Euler equations in a hybrid methodology, In Proceedings of the 19th AIAA/CEAS Aeroacoustics Conference, AIAA 2013 (Vol. 2267, pp. 27-29).

[14] A.H. Kadar, P. Martinez-Lera, V. Korchagin, W. De Roeck, W. Desmet, Stochastic reconstruction of turbulence for trailing-edge noise computation, International Conference on Noise and Vibration Engineering 2016.

[15] Sté, Moreau, P., Henner, M., Iaccarino, G., Wang, M., & Roger, M. (2003). "Analysis of flow conditions in freejet experiments for studying airfoil self-noise". *AIAA journal*, *41*(10), 1895-1905.

[16] Moreau, S., Neal, D., & Foss, J. (2006). "Hot-wire measurements around a controlled diffusion airfoil in an open-jet anechoic wind tunnel". *Journal of fluids engineering*, *128*(4), 699-706.

[17] Wang, M., Moreau, S., Iaccarino, G., & Roger, M. (2009). "LES prediction of wall-pressure fluctuations and noise of a low-speed airfoil". *International journal of aeroacoustics*, *8*(3), 177-197.

[18] Moreau, S., Neal, D., Khalighi, Y., Wang, M., & Iaccarino, G. (2006). "Validation of unstructured-mesh LES of the trailing-edge flow and noise of a controlled diffusion airfoil". In *Proceedings of the Summer Program* (p.1).

[19] J. Christophe, J. Anthoine, S. Moreau, Trailing edge noise of a controlled-diffusion airfoil at moderate and high angle of attack. 15th AIAA/CEAS aeroacoustics conference (2009).

[20] J. Christophe, Application of hybrid methods to high frequency aeroacoustics, PhD thesis, von Karman Institute for Fluid Dynamics and Universite Libre de Bruxelles, 2011.

[21] CFD Direct, OpenFOAM-3.0.1, http://openfoam.org/

[22] Sandia National Laboratory, Kitware Inc, Los Alamos National Laboratory, ParaView-4.4.0, http://www.paraview.org/

THE INTERNATIONAL CONFERENCE ON
WIND ENERGY HARVESTING 2017
20-21 April 2017
Coimbra, Portugal

Paper A4F.14

A SHORT REVIEW OF RECENT RESEARCH ACTIVITIES FOR AERODYNAMIC OPTIMIZATION OF VERTICAL AXIS WIND TURBINES

Abdolrahim Rezaeiha*,[a], Ivo Kalkman†,[a] , Bert Blocken‡,[a,b]

[a]*Building Physics and Services, Department of the Built Environment, Eindhoven University of Technology, P.O. Box 513, 5600 MB Eindhoven, The Netherlands*
[b]*Building Physics Section, Department of Civil Engineering, KU Leuven, Kasteelpark Arenberg 40 – Bus 2447, 3001 Leuven, Belgium*

ABSTRACT

There is a growing interest in wind energy harvesting in the built environment. Vertical axis wind turbines (VAWT) seem to represent an ideal candidate for this purpose due to their omni-directional operation. However, as a result of a comparatively small amount of research on VAWTs during the last decades they fall short of horizontal axis wind turbines (HAWT) with respect to aerodynamic efficiency. Therefore, more research is required in order to optimize VAWT performance. Several research methods including numerical modeling of varying complexity and large-scale wind tunnel measurements have aided the optimization of VAWTs. Designing new airfoils, optimizing blade pitch angle and flow control are some of the adopted approaches to improve VAWT performance. The current study intends to present a short review of conducted research and to propose new directions for future research.

INTRODUCTION

There is a growing interest in wind energy harvesting in the built environment. Vertical axis wind turbines (VAWT) seem to represent an ideal candidate for this purpose due to their omni-directional operation. However, compared to horizontal axis wind turbines (HAWT) they have received a small amount of research during the last decades which has contributed to their lower performance. Additionally, the flow around a VAWT is highly complex. This complexity can be related to several phenomena such as azimuthal variations of vortex shedding, dynamic stall, flow curvature effects and blade-wake interactions [1]. Several research methods have been employed in order to further elucidate these complexities. These methods, with various levels of fidelity, include momentum-based [2], vortex, and vorticity-transport models [3], CFD simulations [4], and wind tunnel experiments [1]. They have been employed to optimize VAWT aerodynamics with respect to airfoil shape [5], solidity [6] and pitch angle [7]. However, the research has not been comprehensive and further research, especially on optimizing the blade shape and the variable pitch angle is needed. Moreover, the application of flow control methods has recently been demonstrated for enhancing VAWT performance [8-11] while it is still at a very preliminary stage and requires enormous research. The current study intends to provide a short review of the conducted research on optimization of VAWT aerodynamics and propose new directions for future research.

The outline of the paper is as follows. An overview of the research methods employed to study VAWTs is presented in section 'VAWT research methods'. Section 'Optimization efforts' reviews the different research activities aimed at improving the performance of VAWTs. The last section provides the future trends and conclusions.

VAWT RESEARCH METHODS

Aerodynamic models

During the last decades, many different numerical models have been developed in order to predict the performance of VAWTs [12]. The earliest models were based on blade element momentum (BEM) theory [13] which were adapted from HAWT BEM models. BEM theory is a method developed in order to calculate the induced velocities by the rotor and couples the blade element theory and momentum theory in order to calculate

* PhD student, email: a.rezaeiha@tue.nl, corresponding author
† Senior research fellow, email: i.m.kalkman@tue.nl
‡ Full professor, email: b.j.e.blocken@tue.nl; bert.blocken@bwk.kuleuven.be

the time-averaged local loads on blades [13]. Single streamtube [14] is the fastest and simplest BEM model to predict the performance of a VAWT [12]. Later, two enhancements were made to the model leading to the multiple streamtube [15] and double-multiple streamtube models [2]. The latter, the most comprehensive model of this type, assumes that the rotor plane consists of multiple streamtubes in the crosswind direction and the incoming flow passes through them. Two tandem actuator disks, representing the upwind and downwind halves of the rotor, apply two separate inductions to the flow [2]. Recent studies [3] showed that the accuracy of BEM-based models is limited since they do not consider the effect of the wake on the flow. In some cases, agreement between predicted overall performance using these models and experiments only occurs due to error cancellation [3]. Furthermore, as these models require the airfoil polar as input to the code, they introduce an uncertainty for cases where dynamic stall happens [16]. Therefore, optimization efforts using these models were excluded from the overview presented study.

Vortex models are moderately complex aerodynamic models based on solution of the vorticity equation, which is derived from the Navier-stokes equations using an inviscid assumption [12]. The airfoil is modeled as a 2D lifting line and the wake is solved as trailing and shed vortices according to the Helmholtz theorem and Kelvin's theorem [17]. These models require the airfoil polar as input which is a drawback for flows on VAWT where dynamic stall might happen.

Panel methods are moderately complex models which are based on the solution of potential flow under the influence of the turbine wake vortex structure [12]. The wake can be either considered fixed or free in this model. This model is superior to vortex methods as it does not require the airfoil polar.

The vorticity-transport model (VTM) is another moderately complex aerodynamic model which can provide the velocity field and wake dynamics as well as the overall performance [3]. This is an inviscid model based on the vorticity equation in which a source term is introduced representing the generated vorticity. The source term consists of the contributions from shed and trailing vortices calculated from lifting line theory.

Viscous CFD simulation is the highest fidelity and most complex numerical method to study VAWT aerodynamics and is the only computational method based on solution of approximate versions of the full Navier-stokes equations [18]. This approach includes the effects of viscosity and can correctly capture the boundary layer development and its effects on the velocity field, and reliably determine the overall performance of the turbine. However, the accuracy of CFD results is highly dependent on many details such as the quality of the mesh, numerical schemes and turbulence modeling [4]. Moreover, it is a computationally expensive method. Given a high-quality mesh and correct simulation setup as well as sufficient computational capacity CFD is a great method for parametric studies and the optimization of VAWTs.

Wind tunnel experiments and field measurements

Wind tunnel experiments are highly valuable for elucidating the complex aerodynamics of VAWTs. In addition, numerical results need to be validated with experimental data in order to verify that they represent the flow physics correctly. Therefore, experiments are an essential part of VAWT research. However, setting up an experiment can be very expensive and time-consuming. An alternative is to conduct field measurements, which have the benefit of having the real atmospheric wind characteristics as input to the turbine. However, they are also very challenging and expensive, and control over measuring conditions is obviously lacking.

Comparison

A comparison of research methods for the investigation of VAWT aerodynamics is provided in Table 1.

Table 1. Comparison of methods for the optimization of VAWT aerodynamics.

	Method	Advantages	Disadvantages
Modeling	BEM models	Easy to implement, computationally inexpensive, rough estimate of performance	Does not represent the correct energy extraction mechanism, limited accuracy, requires airfoil polar as input, very inaccurate after stall
	Vortex model	Good for rough parametric study, moderate computational cost, good estimation of flow field, does not need airfoil polar	Inviscid, inaccurate after stall, overestimation of performance

	Panel methods	Medium fidelity, moderate computational cost, good estimation of flow field, does not need airfoil polar	Inviscid, not suitable for detailed parametric studies
	Vortex-transport model	Medium fidelity, moderate computational cost, good estimation of flow field, does not need airfoil polar	Inviscid, not suitable for detailed parametric studies
	CFD	High fidelity, good for optimization and detailed parametric studies	Computationally expensive, highly dependent on the mesh quality and solution setup
Experiment	Wind tunnel experiment	Necessary for validation of numerical models and CFD, ideal for understanding flow phenomena, good for optimization and parametric studies	Expensive, time-consuming
	Open-field large-scale experiments	Represents the real working conditions	Extremely expensive, no controlled freestream conditions, less suitable for optimization

OPTIMIZATION EFFORTS

Airfoil shape

There has been little research on optimization of aerodynamics of wind turbines mainly because the flow physics were not well understood. The initial VAWT airfoils were not specifically designed for this purpose and were simply selected from the symmetric NACA series. More recently, with further understanding of the complex VAWT flow, new specifically designed airfoils were proposed which were optimized for a multi-Megawatt VAWT for both clean and soiled cases using inviscid panel methods and a genetic algorithm. The objective of the optimization was to increase the aerodynamic performance based on criteria defined by Simão Ferreira and Geurts [5] while taking the structural strength and roughness sensitivity into account. The optimized airfoil achieved a 0.03 higher pressure coefficient (C_P) compared with the typical VAWT symmetric NACA0018 airfoil for a tip speed ratio (TSR) as low as 2.5. This increment gradually decreased to zero for higher TSRs (e.g. 4). However, the optimization was based on an inviscid panel code and the airfoils were optimized for a Reynolds number of 5×10^6 which is higher than typically encountered for small-scale turbines in urban environments. The designed airfoils have not yet been investigated using wind tunnel measurements or high-fidelity CFD simulations.

A CFD study by Mohamed [19] quantified the performance of an H-type VAWT using 20 different symmetric and non-symmetric airfoils for a range of solidities and TSRs. The study employed Unsteady RANS (URANS) using the realizable k-ε turbulence model [20] in order to calculate C_P and C_T. However, the results were only based on sampling during 3 revolutions of the turbine after only 1 initial revolution, which was recently found to be too short to make sure that the final results are unaffected by transient effects and that the C_P has reached a constant value [4]. Moreover, the time step in the study was very large (0.001 s, equal to 6.4° to 9.6° per time step for TSRs of 4 and 6 respectively). The mesh which was used contains only 85,000 cells and the y^+ values attained reached up to 50, which is much coarser than normally needed to capture the flow details of a full-scale H-type VAWT.

Pitch angle

The pitch angle (β) is defined as the angle between the chord line and the tangent to the rotation. The effect of fixed pitch angle was studied using high-fidelity viscous CFD simulations [7]. The study found that applying an optimum β can improve the turbine C_P by up to 6.6%. Changing β also was found to shift the instantaneous loads and moments between upwind and downwind halves of the turbine [7, 21]. The findings of the CFD study revealed the high potential for dynamic blade pitching as a future trend for VAWTs.

Shaft

A high-fidelity CFD simulation found that [22] applying an optimum surface roughness height can regain 69% of the power loss due to the presence of shaft which is equivalent to a 1.7% increase in C_P for an urban VAWT.

The mechanism for power enhancement was shown to be due to a shift in flow regime over the shaft from sub-critical to critical.

Flow control

Any type of local manipulation of the flow, either passive or active, which is applied in order to reach some desired flow characteristics is called flow control [23]. Flow control methods have received a huge amount of research in recent years for applications on aircrafts [24] as well as wind turbines [25]. Complex unsteady nature of flow over a VAWT seems to be an ideal case for implementation of local flow control. Recently several flow control methods; such as trailing-edge flaps [8], leading-edge slot suction/blowing [11], dielectric barrier discharge (DBD) plasma actuators [10], synthetic jets [9] and Gurney flaps [26]; have been successful to control the flow separation or circulation for pitching airfoils. The flow on pitching airfoils is of high similarity to that of VAWTs and helicopters. Therefore, the promising findings suggests that VAWTs also have the potential to take advantage of local flow control in order to improve the performance of the turbine. Therefore, further research on application of flow control for VAWTs is of great interest.

FUTURE TRENDS AND CONCLUSION

From the above the following conclusions and future trends are identified:

- With improved understanding of the complex flow around VAWTs during recent years new optimized airfoils have been introduced. The performance of turbines equipped with these airfoils needs to be studied in detail using high-fidelity CFD simulation and wind tunnel experiments in order to test the improvements.
- Optimization of fixed pitch angle has been shown to improve the performance of VAWTs while shifting the loads between upwind and downwind halves of the turbine. The findings of a study on the instantaneous moment on the blades during a revolution revealed the high potential for dynamic blade pitching for VAWTs where the pitch angle distribution is defined based on optimal values identified using high-fidelity CFD calculations at a fixed pitch angle and/or wind tunnel experiments. Therefore, optimal dynamic blade pitching needs to be investigated as a very promising candidate for performance improvement of VAWTs.
- Flow control has emerged as a very promising research area for wind turbines both using experiments and simulations. Methods such as suction/blowing have been successful in controlling the flow separation while trailing-edge flaps, DBD plasma actuators and Gurney flaps could increase the circulation around the airfoil for the case of pitching airfoils. Due to similarities in the flow for pitching airfoils and VAWTs, the promising achievements for the former proposes the flow control as an intriguing field of research for VAWT performance improvement, although its correct application is highly dependent on a detailed understanding of VAWT flow features.

ACKNOWLEDGEMENTS

The authors would like to acknowledge support from the European Commission's Framework Program Horizon 2020, through the Marie Curie Innovative Training Network (ITN) AEOLUS4FUTURE - Efficient harvesting of the wind energy (H2020-MSCA-ITN-2014: Grant agreement no. 643167) as well as the TU1304 COST ACTION “WINERCOST”.

REFERENCES

[1] Tescione G, Ragni D, He C, Simão Ferreira C, and van Bussel GJW, "Near wake flow analysis of a vertical axis wind turbine by stereoscopic particle image velocimetry," *Renewable Energy,* vol. 70, pp. 47-61, 2014.

[2] Paraschivoiu I, *Wind turbine design: with emphasis on darrieus concept*. Montréal, Québec: Polytechnic International Press, 2009.

[3] Simão Ferreira C, Madsen HA, Barone M, Roscher B, Deglaire P, and Arduin I, "Comparison of aerodynamic models for vertical axis wind turbines," *Journal of Physics: Conference Series,* vol. 524 (012125), 2014.

[4] Rezaeiha A, Kalkman IM, and Blocken B, "CFD simulation of a vertical axis wind turbine operating at a moderate tip speed ratio: guidelines for minimum domain size and azimuthal increment," *Renewable Energy*, 2017. doi:10.1016/j.renene.2017.02.006

[5] Simão Ferreira C and Geurts B, "Aerofoil optimization for vertical-axis wind turbines," *Wind Energy,* vol. 18 (8), pp. 1371-85, 2014.
[6] Li Q, Maeda T, Kamada Y, Murata J, Shimizu K, Ogasawara T, Nakai A, and Kasuya T, "Effect of solidity on aerodynamic forces around straight-bladed vertical axis wind turbine by wind tunnel experiments (depending on number of blades)," *Renewable Energy,* vol. 96, pp. 928-939, 2016.
[7] Rezaeiha A, Kalkman IM, and Blocken B, "Effect of pitch angle on power performance and aerodynamics of a vertical axis wind turbine," *submitted for publication*, 2017.
[8] Ertem S, "Enhancing the features of vertical axis wind turbines with active flap control and airfoil design," MSc, Aerospace Engineering, TU Delft, Netherlands, 2015.
[9] Yen J and Ahmed NA, "Enhancing vertical axis wind turbine by dynamic stall control using synthetic jets," *Journal of Wind Engineering and Industrial Aerodynamics,* vol. 114, pp. 12-17, 2013.
[10] Greenblatt D, Schulman M, and Ben-Harav A, "Vertical axis wind turbine performance enhancement using plasma actuators," *Renewable Energy,* vol. 37 (1), pp. 345-354, 2012. doi:10.1016/j.renene.2011.06.040
[11] Sasson B and Greenblatt D, "Effect of leading-edge slot blowing on a vertical axis wind turbine," *AIAA Journal,* vol. 49 (9), pp. 1932-1942, 2011. doi:10.2514/1.j050851
[12] Islam M, Ting D, and Fartaj A, "Aerodynamic models for Darrieus-type straight-bladed vertical axis wind turbines," *Renewable and Sustainable Energy Reviews,* vol. 12 (4), pp. 1087-1109, 2008.
[13] Glauert H, "Airplane propellers," in *Aerodynamic Theory*. vol. 4, W. F. Durand, Ed., ed Berlin: Division L, Julius Springer, 1935, pp. 169–360.
[14] Templin R, "Aerodynamic performance theory of the NRC vertical-axis wind turbine," Technical Report LTR-LA-160, National Research Council of canada, 1974.
[15] Strickland JH, "The Darrieus turbine: a performance prediction model using multiple streamtubes," Sandia National Laboratories, Technical Report SAND75-0431, 1975.
[16] Zanon A, Giannattasio P, and Simão Ferreira C, "Wake modelling of a VAWT in dynamic stall: impact on the prediction of flow and induction fields," *Wind Energy,* vol. 18 (11), pp. 1855-74, 2014. doi:10.1002/we.1793
[17] Anderson JD, *Fundamental of aerodynamics*. Boston: McGraw-Hill, 2001.
[18] Jin X, Zhao G, Gao K, and Ju W, "Darrieus vertical axis wind turbine: basic research methods," *Renewable and Sustainable Energy Reviews,* vol. 42, pp. 212-225, 2015.
[19] Mohamed MH, "Performance investigation of H-rotor Darrieus turbine with new airfoil shapes," *Energy,* vol. 47 (1), pp. 522-530, 2012. doi:10.1016/j.energy.2012.08.044
[20] Bianchini A, Balduzzi F, Rainbird JM, Peiro J, Graham JMR, Ferrara G, and Ferrari L, "An experimental and numerical assessment of airfoil polars for use in Darrieus wind turbines—part I: flow curvature effects," *Journal of Engineering for Gas Turbines and Power,* vol. 138 (032602), 2015. doi:10.1115/1.4031269
[21] Simão Ferreira C and Scheurich F, "Demonstrating that power and instantaneous loads are decoupled in a vertical-axis wind turbine," *Wind Energy,* vol. 17 (3), pp. 385-396, 2014.
[22] Rezaeiha A, Kalkman IM, and Blocken B, "Effect of the shaft on the aerodynamic performance of an urban vertical axis wind turbine: a numerical study," *submitted for publication*, 2017.
[23] Gad-el-Hak M, *Flow control: passive, active, and reactive flow management*: Cambridge University Press, 2000.
[24] Cattafesta LN and Sheplak M, "Actuators for active flow control," *Annual Review of Fluid Mechanics,* vol. 43 (1), pp. 247-272, 2011. doi:10.1146/annurev-fluid-122109-160634
[25] Johnson SJ, Baker JP, van Dam CP, and Berg D, "An overview of active load control techniques for wind turbines with an emphasis on microtabs," *Wind Energy,* vol. 13 (2-3), pp. 239-253, 2010. doi:10.1002/we.356
[26] Ion M, Radu B, and Horia D, "Theoretical performances of double Gurney flap equipped the VAWTs," *Incas Bulletin,* vol. 4 (4), pp. 93-99, 2012. doi:10.13111/2066-8201.2012.4.4.8

THE INTERNATIONAL CONFERENCE ON
WIND ENERGY HARVESTING 2017
20-21 April 2017
Coimbra, Portugal

Editors:
C. Baniotopoulos
C. Rebelo
L. Simões da Silva
C. Borri
B. Blocken
H. Hemida
M. Veljkovic
T. Morbiato
R. P. Borg
S. Huber
E. Efthymiou

Coimbra, Portugal
2017

Sponsored and supported by:

Printed by:

Distributed by:

Business Center Leonardo da Vinci
Coimbra iParque – Lote 3
3040-540 Antanhol, Portugal
+351 239 098 422
store@cmm.pt

Coimbra, Portugal
2017